UNCLASSIFIED

XEROX
322161
CATALOGED BY ASTIA
AS AD No.

INSTITUTE
FOR
COOPERATIVE
RESEARCH

REPORT No. 47

CORY No. 52

UNCLASSIFIED

104400

BALLISTIC ANALYSIS LABORATORY

PROJECT THOR
TECHNICAL REPORT No. 47
APRIL 1961

THE RESISTANCE OF VARIOUS METALLIC MATERIALS TO PERFORATION BY STEEL FRAGMENTS; EMPIRICAL RELATIONSHIPS FOR FRAGMENT RESIDUAL VELOCITY AND RESIDUAL WEIGHT (U)

TECHNICAL LIBRARY
BLDG. 305
ABERDEEN PROVING GROUND, MD.
STEAP-TL

Per Ltr From DRDAR-TSB
dtd 24 Jan 79 distribution A'
Applied
rk 2/13/79
Per Voron J. Wyatt. Distribution
Unlimited

Contract DA-36-034-509-ORD-29RD
Philadelphia Ordnance District
Ordnance Research and Development Project No. TB3-0238
Department of the Army Project No. DA5B03-03-010

Ballistic Research Laboratories
Aberdeen Proving Ground, Maryland

ASTIA
APR 21 1961
TIPDR

UNCLASSIFIED

[redacted]

UNCLASSIFIED

THE RESISTANCE OF VARIOUS METALLIC MATERIALS TO PERFORATION BY STEEL FRAGMENTS; EMPIRICAL RELATIONSHIPS FOR FRAGMENT RESIDUAL VELOCITY AND RESIDUAL WEIGHT (U)

PROJECT THOR TECHNICAL REPORT NO. 47

APRIL 1961

Ballistic Analysis Laboratory
Institute for Cooperative Research
The Johns Hopkins University
3506 Greenway
Baltimore 18, Maryland

TECHNICAL LIBRARY
BLDG 305
ABERDEEN PROVING GROUND, MD.
STEAP-TL

Contract DA-36-034-509-ORD-29RD
Philadelphia Ordnance District

Ordnance Research and Development Project No. TB3-0238
Department of the Army Project No. DA5B03-05-010

Ballistic Research Laboratories
Aberdeen Proving Ground, Maryland

UNCLASSIFIED

TECHNICAL LIBRARY
U. S ARMY ORDNANCE
ABERDEEN PROVING GROUND, MD.
ORDBG-TL

UNCLASSIFIED
[redacted]

TABLE OF CONTENTS

	Page No.
ABSTRACT	vii
INTRODUCTION	1
EMPIRICAL RELATIONSHIPS	8
RESULTS	15
FRAGMENT SHATTER	24
ADAPTATIONS TO VULNERABILITY ANALYSES	31
MEASURING THE MAXIMUM CAPACITY OF THE RESIDUAL FRAGMENT FOR PERFORATION	33
CONCLUSIONS	43
APPENDICES	47
DISTRIBUTION LIST	365

UNCLASSIFIED

UNCLASSIFIED
[redacted]

LIST OF APPENDICES

Appendix			Page No.
A	Graph Set I:	V_o vs m for Selected Values of e	47
B	Graph Set II:	V_r/V_s and m_r/m_s vs V_s for Selected Values of m_s and θ	79
C	Graph Set III:	V_r vs E for Selected Combinations of m_s, θ, V_s	167
	Graph Set IV:	m_r vs E for Selected Combinations of m_s, θ, V_s	195
	Graph Set V:	$f(m_r, V_r)$ vs E for a Particular Combination of m_s, θ, V_s	223
D	Graph Set VI:	e (inches of Celotex) vs E for Various Combinations of m_s, θ, V_s . .	229
	Graph Set VII:	e (inches of 2024T-3) vs E for Various Combinations of m_s, θ, V_s . .	257
E	Graph Set VIII:	Impact Conditions for Fragment Shatter	
		a. Shatter Criterion: $c' = 0$	285
		b. Shatter Criterion: $c' = 0.25$ . .	295
F	Empirical Treatment of Aluminum Alloys and Homogeneous Steels		305
	Graph Set IX:	V_o vs m for Selected Values of e; Composite Graphs for 2SO, 2024T-3, and 7075T-6	309
	Graph Set X:	V_o vs m for Selected Values of e; Composite Graphs for Homogeneous Steels with Brinell Hardness Values of 100, 300, and 500	313
G	Experimental Data; Steel Fragments Impacting on Various Target Materials		317
H	Other Ballistic Analysis Laboratory Reports Dealing with the Perforation of Target Materials by Fragments and Projectiles		363

UNCLASSIFIED
[redacted]

LIST OF TABLES

Table		Page No.
I	Target Materials	4
II	Summary of Characteristics of Experimental Data	5
III	Fragment Dimensions	6
IV	Constants for the Estimating Equations for Residual Velocity (No Particular Fragment Shape Assumed)	18
V	Constants for the Estimating Equations for Residual Velocity (Compact Fragment Shape Assumed)	19
VI	Constants for the Estimating Equations for V_o (No Particular Fragment Shape Assumed)	20
VII	Constants for the Estimating Equations for V_o (Compact Fragment Shape Assumed)	21
VIII	Constants for the Estimating Equations for m_r (No Particular Fragment Shape Assumed)	22
IX	Constants for the Estimating Equations for m_r (Compact Fragment Shape Assumed)	23
X	Constants for the Estimating Equations for $m_s(c')$; $c' = 0$ (Compact Fragment Shape Assumed)	29
XI	Constants for the Estimating Equations for $m_s(c')$; $c' = 0.25$ (Compact Fragment Shape Assumed)	30
XII	Dual Target Experimental Data; Estimates of the Situation	41
XIII	Steel Fragments Impacting on Magnesium	318
XIV	Steel Fragments Impacting on Aluminum Alloys	324
XV	Steel Fragments Impacting on Titanium Alloy	336
XVI	Steel Fragments Impacting on Cast Iron	341
XVII	Steel Fragments Impacting on Face-Hardened Steel	342
XVIII	Steel Fragments Impacting on Homogeneous Steel of Various Hardnesses	345
XIX	Steel Fragments Impacting on Copper	352
XX	Steel Fragments Impacting on Lead	356
XXI	Steel Fragments Impacting on Tuballoy	360

UNCLASSIFIED
[redacted]

LIST OF FIGURES

Figure		Page No.
1	Thickness of Target Materials vs Areal Density	7
2	The Interaction of V_o Estimates with Estimates of Impact Conditions for Fragment Shatter	27
3	Set-Up for Firings on Dual Targets	40
4-6	V_o vs m for Selected Values of e; Magnesium Alloy	48
7-9	V_o vs m for Selected Values of e; 2024T-3	51
10-12	V_o vs m for Selected Values of e; Titanium Alloy	54
13-15	V_o vs m for Selected Values of e; Cast Iron	57
16-18	V_o vs m for Selected Values of e; Face-Hardened Steel	60
19-21	V_o vs m for Selected Values of e; Mild Homogeneous Steel	63
22-24	V_o vs m for Selected Values of e; Hard Homogeneous Steel	66
25-27	V_o vs m for Selected Values of e; Copper	69
28-30	V_o vs m for Selected Values of e; Lead	72
31-33	V_o vs m for Selected Values of e; Tuballoy	75
34-42	V_r/V_s and m_r/m_s vs V_s for Selected Values of m_s and θ; Magnesium	80
43-51	V_r/V_s and m_r/m_s vs V_s for Selected Values of m_s and θ; 2024T-3	89
52-60	V_r/V_s and m_r/m_s vs V_s for Selected Values of m_s and θ; Titanium Alloy	98
61-66	V_r/V_s and m_r/m_s vs V_s for Selected Values of m_s and θ; Cast Iron	107
67-75	V_r/V_s and m_r/m_s vs V_s for Selected Values of m_s and θ; Face-Hardened Steel	113
76-84	V_r/V_s and m_r/m_s vs V_s for Selected Values of m_s and θ; Mild Steel	122

UNCLASSIFIED
[redacted]

LIST OF FIGURES (Cont)

Figure		Page No.
85-93	V_r/V_s and m_r/m_s vs V_s for Selected Values of m_s and θ; Hard Steel	131
94-102	V_r/V_s and m_r/m_s vs V_s for Selected Values of m_s and θ; Copper	140
103-111	V_r/V_s and m_r/m_s vs V_s for Selected Values of m_s and θ; Lead	149
112-120	V_r/V_s and m_r/m_s vs V_s for Selected Values of m_s and θ; Tuballoy	158
121-147	V_r vs E for Selected Combinations of m_s, θ, V_s	168
148-174	m_r vs E for Selected Combinations of m_s, θ, V_s	196
175-178	$f(m_r, V_r)$ vs E for a Particular Combination of m_s, θ, V_s	224
179-205	e (inches of Celotex) vs E for Various Combinations of m_s, θ, and V_s	230
206-232	e (inches of 2024T-3) vs E for Various Combinations of m_s, θ, and V_s	258
233-241	Impact Conditions for Fragment Shatter; c' = 0	286
242-250	Impact Conditions for Fragment Shatter; c' = 0.25	296
251-253	V_o vs m for Selected Values of e; Composite Graphs for 2SO, 2024T-3, and 7075T-6	310
254-256	V_o vs m for Selected Values of e; Composite Graphs for Homogeneous Steels with Brinell Hardness Values of 100, 300, and 500	314

Following page is blank

UNCLASSIFIED
[redacted]

ABSTRACT

Perforation data for steel fragments impacting on each of ten metallic materials have been collected and analyzed. The experimental data are characterized by fragment sizes from five to 825 grains, striking velocities as high as 12,000 feet per second, and obliquities of strike as high as 80 degrees. Empirical formulas of a given type have been fitted to the data for each target material, thereby relating fragment residual velocity and residual weight, in separate equations, to important impact parameters.

The two sets of estimating equations, used together, serve as a basis for several extensions or applications; these are: 1) the determination of impact conditions for which the fragment disintegrates during perforation, 2) a comparison, for equal weight per unit area of target materials, of the resistance of target materials to perforation, 3) a calibration of the resistance of a target material to perforation in terms of the maximum thickness of a standard medium that the residual fragment can perforate, and 4) a more realistic consideration of the effect of an intermediate target on the potential of the fragment to damage a primary target.

UNCLASSIFIED
[redacted]

INTRODUCTION

For several years, this laboratory has been participating in programs sponsored by the Weapon Systems Laboratory, Ballistic Research Laboratories (BRL), to supply information for vulnerability analysts and weapons designers on the resistance of various materials to perforation by steel fragments and projectiles. These materials usually have some military significance, but do not necessarily constitute primary targets. Their use is justified because they have some property or properties necessary or desirable for a given functional or structural purpose. For example, stainless steel or a magnesium alloy may be a suitable material for some particular function within a jet engine; copper is a useful material for missile nose cones of the heat sink variety; thin gauge mild steel is structurally and economically suitable for military truck hoods and cabs; the skin and structural members of an aircraft may be composed of an aluminum alloy noted for its strength and low density. A vulnerability analyst has to contend with the problem of determining the extent of protection provided by these structural materials even though they may never have been intended as armoring materials.

The bulk of the experimental data required to furnish information on the resistance of these materials to perforation has been provided by BRL. Data from other sources have been included wherever possible. The experimental work is always planned with the intention of making the data, and therefore the study, particularly applicable to problems related to the vulnerability of ground, air, and space targets. Several reports have been published on the analyses of such data; the identification of these reports is given in Appendix H.

Other reports, similar to the present one, but dealing with non-metallic target materials, are planned for the future; such materials include nose-cone materials, lightweight armors, transparencies, structural plastics, and foams.

Additional studies will be made of fragment shapes and materials other than those considered here, the relationship of hole size to impact parameters, and the results of fragment impact in terms of the numbers, weights, velocities, and spatial distribution of particles formed from the impact.

The objectives of this study are 1) the consolidation, revision, and extension of information appearing in earlier reports on the perforation of materials by steel fragments, 2) the consideration of additional target materials not discussed in those earlier reports, 3) the determination of the effect of extending the upper limit of the experimental fragment striking velocities from 6000 fps to 12,000 fps, 4) the establishment of a technique for estimating fragment residual weight as well as fragment residual velocity, 5) the determination of sets of impact conditions for which the fragment shatters during the perforation of the target, 6) the formulation of a useful method for comparing target materials in their resistance to perforation by steel fragments, and 7) the establishment of a technique for estimating the maximum capacity of the residual fragment for additional perforation assuming the perforation of an initial target material with known impact parameters.

The ambitious scope of this work emphasizes the need for an empirical attack to penetration problems. This approach becomes more attractive when it is allied with high-speed computer facilities which help to turn out practical results very rapidly. The technique is believed

entirely adequate wherever good predictions over broad ranges of impact parameters are preferred to pinpoint accuracy for a few narrow sets of conditions.

The empirical formulas include the important impact parameters and are established from a relatively small, appropriate collection of experimental data.

For the BRL experimental data, compact steel (SAE 1020) fragments in the shape of short cylinders and cube-on-cylinders were used in single-shot firings. These fragments varied in size from five to 475 grains. Striking velocities as high as 12,000 fps were obtained using light-gas guns. Conventional powder guns were used for the low velocity rounds. Residual velocities were obtained, in general, by the use of break-wire screens and Potter counter chronographs.

The conditions for each round within the experimental data are tabulated in Appendix G. It will be noted that a greater effort was made to secure experimental data for some target materials than for others; this reflects the relative military importance or the cost of these target materials, or the explanation may simply be related to the difficulty of obtaining appropriate thicknesses of certain target materials.

The target materials selected for inclusion in this report along with their designations are listed in Table I which follows. Table II summarizes the characteristics of the experimental data. Table III provides the dimensions and weights of fragments used in collecting the experimental data.

Table I

Target Materials

Name	Identification	Density (lb/ft^3)	BHN
Magnesium Alloys	FS-1 (Dow Chemical); AZ92	110, 114	72
Aluminum Alloy *	2024T-3 and 2024T-4	173	120
Titanium Alloys	Ti 6Al 4V; Ti 7Mn	276, 284	190
Cast Iron	Ductile Nodular Graphitic (60-45-18) ASTM-A339-51T	450	150-220
Face-Hardened Steel		485	(Front) 480-510 (Rear) 331-365
Homogeneous Steel		485	
a. Mild			150
b. Hard			380
Copper	Elec. Tough Pitch; QQC 502	556	42
Lead	Comm. Pure (No Sb) B-29-40-t	687	5.5
Tuballoy	Depleted Uranium or U_{238}	1167	235-245

* Throughout the text, wherever reference is made to 2024T-3, the remark applies equally well to 2024T-4, since both alloys were used interchangeably in the experimental work.

UNCLASSIFIED

Table II

Summary of Characteristics of Experimental Data

Target Material	Target Thickness Range (inches)	Areal Density Range (lb/ft^2)	Obliquity Range (degrees)	Striking Velocity Range (fps)	Fragment Size Range (grains)
Magnesium Alloys	0.05 - 3.00	0.5 - 28	0 - 80	500 - 10,500	15 - 240
2024T-3	0.02 - 2.00	0.3 - 29	0 - 80	1200 - 11,000	5 - 240
Titanium Alloys	0.04 - 1.20	1 - 28	0 - 80	700 - 10,400	30 - 240
Cast Iron	0.19 - 0.56	7 - 21	0 - 45	1900 - 6100	15 - 240
Face-Hardened Steel	0.14 - 0.50	5 - 20	0 - 70	2500 - 9800	15 - 240
Homogeneous Steel	0.03 - 1.00	1 - 40	0 - 70	600 - 12,000	5 - 825
Copper	0.06 - 1.00	3 - 46	0 - 70	1100 - 11,400	15 - 240
Lead	0.07 - 1.00	4 - 57	0 - 70	500 - 10,400	15 - 240
Tuballoy	0.10 - 0.20	10 - 19	0 - 60	4500 - 10,100	30 - 475

UNCLASSIFIED

UNCLASSIFIED

Note: Graphs in the appendices contain contours which, for the most part, are limited by the intervals of the experimental data, as shown above. Some minor extrapolations outside these intervals have been made. Thus, for example, no commitment is made on Cast Iron at fragment velocities above 6000 fps or at 70° obliquity. Similarly, the contours for Face-Hardened Steel begin at an areal density of 5 lb/ft^2.

Table III

Fragment Dimensions

TYPE I

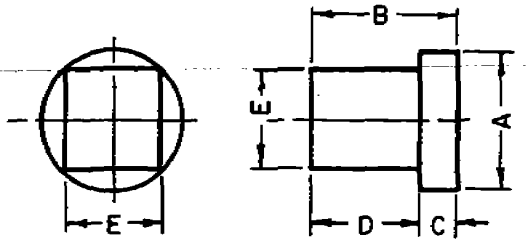

TYPE II

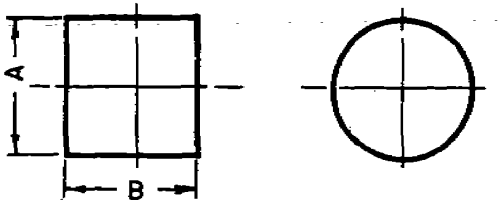

TYPE	A	B	C	D	E	wt (grains)
I	.587	.579	.225	.354	.414	240
I	.499	.389	.170	.219	.353	120
I	.399	.303	.131	.172	.282	60
I	.299	.282	.115	.167	.211	30
I	.233	.230	.093	.137	.167	15
II	.587	.450				240
II	.499	.313				120
II	.399	.243				60
II	.299	.213				30
II	.233	.180				15
II	.687	.654				475

(All dimensions in inches)

UNCLASSIFIED [redacted]

UNCLASSIFIED [redacted]

[redacted]

UNCLASSIFIED

Thickness of Target Materials vs Areal Density

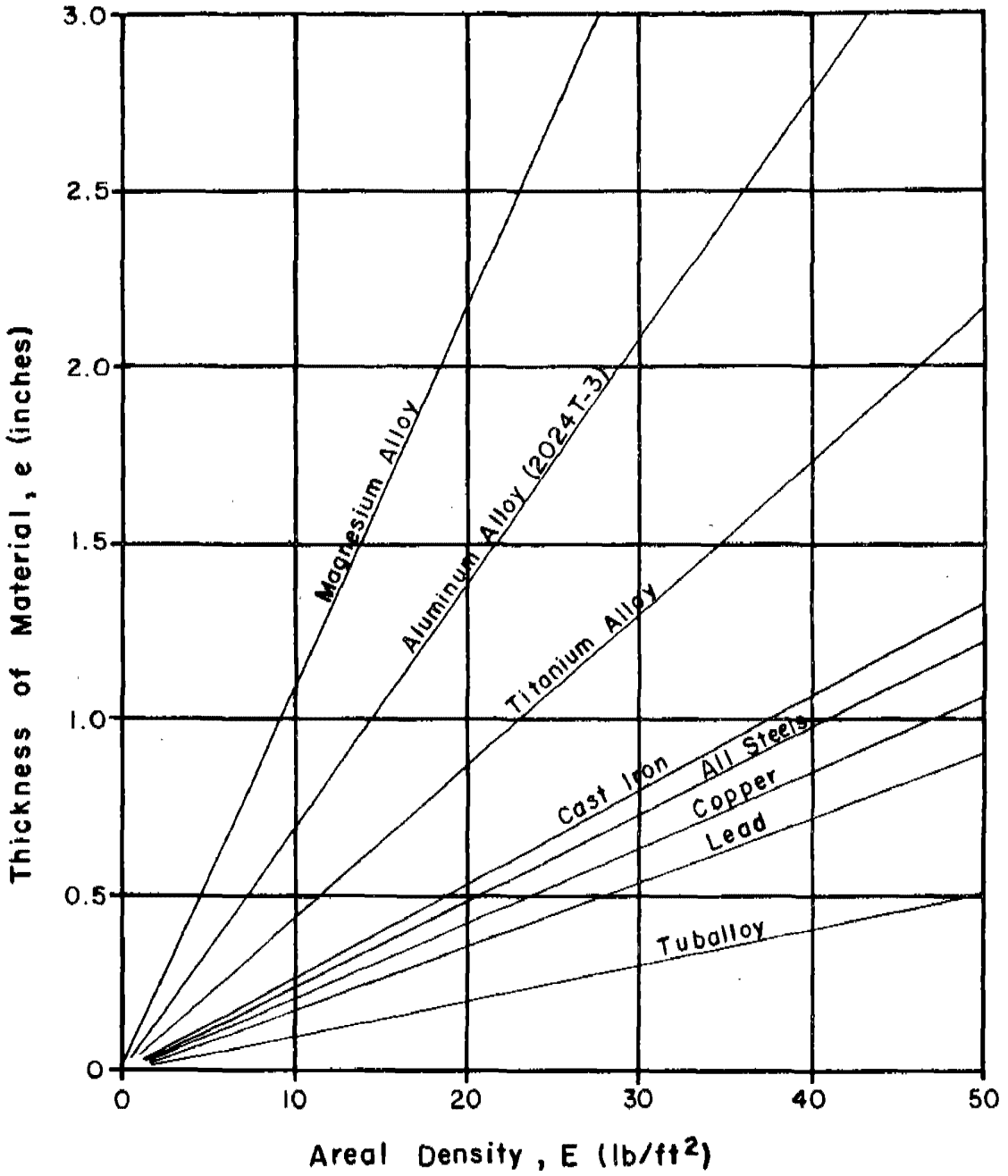

Fig. 1

UNCLASSIFIED

[redacted]

EMPIRICAL RELATIONSHIPS

The resistance of a material to perforation by steel fragments has been measured in many ways. Here, the assumption is made that this resistance can be related to the losses in weight and velocity sustained by the fragment during perforation. Accordingly, experimental data have been collected for steel fragments impacting on each material of a variety of metallic target materials. Those data cases where perforation was achieved were singled out for the analysis. Measurements of both the residual velocity and the residual weight were noted. These measurements refer to the largest piece of the original fragment which perforates the plate.

In Technical Report No. 36 (see Appendix H), a method is described for obtaining empirical equations from residual velocity data to relate residual velocity to important impact parameters. The type of equation proposed is:

$$V_r = V_s - 10^c \, (eA)^{\alpha} \, m_s^{\beta} \, (\sec \theta)^{\gamma} \, V_s^{\lambda} \, ,$$

where V_r is the fragment residual velocity in fps,

V_s is the fragment striking velocity in fps,

e is the target thickness in inches,

A is the average impact area of the fragment in square inches,

m_s is the weight of the original fragment in grains,

θ is the angle between the trajectory of the fragment and the normal to the target material, and

$c, \alpha, \beta, \gamma, \lambda$ are constants determined separately for each material.

The derived values of the constants specifying the estimating equation for fragment residual velocity for each target material are tabulated in Tables IV and V of the Results Section.

The exponential form of this equation is simple and practical and includes the important impact parameters. The form has the additional merit of being convertible into a corresponding logarithmic form which is useful because of its linearity.

For a comparison of the resistances of target materials to perforation by fragments, it has been found useful to introduce another variable, "E", into the estimating equation. The new variable refers to the areal density of the target material and is measured in pounds per square foot. It is obtained by multiplying the target thickness in feet by the density of the target material in pounds per cubic foot. By altering the formulas so that the thickness parameter is replaced by the areal density parameter, it becomes possible to compare the resistance of target materials to perforation on an equal target weight basis.

The criterion for goodness of fit of the estimating equation is the magnitude of σ defined below. If $|\Delta V_r|_i$ is the magnitude of the error made in estimating the fragment residual velocity in the i-th set of N sets of experimental conditions, then

$$\sigma^2 = \frac{\sum_{i=1}^{N} |\Delta V_r|_i^2}{N} .$$

It is understood that the selection of fit for each target material is made to correspond with the lowest obtainable value of σ. The value of σ for each residual velocity estimating equation is given in Table IV of the Results Section.

The following method is employed to obtain an empirical formula for estimating residual velocity for steel fragments impacting on each target material. The basic formula is converted into the associated logarithmic form:

$$\log (V_s - V_r) = c + \alpha \log (eA) + \beta \log m_s + \gamma \log \sec \theta + \lambda \log V_s .$$

With this linear form, the method of least squares is employed to determine a satisfactory set of values for c, α, β, γ, λ.

Admittedly, this procedure minimizes S, defined below, rather than σ.

$$S^2 = \frac{\sum_{i=1}^{N} \left\{ \left[\log(V_s - V_r)\right]_{exp} - \left[\log(V_s - V_r)\right]_{calc} \right\}_i^2}{N} ,$$

where the subscripts "exp" and "calc" refer to experimental and calculated values respectively. This method of calculating the constants has proved to be entirely satisfactory. It is often possible, by slight alterations of the constants, to improve the fit of the estimating equation. Experience has shown, however, that the minor improvements obtainable do not justify the effort.

For the type of equation assumed, it is possible to solve for V_s when V_r is zero. This striking velocity shall be designated V_o. The constants which define the V_o equation for each target material are specified in Tables VI and VII of the Results Section. The significance of V_o has been established in previous reports by this laboratory where V_o has been found to be a good analytical approximation to the protection velocity; the latter is defined to be the highest striking velocity below the ballistic limit for which the probability of perforation is zero. In other words, the V_o values are estimates of the limiting striking velocities for which the target always prevents perforation by the fragment. A set of graphs featuring V_o values for each target material is included in Appendix A.

* * * *

In an analogous manner, an empirical equation is developed for each target material for estimating fragment residual weight. The form of the equation fitted to the data for each target material is:

$$m_s - m_r = 10^c \, (eA)^\alpha \, m_s^\beta \, (\sec \theta)^\gamma \, V_s^\lambda \, ,$$

where the only new symbol is m_r, the weight in grains of the largest piece of the original fragment which perforates the target. To accommodate a similar least squares treatment on the associated logarithmic equation, the assumption is made that the minimum loss in fragment weight is one grain rather than zero grains. The criterion of goodness of fit is σ^* defined below. If $|\Delta m_r|_i$ is the magnitude of the error in estimating the fragment residual weight in the i-th set of N sets of experimental conditions, then

$$(\sigma^*)^2 = \frac{\sum_{i=1}^{N} |\Delta m_r|_i^2}{N} \, .$$

The values of the constants specifying the equation for estimating fragment residual weight for each target material are given in Tables VIII and IX of the Results Section.

With low striking velocities, the loss in weight of a fragment during perforation is small and is usually ignored. In such cases, the residual velocity, alone, serves as a good measure of the resistance of the target to perforation and the capacity of the residual fragment for perforating another target. As striking velocity increases, the break-up of the fragment becomes more and more pronounced until this aspect of the impact must be taken into account. The residual weight of the fragment must

be known as well as the residual velocity before any reasonable estimate can be made of the capacity of the fragment for perforating another target.

Fragment recovery after impact is accomplished by the use of a bank of fiberboard ("celotex") sheets. The residual fragment is located within this bank, weighed, and saved in a small manila envelope marked to show the impact condition and the depth of penetration into the celotex. More refined techniques and other recovery materials are in use, but recovery in celotex was adopted as the most practical method for this study. The weight of the residual fragment together with the depth of penetration into celotex suggest a striking velocity on the celotex which serves as a rough check on the residual velocity recorded for the fragment. Even this simple recovery technique is tedious and time-consuming, but for the objectives of this report, the derived information was deemed important enough to outweigh these disadvantages.

In many experimental cases, the weight of the largest piece of residual fragment approximates the total weight of fragment perforating the barrier target. At any rate, the capacity of a fragment to perforate a primary target beyond an initial barrier can be conservatively estimated by considering only the largest piece of fragment which perforates the barrier. This approach is justified whenever the hypothetical primary target is one for which damage from the impact of small, slow-moving particles is not anticipated, i.e., damage to such a target will essentially be that caused by the largest, fastest particle that impacts on it. Incidentally, such a tough, internal component is a common element of modern targets such as guided missiles and aircraft. These components are often large and difficult to protect, so that they contribute heavily to the vulnerability of the target.

On the other hand, when a large, hypothetical, primary target is extremely vulnerable to impact, even from a small, slow fragment, then a solution based on the largest, fastest fragment is helpful but inadequate. A typical high-speed impact may result in one main fragment particle, several smaller fragment particles, and several spall particles of variable size issuing from the rear surface of the target. If any one of several of these particles can damage the primary target, then it becomes necessary to account for the total number, sizes, and velocities of these particles before a proper measure of the lethality of the fragment-producing weapon can be made.

In the laboratory, it is more practical to keep track of the largest portion of residual fragment than to recover every portion of residual fragment regardless of size. Ideal information would provide the weight, speed, and direction of each particle of the original fragment that successfully perforates the target material as well as the weight, speed, and direction of every spall particle.

* * * *

Sets of graphs for estimating both fragment residual velocity and residual weight are presented in Appendix B. The use of double ordinates in these graphs requires some explanation. Two sets of thickness contours are to be found on each graph of this type. The thickness contours drawn with solid lines refer to the left-hand ordinate; the dashed contours refer to the right-hand ordinate. Thus, for a given graph and a given striking velocity, two ratios are found. The contours are shown only where both ratios are positive. The dotted lines on these graphs suggest that the associated residual velocities apply to a particle of insignificant weight (no more than one or two grains).

No commitment is made on the spall particles which are formed from the plate material. Limited observations of spall patterns reveal wide experimental fluctuations in the number, size, and velocity of the spall particles from one round to the next where the same impact conditions are employed.

The previous remarks emphasize the need for using the empirical equations for residual weight and residual velocity jointly. In this way, it will become apparent where the results are valid. The double-ordinate graphs clearly display the regions of validity, i.e., where both ratios are positive.

For the empirical treatment of homogeneous steels and aluminum alloys, reference is made to Appendix F, since a more complicated technique is required to account for variations of target materials in hardness when these target materials have essentially the same chemical composition.

[redacted]

RESULTS

The empirical formulas developed from the experimental data on each of the metallic targets for the purpose of estimating residual velocity are of the form:

$$V_r = V_s - 10^c \, (eA)^{\alpha} \, m_s^{\beta} \, (\sec \theta)^{\gamma} \, V_s^{\lambda} \quad .$$

The values of c, α, β, γ, and λ are tabulated in Table IV for each of the metallic targets. In addition, the sample size N of experimental data and the value of σ are displayed.

For fragments of a given shape, these formulas can be simplified by removal of the impact parameter A to the form:

$$V_r = V_s - 10^{c*} \, e^{\alpha} \, m_s^{\beta*} \, (\sec \theta)^{\gamma} \, V_s^{\lambda} \quad ,$$

since for any shape approximating that of a regular convex polyhedron, the average presented area is nearly directly proportional to the two-thirds power of the mass.

Note that whenever a form of the estimating equation is desired which omits the impact parameter A, then some assumption has to be made about the shape of the fragments under consideration. Whenever the fragments under consideration are similar in configuration to those used in the experimental work for this report, it can be assumed that the simplified equations, graphs, and conclusions based on the master estimating equations apply. In fact, predictions from these equations for extrapolations to bullets with length to diameter ratios approximately equal to three, show good agreement with experimental results. If the fragments under consideration have large length to diameter ratios, like some flechettes, then it is not yet clear how well these estimating equations would apply. The

[redacted]

experimental data which have been used to fix the estimating equations involve compact fragments, i.e., fragments with length to diameter ratios close to unity. The simplified equations for non-compact fragments would be different than those used here since some new relationship between average impact area and fragment weight would be appropriate.

The values of c^*, α, β^*, γ, and λ for the equations associated with compact fragments are tabulated in Table V.

The V_o formulas derived from the empirical residual velocity formulas are of the form:

$$V_o = 10^{c_1} (eA)^{\alpha_1} m_s^{\beta_1} (\sec \theta)^{\gamma_1} .$$

The values for c_1, α_1, β_1, and γ_1 for each target material are tabulated in Table VI.

For fragments of a given shape, these formulas can be simplified, as before, to the form:

$$V_o = 10^{c_1^*} e^{\alpha_1} m_s^{\beta_1^*} (\sec \theta)^{\gamma_1} .$$

The values of c_1^*, α_1, β_1^* and γ_1 for the equations associated with compact fragments are tabulated in Table VII.

The empirical formulas developed from the experimental data for the purpose of estimating fragment residual weight are of the form:

$$m_r = m_s - 10^c (eA)^{\alpha} m_s^{\beta} (\sec \theta)^{\gamma} V_s^{\lambda} .$$

The values of c, α, β, γ, and λ are tabulated in Table VIII for each target material. In addition, the sample size N^* of experimental data for the residual weight equation and the value of σ^* are noted.

[redacted]

For fragments of a given shape, these formulas can be simplified by removal of the impact parameter A, as before, to the form:

$$m_r = m_s - 10^{c^*} e^{\alpha} m_s^{\beta^*} (\sec \theta)^{\gamma} V_s^{\lambda} \quad .$$

The resulting values of c^*, α, β^*, γ, and λ for the equations associated with compact fragments are tabulated in Table IX.

[redacted]

Table IV

Constants for the Estimating Equations for Residual Velocity

(No Particular Fragment Shape Assumed)

Form of Equation: $V_r = V_s - 10^c (eA)^\alpha m_s^\beta (\sec\theta)^\gamma V_s^\lambda$

$\frac{V_r}{V_s^\lambda} = \frac{10^c (eA)^\alpha m_s^\beta (\sec\theta)^\gamma V_s^\lambda}{V_s^\lambda}$

Target Material	c	α	β	γ	λ	N	σ
Magnesium	6.904	1.092	-1.170	1.050	-0.087	85	600
Aluminum Alloy 2024T-3	7.047	1.029	-1.072	1.251	-0.139	189	400
Titanium Alloy	6.292	1.103	-1.095	1.369	0.167	51	703
Cast Iron	4.840	1.042	-1.051	1.028	0.523	28	195
Face-Hardened Steel	4.356	0.674	-0.791	0.989	0.434	55	546
Mild Homogeneous Steel	6.399	0.889	-0.945	1.262	0.019	117	516
Hard Homogeneous Steel	6.475	0.889	-0.945	1.262	0.019		
Copper	2.785	0.678	-0.730	0.846	0.802	49	562
Lead	1.999	0.499	-0.502	0.655	0.818	71	700
Tuballoy	2.537	0.583	-0.603	0.865	0.828	92	291

Thor Exponent Conversion

$$V_s - V_R = 10^{c} (eA)^{\alpha} m_s^{\beta} (\sec\theta)^{\gamma} V_s^{\lambda}$$

$$(eA)^{\alpha} \longrightarrow \left[\frac{1}{(2.54)^3}\right]^{\alpha}$$ converts cm to ins.

$$m_s^{\beta} \longrightarrow \left[\frac{2000}{453.9524}\right]^{\beta}$$ converts grams to grains

$$\left[\frac{V_s^{\lambda}}{V_s - V_R}\right] \longrightarrow (0.0328084)^{\lambda-1}$$ converts cm/sec to ft/sec

Then $C = c' + \log_{10}\left[\left(\frac{1}{(2.54)^3}\right)^{\alpha}\left(\frac{2000}{453.9524}\right)^{\beta}(0.0328084)^{\lambda-1}\right]$

Table V

Constants for the Estimating Equations for Residual Velocity

(Compact Fragment Shape Assumed)

Form of Equation: $V_r = V_s - 10^{c^*} e^{\alpha} m_s^{\beta^*} (\sec \theta)^{\gamma} V_s^{\lambda}$

Target Material	c^*	α	β^*	γ	λ
Magnesium	4.596	1.092	-0.442	1.050	-0.087
Aluminum Alloy 2024T-3	4.872	1.029	-0.386	1.251	-0.139
Titanium Alloy	3.960	1.103	-0.359	1.369	0.167
Cast Iron	2.638	1.042	-0.356	1.028	0.523
Face-Hardened Steel	2.931	0.674	-0.341	0.989	0.434
Mild Homogeneous Steel	4.520	0.889	-0.352	1.262	0.019
Hard Homogeneous Steel	4.596	0.889	-0.352	1.262	0.019
Copper	1.351	0.678	-0.278	0.846	0.802
Lead	0.944	0.499	-0.170	0.655	0.818
Tuballoy	1.305	0.583	-0.214	0.865	0.828

Table VI

Constants for the Estimating Equations for V_o

(No Particular Fragment Shape Assumed)

Form of Equation: $V_o = 10^{c_1} (eA)^{\alpha_1} m_s^{\beta_1} (\sec \theta)^{\gamma_1}$

Target Material	c_1	α_1	β_1	γ_1
Magnesium	6.349	1.004	-1.076	0.966
Aluminum Alloy 2024T-3	6.185	0.903	-0.941	1.098
Titanium Alloy	7.552	1.325	-1.314	1.643
Cast Iron	10.153	2.186	-2.204	2.156
Face-Hardened Steel	7.694	1.191	-1.397	1.747
Mild Homogeneous Steel	6.523	0.906	-0.963	1.286
Hard Homogeneous Steel	6.601	0.906	-0.963	1.286
Copper	14.065	3.476	-3.687	4.270
Lead	10.955	2.735	-2.753	3.590
Tuballoy	14.773	3.393	-3.510	5.037

Table VII

Constants for the Estimating Equations for V_o

(Compact Fragment Shape Assumed)

Form of Equation: $V_o = 10^{c_1^*} e^{\alpha_1} m_s^{\beta_1^*} (\sec \theta)^{\gamma_1}$

Target Material	c_1^*	α_1	β_1^*	γ_1
Magnesium	4.226	1.004	-0.406	0.966
Aluminum Alloy 2024T-3	4.276	0.903	-0.339	1.098
Titanium Alloy	4.753	1.325	-0.431	1.643
Cast Iron	5.533	2.186	-0.747	2.156
Face-Hardened Steel	5.178	1.191	-0.603	1.747
Mild Homogeneous Steel	4.608	0.906	-0.359	1.286
Hard Homogeneous Steel	4.685	0.906	-0.359	1.286
Copper	6.823	3.426	-1.403	4.270
Lead	5.175	2.735	-0.930	3.540
Tuballoy	7.602	3.393	-1.248	5.037

[redacted]

Table VIII

Constants for the Estimating Equations for m_r

(No Particular Fragment Shape Assumed)

Form of Equation: $m_r = m_s - 10^c \, (eA)^{\alpha} \, m_s^{\beta} \, (\sec \theta)^{\gamma} \, V_s^{\lambda}$

Target Material	c	α	β	γ	λ	N*	σ*
Magnesium	-5.945	0.285	0.803	-0.172	1.519	105	11
Aluminum Alloy 2024T-3	-6.663	0.227	0.694	-0.361	1.901	172	22
Titanium Alloy	2.318	1.086	-0.748	1.327	0.459	107	16
Cast Iron	-9.703	0.162	0.673	2.091	2.710	29	13
Face-Hardened Steel	1.195	0.234	0.744	0.469	0.483	54	28
Mild Homogeneous Steel	-2.507	0.138	0.835	0.143	0.761	31	20
Hard Homogeneous Steel	-2.264	0.346	0.629	0.327	0.880	27	29
Copper	-5.489	0.340	0.568	1.422	1.650	70	25
Lead	-1.856	0.506	0.350	0.777	0.934	54	26
Tuballoy	-3.379	0.560	0.447	0.640	1.381	148	30

these don't make sense

negative

[redacted]

Table IX

Constants for the Estimating Equations for m_r

(Compact Fragment Shape Assumed)

Form of Equation: $m_r = m_s - 10^{c^*} e^{\alpha} m_s^{\beta^*} (\sec \theta)^{\gamma} V_s^{\lambda}$

Target Material	c^*	α	β^*	γ	λ
Magnesium	-6.547	0.285	0.993	-0.172	1.519
Aluminum Alloy 2024T-3	-7.142	0.227	0.845	-0.361	1.901
Titanium Alloy	0.023	1.086	-0.024	1.327	0.459
Cast Iron	-10.046	0.162	0.782	2.091	2.710
Face-Hardened Steel	-1.690	0.234	0.900	0.469	0.483
Mild Homogeneous Steel	-2.798	0.138	0.926	0.143	0.761
Hard Homogeneous Steel	-2.994	0.346	0.859	0.327	0.880
Copper	-6.207	0.340	0.794	1.422	1.650
Lead	-2.926	0.506	0.687	0.777	0.934
Tuballoy	-4.564	0.560	0.821	0.640	1.381

FRAGMENT SHATTER

A form of the estimating equation for predicting fragment residual weight is:

$$m_s - m_r = k\, e^{\alpha}\, m_s^{\beta}\, (\sec\theta)^{\gamma}\, V_s^{\lambda} \;.$$

The omission of the parameter, A, the average presented area of the fragment, implies that fragments of a fixed shape are under consideration. The question naturally arises: Is it possible to develop a useful auxiliary equation, in a manner similar to that of obtaining a V_o equation from the estimating equation for predicting residual velocity?

Observations of the double-ordinate graphs in Set II of Appendix B show many of the thickness contours, which relate to fragment residual weight, with intercepts on the striking velocity axis at velocities less than 10,000 fps. The conditions corresponding to these intercepts are significant in that the fragment is much heavier and/or moving much faster than needed to defeat the target. Originally, no special attempt was made to locate these intercepts, the main effort being made to establish a useful estimating equation for predicting fragment residual weight. For each of the dense target materials, the data contain cases where very little or none of the original fragment is recorded as having passed through the target and having been found in the collecting medium. Since fragment residual weight decreases with an increase in striking velocity, for all target materials, the question of the existence of sets of impact conditions for which perforation occurs and the fragment residual weight is essentially zero, becomes of foremost importance. As a consequence, more experimental data were collected for impact conditions near the anticipated intercepts to determine whether the results substantiated the extrapolations to these

intercepts. At the same time, these additional data served to improve the estimates of the locations of the intercepts.

If, within the estimating equation for predicting fragment residual weight,

$$m_r = c' m_s,$$

then

$$m_s = \left[\frac{k}{1-c'}\right]^{\frac{1}{1-\beta}} e^{\frac{\alpha}{1-\beta}} (\sec\theta)^{\frac{\gamma}{1-\beta}} V_s^{\frac{\lambda}{1-\beta}} .$$

Let this parameter m_s, under the qualification that $m_r = c' m_s$, be called $m_s(c')$. The significance of c' is that it represents the ratio of fragment residual weight to striking weight. When $c' = 0$, it follows that no residual piece of the original fragment is expected to have any measureable or appreciable weight, whereas the target may nevertheless be perforated. With existing laboratory facilities, it is difficult to obtain precise data near the intercepts, because when extreme fragment break-up occurs, the likelihood of overlooking small portions of the original fragment in the collecting medium increases. The choice of c' close to but not equal to zero may not provide equally useful information, but this information may be more closely associated with experimental accuracy and fact.

The graphs in Appendix E for $c' = 0$ relate shatter velocity to the striking weight of the fragment. The thickness contours on these graphs are displayed only where perforation is anticipated. This point emphasizes the need for using the $m_s(c')$ equations in conjunction with the V_o equations or graphs; the V_o equations or graphs indicate the lower limits of the regions of validity of the thickness contours in the graphs of Appendix E. If the

$m_s(c')$ equations are used indiscriminately, they might suggest a condition for fragment shatter where only a partial penetration would occur.

To illustrate, a portion of a graph in Graph Set VIII is reproduced in Figure 2 which follows. The conditions that are sampled in this figure are 0.125" of Face-Hardened Steel impacted upon by a fragment at 60° obliquity. The value of c', the shatter criterion, is taken as zero. If the V_o contour corresponding to the impact conditions is inserted as well onto this graph, the m_s, V_s plane is thereby divided into three regions: 1) no perforation, 2) perforation with $m_r \geq 0$, and 3) perforation with $m_r = 0$. It becomes obvious why the "shatter line" is not extended below the V_o line.

It is to be noted that most of the present estimates for fragment shatter lie outside the main region of experimentation. These extrapolated estimates may nevertheless prove useful until better estimates are possible as a result of improved launching devices which will permit higher striking velocities.

Until a much greater experimental effort is made to obtain detailed data corresponding to the intercept conditions, a safer interpretation of the graphs in Appendix E for $c' = 0$ is to regard the shatter velocity as the striking velocity for which extreme break-up of the fragment will occur, rather than to assume that absolutely no portion of the original fragment passes through the target.

When c' is chosen as 0.25, a second, more conservative, family of graphs is evolved, as shown in Appendix E. A comparison of corresponding graphs in these two families suggests how much the velocity must be increased to cause the additional fragment break-up as evidenced by the variation in the two values of c'.

The Interaction of V_0 Estimates with Estimates of Impact Conditions for Fragment Shatter

Target Material: Face-Hardened Steel
Target Thickness: e = 0.125"

Obliquity: $\theta = 60°$
Shatter Criterion: $c' = 0$

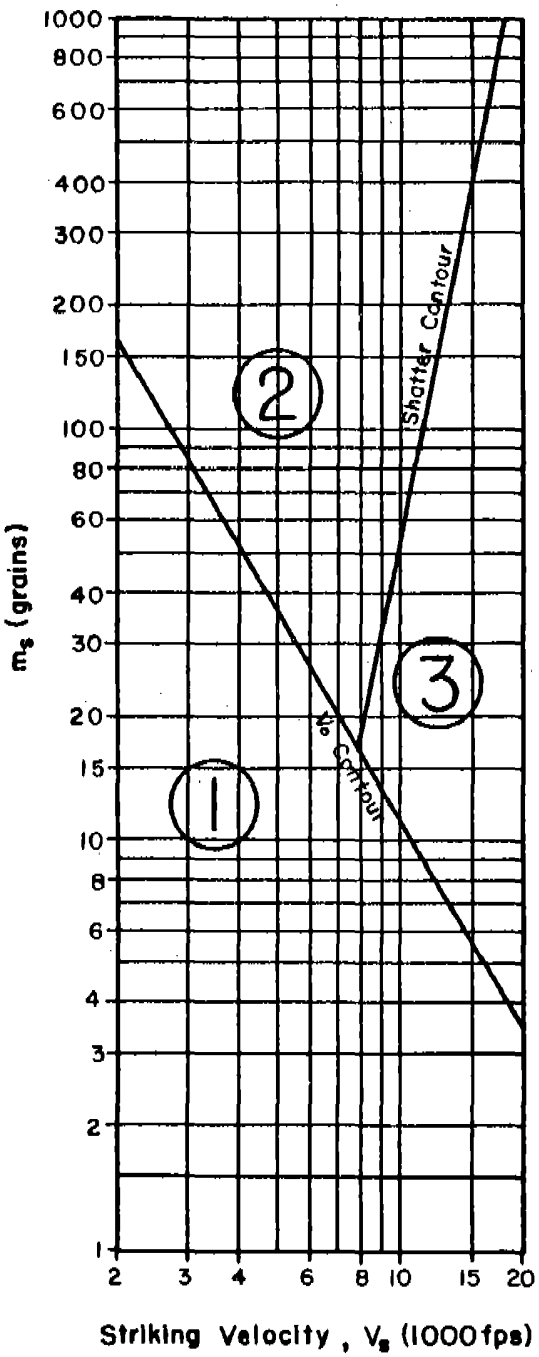

Legend
① No Perforation
② Perforation $m_r \geq 0$
③ Perforation $m_r = 0$

Fig. 2

If the equation for m_s (c') is of the form

$$m_s(c') = 10^K e^{\alpha'} (\sec \theta)^{\gamma'} V_s^{\lambda'} ,$$

then the values of K, α', γ', and λ' for each target material except Magnesium are listed in Tables X and XI for c'= 0 and c'= 0.25 respectively. The omission of Magnesium is a result of the inability of this low-density material to cause severe fragment break-up within the interval of striking velocities (12,000 fps maximum) used in the experimental firings.

Table X

Constants for the Estimating Equations for $m_s(c')$; $c' = 0$

(Compact Fragment Shape Assumed)

Form of Equation: $m_s(c') = 10^K e^{\alpha'} (\sec \theta)^{\gamma'} V_s^{\lambda'}$

Target Material	K	α'	γ'	λ'
Magnesium*	-------	------	------	--------
2024T-3	-46.122	1.464	-2.328	12.277
Titanium	0.022	1.060	1.295	0.448
Cast Iron	-45.980	0.742	9.570	12.405
Face-Hardened Steel	-16.913	2.344	4.690	4.834
Mild Homogeneous Steel	-38.061	1.872	1.945	10.348
Hard Homogeneous Steel	-21.302	2.458	2.326	6.258
Copper	-30.136	1.650	6.904	8.012
Lead	-9.346	1.616	2.481	2.983
Tuballoy	-25.466	3.127	3.571	7.708

* Within the limitations of the experimental data, this material did not cause the steel fragments to break up considerably upon impact. Higher striking velocities than those that are now obtainable in the laboratory would be required to produce the necessary information to establish a working set of constants for the $m_s(c')$ equations for this material.

Table XI

Constants for the Estimating Equations for $m_s(c')$; $c' = 0.25$

(Compact Fragment Shape Assumed)

Form of Equation: $m_s(c') = 10^K e^{\alpha'} (\sec \theta)^{\gamma'} V_s^{\lambda'}$

Target Material	K	α'	γ'	λ'
Magnesium*	--------	-----	------	------
2024T-3	-45.315	1.464	-2.328	12.277
Titanium	0.144	1.060	1.295	0.448
Cast Iron	-45.408	0.742	9.570	12.405
Face-Hardened Steel	-15.662	2.344	4.690	4.834
Mild Homogeneous Steel	-36.361	1.872	1.945	10.348
Hard Homogeneous Steel	-20.413	2.458	2.326	6.258
Copper	-29.529	1.650	6.904	8.012
Lead	-8.947	1.616	2.481	2.983
Tuballoy	-24.768	3.127	3.571	7.708

* Within the limitations of the experimental data, this material did not cause the steel fragments to break up considerably upon impact. Higher striking velocities than those that are now obtainable in the laboratory would be required to produce the necessary information to establish a working set of constants for the $m_s(c')$ equations for this material.

ADAPTATIONS TO VULNERABILITY ANALYSES

The vulnerability analyst, calculating the effects of a hypothetical fragmenting weapon as used against some primary target, usually relies on experimental evidence from fragments fired singly against facsimile or mock-up targets. The target is considered as an assembly of sets of vital components shielded by structural "shell" members or other components. Firings are conducted to determine the level and extent of damage required to "defeat" or "kill" each vital component under various kill criteria. These firings provide an empirical relation between the conditional probability of killing each vital component, given a hit, and some appropriate function of the weight and velocity of the impacting fragment.

Assuming that such a relationship is established, one can proceed with the analysis when the impact weight and velocity of the fragment are known. If the fragment impinges first on some barrier target, then it is important to be able to estimate the losses sustained by the fragment in both weight and velocity during the perforation of this barrier.

The advent of guided missiles and other space targets has forced vulnerability analysts to consider higher and higher impact velocities. With these higher striking velocities, the loss of fragment weight during perforation becomes more pronounced. While the significance of fragment break-up has been acknowledged for some time, there has hitherto been no systematic technique to account for this aspect of the impact.

The present study makes it possible to more fully account for the effect of barrier targets, as represented by any one of the ten metallic materials, on the original fragment. The appropriate estimating equations can be used to provide estimates of the fragment residual weight and velocity for a hypothetical impact situation.

The analyst can then evaluate any suitable function of fragment weight and velocity to determine the probability of killing a particular component. It is, of course, the responsibility of the analyst to determine the function of fragment weight and velocity to be used with each component type. The function that is chosen will depend on the type of component and the criterion for damage. Finally, the corresponding probability of killing or damaging the primary target is obtained; this kill probability will inevitably be more precise and more realistic.

In Graph Set V of Appendix C, for a fixed combination of m_s, θ, and V_s, four different functions of m_r and V_r are plotted against target areal density. These graphs serve to show that the ordering of the contours for the target materials varies with the function of m_r and V_r being used. Therefore, any comparison of the resistance of target materials, using as a basis some selected function of m_r and V_r, is weakened by this arbitrary selection. Nevertheless, some particular function of m_r and V_r may be entirely appropriate as a measure of the probability of killing a given component.

MEASURING THE MAXIMUM CAPACITY OF THE RESIDUAL FRAGMENT FOR PERFORATION

Establishing minimum requirements for perforation of these metallic materials is needed, but this knowledge is hardly useful in estimating the capacity for additional perforation when these minimum requirements are exceeded. How is this capacity for additional perforation to be measured? Several techniques have been considered and some will be discussed in this section.

Usually, the metallic materials are not themselves primary targets, so their perforation by fragments is of interest mainly in the sense of the resulting changes in the characteristics of the fragment during perforation. The two outstanding characteristics which are related to the capacity of a fragment for perforation are the weight and velocity of the fragment. Thus it is important to be able to estimate the losses in both fragment weight and velocity during perforation. When these factors are properly estimated, it becomes possible to make a first order approximation on the maximum capacity of the residual fragment for perforation. With the advent of fragment break-up, it becomes necessary to compromise in this matter by assuming that this capacity can be estimated by considering only the largest piece of fragment which perforates the target material along with the associated residual velocity. This compromise does not destroy the significance of the technique for measuring the capacity of the residual fragment for perforation, since the largest portion of the residual fragment is the only portion that matters for the tough, primary target. These tough, primary targets exist and are a major concern to vulnerability analysts and weapons designers.

By means of the empirical formulas developed for relating fragment residual velocity and residual weight to the main impact parameters, one can

estimate the values of those two characteristics of the residual fragment. Admittedly, particles of residual fragment other than the largest particle and spall (fragments of target material) issuing from the target material at time of impact are not considered. Usually, the most lethal element resulting from an impact for which there is a perforation is the largest particle of residual fragment. This is the particle which most regularly penetrates deepest into the catch-all medium behind the target material in the experimental work.

The initial effort to compare the resistance of target materials to perforation used separate plots of fragment residual velocity and residual weight, each related to areal density of metallic target material. These sets of graphs, displayed in Appendix C, are useful to the vulnerability analyst who can relate the probability of damaging a primary target to some suitable function of fragment impact weight and velocity. For the comparison, however, these sets of graphs are not extremely helpful since neither set necessarily provides, in itself, the required information.

For example, how does one compare the relative capacity for perforation of 1) a residual fragment with low weight and high velocity, and 2) a residual fragment with high weight and low velocity?

For the condition that the original target materials are perforated, a more useful comparison of the resistance of these materials can be obtained by examining the capacity of the residual fragment to perforate a calibrating material. The latter may be arbitrarily selected.

The empirical formulas feature a single exponent for the product of target thickness and average presented area of the fragment. This, in effect, suggests that if certain results are anticipated for a given impact

condition, then the same results should be expected for, say, an impact situation where the target thickness is halved and the fragment shape is altered so that the average presented area is doubled. As long as the product of target thickness and fragment impact area remains constant, the same results are expected. This assumption has been found tenable at least for those fragment shapes which are not distantly removed from compact shapes.

For purposes of calibration, the simplest impact situation (i.e., normal impact) is assumed for the angle of impact of the residual fragment on the calibrating material regardless of the angle of impact on the initial target material.

The impact parameters which determine the capacity of a steel fragment for perforation of a given medium include the fragment weight, velocity, shape, and the angle of obliquity. Estimates of the first two characteristics are provided by the empirical formulas. The shape of the largest portion of residual fragment is usually similar to the shape of the original fragment whenever the residual fragment is of appreciable size. There is a tendency for the fragment to be squashed and thereby rendered less compact.

At low impact velocities, fragments tend to perforate thin targets by shearing or tearing while the fragment itself sustains little deformation. As the striking velocity and the target thickness increase, the fragment tends to "mash and mushroom" on the impacted side, and also to fracture, both axially and longitudinally, due to shock. This tendency appears to depend on the relative dimensions of the fragment and the thickness of the target. With hypervelocity impact, the fragment tends to flow radially and then back together with the target material. This phenomenon can be visualized as a fragment literally turning itself inside out and

stretching to pieces. Variations of this phenomenon occur with changes in target materials, but various stages of the phenomenon have been observed in the recovered fragments from the present body of experimental data. Finally, for an extreme set of impact conditions, it becomes practically impossible to recognize the remains of the original impacting fragment, with traces of pulverized fragment embedded within or fused with or even alloyed with the target material and the spall.

When there is considerable break-up of the fragment during the perforation of the initial target material, the residual fragment may have a shape other than that which could reasonably be called compact. In such cases, the residual fragment may have an average presented area (assuming random orientation) of two to three times that of a compact fragment of the same weight. It is also of importance to recognize that, for a non-compact fragment, there is a greater interval between the minimum and the maximum presented areas than for a compact fragment of the same weight. This implies a greater variation in performance for the non-compact, residual fragment against a given primary target.

Furthermore, recovered portions of fragments after impact reveal, in many cases, a shredded appearance suggesting much less unity than the original fragment. Such a particle appears more susceptible to further break-up on the impact of another target than an unweakened particle of the same weight. This increased susceptibility to break-up could result in a lower capacity for additional perforation.

The importance of each particle which is formed from an impact of a fragment upon some barrier target is relative to the vulnerability of the primary target to particle impact. If the primary target is extremely

sensitive to such impact, it is important to know how many particles are formed, and the weight and velocity characteristics of each particle. If the primary target is one which is not likely to be damaged by the impact of small, slow particles, then these particles can be ignored.

The present report deals primarily with the characteristics of the largest particle of fragment origin resulting from impact on a barrier target. From the point of view of protecting the primary target, if the primary target can withstand the impact of the largest, fastest-moving particle of fragment origin, then it is reasonable to assume that the primary target can withstand the impact of all particles.

A basis will now be established for measuring the maximum capacity of the largest particle of residual fragment for perforation of a second medium. The maximum thickness of this medium which can be perforated by the largest portion of residual fragment, striking the calibrating medium at normal impact, will be used as the measure. To arrive at this measure, estimates of the fragment residual weight and velocity are required. To favor this residual fragment, it will be assumed that this particle has the same capacity for perforation as an unfired, pre-formed fragment of the same weight.

Sets of graphs, relating maximum thickness of calibrating material that can be perforated to areal density of the metallic target materials for each of twenty-seven combinations of fragment weight, velocity, and angle of obliquity, are displayed in Appendix D. Two media, celotex and 2024T-3, have been selected as calibrating materials. The first represents a "soft" primary target while the second represents a tougher primary target.

Under the assumptions which have been clearly stated, it is a simple matter to use these graphs to compare the resistance of the metallic materials to perforation by steel fragments. For a given value of areal density, the "best" material is that one which allows the least perforation of calibrating medium.

If the change in shape of the residual fragment and the weakened condition are taken into account, lower estimates of maximum thicknesses of the calibrating medium will result. For purposes of comparison of the resistance of the initial target materials to perforation, this would not be necessary.

A substantial number of dual target firings (See Fig. 3) were conducted at BRL with the second target chosen as 2024T-3 or 2024T-4 in all cases. The thickness of aluminum alloy was selected for each round to correspond to the maximum thickness that the residual fragment could perforate. In this experiment, several barriers were placed in the path of the oncoming fragment. The initial barrier target was one of the ten structural metallic materials with the remainder of details defining the initial impact selected to ensure perforation. The second target, aluminum alloy, was placed perpendicular to the original fragment trajectory; the thickness of the second target used was calculated to be the maximum needed to stop the residual fragment. Finally, a bank of celotex was placed parallel to and behind the aluminum alloy. All the barriers were placed close to but not touching each other to cut down on the effect of fragment slow-down. The thickness of aluminum alloy for each round was estimated from the V_o equation for this material, using as input data, the residual weight and velocity of the fragment computed from the appropriate estimating equations, an assumption of normal impact, and an assumption that

the residual fragment is of a compact shape like the original fragment. In 34 rounds of dual target firings, with a wide variety of impact conditions, the results indicate that perforation of the calibrating material was accomplished (when perforation was not anticipated) in only about 5% of the cases. In the remainder of the cases, the particles of residual fragment expended themselves in the calibrating material. (See Table XII.)

In view of the many calculations required to determine the maximum thickness of calibrating material needed to stop the residual fragment, the results of this experiment can be regarded as successful. This technique does tend to estimate this maximum thickness conservatively. Certainly if the distortion, change in shape, and weakened condition of the residual fragment are taken into account, some lesser thickness of calibrating material would be found equally adequate to stop the residual fragment.

[redacted]

Set-Up for Firings on Dual Targets

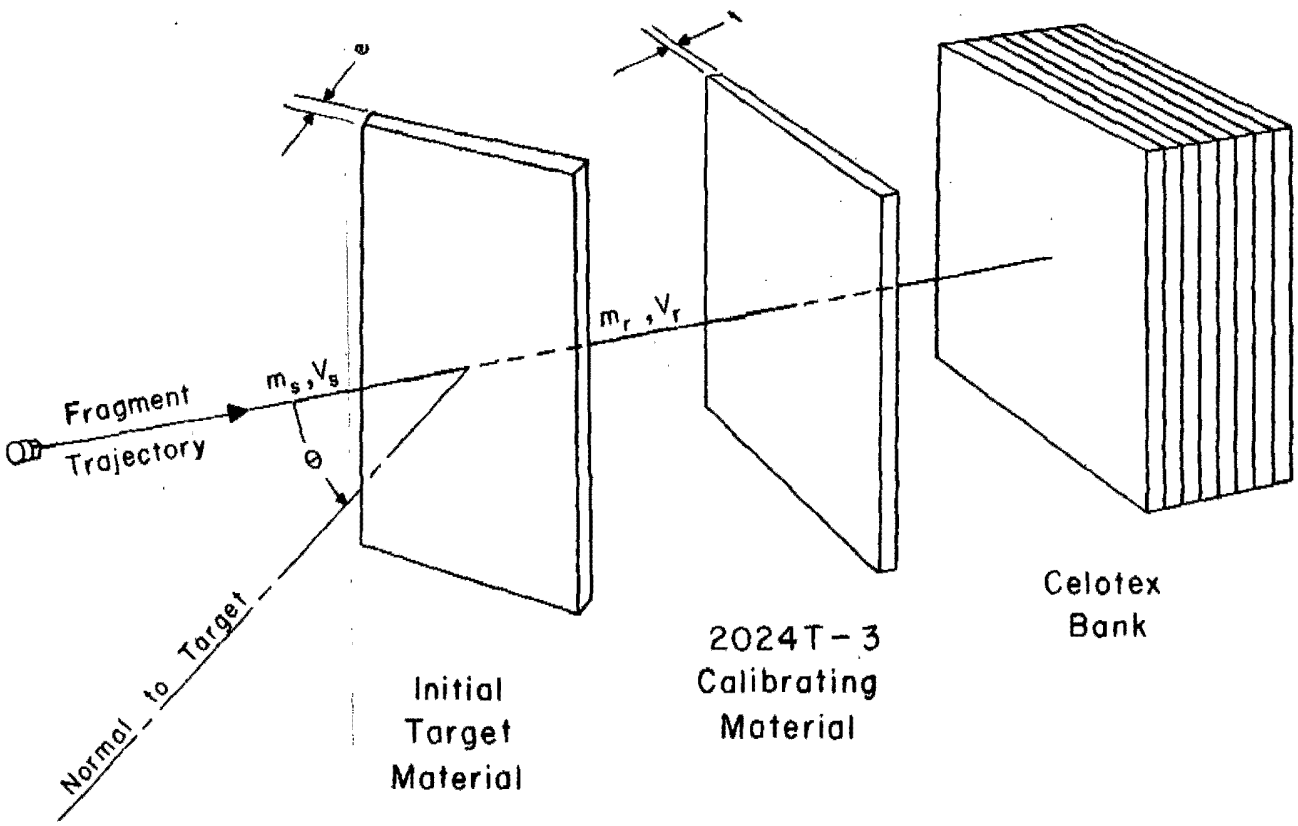

Fig. 3

[redacted]

Table XII: Dual Target Experimental Data; Estimates of the Situation

BAL Data No.	Impact Situation: Initial Target Material	Target Thickness	Fragment Weight	Obliquity of Strike	Striking Velocity	Estimates of the Situation: Estimated Residual Weight	Estimated Residual Velocity	Thickness* of 2024T-3	Actual Thickness of 2024T-3 Used	Results of the Impact: Perforation of Target Material	Hole Size in Target Material	Perforation of 2024T-3	Celotex Penetrated	Comments
		e(in.)	m_s(grains)	θ(degrees)	V_s(fps)	m_r(grains)	V_r(fps)	t_{max}(in.)	t(in.)	Yes-No	in.^{2}	Yes-No	in.	
1	Magnesium	0.495	30	0	2935	28.7	908	0.122	0.124	Yes	0.1	Yes	2.5	A
2	Titanium	0.274	120	0	3530	111.2	2003	0.488	0.374	Yes	0.3	No	--	
3	F.H.S.	0.139	240	0	3020	154.5	1895	0.536	0.505	Yes	0.5	Yes	8.0	A
4	H.H.S.	0.080	30	0	5600	14.4	4114	0.503	0.500	Yes	0.2	No	--	
5	Lead	0.375	120	0	5920	55.6	3017	0.592	0.124	Yes	2.8	No	--	
6	Copper	0.500	240	0	5820	177.4	2621	0.782	0.750	Yes	2.1	No	--	
7	Magnesium	0.310	30	0	8646	24.3	7540	1.198	1.000	Yes	0.2	No	--	
8	Titanium	0.500	60	0	8177	32.0	3801	0.622	0.750	Yes	0.4	No	--	
9	M.S.	0.500	240	0	8973	4.0	5890	0.463	0.250	Yes	1.4	Yes	3.5	B
10	Lead	0.074	30	60	3050	20.0	1554	0.193	0.185	Yes	0.5	No	--	
11	M.S.	0.132	120	60	2935	71.2	107	0.016	0.049	Yes	0.5	No	--	
12	Copper	0.248	240	60	2930	197.4	870	0.240	0.250	No	1.0	No	--	C
13	M.S.	0.102	30	60	5660	8.5	1949	0.181	0.187	Yes	0.3	No	--	
14	H.H.S.	0.125	120	60	5680	43.8	2427	0.416	0.375	Yes	0.7	No	--	
15	F.H.S.	0.139	240	60	5515	81.5	2614	0.583	0.253	Yes	0.9	Yes	4.5	B
16	Lead	0.070	30	60	8872	3.4	5388	0.396	0.300	Yes	0.9	No	--	
17	M.S.	0.030	60	60	8404	13.4	7418	0.941	0.950	Yes	0.4	No	--	

* Estimated maximum thickness of 2024T-3 calibrating material that can be perforated by the residual fragment
A: Perforation of calibrating material not anticipated
B: Lower thickness of calibrating material used than t_{max}
C: Fragment ricochetted after making hole in target

M.S.: Mild Steel
H.H.S.: Hard Homogeneous Steel
F.H.S.: Face-Hardened Steel

Table XII: Dual Target Experimental Data; Estimates of the Situation (Cont)

BAL Data No.	Impact Situation: Initial Target Material	Target Thickness e(in.)	Fragment Weight m_s(grains)	Obliquity of Strike θ(degrees)	Striking Velocity V_s(fps)	Estimates of the Situation: Estimated Residual Weight m_r(grains)	Estimated Residual Velocity V_r(fps)	Thickness of 2024T-3 * t_{max}(in.)	Actual Thickness of 2024T-3 Used t(in.)	Results of the Impact: Perforation of Target Material Yes-No	Hole Size in Target Material in.^{2}	Perforation of 2024T-3 Yes-No	Celotex Penetrated in.	Comments
18	H.H.S.	0.128	240	60	9093	29.2	6467	1.082	0.625	Yes	1.1	Yes	0.5	B
19	Copper	0.060	30	70	2890	21.5	979	0.119	0.125	Yes	0.4	No	--	
20	Magnesium	0.310	120	70	3055	116.4	1432	0.341	0.253	Yes	0.7	No	--	
21	Titanium	0.127	240	70	2490	226.8	402	0.108	0.253	Yes	2.2	No	--	
22	Lead	0.135	30	70	5410	< 1.0	1272	0.050	0.185	Yes	0.5	No	--	
23	F.H.S.	0.139	120	70	6290	11.9	626	0.058	0.073	Yes	0.8	No	--	
24	H.H.S.	0.080	240	70	5690	105.7	2923	0.728	0.090	Yes	1.3	Yes	11.5	B
25	Magnesium	0.500	30	70	8841	24.4	3100	0.448	0.500	Yes	0.3	No	--	
26	2024T-3	0.250	60	70	8746	24.5	4766	0.723	0.750	Yes	0.7	No	--	
27	2024T-3	0.500	60	0	7807	10.8	5651	0.641	0.500	Yes	0.5	No	--	
28	2024T-3	0.375	30	60	8135	8.4	3178	0.309	0.250	Yes	0.5	No	--	
29	2024T-3	0.500	240	0	4700	179.4	3345	1.030	1.000	Yes	0.6	No	--	
30	Copper	0.124	30	0	5010	48.9	3391	0.647	0.500	Yes	0.7	No	--	
31	Tuballoy	0.100	30	0	5572	11.7	2343	0.249	0.250	Yes	0.2	No	--	
32	Tuballoy	0.100	240	60	4640	117.8	1404	0.336	0.500	Yes	1.0	No	--	
33	F.H.S.	0.139	240	0	3010	154.5	1886	0.516	0.253	Yes	0.4	Yes	11.0	B
34	F.H.S.	0.139	240	60	4930	89.9	2167	0.492	0.374	Yes	1.0	No	--	

* Estimated maximum thickness of 2024T-3 calibrating material that can be perforated by the residual fragment

B: Lower thickness of calibrating material used than t_{max}

M.S.: Mild Steel
H.H.S.: Hard-Homogeneous Steel
F.H.S.: Face-Hardened Steel

CONCLUSIONS

The description of the impact situation and the results of the impact can be given, in a simplified way, in terms of the following outline.

Impact Conditions

1. Fragment:
   - material
   - size (m_s)
   - shape
2. Target:
   - material
   - density } areal density (E)
   - thickness (e) }
3. Other:
   - striking velocity (V_s)
   - angle of obliquity of strike (θ)

Results of Impact

1. Perforation or Partial Penetration
2. Residual Fragment (largest piece):
   - weight (m_r)
   - condition
   - shape
   - velocity (V_r)
3. Spall:
   - weight } of each particle
   - shape }
   - velocity }
4. Target:
   - hole size

It is of interest to observe how certain changes in impact conditions affect the results of the impact. Only the weight and velocity of the largest portion of residual fragment are being considered as results of the impact, assuming of course that target perforation has taken place. The capacity of the residual fragment for additional perforation is related to both of these characteristics of the residual fragment (as well as other characteristics, e.g., shape, condition).

1. For all metallic target materials, the fragment residual velocity <u>increases</u> when any one of the following changes in impact conditions occurs:

a) a decrease in target thickness,

b) a decrease in obliquity of strike,

c) an increase in fragment weight,

d) a decrease in the average presented area of the fragment,

e) an increase in striking velocity.

2. For all metallic target materials, the fragment residual weight <u>decreases</u> when any one of the following changes in impact conditions occurs:

a) an increase in target thickness,

b) an increase in the striking velocity,

c) an increase in the average presented area of the fragment.

3. Increasing the striking velocity of a fragment does not necessarily increase the capacity of the residual fragment for perforation of some medium, all other impact conditions being fixed.

4. In view of the decrease in fragment residual weight with an increase in fragment striking velocity, it becomes apparent that fragments at sufficiently high velocity will be thwarted by even very thin targets, regardless of the target material; holes in the target may result, but very little, if any, of the original fragment will pass through in a single piece of appreciable weight. Spall, thus, increases in importance relative to the residual fragment when the striking velocity is sufficiently high.

5. Soft, high density target materials such as lead and copper are materials with low resistance to perforation at low striking velocities. As the striking velocity increases, this resistance to perforation improves until at a striking velocity of 9000 fps, these soft, high density materials

compare favorably even with hard steels in their resistance to perforation. This comparison becomes all the more striking as the obliquity increases.

6. High density target materials, in general, cause more break-up of the fragment, for equal areal densities of target.

7. For a given areal density of target, the fragment residual weight varies much more with the target material than does the fragment residual velocity.

8. A technique to measure the maximum capacity of the residual fragment for additional perforation has been defined and successfully tested. Whereas this measure tends to be conservative (the technique predicts, in general, that the fragment can perforate more than what seems possible), a firm basis has been established upon which improvements can be made when it becomes possible to account for more refined aspects of the results of the impact.

Following page is blank

Appendix A

Graph Set I: V_o vs m for Selected Values of e

Figs. 4-33

Note: V_o is the value of striking velocity, V_s, obtained from the empirical formulas by setting the residual velocity, V_r, equal to zero. The significance of the V_o values has been established in previous reports by this laboratory where V_o has been found to be a good analytical approximation to the protection velocity; the latter is defined to be the highest striking velocity below the ballistic limit for which the probability of perforation is zero. In other words, the V_o values are estimates of the limiting striking velocities for which the target always prevents perforation by the fragment.

V_o vs Fragment Weight for Selected Target Thicknesses

Obliquity: 0°

Target Material: Magnesium Alloy

Fragment:

Type: BRL Pre-formed

Material: Steel, SAE 1020

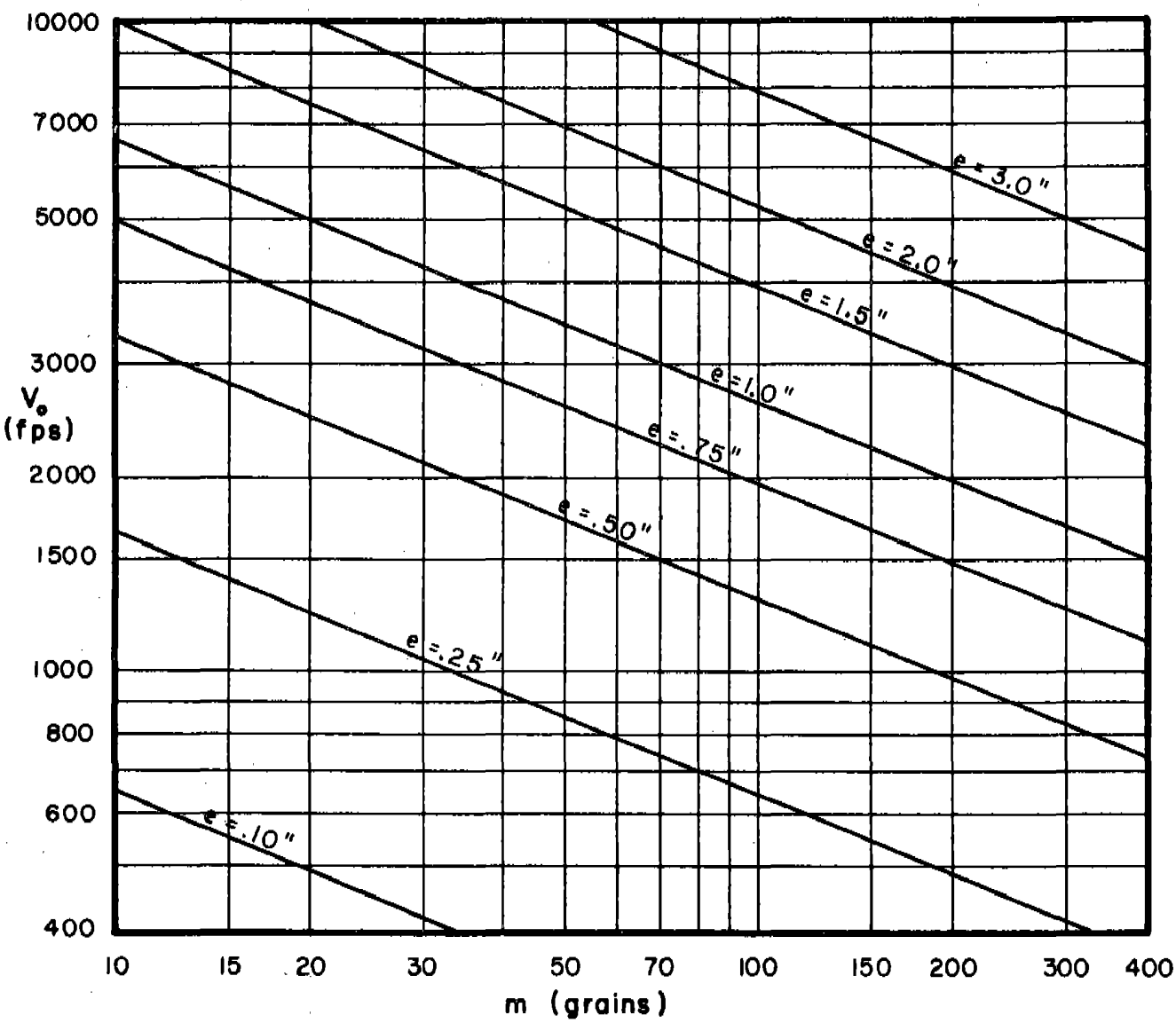

Fig. 4

[redacted]

V_o vs Fragment Weight for Selected Target Thicknesses

Obliquity: 60°

Target Material: Magnesium Alloy

Fragment:

Type: BRL Pre-formed

Material: Steel, SAE 1020

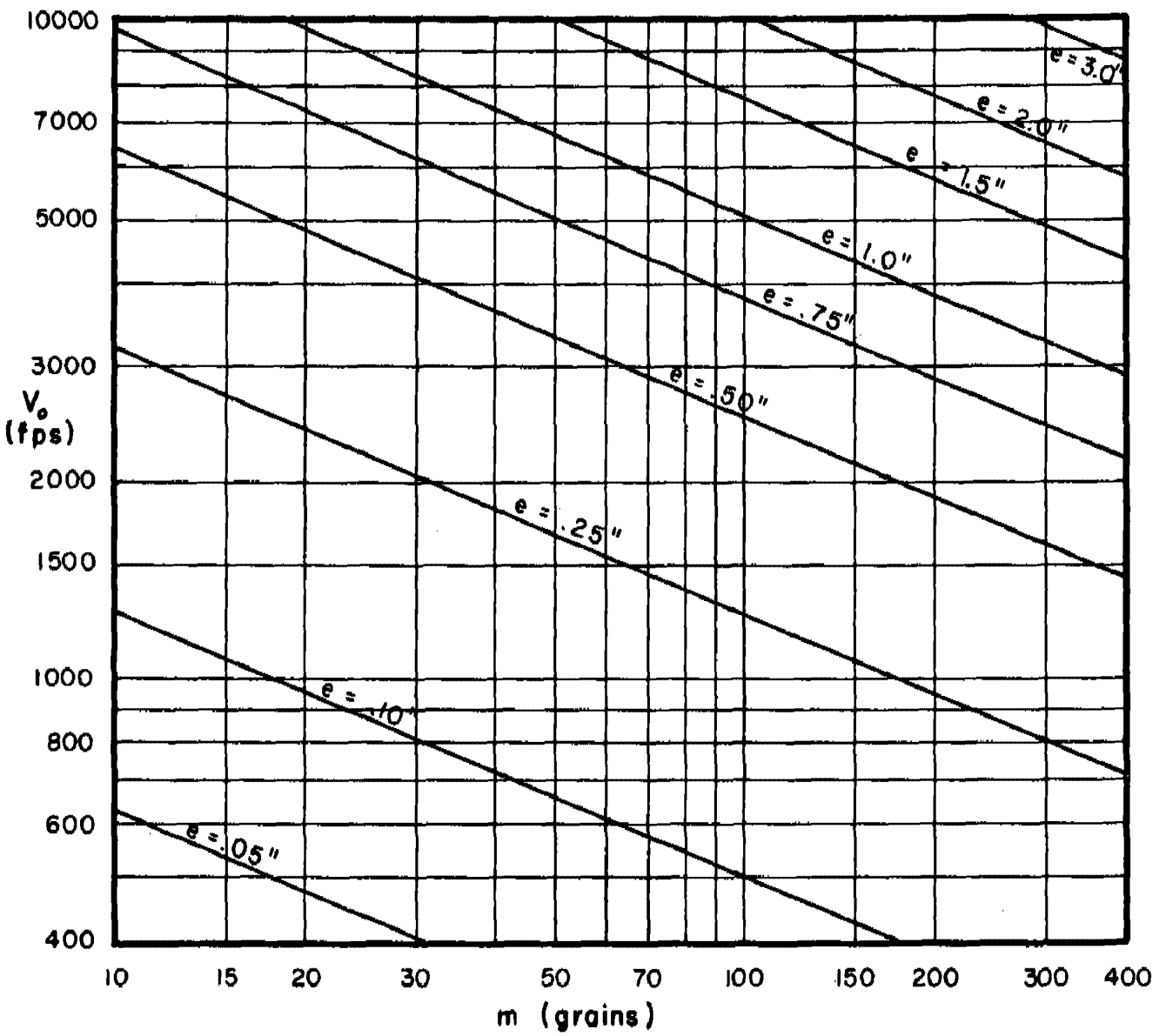

Fig. 5

[redacted]

V_o vs Fragment Weight for Selected Target Thicknesses

Obliquity: 70°

Target Material: Magnesium Alloy

Fragment:

Type: BRL Pre-formed

Material: Steel, SAE 1020

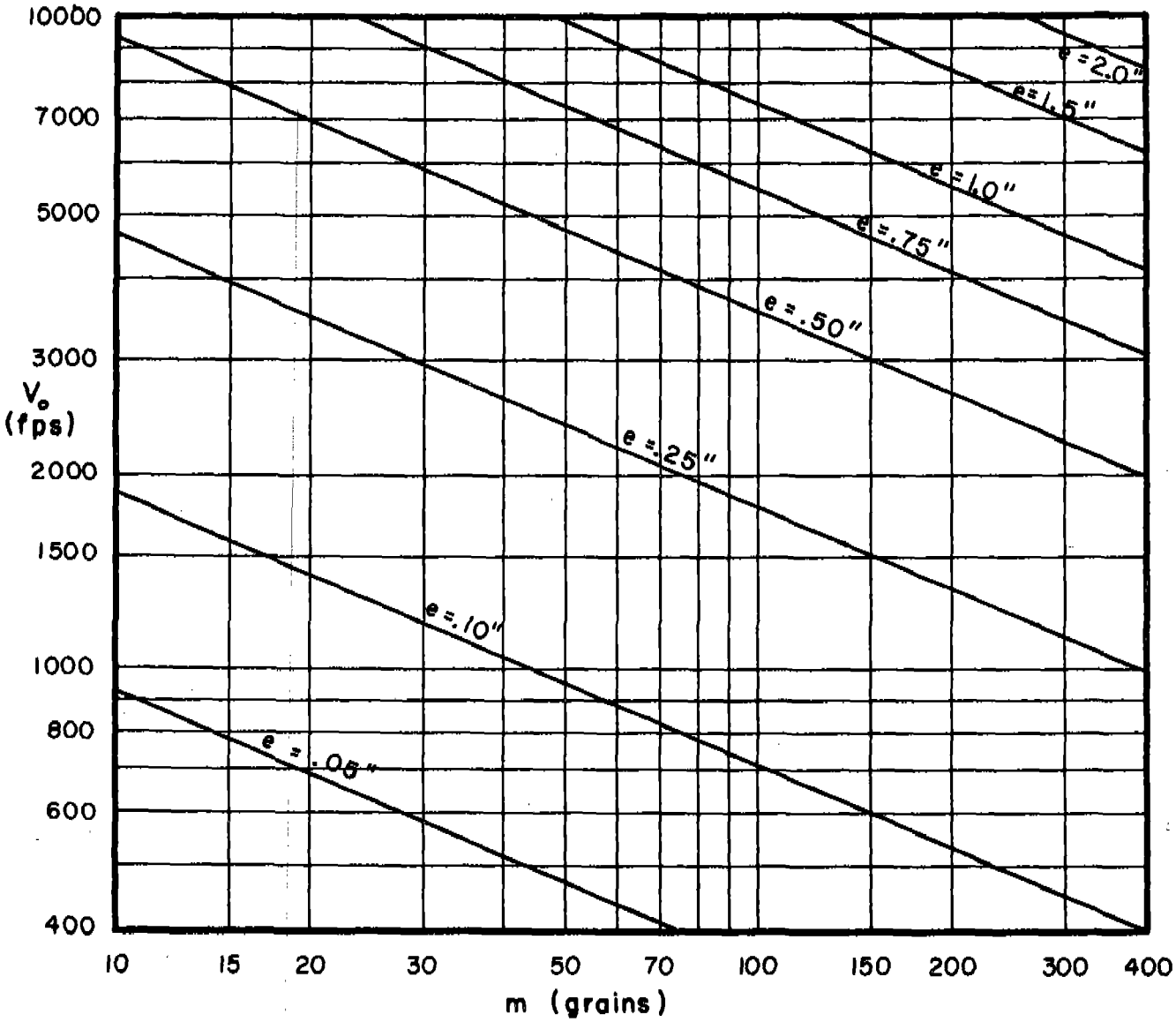

Fig. 6

[redacted]

V_o vs Fragment Weight for Selected Target Thicknesses

Obliquity: 0°

Target Material: 2024T-3

Fragment:

Type: BRL Pre-formed

Material: Steel, SAE 1020

V_o = LIMIT VELOCITY

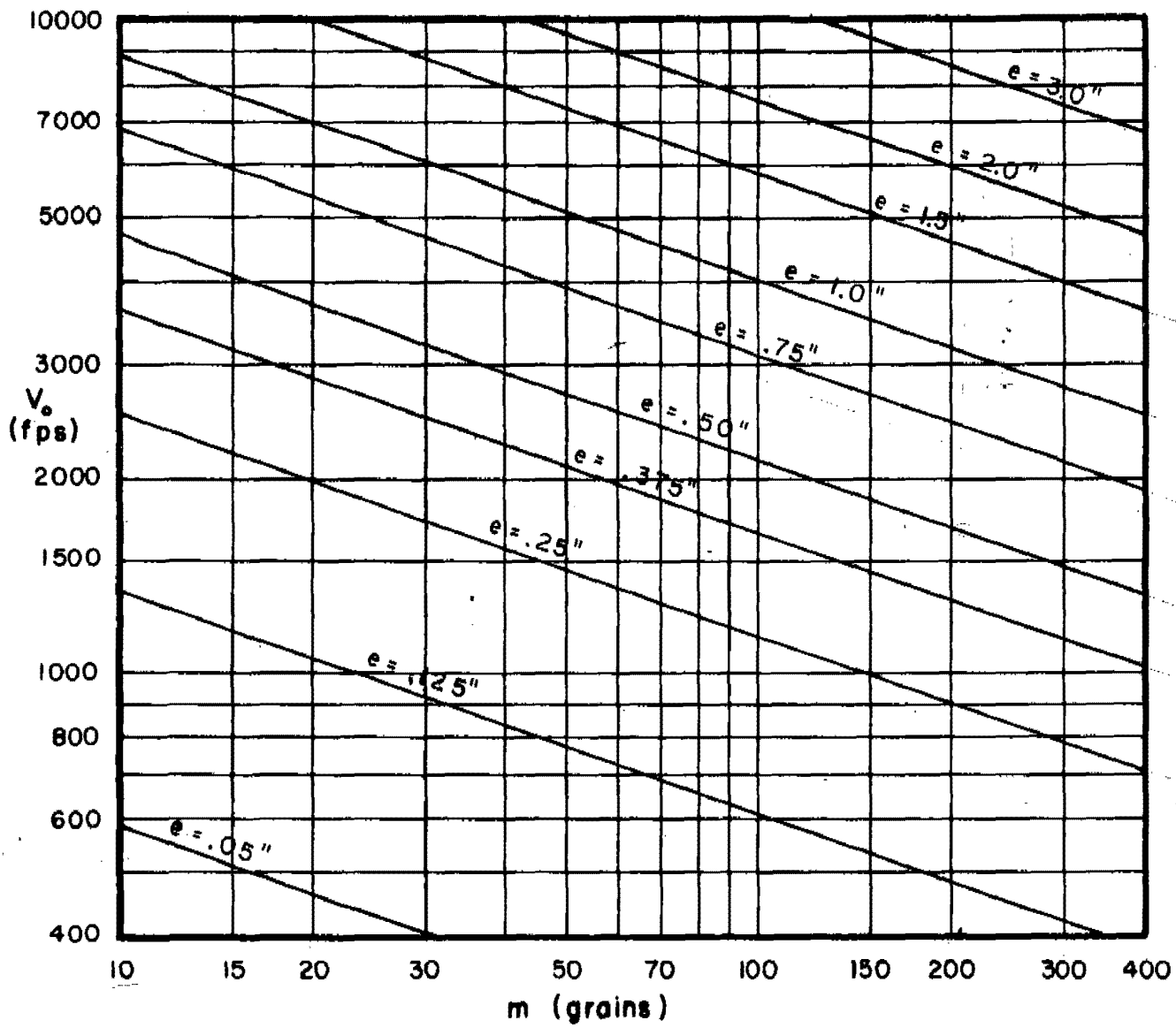

Fig. 7

[redacted]

V_o vs Fragment Weight for Selected Target Thicknesses

Obliquity: 60°

Target Material: 2024T-3

Fragment:

Type: BRL Pre-formed

Material: Steel, SAE 1020

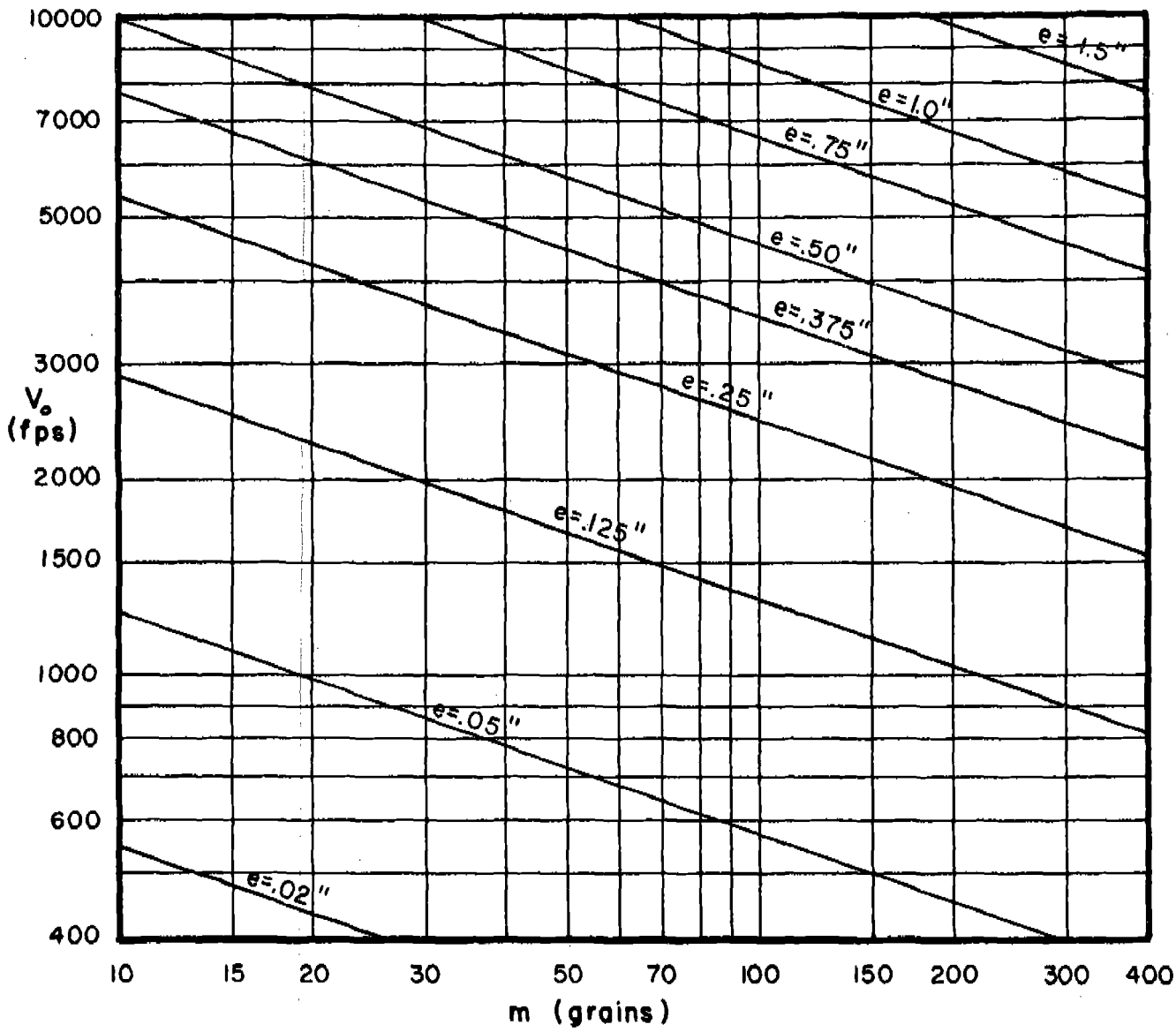

Fig. 8

V_o vs Fragment Weight for Selected Target Thicknesses

Obliquity: 70°

Target Material: 2024T-3

Fragment:

Type: BRL Pre-formed

Material: Steel, SAE 1020

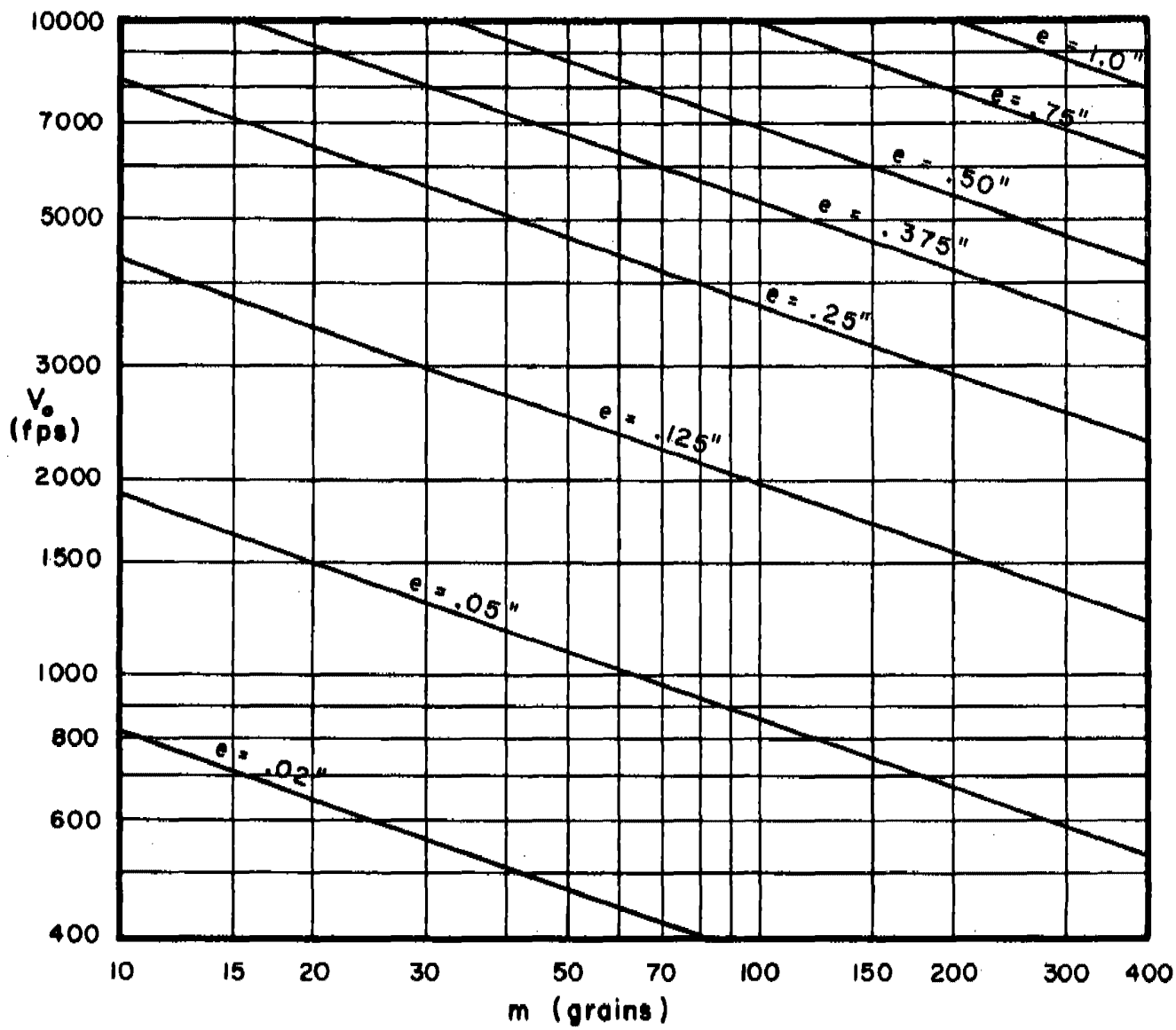

Fig. 9

V_o vs Fragment Weight for Selected Target Thicknesses

Obliquity: 0°

Target Material: Titanium Alloy

Fragment:

Type: BRL Pre-formed

Material: Steel, SAE 1020

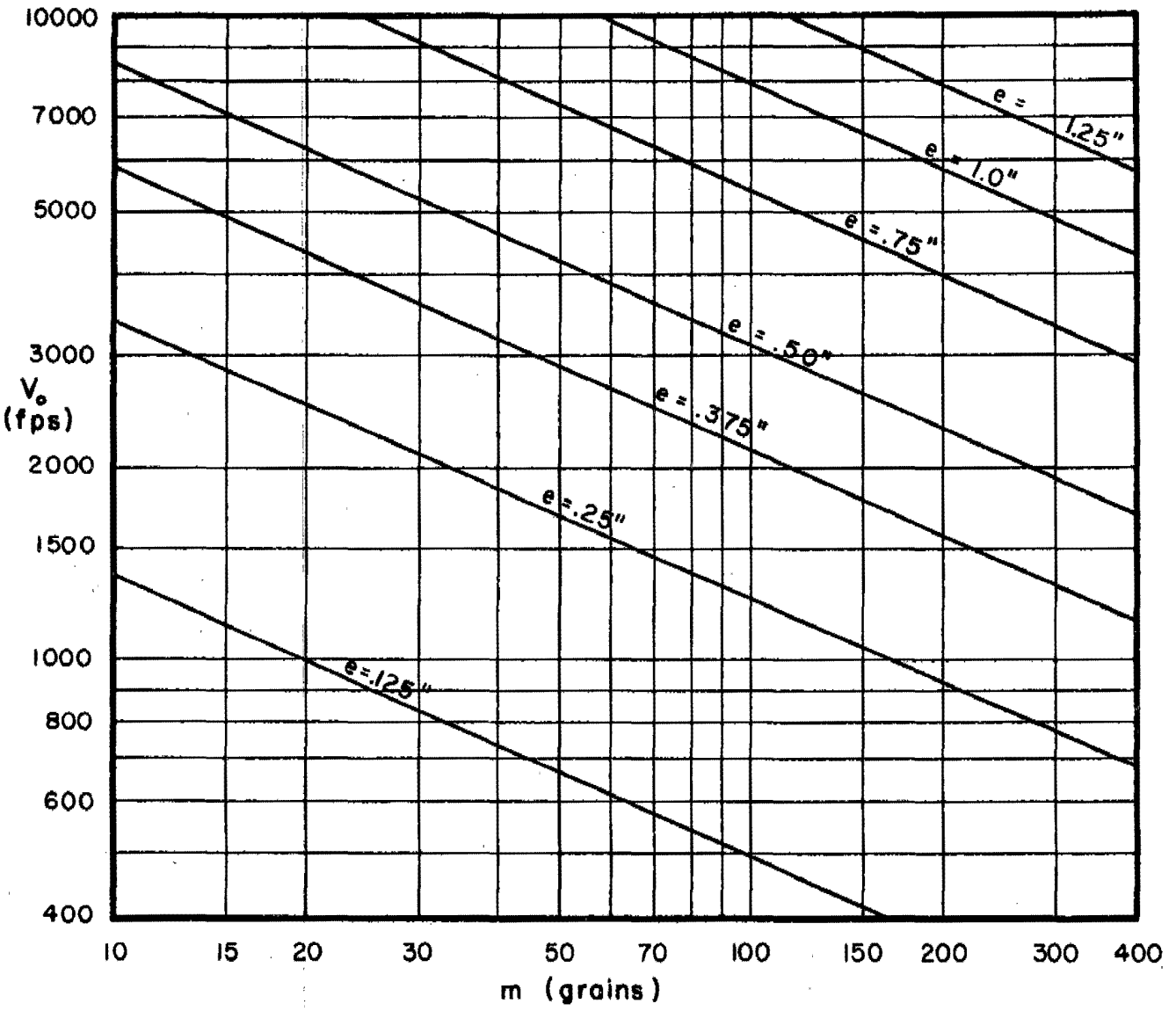

Fig. 10

[redacted]

V_o vs Fragment Weight for Selected Target Thicknesses

Obliquity: 60°

Target Material: Titanium Alloy

Fragment:

Type: BRL Pre-formed

Material: Steel, SAE 1020

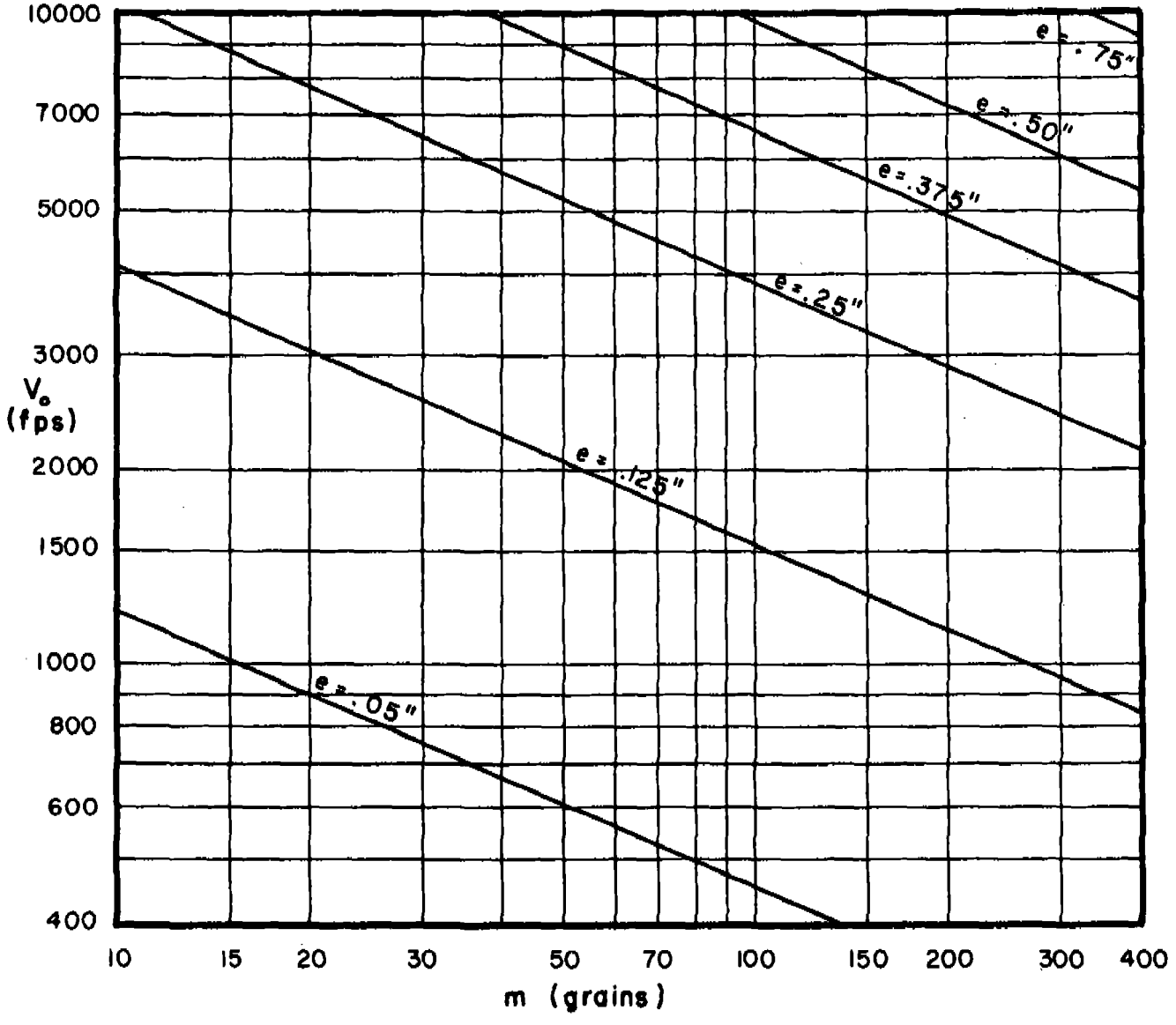

Fig. 11

[redacted]

V_o vs Fragment Weight for Selected Target Thicknesses

Obliquity: 70°

Target Material: Titanium Alloy

Fragment:

Type: BRL Pre-formed

Material: Steel, SAE 1020

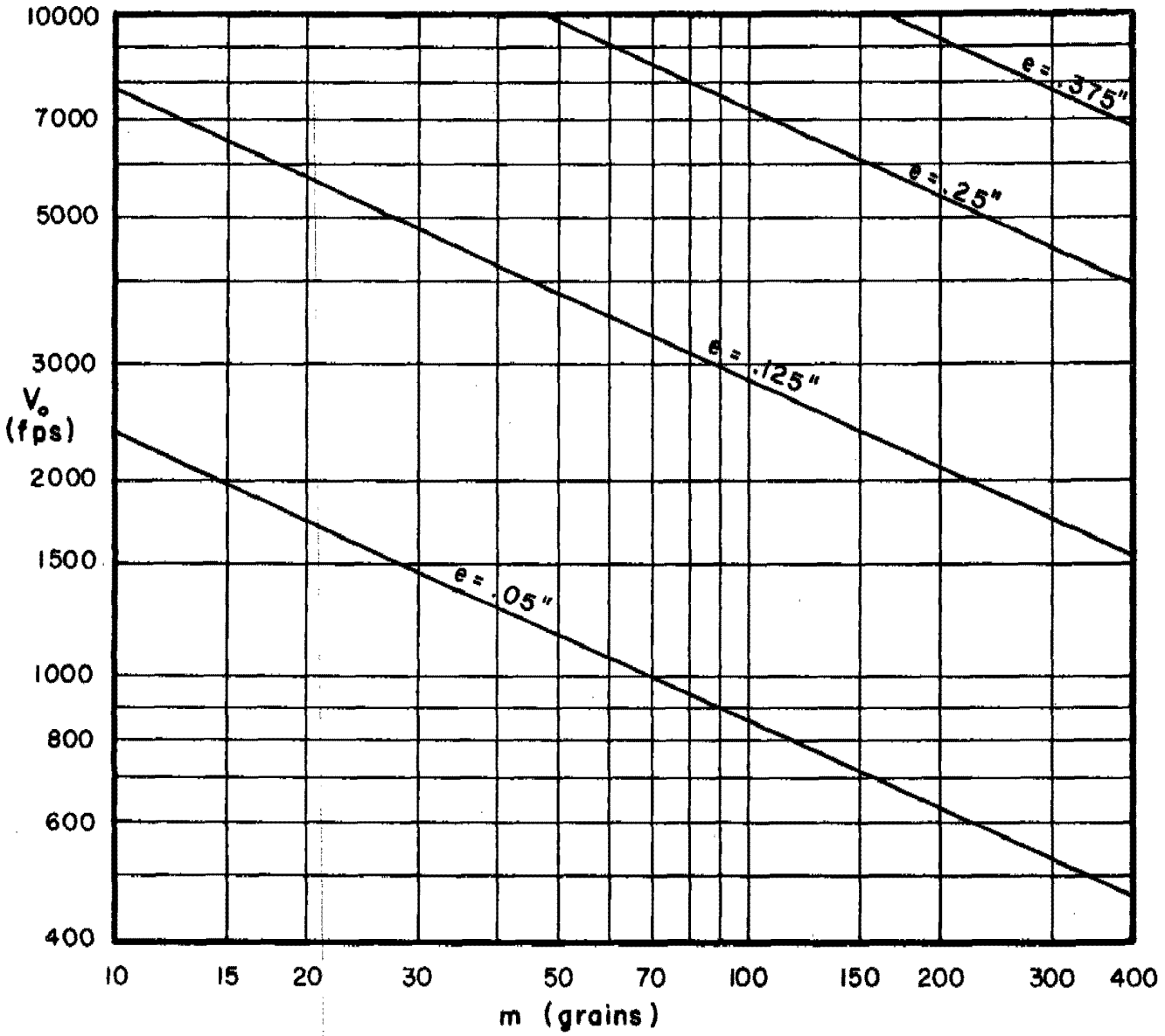

Fig. 12

V_o vs Fragment Weight for Selected Target Thicknesses

Obliquity: 0°

Target Material: Cast Iron *

Fragment:

Type: BRL Pre-formed

Material: Steel, SAE 1020

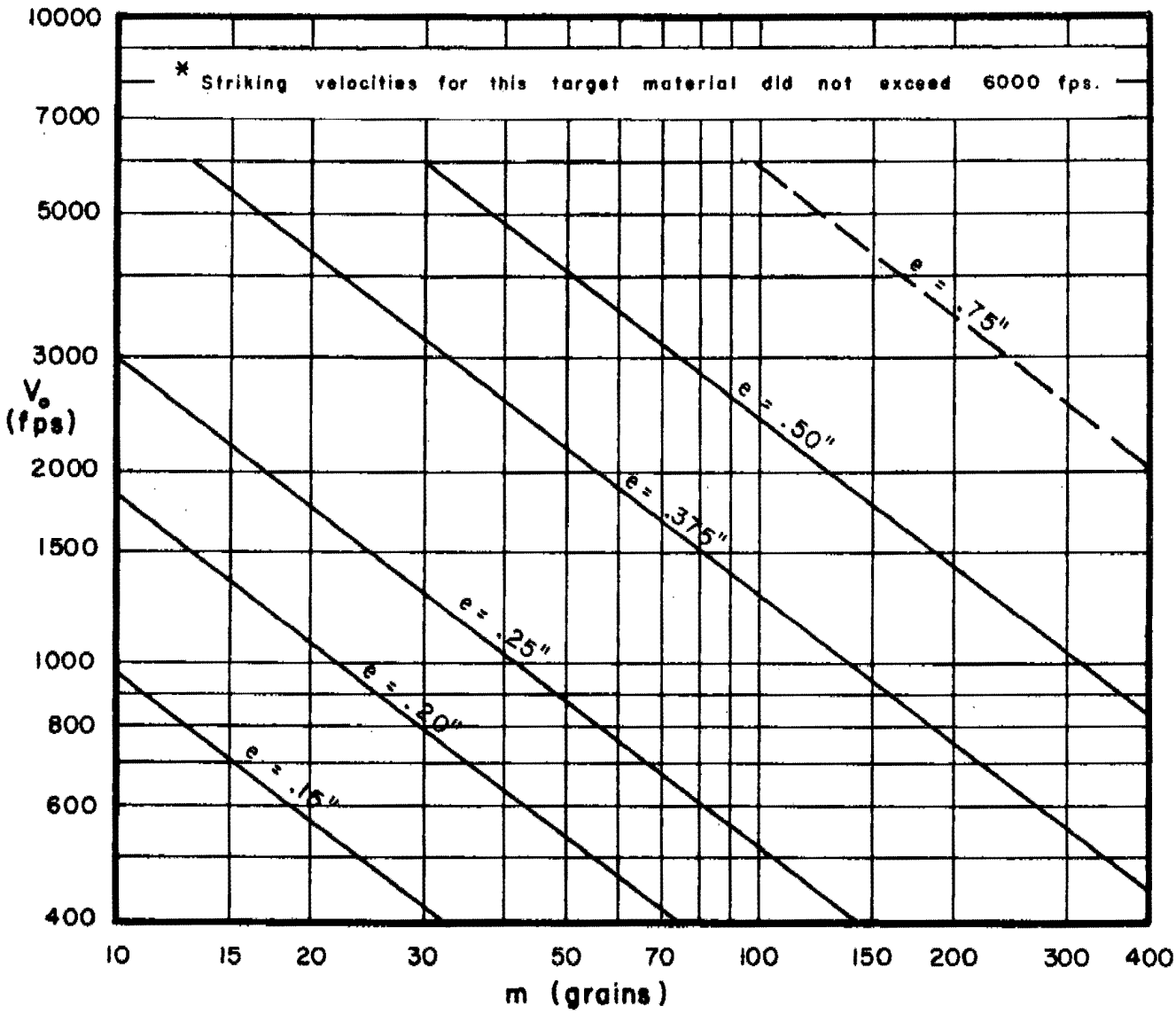

Fig. 13

[redacted]

V_o vs Fragment Weight for Selected Target Thicknesses

Obliquity: 45°

Target Material: Cast Iron *

Fragment:

Type: BRL Pre-formed

Material: Steel, SAE 1020

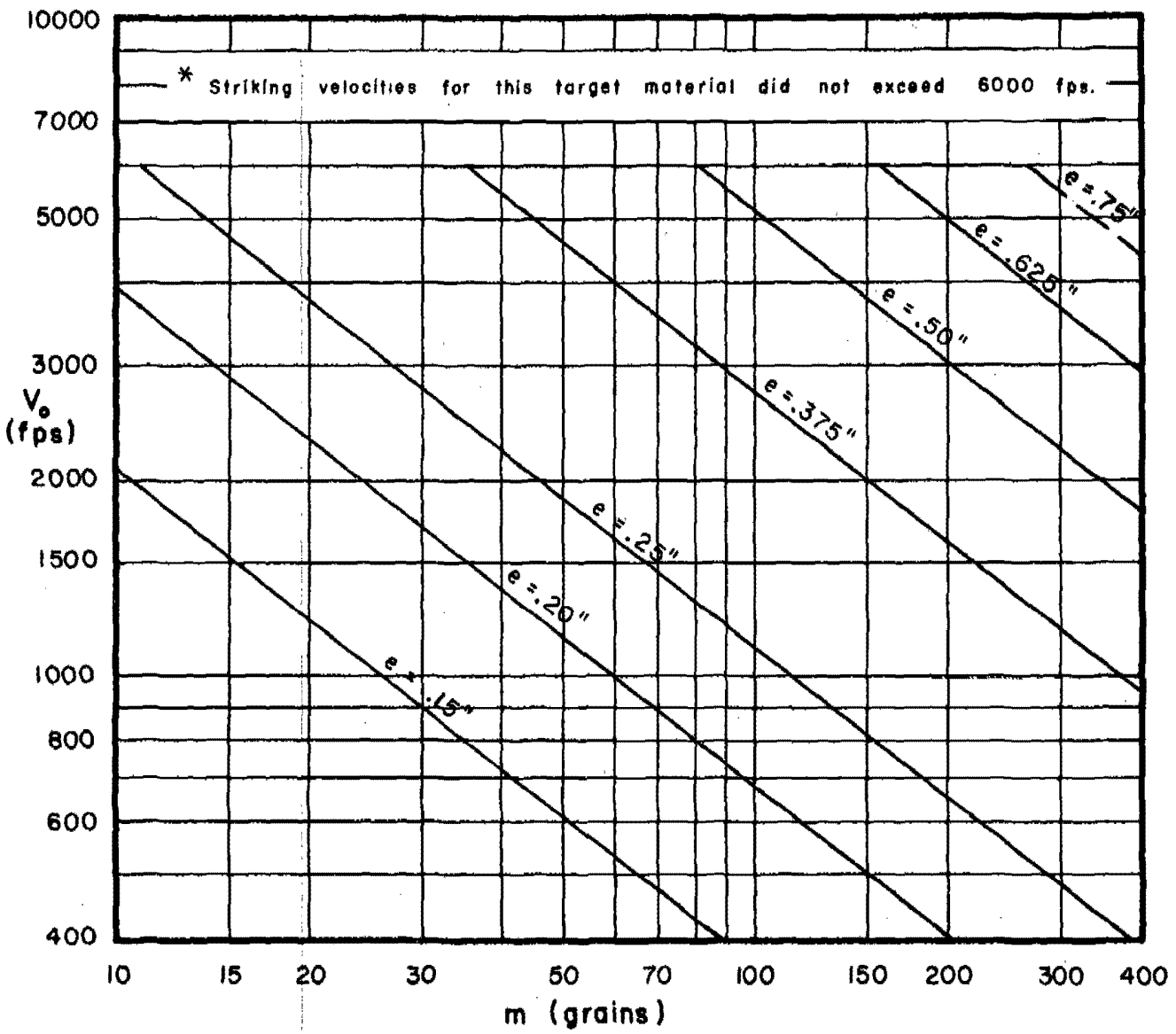

Fig. 14

[redacted]

[redacted]

V_o vs Fragment Weight for Selected Target Thicknesses

Obliquity: 60°

Target Material: Cast Iron*

Fragment:

Type: BRL Pre-formed

Material: Steel, SAE 1020

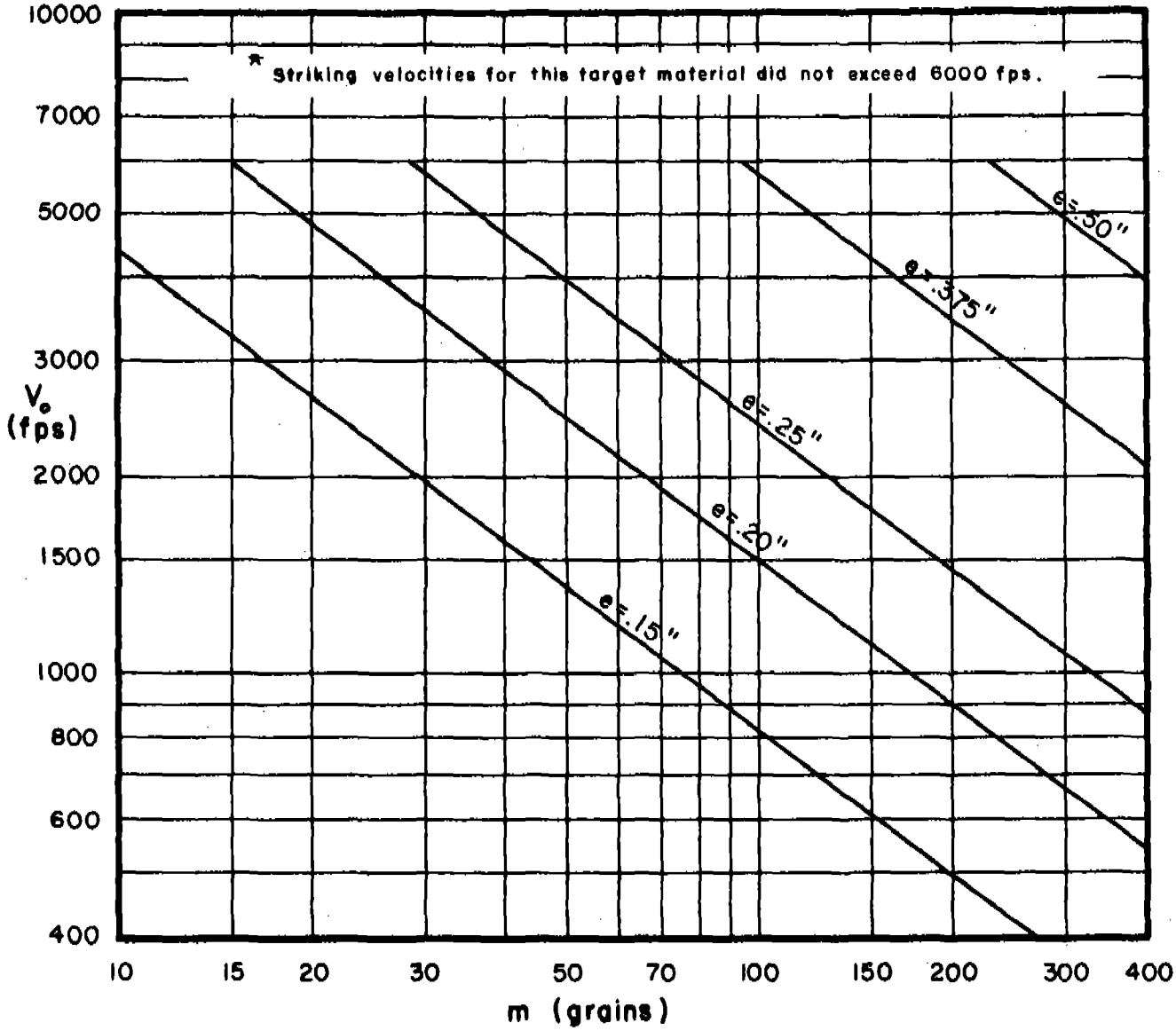

Fig. 15

[redacted]

V_o vs Fragment Weight for Selected Target Thicknesses

Obliquity: 0°

Target Material:

Face-Hardened Steel

Fragment:

Type: BRL Pre-formed

Material: Steel, SAE 1020

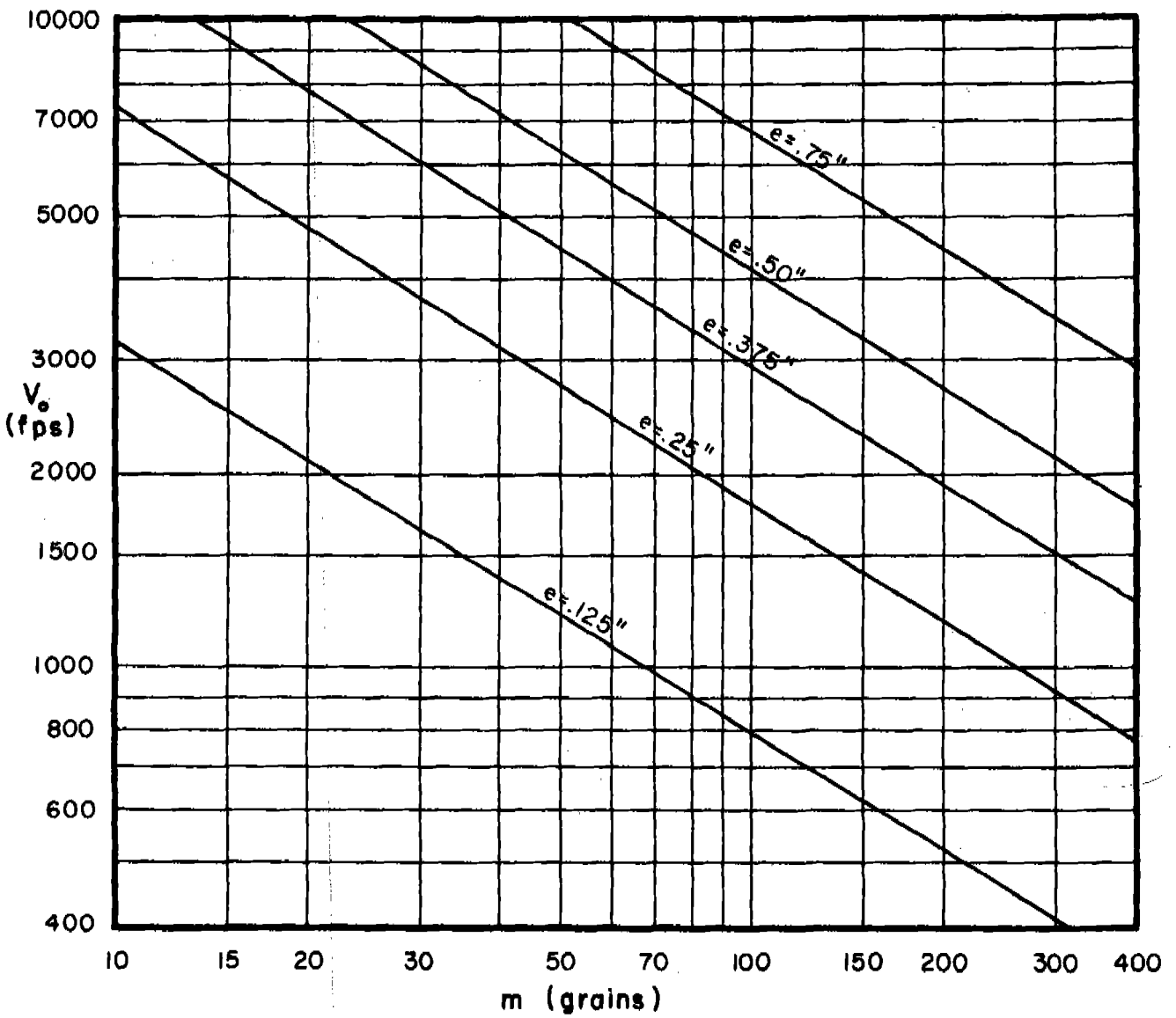

Fig. 16

[redacted]

V_o vs Fragment Weight for Selected Target Thicknesses

Obliquity: 60°

Target Material:
Face-Hardened Steel

Fragment:
Type: BRL Pre-formed
Material: Steel, SAE 1020

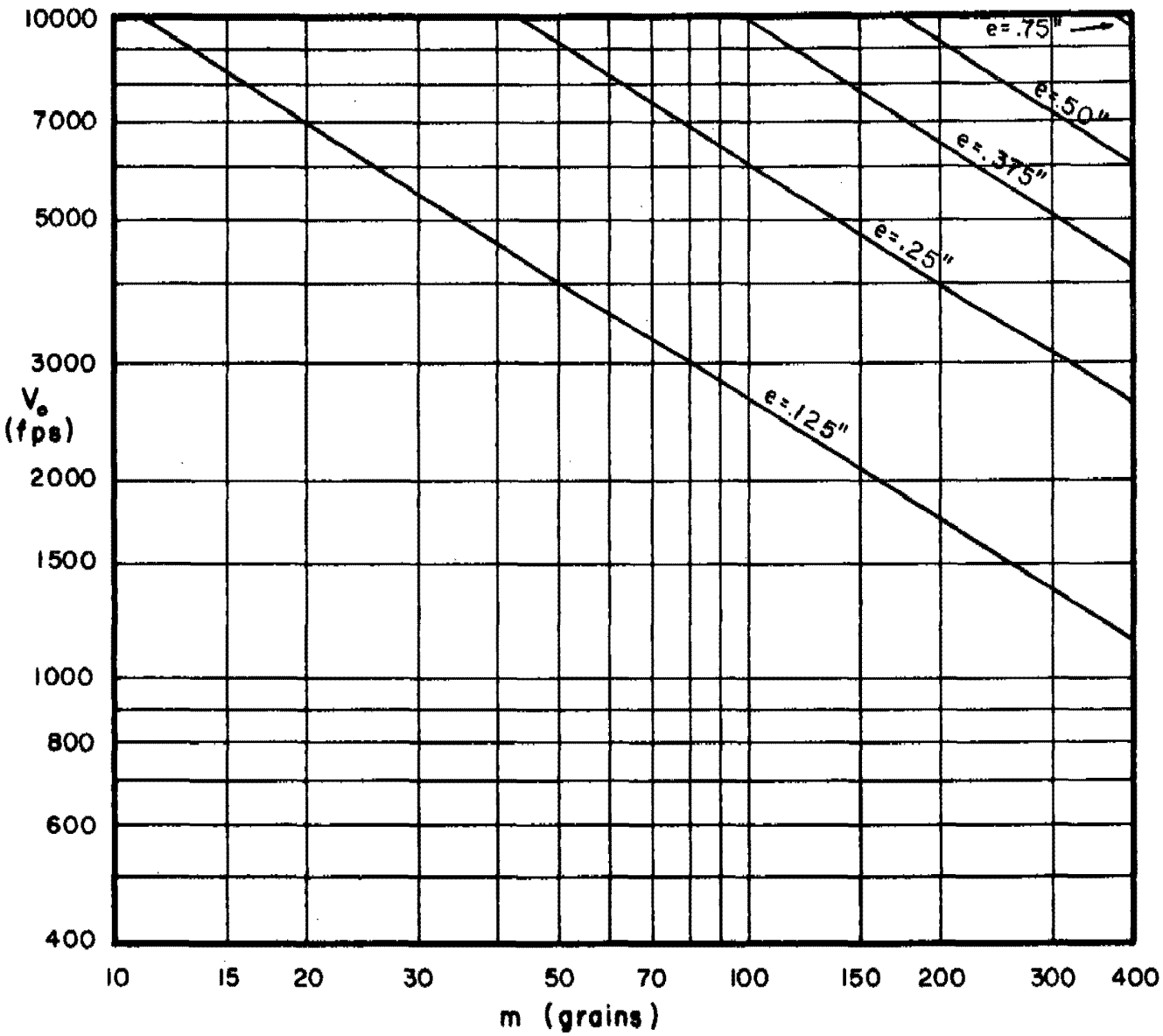

Fig. 17

[redacted]

V_o vs Fragment Weight for Selected Target Thicknesses

Obliquity: 70°

Target Material:

Face-Hardened Steel

Fragment:

Type: BRL Pre-formed

Material: Steel, SAE 1020

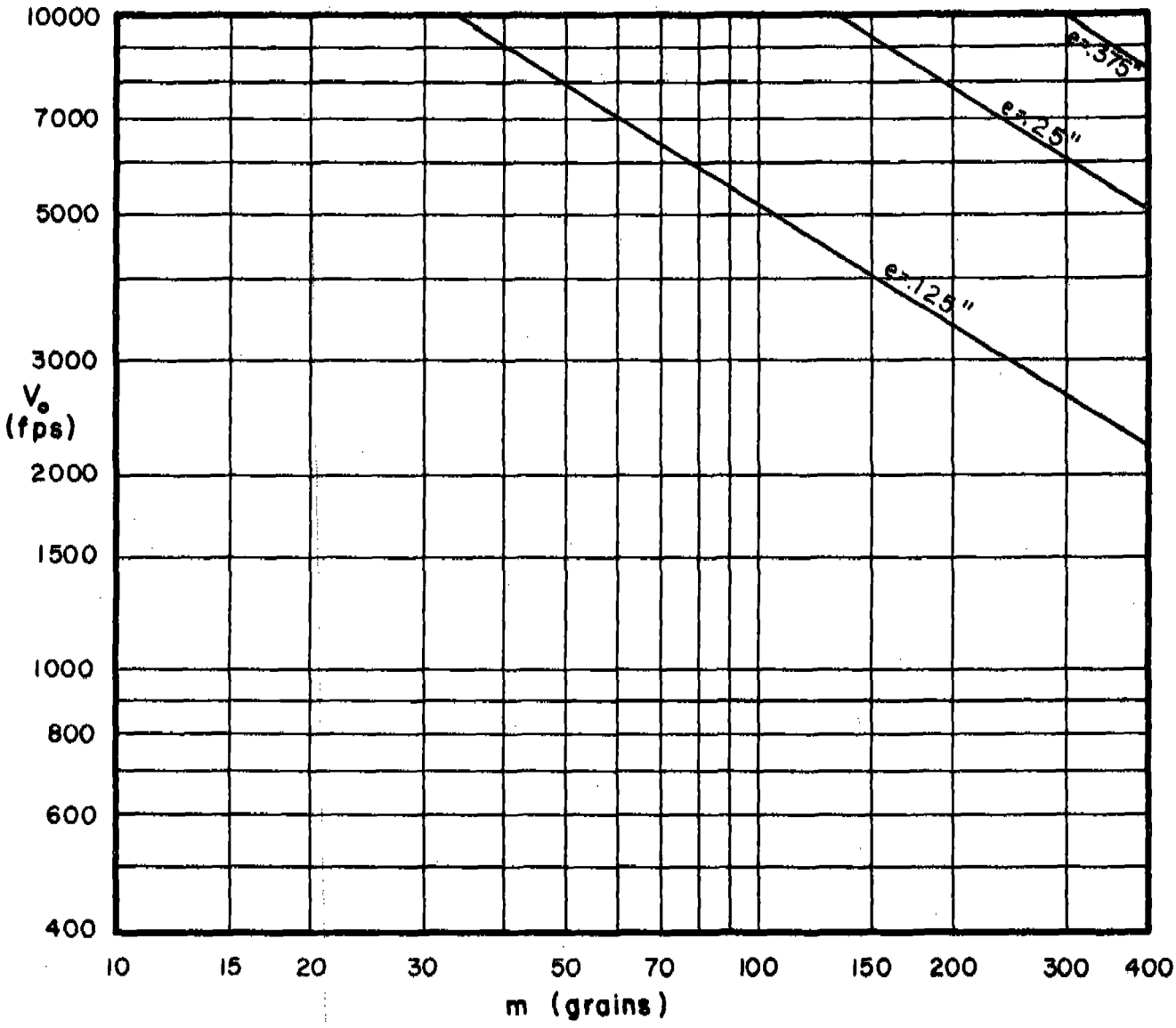

Fig. 18

V_o vs Fragment Weight for Selected Target Thicknesses

Obliquity: 0°

Target Material:

Mild Steel, BHN ~ 150

Fragment:

Type: BRL Pre-formed

Material: Steel, SAE 1020

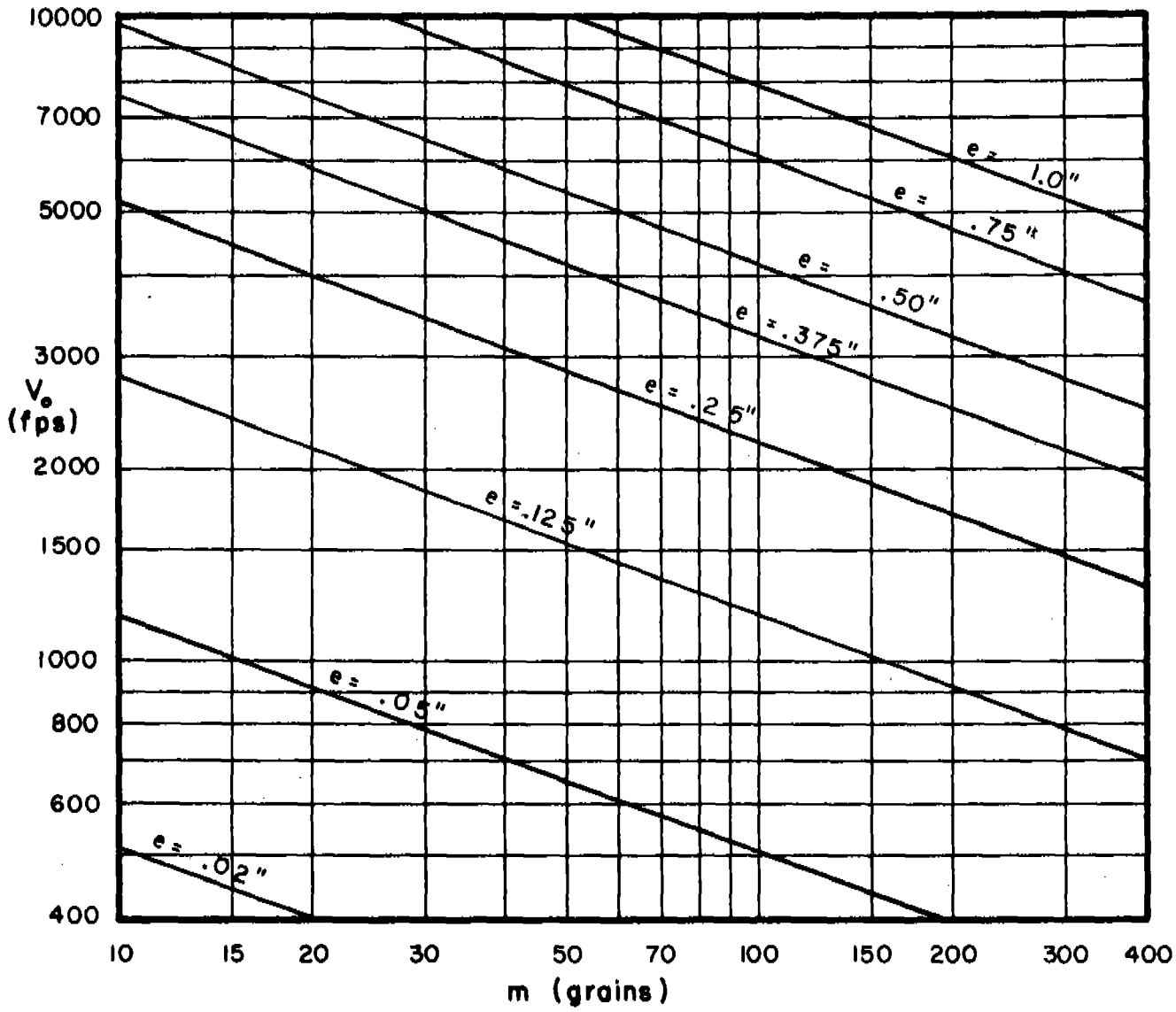

Fig. 19

V_o vs Fragment Weight for Selected Target Thicknesses

Obliquity: 60°

Target Material:

Mild Steel, BHN ~ 150

Fragment:

Type: BRL Pre-formed

Material: Steel, SAE 1020

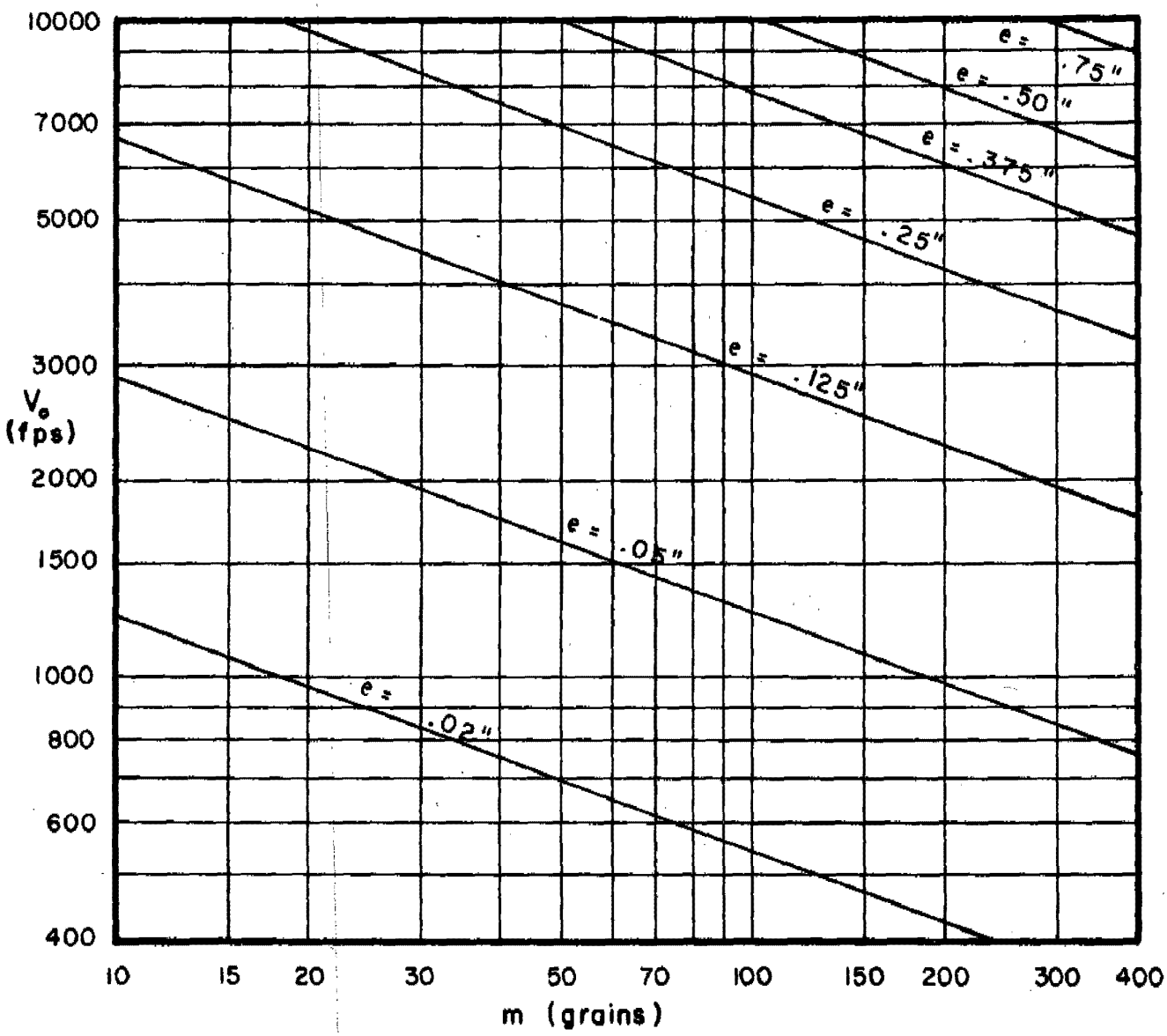

Fig. 20

[redacted]

V_o vs Fragment Weight for Selected Target Thicknesses

Obliquity: 70°

Target Material:

Mild Steel, BHN ~ 150

Fragment:

Type: BRL Pre-formed

Material: Steel, SAE 1020

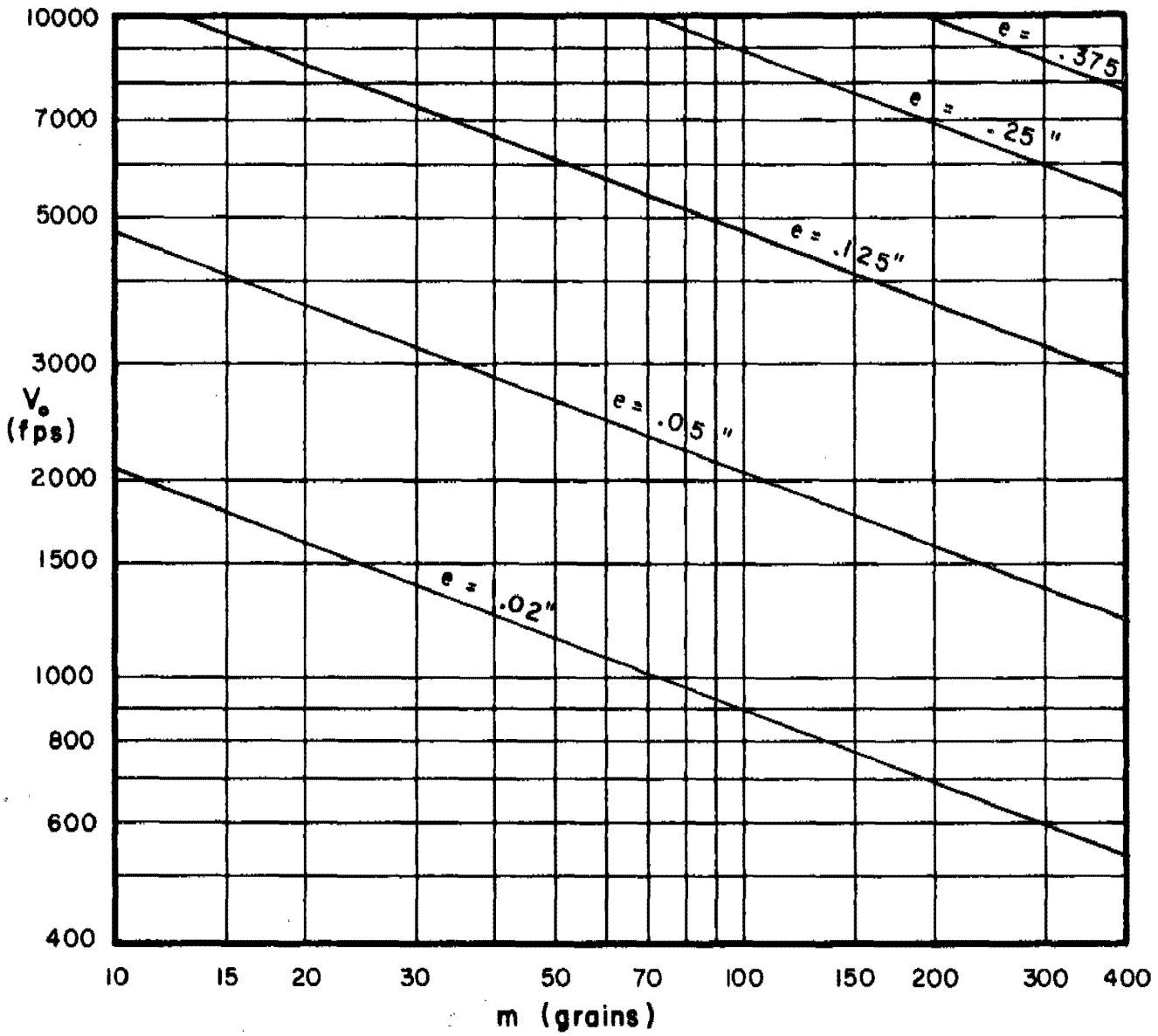

Fig. 21

[redacted]

[redacted]

V_o vs Fragment Weight for Selected Target Thicknesses

Obliquity: 0°

Target Material:

Hard Homogeneous Steel

Fragment:

Type: BRL Pre-formed

Material: Steel, SAE 1020

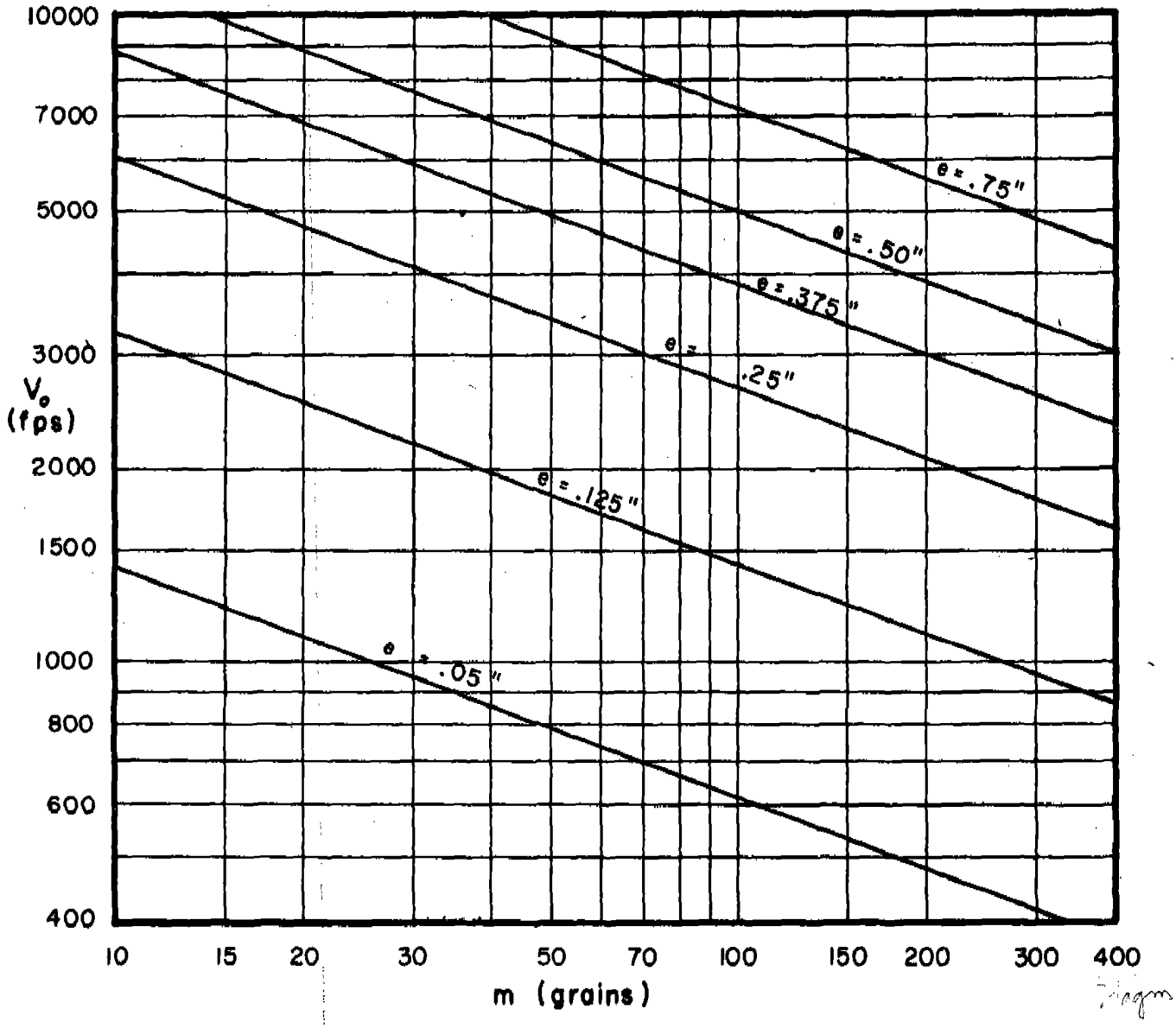

Fig. 22

[redacted]

[redacted]

V_o vs Fragment Weight for Selected Target Thicknesses

Obliquity: 60°

Target Material:

Hard Homogeneous Steel

Fragment:

Type: BRL Pre-formed

Material: Steel, SAE 1020

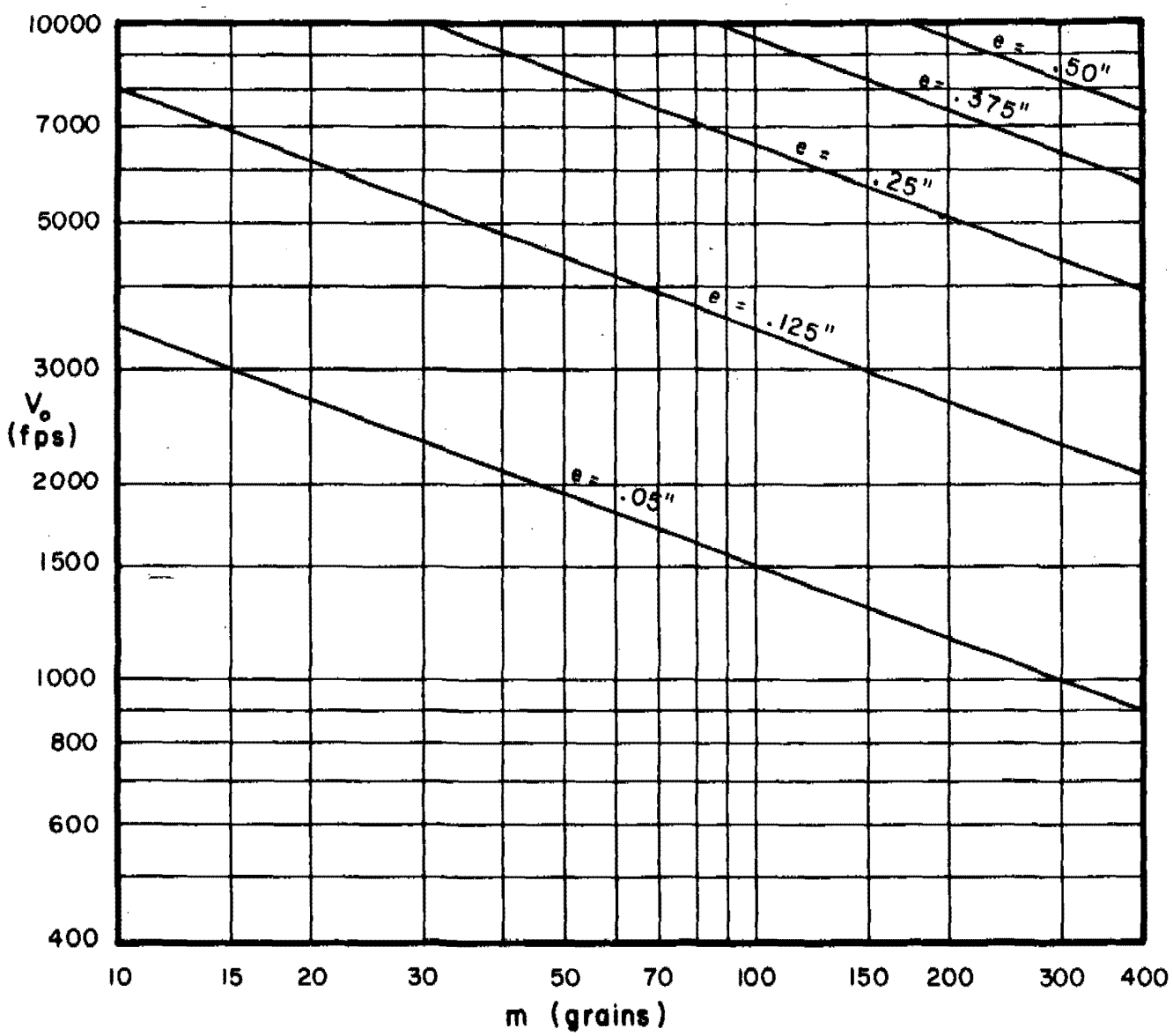

Fig. 23

[redacted]

V_o vs Fragment Weight for Selected Target Thicknesses

Obliquity: 70°

Target Material:

Hard Homogeneous Steel

Fragment:

Type: BRL Pre-formed

Material: Steel, SAE 1020

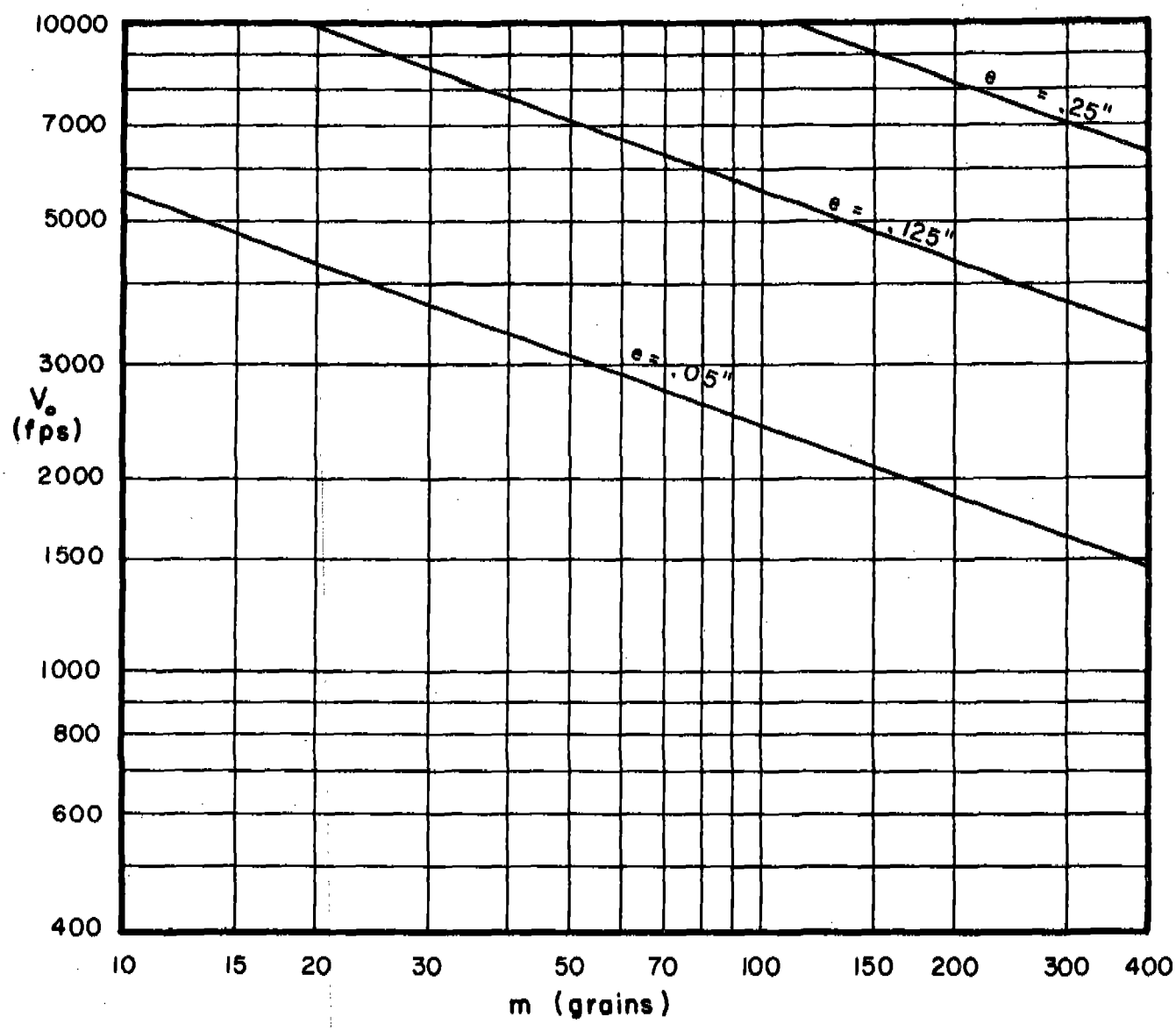

Fig. 24

[redacted]

V_o vs Fragment Weight for Selected Target Thicknesses

Obliquity: 0°

Target Material: Copper

Fragment:

Type: BRL Pre-formed

Material: Steel, SAE 1020

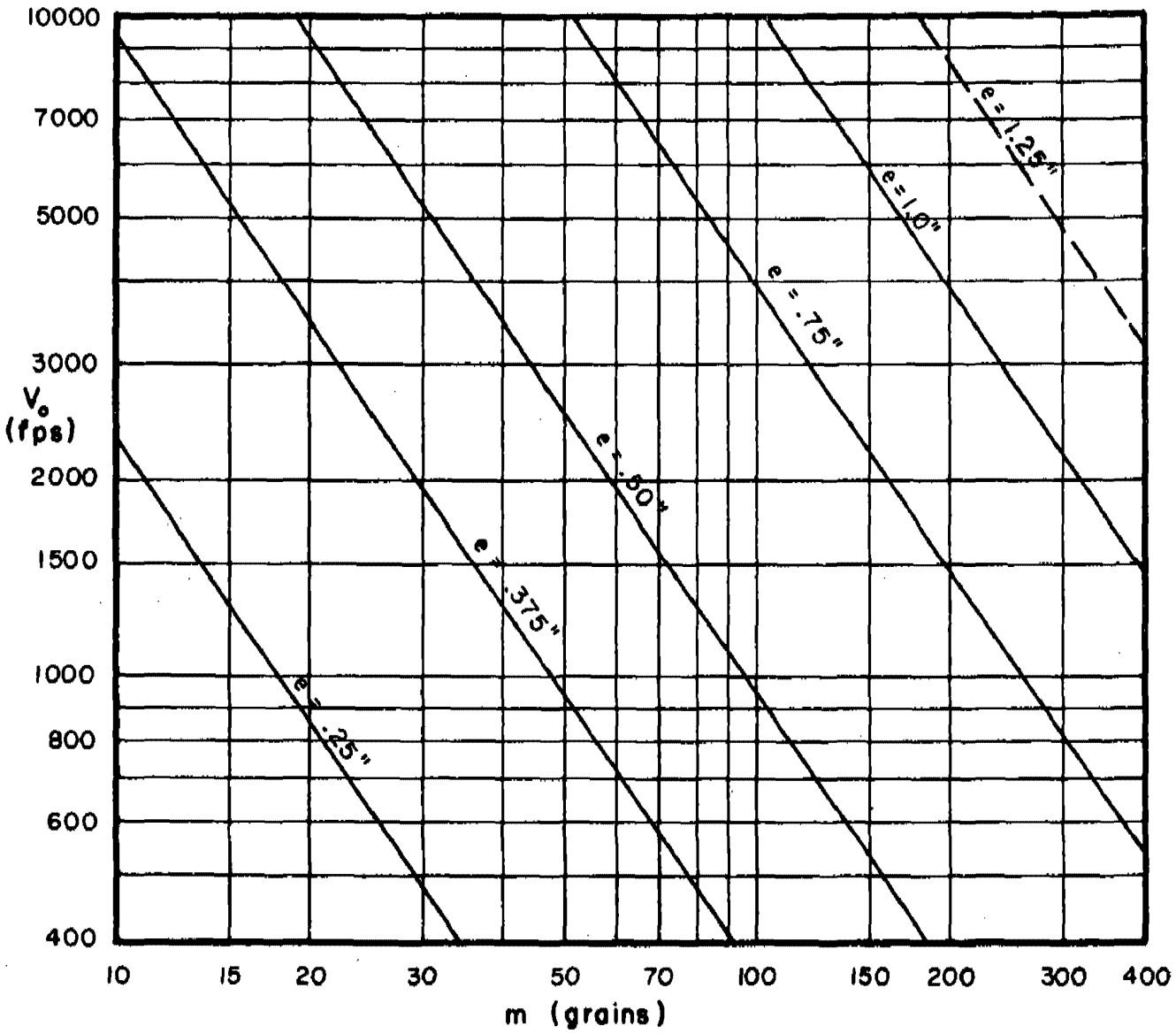

Fig. 25

[redacted]

[redacted]

V_o vs Fragment Weight for Selected Target Thicknesses

Obliquity: 60°

Target Material: Copper

Fragment:

Type: BRL Pre-formed

Material: Steel, SAE 1020

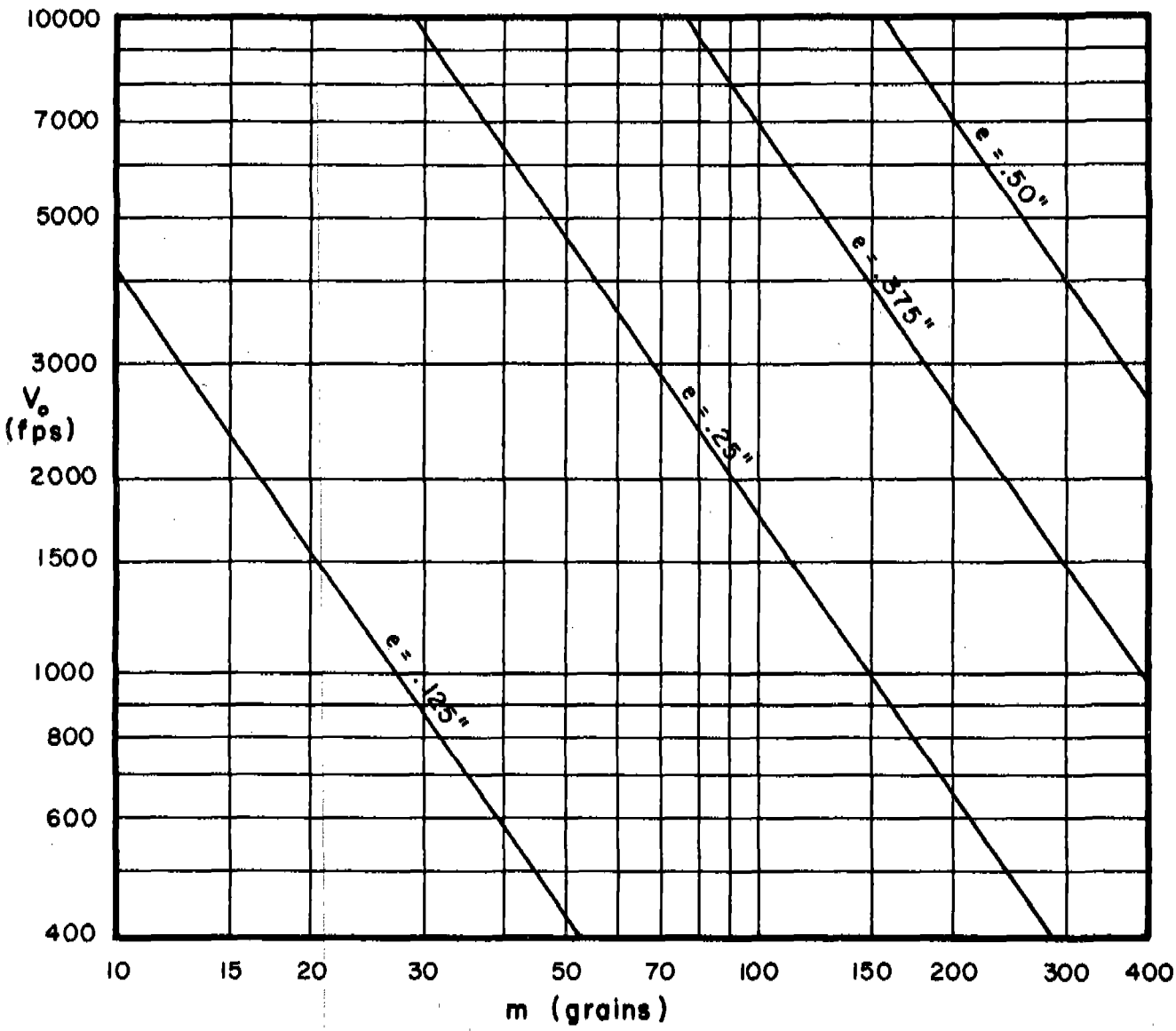

Fig. 26

[redacted]

[redacted]

V_o vs Fragment Weight for Selected Target Thicknesses

Obliquity: 70°

Target Material: Copper

Fragment:

Type: BRL Pre-formed

Material: Steel, SAE 1020

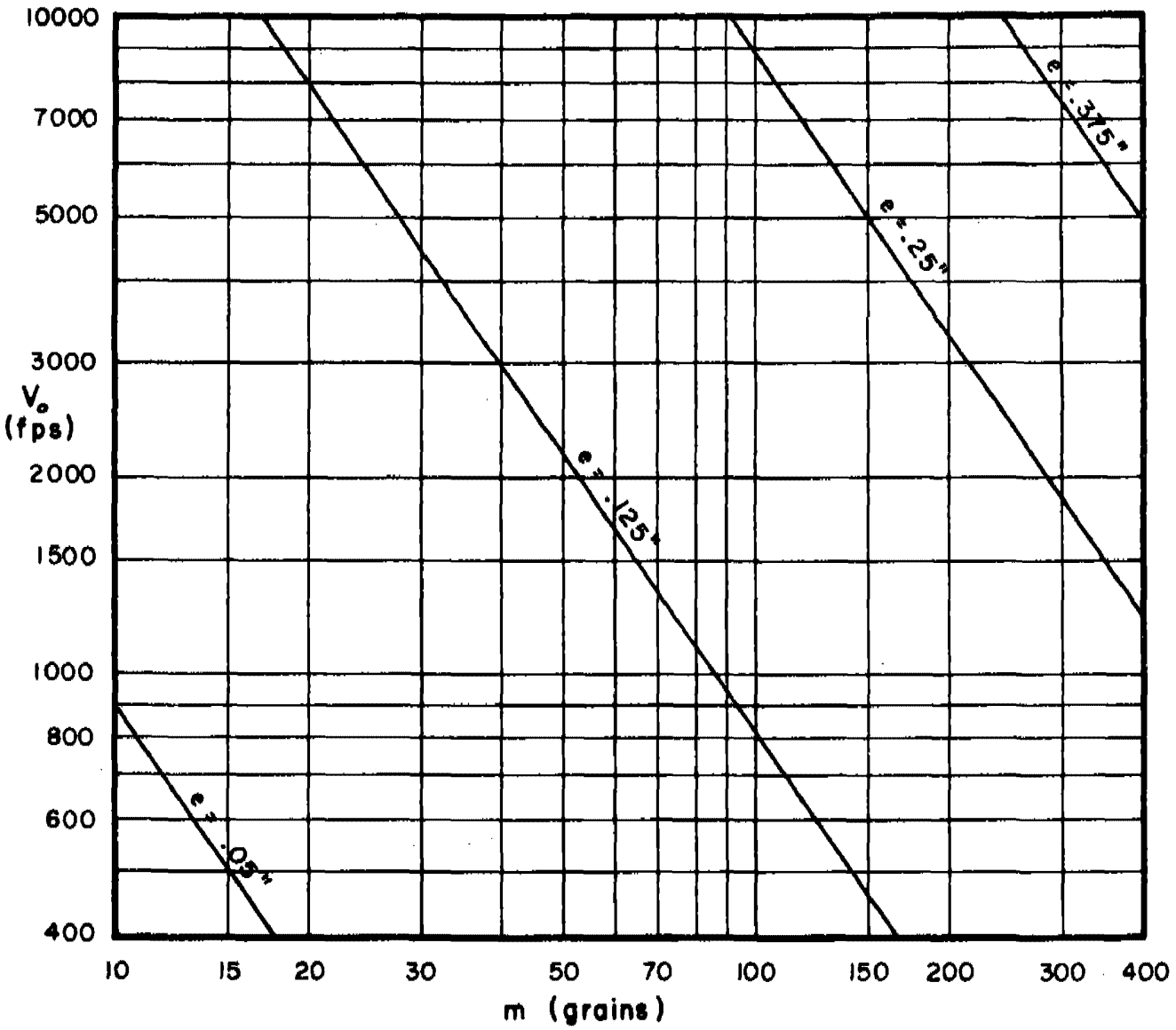

Fig. 27

[redacted]

[redacted]

V_o vs Fragment Weight for Selected Target Thicknesses

Obliquity: 0°

Target Material: Lead

Fragment:

Type: BRL Pre-formed

Material: Steel, SAE 1020

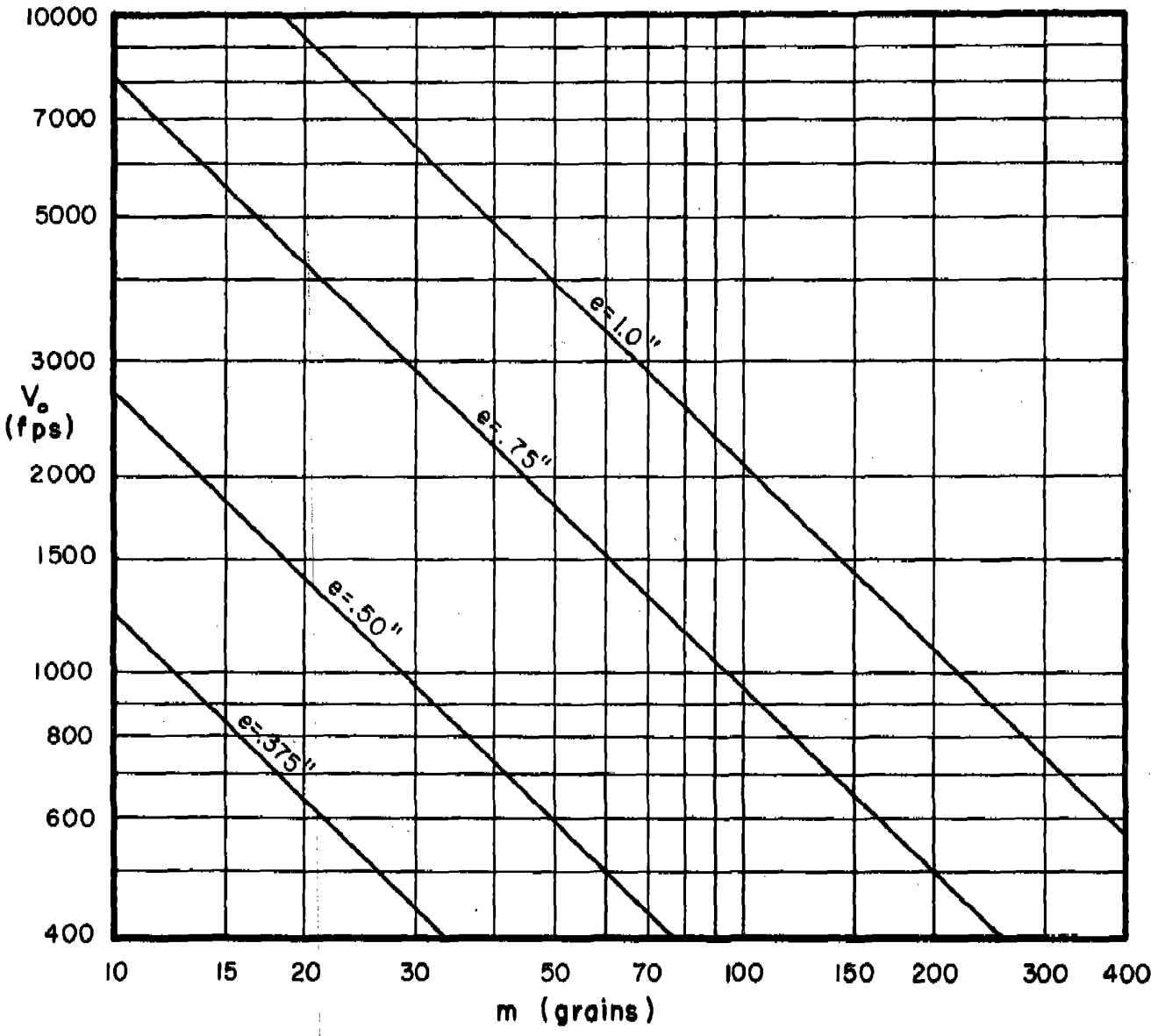

Fig. 28

[redacted]

[redacted]

V_o vs Fragment Weight for Selected Target Thicknesses

Obliquity: 60°

Target Material: Lead

Fragment:

Type: BRL Pre-formed

Material: Steel, SAE 1020

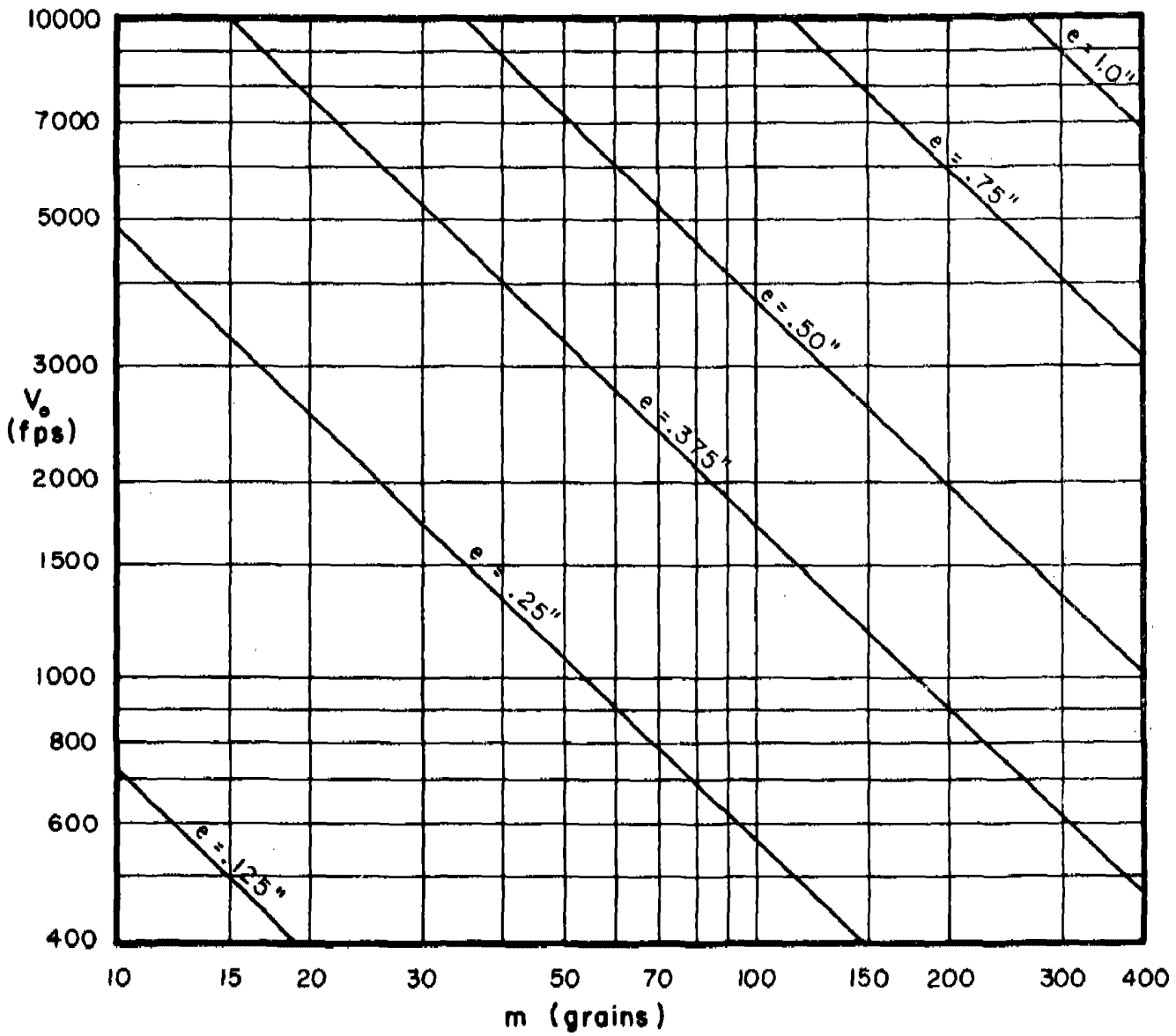

Fig. 29

[redacted]

[redacted]

V_o vs Fragment Weight for Selected Target Thicknesses

Obliquity: 70°

Target Material: Lead

Fragment:

Type: BRL Pre-formed

Material: Steel, SAE 1020

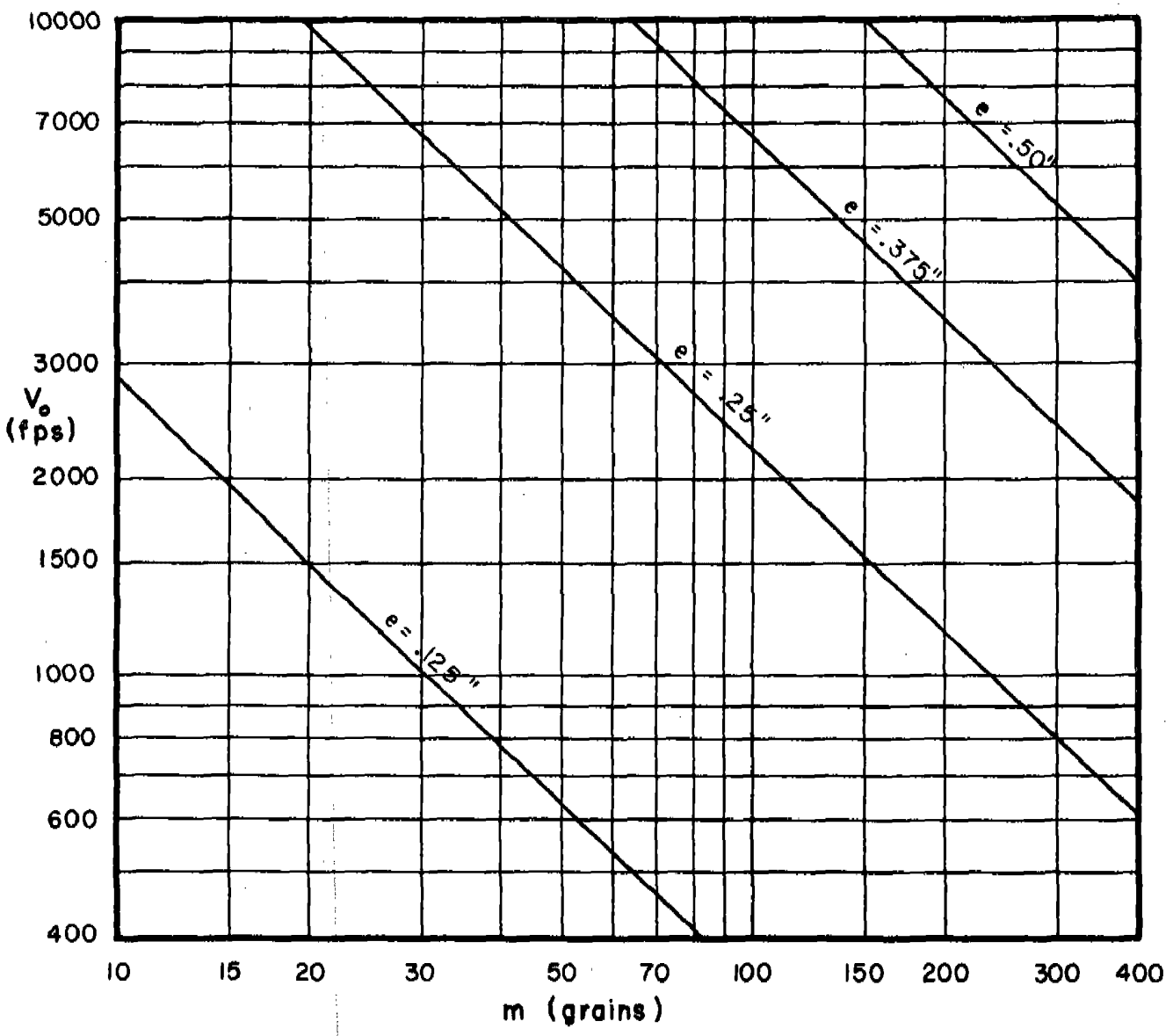

Fig. 30

[redacted]

[redacted]

V_o vs Fragment Weight for Selected Target Thicknesses

Obliquity: 0°

Target Material: Tuballoy

Fragment:

Type: BRL Pre-formed

Material: Steel, SAE 1020

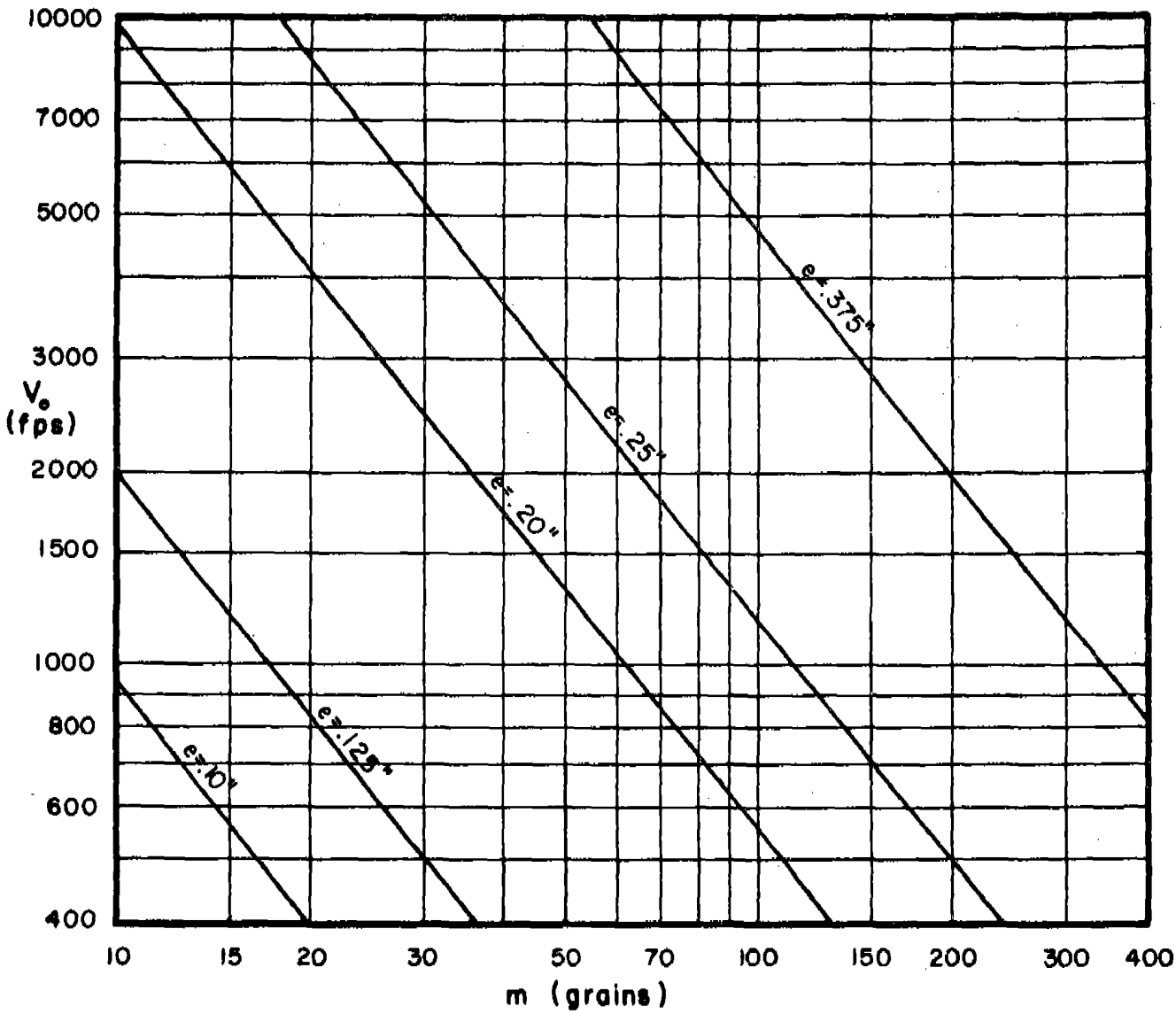

Fig. 31

[redacted]

V_o vs Fragment Weight for Selected Target Thicknesses

Obliquity: 60°

Target Material: Tuballoy

Fragment:

Type: BRL Pre-formed

Material: Steel, SAE 1020

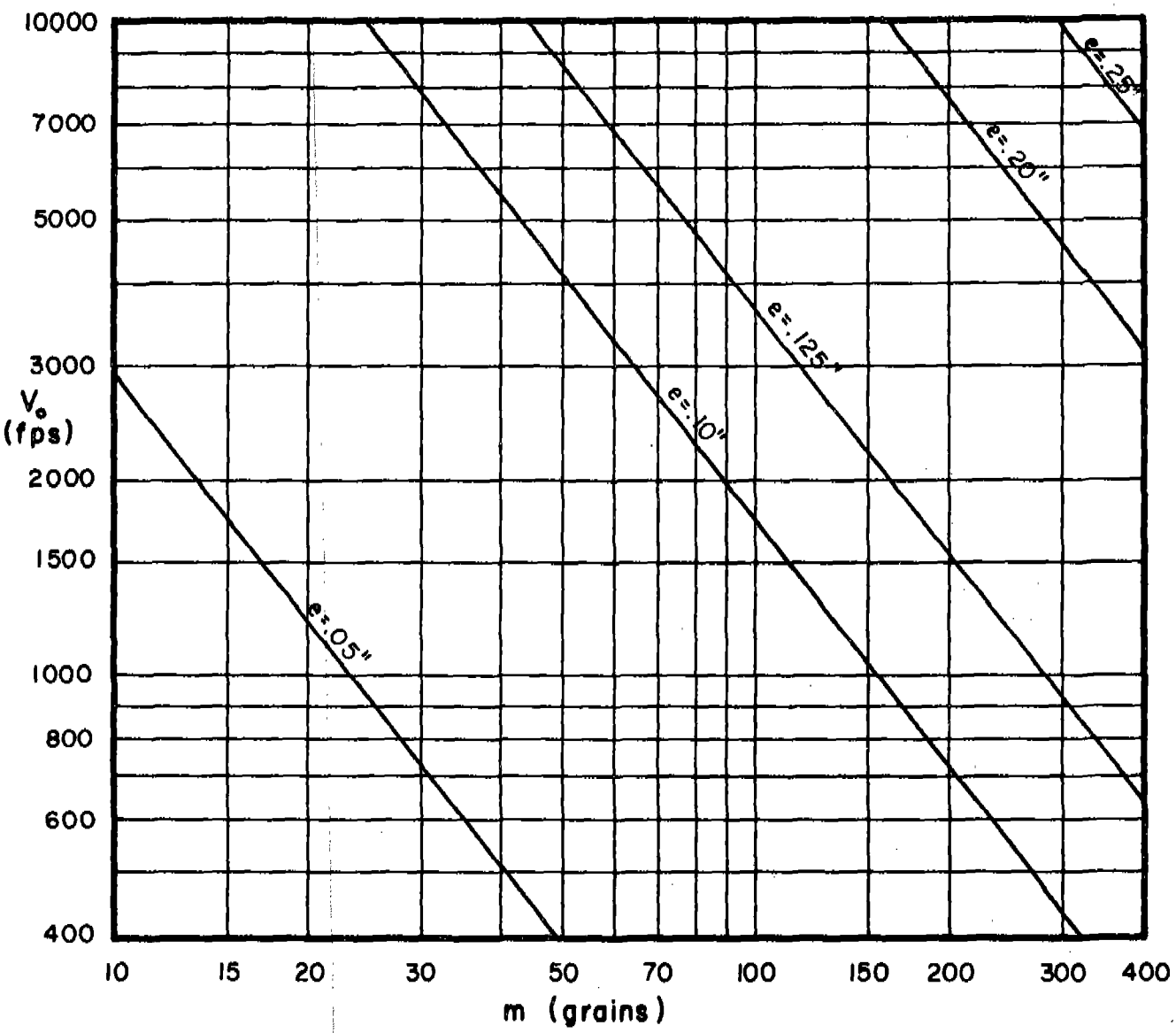

Fig. 32

[redacted]

V_o vs Fragment Weight for Selected Target Thicknesses

Obliquity: 70°

Target Material: Tuballoy

Fragment:

Type: BRL Pre-formed

Material: Steel, SAE 1020

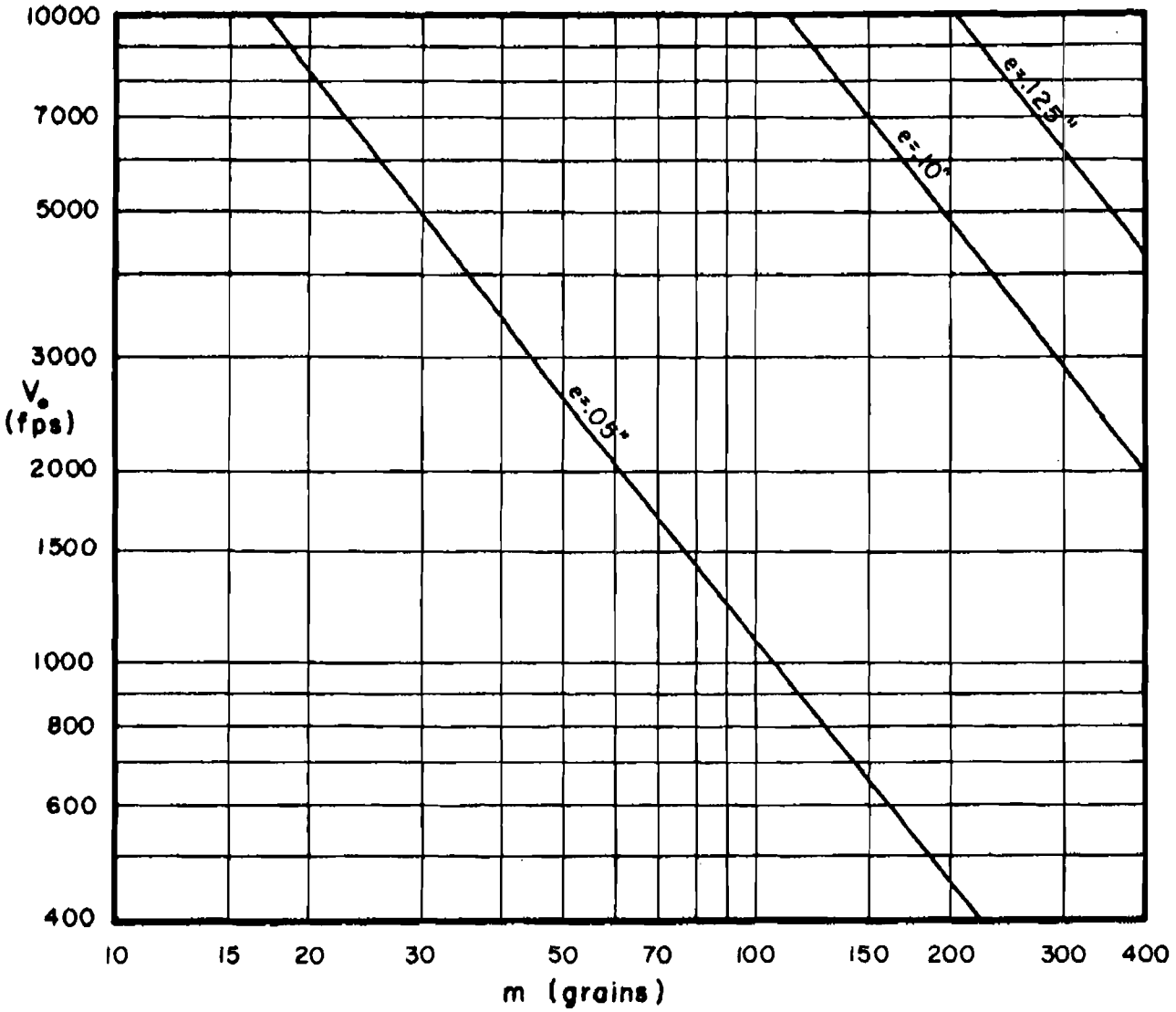

Fig. 33

Following page is blank

[redacted]

[redacted]

Appendix B

Graph Set II: $\frac{V_r}{V_s}$ and $\frac{m_r}{m_s}$ vs V_s for Selected Values of m_s and θ

Figs. 34-120

Note: The use of double ordinates in these graphs requires some explanation. Two sets of thickness contours are to be found on each graph of this type. The thickness contours drawn with solid lines refer to the left-hand ordinate; the dashed contours refer to the right-hand ordinate. Thus, for a given graph and a given striking velocity, two ratios are found. The contours are shown only where both ratios are positive. The dotted lines on these graphs suggest that the associated residual velocities apply to a particle of insignificant weight. These remarks emphasize the need for using the empirical equations for residual velocity and residual weight jointly. In this way, it becomes apparent where the estimates are valid, i.e., where both estimates are positive.

[redacted]

$\frac{V_r}{V_s}$ and $\frac{m_r}{m_s}$ vs V_s for Selected Target Thicknesses

Target: Magnesium Alloy

Obliquity: 0°

Fragment Size: 30 grains

Dashed Thickness Contours Refer to $\frac{m_r}{m_s}$ Ordinate

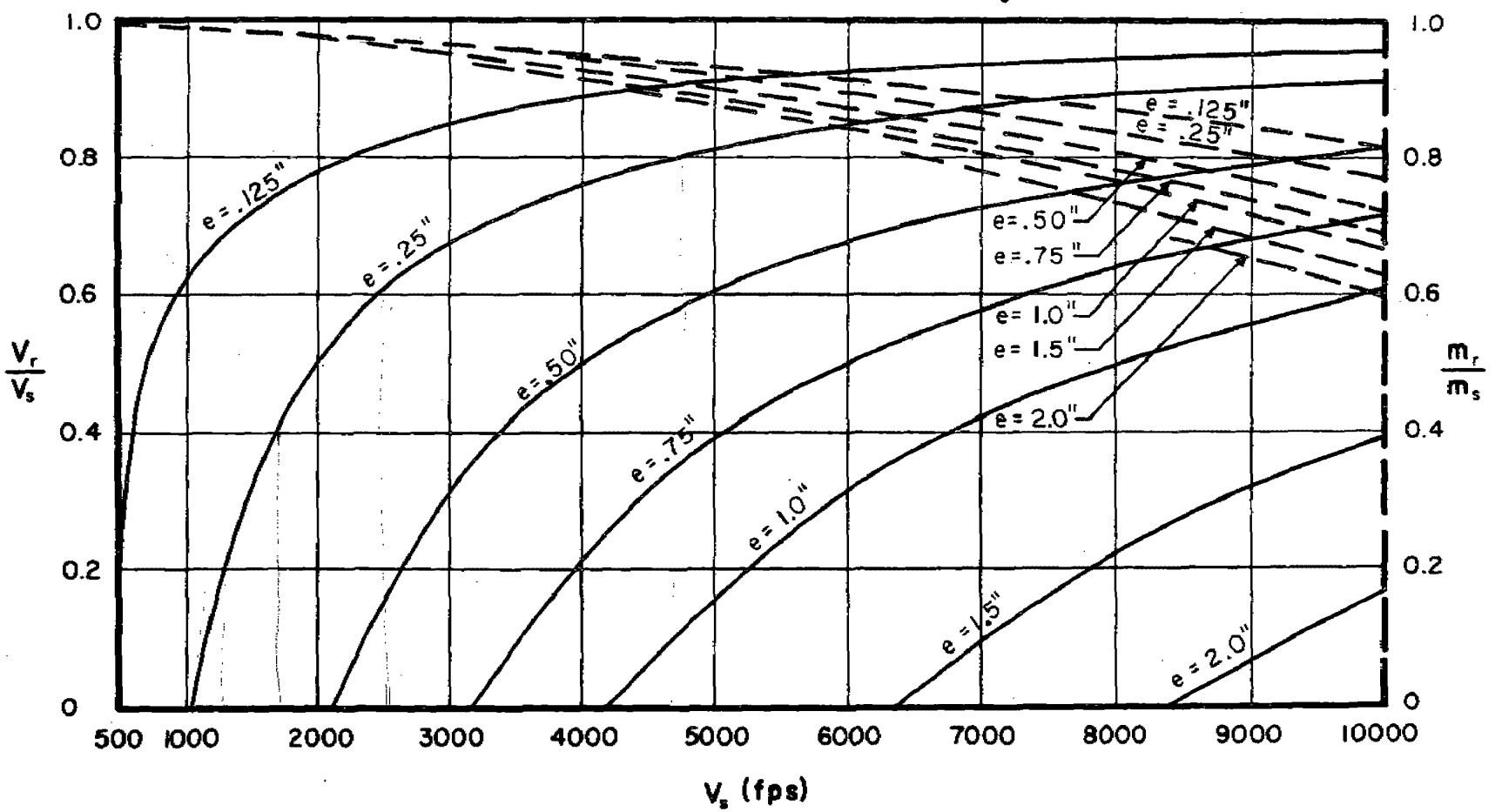

Fig. 34

$\frac{V_r}{V_s}$ and $\frac{m_r}{m_s}$ vs V_s for Selected Target Thicknesses

Target: Magnesium Alloy

Obliquity: 60°

Fragment Size: 30 grains

Dashed Thickness Contours Refer to $\frac{m_r}{m_s}$ Ordinate

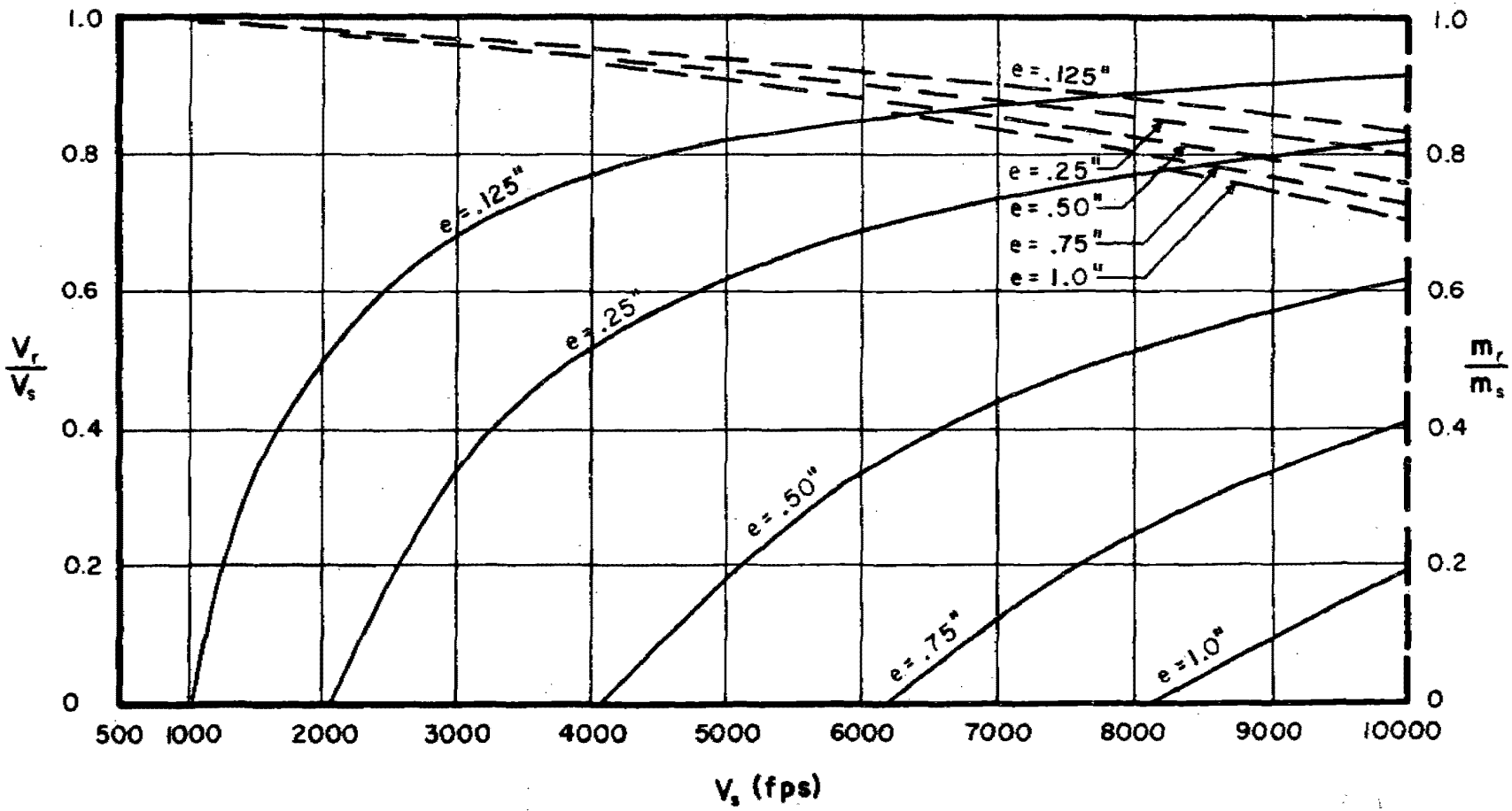

Fig. 35

$\frac{V_r}{V_s}$ and $\frac{m_r}{m_s}$ vs V_s for Selected Target Thicknesses

Target: Magnesium Alloy

Obliquity: 70°

Fragment Size: 30 grains

Dashed Thickness Contours Refer to $\frac{m_r}{m_s}$ Ordinate

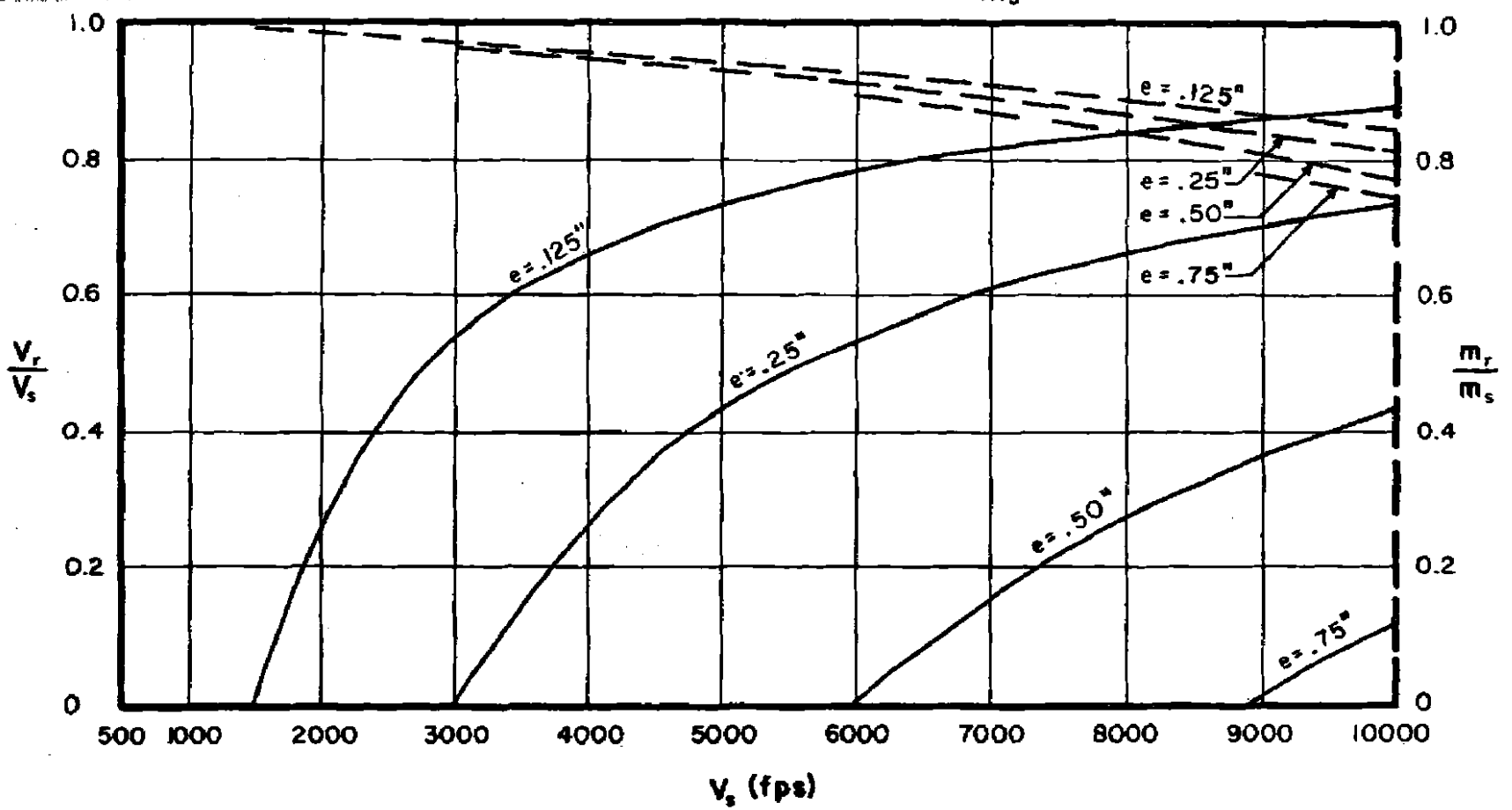

Fig. 36

$\frac{V_r}{V_s}$ and $\frac{m_r}{m_s}$ vs V_s for Selected Target Thicknesses

Target: Magnesium Alloy

Obliquity: 0°

Fragment Size: 100 grains

Dashed Thickness Contours Refer to $\frac{m_r}{m_s}$ Ordinate

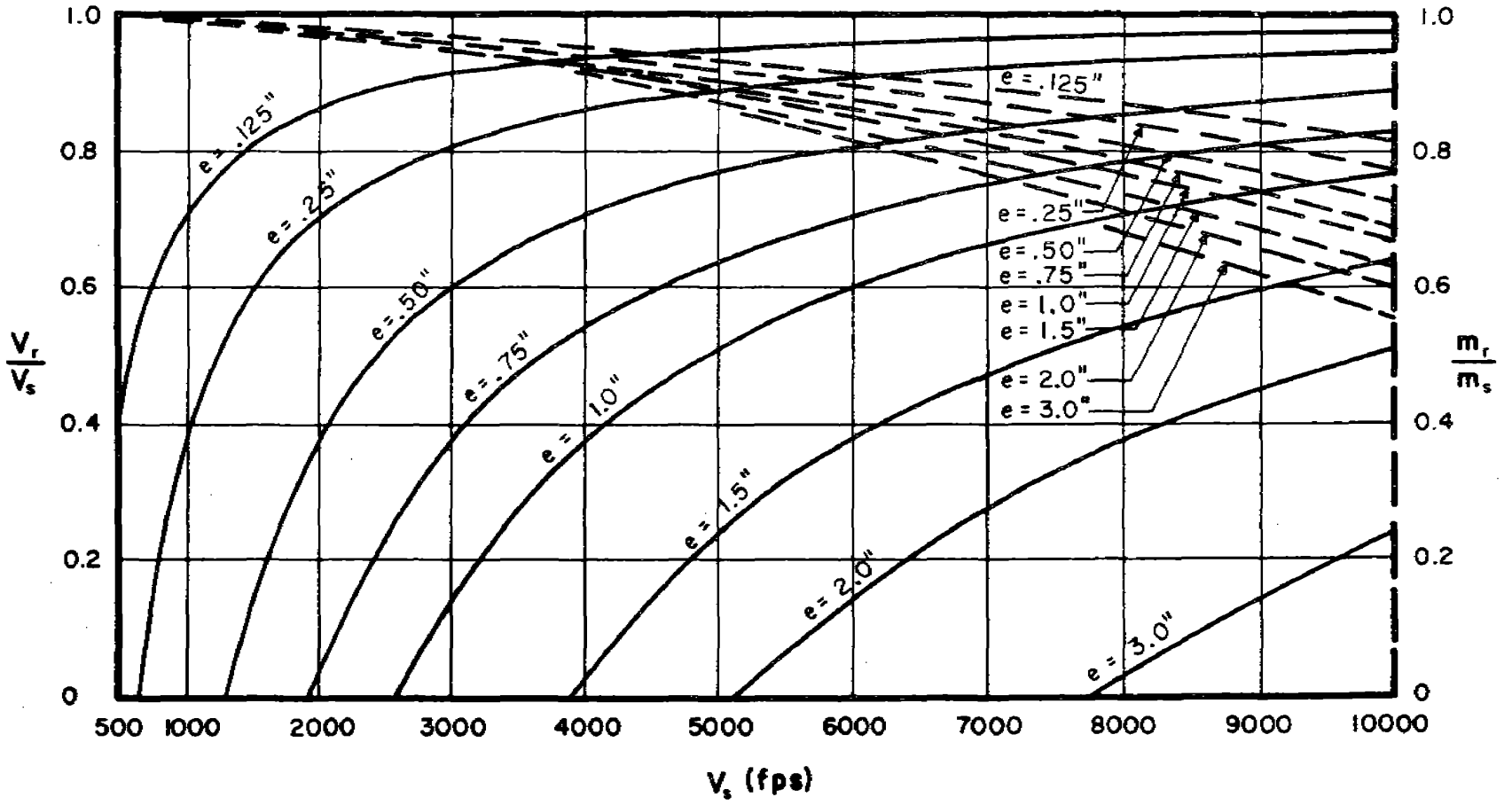

Fig. 37

$\frac{V_r}{V_s}$ and $\frac{m_r}{m_s}$ vs V_s for Selected Target Thicknesses

Target: Magnesium Alloy

Obliquity: 60°

Fragment Size: 100 grains

Dashed Thickness Contours Refer to $\frac{m_r}{m_s}$ Ordinate

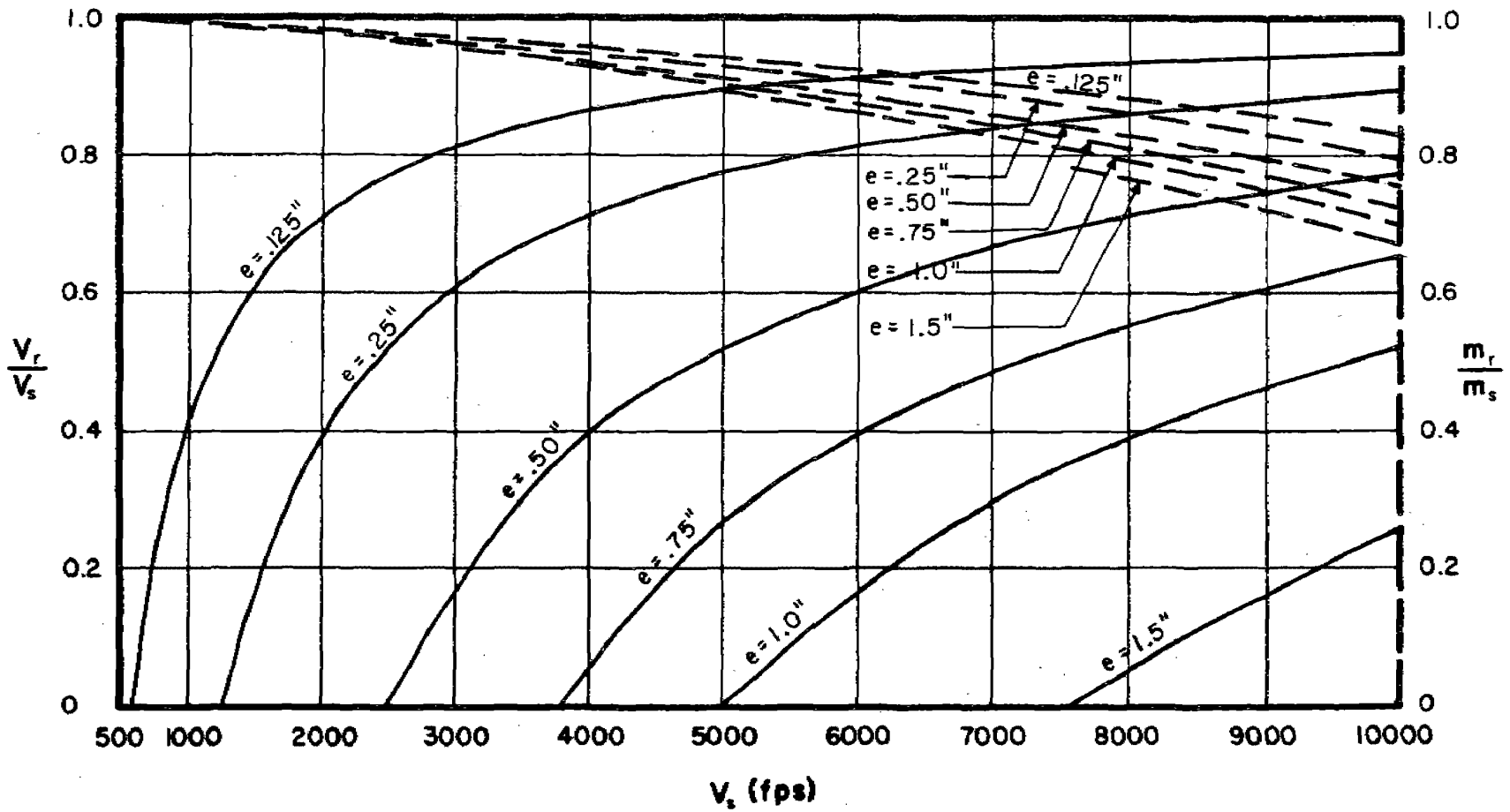

Fig. 38

$\frac{V_r}{V_s}$ and $\frac{m_r}{m_s}$ vs V_s for Selected Target Thicknesses

Target: Magnesium Alloy

Obliquity: 70°

Fragment Size: 100 grains

Dashed Thickness Contours Refer to $\frac{m_r}{m_s}$ Ordinate

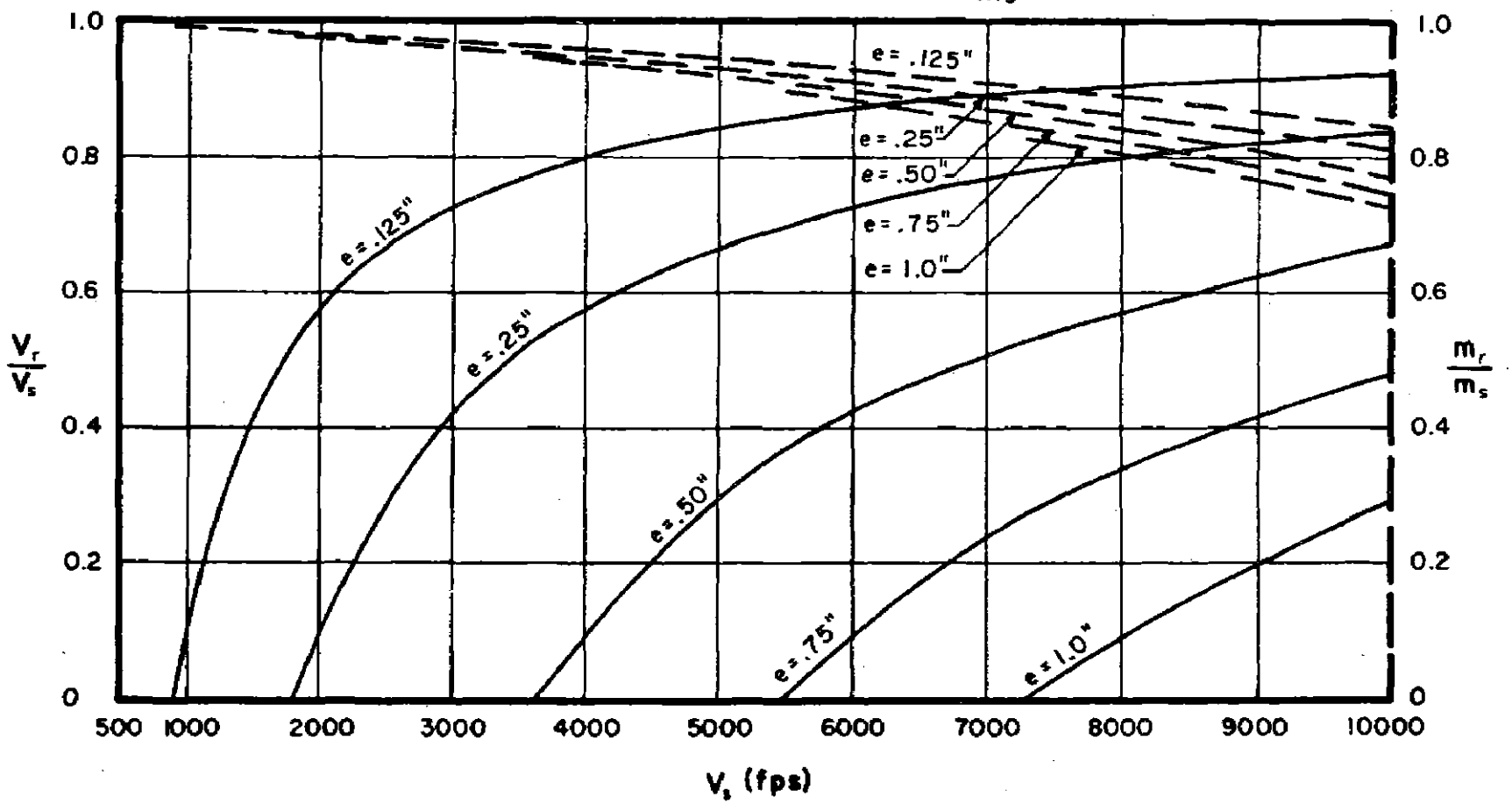

Fig. 39

$\frac{V_r}{V_s}$ and $\frac{m_r}{m_s}$ vs V_s for Selected Target Thicknesses

Target: Magnesium Alloy

Obliquity: 0°

Fragment Size: 300 grains

Dashed Thickness Contours Refer to $\frac{m_r}{m_s}$ Ordinate

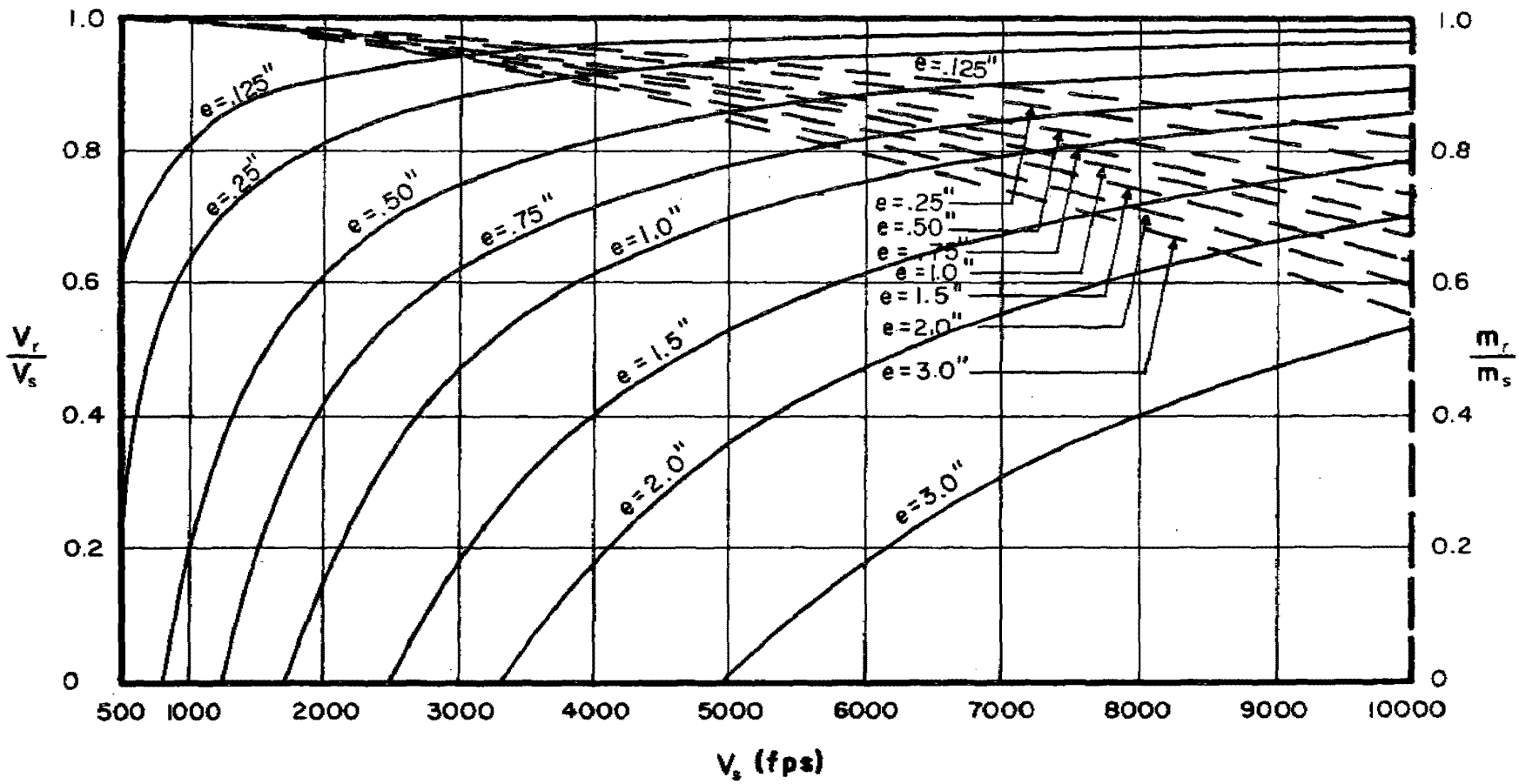

Fig. 40

$\frac{V_r}{V_s}$ and $\frac{m_r}{m_s}$ vs V_s for Selected Target Thicknesses

Target: Magnesium Alloy

Obliquity: 60°

Fragment Size: 300 grains

Dashed Thickness Contours Refer to $\frac{m_r}{m_s}$ Ordinate

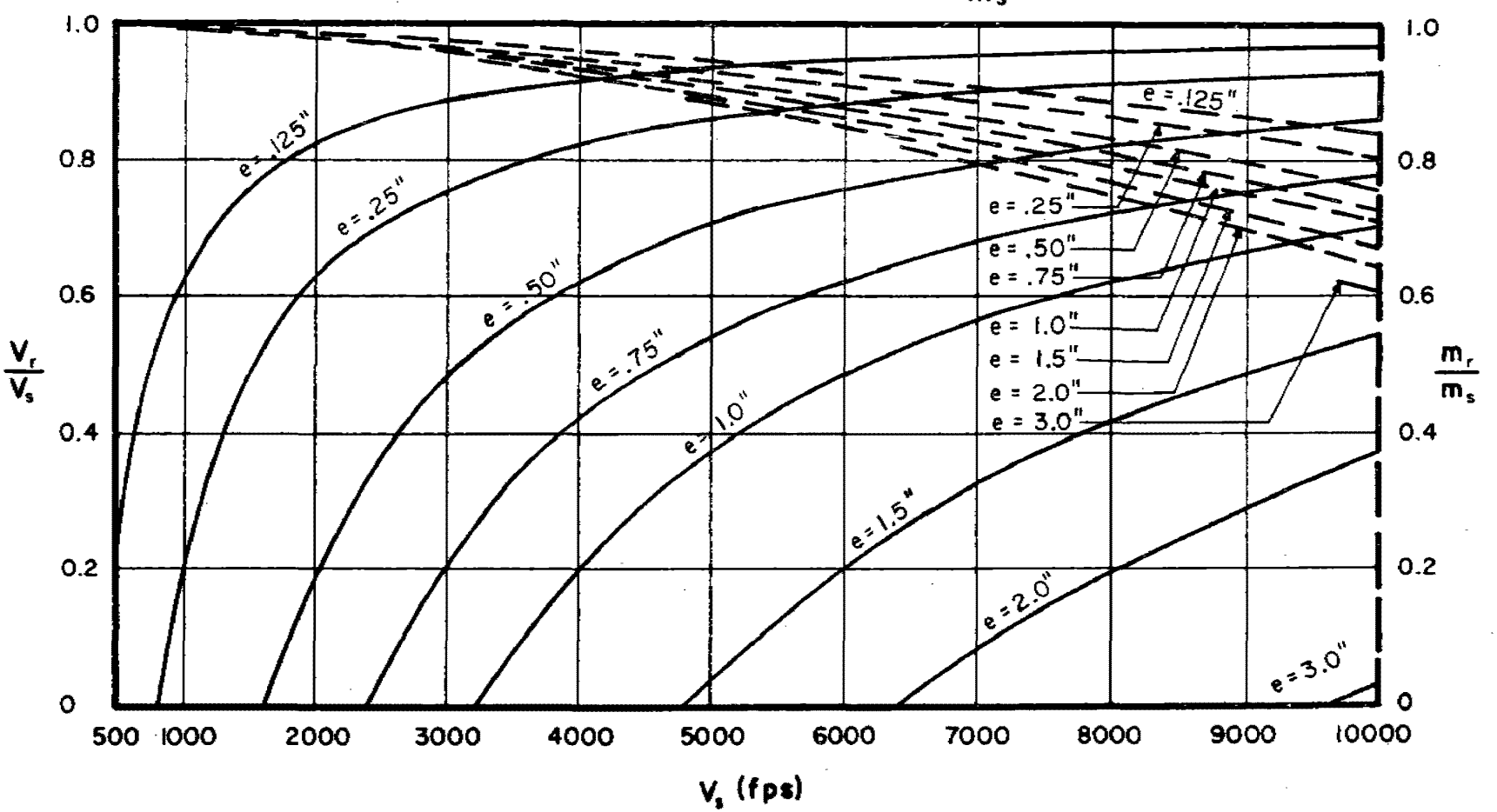

Fig. 41

$\frac{V_r}{V_s}$ and $\frac{m_r}{m_s}$ vs V_s for Selected Target Thicknesses

Target: Magnesium Alloy

Obliquity: 70°

Fragment Size: 300 grains

Dashed Thickness Contours Refer to $\frac{m_r}{m_s}$ Ordinate

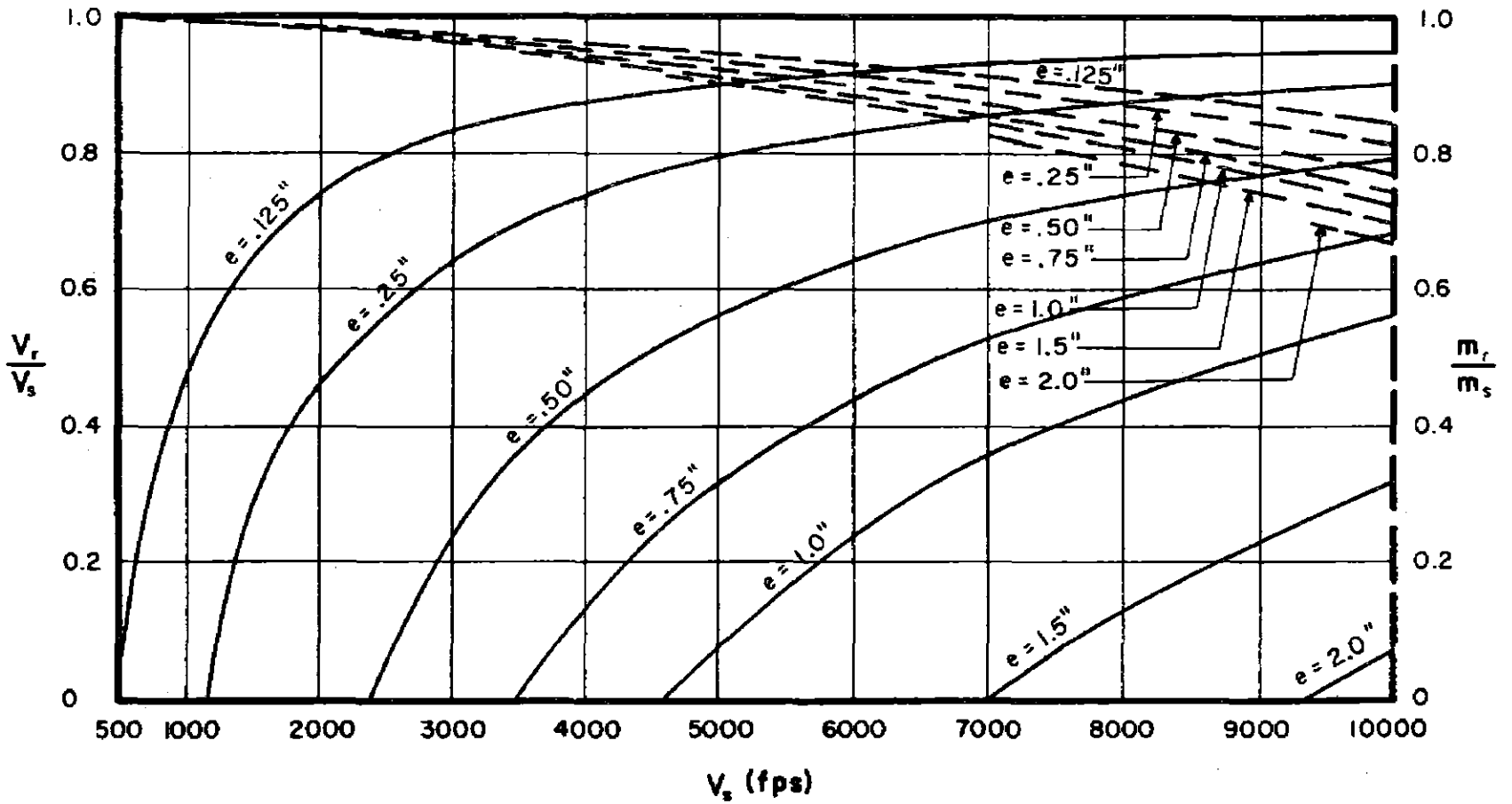

Fig. 42

$\frac{V_r}{V_s}$ and $\frac{m_r}{m_s}$ vs V_s for Selected Target Thicknesses

Target: Aluminum Alloy, 2024 T-3

Obliquity: 0°

Fragment Size: 30 grains

Dashed Thickness Contours Refer to $\frac{m_r}{m_s}$ Ordinate

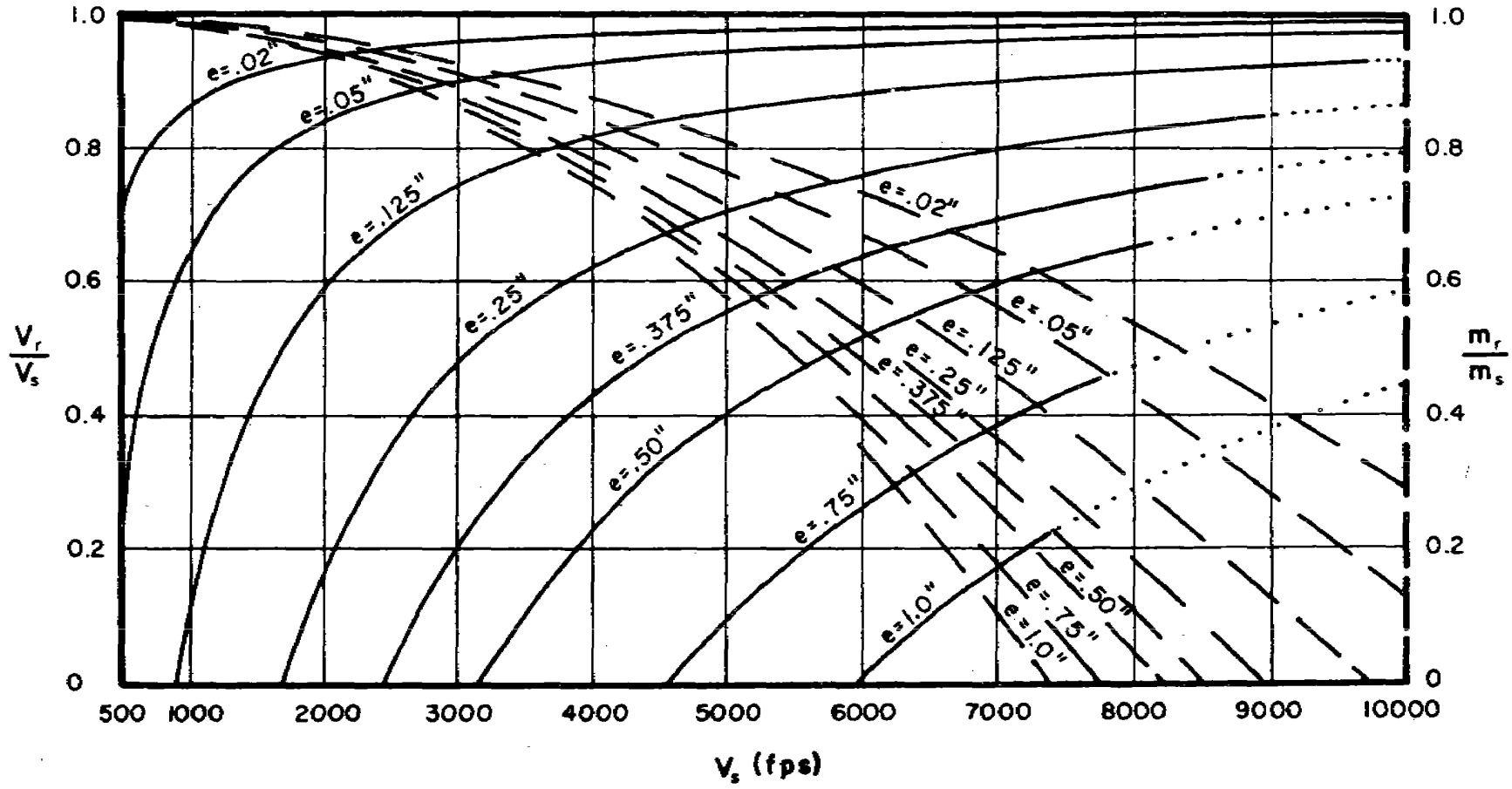

Fig. 43

$\frac{V_r}{V_s}$ and $\frac{m_r}{m_s}$ vs V_s for Selected Target Thicknesses

Target: Aluminum Alloy, 2024T-3

Obliquity: 60°

Fragment Size: 30 grains

Dashed Thickness Contours Refer to $\frac{m_r}{m_s}$ Ordinate

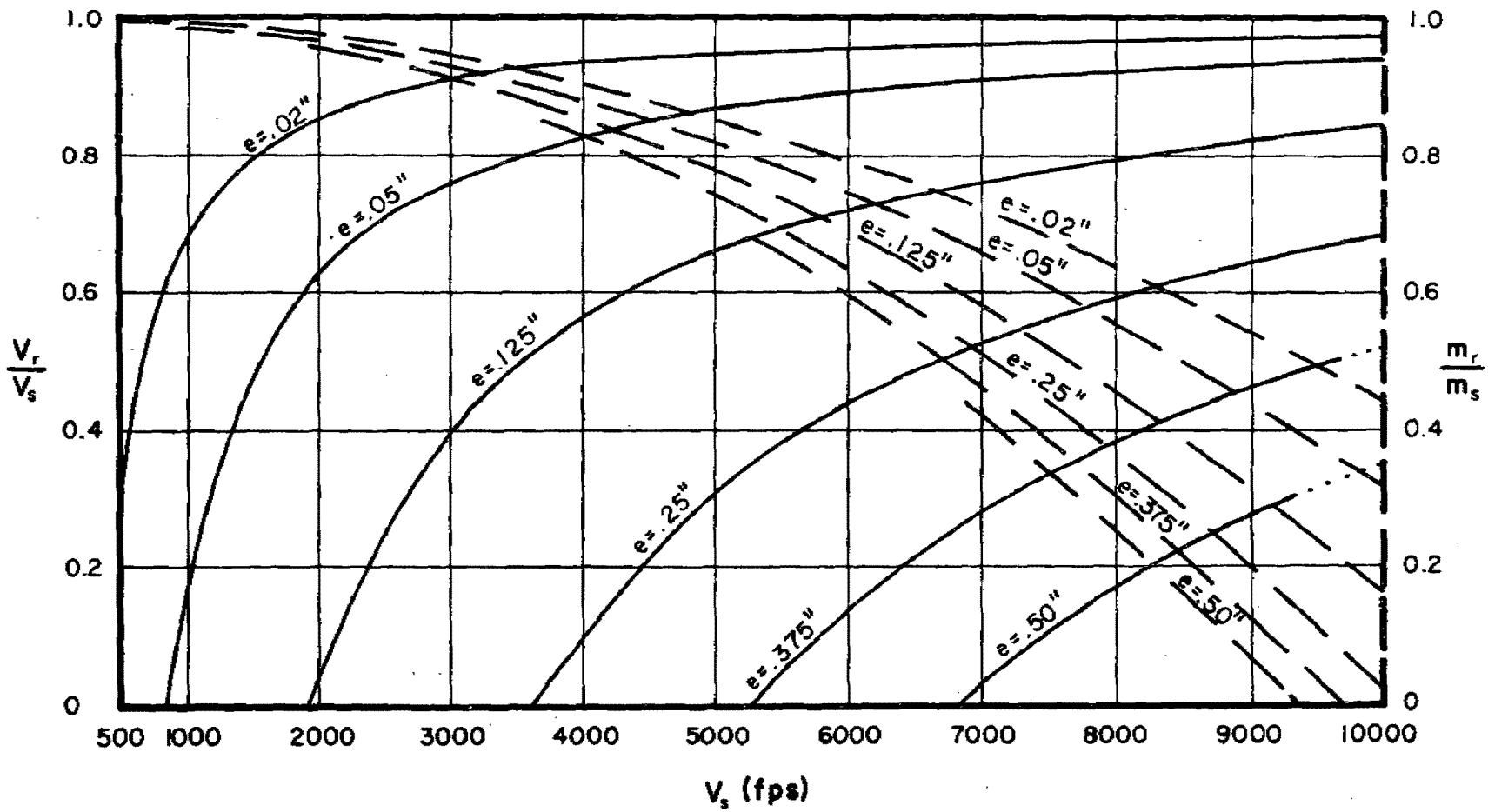

Fig. 44

$\frac{V_r}{V_s}$ and $\frac{m_r}{m_s}$ vs V_s for Selected Target Thicknesses

Target: Aluminum Alloy, 2024 T-3

Obliquity: 70°

Fragment Size: 30 grains

Dashed Thickness Contours Refer to $\frac{m_r}{m_s}$ Ordinate

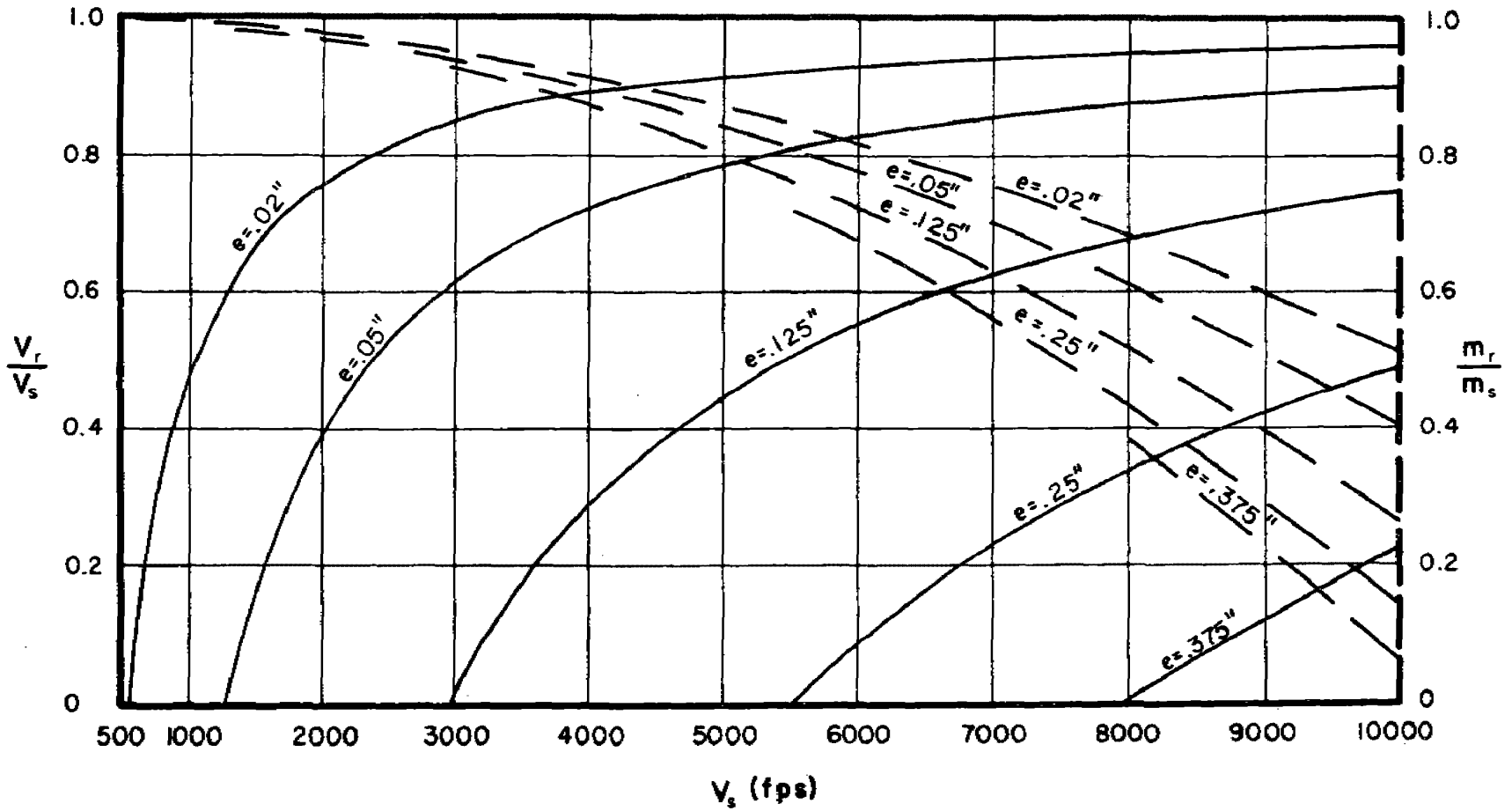

Fig. 45

$\frac{V_r}{V_s}$ and $\frac{m_r}{m_s}$ vs V_s for Selected Target Thicknesses

Target: Aluminum Alloy, 2024T-3

Obliquity: 0°

Fragment Size: 100 grains

Dashed Thickness Contours Refer to $\frac{m_r}{m_s}$ Ordinate

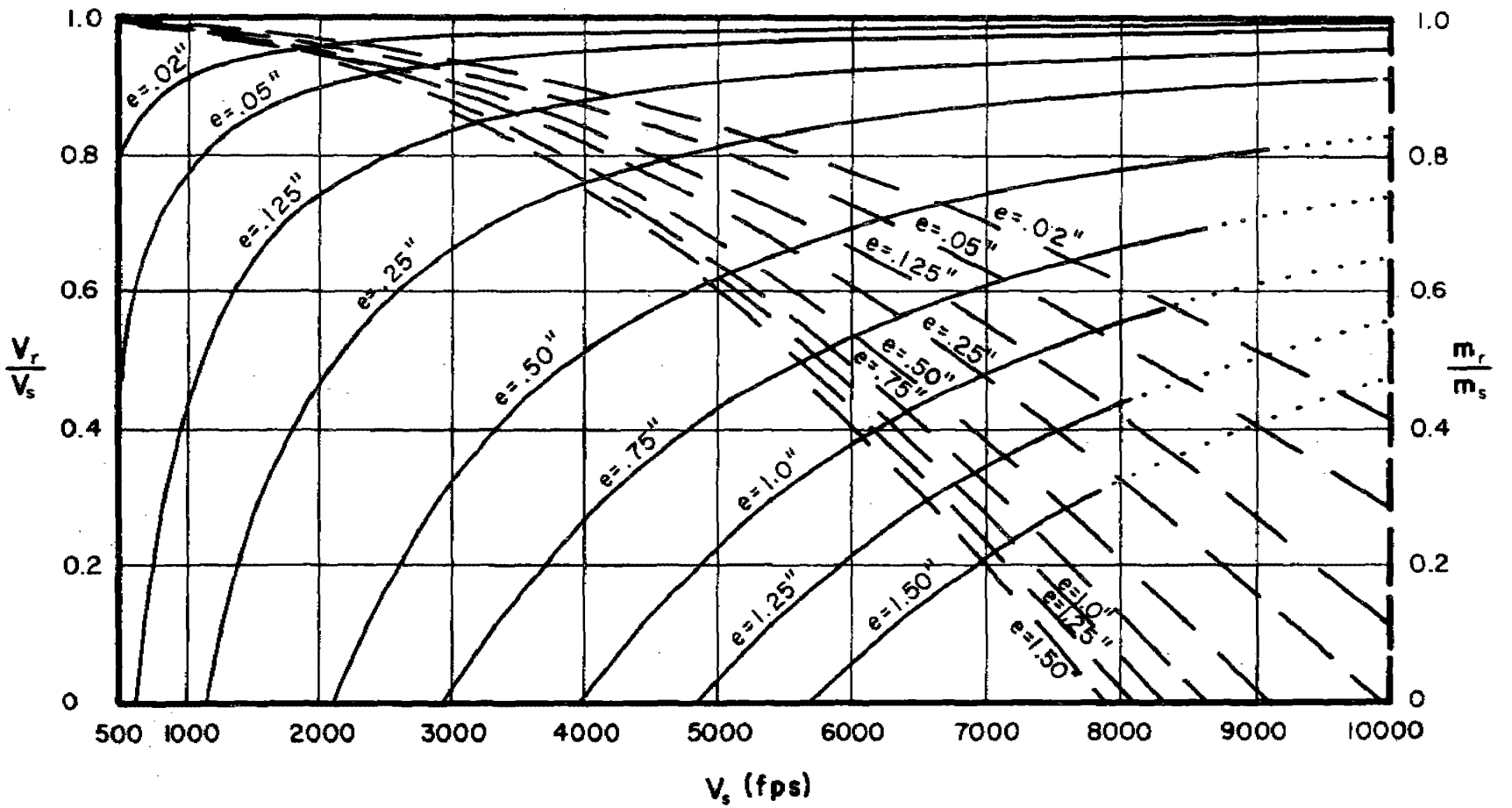

Fig. 46

$\frac{V_r}{V_s}$ and $\frac{m_r}{m_s}$ vs V_s for Selected Target Thicknesses

Target: Aluminum Alloy, 2024 T-3

Obliquity: 60°

Fragment Size: 100 grains

Dashed Thickness Contours Refer to $\frac{m_r}{m_s}$ Ordinate

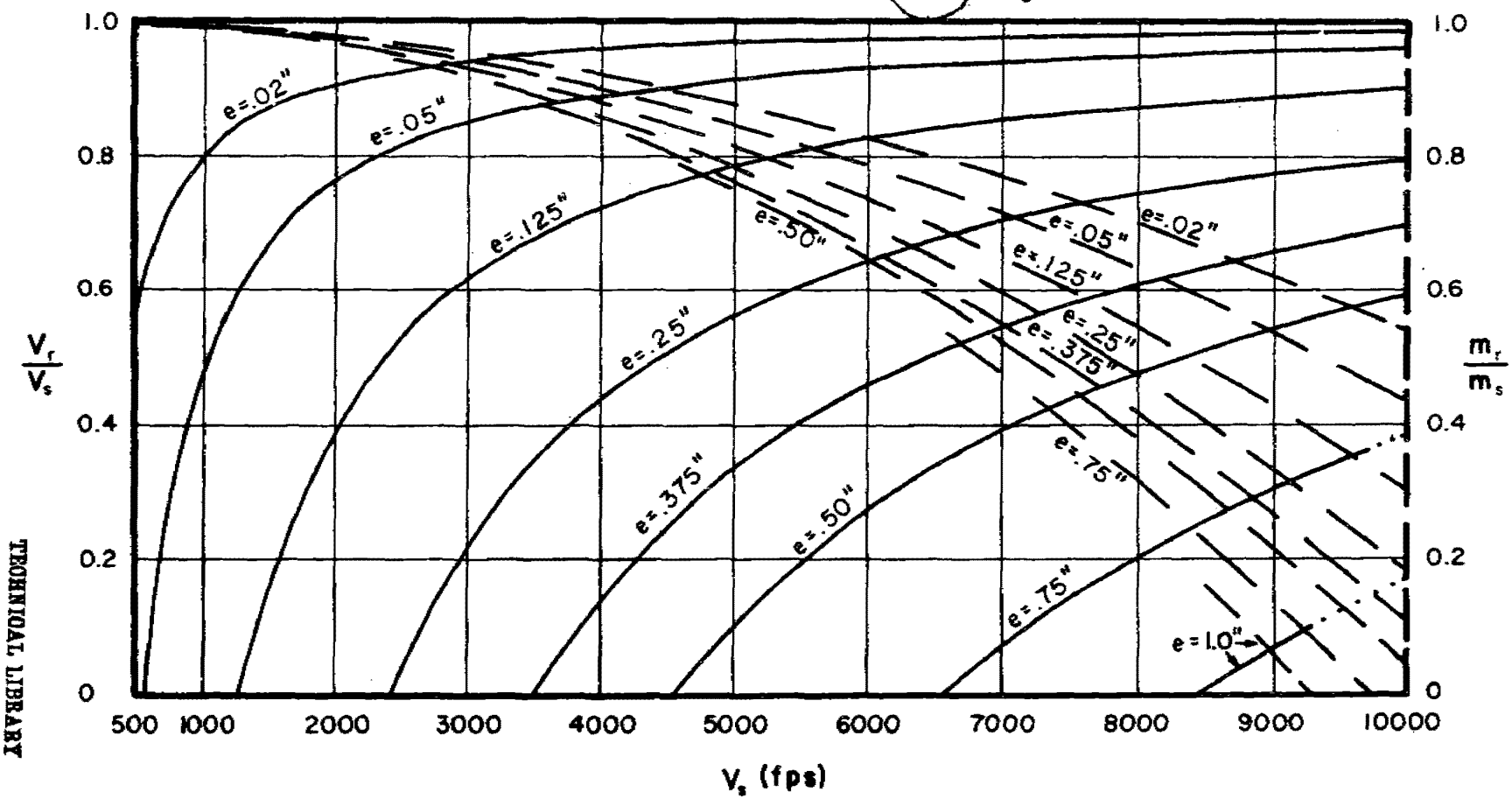

Fig. 47

TECHNICAL LIBRARY
U. S. ARMY ORDNANCE
ABERDEEN PROVING GROUND, MD.
ORDBG-TL

$\frac{V_r}{V_s}$ and $\frac{m_r}{m_s}$ vs V_s for Selected Target Thicknesses

Target: Aluminum Alloy, 2024T-3

Obliquity: 70°

Fragment Size: 100 grains

Dashed Thickness Contours Refer to $\frac{m_r}{m_s}$ Ordinate

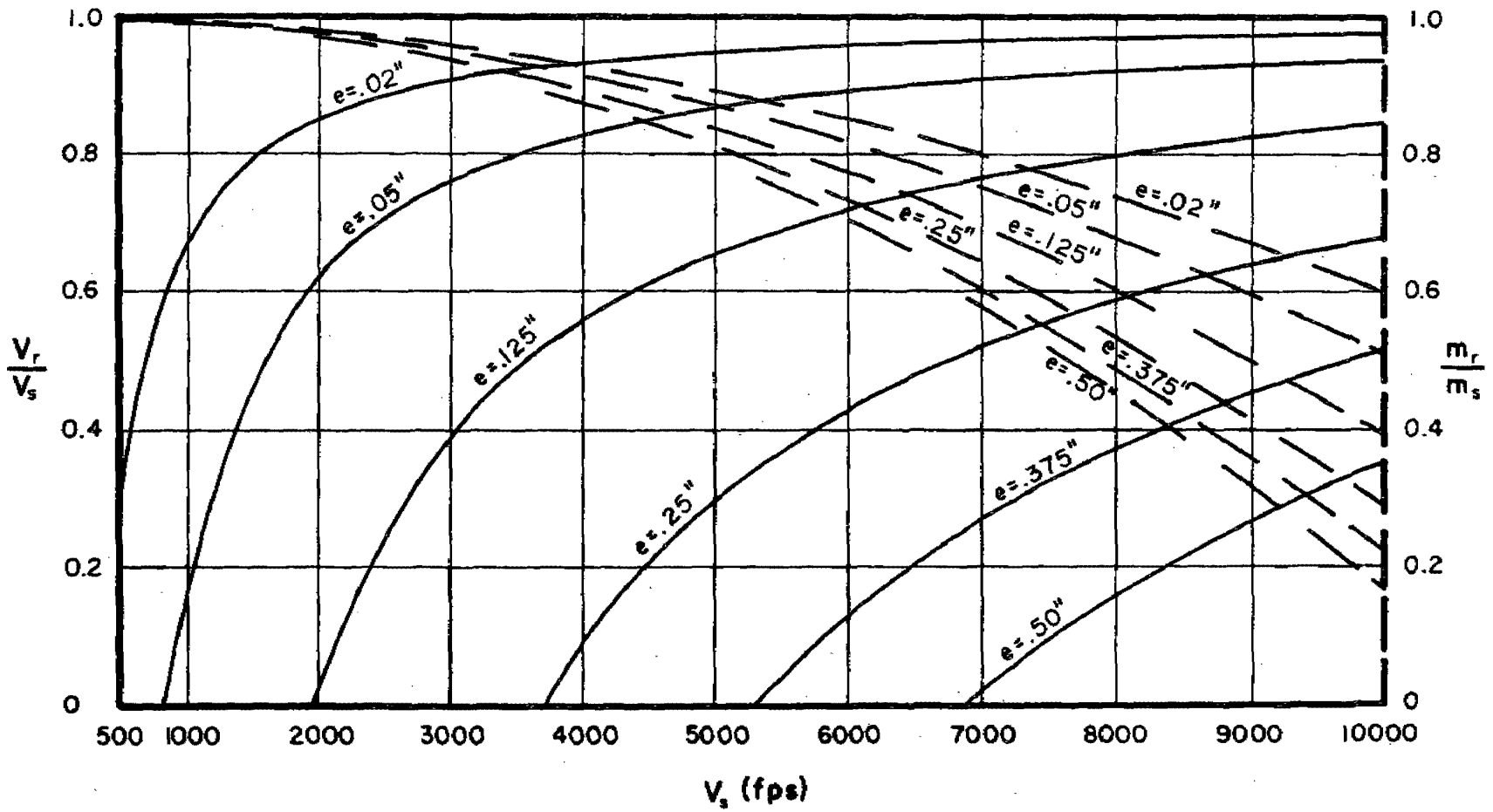

Fig. 48

$\frac{V_r}{V_s}$ and $\frac{m_r}{m_s}$ vs V_s for Selected Target Thicknesses

Target: Aluminum Alloy, 2024T-3

Obliquity: 0°

Fragment Size: 300 grains

Dashed Thickness Contours Refer to $\frac{m_r}{m_s}$ Ordinate

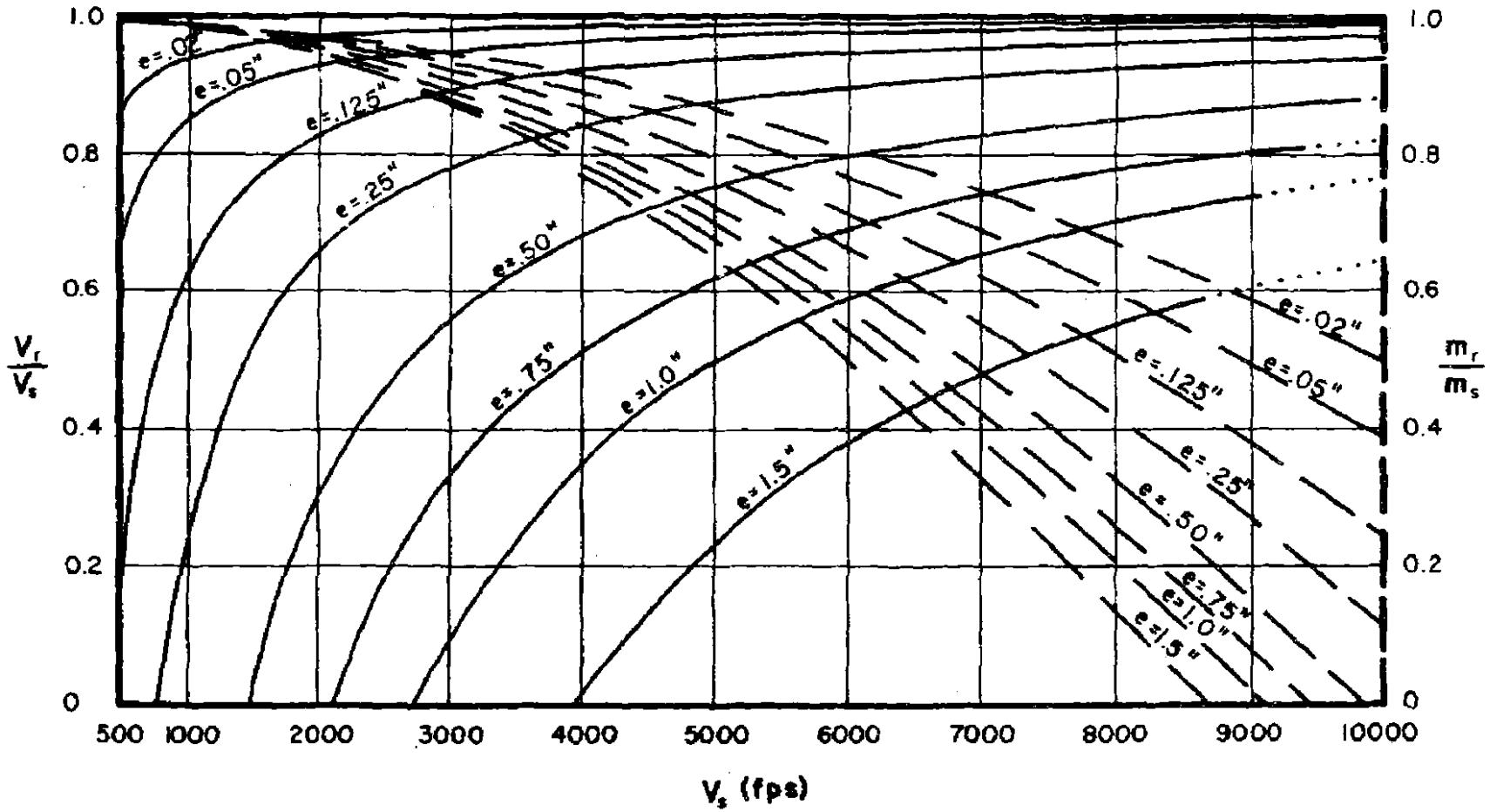

Fig. 49

$\frac{V_r}{V_s}$ and $\frac{m_r}{m_s}$ vs V_s for Selected Target Thicknesses

Target: Aluminum Alloy, 2024 T-3

Obliquity: 60°

Fragment Size: 300 grains

Dashed Thickness Contours Refer to $\frac{m_r}{m_s}$ Ordinate

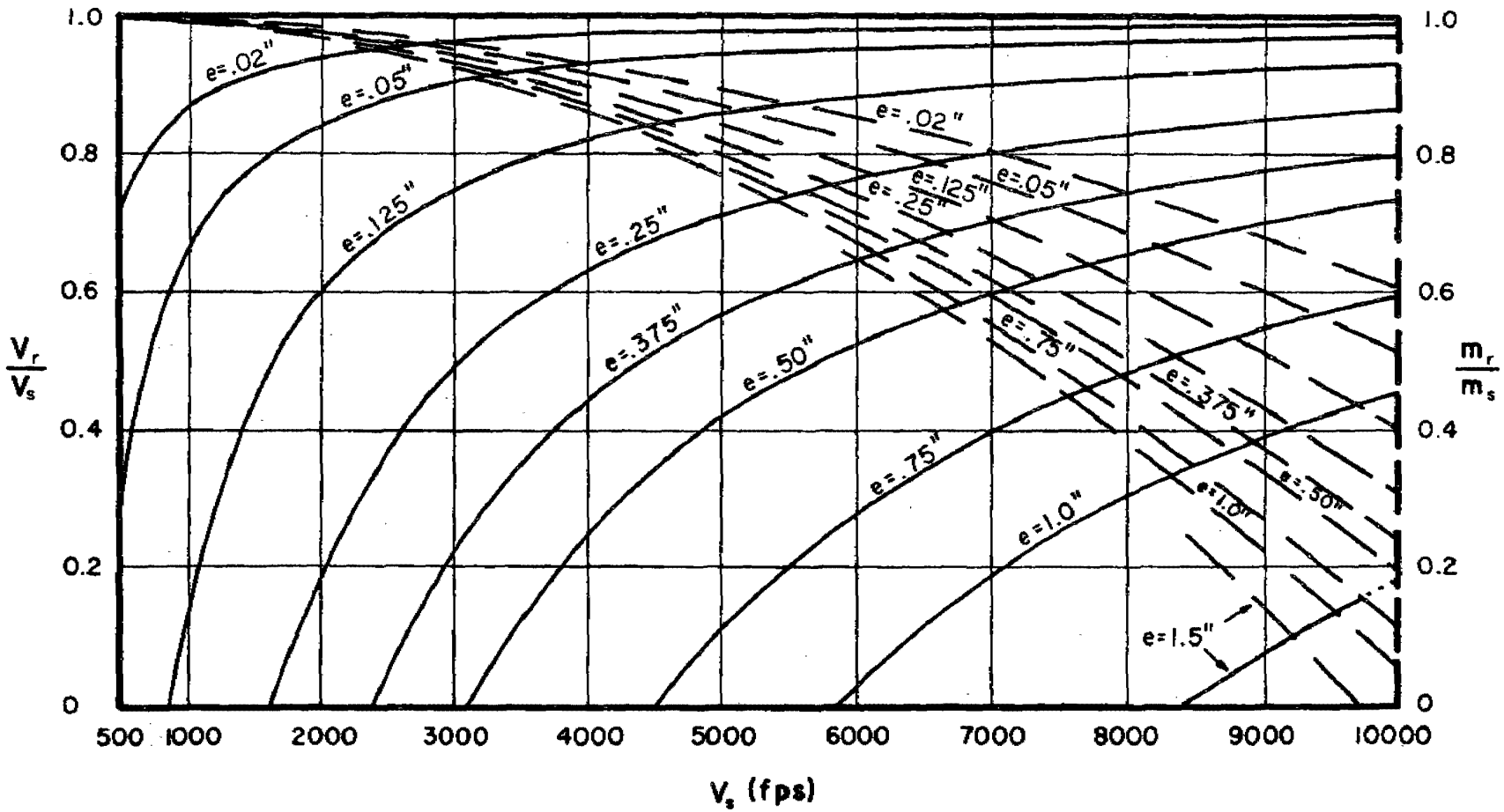

Fig. 50

$\frac{V_r}{V_s}$ and $\frac{m_r}{m_s}$ vs V_s for Selected Target Thicknesses

Target: Aluminum Alloy, 2024T-3

Obliquity: 70°

Fragment Size: 300 grains

Dashed Thickness Contours Refer to $\frac{m_r}{m_s}$ Ordinate

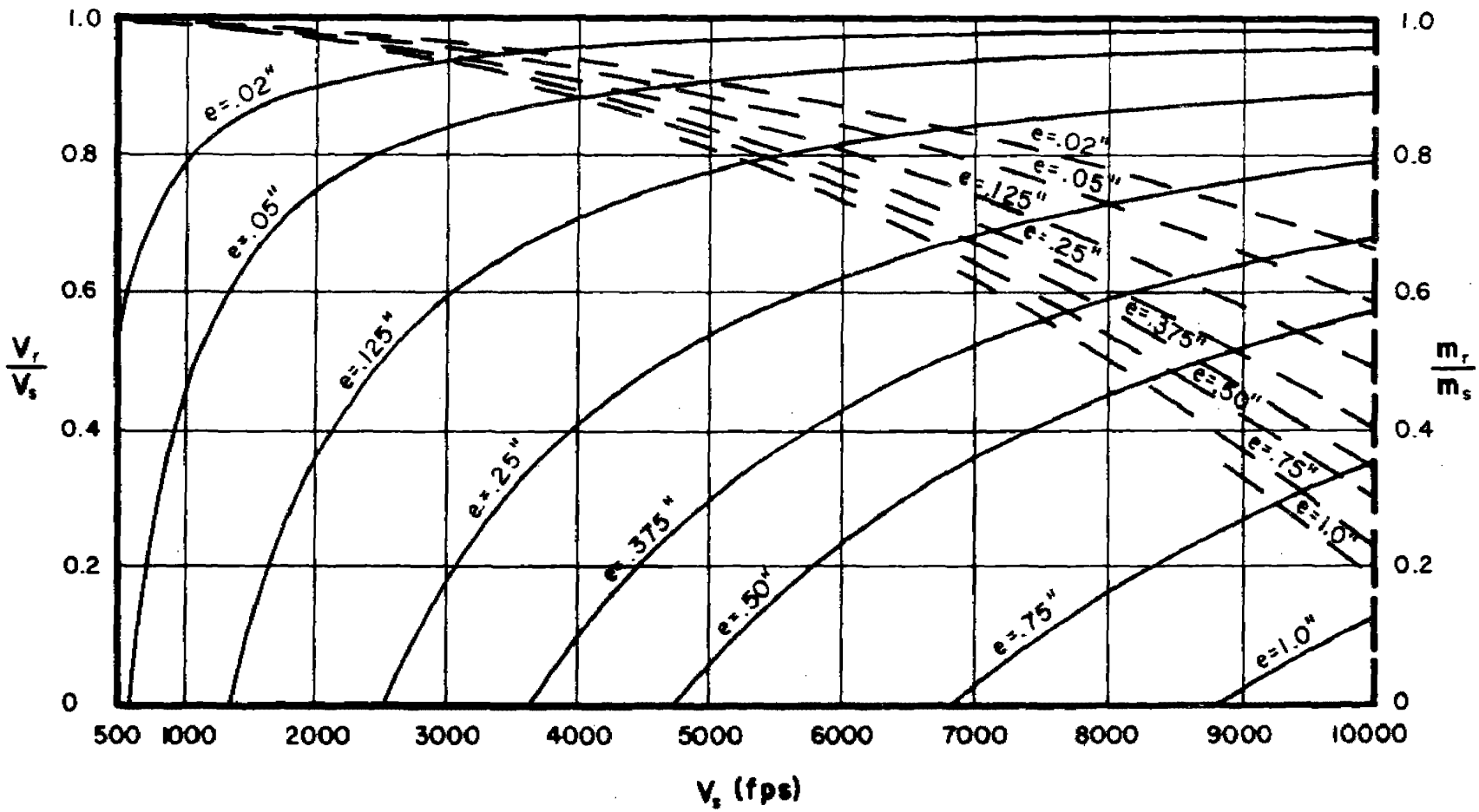

Fig. 51

$\frac{V_r}{V_s}$ and $\frac{m_r}{m_s}$ vs V_s for Selected Target Thicknesses

Target: Titanium Alloy

Obliquity: 0°

Fragment Size: 30 grains

Dashed Thickness Contours Refer to $\frac{m_r}{m_s}$ Ordinate

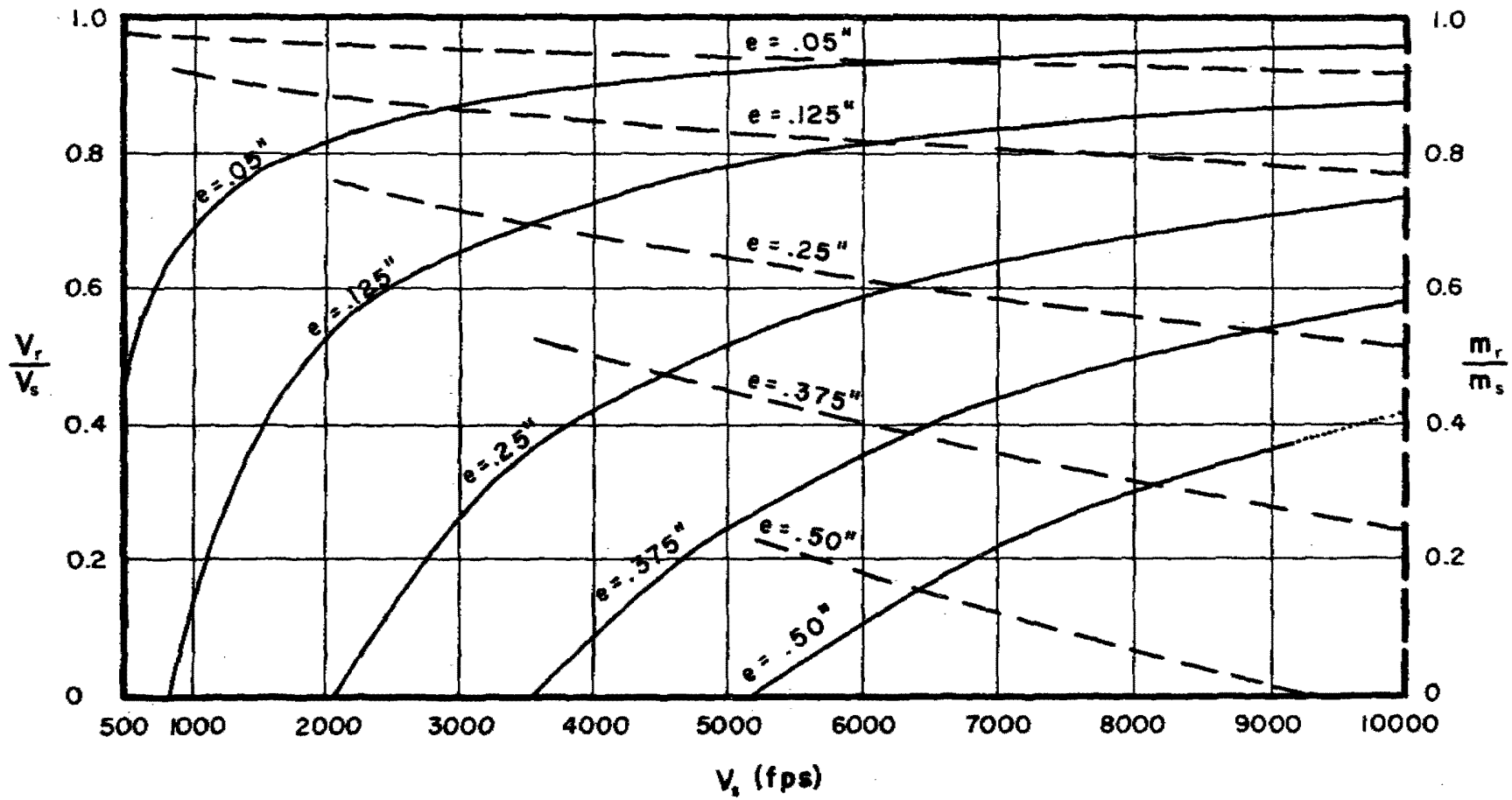

Fig. 52

$\frac{V_r}{V_s}$ and $\frac{m_r}{m_s}$ vs V_s for Selected Target Thicknesses

Target: Titanium Alloy

Obliquity: 60°

Fragment Size: 30 grains

Dashed Thickness Contours Refer to $\frac{m_r}{m_s}$ Ordinate

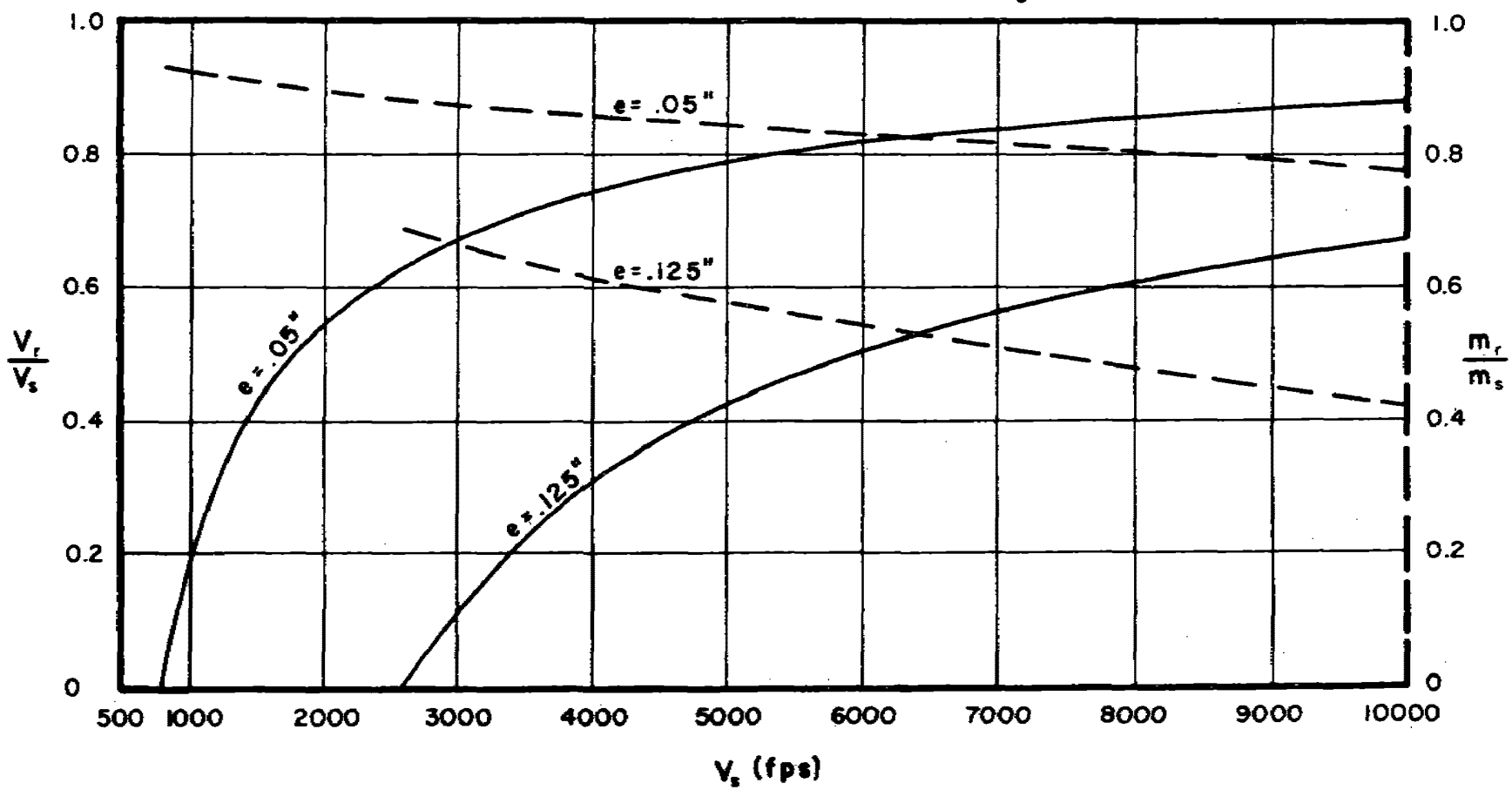

Fig. 53

$\frac{V_r}{V_s}$ and $\frac{m_r}{m_s}$ vs V_s for Selected Target Thicknesses

Target: Titanium Alloy

Obliquity: 70°

Fragment Size: 30 grains

Dashed Thickness Contours Refer to $\frac{m_r}{m_s}$ Ordinate

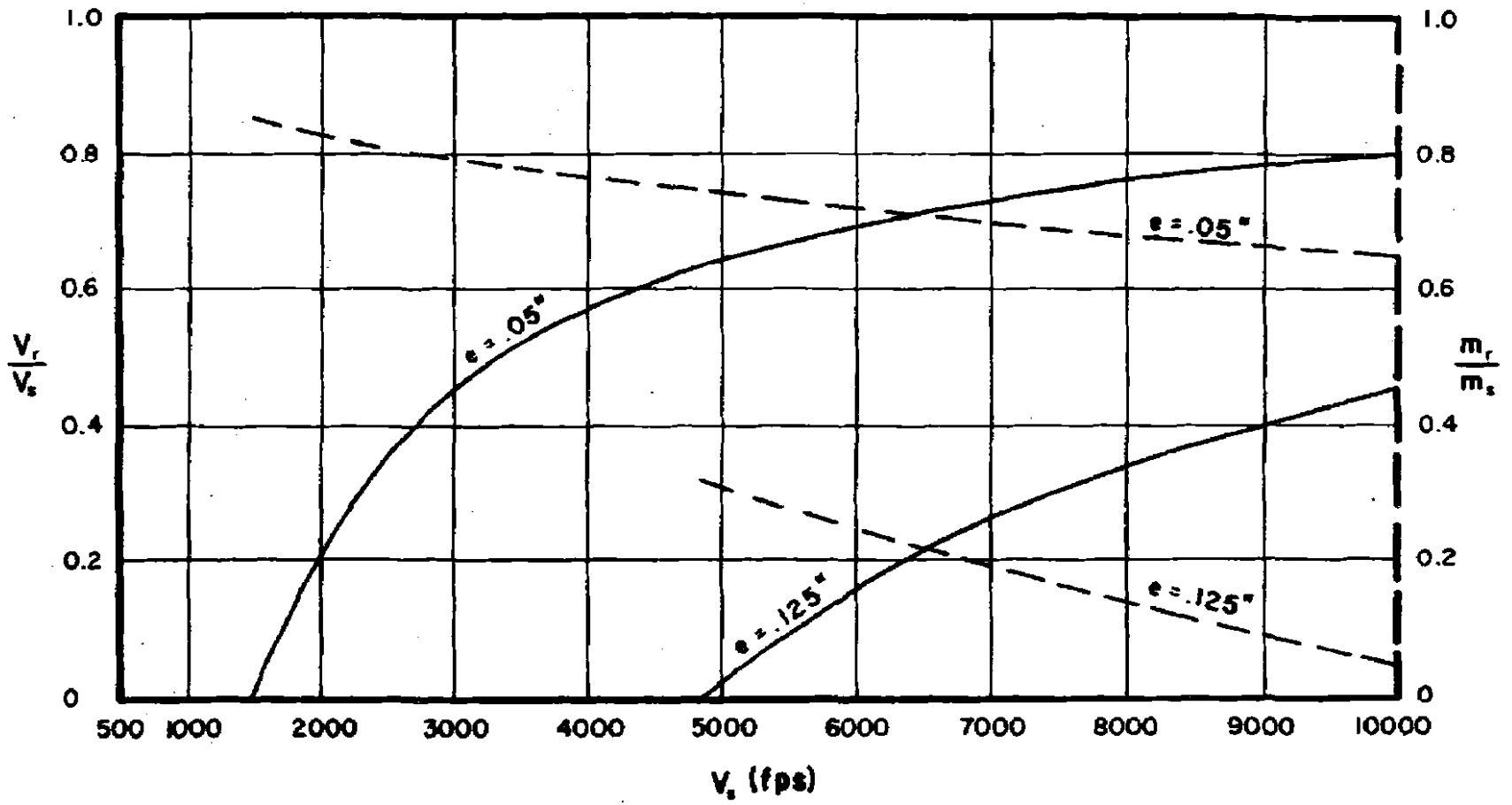

Fig. 54

$\frac{V_r}{V_s}$ and $\frac{m_r}{m_s}$ vs V_s for Selected Target Thicknesses

Target: Titanium Alloy

Obliquity: 0°

Fragment Size: 100 grains

Dashed Thickness Contours Refer to $\frac{m_r}{m_s}$ Ordinate

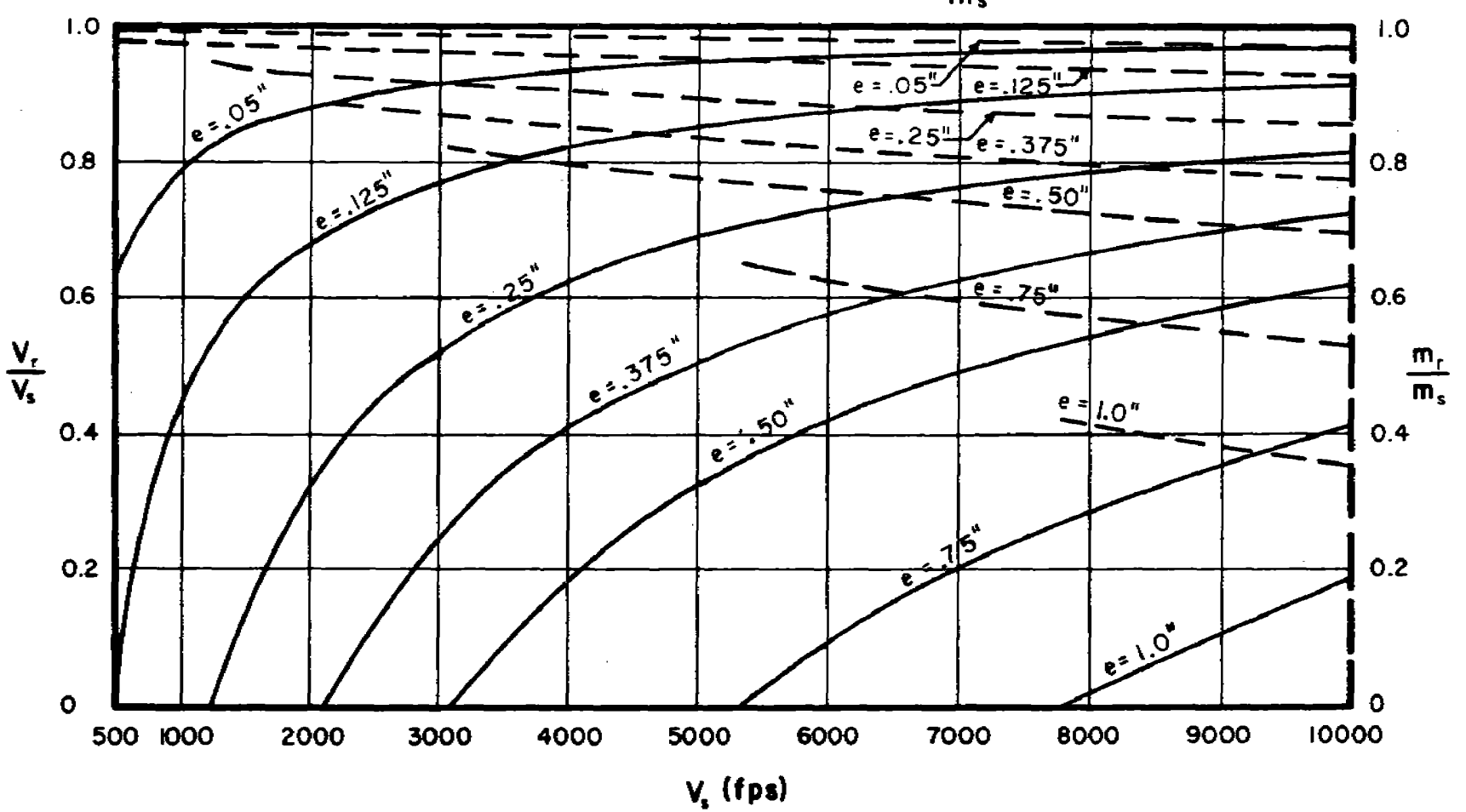

Fig. 55

$\frac{V_r}{V_s}$ and $\frac{m_r}{m_s}$ vs V_s for Selected Target Thicknesses

Target: Titanium Alloy

Obliquity: 60°

Fragment Size: 100 grains

Dashed Thickness Contours Refer to $\frac{m_r}{m_s}$ Ordinate

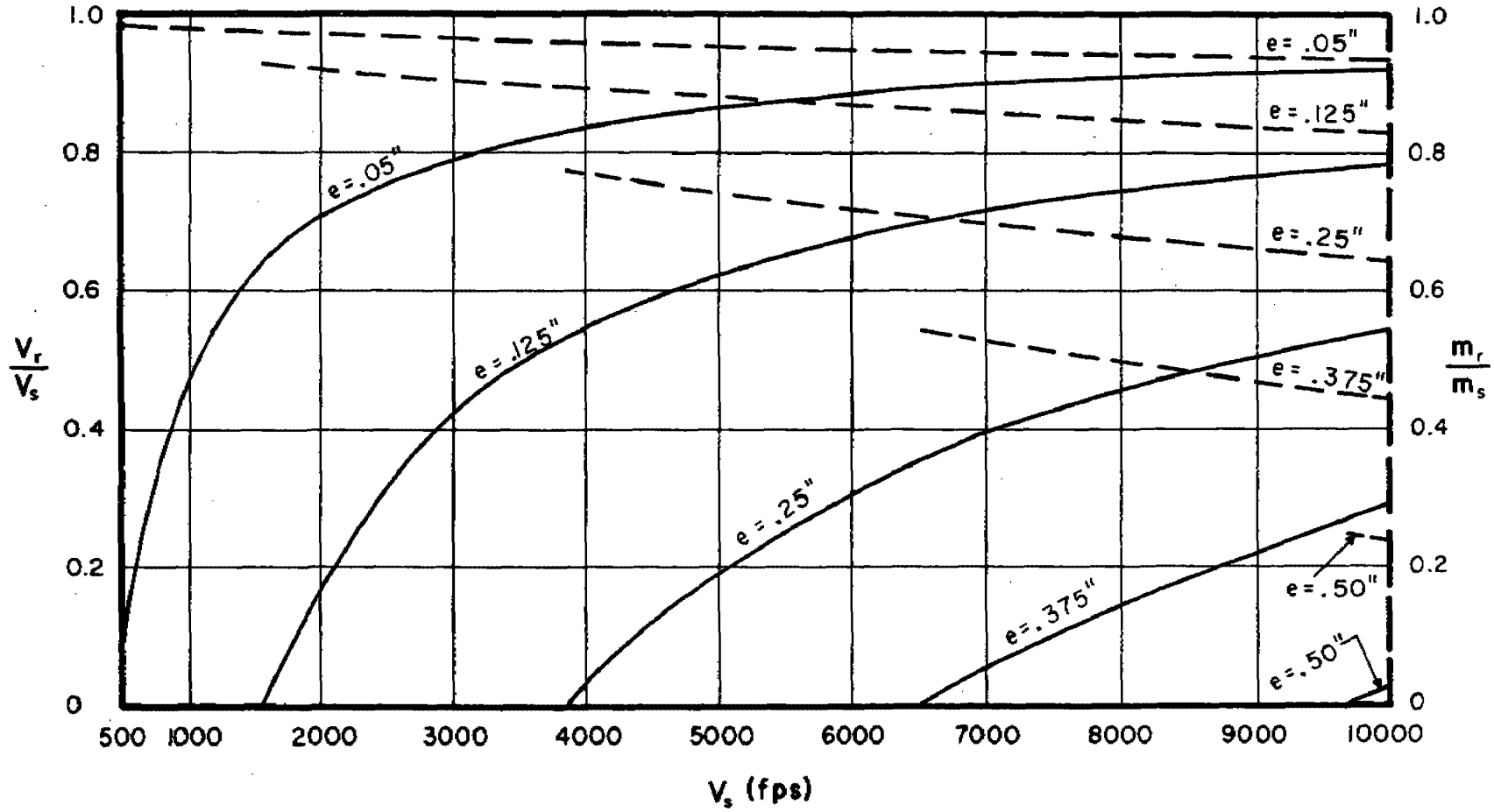

Fig. 56

$\frac{V_r}{V_s}$ and $\frac{m_r}{m_s}$ vs V_s for Selected Target Thicknesses

Target: Titanium Alloy

Obliquity: 70°

Fragment Size: 100 grains

Dashed Thickness Contours Refer to $\frac{m_r}{m_s}$ Ordinate

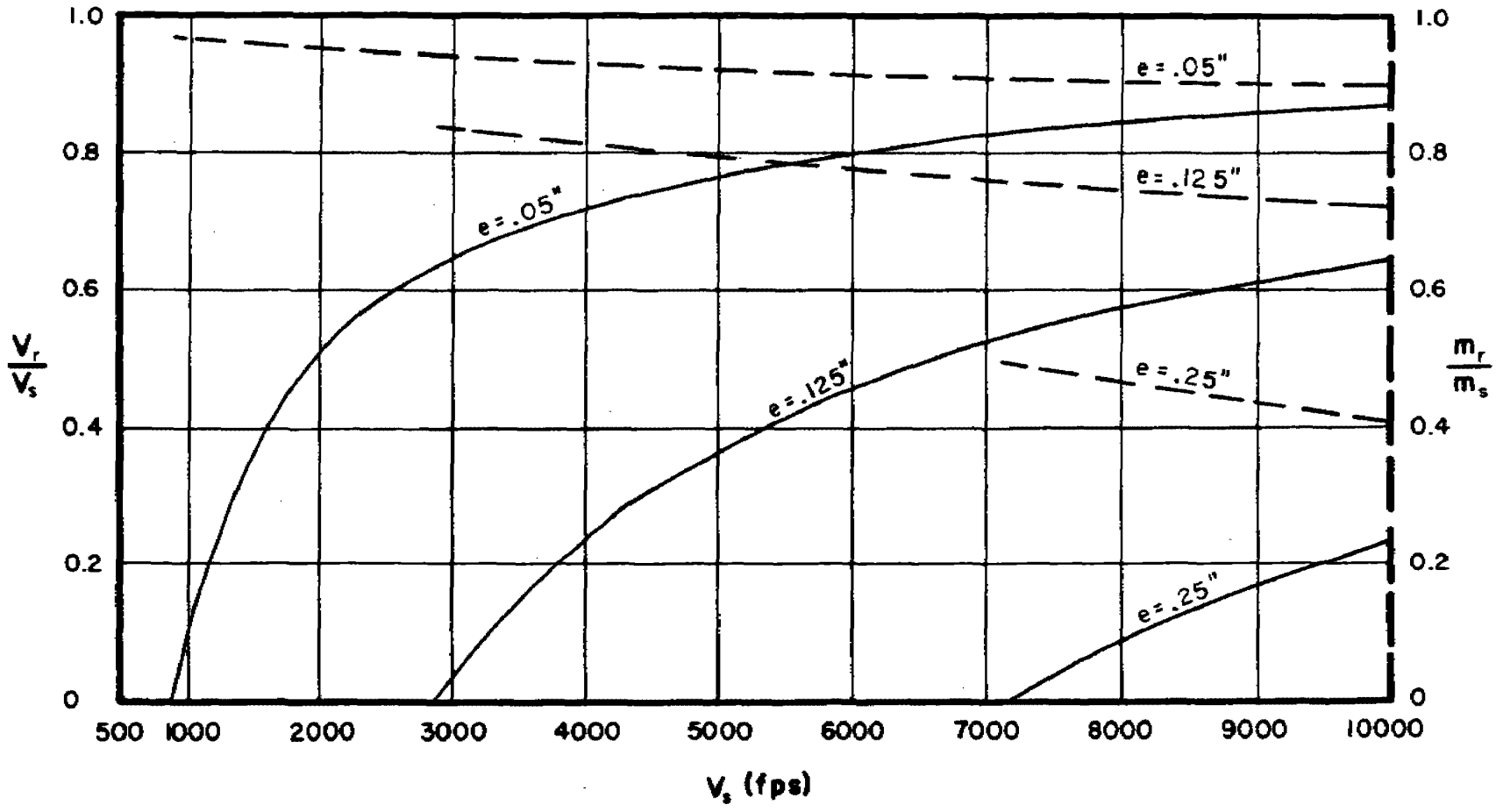

Fig. 57

$\frac{V_r}{V_s}$ and $\frac{m_r}{m_s}$ vs V_s for Selected Target Thicknesses

Target: Titanium Alloy

Obliquity: 0°

Fragment Size: 300 grains

Dashed Thickness Contours Refer to $\frac{m_r}{m_s}$ Ordinate

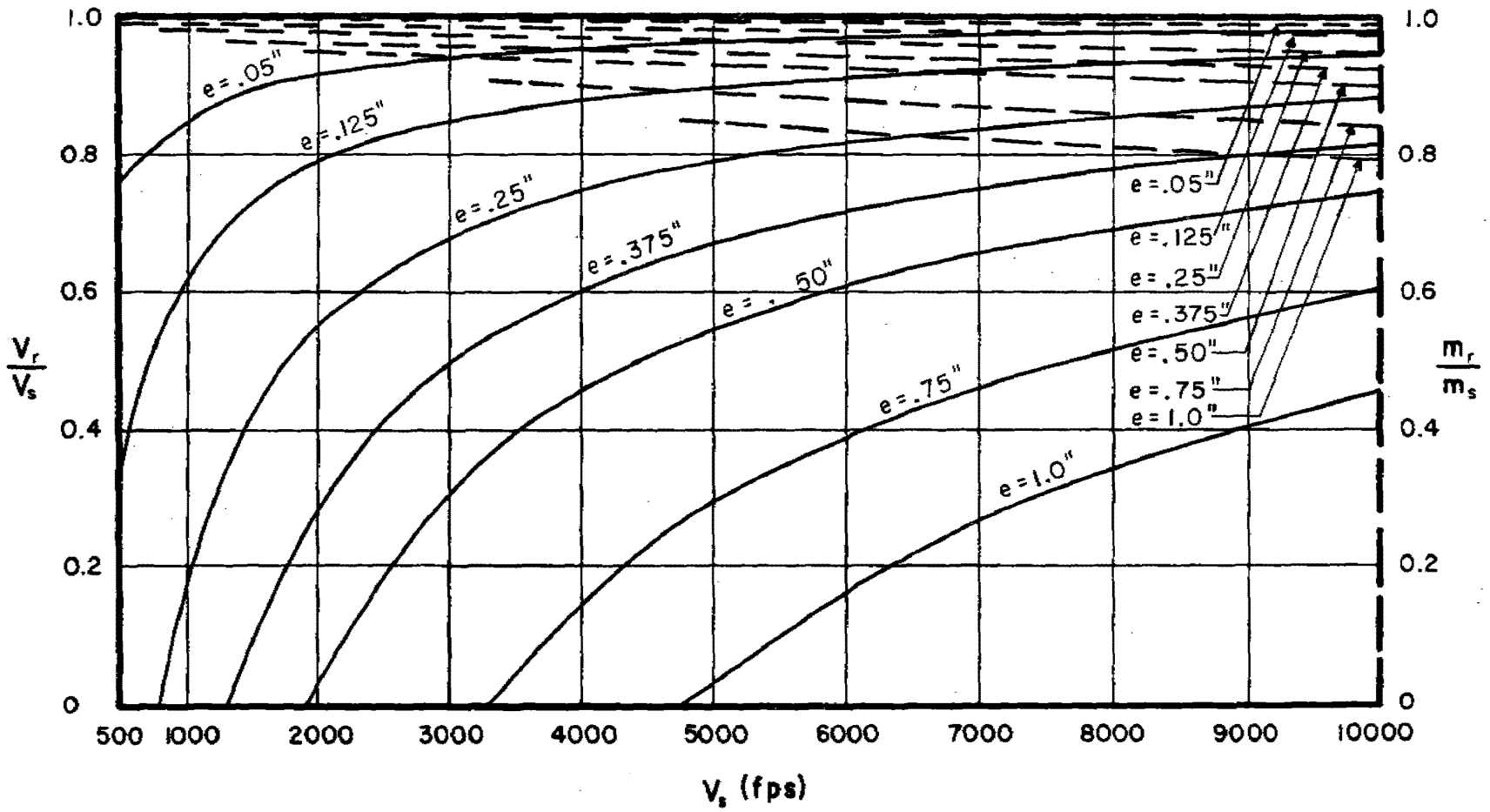

Fig. 58

$\frac{V_r}{V_s}$ and $\frac{m_r}{m_s}$ vs V_s for Selected Target Thicknesses

Target: Titanium Alloy

Obliquity: 60°

Fragment Size: 300 grains

Dashed Thickness Contours Refer to $\frac{m_r}{m_s}$ Ordinate

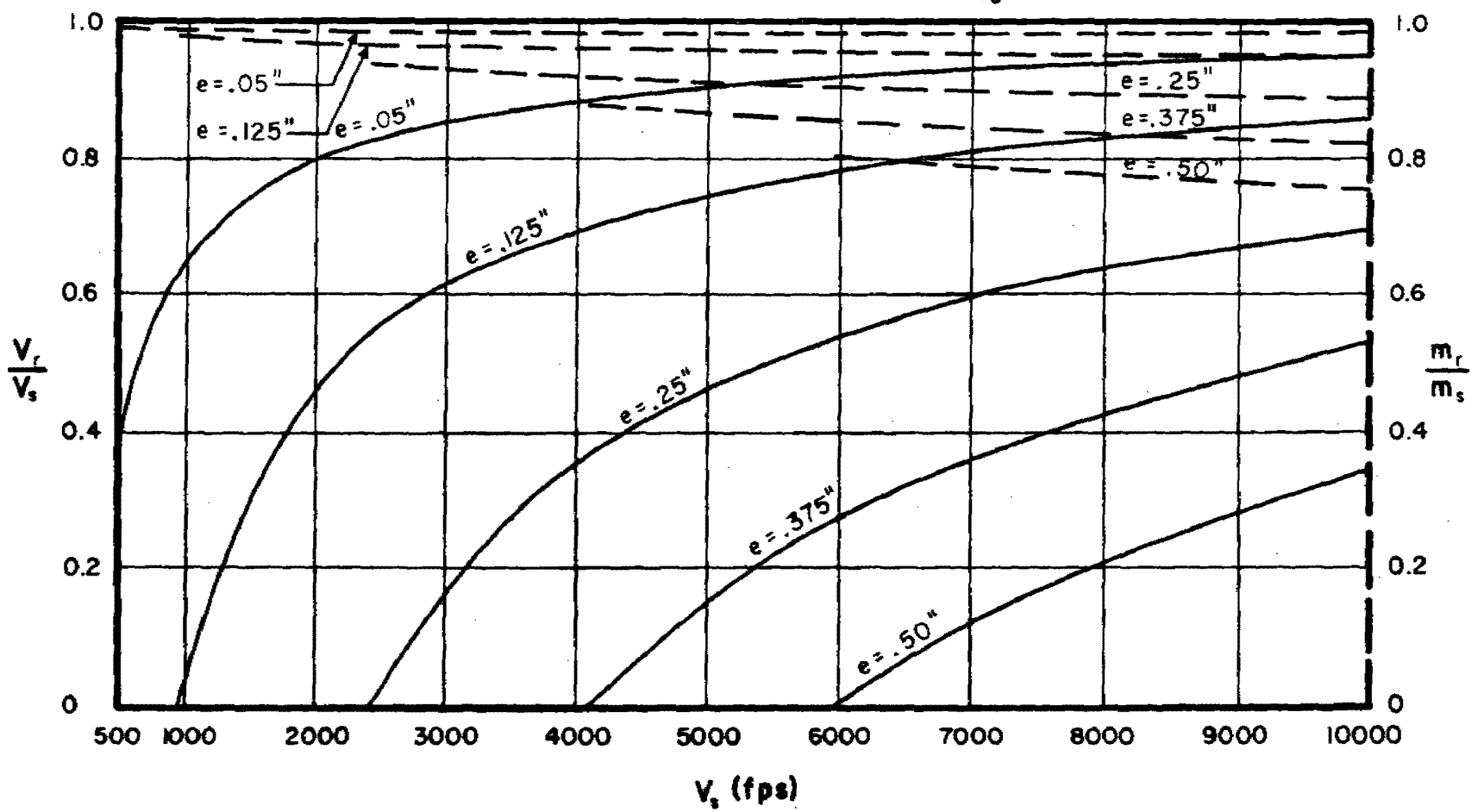

Fig. 59

$\frac{V_r}{V_s}$ and $\frac{m_r}{m_s}$ vs V_s for Selected Target Thicknesses

Target: Titanium Alloy

Obliquity: 70°

Fragment Size: 300 grains

Dashed Thickness Contours Refer to $\frac{m_r}{m_s}$ Ordinate

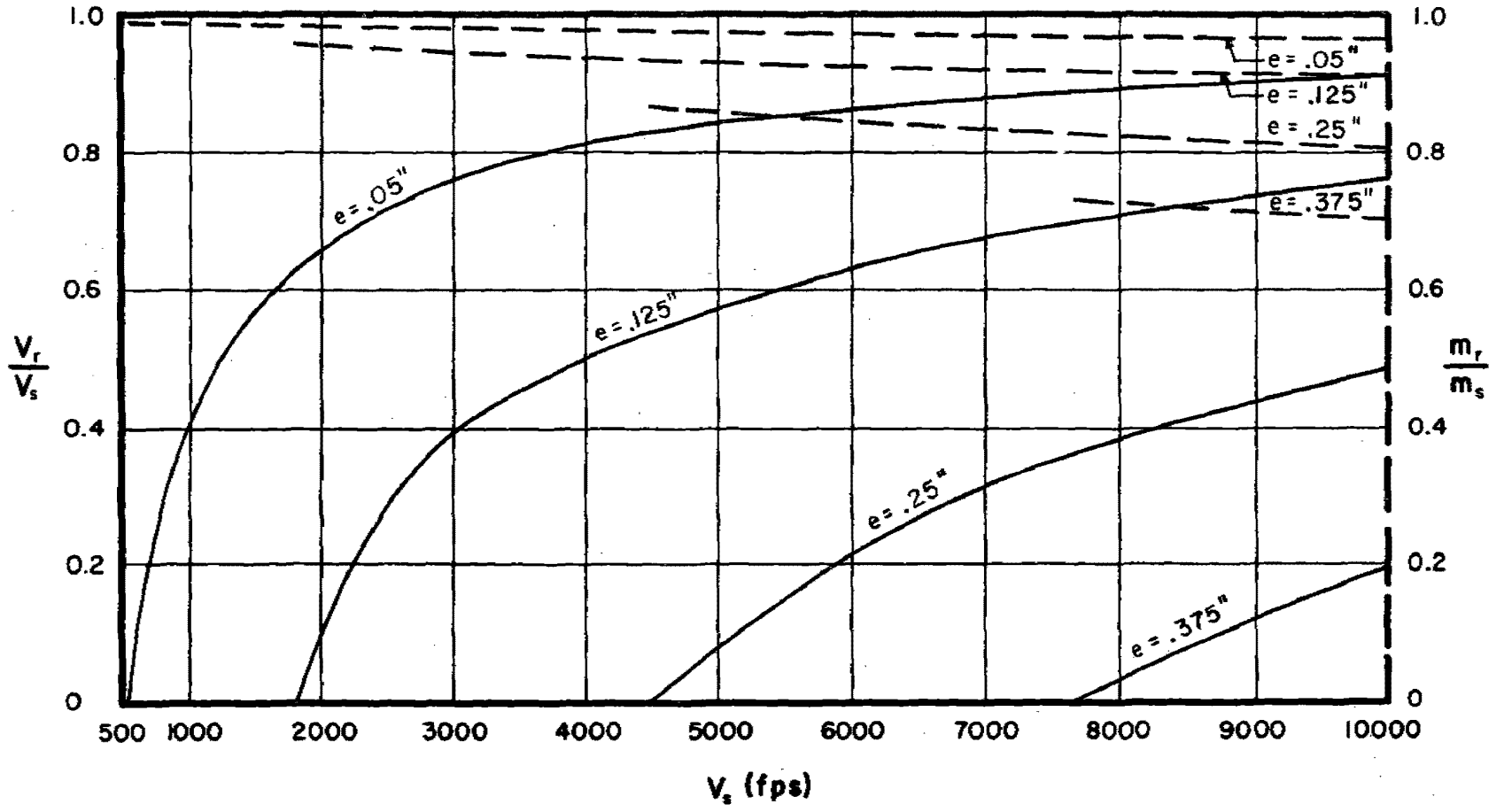

Fig. 60

$\frac{V_r}{V_s}$ and $\frac{m_r}{m_s}$ vs V_s for Selected Target Thicknesses

Target: Cast Iron

Obliquity: 0°

Fragment Size: 30 grains

Dashed Thickness Contours Refer to $\frac{m_r}{m_s}$ Ordinate

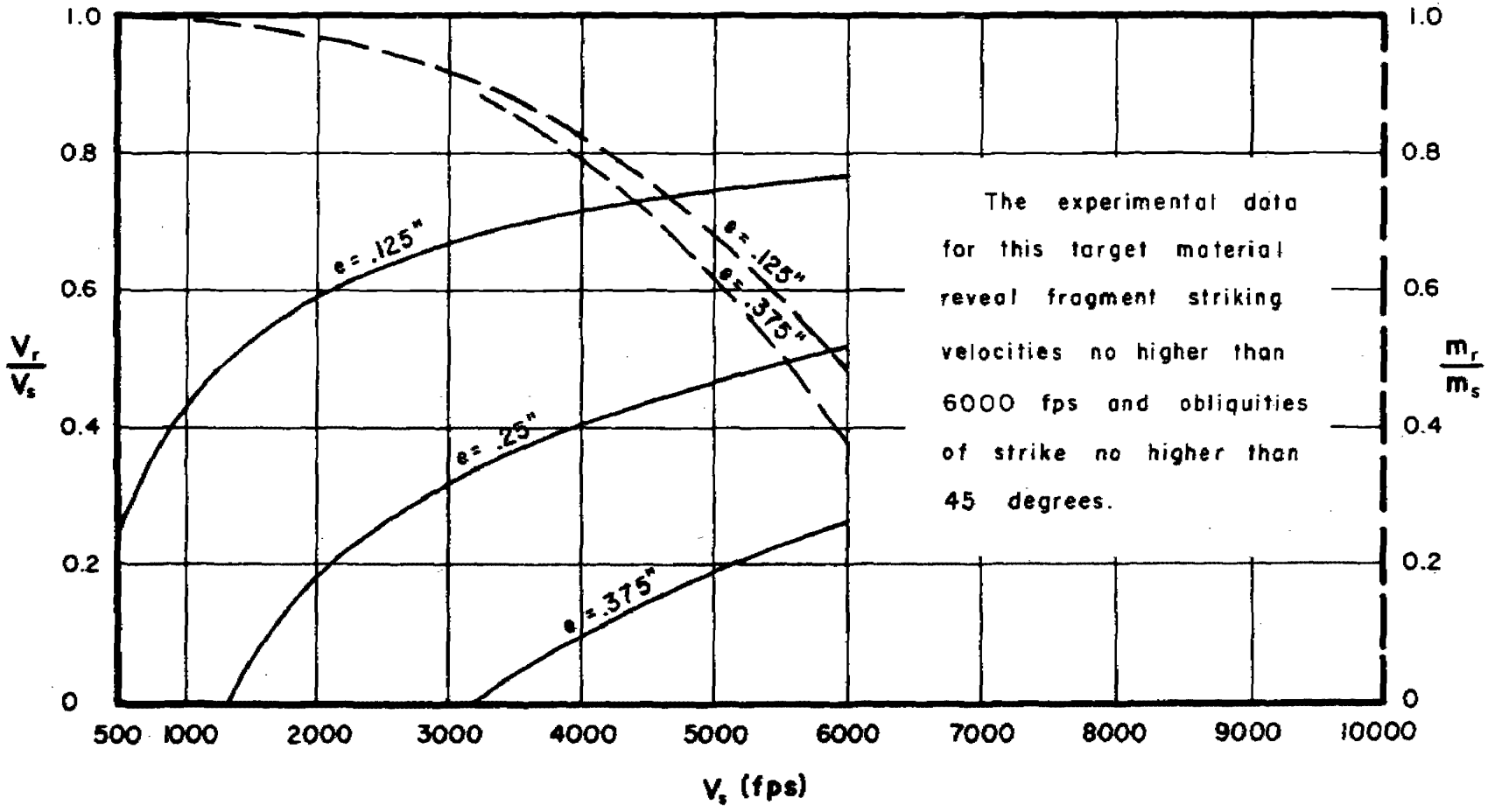

Fig. 61

[redacted]

$\frac{V_r}{V_s}$ and $\frac{m_r}{m_s}$ vs V_s for Selected Target Thicknesses

Target: Cast Iron

Obliquity: 60°

Fragment Size: 30 grains

Dashed Thickness Contours Refer to $\frac{m_r}{m_s}$ Ordinate

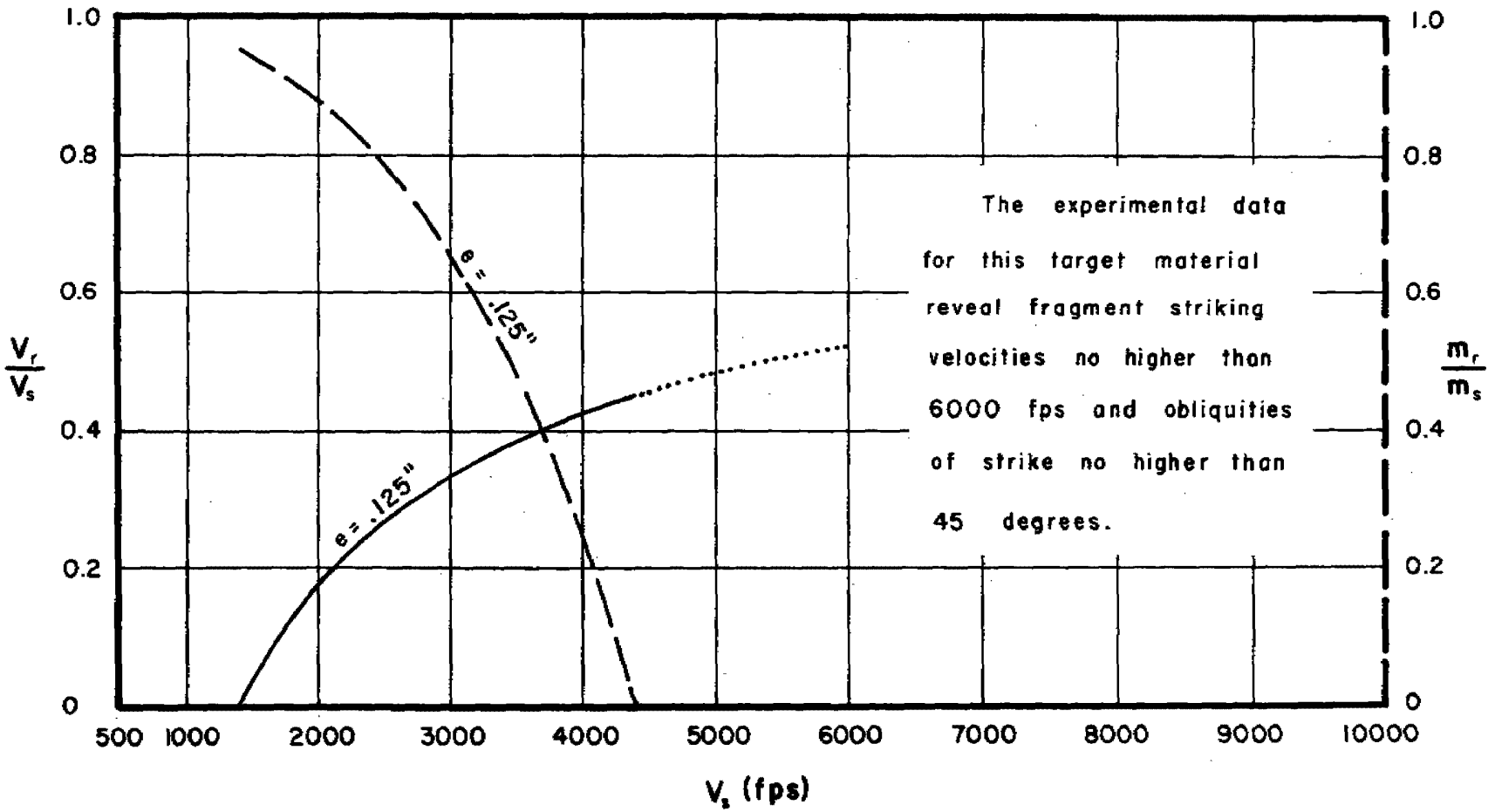

Fig. 62

[redacted]

$\frac{V_r}{V_s}$ and $\frac{m_r}{m_s}$ vs V_s for Selected Target Thicknesses

Target: Cast Iron

Obliquity: 0°

Fragment Size: 100 grains

Dashed Thickness Contours Refer to $\frac{m_r}{m_s}$ Ordinate

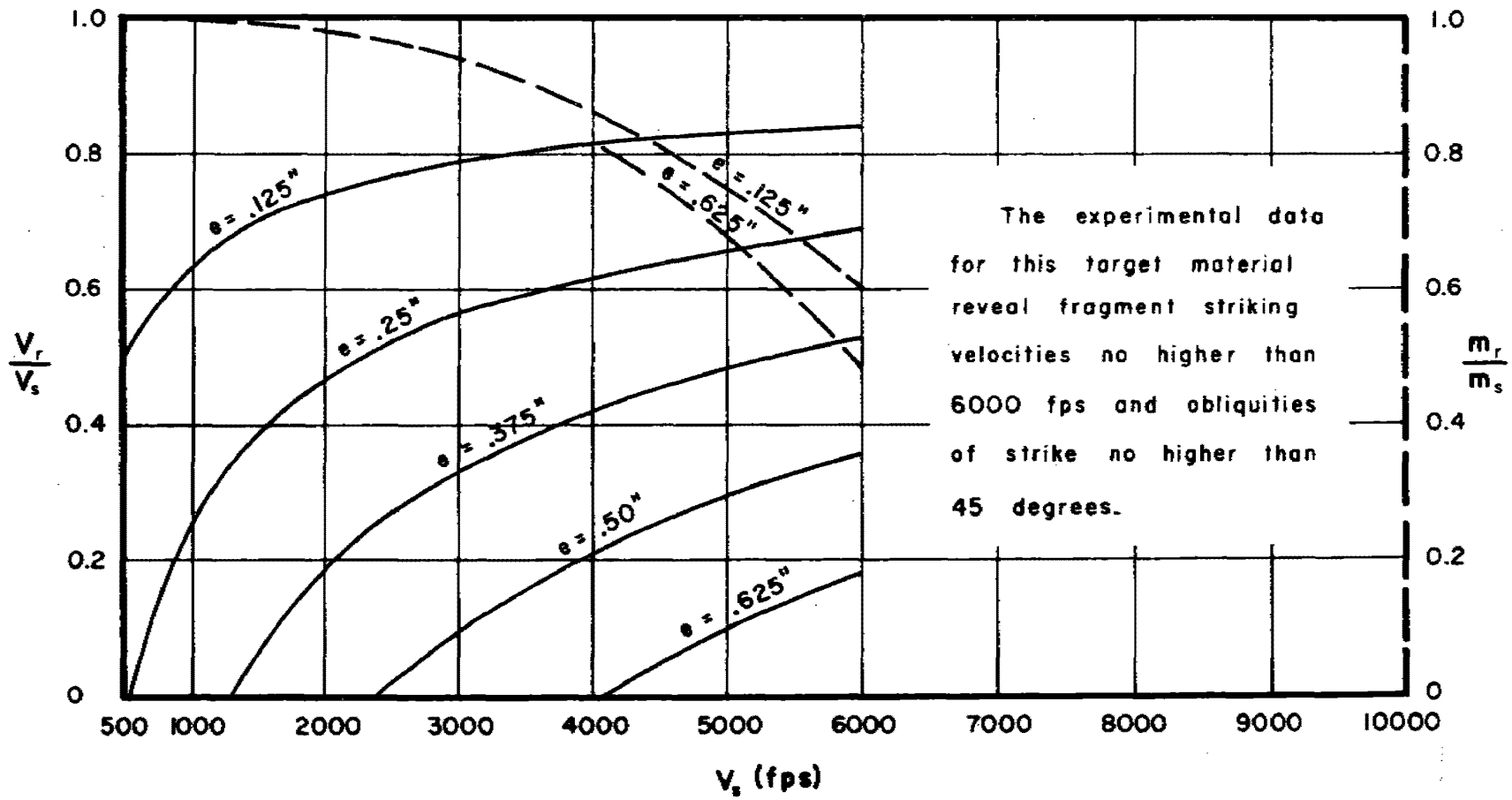

Fig. 63

$\frac{V_r}{V_s}$ and $\frac{m_r}{m_s}$ vs V_s for Selected Target Thicknesses

Target: Cast Iron

Obliquity: 60°

Fragment Size: 100 grains

Dashed Thickness Contours Refer to $\frac{m_r}{m_s}$ Ordinate

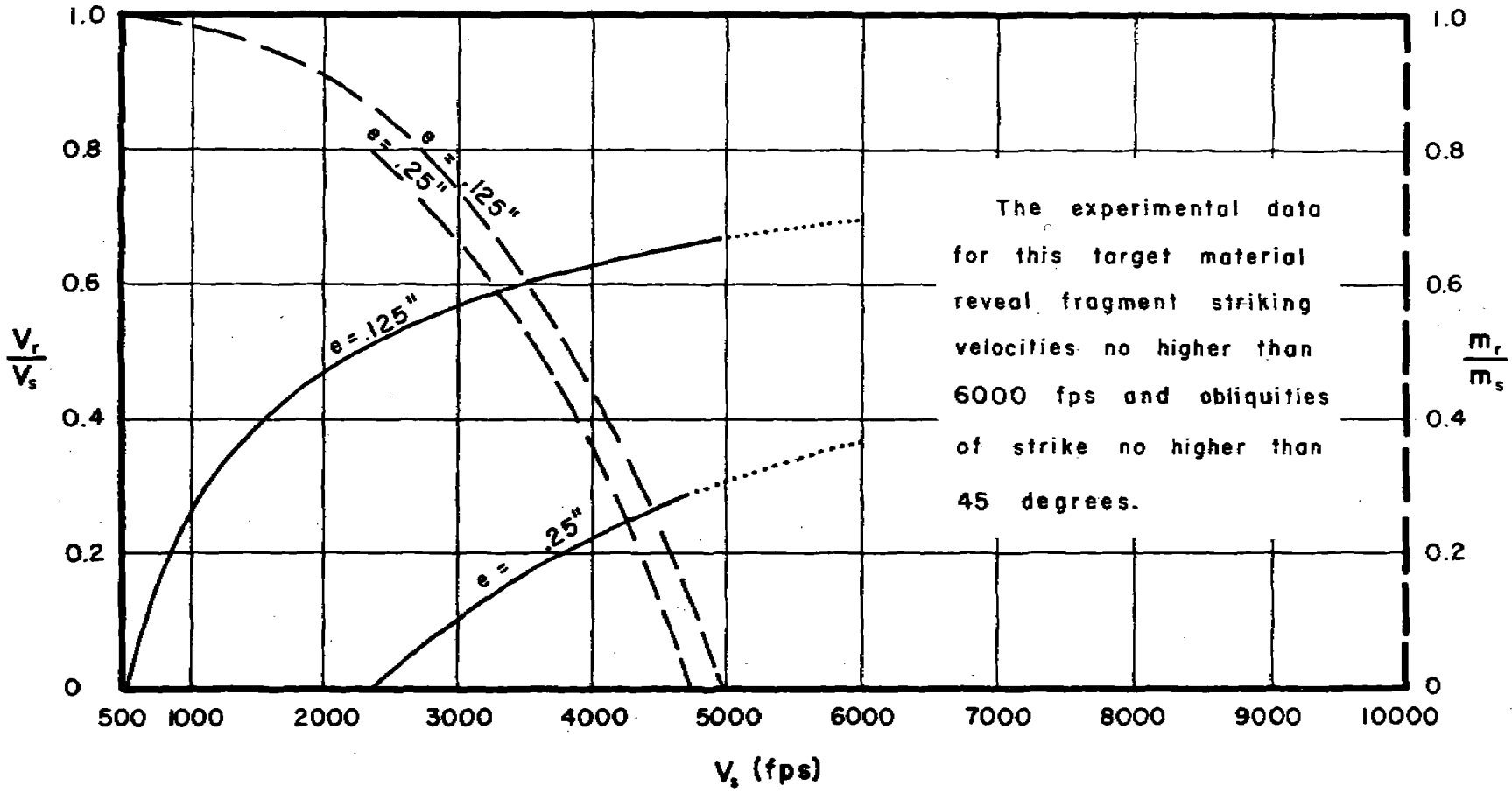

Fig. 64

$\frac{V_r}{V_s}$ and $\frac{m_r}{m_s}$ vs V_s for Selected Target Thicknesses

Target: Cast Iron

Obliquity: 0°

Fragment Size: 300 grains

Dashed Thickness Contours Refer to $\frac{m_r}{m_s}$ Ordinate

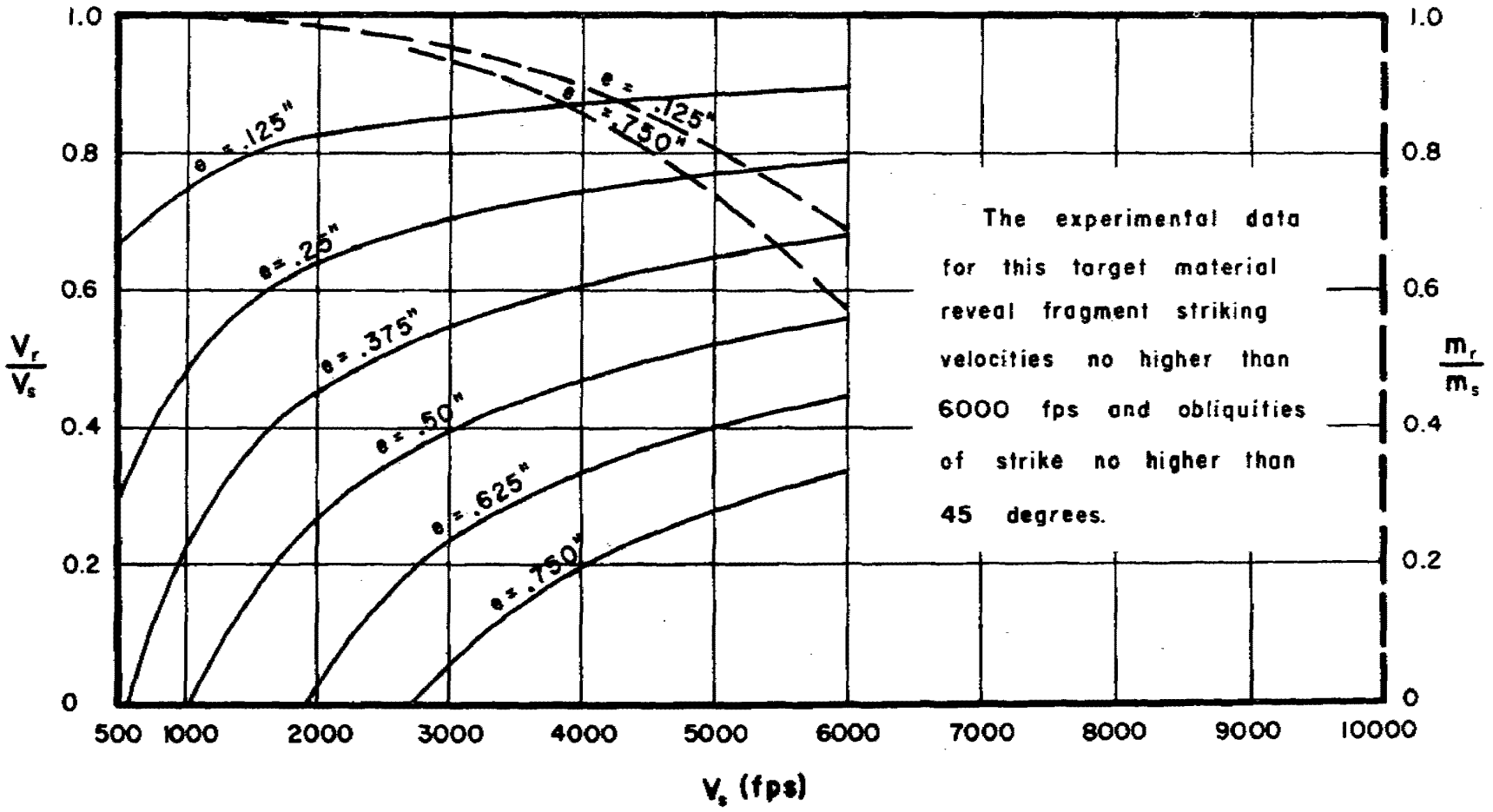

Fig. 65

$\frac{V_r}{V_s}$ and $\frac{m_r}{m_s}$ vs V_s for Selected Target Thicknesses

Target: Face-Hardened Steel

Obliquity: 60°

Fragment Size: 30 grains

Dashed Thickness Contours Refer to $\frac{m_r}{m_s}$ Ordinate

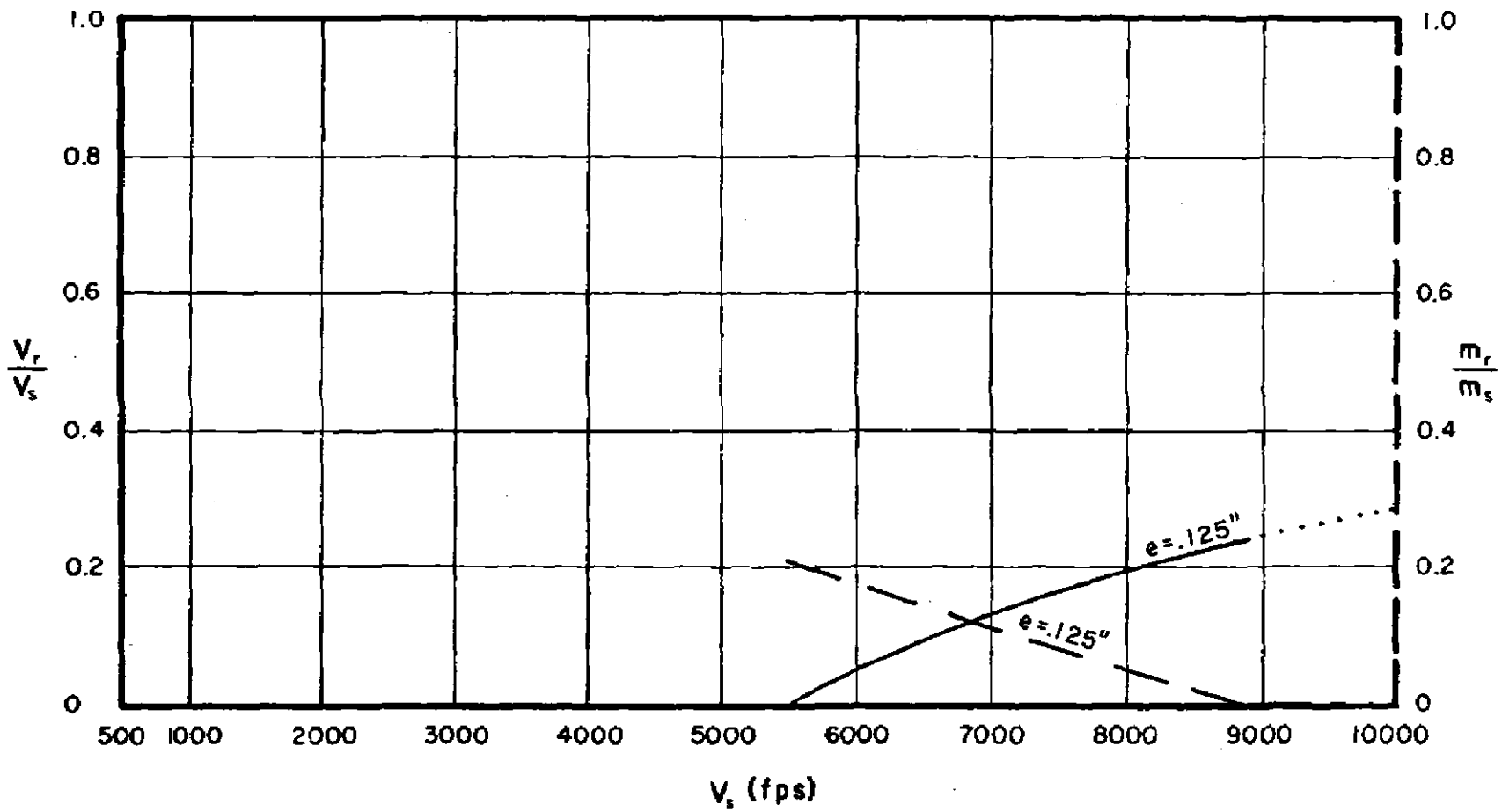

Fig. 68

$\frac{V_r}{V_s}$ and $\frac{m_r}{m_s}$ vs V_s for Selected Target Thicknesses

Target: Face-Hardened Steel

Obliquity: 70°

Fragment Size: 30 grains

Dashed Thickness Contours Refer to $\frac{m_r}{m_s}$ Ordinate

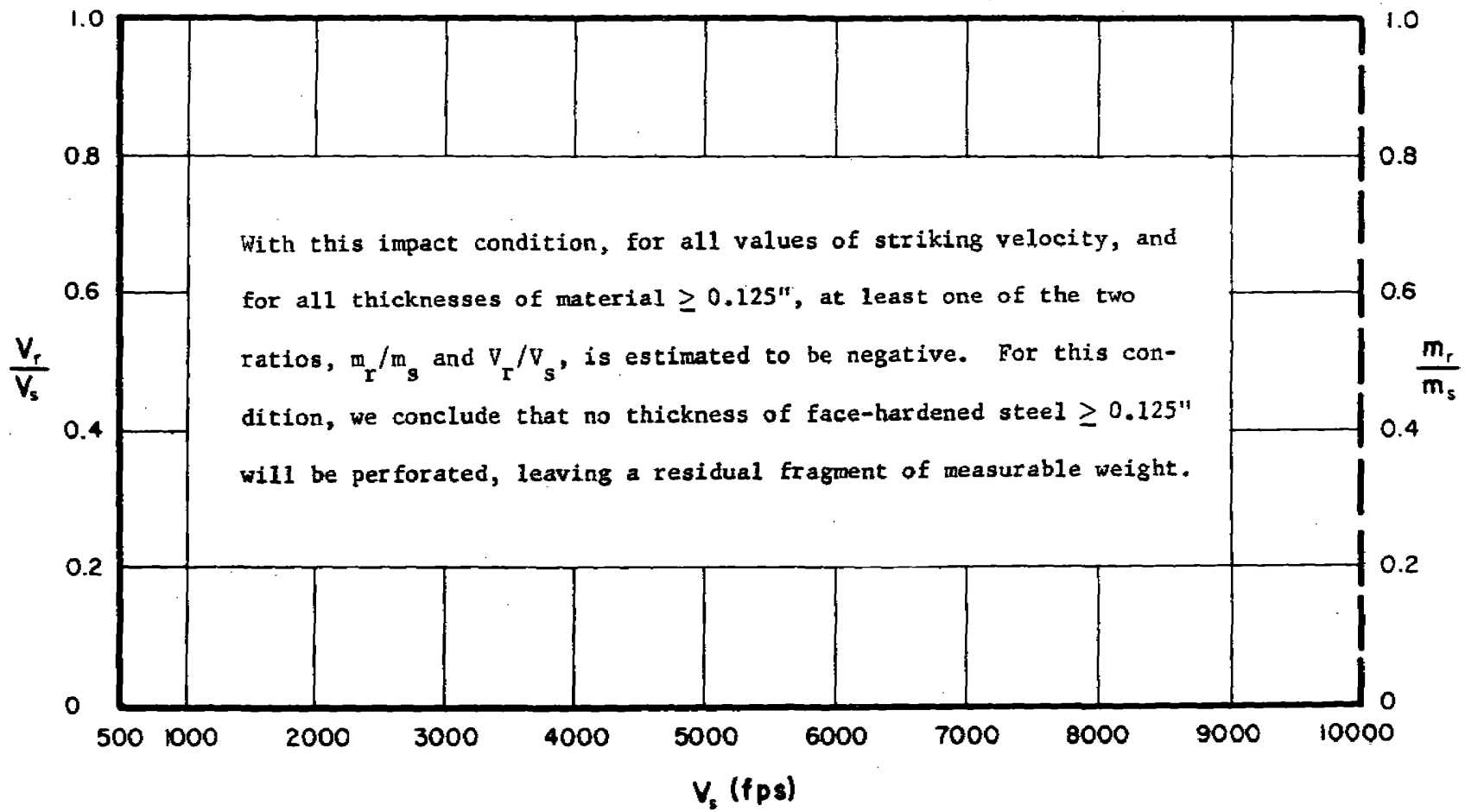

Fig. 69

$\frac{V_r}{V_s}$ and $\frac{m_r}{m_s}$ vs V_s for Selected Target Thicknesses

Target: Face-Hardened Steel

Obliquity: 0°

Fragment Size: 100 grains

Dashed Thickness Contours Refer to $\frac{m_r}{m_s}$ Ordinate

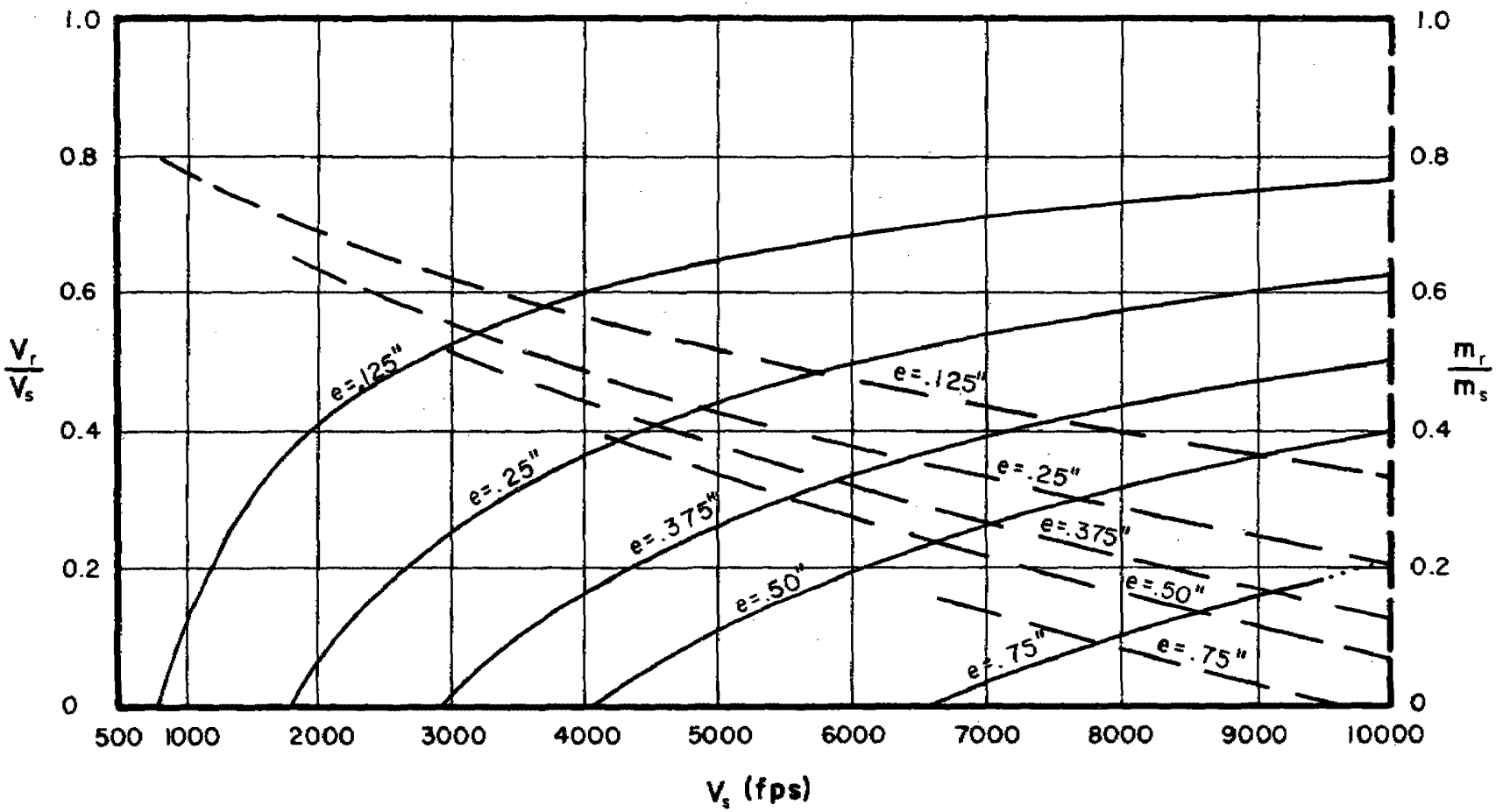

Fig. 70

$\frac{V_r}{V_s}$ and $\frac{m_r}{m_s}$ vs V_s for Selected Target Thicknesses

Target: Face-Hardened Steel

Obliquity: 60°

Fragment Size: 100 grains

Dashed Thickness Contours Refer to $\frac{m_r}{m_s}$ Ordinate

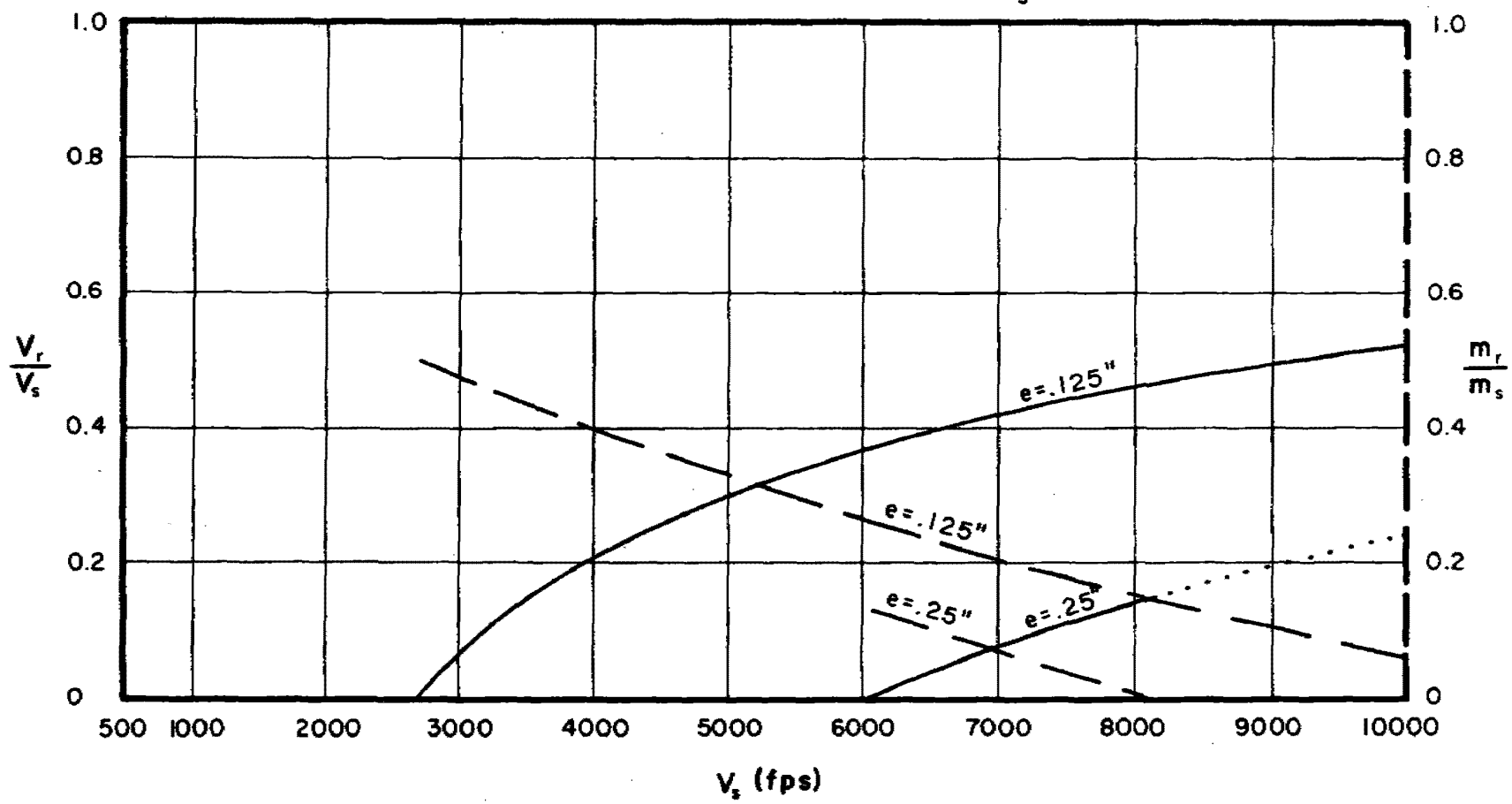

Fig. 71

$\frac{V_r}{V_s}$ and $\frac{m_r}{m_s}$ vs V_s for Selected Target Thicknesses

Target: Face-Hardened Steel

Obliquity: 70°

Fragment Size: 100 grains

Dashed Thickness Contours Refer to $\frac{m_r}{m_s}$ Ordinate

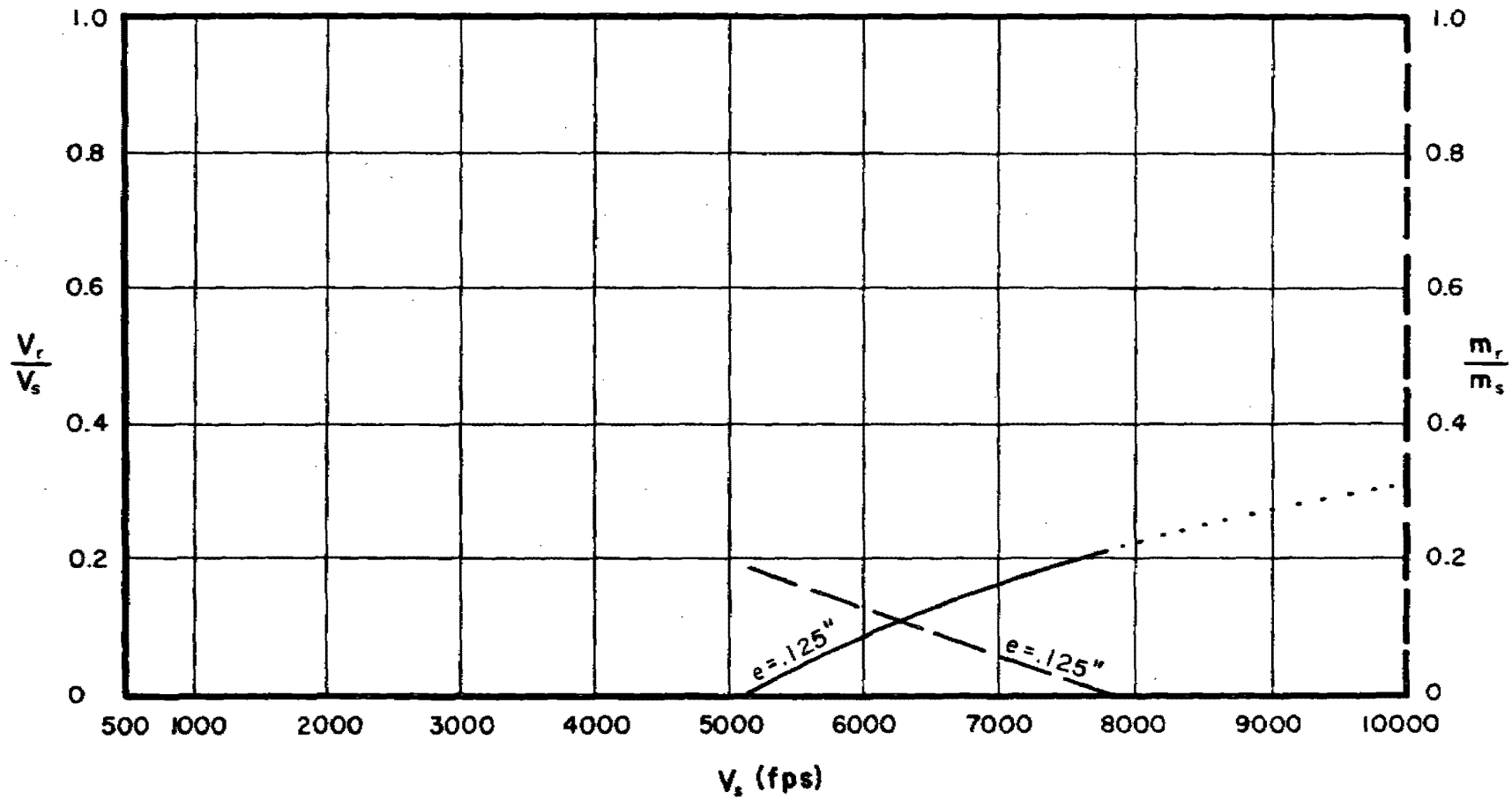

Fig. 72

$\frac{V_r}{V_s}$ and $\frac{m_r}{m_s}$ vs V_s for Selected Target Thicknesses

Target: Face-Hardened Steel

Obliquity: 0°

Fragment Size: 300 grains

Dashed Thickness Contours Refer to $\frac{m_r}{m_s}$ Ordinate

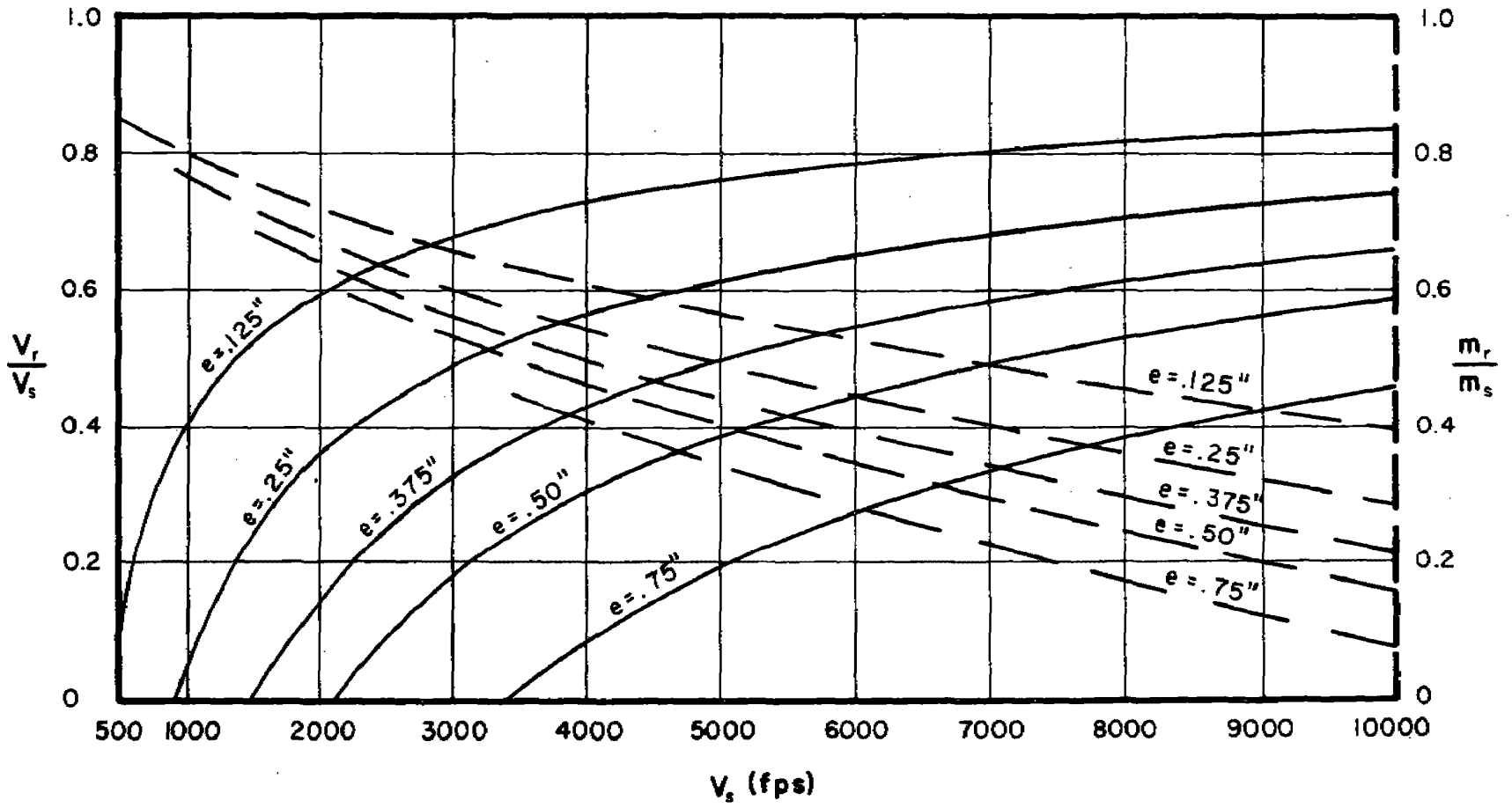

Fig. 73

$\frac{V_r}{V_s}$ and $\frac{m_r}{m_s}$ vs V_s for Selected Target Thicknesses

Target: Face-Hardened Steel

Obliquity: 60°

Fragment Size: 300 grains

Dashed Thickness Contours Refer to $\frac{m_r}{m_s}$ Ordinate

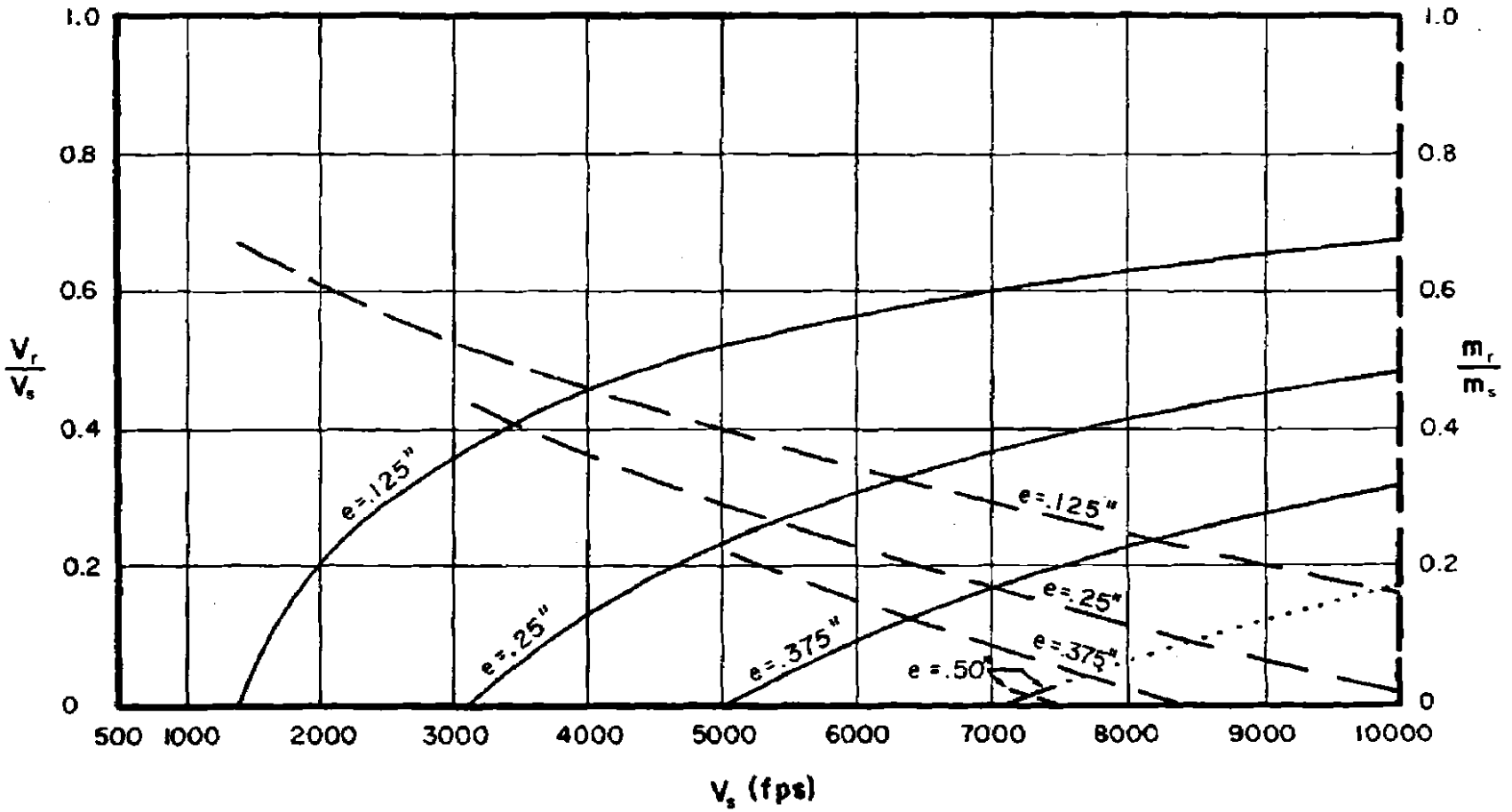

Fig. 74

$\frac{V_r}{V_s}$ and $\frac{m_r}{m_s}$ vs V_s for Selected Target Thicknesses

Target: Face-Hardened Steel

Obliquity: 70°

Fragment Size: 300 grains

Dashed Thickness Contours Refer to $\frac{m_r}{m_s}$ Ordinate

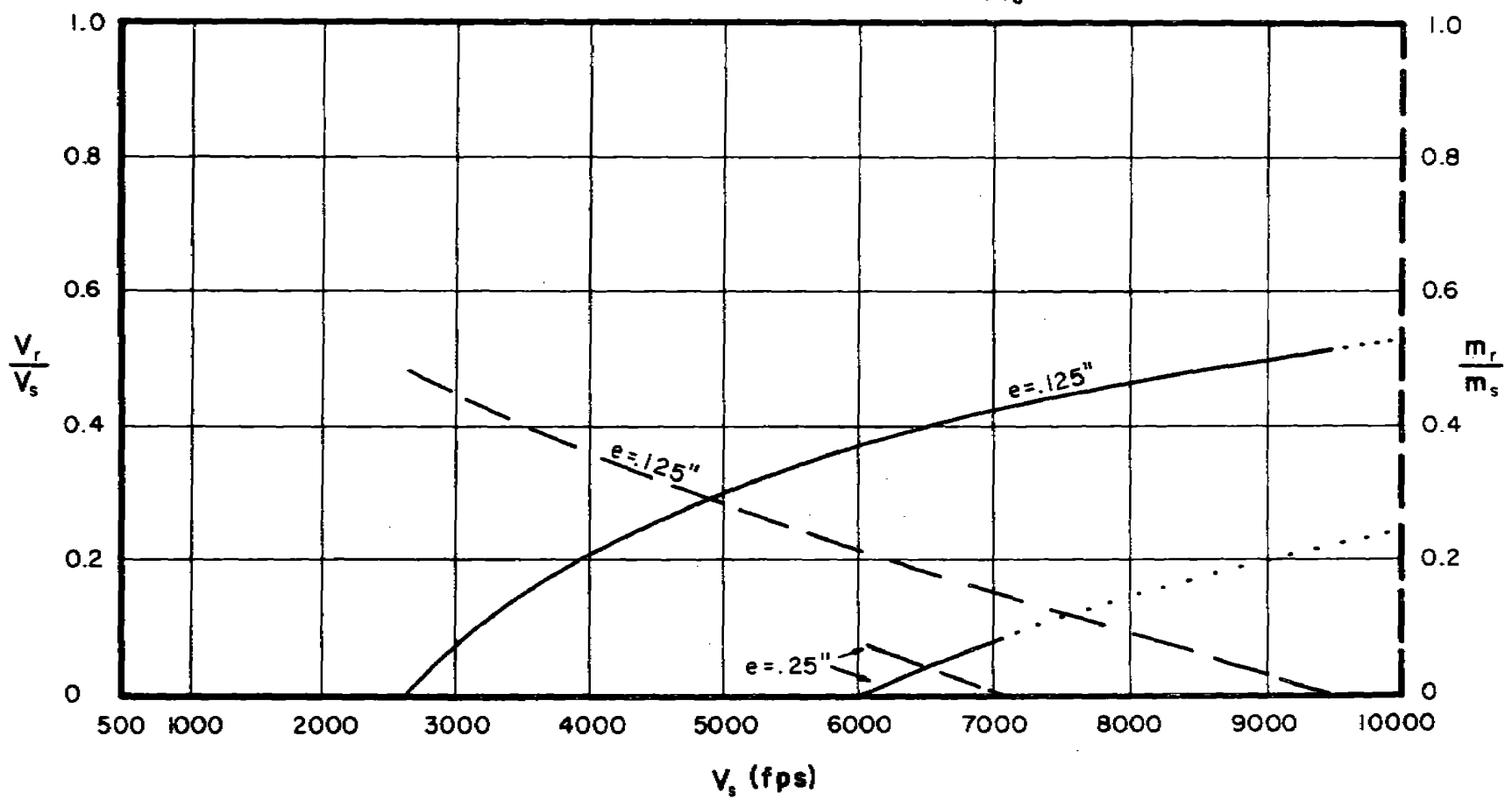

Fig. 75

$\frac{V_r}{V_s}$ and $\frac{m_r}{m_s}$ vs V_s for Selected Target Thicknesses

Target: Mild Steel, BHN ~ 150

Obliquity: 0°

Fragment Size: 30 grains

Dashed Thickness Contours Refer to $\frac{m_r}{m_s}$ Ordinate

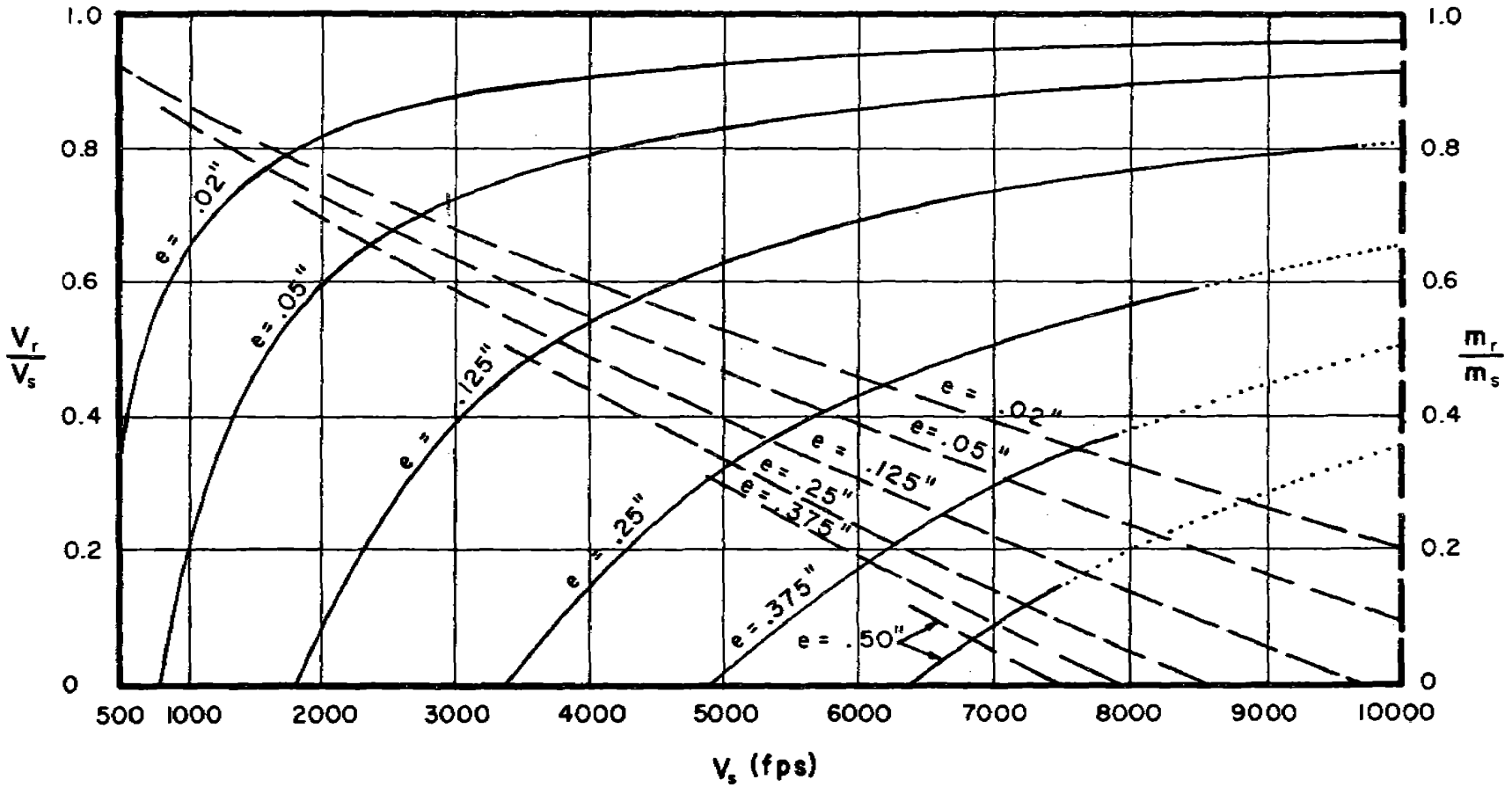

Fig. 76

$\frac{V_r}{V_s}$ and $\frac{m_r}{m_s}$ vs V_s for Selected Target Thicknesses

Target: Mild Steel, BHN ~ 150

Obliquity: 60°

Fragment Size: 30 grains

Dashed Thickness Contours Refer to $\frac{m_r}{m_s}$ Ordinate

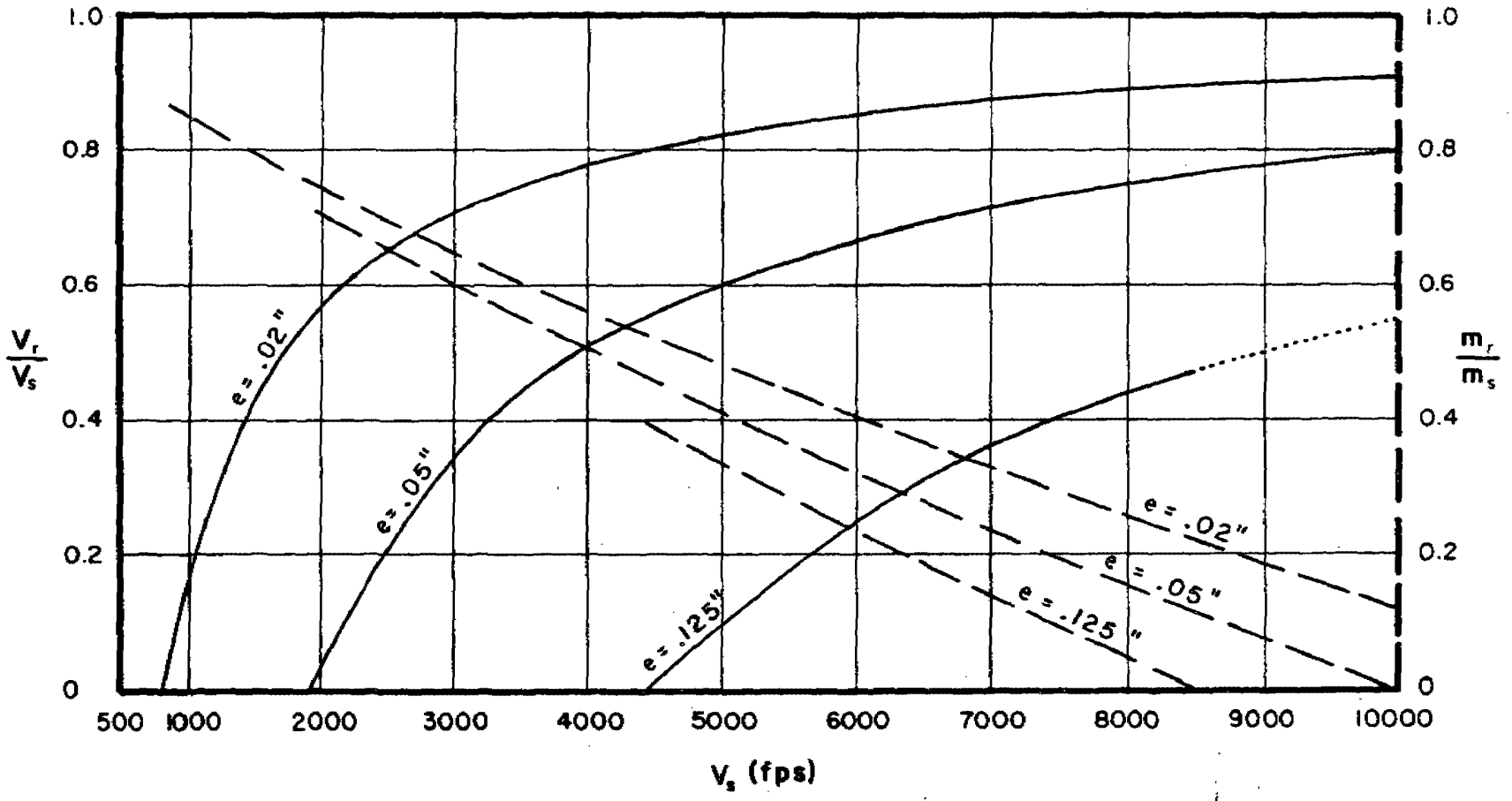

Fig. 77

CONFIDENTIAL

$\frac{V_r}{V_s}$ and $\frac{m_r}{m_s}$ vs V_s for Selected Target Thicknesses

Target: Mild Steel, BHN ~ 150

Obliquity: 70°

Fragment Size: 30 grains

Dashed Thickness Contours Refer to $\frac{m_r}{m_s}$ Ordinate

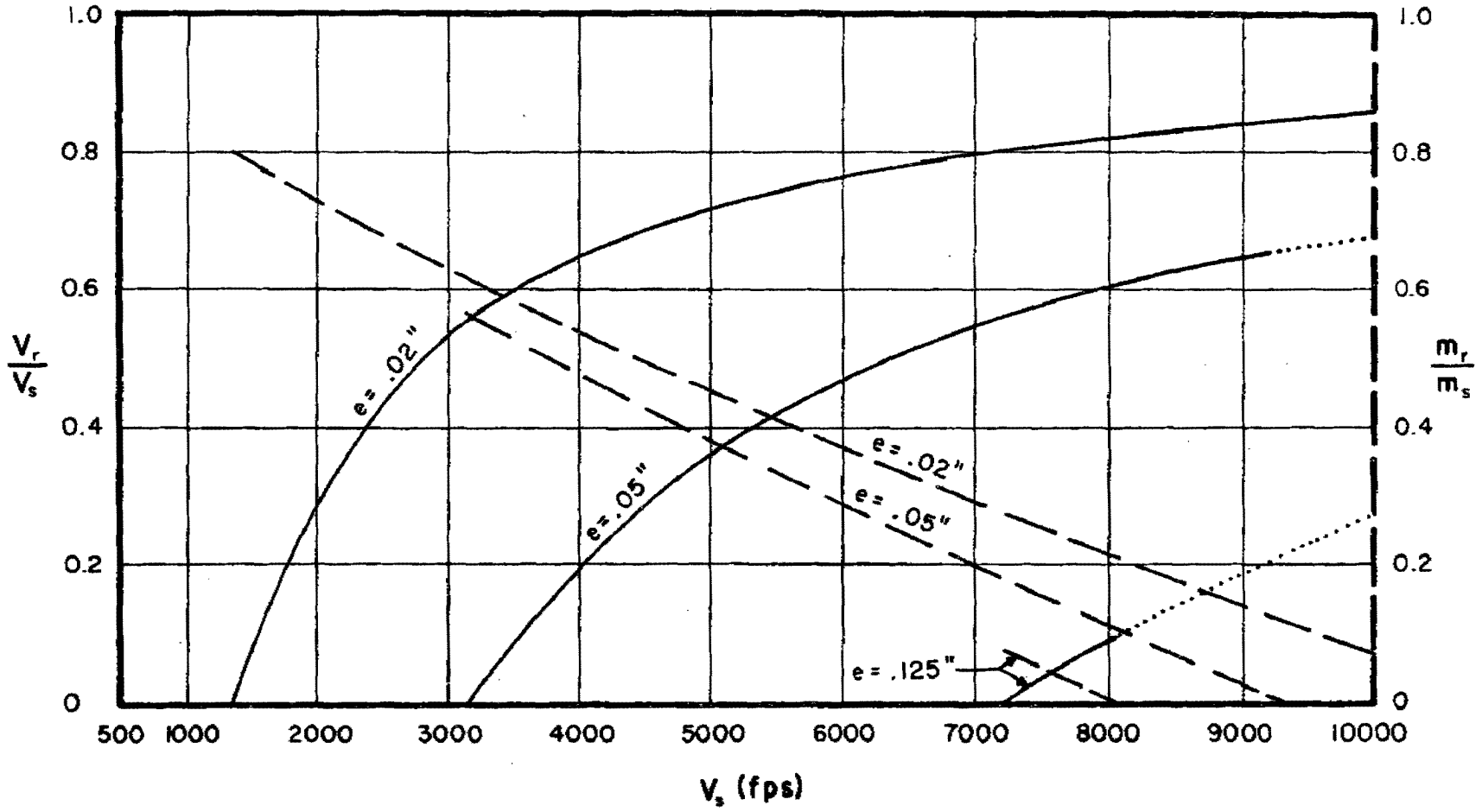

Fig. 78

CONFIDENTIAL

$\frac{V_r}{V_s}$ and $\frac{m_r}{m_s}$ vs V_s for Selected Target Thicknesses

Target: Mild Steel, BHN ~ 150

Obliquity: 0°

Fragment Size: 100 grains

Dashed Thickness Contours Refer to $\frac{m_r}{m_s}$ Ordinate

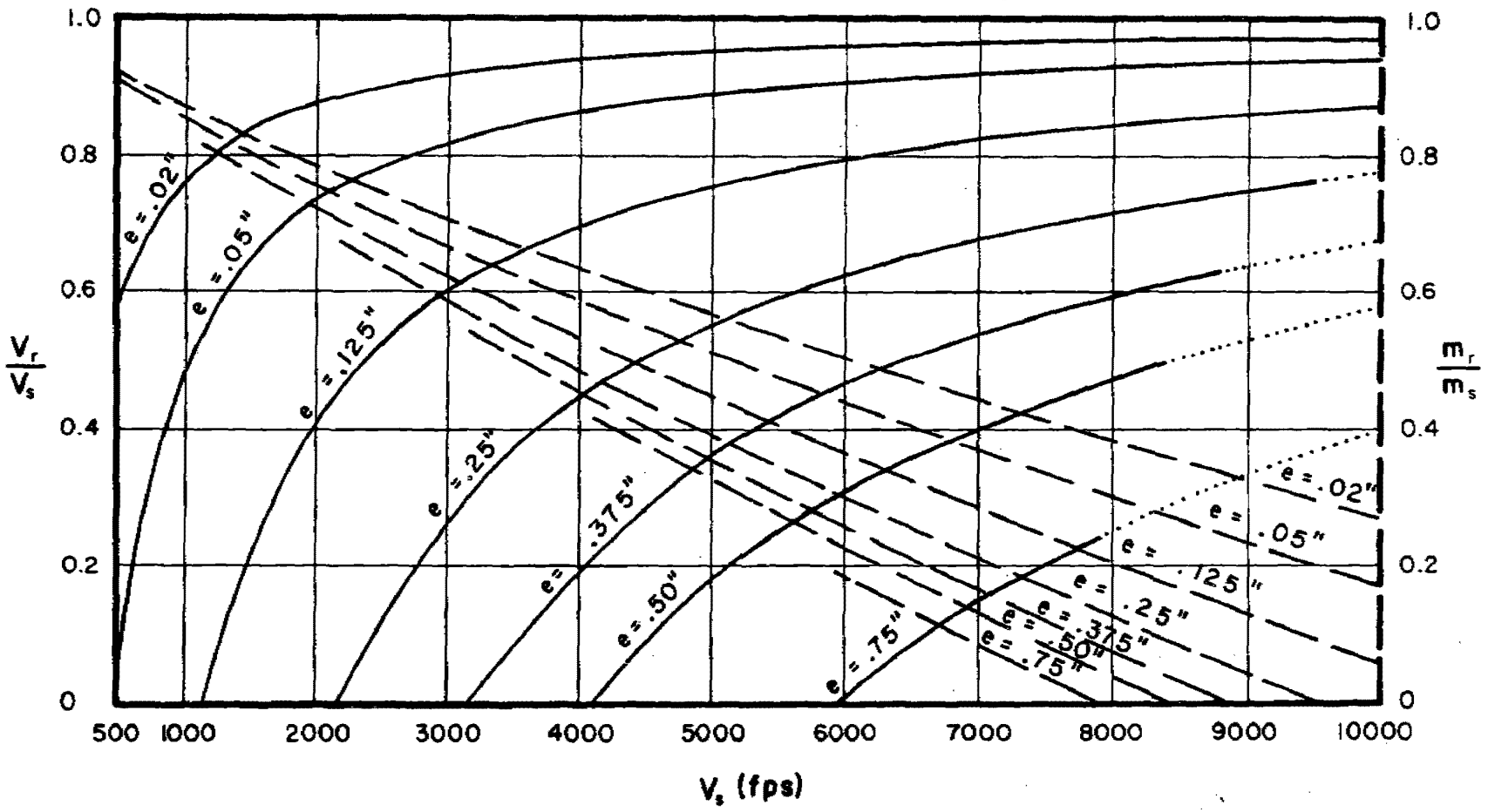

Fig. 79

$\frac{V_r}{V_s}$ and $\frac{m_r}{m_s}$ vs V_s for Selected Target Thicknesses

Target: Mild Steel, BHN~150

Obliquity: 60°

Fragment Size: 100 grains

Dashed Thickness Contours Refer to $\frac{m_r}{m_s}$ Ordinate

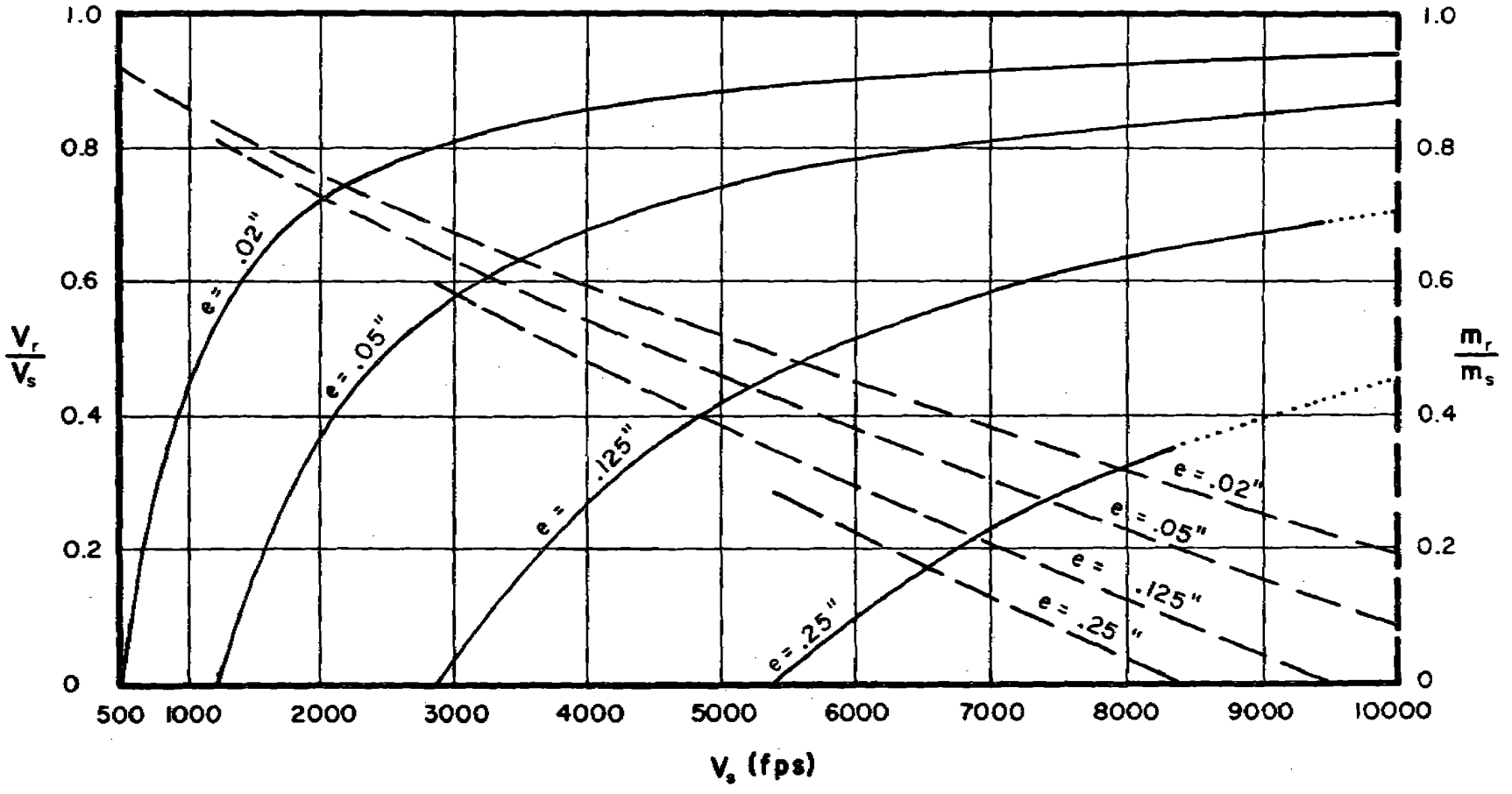

Fig. 80

$\frac{V_r}{V_s}$ and $\frac{m_r}{m_s}$ vs V_s for Selected Target Thicknesses

Target: Mild Steel, BHN ~ 150

Obliquity: 70°

Fragment Size: 100 grains

Dashed Thickness Contours Refer to $\frac{m_r}{m_s}$ Ordinate

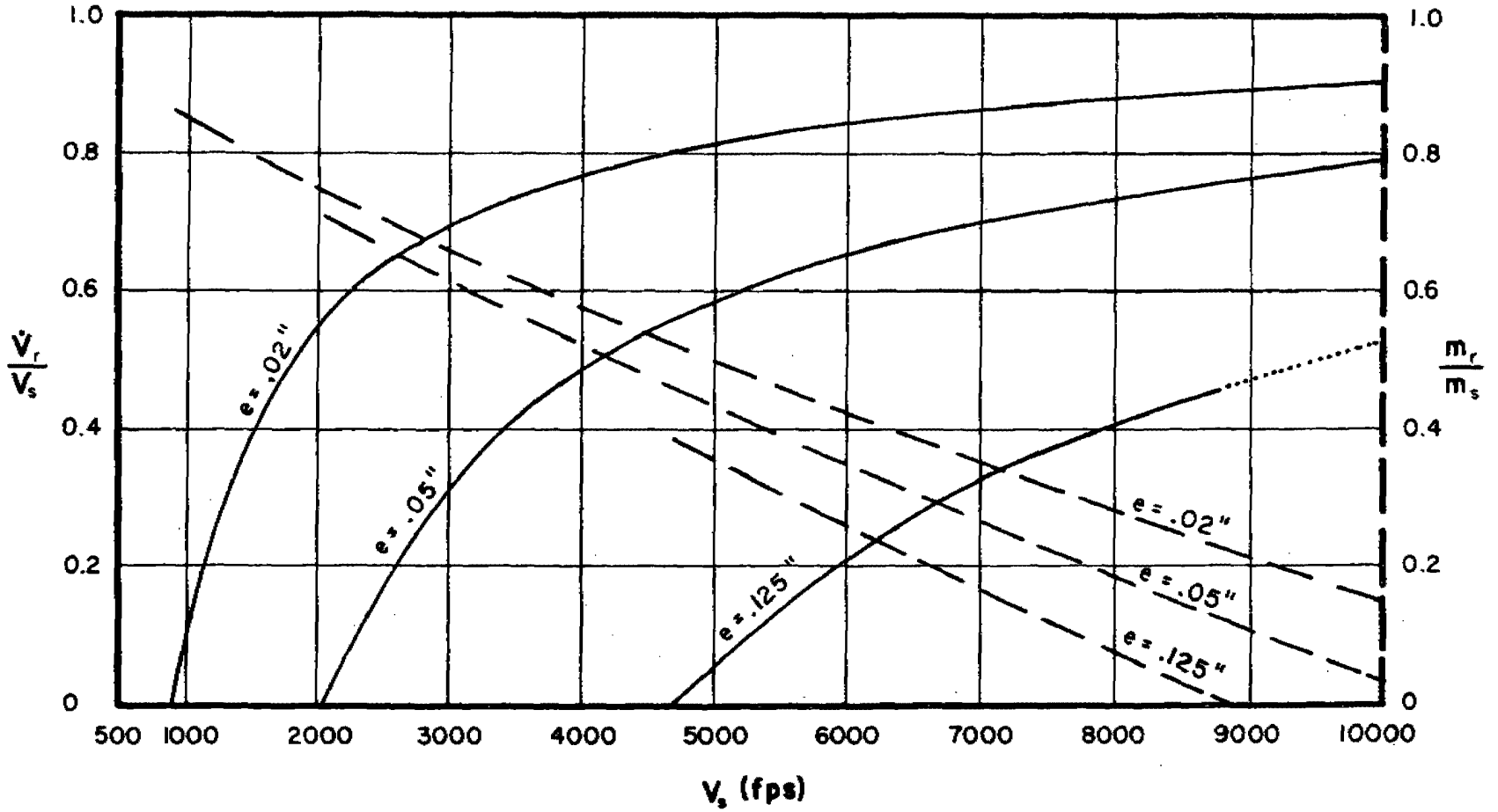

Fig. 81

[redacted]

[redacted]

[redacted]

$\frac{V_r}{V_s}$ and $\frac{m_r}{m_s}$ vs V_s for Selected Target Thicknesses

Target: Mild Steel, BHN ~ 150

Obliquity: 0°

Fragment Size: 300 grains

Dashed Thickness Contours Refer to $\frac{m_r}{m_s}$ Ordinate

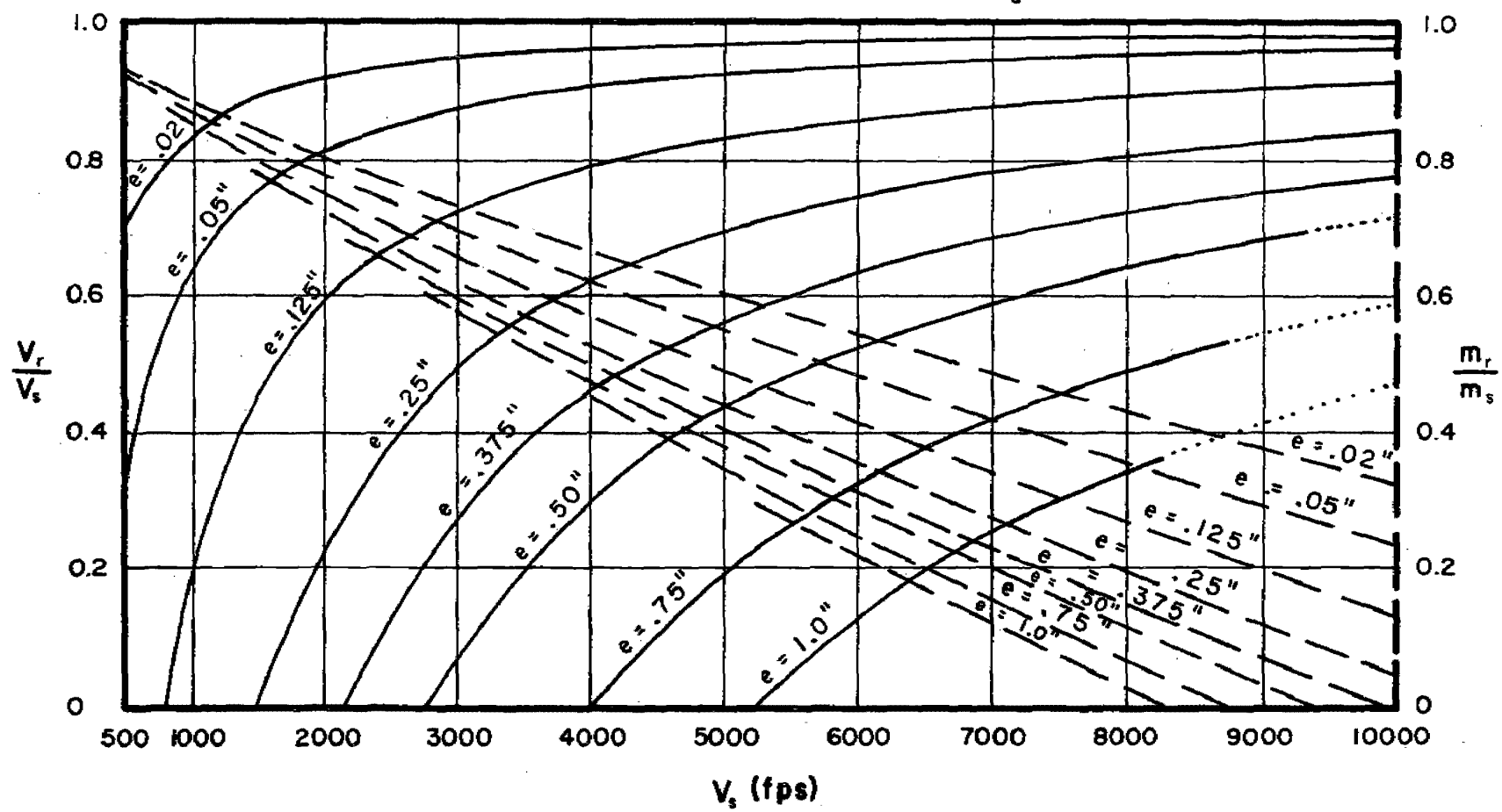

Fig. 82

[redacted]

$\frac{V_r}{V_s}$ and $\frac{m_r}{m_s}$ vs V_s for Selected Target Thicknesses

Target: Mild Steel, BHN ~ 150

Obliquity: 60°

Fragment Size: 300 grains

Dashed Thickness Contours Refer to $\frac{m_r}{m_s}$ Ordinate

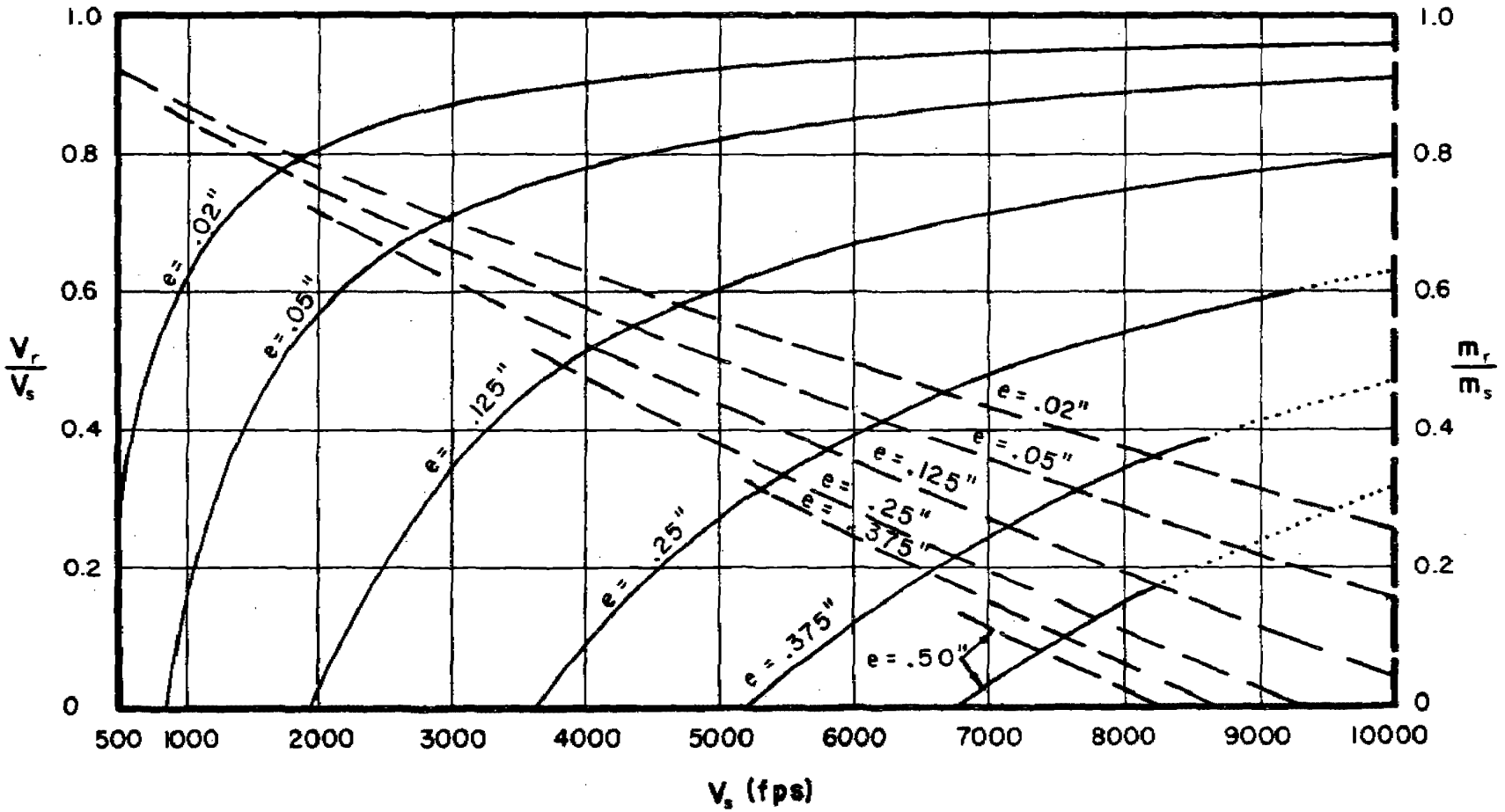

Fig. 83

$\frac{V_r}{V_s}$ and $\frac{m_r}{m_s}$ vs V_s for Selected Target Thicknesses

Target: Mild Steel, BHN ~ 150

Obliquity: 70°

Fragment Size: 300 grains

Dashed Thickness Contours Refer to $\frac{m_r}{m_s}$ Ordinate

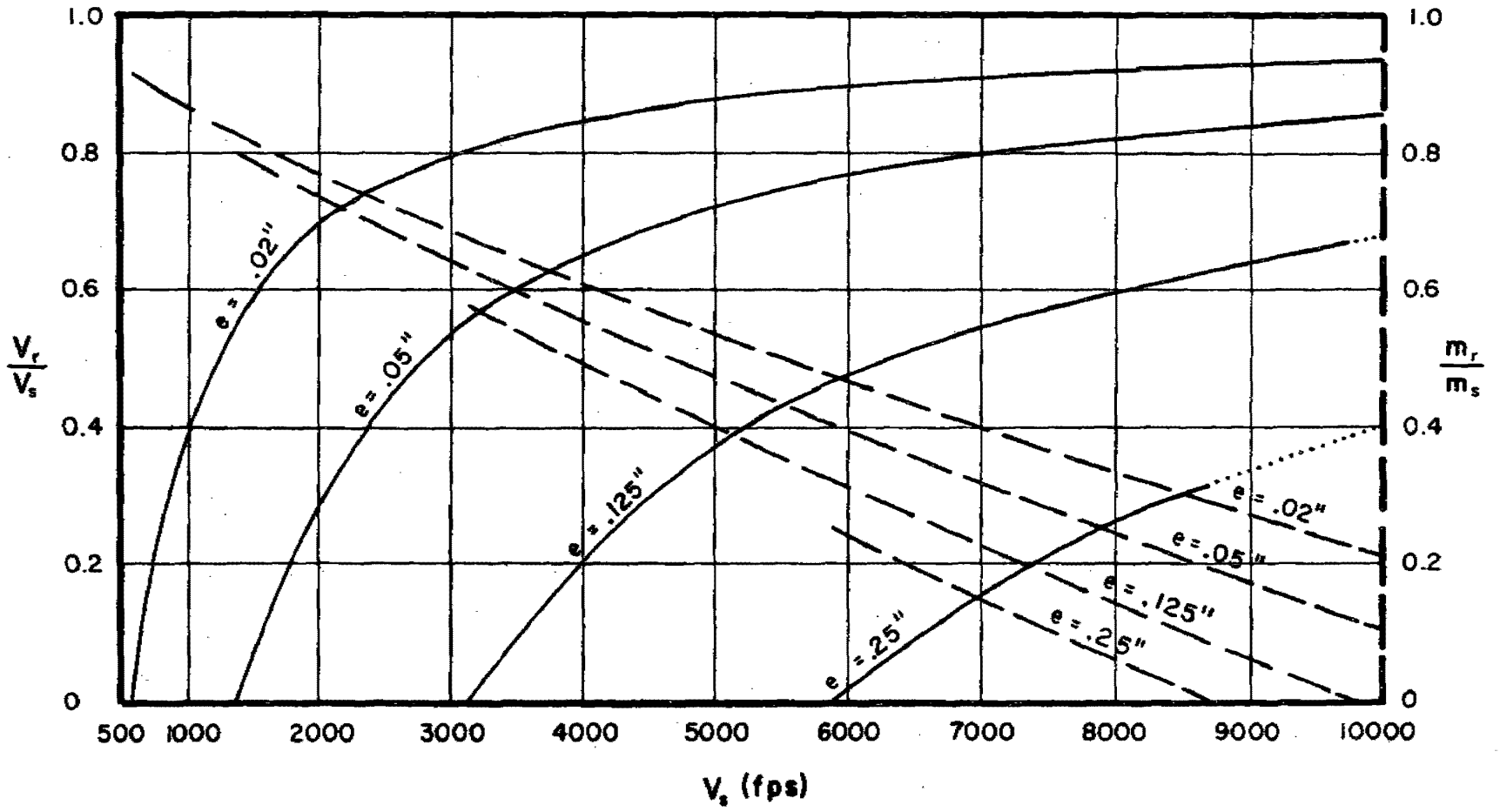

Fig. 84

$\frac{V_r}{V_s}$ and $\frac{m_r}{m_s}$ vs V_s for Selected Target Thicknesses

Target: Hard Homogeneous Steel

Obliquity: 0°

Fragment Size: 30 grains

Dashed Thickness Contours Refer to $\frac{m_r}{m_s}$ Ordinate

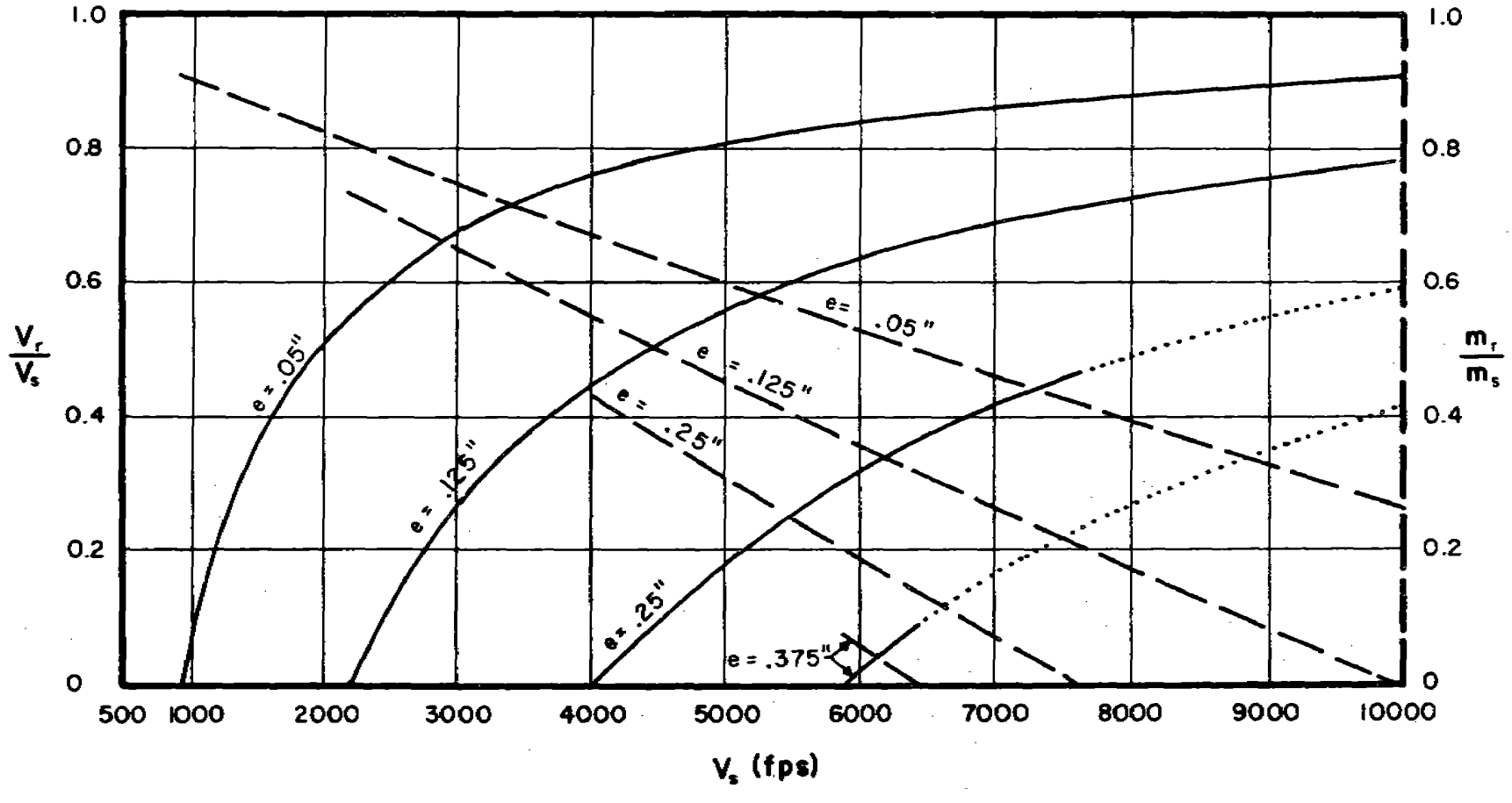

Fig. 85

$\frac{V_r}{V_s}$ and $\frac{m_r}{m_s}$ vs V_s for Selected Target Thicknesses

Target: Hard Homogeneous Steel

Obliquity: 60°

Fragment Size: 30 grains

Dashed Thickness Contours Refer to $\frac{m_r}{m_s}$ Ordinate

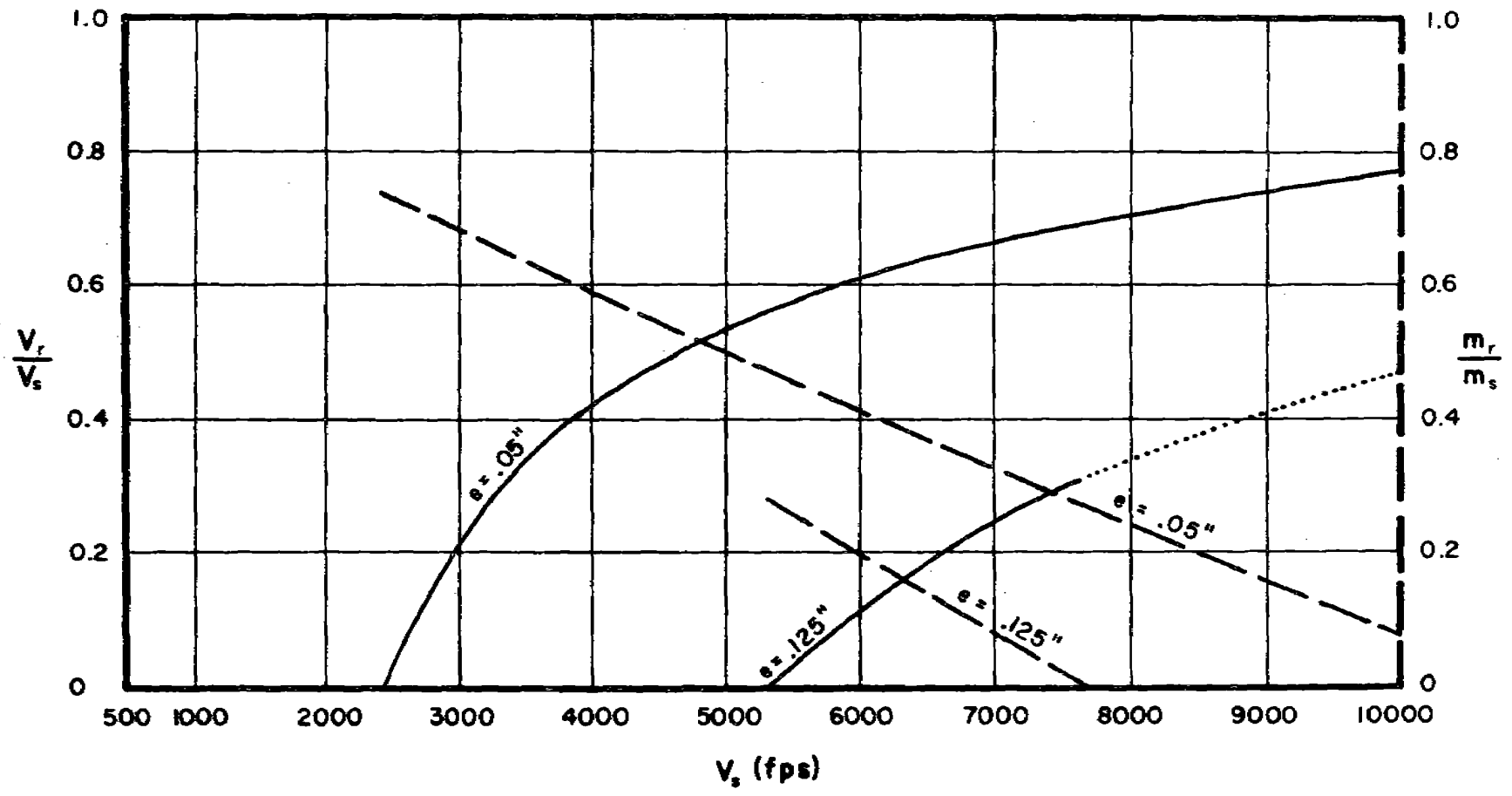

Fig. 86

$\frac{V_r}{V_s}$ and $\frac{m_r}{m_s}$ vs V_s for Selected Target Thicknesses

Target: Hard Homogeneous Steel

Obliquity: 70°

Fragment Size: 30 grains

Dashed Thickness Contours Refer to $\frac{m_r}{m_s}$ Ordinate

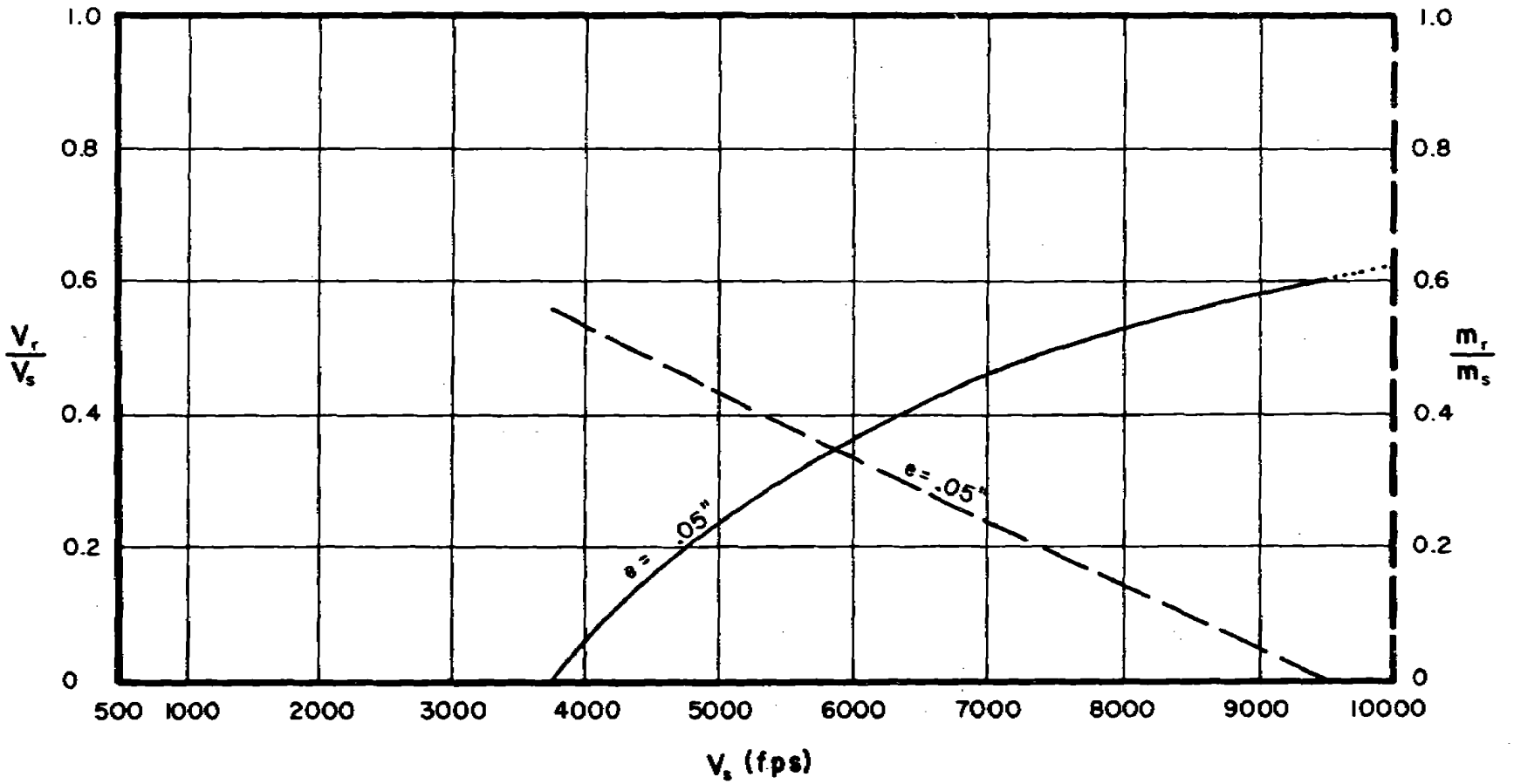

Fig. 87

$\frac{V_r}{V_s}$ and $\frac{m_r}{m_s}$ vs V_s for Selected Target Thicknesses

Target: Hard Homogeneous Steel

Obliquity: 0°

Fragment Size: 100 grains

Dashed Thickness Contours Refer to $\frac{m_r}{m_s}$ Ordinate

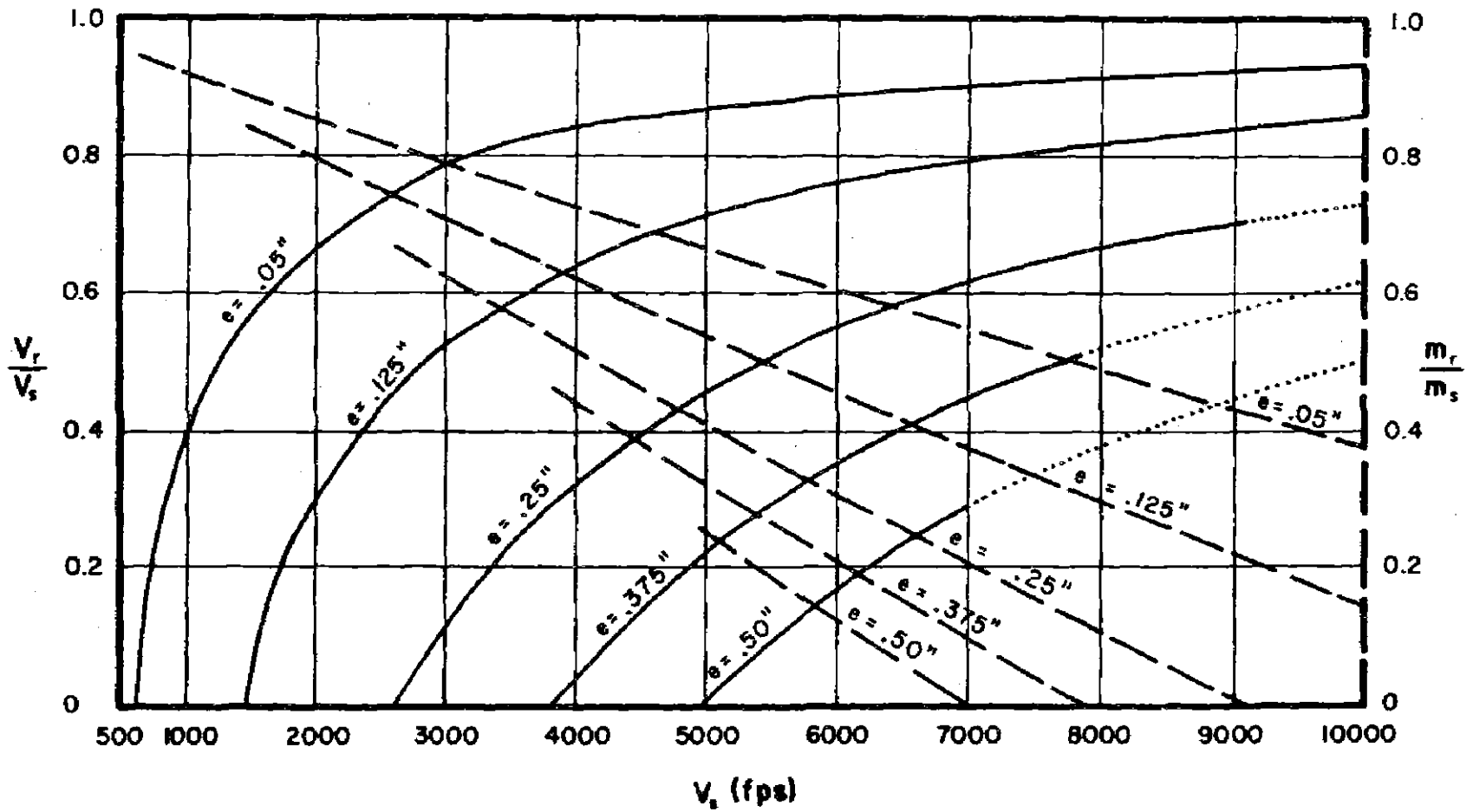

Fig. 88

$\frac{V_r}{V_s}$ and $\frac{m_r}{m_s}$ vs V_s for Selected Target Thicknesses

Target: Hard Homogeneous Steel

Obliquity: 60°

Fragment Size: 100 grains

Dashed Thickness Contours Refer to $\frac{m_r}{m_s}$ Ordinate

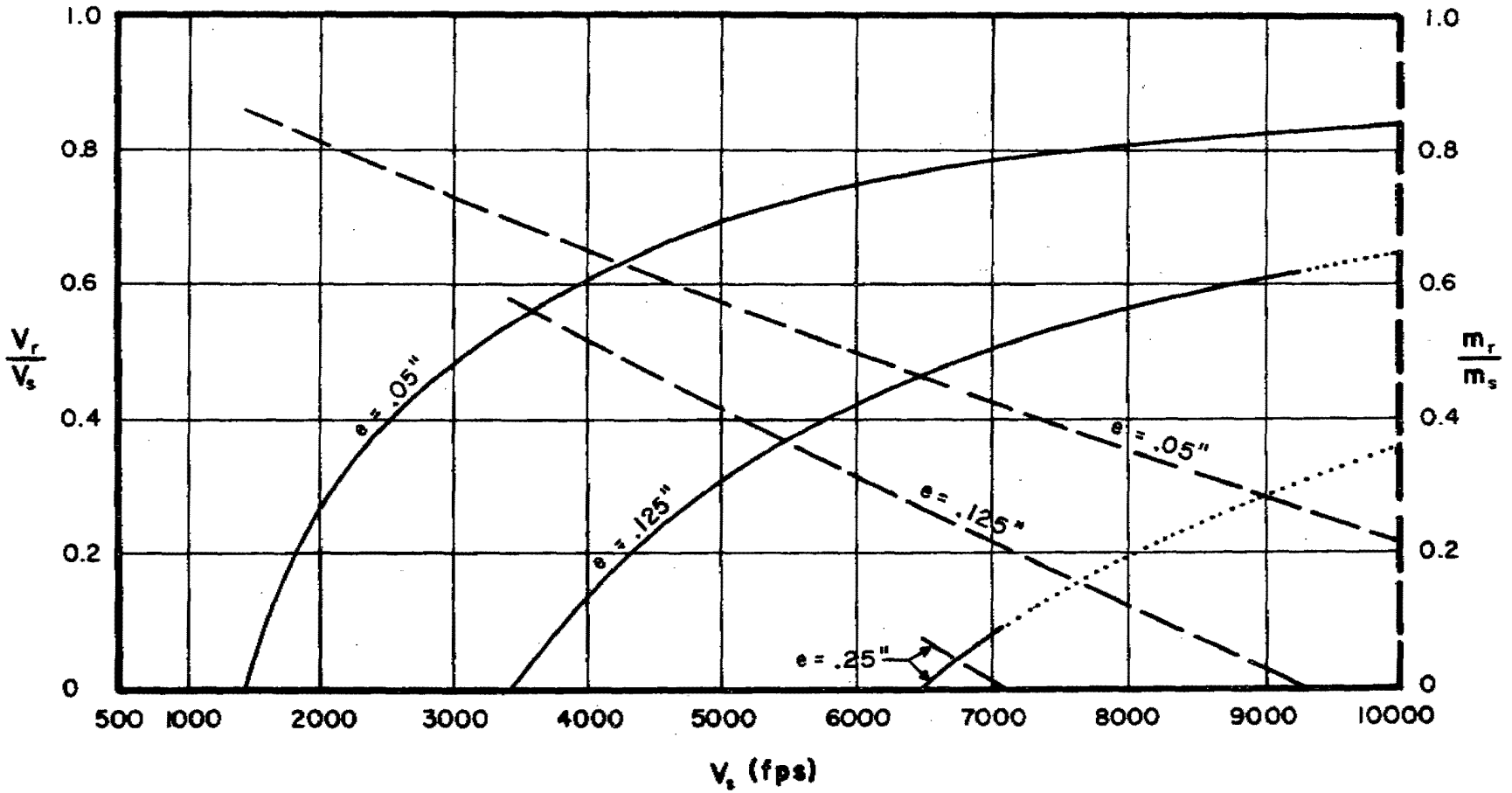

Fig. 89

$\frac{V_r}{V_s}$ and $\frac{m_r}{m_s}$ vs V_s for Selected Target Thicknesses

Target: Hard Homogeneous Steel

Obliquity: 70°

Fragment Size: 100 grains

Dashed Thickness Contours Refer to $\frac{m_r}{m_s}$ Ordinate

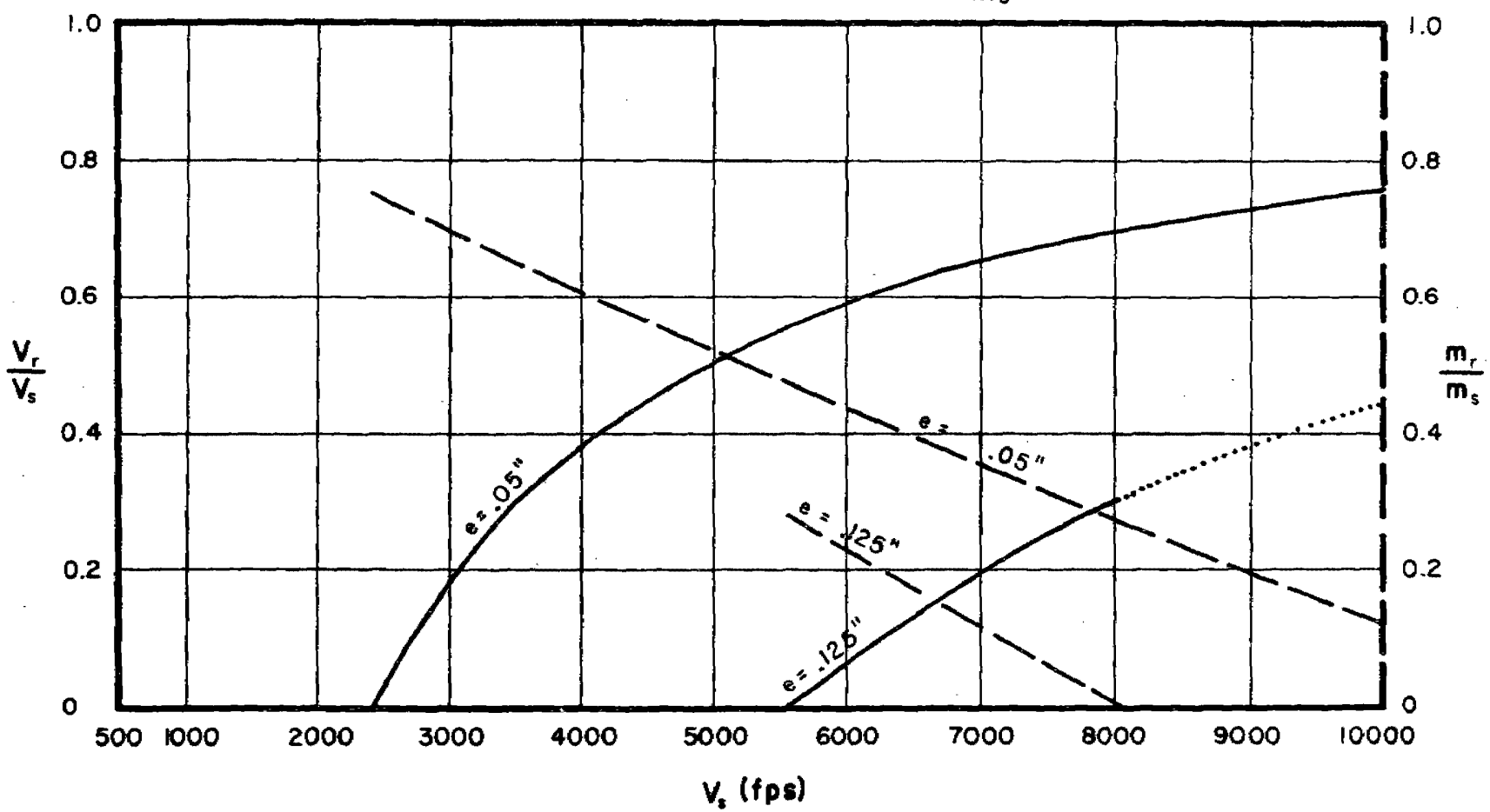

Fig. 90

$\frac{V_r}{V_s}$ and $\frac{m_r}{m_s}$ vs V_s for Selected Target Thicknesses

Target: Hard Homogeneous Steel

Obliquity: 0°

Fragment Size: 300 grains

Dashed Thickness Contours Refer to $\frac{m_r}{m_s}$ Ordinate

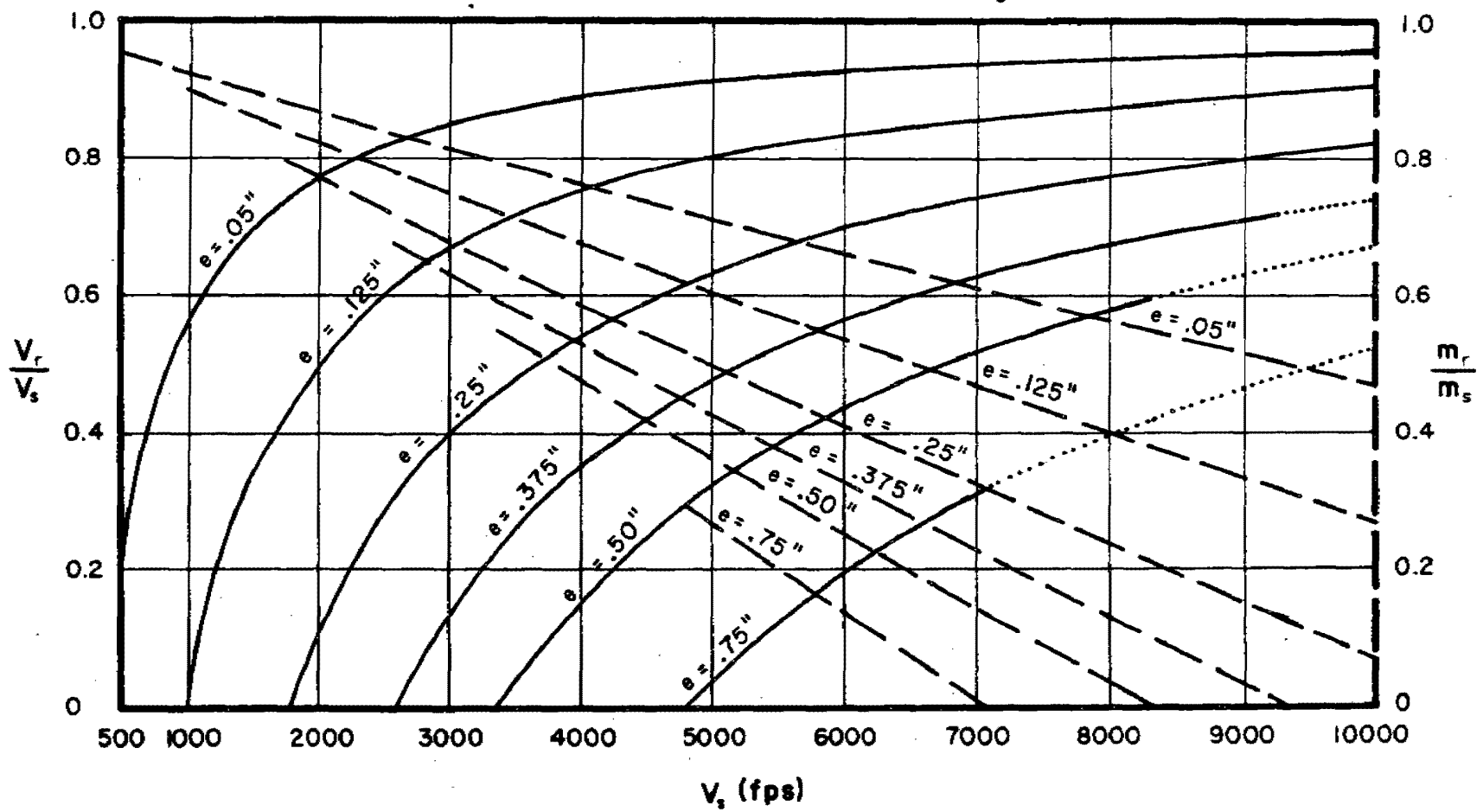

Fig. 91

TECHNICAL LIBRARY
BLDG. 305
ABERDEEN PROVING GROUND, MD.
STEAP-TL

$\frac{V_r}{V_s}$ and $\frac{m_r}{m_s}$ vs V_s for Selected Target Thicknesses

Target: Hard Homogeneous Steel

Obliquity: 60°

Fragment Size: 300 grains

Dashed Thickness Contours Refer to $\frac{m_r}{m_s}$ Ordinate

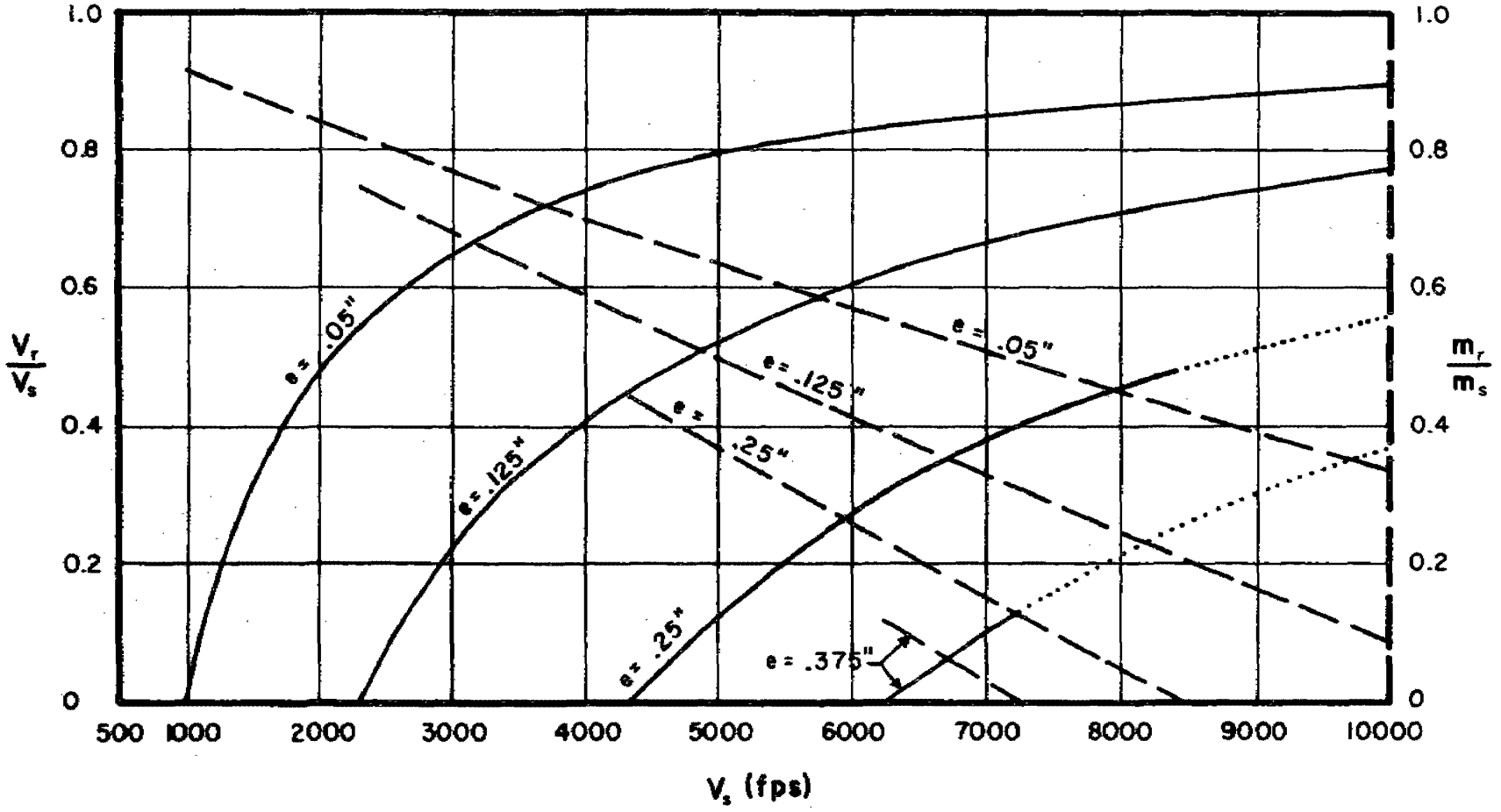

Fig. 92

$\frac{V_r}{V_s}$ and $\frac{m_r}{m_s}$ vs V_s for Selected Target Thicknesses

Target: Hard Homogeneous Steel

Obliquity: 70°

Fragment Size: 300 grains

Dashed Thickness Contours Refer to $\frac{m_r}{m_s}$ Ordinate

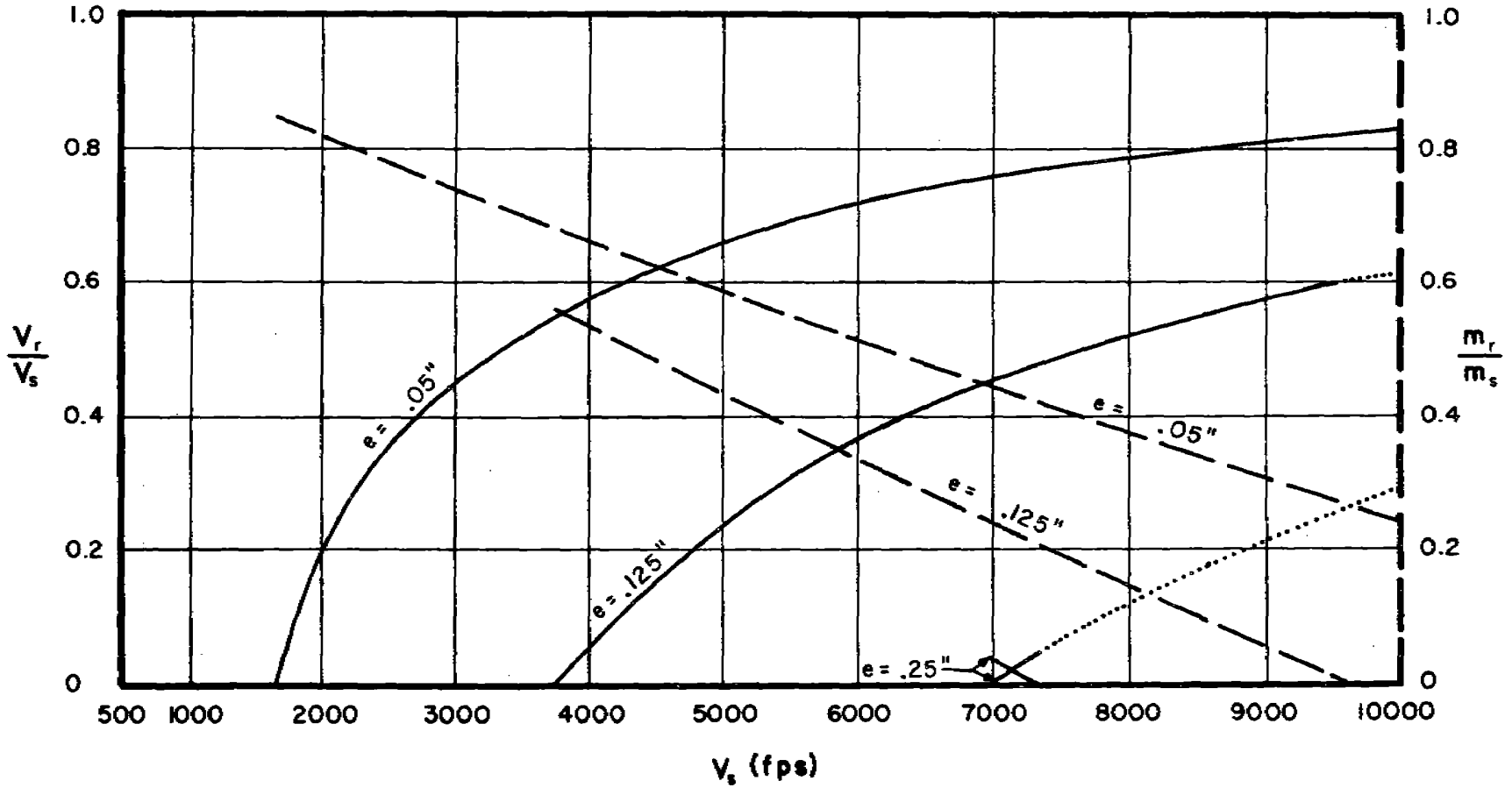

Fig. 93

$\frac{V_r}{V_s}$ and $\frac{m_r}{m_s}$ vs V_s for Selected Target Thicknesses

Target: Copper

Obliquity: 0°

Fragment Size: 30 grains

Dashed Thickness Contours Refer to $\frac{m_r}{m_s}$ Ordinate

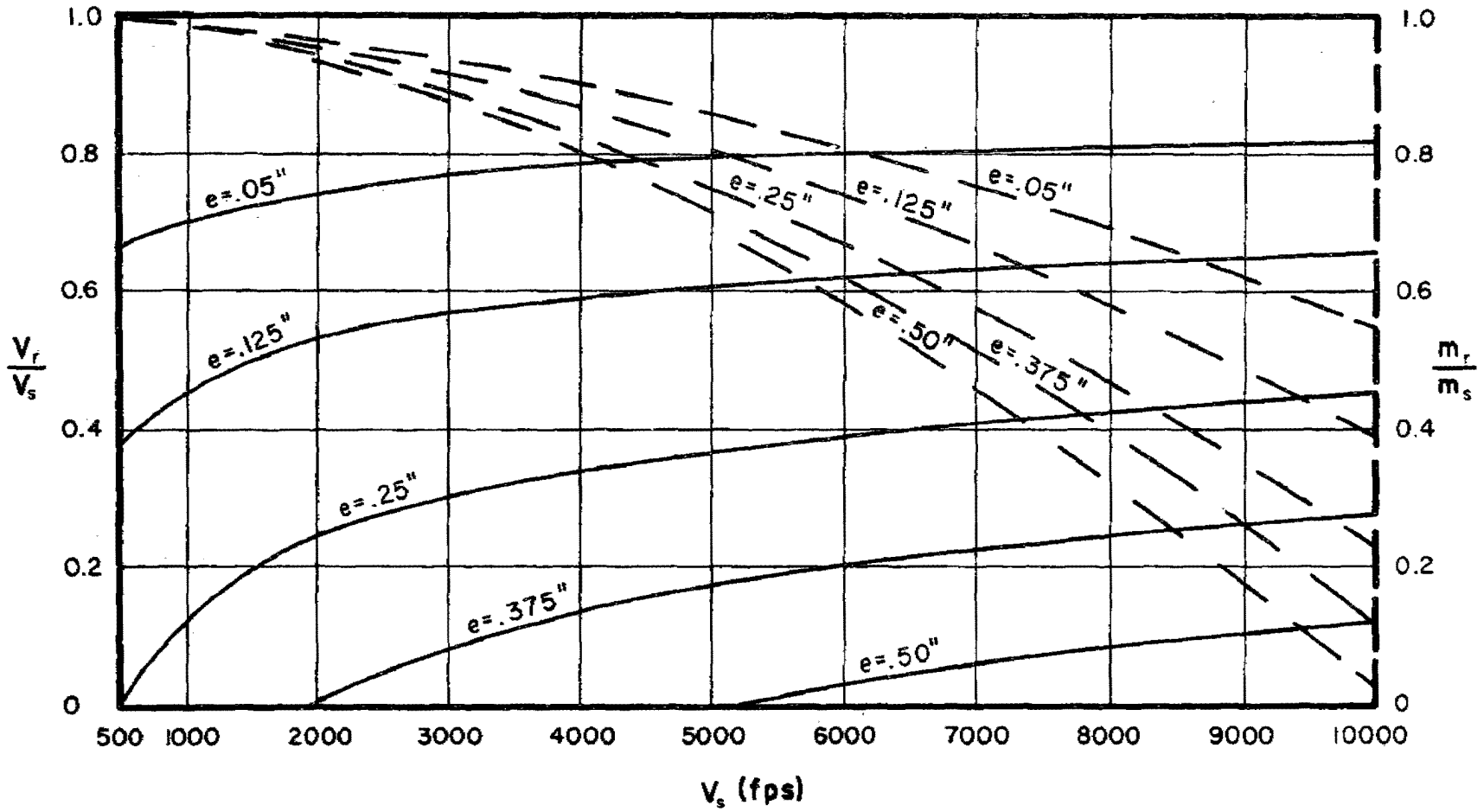

Fig. 94

$\frac{V_r}{V_s}$ and $\frac{m_r}{m_s}$ vs V_s for Selected Target Thicknesses

Target: Copper

Obliquity: 60°

Fragment Size: 30 grains

Dashed Thickness Contours Refer to $\frac{m_r}{m_s}$ Ordinate

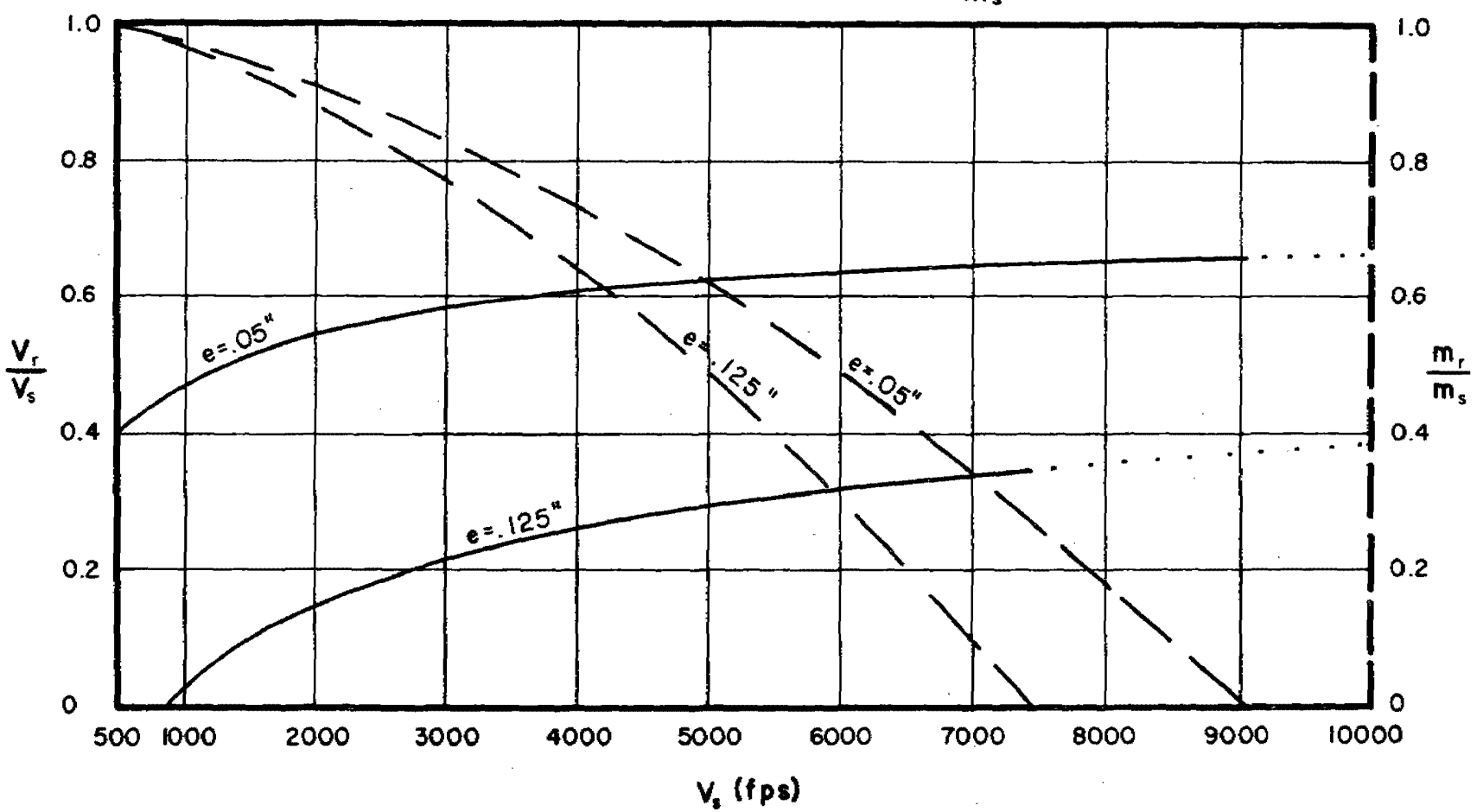

Fig. 95

$\frac{V_r}{V_s}$ and $\frac{m_r}{m_s}$ vs V_s for Selected Target Thicknesses

Target: Copper

Obliquity: 70°

Fragment Size: 30 grains

Dashed Thickness Contours Refer to $\frac{m_r}{m_s}$ Ordinate

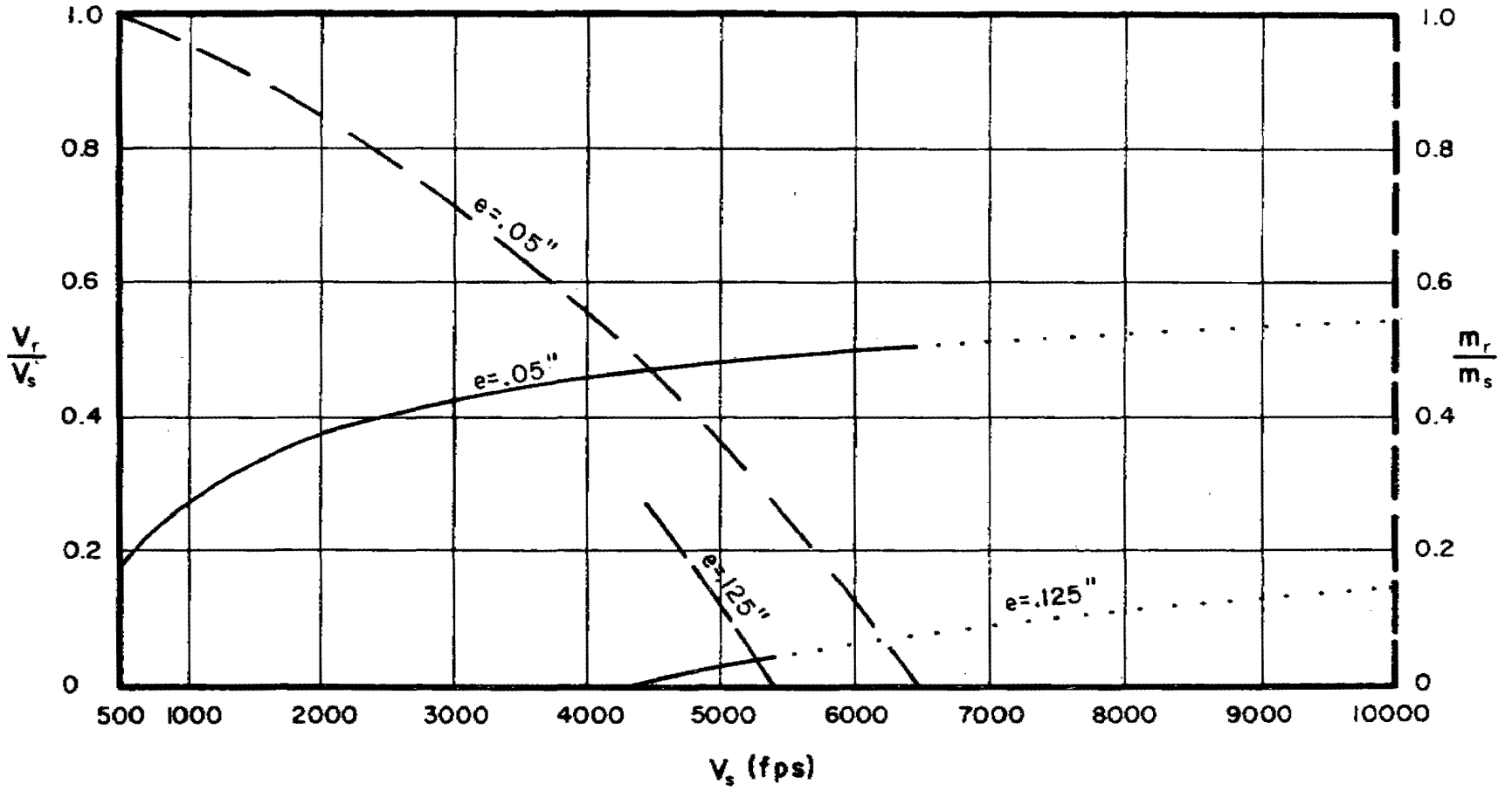

Fig. 96

$\frac{V_r}{V_s}$ and $\frac{m_r}{m_s}$ vs V_s for Selected Target Thicknesses

Target: Copper

Obliquity: 0°

Fragment Size: 100 grains

Dashed Thickness Contours Refer to $\frac{m_r}{m_s}$ Ordinate

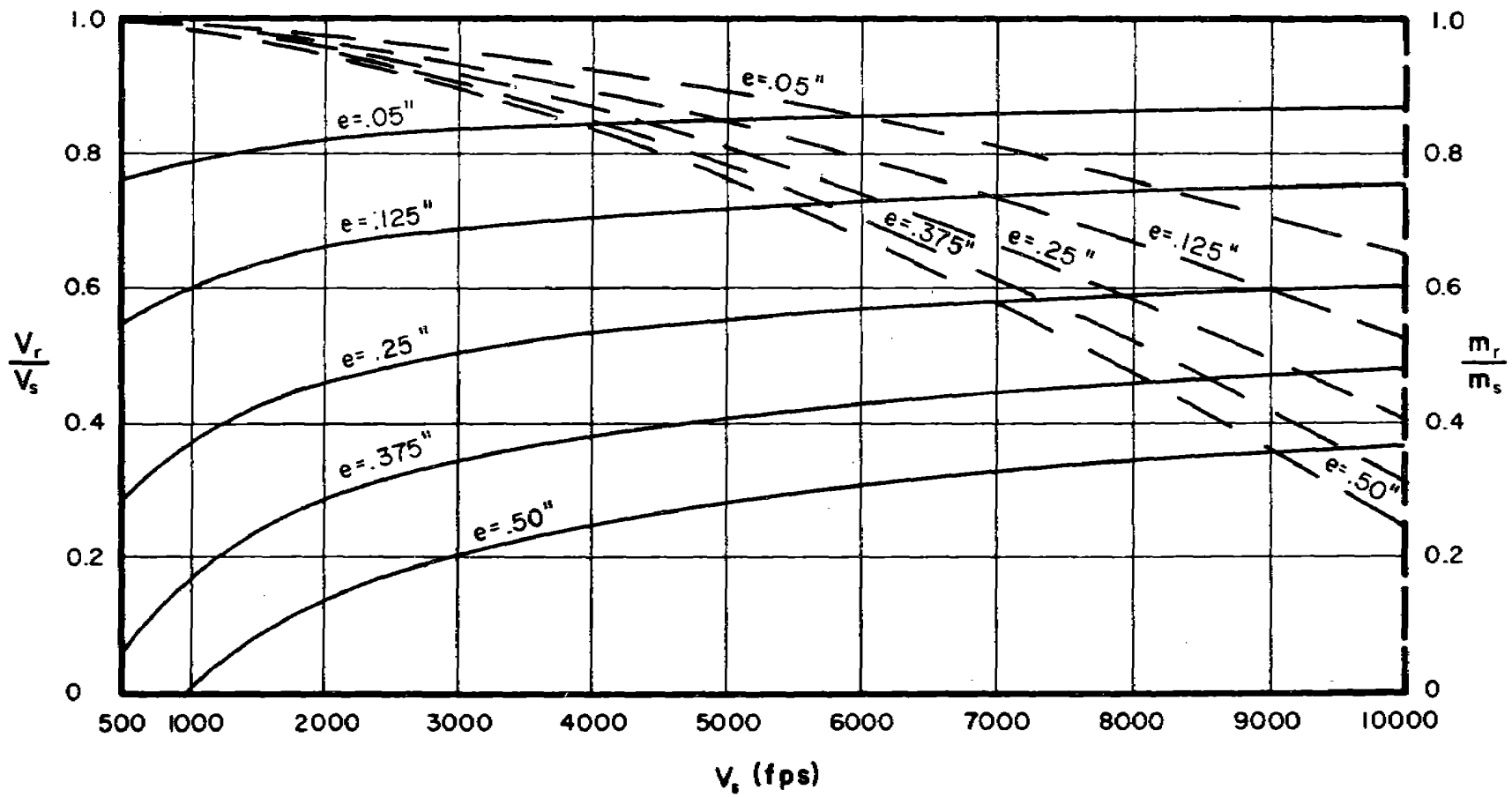

Fig. 97

$\frac{V_r}{V_s}$ and $\frac{m_r}{m_s}$ vs V_s for Selected Target Thicknesses

Target: Copper

Obliquity: 60°

Fragment Size: 100 grains

Dashed Thickness Contours Refer to $\frac{m_r}{m_s}$ Ordinate

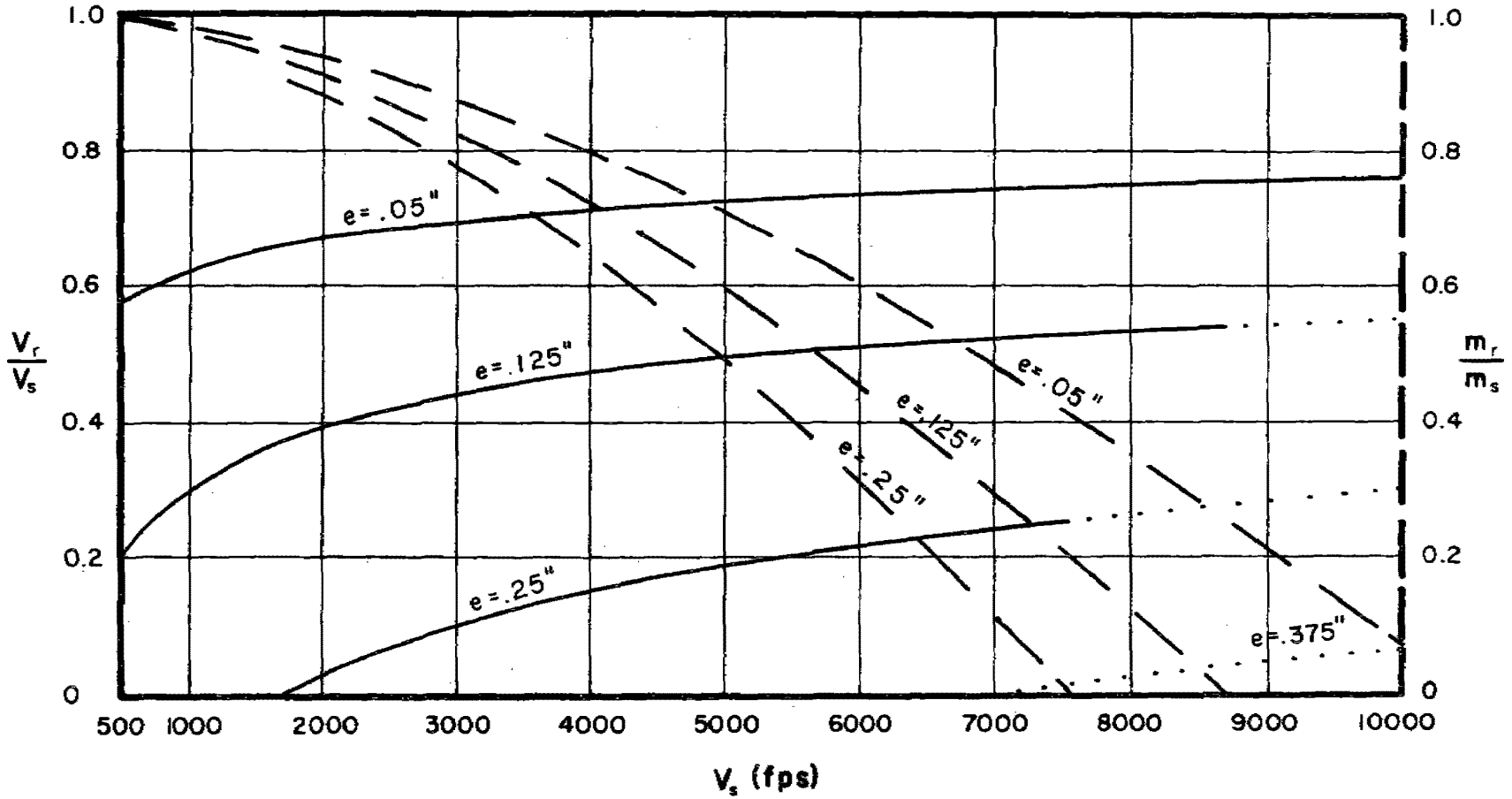

Fig. 98

$\frac{V_r}{V_s}$ and $\frac{m_r}{m_s}$ vs V_s for Selected Target Thicknesses

Target: Copper

Obliquity: 70°

Fragment Size: 100 grains

Dashed Thickness Contours Refer to $\frac{m_r}{m_s}$ Ordinate

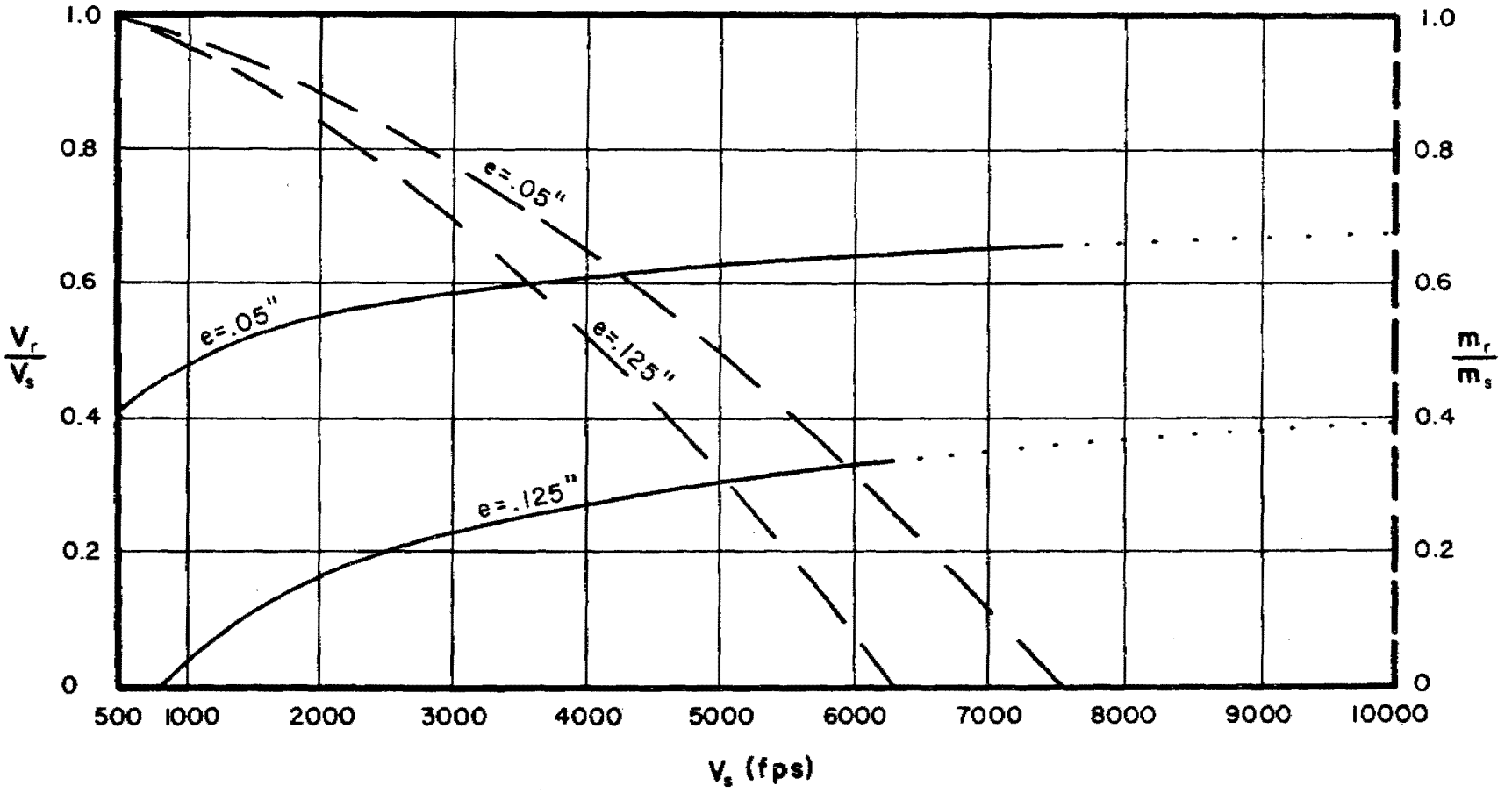

Fig. 99

$\frac{V_r}{V_s}$ and $\frac{m_r}{m_s}$ vs V_s for Selected Target Thicknesses

Target: Copper

Obliquity: 0°

Fragment Size: 300 grains

Dashed Thickness Contours Refer to $\frac{m_r}{m_s}$ Ordinate

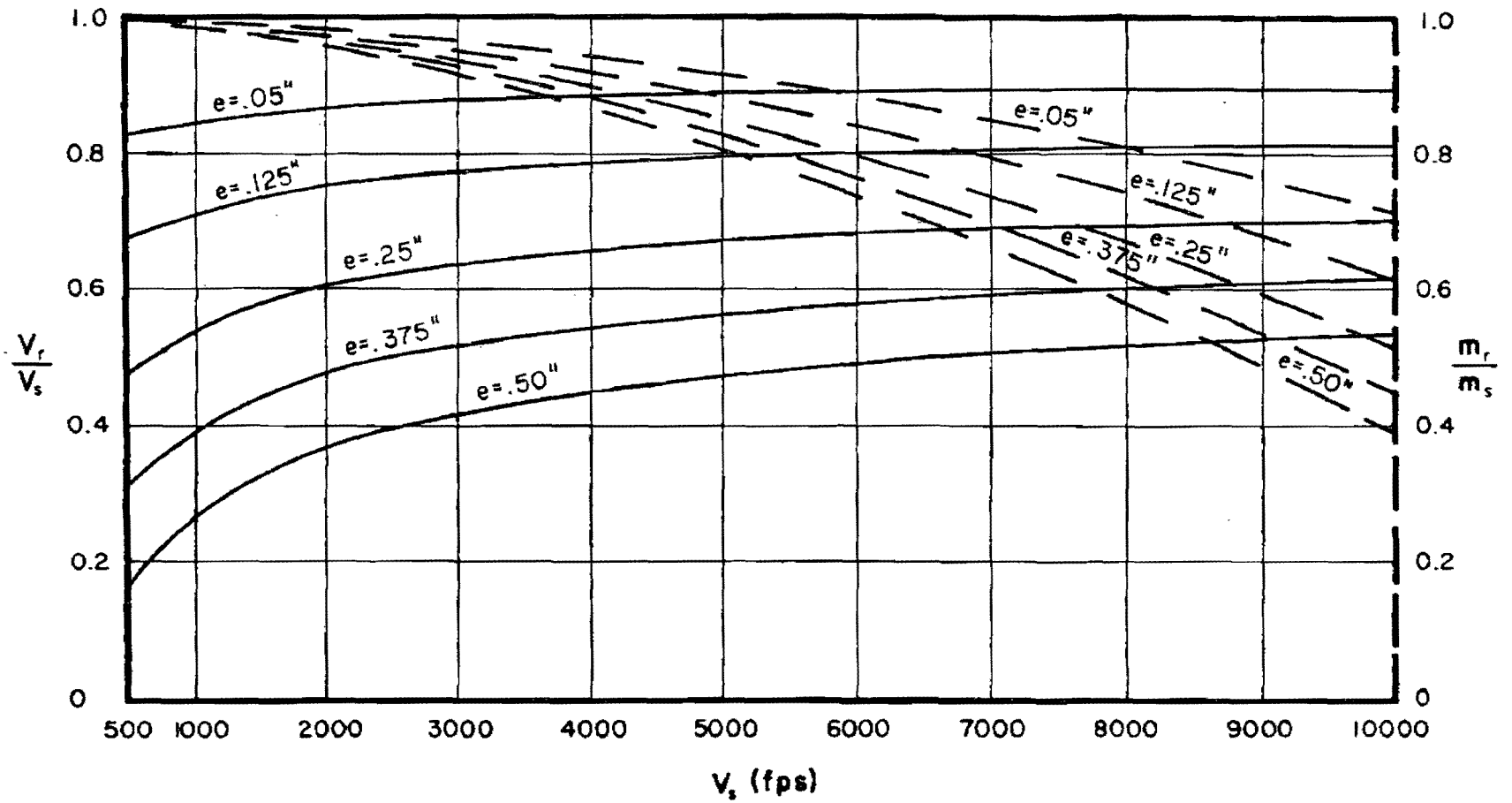

Fig. 100

$\frac{V_r}{V_s}$ and $\frac{m_r}{m_s}$ vs V_s for Selected Target Thicknesses

Target: Copper

Obliquity: 60°

Fragment Size: 300 grains

Dashed Thickness Contours Refer to $\frac{m_r}{m_s}$ Ordinate

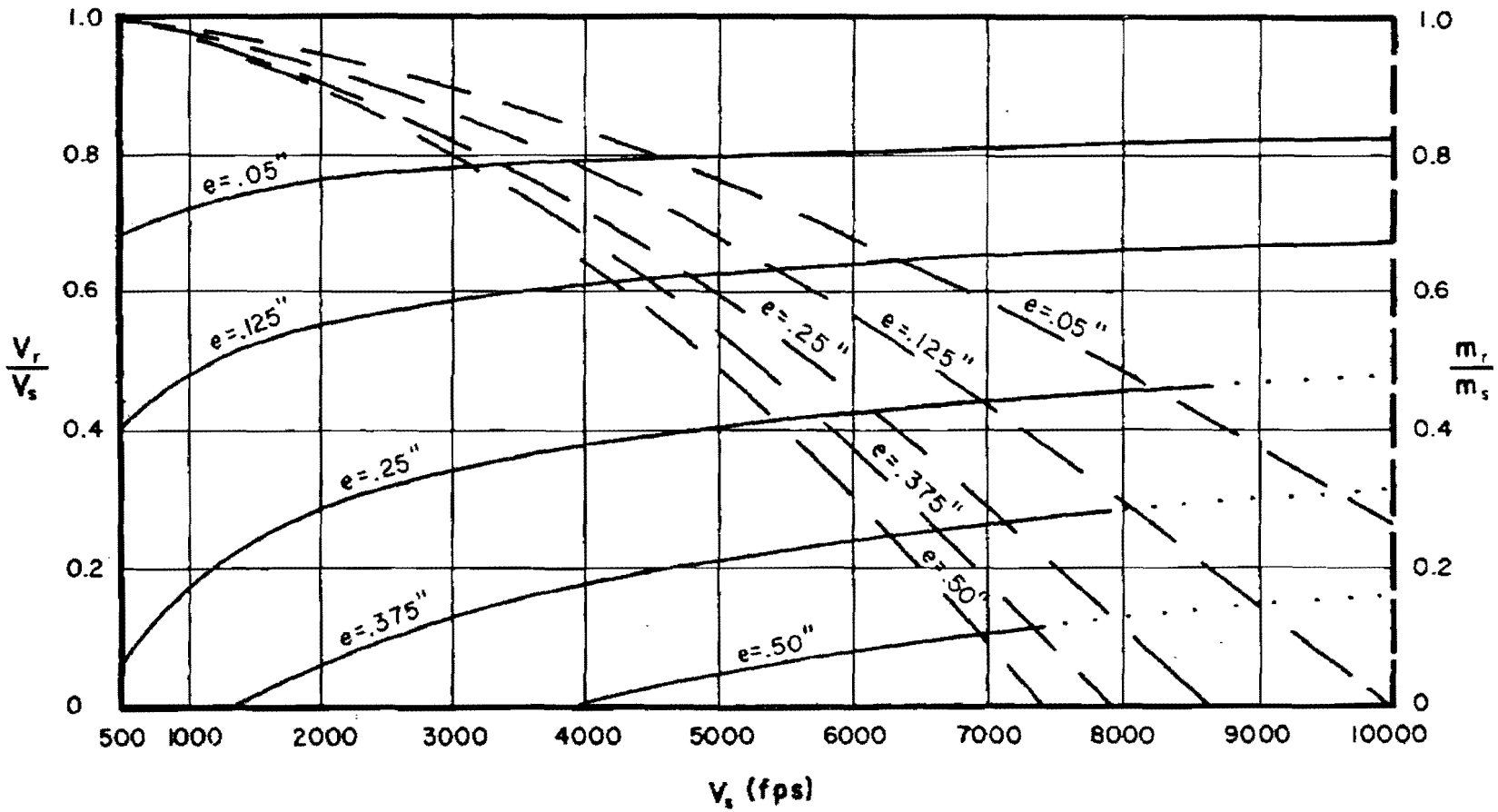

Fig. 101

$\frac{V_r}{V_s}$ and $\frac{m_r}{m_s}$ vs V_s for Selected Target Thicknesses

Target: Copper

Obliquity: 70°

Fragment Size: 300 grains

Dashed Thickness Contours Refer to $\frac{m_r}{m_s}$ Ordinate

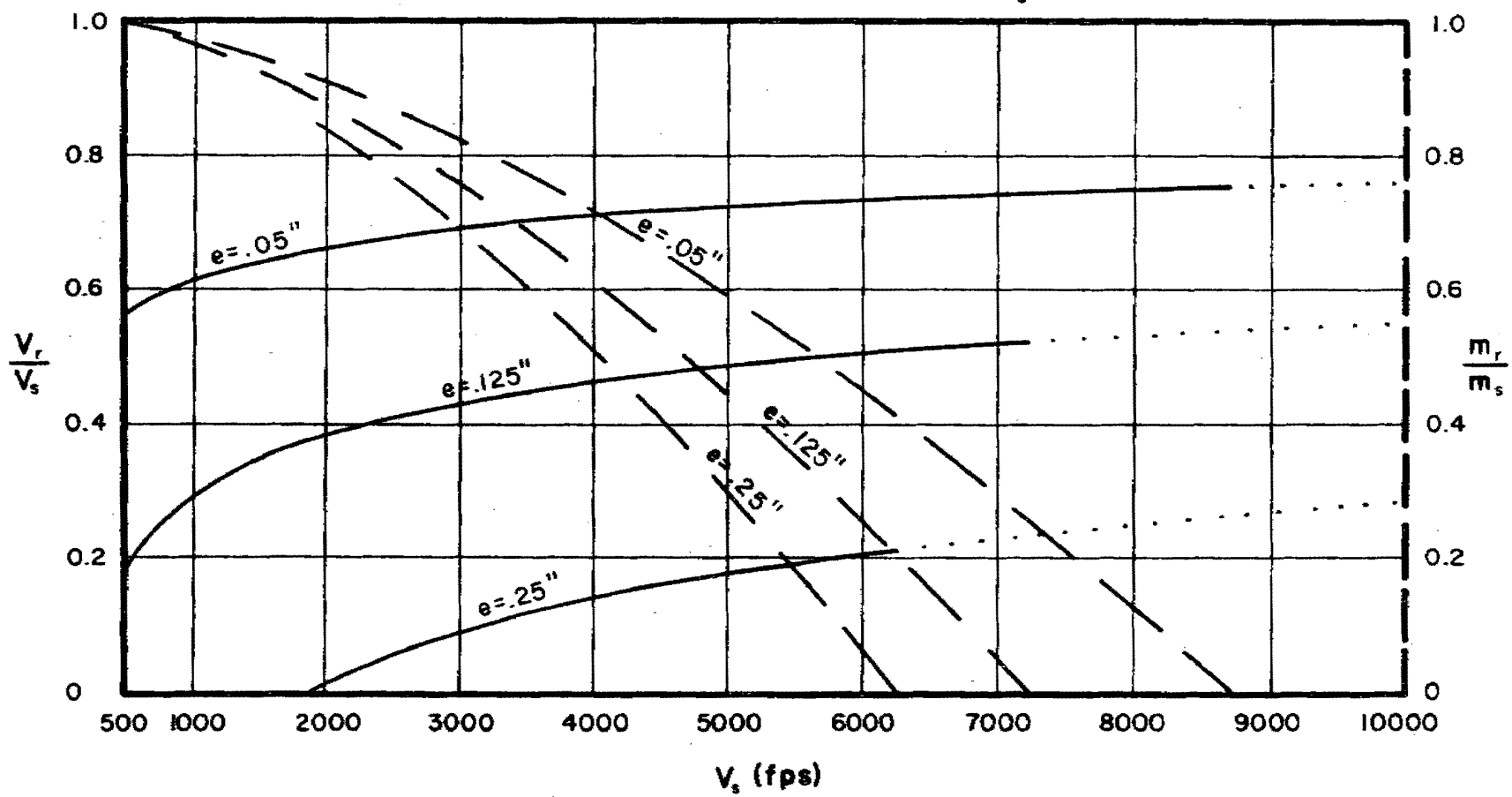

Fig. 102

$\frac{V_r}{V_s}$ and $\frac{m_r}{m_s}$ vs V_s for Selected Target Thicknesses

Target: Lead

Obliquity: 0°

Fragment Size: 30 grains

Dashed Thickness Contours Refer to $\frac{m_r}{m_s}$ Ordinate

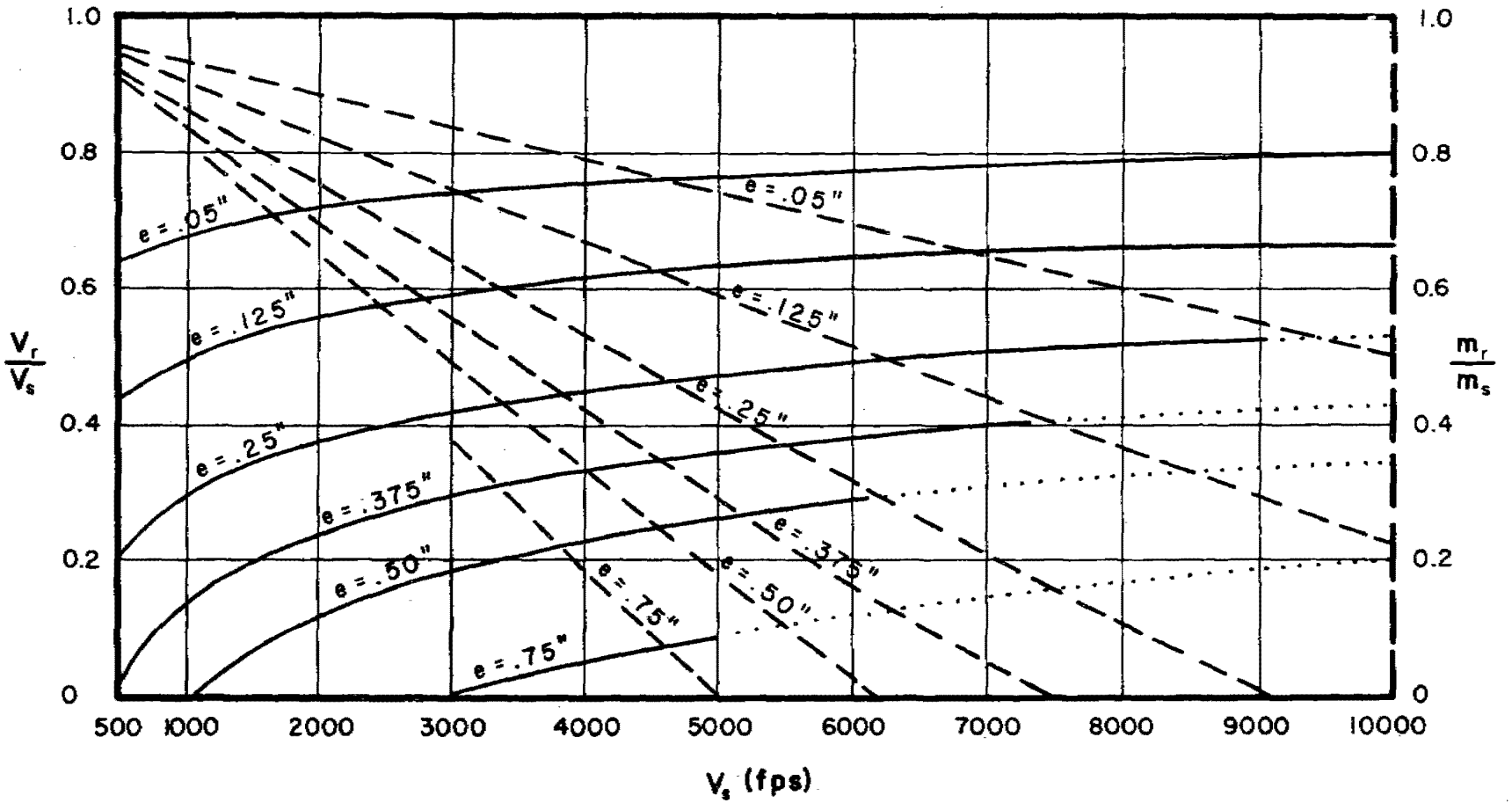

Fig. 103

$\frac{V_r}{V_s}$ and $\frac{m_r}{m_s}$ vs V_s for Selected Target Thicknesses

Target: Lead

Obliquity: 60°

Fragment Size: 30 grains

Dashed Thickness Contours Refer to $\frac{m_r}{m_s}$ Ordinate

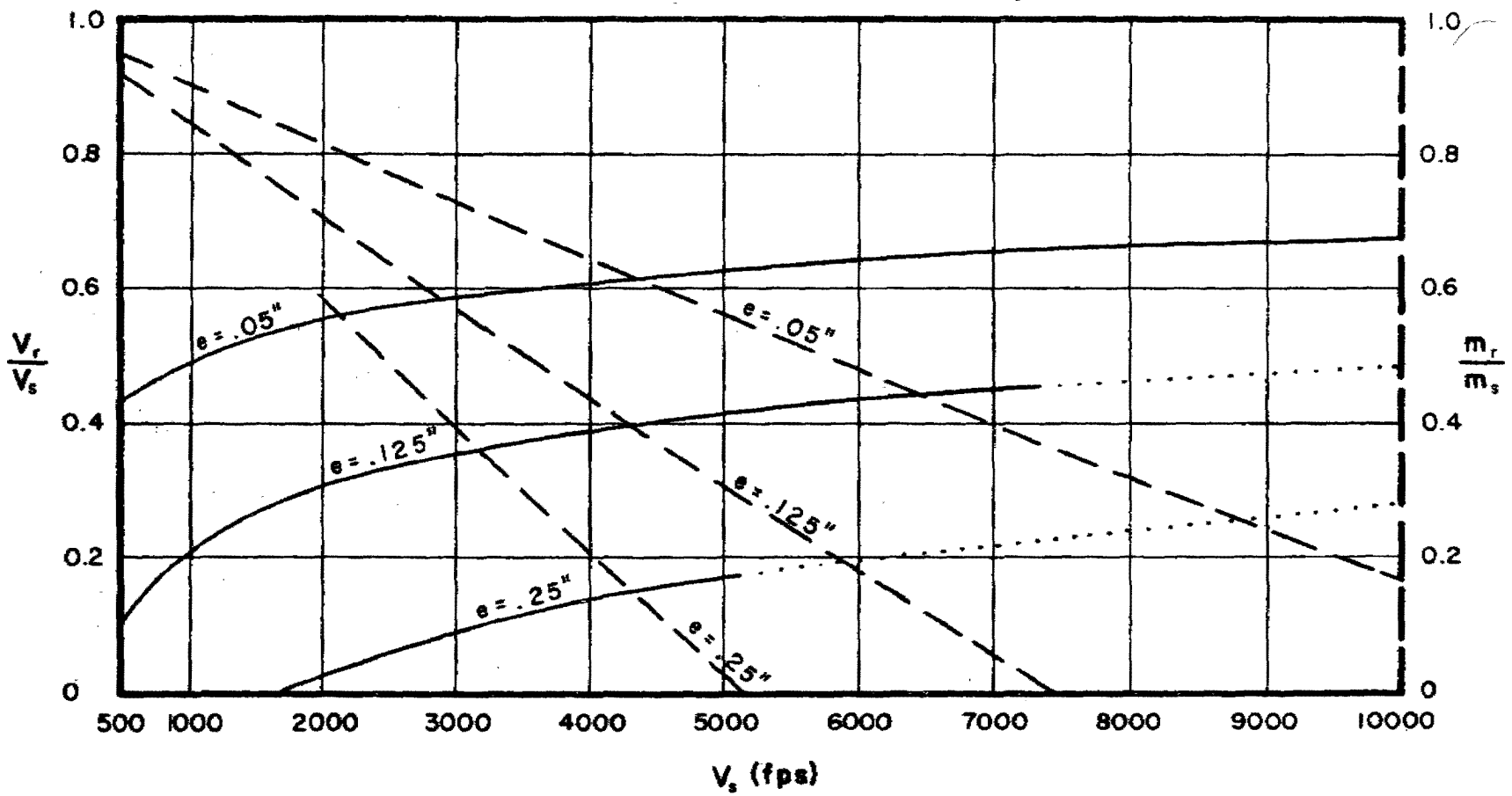

Fig. 104

$\frac{V_r}{V_s}$ and $\frac{m_r}{m_s}$ vs V_s for Selected Target Thicknesses

Target: Lead

Obliquity: 70°

Fragment Size: 30 grains

Dashed Thickness Contours Refer to $\frac{m_r}{m_s}$ Ordinate

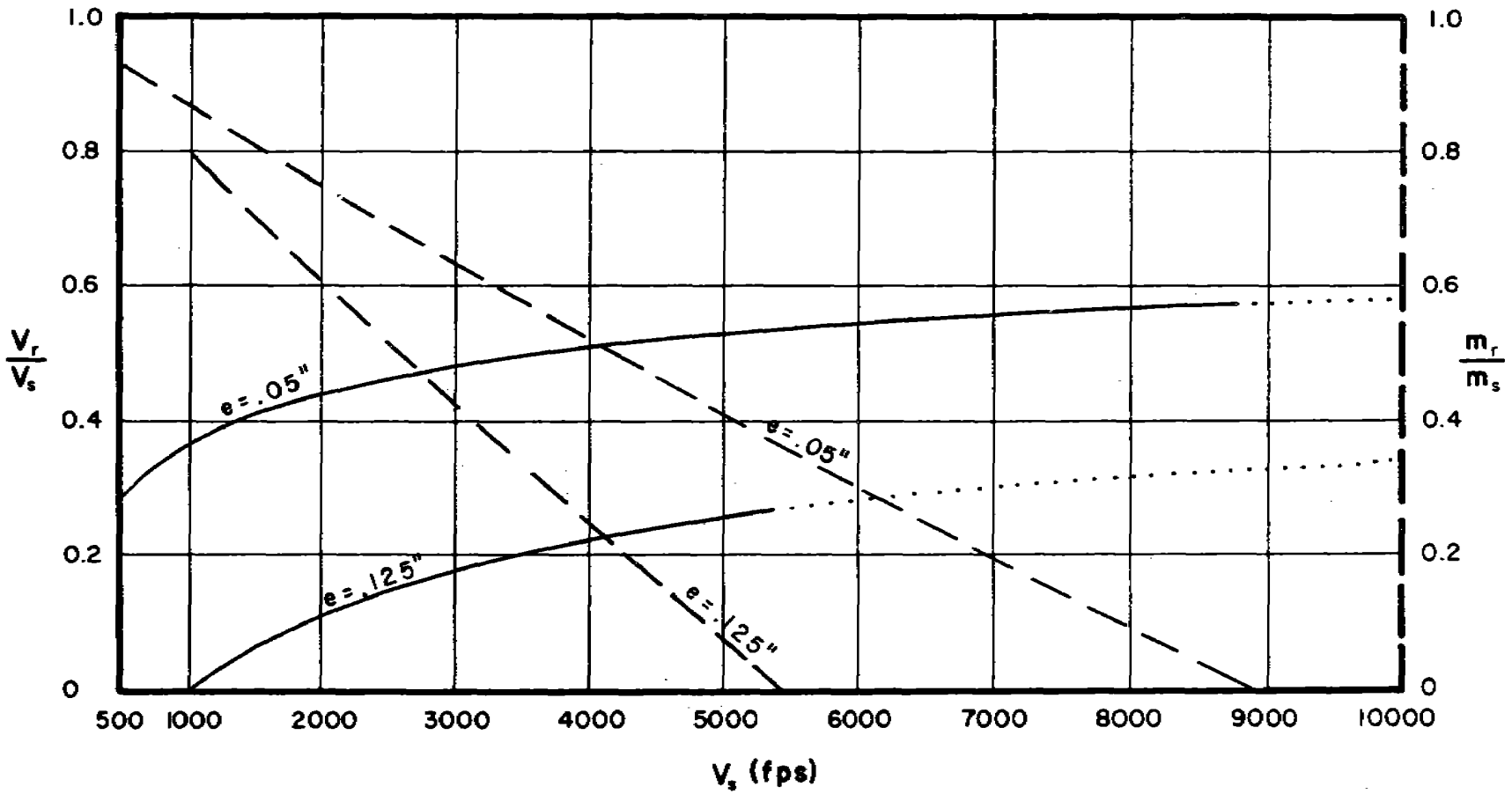

Fig. 105

$\frac{V_r}{V_s}$ and $\frac{m_r}{m_s}$ vs V_s for Selected Target Thicknesses

Target: Lead

Obliquity: 0°

Fragment Size: 100 grains

Dashed Thickness Contours Refer to $\frac{m_r}{m_s}$ Ordinate

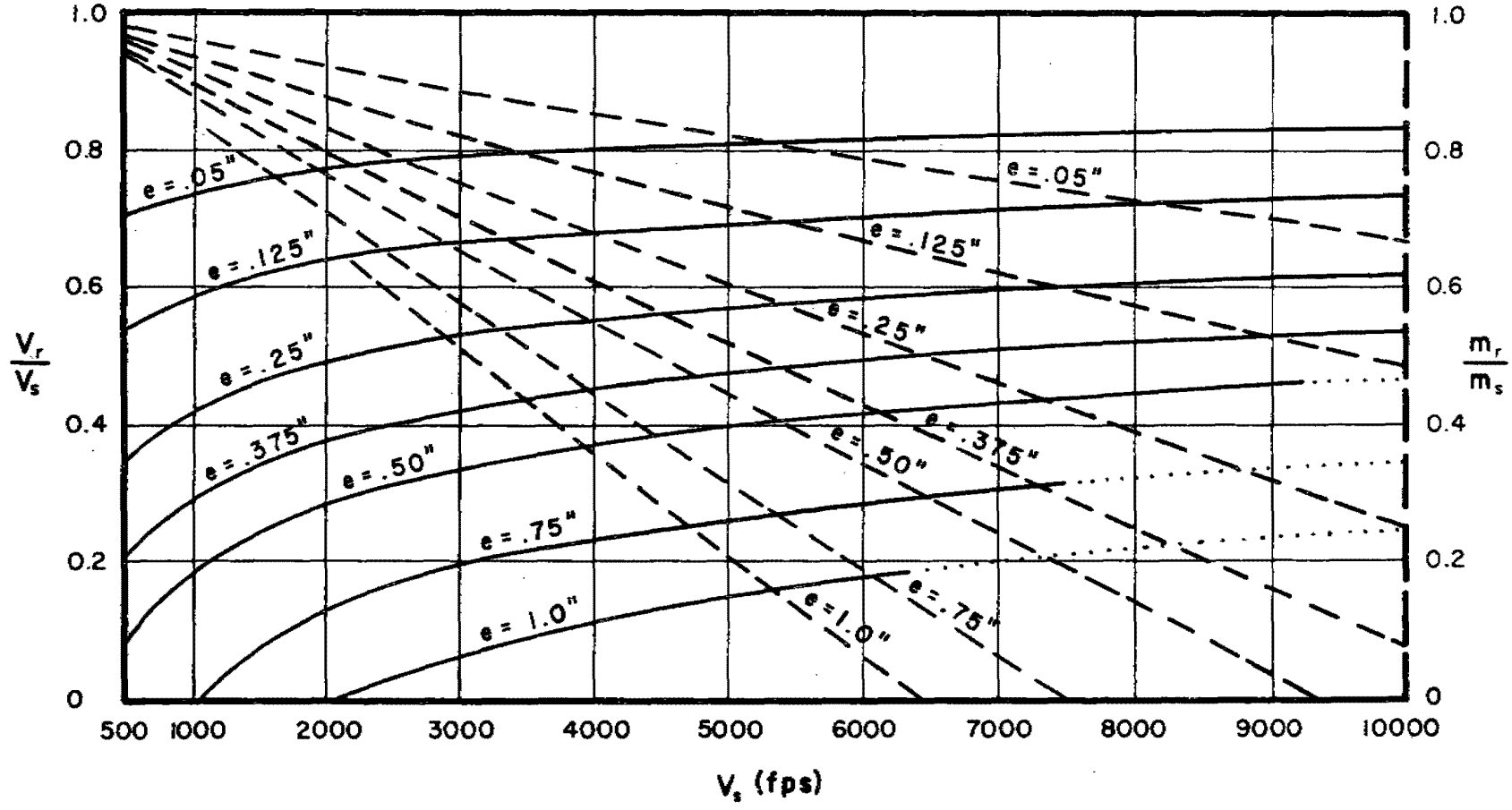

Fig. 106

$\frac{V_r}{V_s}$ and $\frac{m_r}{m_s}$ vs V_s for Selected Target Thicknesses

Target: Lead

Obliquity: 60°

Fragment Size: 100 grains

Dashed Thickness Contours Refer to $\frac{m_r}{m_s}$ Ordinate

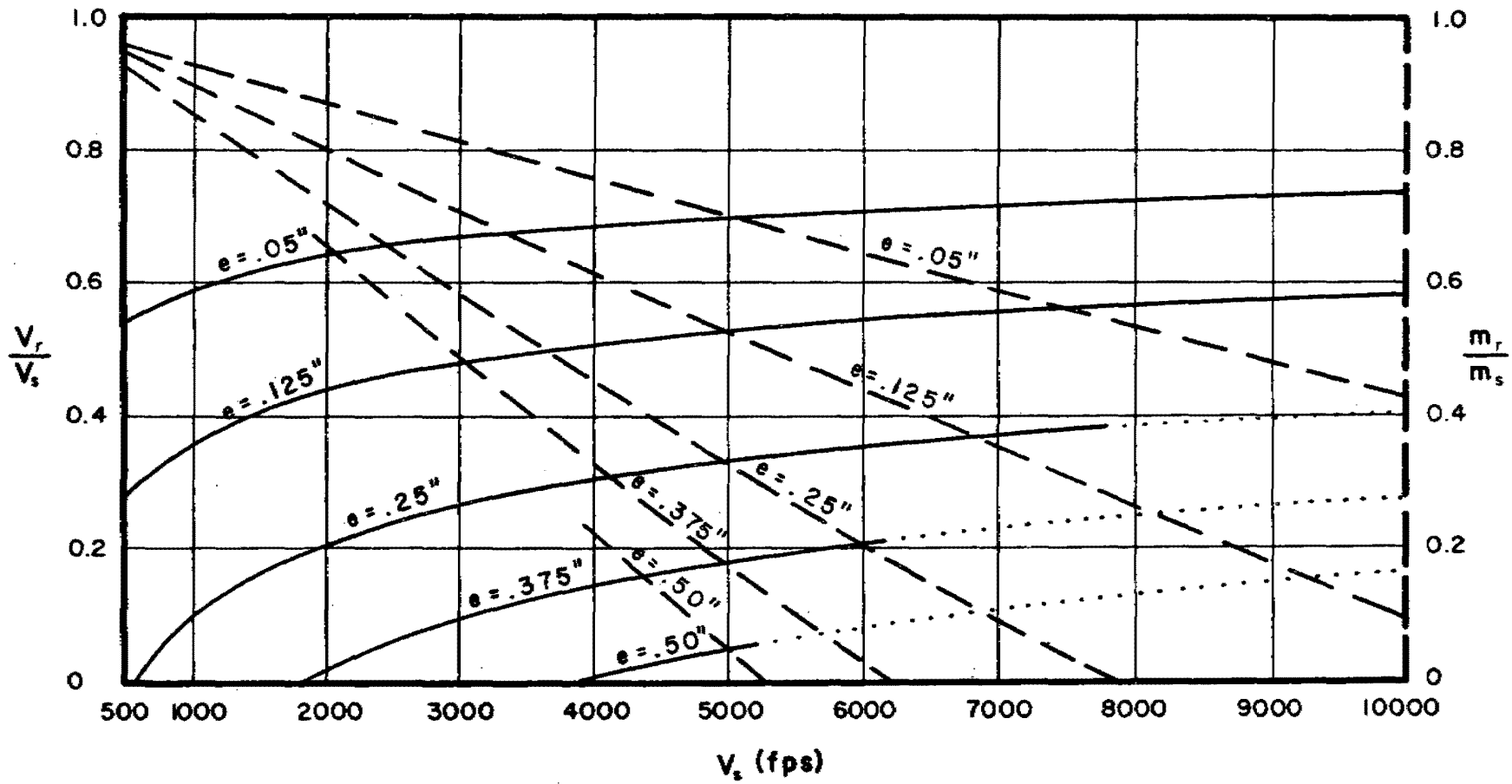

Fig. 107

$\frac{V_r}{V_s}$ and $\frac{m_r}{m_s}$ vs V_s for Selected Target Thicknesses

Target: Lead

Obliquity: 70°

Fragment Size: 100 grains

Dashed Thickness Contours Refer to $\frac{m_r}{m_s}$ Ordinate

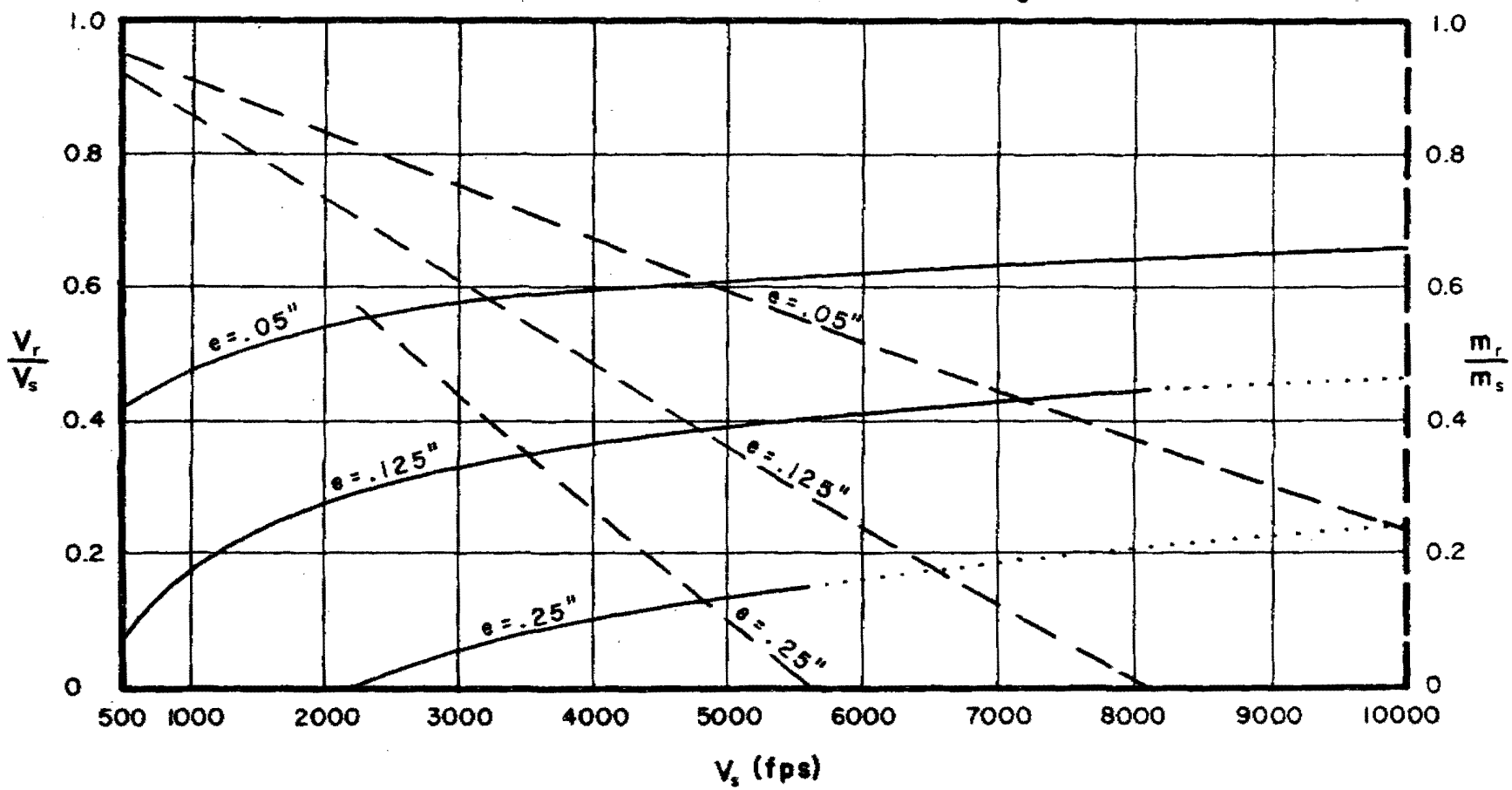

Fig. 108

$\frac{V_r}{V_s}$ and $\frac{m_r}{m_s}$ vs V_s for Selected Target Thicknesses

Target: Lead

Obliquity: 0°

Fragment Size: 300 grains

Dashed Thickness Contours Refer to $\frac{m_r}{m_s}$ Ordinate

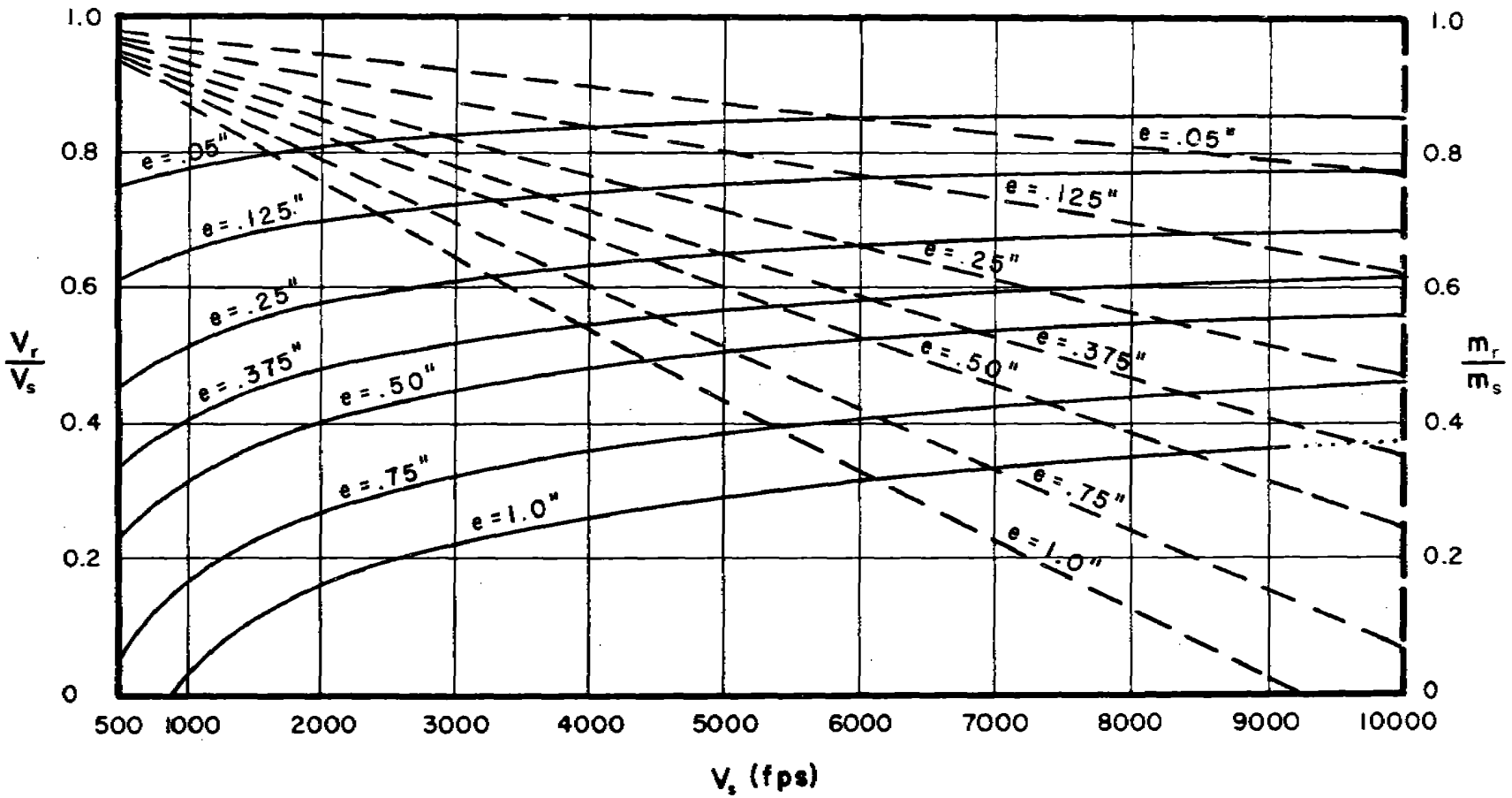

Fig. 109

$\frac{V_r}{V_s}$ and $\frac{m_r}{m_s}$ vs V_s for Selected Target Thicknesses

Target: Lead

Obliquity: 60°

Fragment Size: 300 grains

Dashed Thickness Contours Refer to $\frac{m_r}{m_s}$ Ordinate

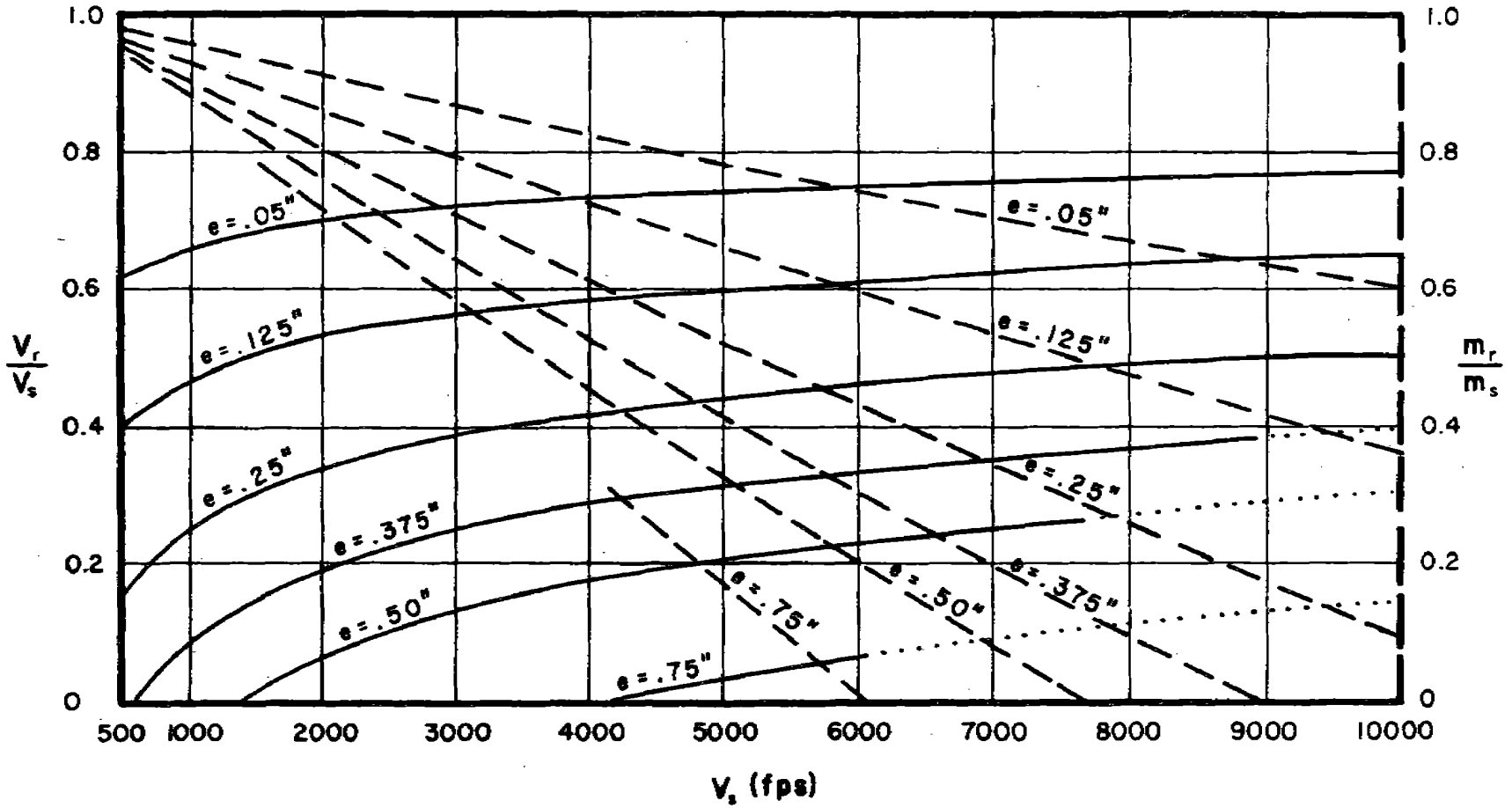

Fig. 110

$\frac{V_r}{V_s}$ and $\frac{m_r}{m_s}$ vs V_s for Selected Target Thicknesses

Target: Lead

Obliquity: 70°

Fragment Size: 300 grains

Dashed Thickness Contours Refer to $\frac{m_r}{m_s}$ Ordinate

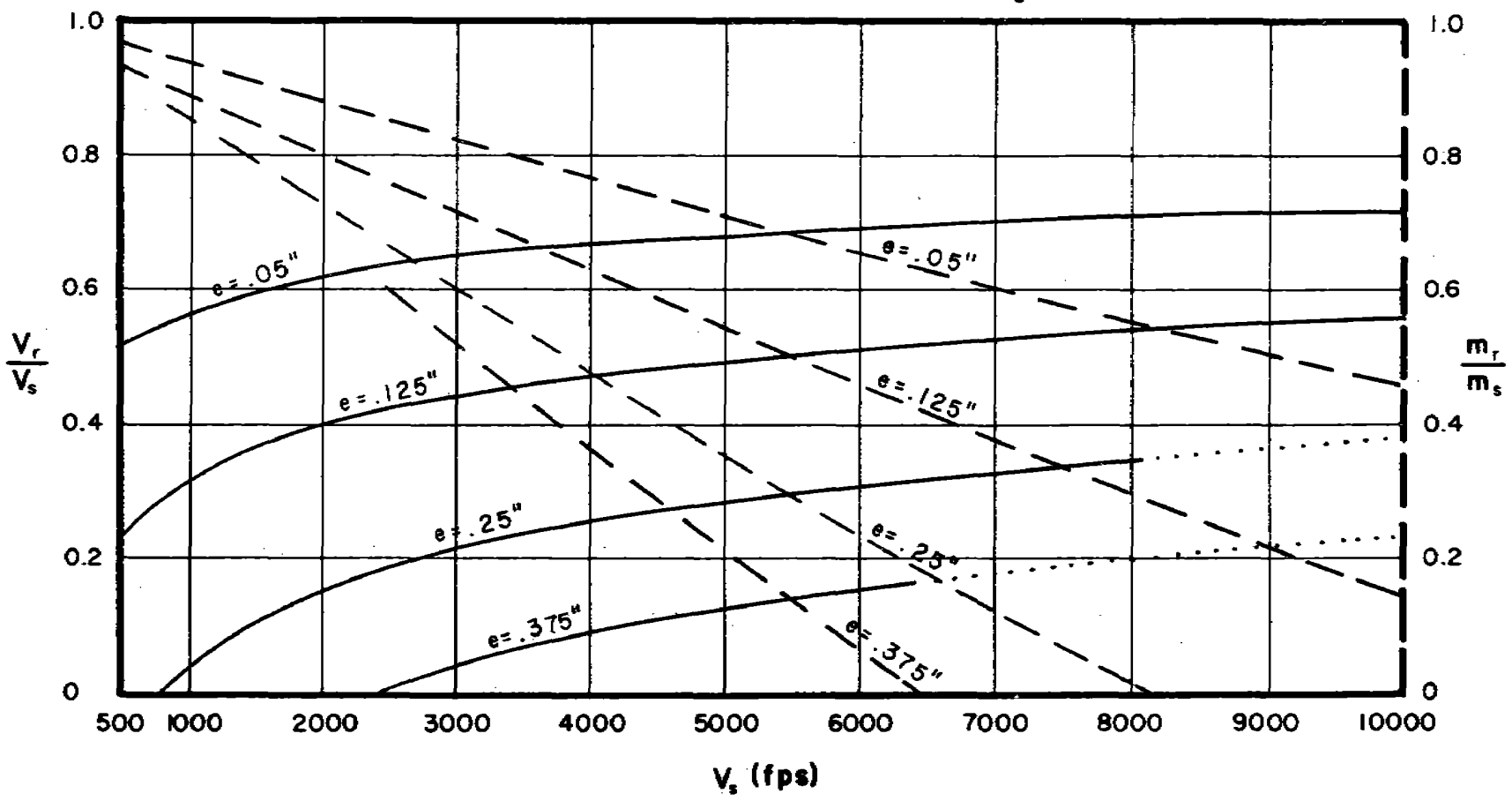

Fig. 111

$\frac{V_r}{V_s}$ and $\frac{m_r}{m_s}$ vs V_s for Selected Target Thicknesses

Target: Tuballoy

Obliquity: 0°

Fragment Size: 30 grains

Dashed Thickness Contours Refer to $\frac{m_r}{m_s}$ Ordinate

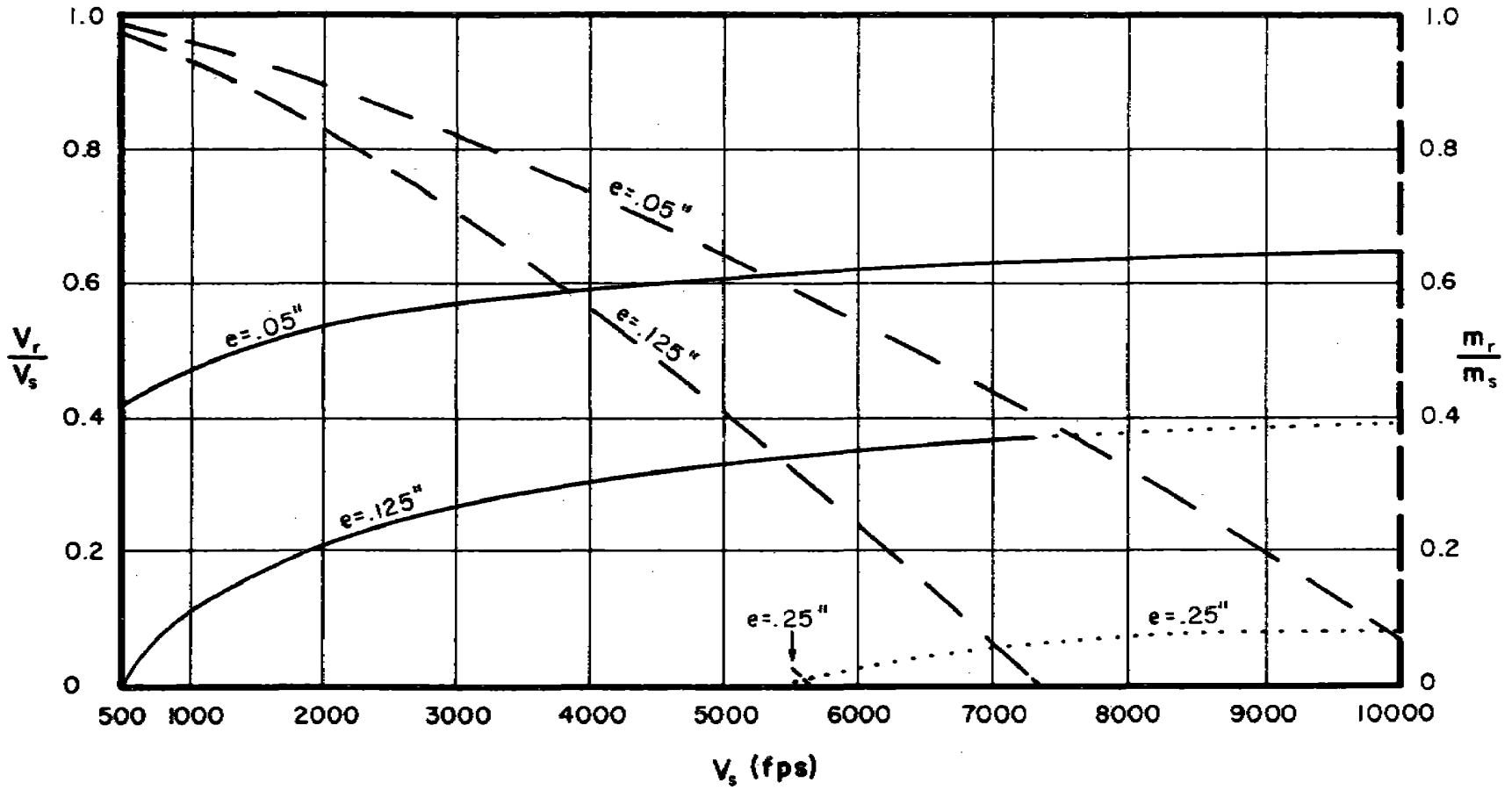

Fig. 112

$\frac{V_r}{V_s}$ and $\frac{m_r}{m_s}$ vs V_s for Selected Target Thicknesses

Target: Tuballoy

Obliquity: 60°

Fragment Size: 30 grains

Dashed Thickness Contours Refer to $\frac{m_r}{m_s}$ Ordinate

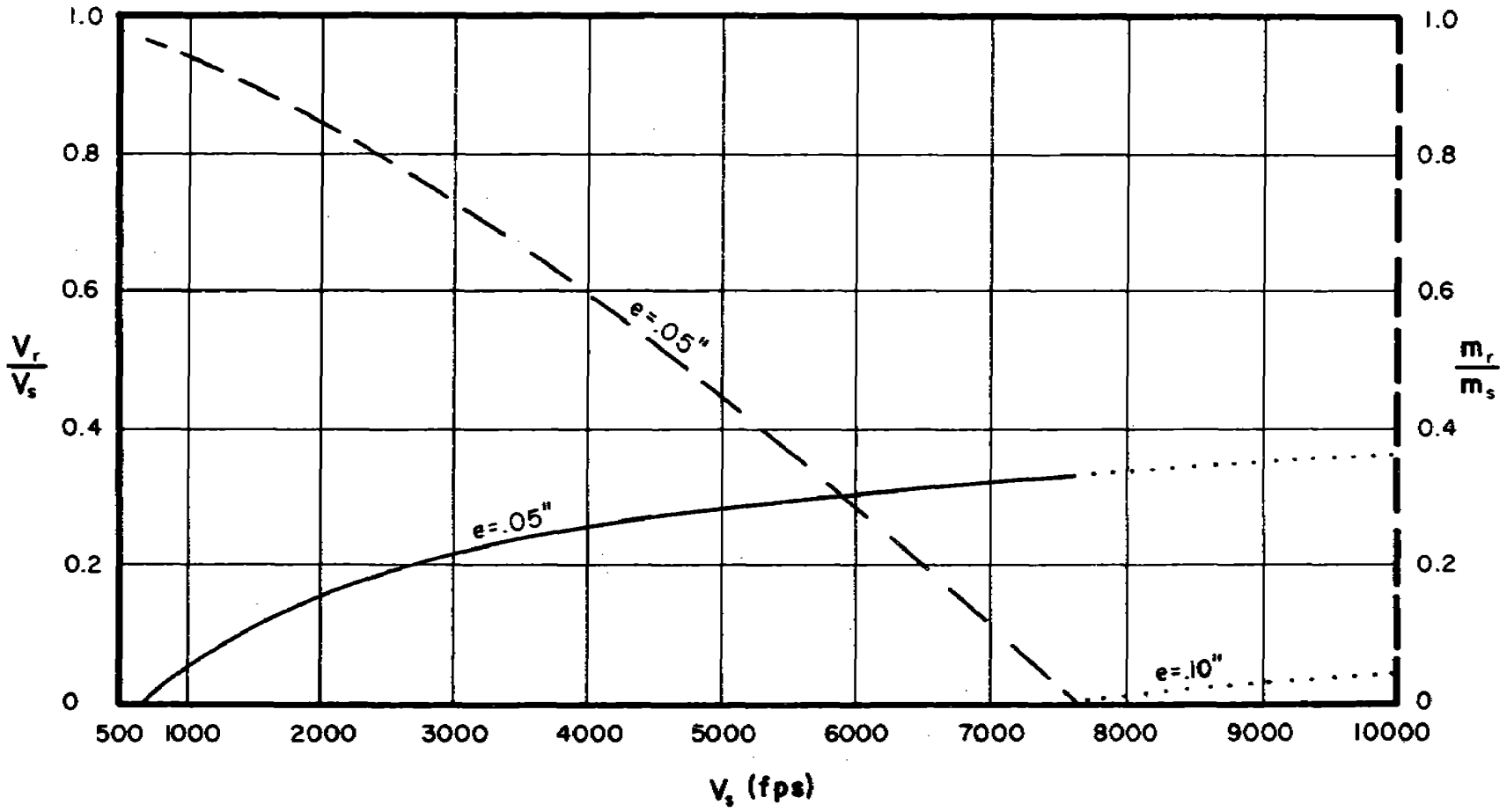

Fig. 113

$\frac{V_r}{V_s}$ and $\frac{m_r}{m_s}$ vs V_s for Selected Target Thicknesses

Target: Tuballoy

Obliquity: 70°

Fragment Size: 30 grains

Dashed Thickness Contours Refer to $\frac{m_r}{m_s}$ Ordinate

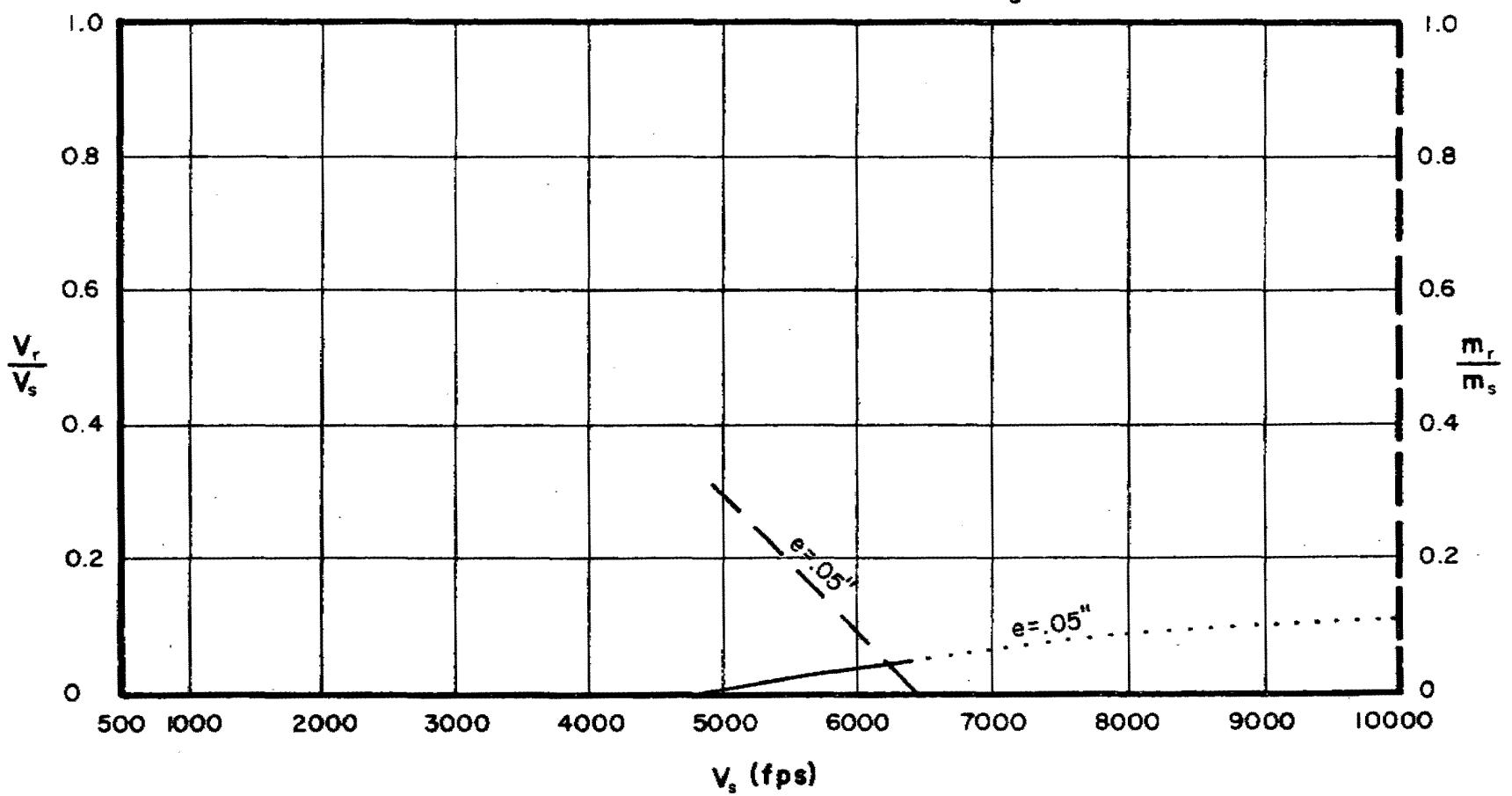

Fig. 114

$\frac{V_r}{V_s}$ and $\frac{m_r}{m_s}$ vs V_s for Selected Target Thicknesses

Target: Tuballoy

Obliquity: 0°

Fragment Size: 100 grains

Dashed Thickness Contours Refer to $\frac{m_r}{m_s}$ Ordinate

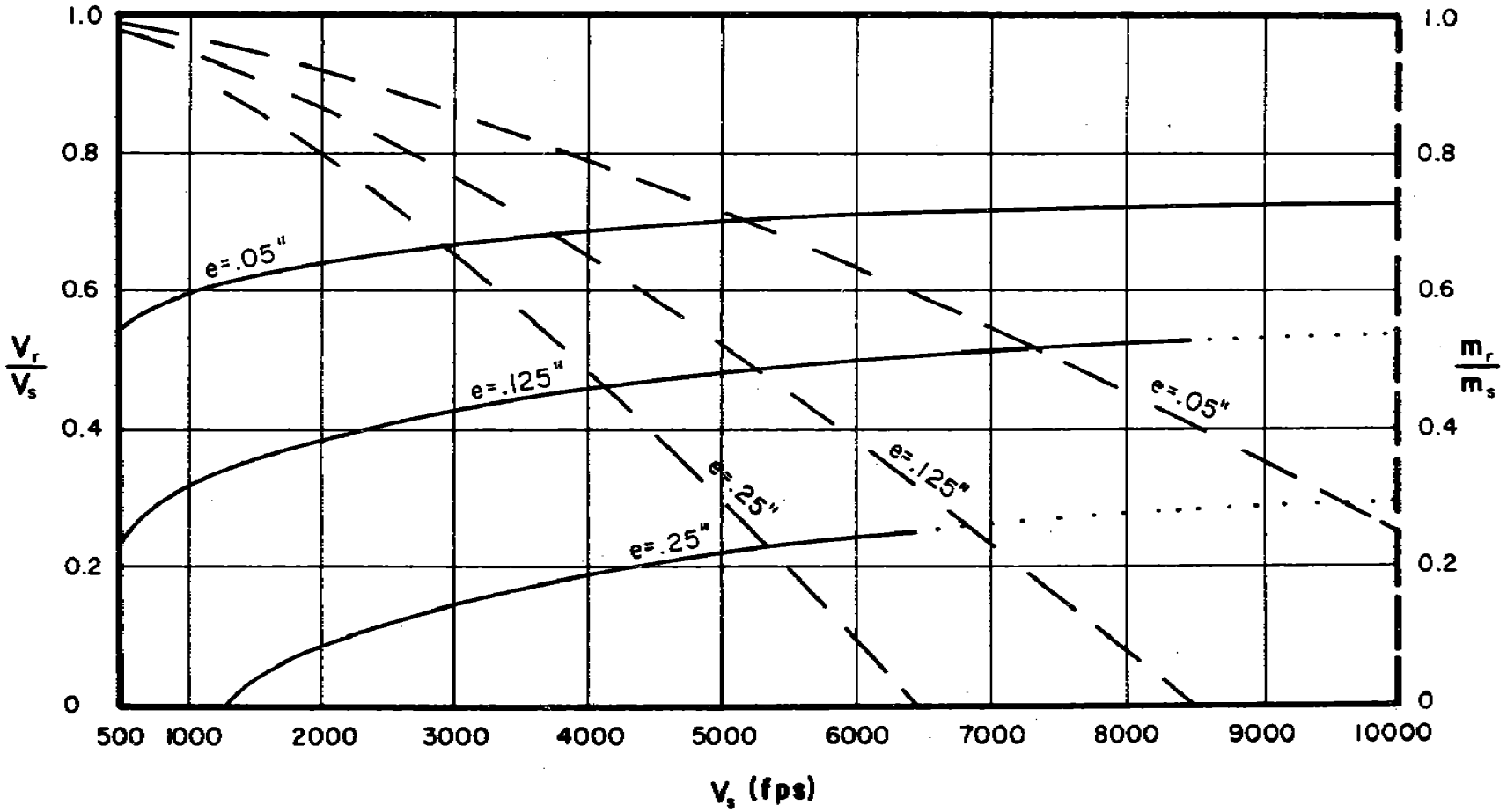

Fig. 115

$\frac{V_r}{V_s}$ and $\frac{m_r}{m_s}$ vs V_s for Selected Target Thicknesses

Target: Tuballoy

Obliquity: 60°

Fragment Size: 100 grains

Dashed Thickness Contours Refer to $\frac{m_r}{m_s}$ Ordinate

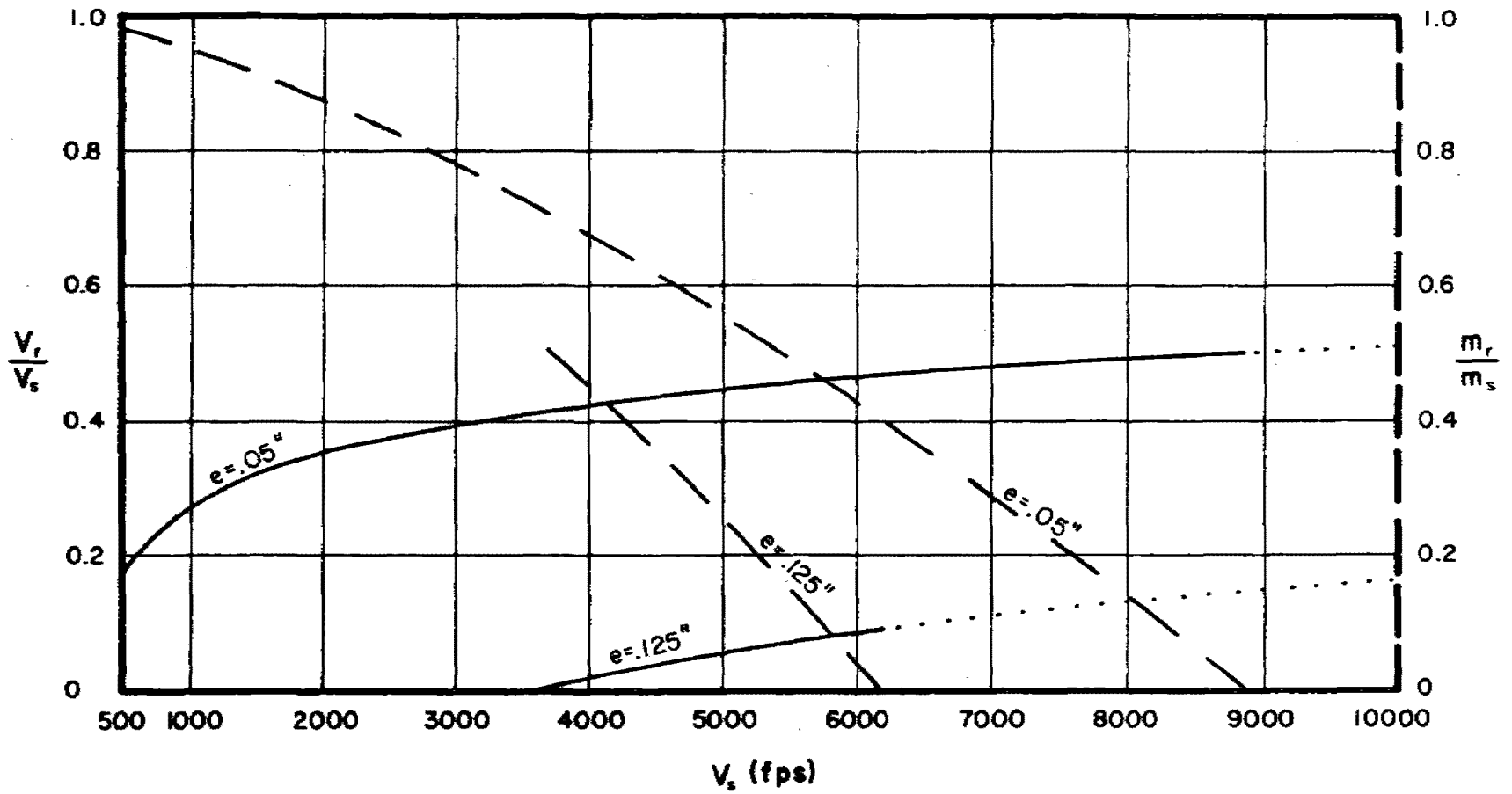

Fig. 116

$\frac{V_r}{V_s}$ and $\frac{m_r}{m_s}$ vs V_s for Selected Target Thicknesses

Target: Tuballoy

Obliquity: 70°

Fragment Size: 100 grains

Dashed Thickness Contours Refer to $\frac{m_r}{m_s}$ Ordinate

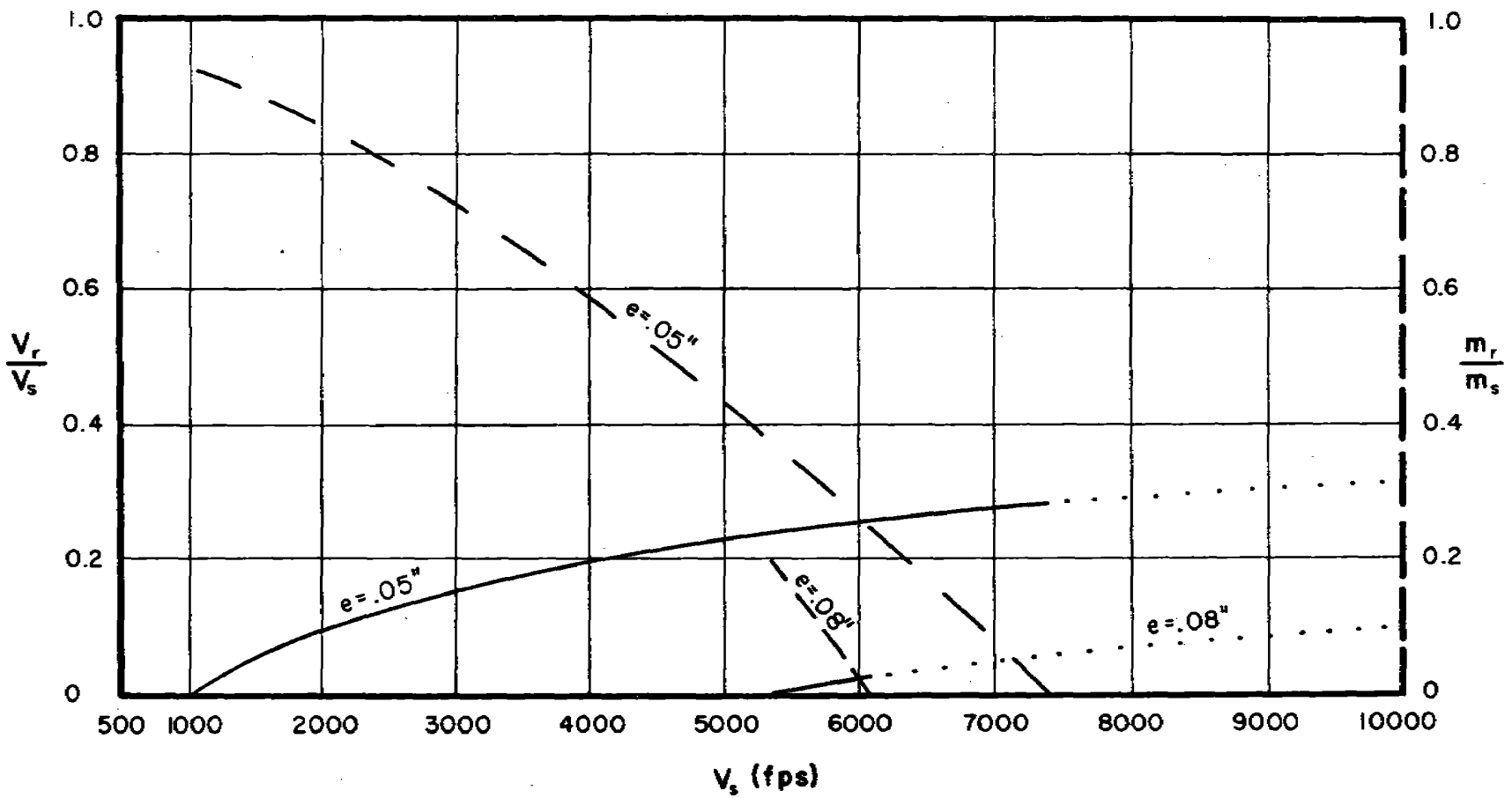

Fig. 117

$\frac{V_r}{V_s}$ and $\frac{m_r}{m_s}$ vs V_s for Selected Target Thicknesses

Target: Tuballoy

Obliquity: 0°

Fragment Size: 300 grains

Dashed Thickness Contours Refer to $\frac{m_r}{m_s}$ Ordinate

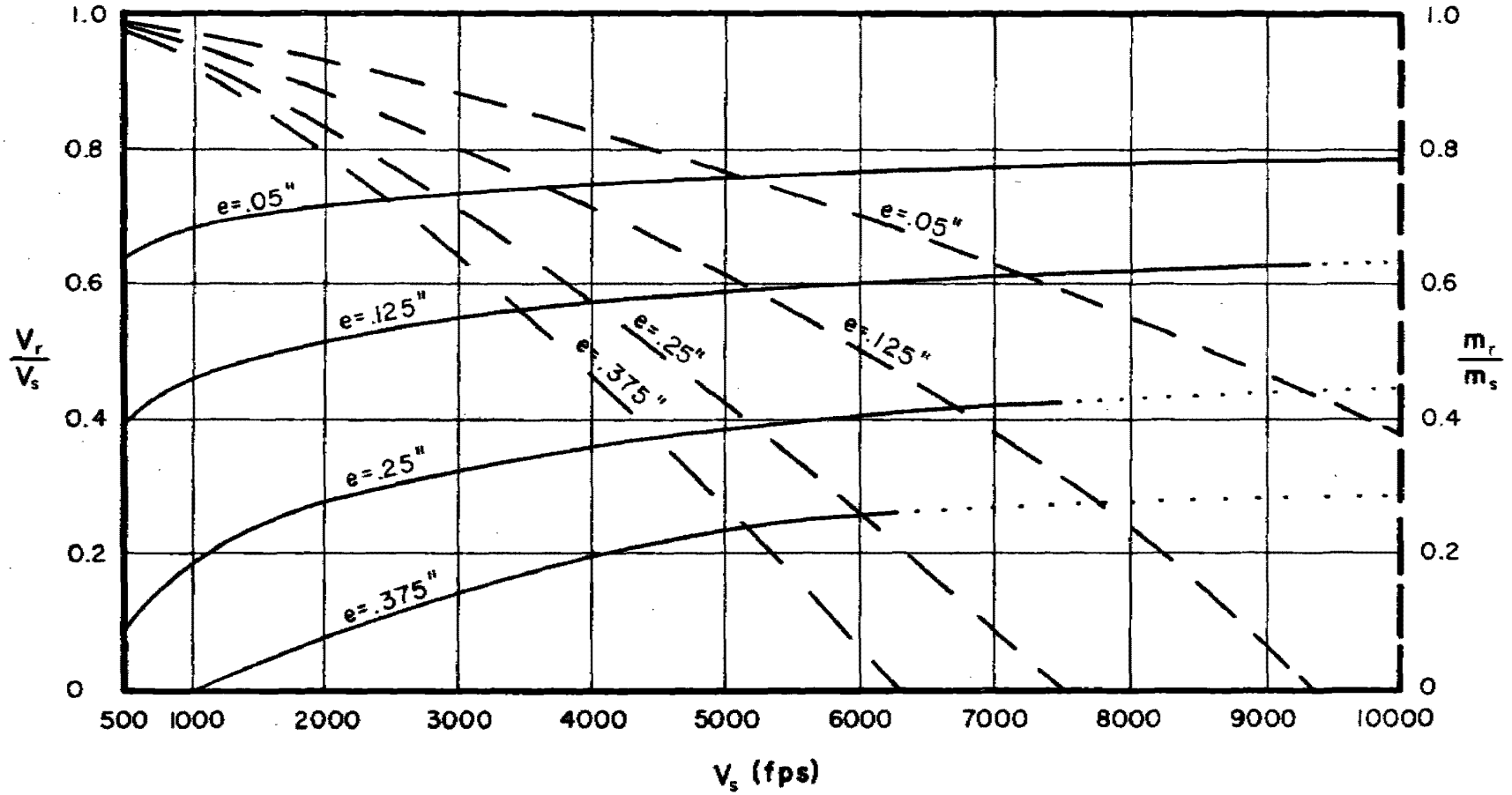

Fig. 118

$\frac{V_r}{V_s}$ and $\frac{m_r}{m_s}$ vs V_s for Selected Target Thicknesses

Target: Tuballoy

Obliquity: 60°

Fragment Size: 300 grains

Dashed Thickness Contours Refer to $\frac{m_r}{m_s}$ Ordinate

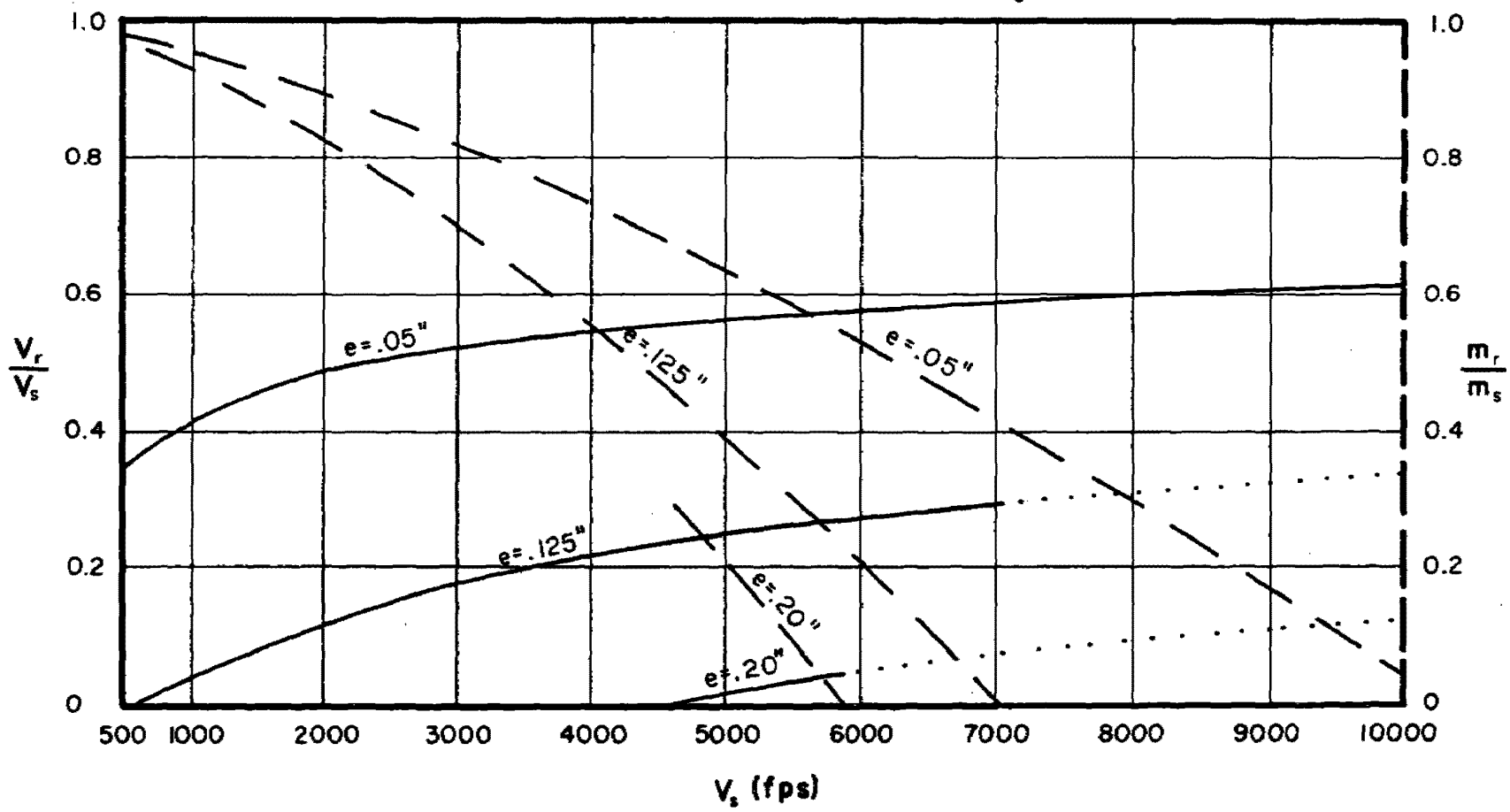

Fig. 119

$\frac{V_r}{V_s}$ and $\frac{m_r}{m_s}$ vs V_s for Selected Target Thicknesses

Target: Tuballoy

Obliquity: 70°

Fragment Size: 300 grains

Dashed Thickness Contours Refer to $\frac{m_r}{m_s}$ Ordinate

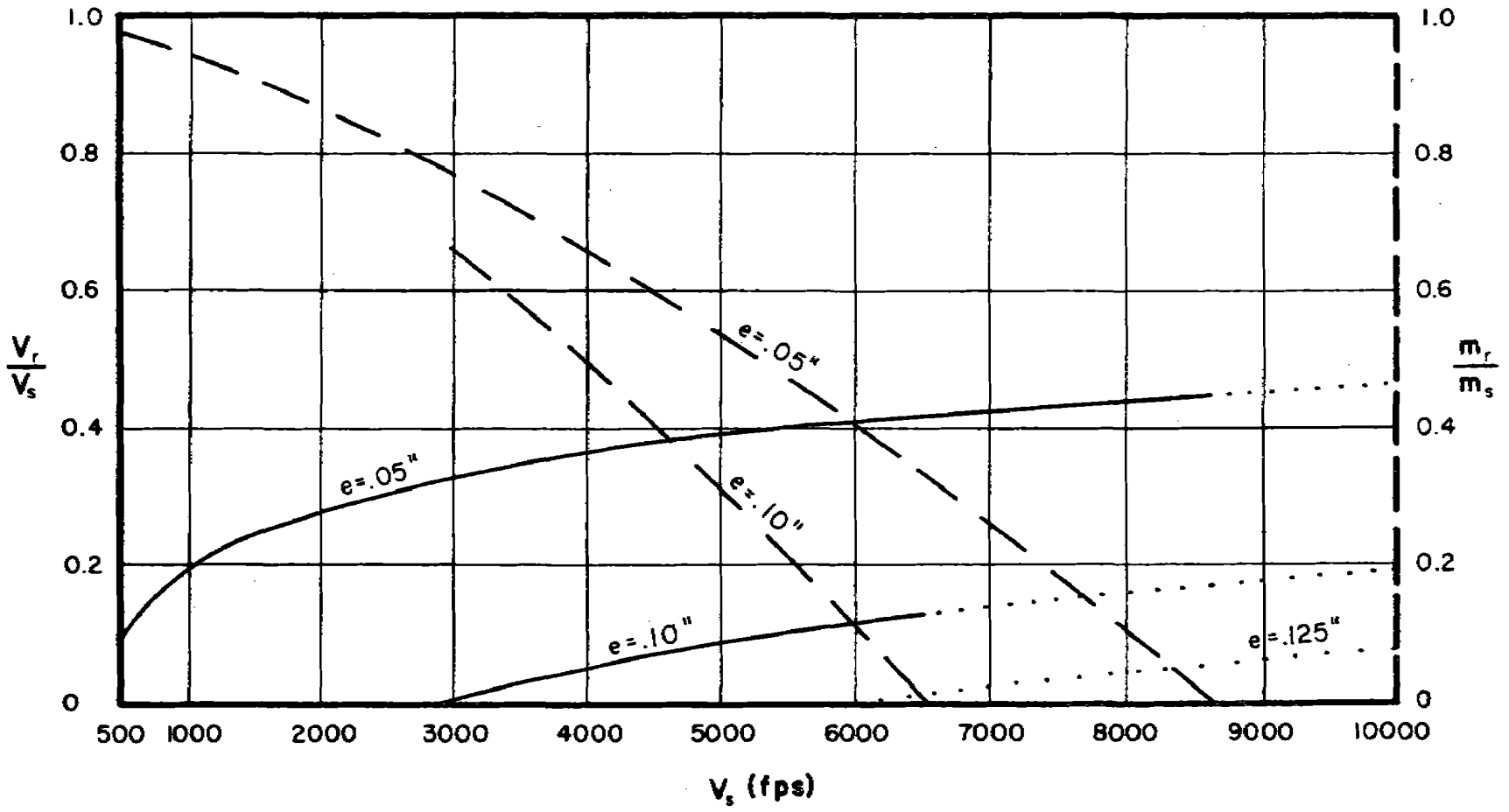

Fig. 120

[redacted]

Appendix C

Graph Set III: V_r vs E for Various Combinations of m_s, θ, and V_s

Figs. 121-147

Note: Within these sets of graphs, a contour for a particular material is shown only for those values of the abscissa for which m_r and V_r are both positive. Furthermore, the contours are not significantly extrapolated beyond the interval of thicknesses of target material employed in the basic experiments. This explains, for example, why the contours for face-hardened steel start at a value of E of 5 lb/ft^2 corresponding to a minimum experimental thickness of 0.125". No contours for cast iron appear on graphs for conditions of either 9000 fps or 70° obliquity for the reason that the experimental data did not cover these conditions. However, a contour for a given material may not appear on a graph simply because there is no permissible value of E for which both m_r and V_r are positive under the conditions for that graph.

[redacted]

[redacted]

V_r vs E for Various Combinations of m_s, θ, and V_s

m_s = 30 grains θ = 0 degrees V_s = 3000 fps

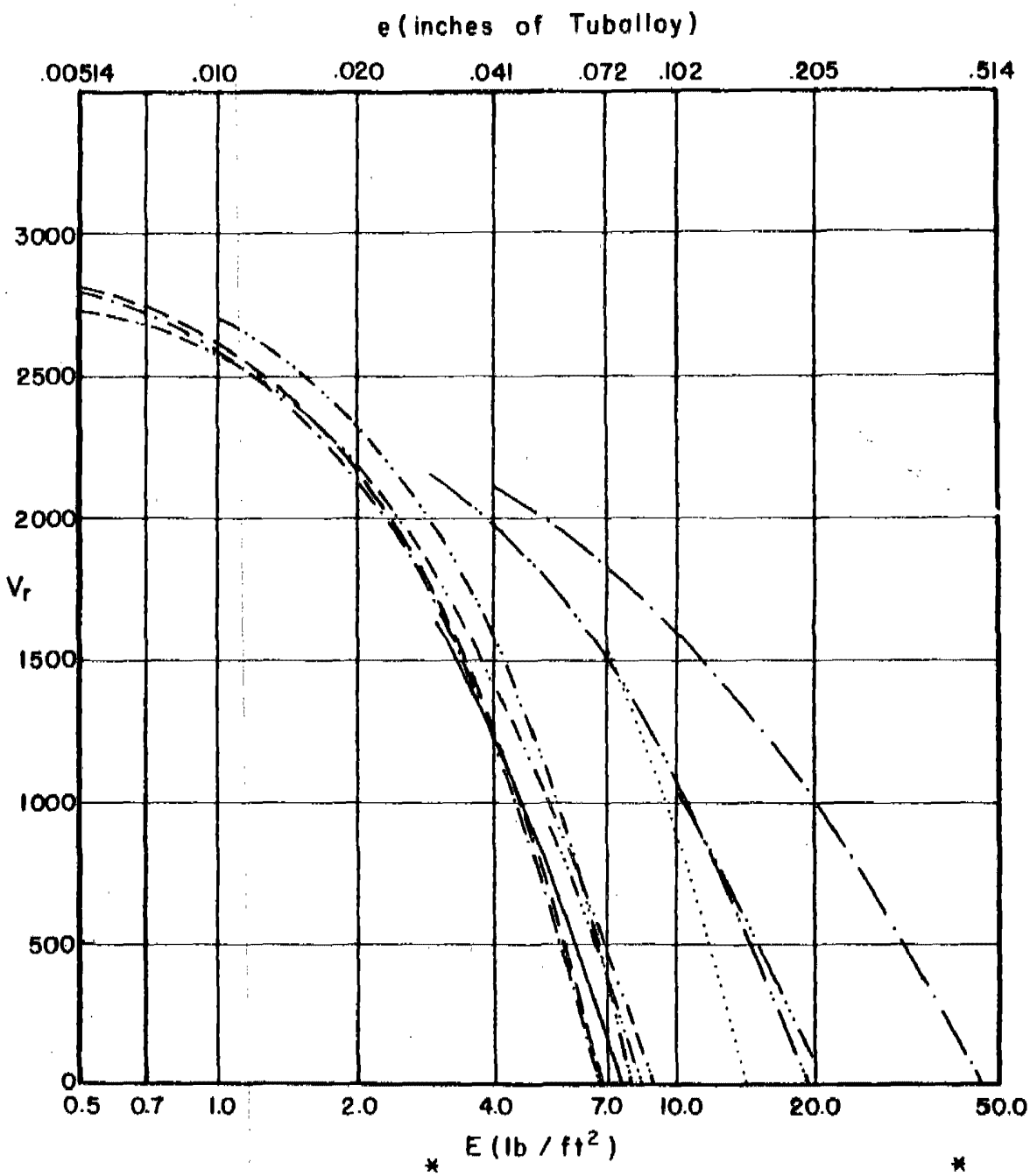

		*			*
Magnesium	———	10.58	F.H. Steel	—·—·—	2.41
2024 T-3	—·—·—	6.65	Hard Steel	———	2.41
Titanium	—··—··—	4.17	Copper	—··—	2.10
Cast Iron	·····	2.59	Lead	—·—	1.70
Mild Steel	—··—	2.41	Tuballoy	—···—	1.00

*Ratio of Material Thickness Relative to a Unit Thickness of Tuballoy

Fig. 121

[redacted]

[redacted]

V_r vs E for Various Combinations of m_s, θ, and V_s

m_s = 100 grains θ = 0 degrees V_s = 3000 fps

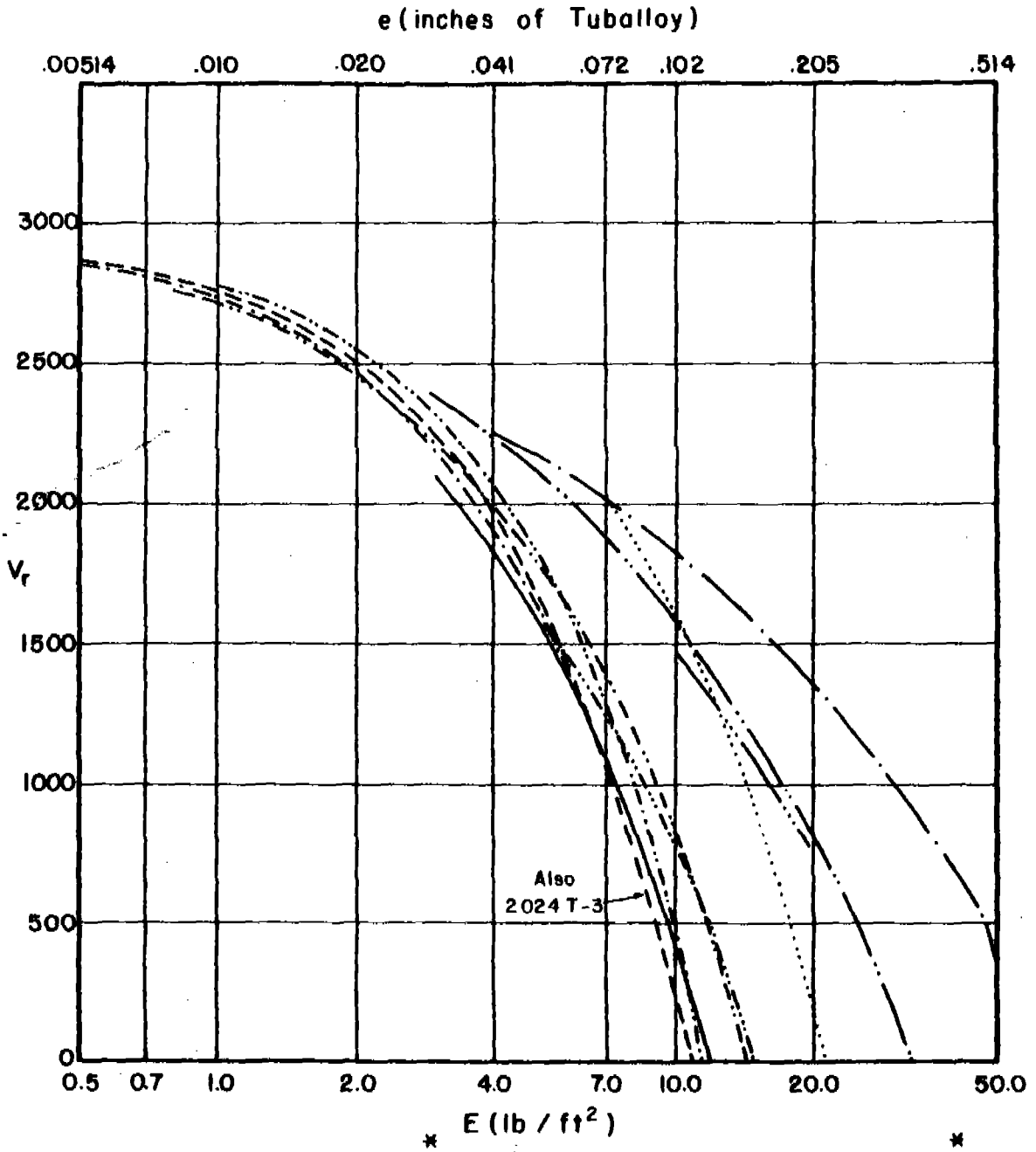

		*			*
Magnesium	— — — —	10.58	F.H. Steel	—··—··—	2.41
2024 T-3	—·—·—	6.65	Hard Steel	———	2.41
Titanium	—··—··—	4.17	Copper	—··—	2.10
Cast Iron	·····	2.59	Lead	—·—	1.70
Mild Steel	—··— —	2.41	Tuballoy	—···—	1.00

*Ratio of Material Thickness Relative to a Unit Thickness of Tuballoy

Fig. 122

[redacted]

[redacted]

V_r vs E for Various Combinations of m_s, θ, and V_s

m_s = 300 grains θ = 0 degrees V_s = 3000 fps

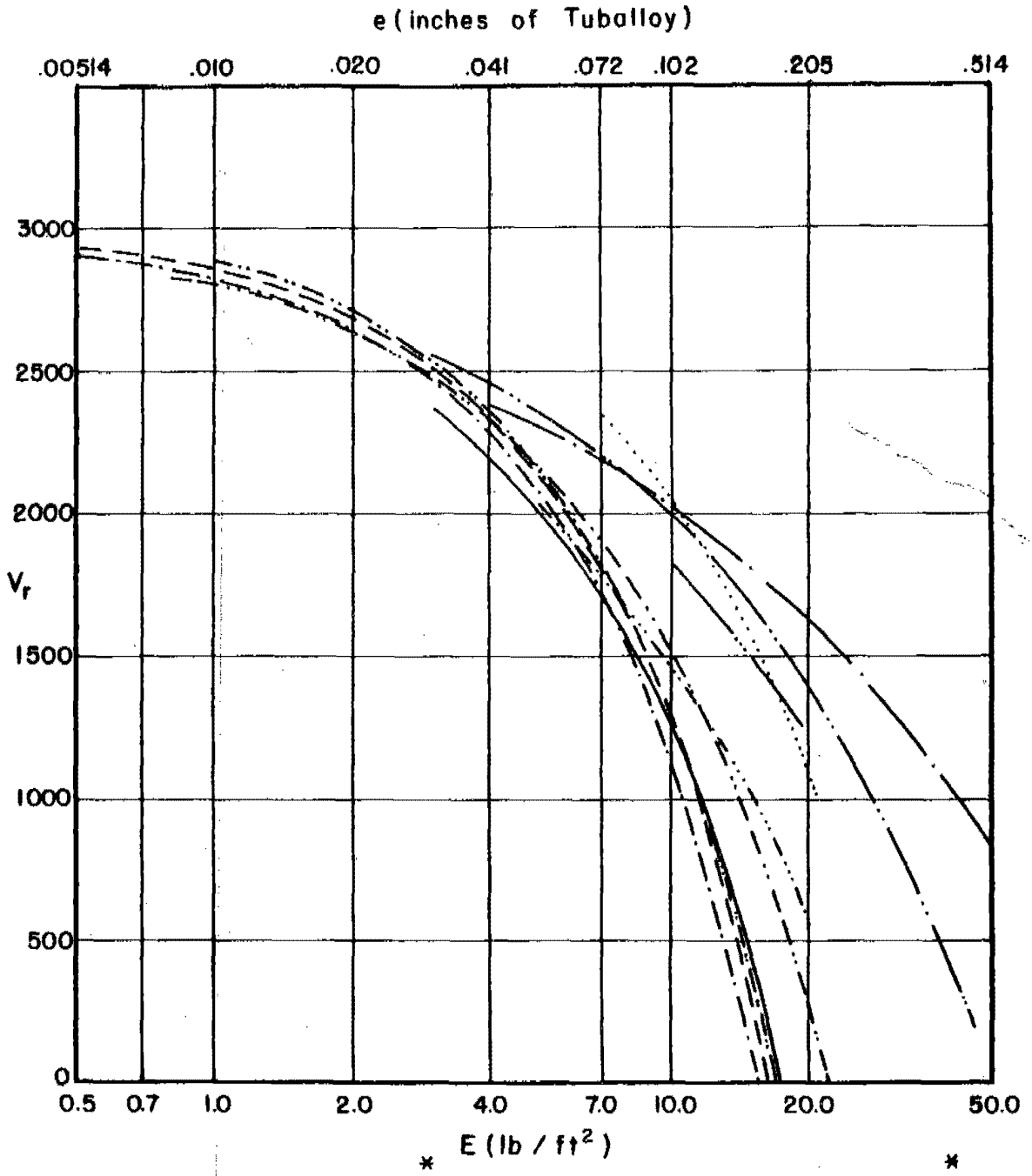

		*			*
Magnesium	— — — —	10.58	F.H. Steel	—·····—·····—	2.41
2024 T-3	—·—·—·—	6.65	Hard Steel	————	2.41
Titanium	—··—··—	4.17	Copper	—··—	2.10
Cast Iron	·····	2.59	Lead	—·—	1.70
Mild Steel	— —··— —	2.41	Tuballoy	—····—	1.00

*Ratio of Material Thickness Relative to a Unit Thickness of Tuballoy

Fig. 123

[redacted]

[redacted]

V_r vs E for Various Combinations of m_s, θ, and V_s

m_s = 30 grains θ = 60 degrees V_s = 3000 fps

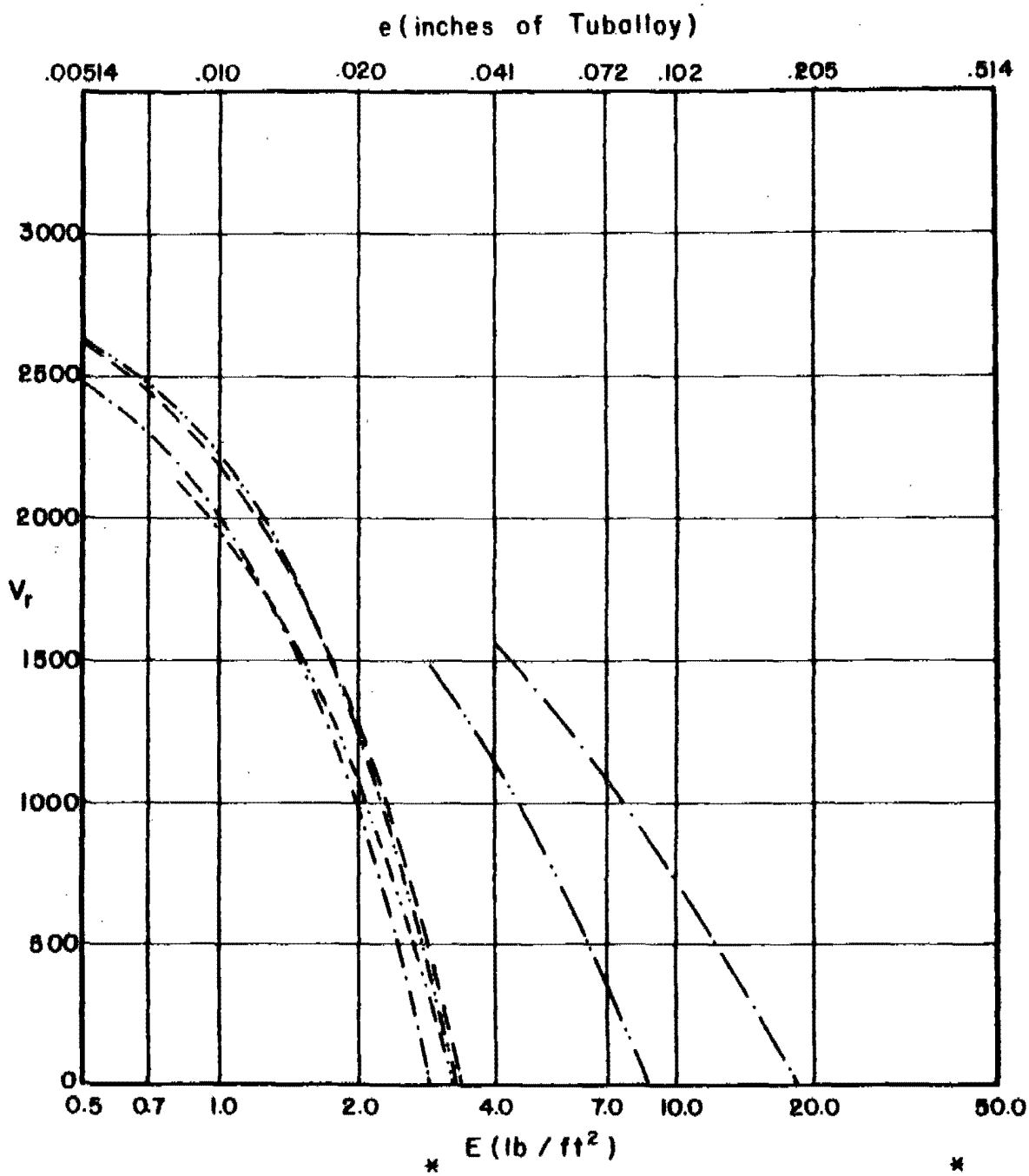

		*			*
Magnesium	— — — —	10.58	F.H. Steel	—·····—·····—	2.41
2024 T-3	—·—·—·—	6.65	Hard Steel	————	2.41
Titanium	—··—··—··	4.17	Copper	—··—	2.10
Cast Iron	·····	2.59	Lead	—·—	1.70
Mild Steel	— —··— —	2.41	Tuballoy	—···—	1.00

*Ratio of Material Thickness Relative to a Unit Thickness of Tuballoy

Fig. 124

[redacted]

[redacted]

V_r vs E for Various Combinations of m_s, θ, and V_s

m_s = 100 grains θ = 60 degrees V_s = 3000 fps

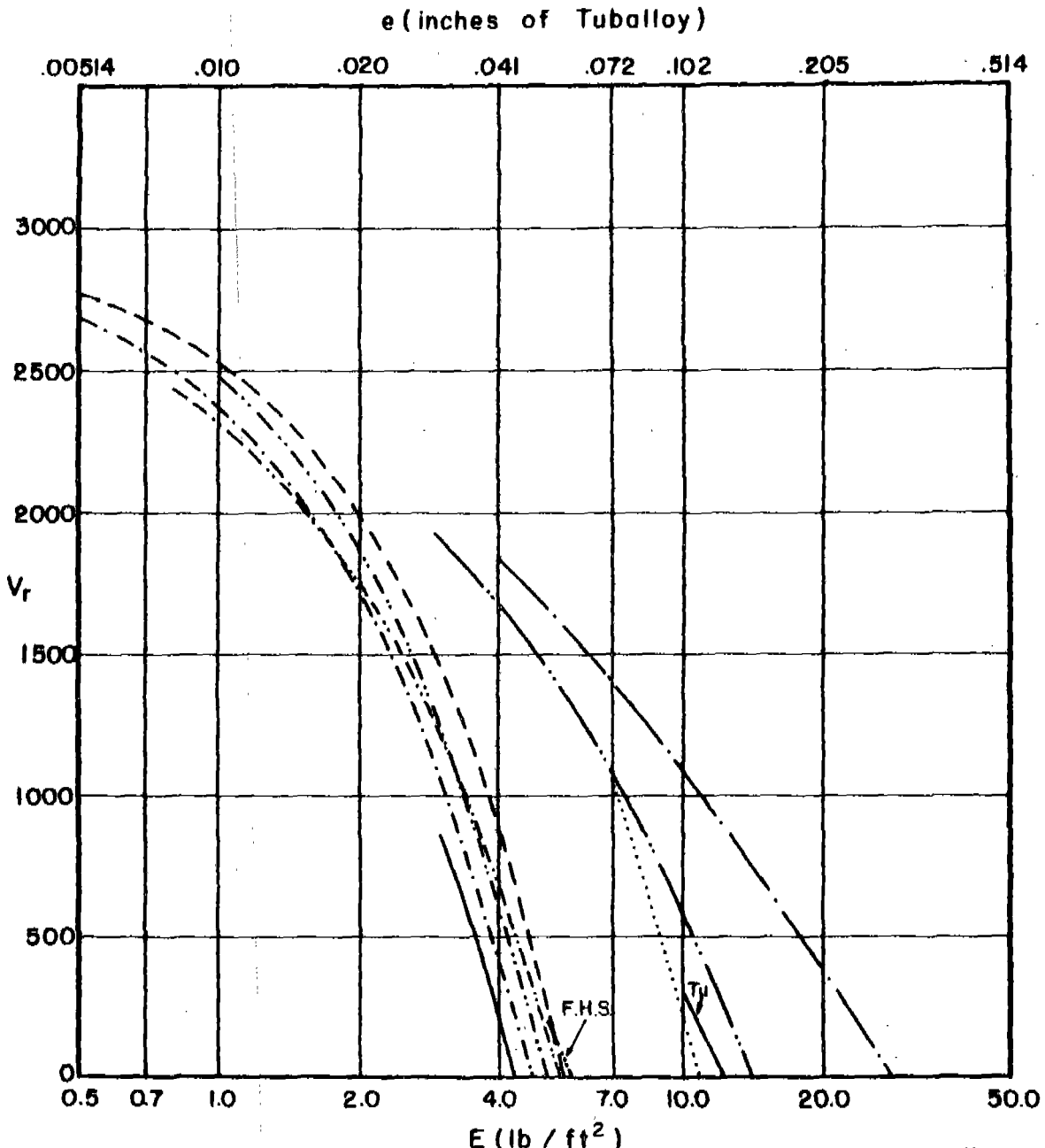

		*			*
Magnesium	— — — —	10.58	F.H. Steel	—·····—·····—	2.41
2024 T-3	—·—·—·—	6.65	Hard Steel	————	2.41
Titanium	—··—··—	4.17	Copper	—··——	2.10
Cast Iron	·····	2.59	Lead	—·—·—	1.70
Mild Steel	—··—·—	2.41	Tuballoy	—····—	1.00

*Ratio of Material Thickness Relative to a Unit Thickness of Tuballoy

Fig. 125

[redacted]

[redacted]

V_r vs E for Various Combinations of m_s, θ, and V_s

m_s = 300 grains θ = 60 degrees V_s = 3000 fps

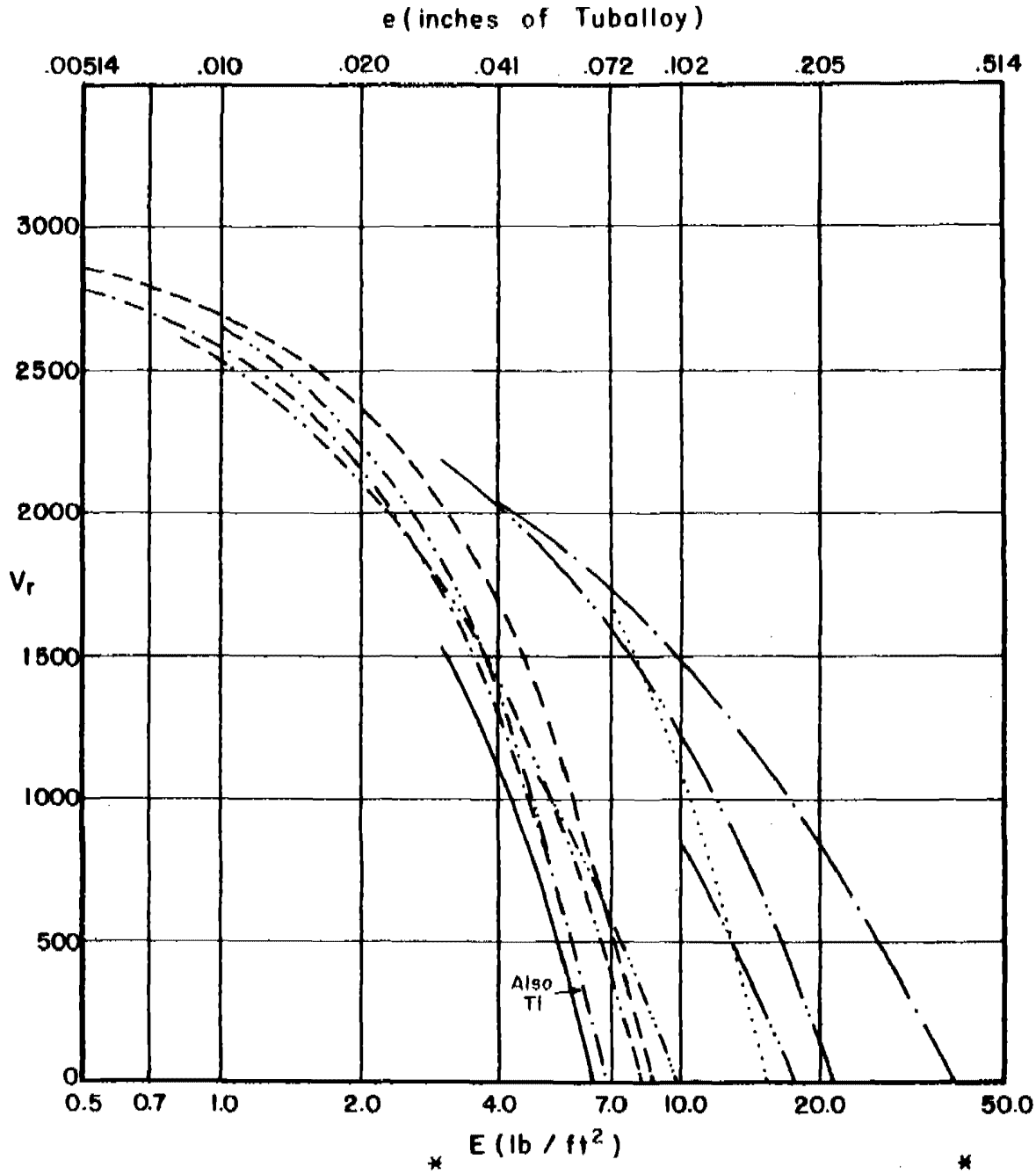

		*			*
Magnesium	— — — —	10.58	F.H. Steel	—··—··—	2.41
2024 T-3	—·—·—	6.65	Hard Steel	———	2.41
Titanium	—··—··—	4.17	Copper	—··—	2.10
Cast Iron	·····	2.59	Lead	—·—	1.70
Mild Steel	— —··— —	2.41	Tuballoy	—···—	1.00

*Ratio of Material Thickness Relative to a Unit Thickness of Tuballoy

Fig. 126

[redacted]

V_r vs E for Various Combinations of m_s, θ, and V_s

$m_s = 30$ grains $\theta = 70$ degrees $V_s = 3000$ fps

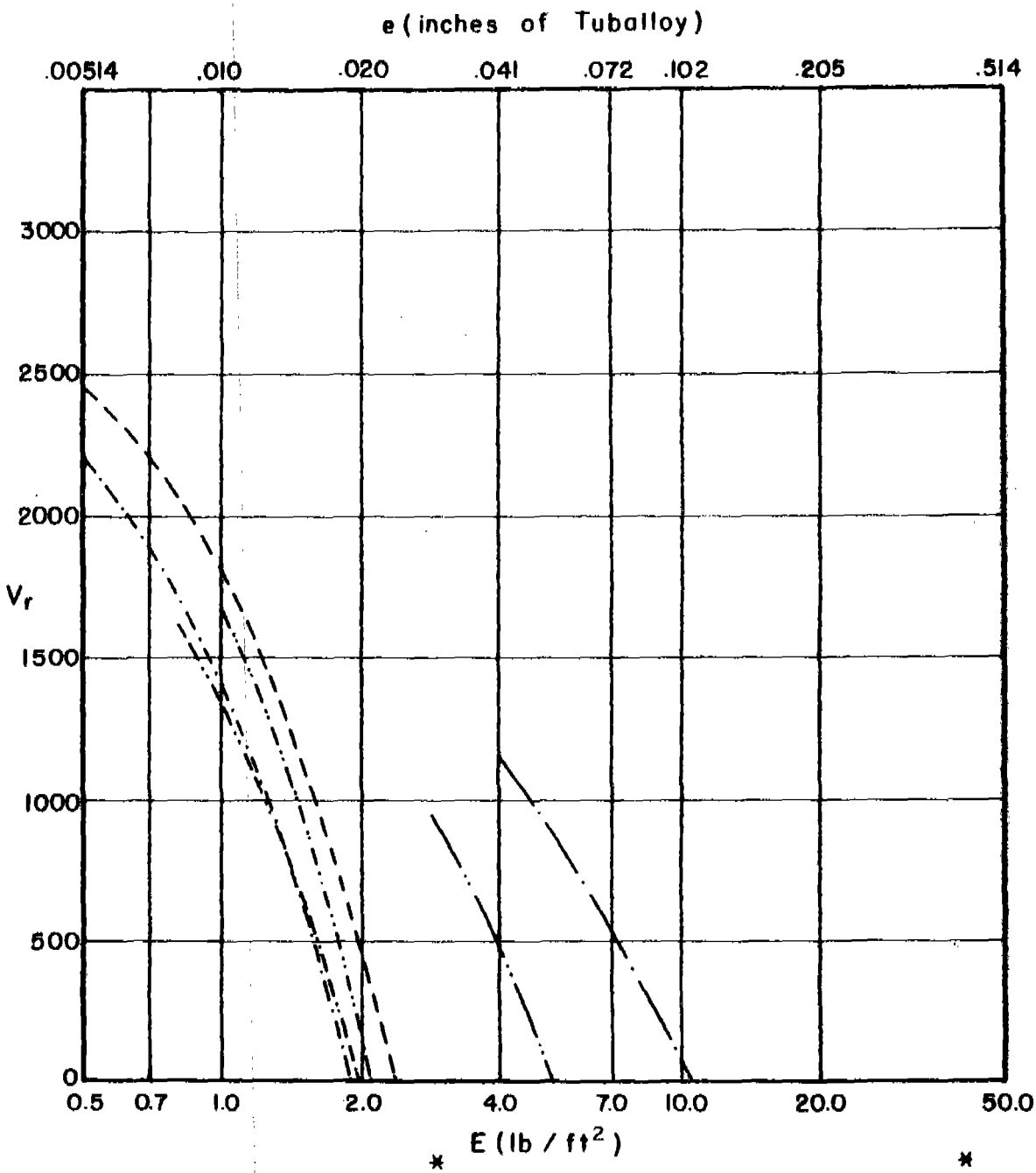

		*			*
Magnesium	— — — —	10.58	F.H. Steel	—··—··—	2.41
2024 T-3	—·—·—	6.65	Hard Steel	———	2.41
Titanium	—··—··—	4.17	Copper	—··—	2.10
Cast Iron	·····	2.59	Lead	—·—	1.70
Mild Steel	— —··— —	2.41	Tuballoy	—··—	1.00

*Ratio of Material Thickness Relative to a Unit Thickness of Tuballoy

Fig. 127

[redacted]

V_r vs E for Various Combinations of m_s, θ, and V_s

m_s = 100 grains θ = 70 degrees V_s = 3000 fps

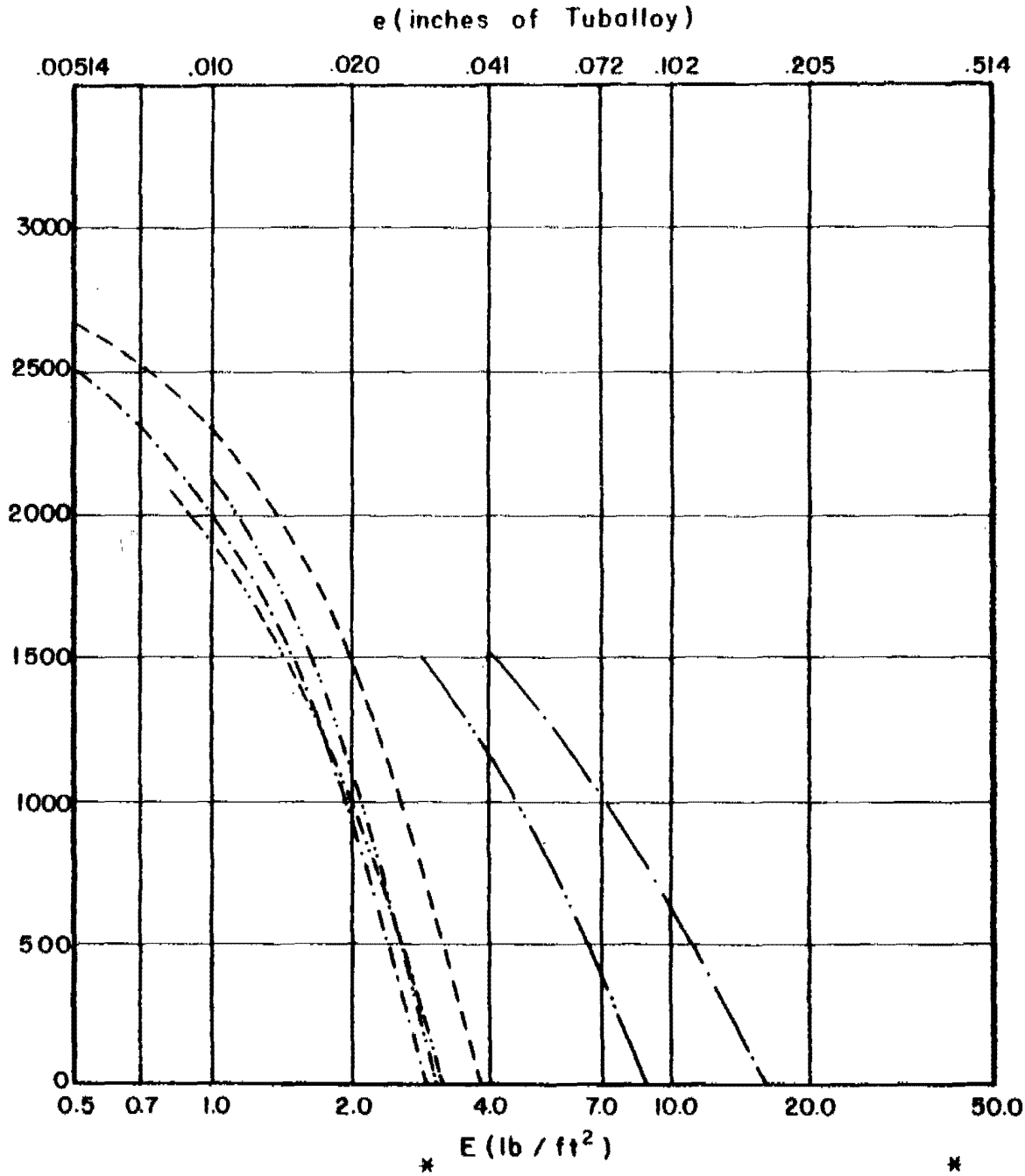

		*			*
Magnesium	— — — —	10.58	F.H. Steel	—··—··—	2.41
2024 T-3	—·—·—	6.65	Hard Steel	———	2.41
Titanium	—··—··—	4.17	Copper	—··—	2.10
Cast Iron	·····	2.59	Lead	—·—	1.70
Mild Steel	— —··— —	2.41	Tuballoy	—··—	1.00

*Ratio of Material Thickness Relative to a Unit Thickness of Tuballoy

Fig. 128

[redacted]

V_r vs E for Various Combinations of m_s, θ, and V_s

m_s = 300 grains θ = 70 degrees V_s = 3000 fps

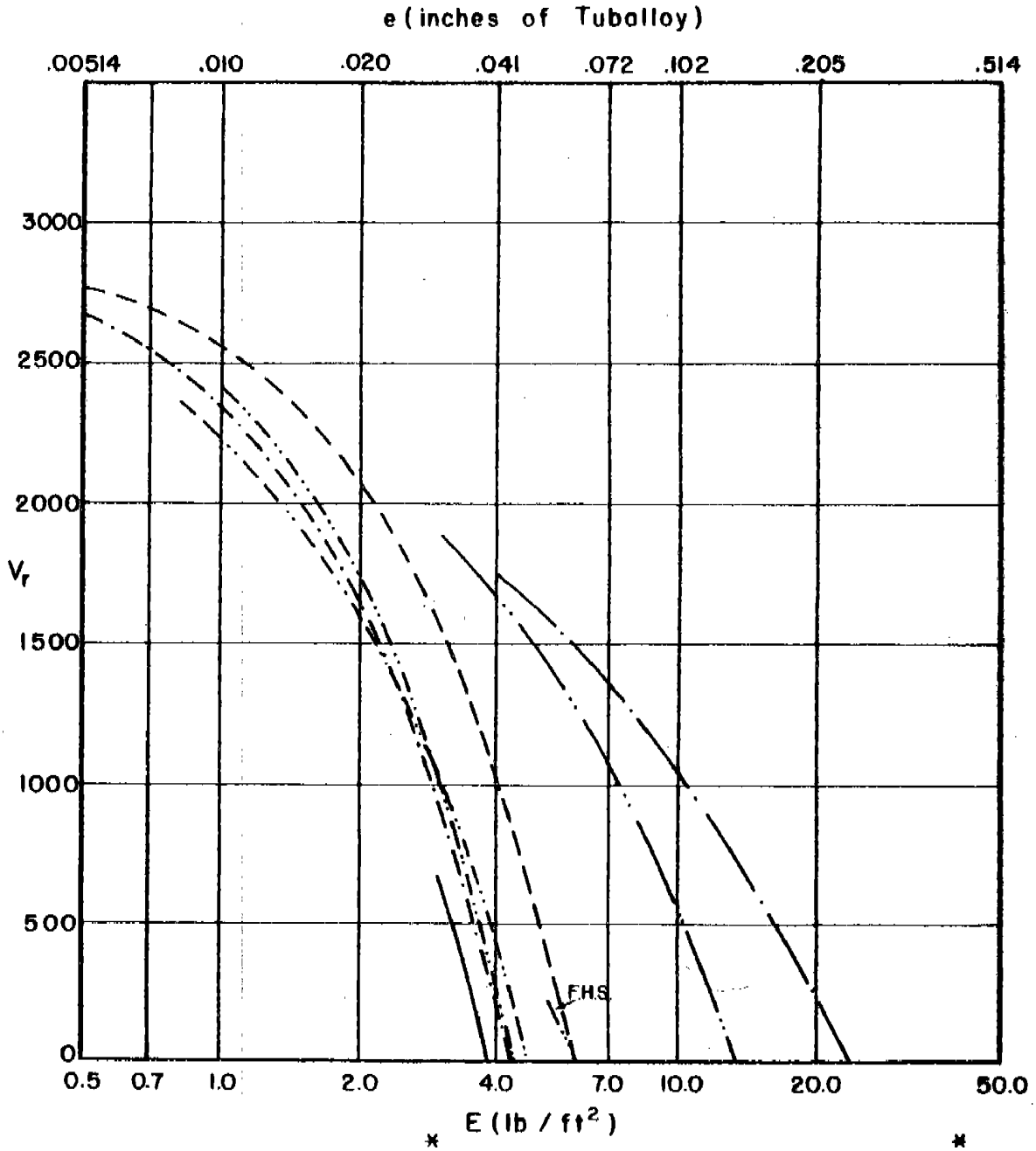

		*			*
Magnesium	— — — —	10.58	F.H. Steel	—··—··—	2.41
2024 T-3	—·—·—	6.65	Hard Steel	————	2.41
Titanium	—··—··—	4.17	Copper	—··—	2.10
Cast Iron	·····	2.59	Lead	—·—	1.70
Mild Steel	—··—	2.41	Tuballoy	—··—	1.00

*Ratio of Material Thickness Relative to a Unit Thickness of Tuballoy

Fig. 129

V_r vs E for Various Combinations of m_s, θ, and V_s

m_s = 30 grains θ = 0 degrees V_s = 6000 fps

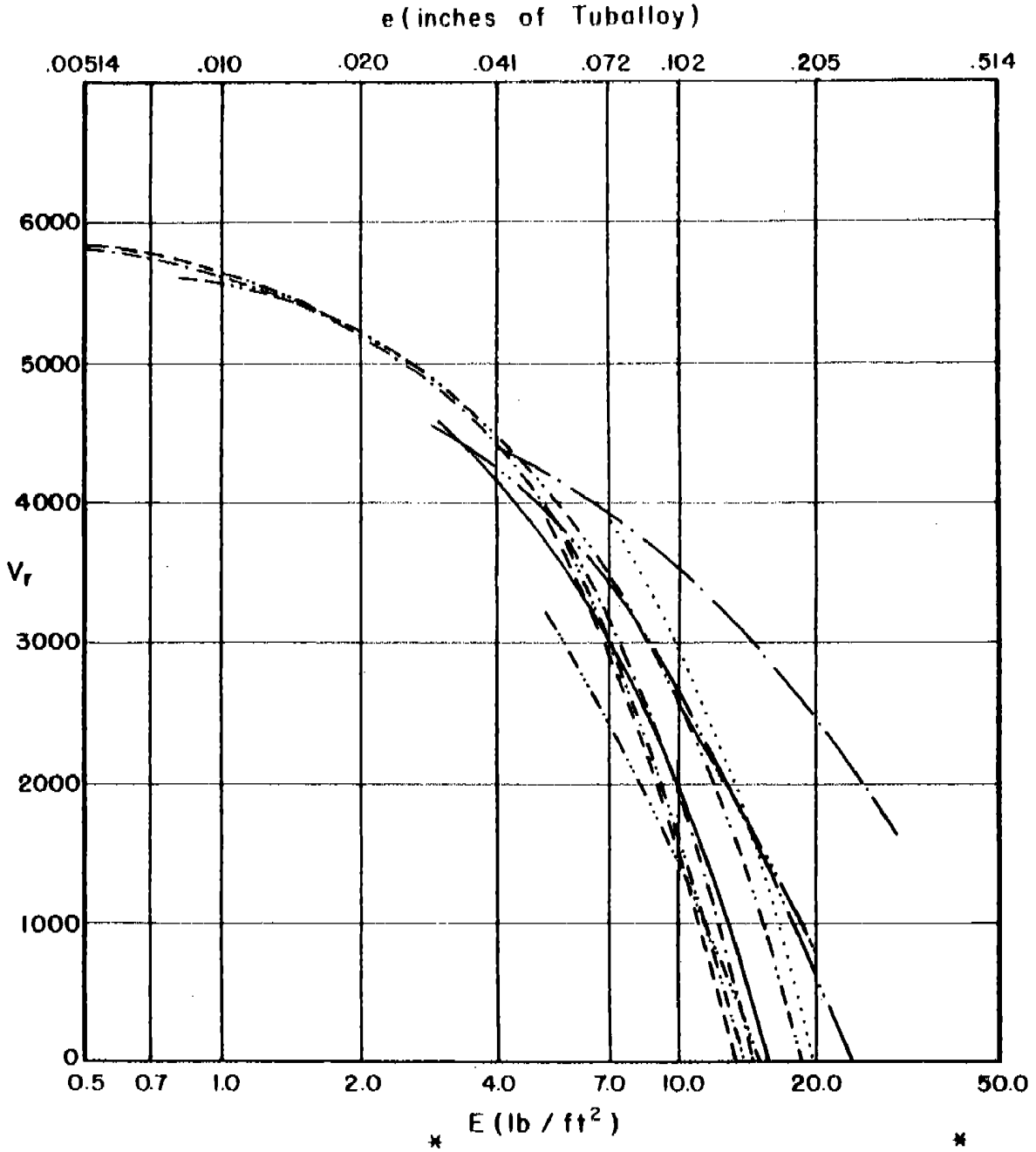

		*			*
Magnesium	— — — —	10.58	F.H. Steel	—·—·—	2.41
2024 T-3	—·—·—	6.65	Hard Steel	———	2.41
Titanium	—··—··—	4.17	Copper	—··—	2.10
Cast Iron	·····	2.59	Lead	—·—	1.70
Mild Steel	— —··— —	2.41	Tuballoy	—··—	1.00

*Ratio of Material Thickness Relative to a Unit Thickness of Tuballoy

Fig. 130

[redacted]

V_r vs E for Various Combinations of m_s, θ, and V_s

m_s = 100 grains θ = 0 degrees V_s = 6000 fps

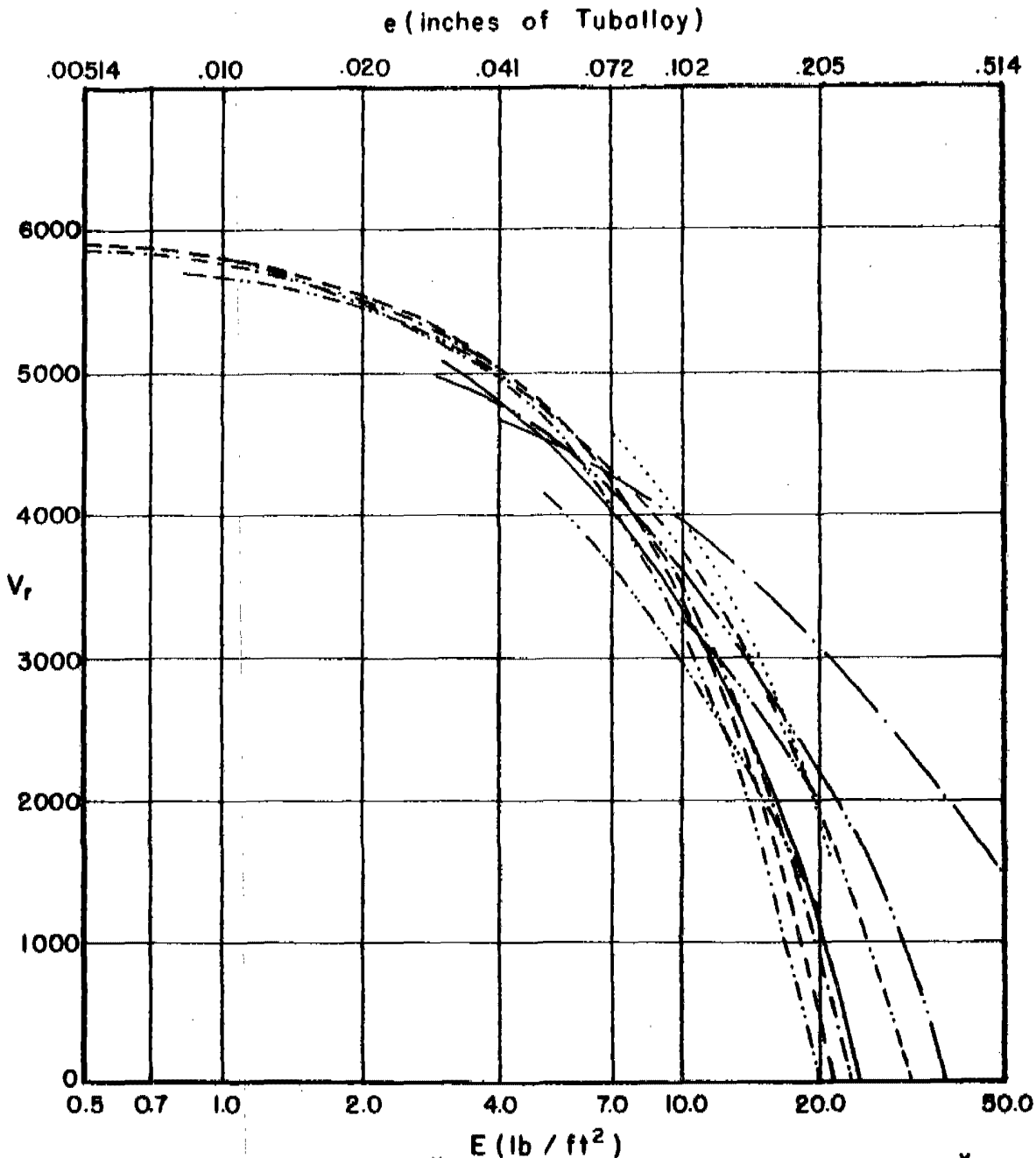

		*			*
Magnesium	— — — —	10.58	F.H. Steel	—··—··—	2.41
2024 T-3	—·—·—	6.65	Hard Steel	———	2.41
Titanium	—··—··—	4.17	Copper	—··—	2.10
Cast Iron	·····	2.59	Lead	—·—	1.70
Mild Steel	— —··— —	2.41	Tuballoy	—··—	1.00

*Ratio of Material Thickness Relative to a Unit Thickness of Tuballoy

Fig. 131

[redacted]

[redacted]

V_r vs E for Various Combinations of m_s, θ, and V_s

m_s = 300 grains θ = 0 degrees V_s = 6000 fps

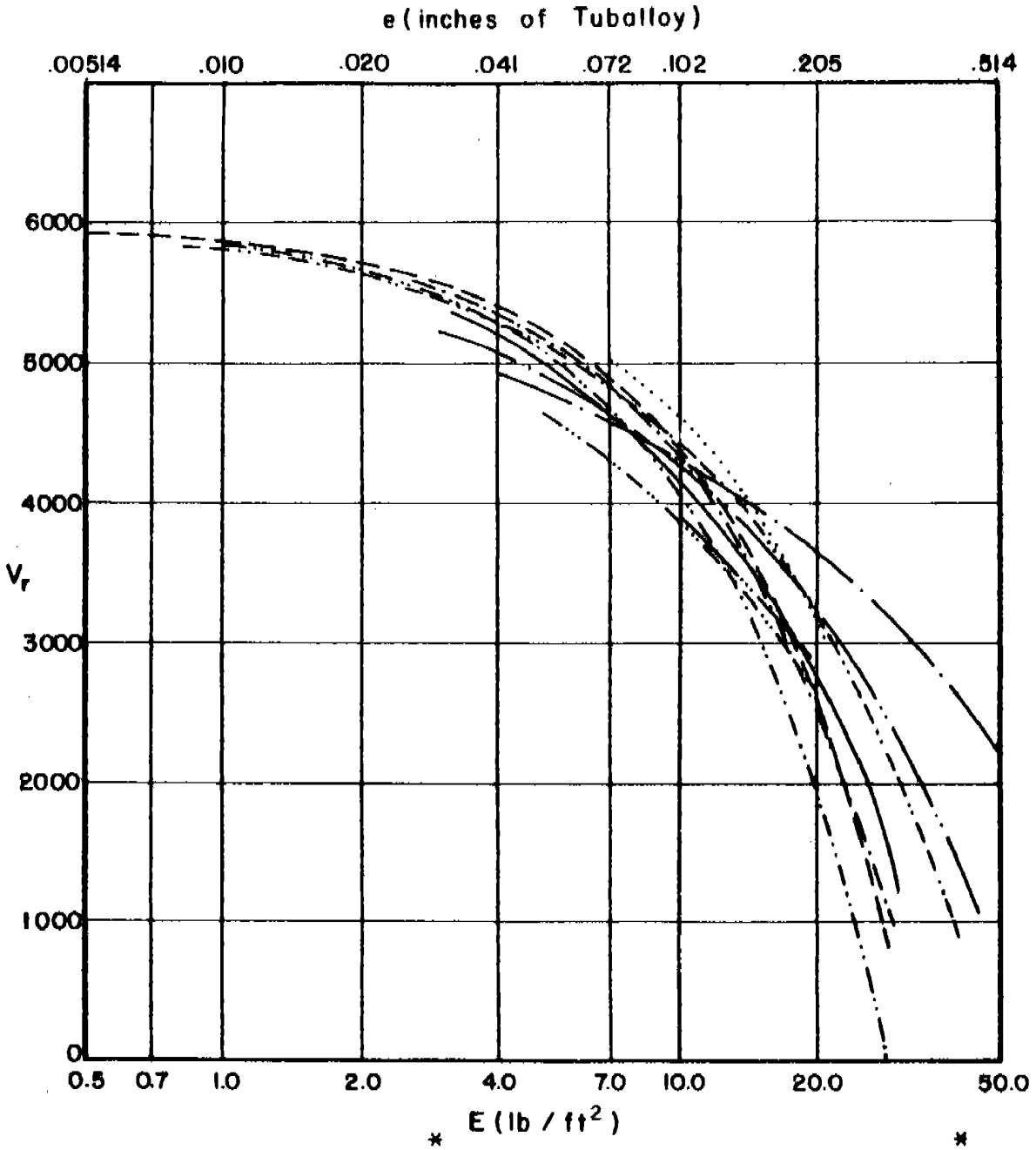

		*			*
Magnesium	— — — —	10.58	F. H. Steel	—·· —··	2.41
2024 T-3	—·—·—	6.65	Hard Steel	———	2.41
Titanium	—··—··—	4.17	Copper	—··—	2.10
Cast Iron	·····	2.59	Lead	—·—	1.70
Mild Steel	— —··— —	2.41	Tuballoy	—··—	1.00

*Ratio of Material Thickness Relative to a Unit Thickness of Tuballoy

Fig. 132

[redacted]

[redacted]

V_r vs E for Various Combinations of m_s, θ, and V_s

m_s = 30 grains θ = 60 degrees V_s = 6000 fps

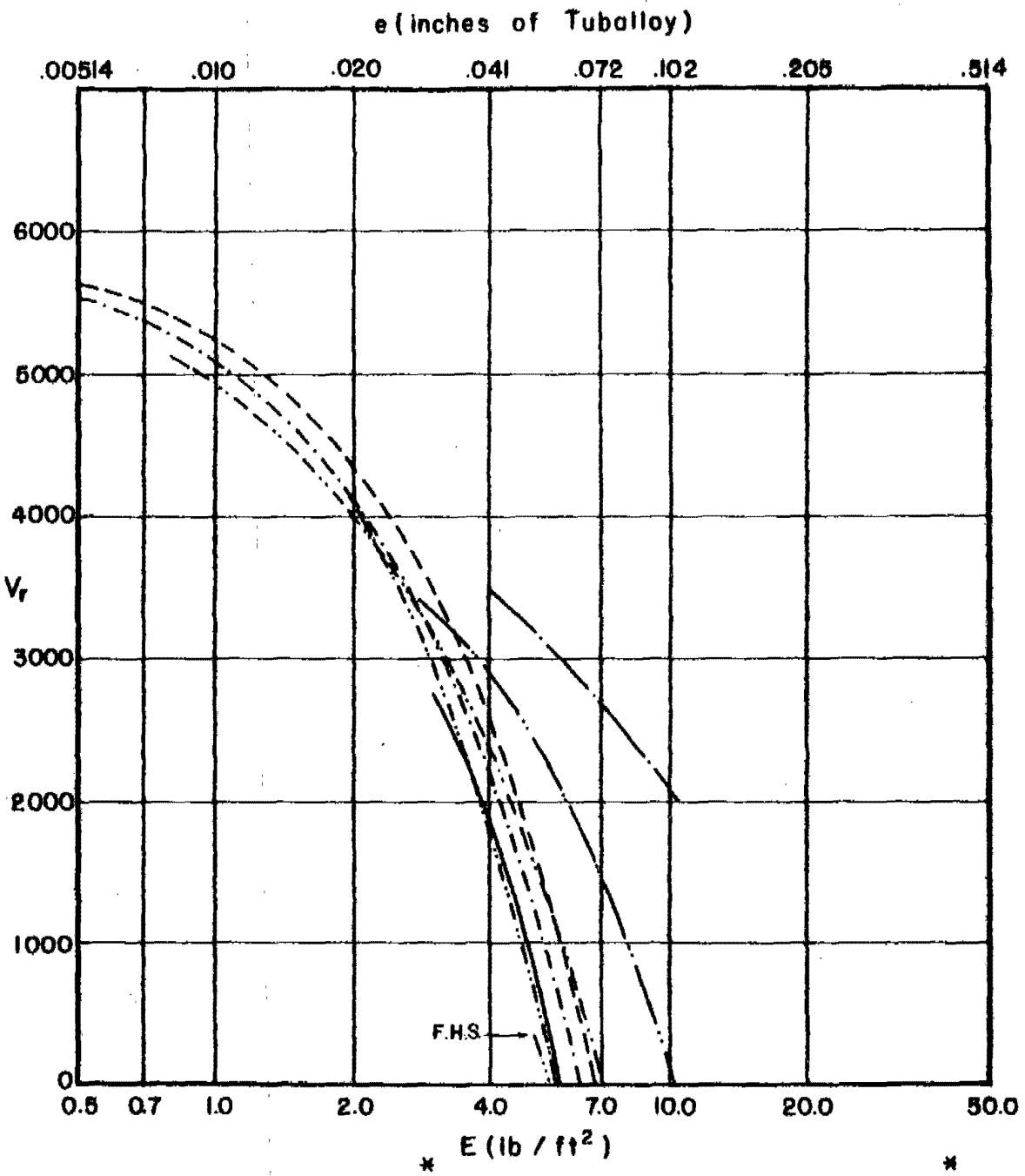

		*			*
Magnesium	— — — —	10.58	F.H. Steel	—··—··—	2.41
2024 T-3	—·—·—	6.65	Hard Steel	———	2.41
Titanium	—··—··—	4.17	Copper	—··—	2.10
Cast Iron	·····	2.59	Lead	—·—	1.70
Mild Steel	— —··— —	2.41	Tuballoy	—···—	1.00

*Ratio of Material Thickness Relative to a Unit Thickness of Tuballoy

Fig. 133

[redacted]

[redacted]

V_r vs E for Various Combinations of m_s, θ, and V_s

m_s = 100 grains θ = 60 degrees V_s = 6000 fps

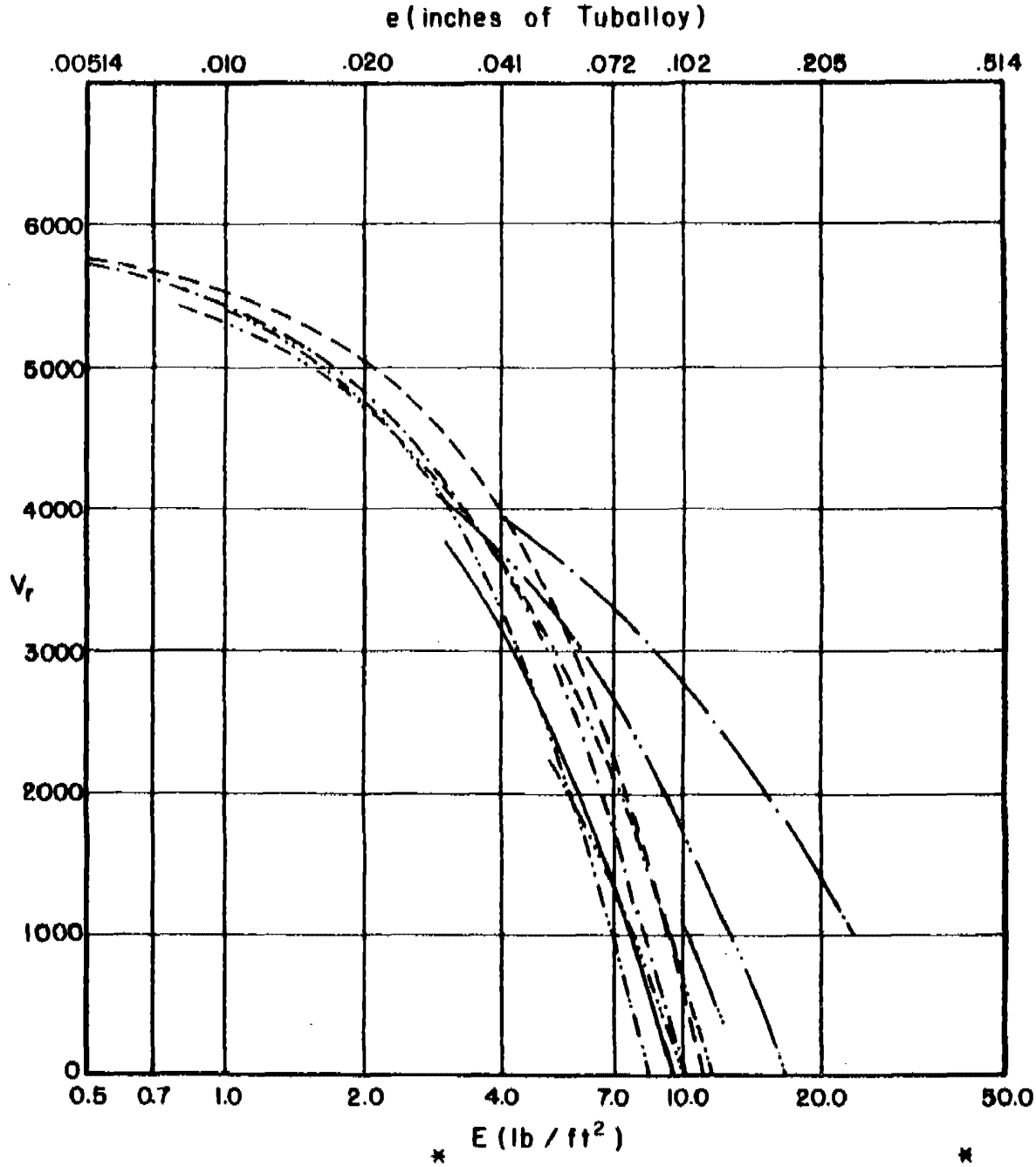

		*			*
Magnesium	— — — —	10.58	F.H. Steel	—··—··—	2.41
2024 T-3	—·—·—	6.65	Hard Steel	———	2.41
Titanium	—··—··—	4.17	Copper	—··—	2.10
Cast Iron	·····	2.59	Lead	—·—	1.70
Mild Steel	— —··— —	2.41	Tuballoy	—···—	1.00

*Ratio of Material Thickness Relative to a Unit Thickness of Tuballoy

Fig. 134

[redacted]

[redacted]

V_r vs E for Various Combinations of m_s, θ, and V_s

m_s = 300 grains θ = 60 degrees V_s = 6000 fps

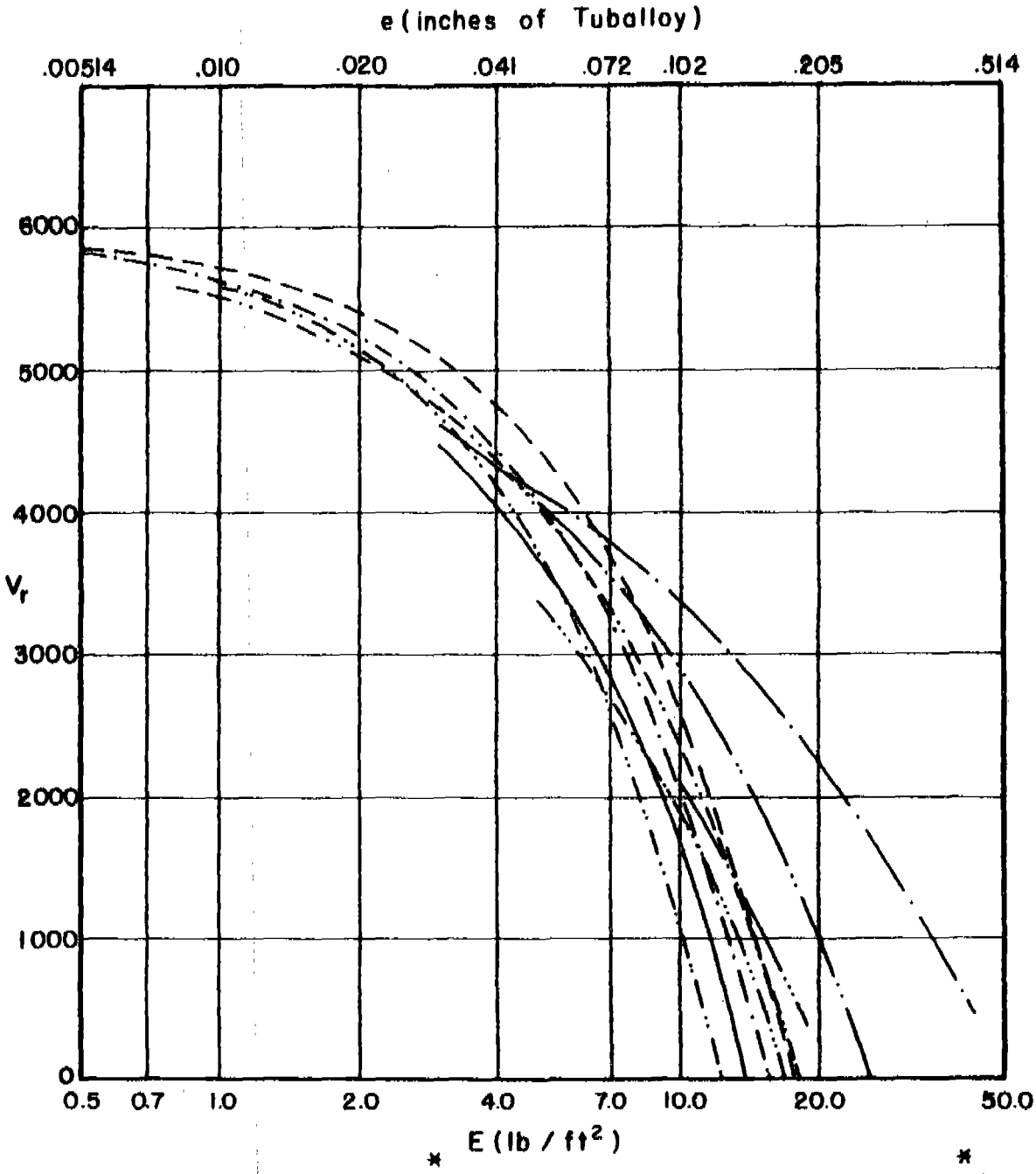

		*			*
Magnesium	— — — —	10.58	F. H. Steel	—··—··—	2.41
2024 T-3	—·—·—	6.65	Hard Steel	———	2.41
Titanium	—··—··—	4.17	Copper	—··—	2.10
Cast Iron	·····	2.59	Lead	—·—	1.70
Mild Steel	—··— —	2.41	Tuballoy	—···—	1.00

*Ratio of Material Thickness Relative to a Unit Thickness of Tuballoy

Fig. 135

[redacted]

[redacted]

V_r vs E for Various Combinations of m_s, θ, and V_s

m_s = 30 grains θ = 70 degrees V_s = 6000 fps

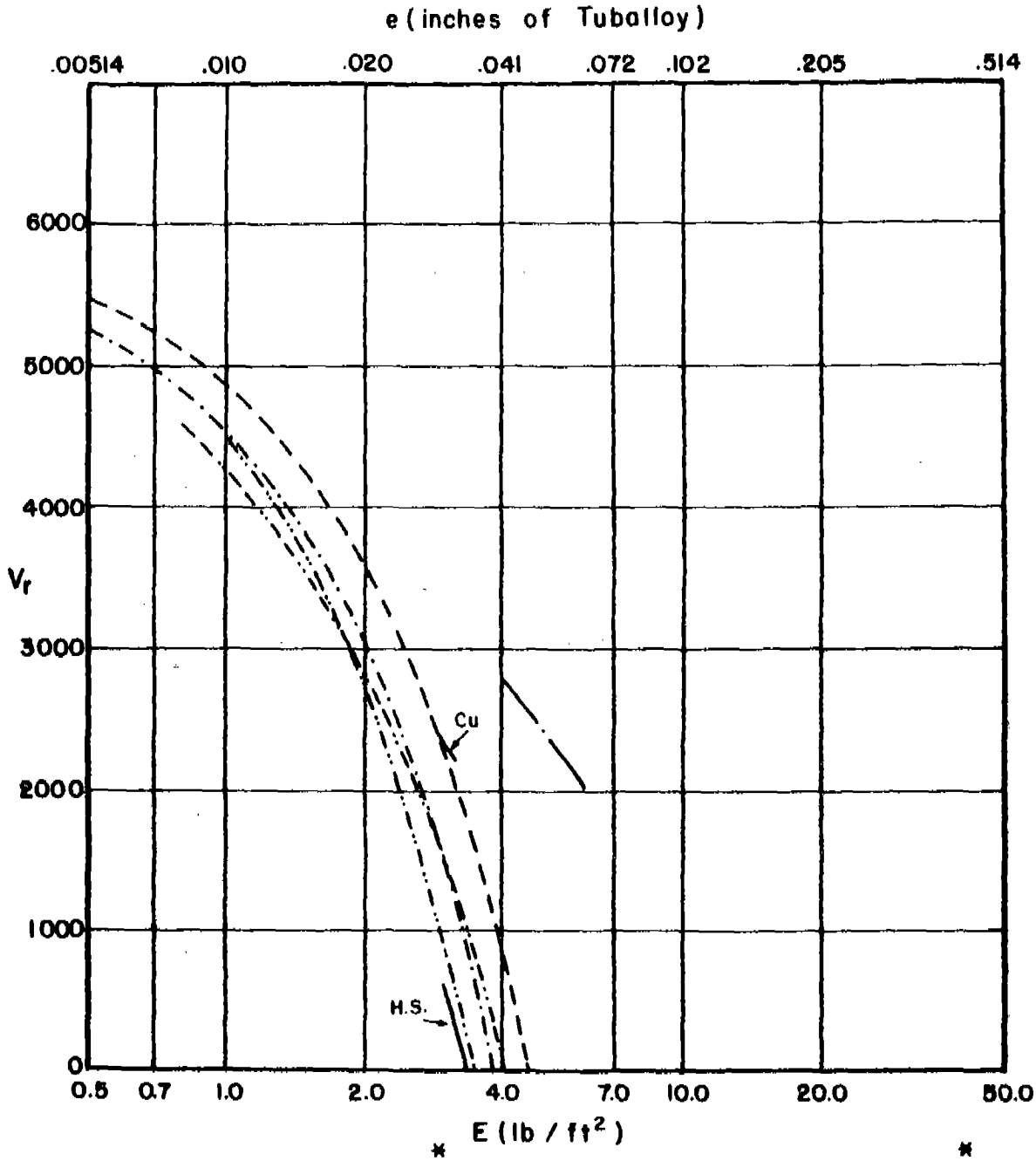

		*			*
Magnesium	— — — —	10.58	F. H. Steel	—··—··—	2.41
2024 T-3	—·—·—	6.65	Hard Steel	———	2.41
Titanium	—··—··—	4.17	Copper	—··—	2.10
Cast Iron	·····	2.59	Lead	—·—	1.70
Mild Steel	— —··— —	2.41	Tuballoy	—···—	1.00

*Ratio of Material Thickness Relative to a Unit Thickness of Tuballoy

Fig. 136

[redacted]

[redacted]

V_r vs E for Various Combinations of m_s, θ, and V_s

m_s = 100 grains θ = 70 degrees V_s = 6000fps

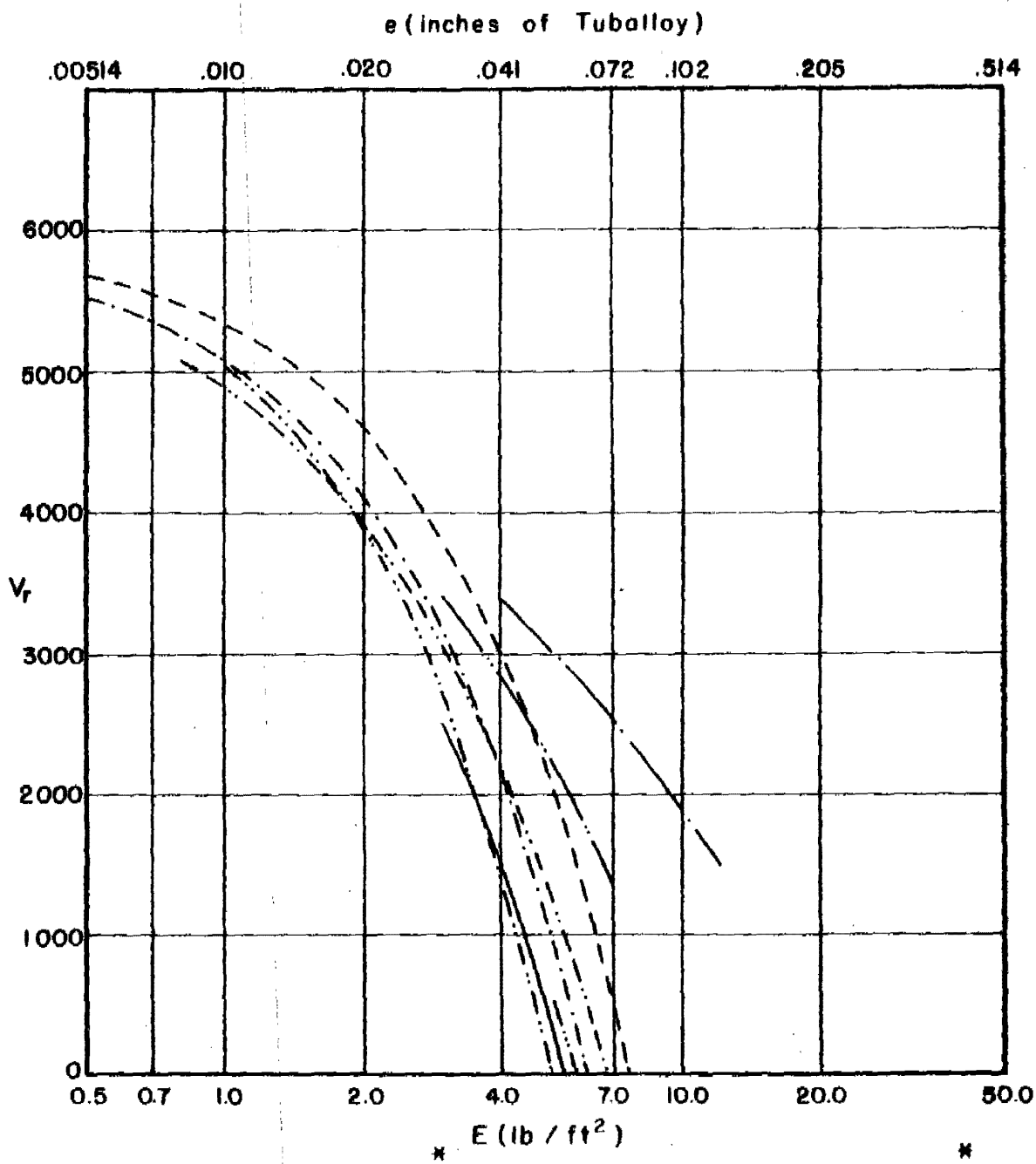

		*			*
Magnesium	— — — —	10.58	F.H. Steel	—··—··—	2.41
2024 T-3	—·—·—·—	6.65	Hard Steel	———	2.41
Titanium	—··—··—	4.17	Copper	—··—	2.10
Cast Iron	·····	2.59	Lead	—·—	1.70
Mild Steel	—··— —	2.41	Tuballoy	—···—	1.00

*Ratio of Material Thickness Relative to a Unit Thickness of Tuballoy

Fig. 137

[redacted]

[redacted]

V_r vs E for Various Combinations of m_s, θ, and V_s

m_s = 300 grains θ = 70 degrees V_s = 6000 fps

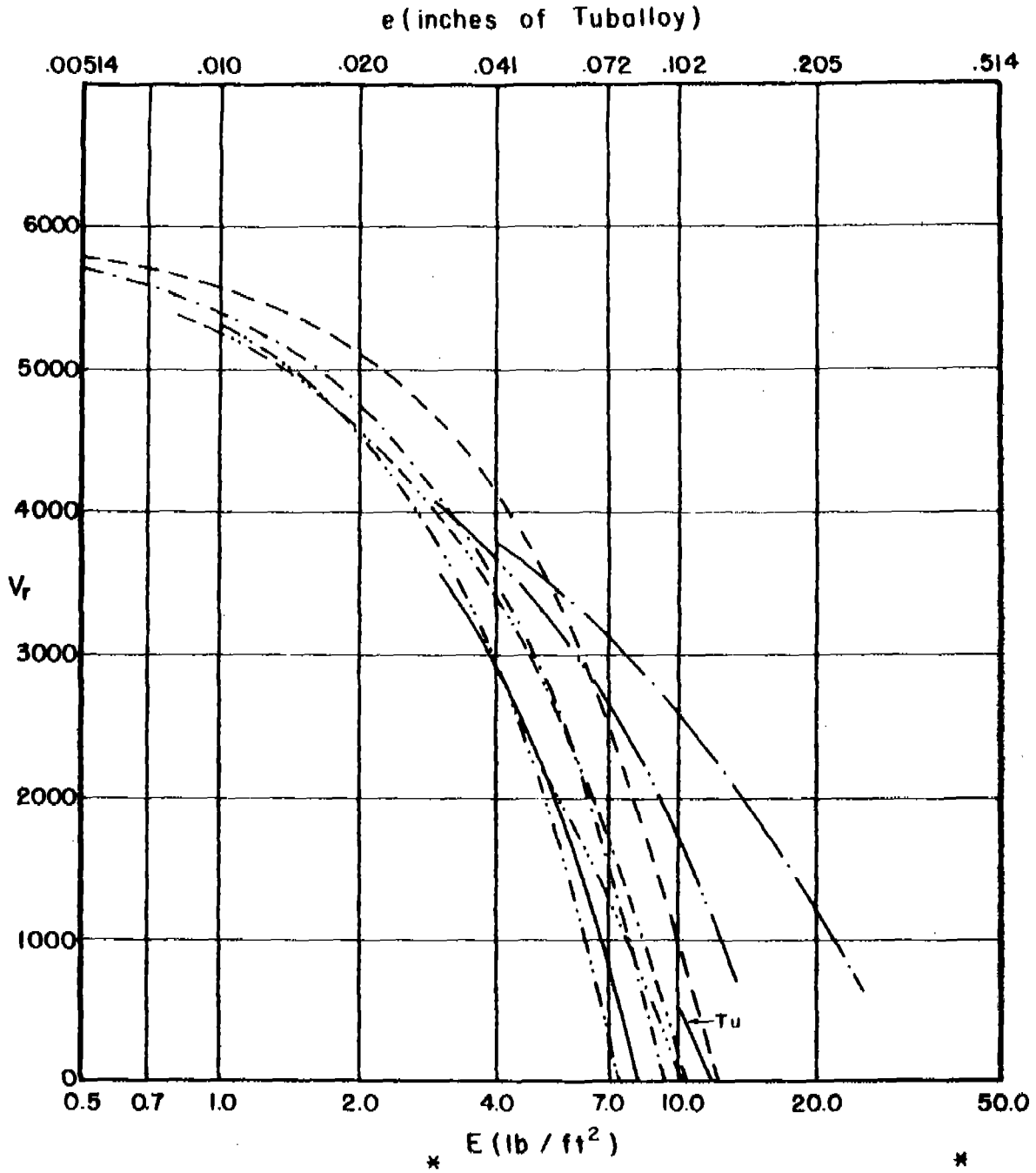

		*			*
Magnesium	— — — —	10.58	F. H. Steel	—··—··—	2.41
2024 T-3	—·—·—	6.65	Hard Steel	———	2.41
Titanium	—··—··—	4.17	Copper	—··—	2.10
Cast Iron	·····	2.59	Lead	—·—	1.70
Mild Steel	— —··— —	2.41	Tuballoy	—···—	1.00

*Ratio of Material Thickness Relative to a Unit Thickness of Tuballoy

Fig. 138

[redacted]

[redacted]

V_r vs E for Various Combinations of m_s, θ, and V_s

m_s = 30 grains θ = 0 degrees V_s = 9000 fps

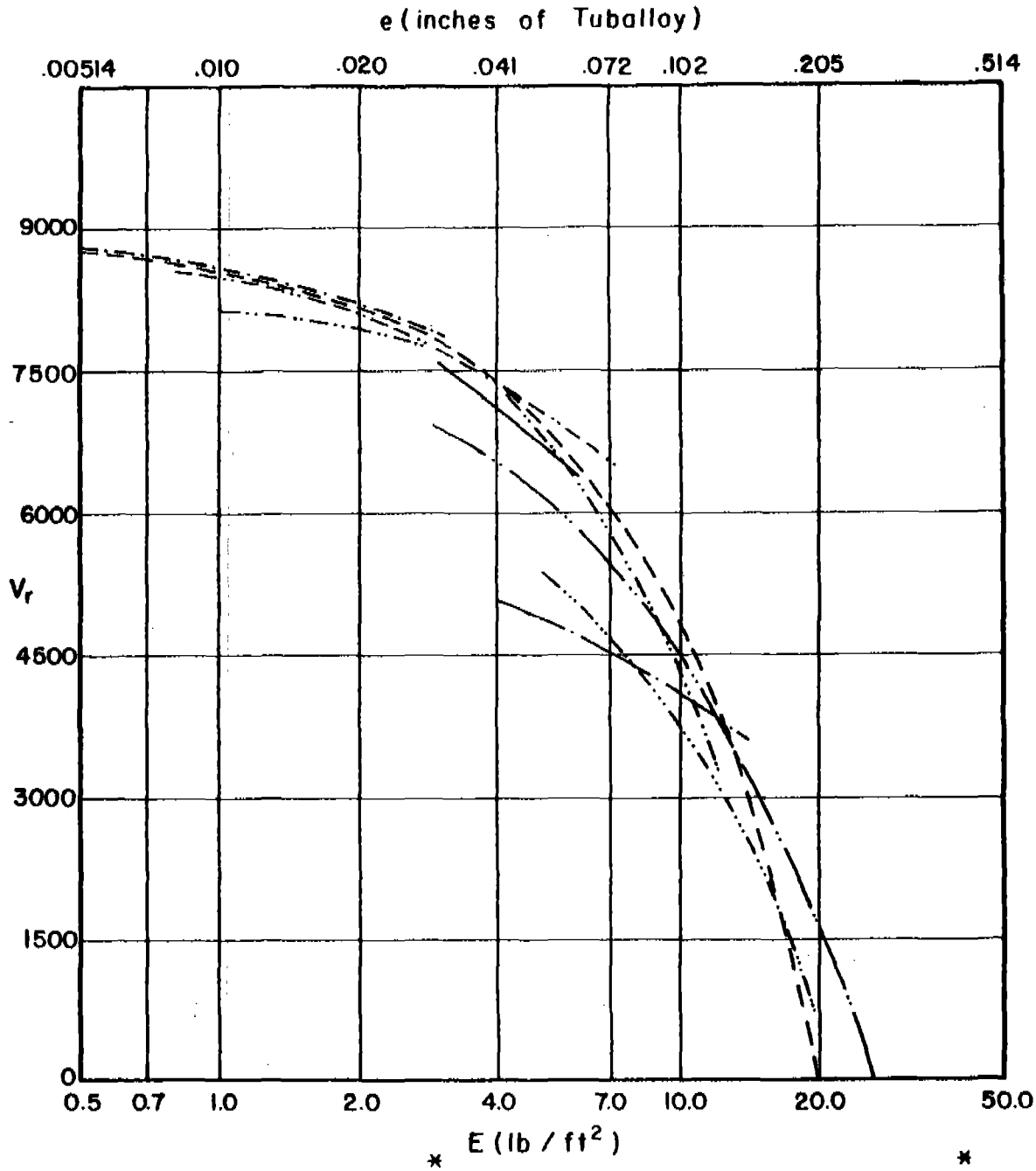

		*			*
Magnesium	— — — — —	10.58	F.H. Steel	—··—··—	2.41
2024 T-3	—·—·—	6.65	Hard Steel	———	2.41
Titanium	—··—··—	4.17	Copper	—··—	2.10
Cast Iron	·····	2.59	Lead	—·—	1.70
Mild Steel	— —··— —	2.41	Tuballoy	—···—	1.00

*Ratio of Material Thickness Relative to a Unit Thickness of Tuballoy

Fig. 139

[redacted]

[redacted]

V_r vs E for Various Combinations of m_s, θ, and V_s

m_s = 100 grains θ = 0 degrees V_s = 9000 fps

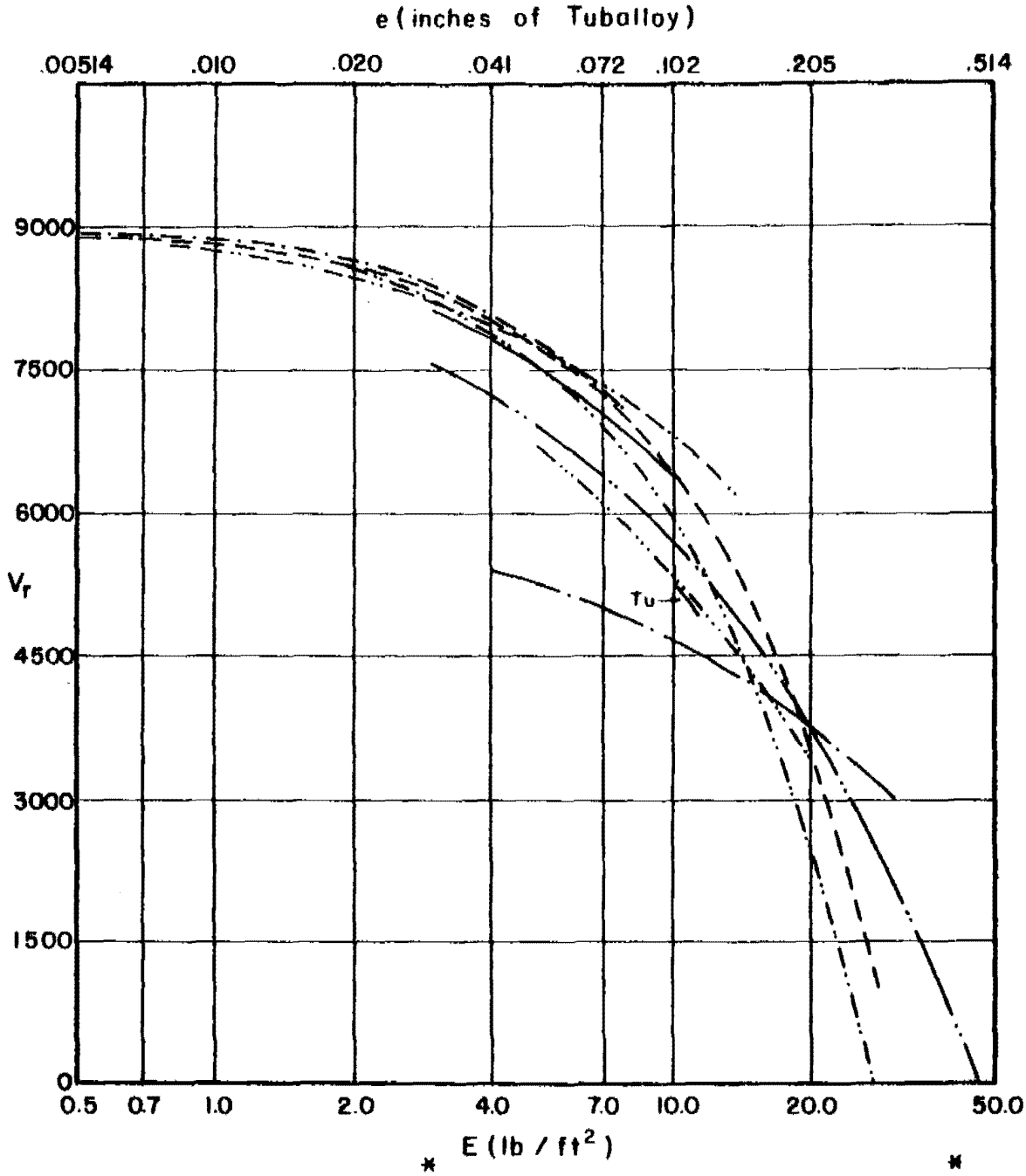

		*			*
Magnesium	— — — —	10.58	F.H. Steel	—··—··—	2.41
2024 T-3	—·—·—	6.65	Hard Steel	———	2.41
Titanium	—··—··—	4.17	Copper	—··—	2.10
Cast Iron	·····	2.59	Lead	—·—	1.70
Mild Steel	— —··— —	2.41	Tuballoy	—··—	1.00

*Ratio of Material Thickness Relative to a Unit Thickness of Tuballoy

Fig. 140

[redacted]

[redacted]

V_r vs E for Various Combinations of m_s, θ, and V_s

m_s = 300 grains θ = 0 degrees V_s = 9000 fps

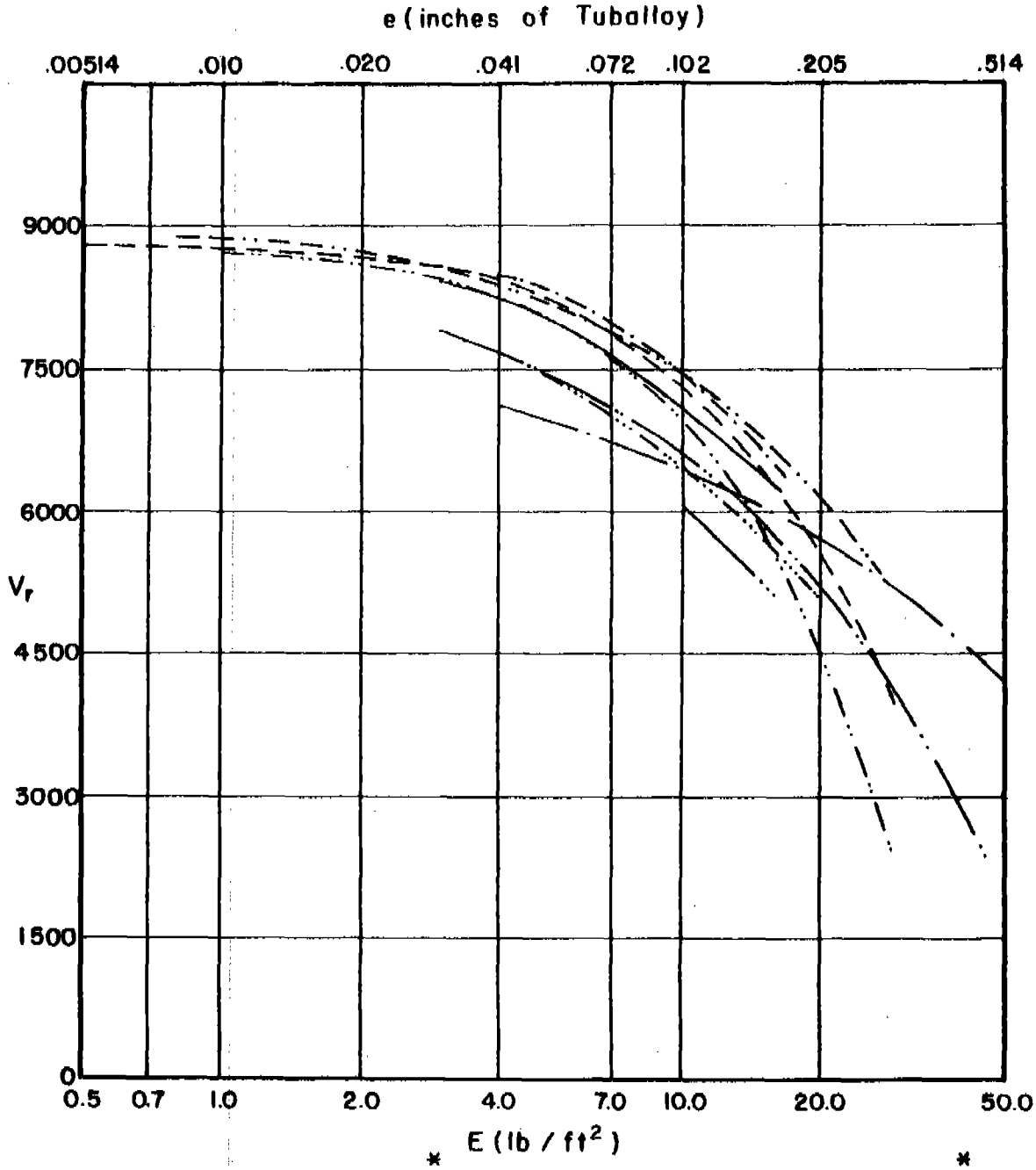

		*			*
Magnesium	— — — —	10.58	F. H. Steel	—··—··—	2.41
2024 T-3	—·—·—	6.65	Hard Steel	———	2.41
Titanium	—··—··—	4.17	Copper	—·—·—	2.10
Cast Iron	·····	2.59	Lead	—·—	1.70
Mild Steel	—··—··—	2.41	Tuballoy	—··—	1.00

*Ratio of Material Thickness Relative to a Unit Thickness of Tuballoy

Fig. 141

[redacted]

[redacted]

V_r vs E for Various Combinations of m_s, θ, and V_s

m_s = 30 grains θ = 60 degrees V_s = 9000 fps

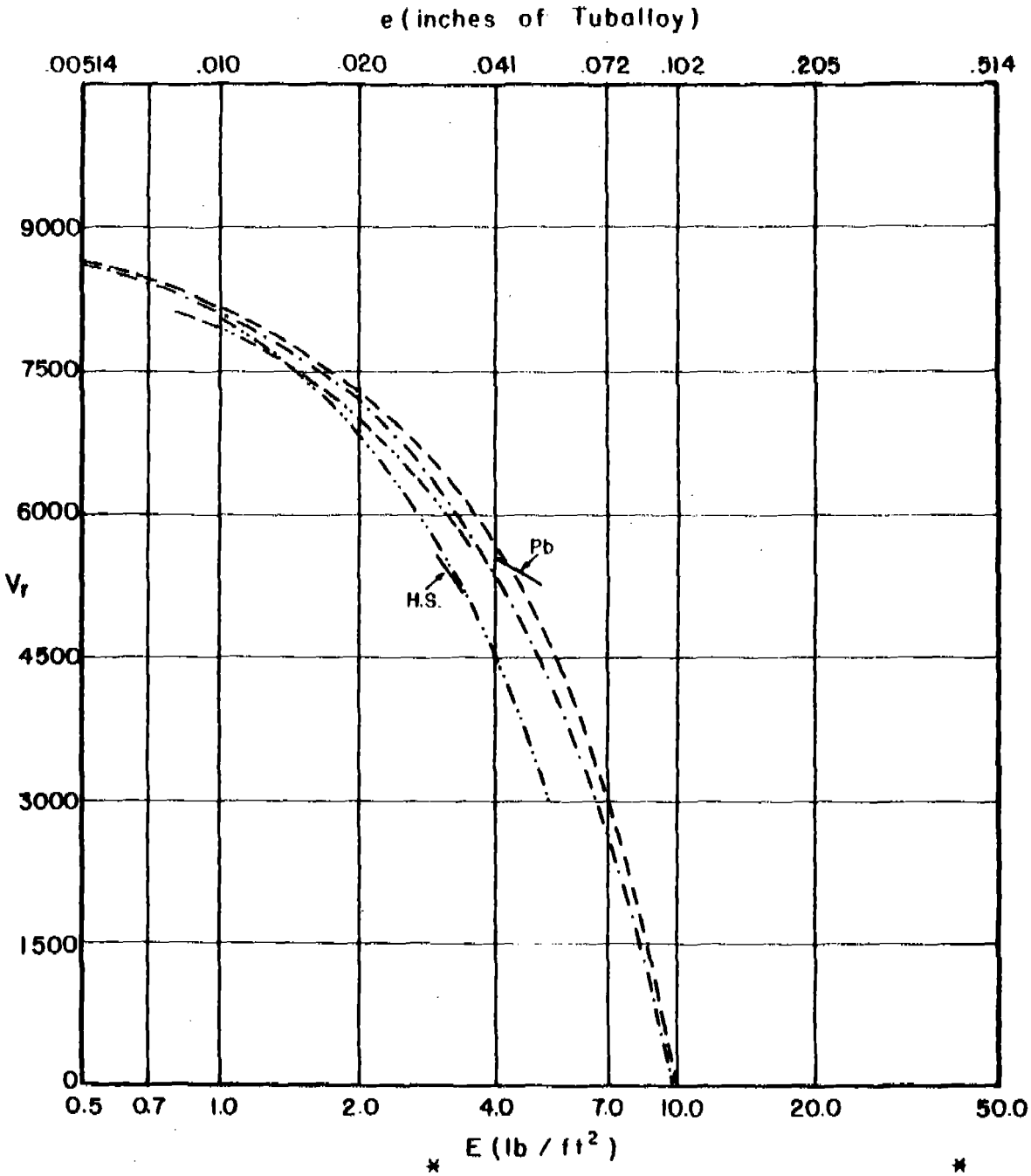

		*			*
Magnesium	— — — —	10.58	F.H. Steel	—·—·—	2.41
2024 T-3	—·—·—	6.65	Hard Steel	———	2.41
Titanium	—··—··—	4.17	Copper	—··—	2.10
Cast Iron	·····	2.59	Lead	—·—	1.70
Mild Steel	— —··— —	2.41	Tuballoy	—··—	1.00

*Ratio of Material Thickness Relative to a Unit Thickness of Tuballoy

Fig. 142

[redacted]

[redacted]

V_r vs E for Various Combinations of m_s, θ, and V_s

m_s = 100 grains θ = 60 degrees V_s = 9000 fps

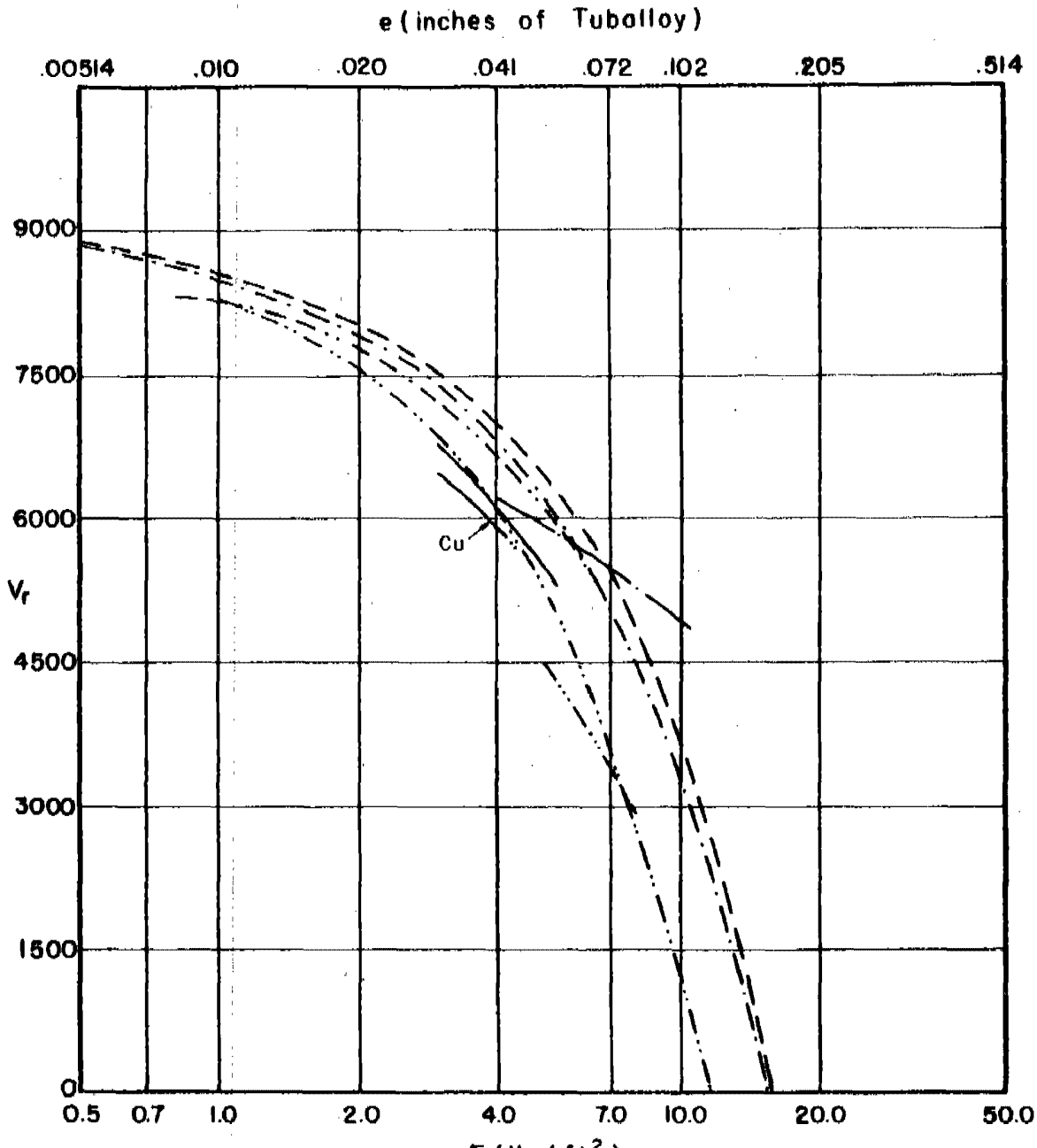

		*			*
Magnesium	— — — —	10.58	F.H. Steel	—·····—·····—	2.41
2024 T-3	—·—·—·—	6.65	Hard Steel	————	2.41
Titanium	—··—··—	4.17	Copper	—··—··—	2.10
Cast Iron	·····	2.59	Lead	—·—·—	1.70
Mild Steel	— —··— —	2.41	Tuballoy	—··—··—	1.00

*Ratio of Material Thickness Relative to a Unit Thickness of Tuballoy

Fig. 143

[redacted]

[redacted]

V_r vs E for Various Combinations of m_s, θ, and V_s

m_s = 300 grains θ = 60 degrees V_s = 9000 fps

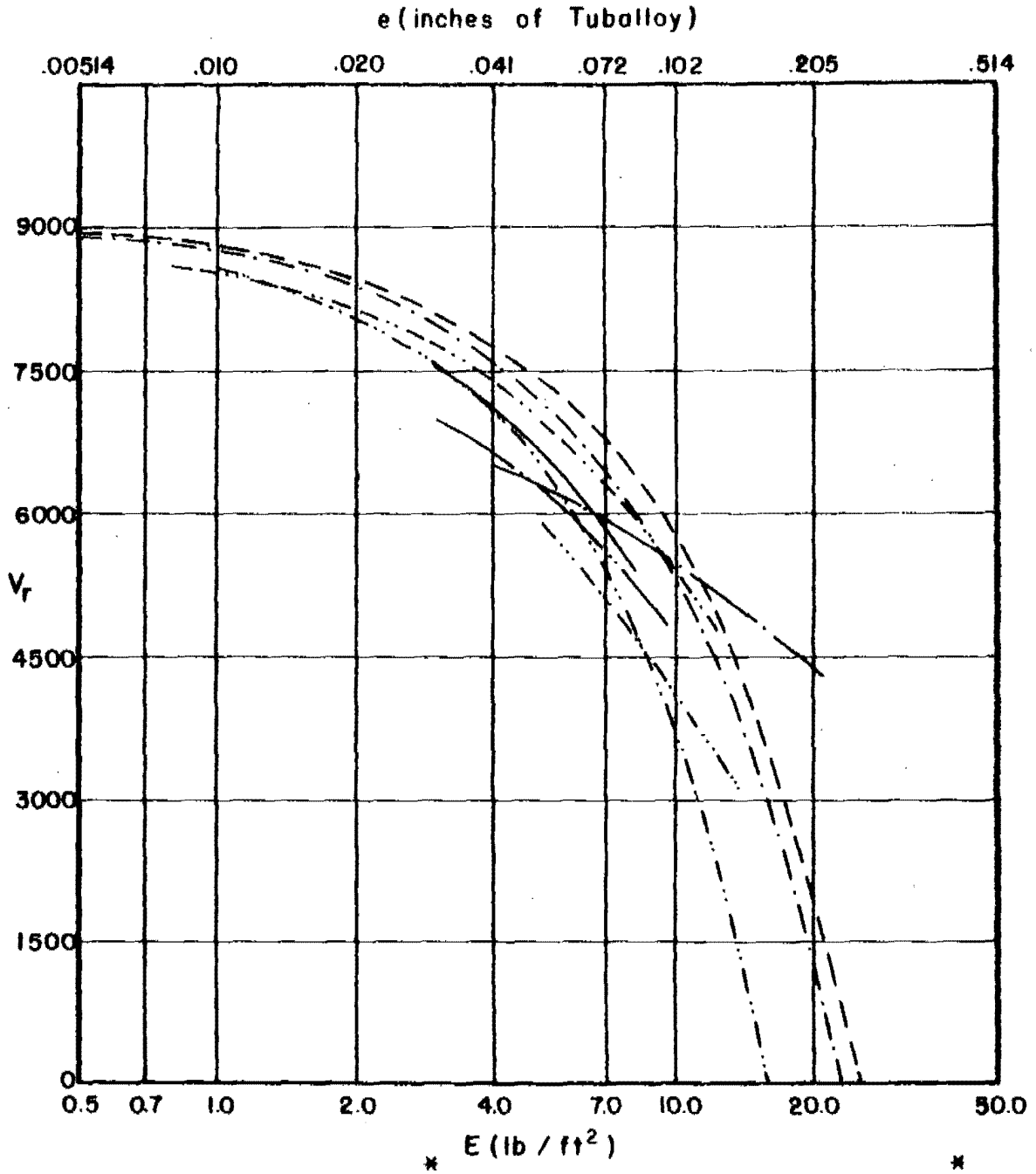

Magnesium	— — — —	10.58*	F.H. Steel	—·—·—	2.41*
2024 T-3	—·—·—	6.65	Hard Steel	———	2.41
Titanium	—··—··—	4.17	Copper	—··—	2.10
Cast Iron	·····	2.59	Lead	—·—	1.70
Mild Steel	— —·— —	2.41	Tuballoy	—···—	1.00

*Ratio of Material Thickness Relative to a Unit Thickness of Tuballoy

Fig. 144

[redacted]

[redacted]

V_r vs E for Various Combinations of m_s, θ, and V_s

m_s = 30 grains θ = 70 degrees V_s = 9000 fps

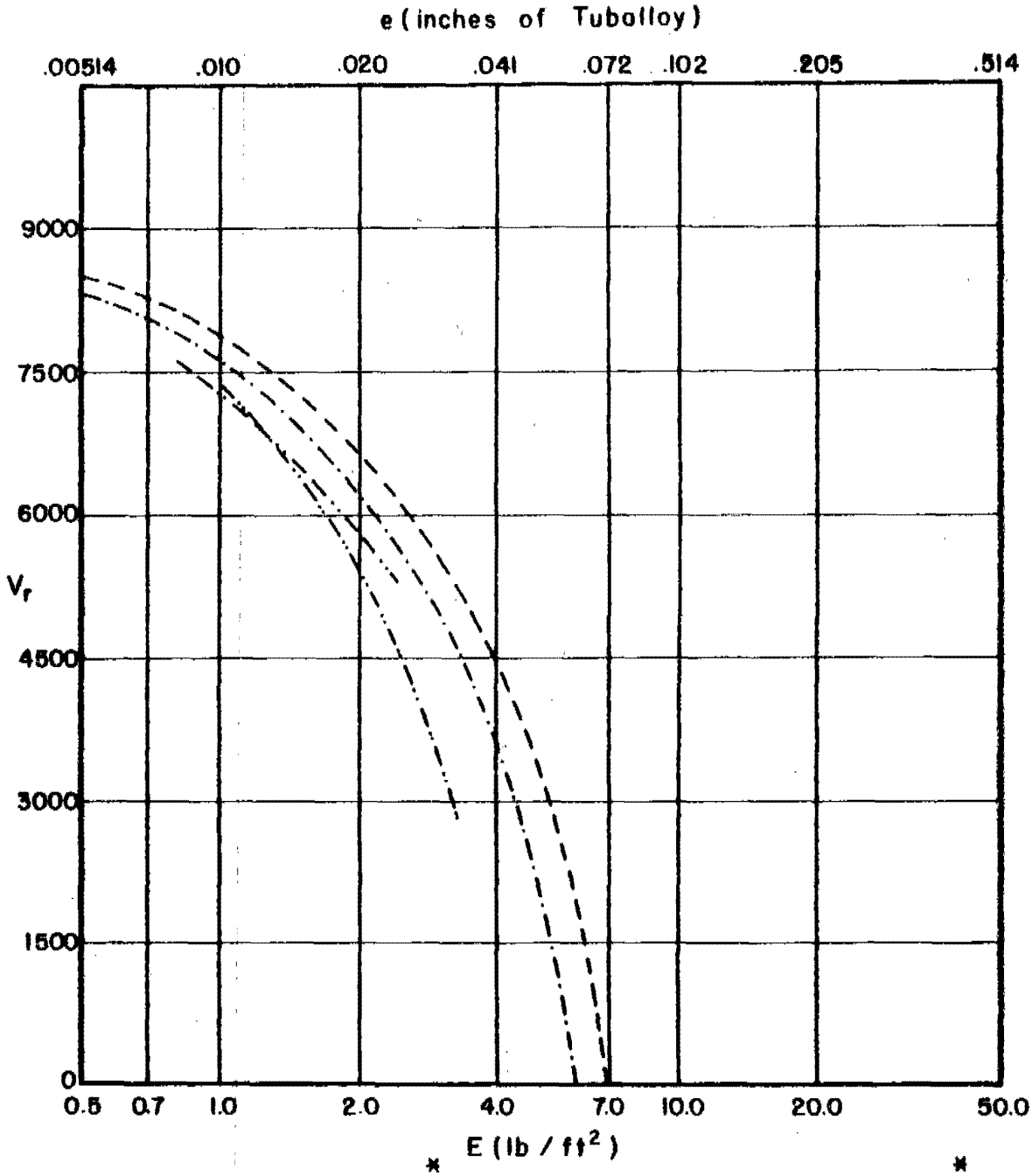

		*			*
Magnesium	— — — — —	10.58	F.H. Steel	—··—··—	2.41
2024 T-3	—·—·—·—	6.65	Hard Steel	————	2.41
Titanium	—··—··—	4.17	Copper	—··—	2.10
Cast Iron	·····	2.59	Lead	—·—	1.70
Mild Steel	— —·— —	2.41	Tuballoy	—··—	1.00

*Ratio of Material Thickness Relative to a Unit Thickness of Tuballoy

Fig. 145

[redacted]

[redacted]

V_r vs E for Various Combinations of m_s, θ, and V_s

m_s = 100 grains θ = 70 degrees V_s = 9000 fps

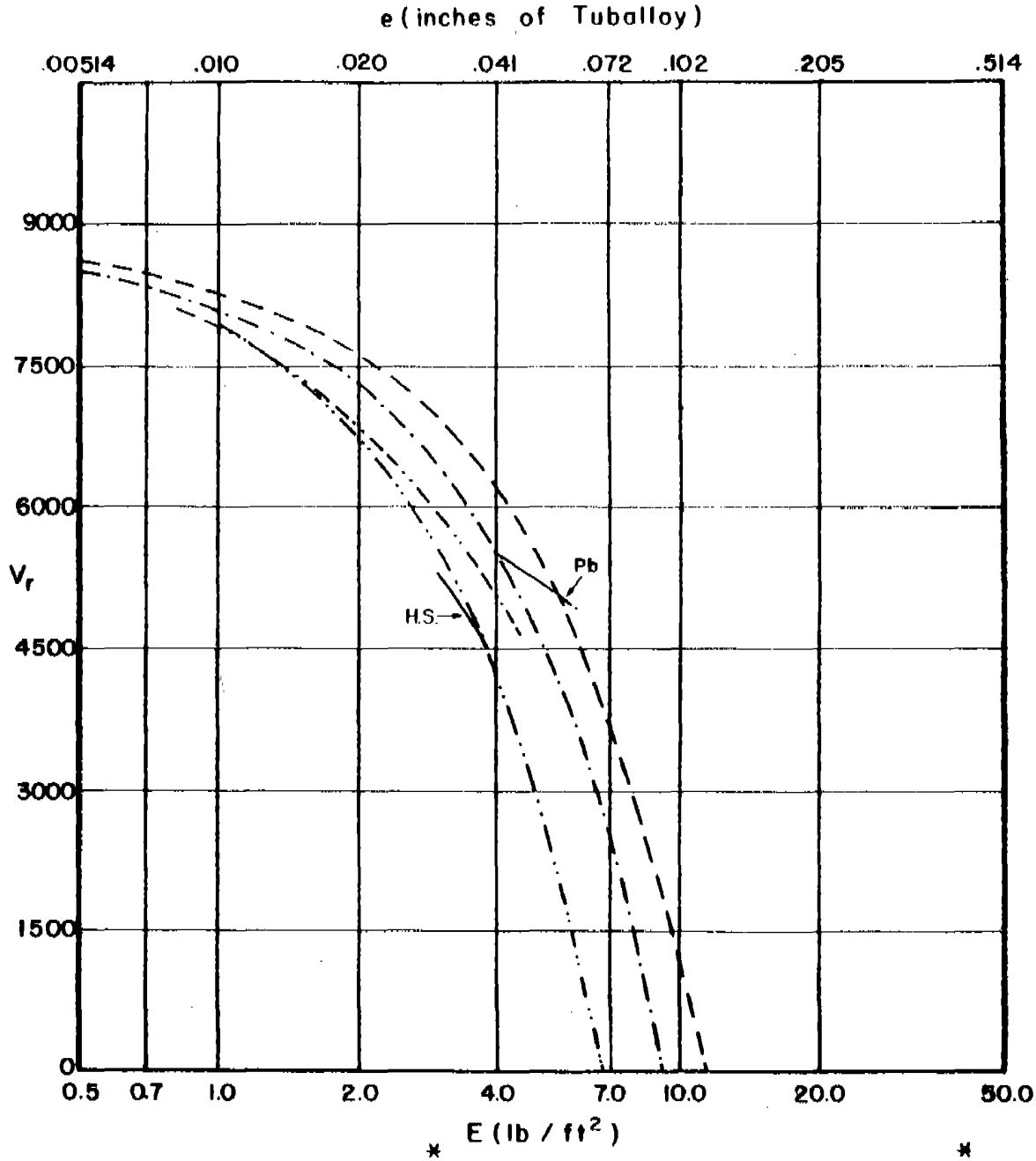

		*			*
Magnesium	— — — —	10.58	F.H. Steel	—··—··—	2.41
2024 T-3	—·—·—	6.65	Hard Steel	———	2.41
Titanium	—··—··—	4.17	Copper	—··—	2.10
Cast Iron	·····	2.59	Lead	—·—	1.70
Mild Steel	— —··— —	2.41	Tuballoy	—···—	1.00

*Ratio of Material Thickness Relative to a Unit Thickness of Tuballoy

Fig. 146

[redacted]

TECHNICAL LIBRARY
U. S. ARMY ORDNANCE
ABERDEEN PROVING GROUND, MD.
ORDBG-TL

[redacted]

V_r vs E for Various Combinations of m_s, θ, and V_s

m_s = 300 grains θ = 70 degrees V_s = 9000 fps

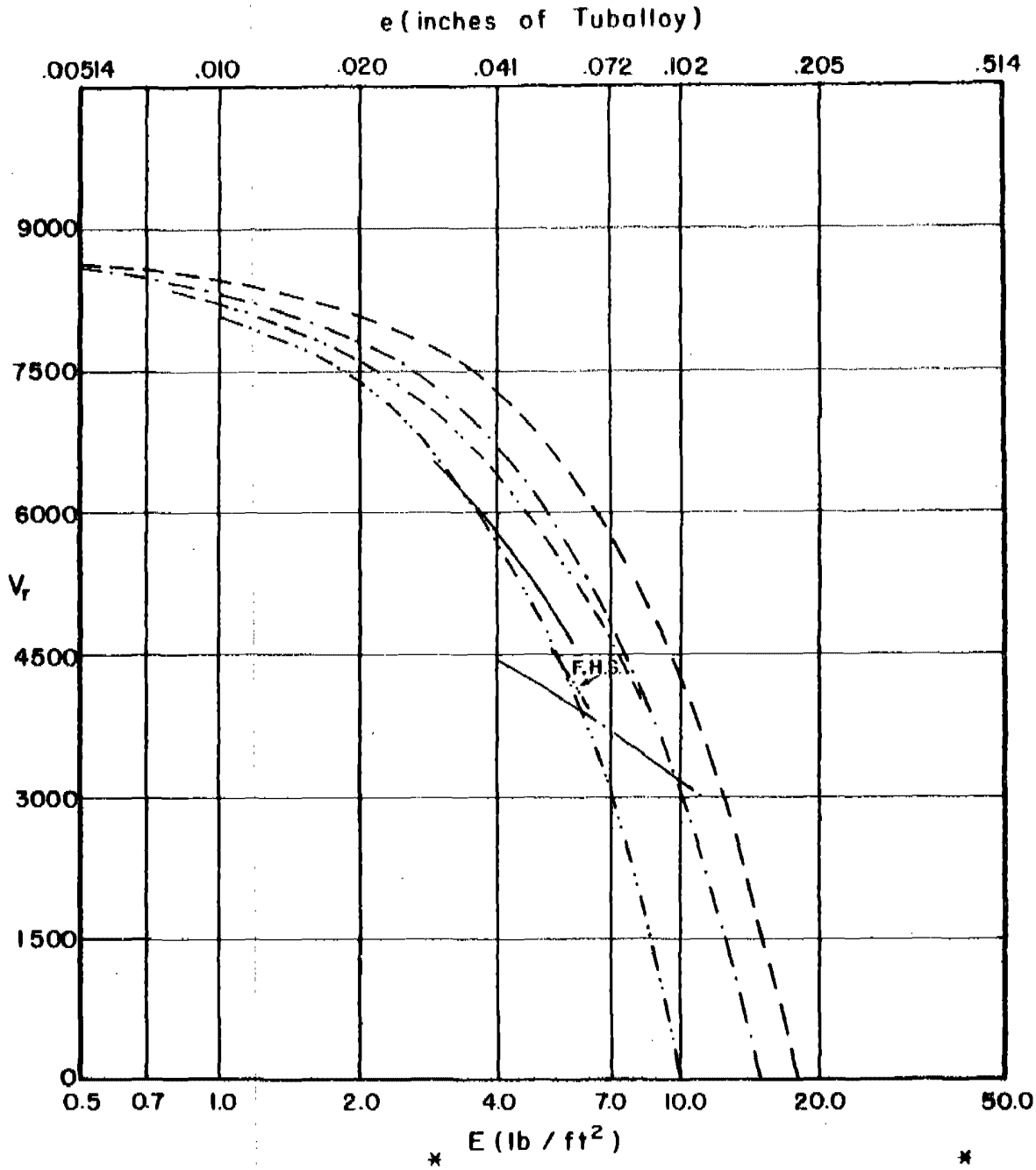

		*			*
Magnesium	— — — —	10.58	F.H. Steel	—·—·—	2.41
2024 T-3	—·—·—	6.65	Hard Steel	———	2.41
Titanium	—··—··—	4.17	Copper	—··—	2.10
Cast Iron	·····	2.59	Lead	—·—	1.70
Mild Steel	— —··— —	2.41	Tuballoy	—··—	1.00

*Ratio of Material Thickness Relative to a Unit Thickness of Tuballoy

Fig. 147

[redacted]

[redacted]

Appendix C

Graph Set IV: m_r vs E for Various Combinations of m_s, θ, and V_s

Figs. 148-174

Note: Within these sets of graphs, a contour for a particular material is shown only for those values of the abscissa for which m_r and V_r are both positive. Furthermore, the contours are not significantly extrapolated beyond the interval of thicknesses of target material employed in the basic experiments. This explains, for example, why the contours for face-hardened steel start at a value of E of 5 lb/ft^2 corresponding to a minimum experimental thickness of 0.125". No contours for cast iron appear on graphs for conditions of either 9000 fps or 70° obliquity for the reason that the experimental data did not cover these conditions. However, a contour for a given material may not appear on a graph simply because there is no permissible value of E for which both m_r and V_r are positive under the conditions for that graph.

[redacted]

[redacted]

m_r vs E for Various Combinations of m_s, θ, and V_s

m_s = 30 grains θ = 0 degrees V_s = 3000 fps

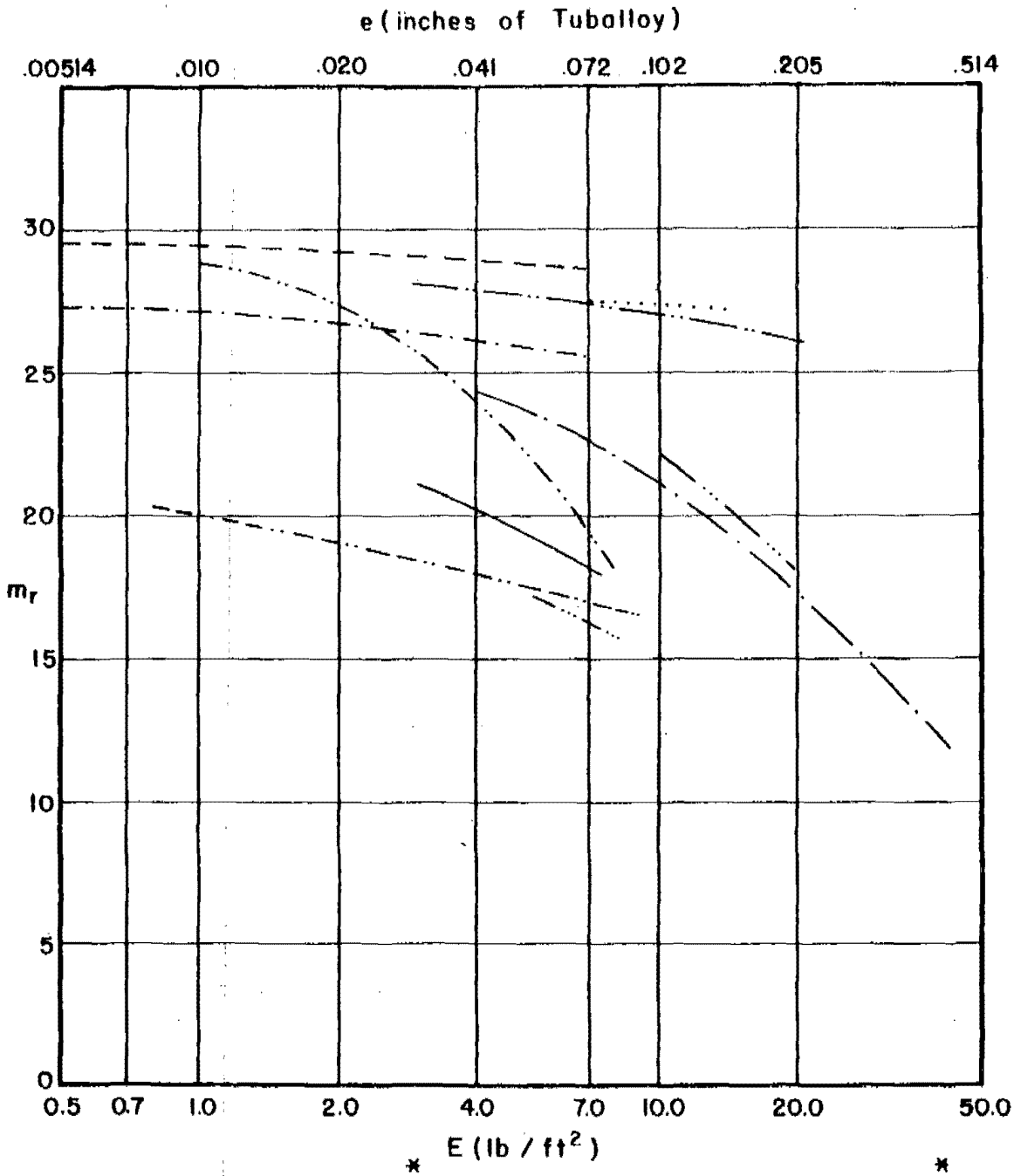

		*			*
Magnesium	— — — —	10.58	F.H. Steel	—··—··—	2.41
2024 T-3	—·—·—	6.65	Hard Steel	———	2.41
Titanium	—··—··—	4.17	Copper	—··—	2.10
Cast Iron	·····	2.59	Lead	—·—	1.70
Mild Steel	— —··— —	2.41	Tuballoy	—···—	1.00

*Ratio of Material Thickness Relative to a Unit Thickness of Tuballoy

Fig. 148

[redacted]

[redacted]

m_r vs E for Various Combinations of m_s, θ, and V_s

m_s = 100 grains θ = 0 degrees V_s = 3000 fps

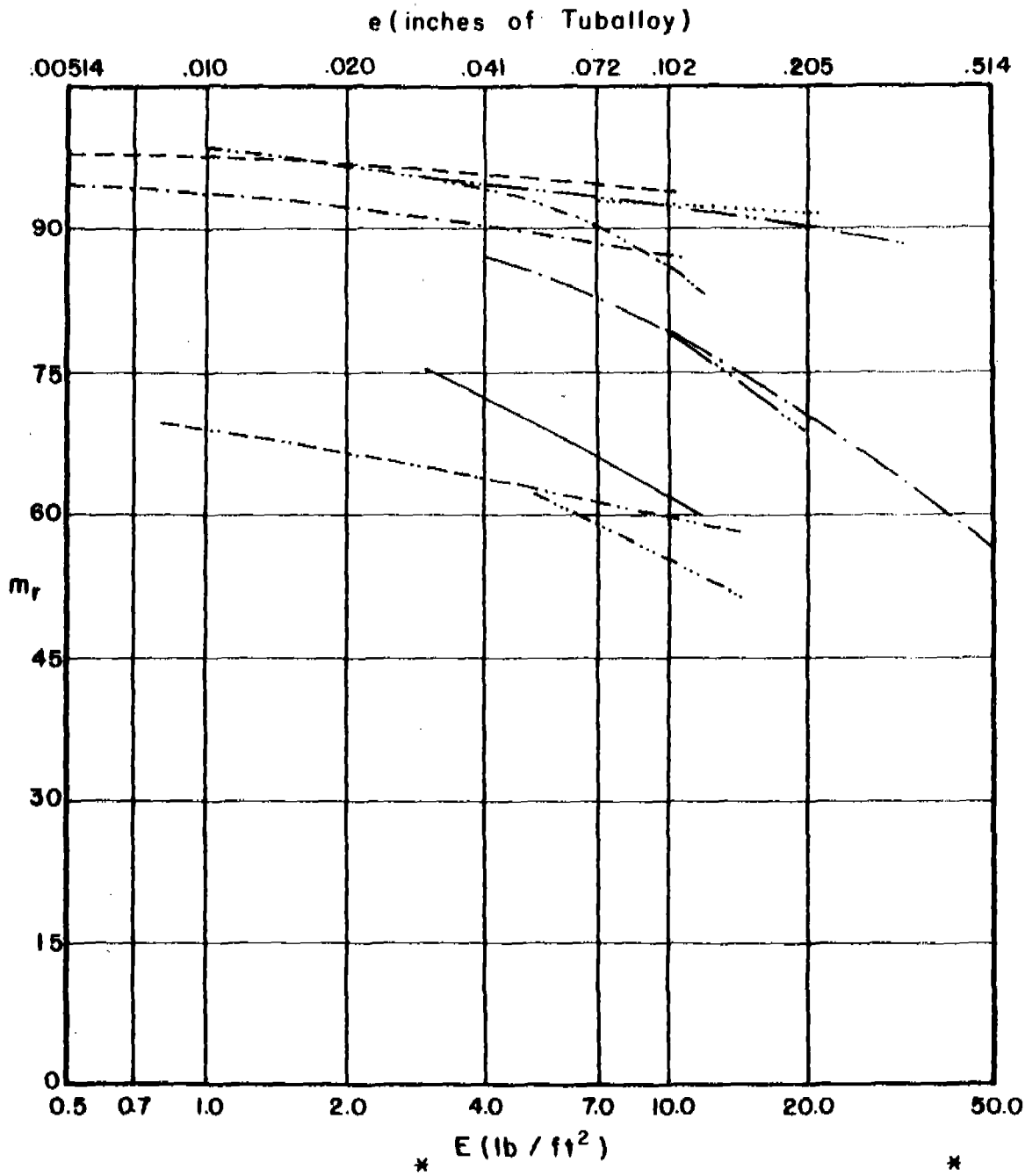

		*			*
Magnesium	— — — —	10.58	F.H. Steel	—··—··—	2.41
2024 T-3	—·—·—	6.65	Hard Steel	———	2.41
Titanium	—··—··—	4.17	Copper	—··—	2.10
Cast Iron	·····	2.59	Lead	—·—	1.70
Mild Steel	— —··— —	2.41	Tuballoy	—···—	1.00

*Ratio of Material Thickness Relative to a Unit Thickness of Tuballoy

Fig. 149

[redacted]

[redacted]

m_r vs E for Various Combinations of m_s, θ, and V_s

m_s = 300 grains θ = 0 degrees V_s = 3000 fps

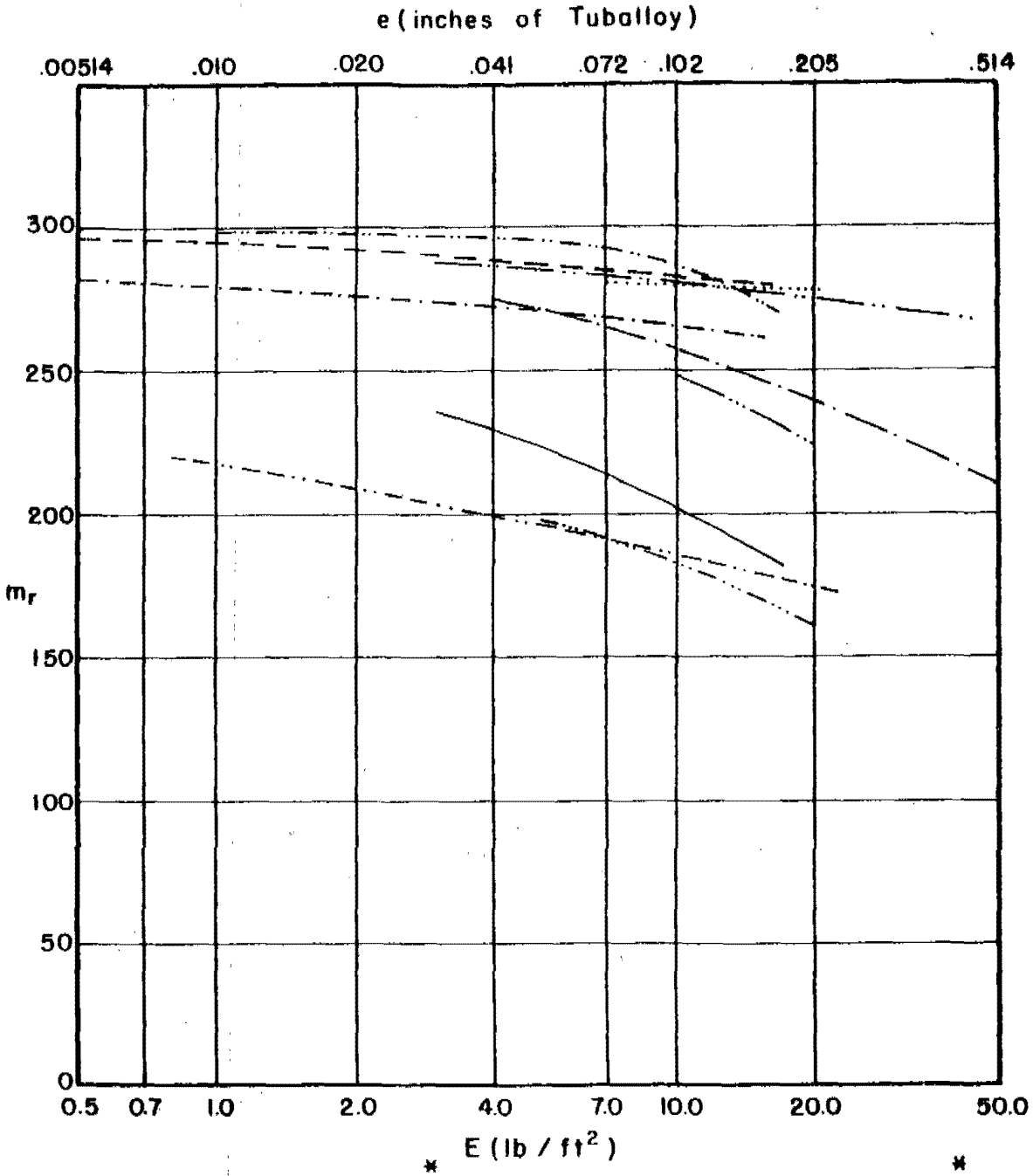

		*			*
Magnesium	———	10.58	F.H. Steel	—·—·—	2.41
2024 T-3	—·—·—	6.65	Hard Steel	———	2.41
Titanium	—··—··—	4.17	Copper	—··—	2.10
Cast Iron	·····	2.59	Lead	—·—	1.70
Mild Steel	—··—	2.41	Tuballoy	—··—	1.00

*Ratio of Material Thickness Relative to a Unit Thickness of Tuballoy

Fig. 150

[redacted]

[redacted]

m_r vs E for Various Combinations of m_s, θ, and V_s

m_s = 30 grains θ = 60 degrees V_s = 3000 fps

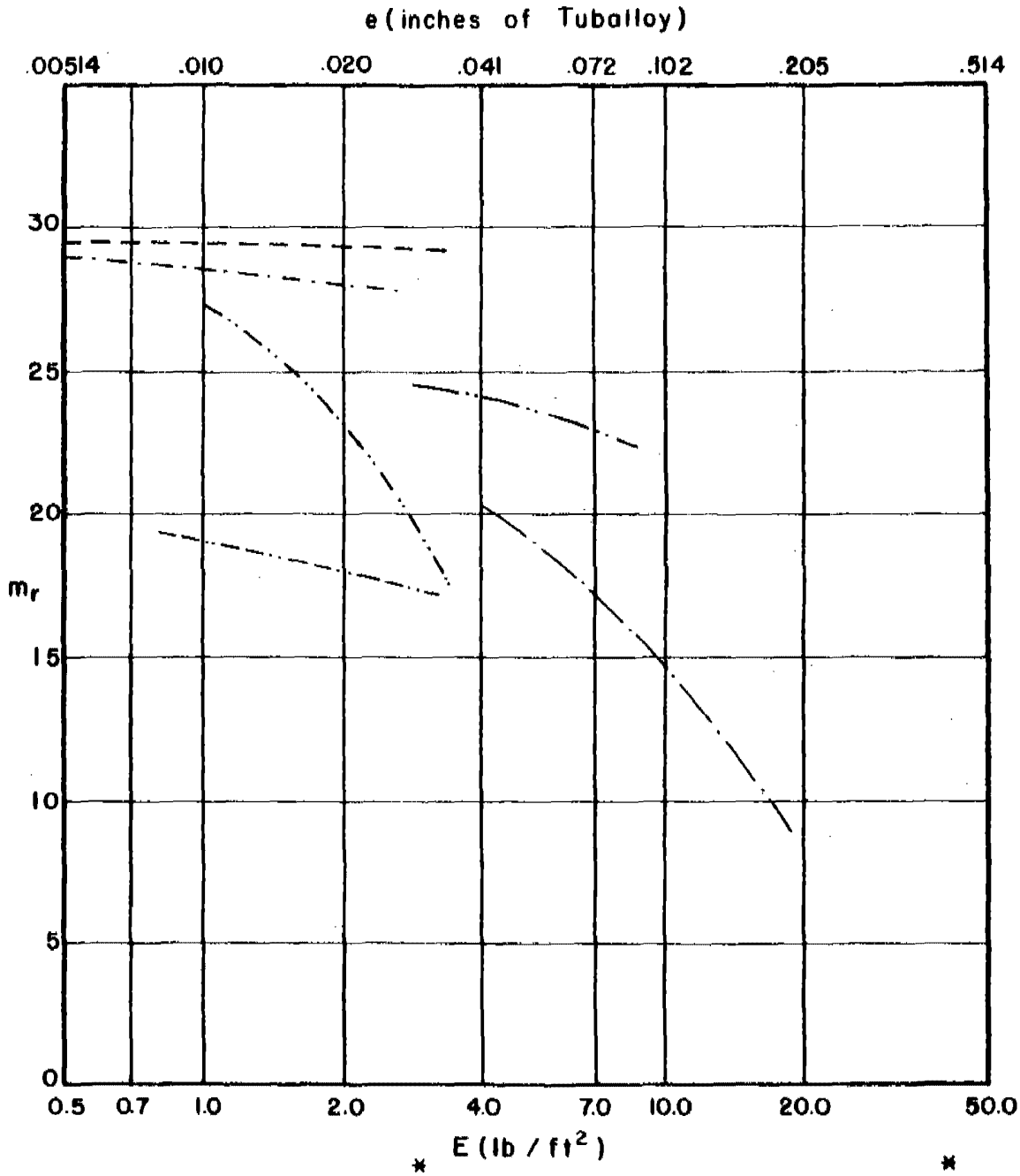

		*			*
Magnesium	— — — —	10.58	F. H. Steel	—··—··—	2.41
2024 T-3	—·—·—	6.65	Hard Steel	———	2.41
Titanium	—··—··—	4.17	Copper	—··—	2.10
Cast Iron	·····	2.59	Lead	—·—	1.70
Mild Steel	—··— —	2.41	Tuballoy	—··—	1.00

*Ratio of Material Thickness Relative to a Unit Thickness of Tuballoy

Fig. 151

[redacted]

[redacted]

m_r vs E for Various Combinations of m_s, θ, and V_s

m_s = 100 grains θ = 60 degrees V_s = 3000 fps

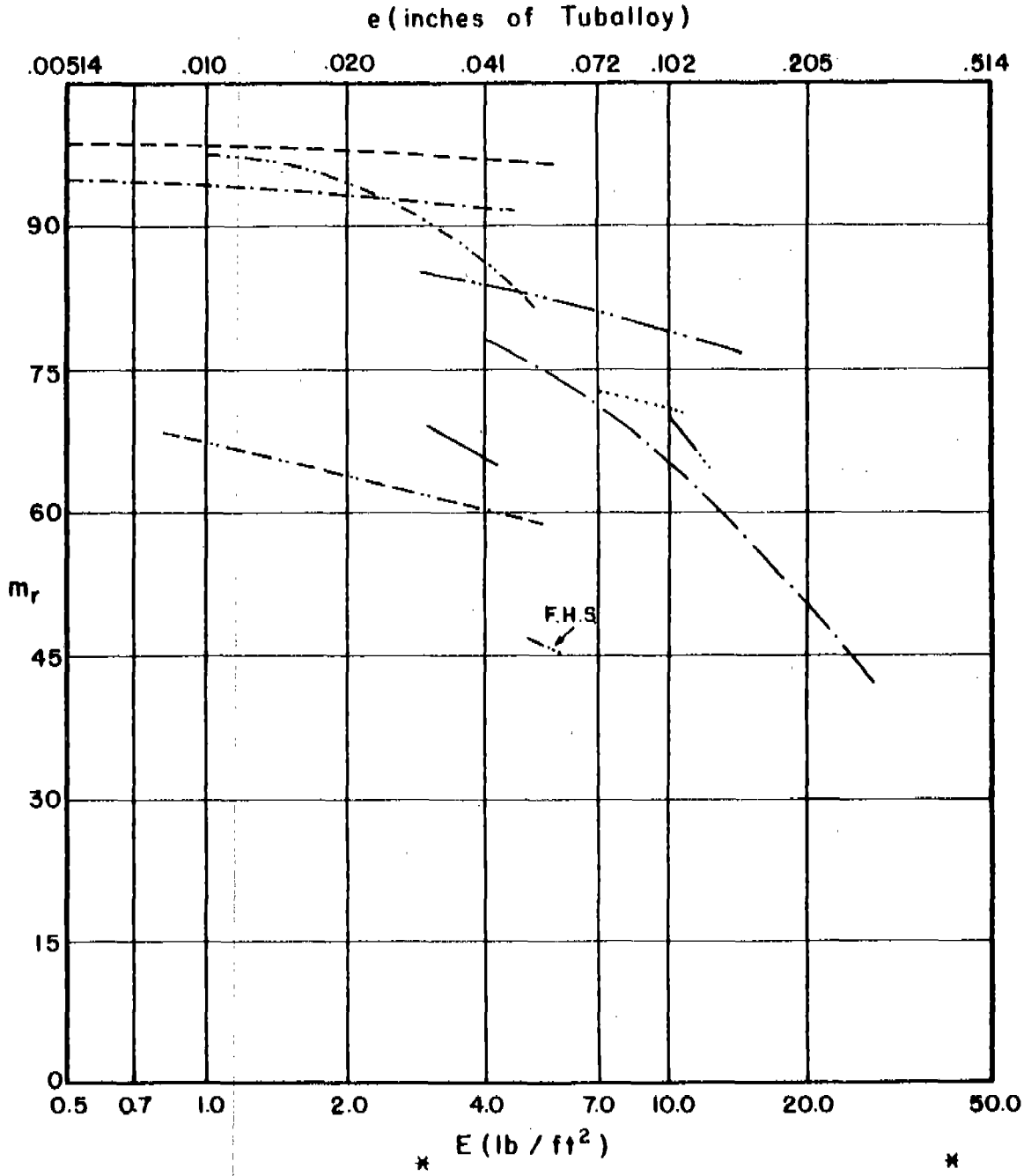

		*			*
Magnesium	— — — —	10.58	F.H. Steel	—·—·—	2.41
2024 T-3	—·—·—	6.65	Hard Steel	———	2.41
Titanium	—··—··—	4.17	Copper	—··—	2.10
Cast Iron	·····	2.59	Lead	—·—	1.70
Mild Steel	—··—	2.41	Tuballoy	—···—	1.00

*Ratio of Material Thickness Relative to a Unit Thickness of Tuballoy

Fig. 152

[redacted]

[redacted]

m_r vs E for Various Combinations of m_s, θ, and V_s

m_s = 300 grains θ = 60 degrees V_s = 3000 fps

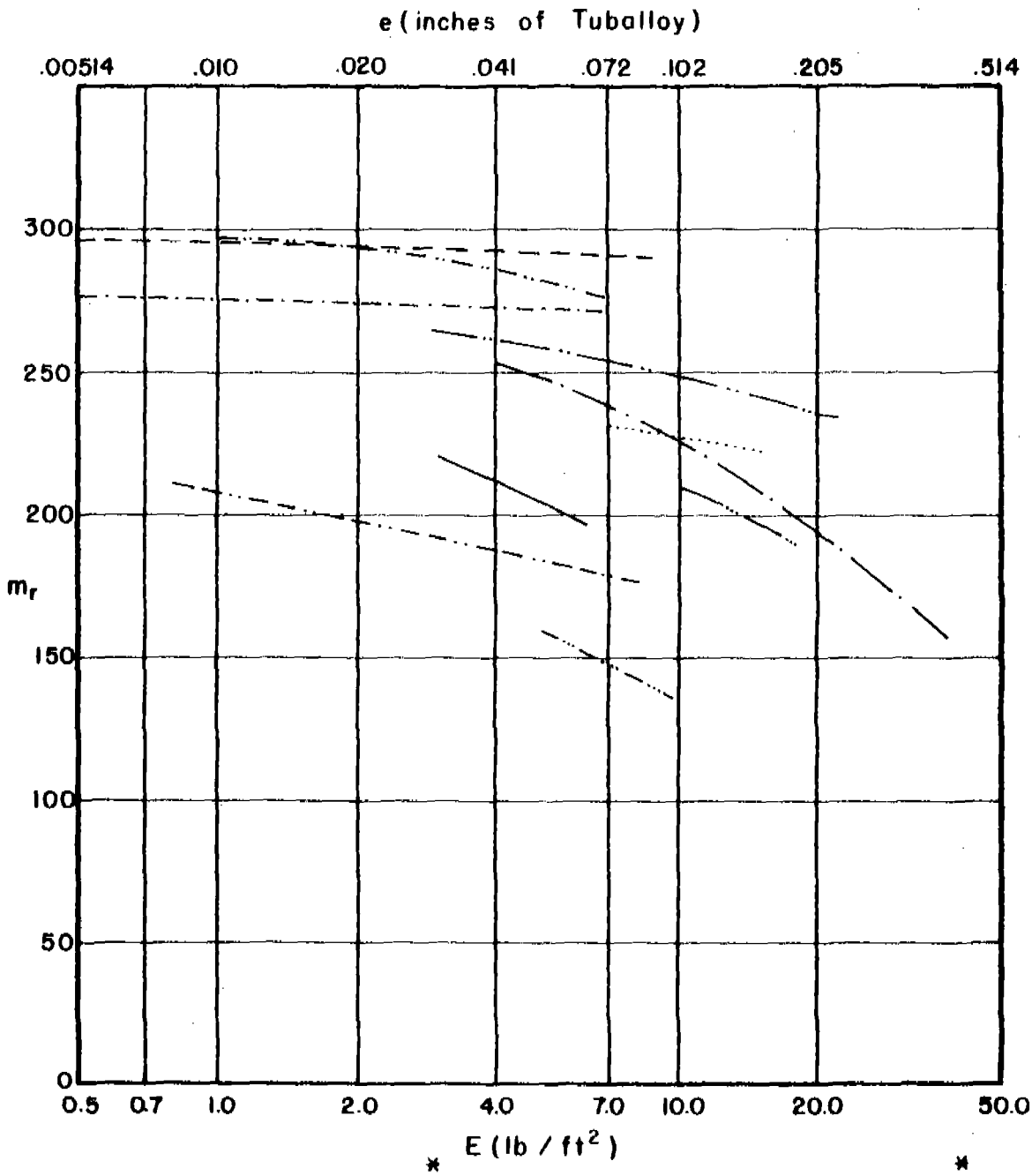

		*			*
Magnesium	— — — —	10.58	F.H. Steel	—··—··—	2.41
2024 T-3	—·—·—	6.65	Hard Steel	———	2.41
Titanium	—··—··—	4.17	Copper	—··—	2.10
Cast Iron	·····	2.59	Lead	—·—	1.70
Mild Steel	— —··— —	2.41	Tuballoy	—··—	1.00

*Ratio of Material Thickness Relative to a Unit Thickness of Tuballoy

Fig. 153

[redacted]

[redacted]

m_r vs E for Various Combinations of m_s, θ, and V_s

m_s = 30 grains θ = 70 degrees V_s = 3000 fps

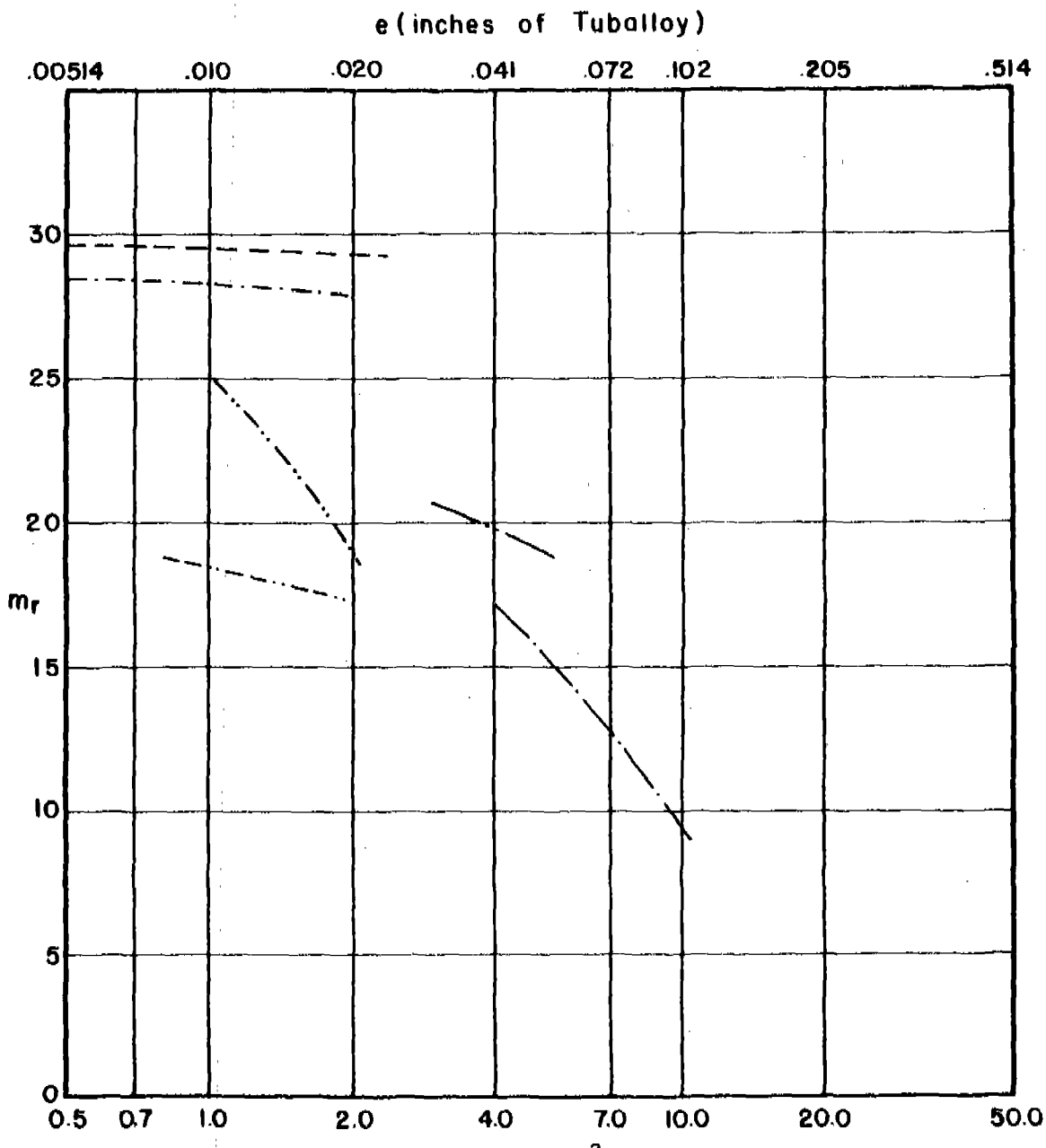

		*			*
Magnesium	———	10.58	F.H. Steel	—··—··—	2.41
2024 T-3	—·—·—	6.65	Hard Steel	———	2.41
Titanium	—··—··—	4.17	Copper	—··—	2.10
Cast Iron	·····	2.59	Lead	—·—	1.70
Mild Steel	—··—	2.41	Tuballoy	—···—	1.00

*Ratio of Material Thickness Relative to a Unit Thickness of Tuballoy

Fig. 154

[redacted]

[redacted]

m_r vs E for Various Combinations of m_s, θ, and V_s

m_s = 100 grains θ = 70 degrees V_s = 3000 fps

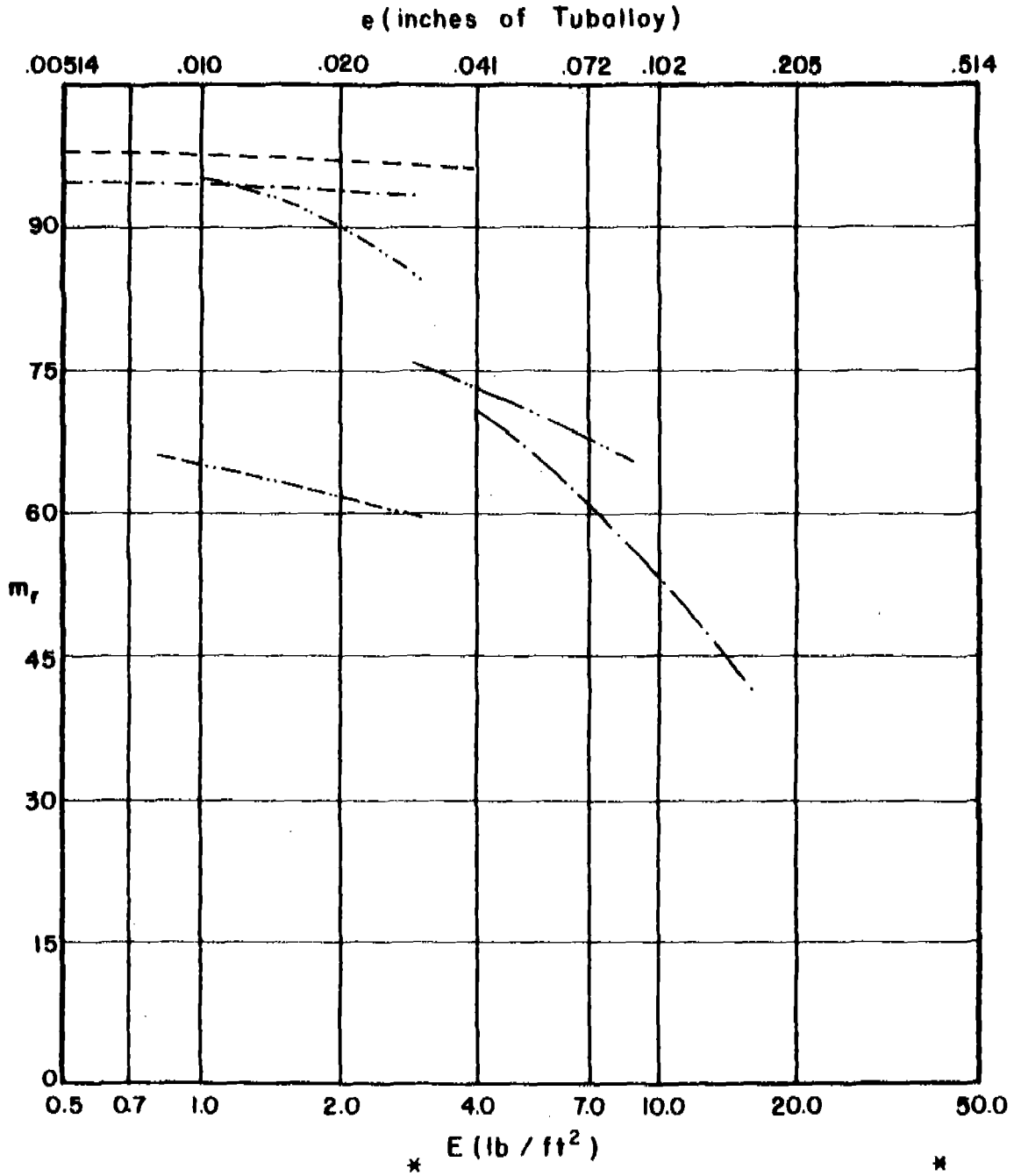

		*			*
Magnesium	— — — —	10.58	F.H. Steel	—··—··—	2.41
2024 T-3	—·—·—	6.65	Hard Steel	———	2.41
Titanium	—··—··—	4.17	Copper	—··—	2.10
Cast Iron	·····	2.59	Lead	—·—	1.70
Mild Steel	— —··— —	2.41	Tuballoy	—··—	1.00

*Ratio of Material Thickness Relative to a Unit Thickness of Tuballoy

Fig. 155

[redacted]

[redacted]

m_r vs E for Various Combinations of m_s, θ, and V_s

m_s = 300 grains θ = 70 degrees V_s = 3000 fps

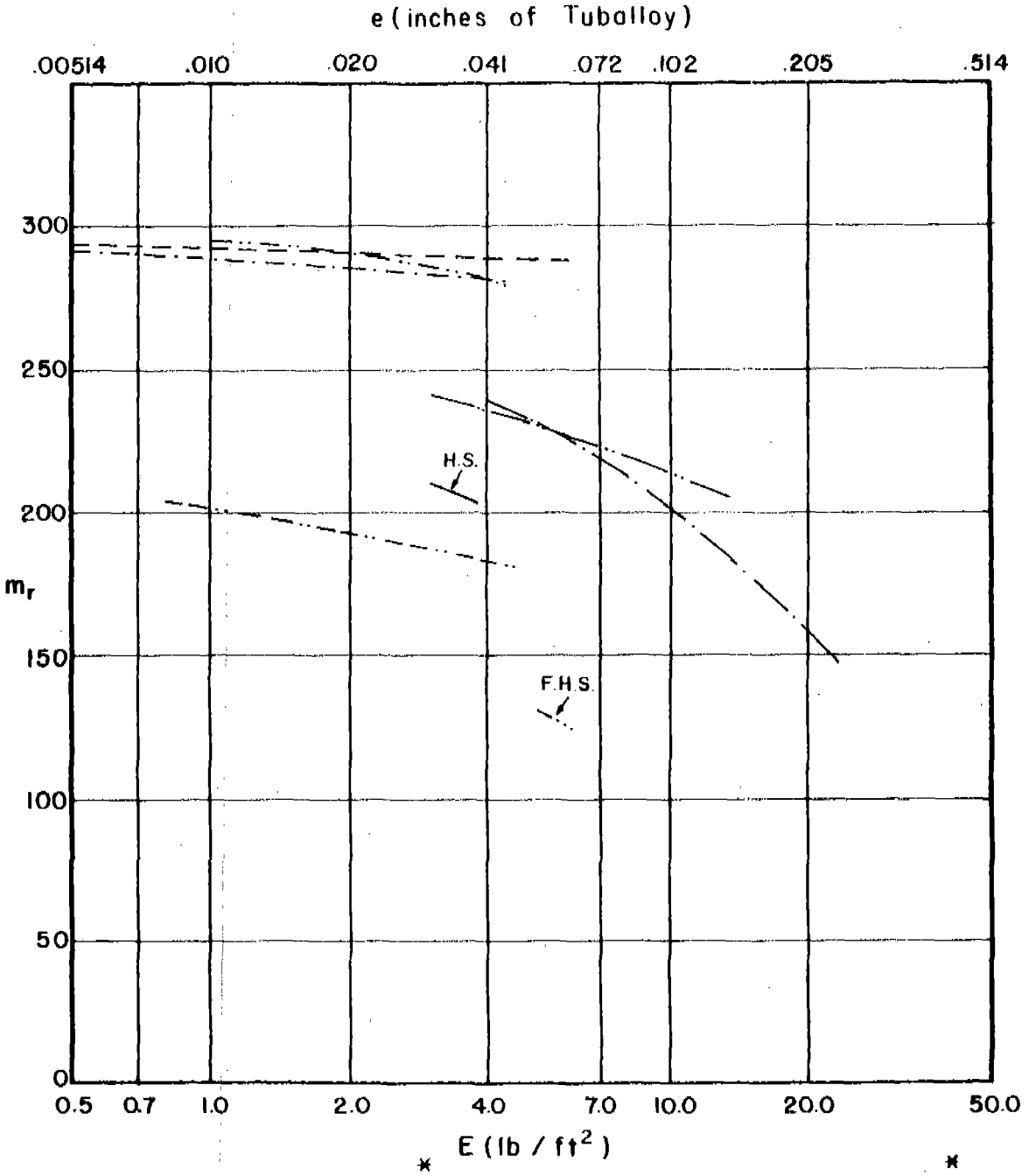

		*			*
Magnesium	— — — —	10.58	F. H. Steel	—·—·—	2.41
2024 T-3	—·—·—	6.65	Hard Steel	———	2.41
Titanium	—··—··—	4.17	Copper	—··—	2.10
Cast Iron	·····	2.59	Lead	—·—	1.70
Mild Steel	— —··— —	2.41	Tuballoy	—····—	1.00

*Ratio of Material Thickness Relative to a Unit Thickness of Tuballoy

Fig. 156

[redacted]

[redacted]

m_r vs E for Various Combinations of m_s, θ, and V_s

m_s = 30 grains θ = 0 degrees V_s = 6000 fps

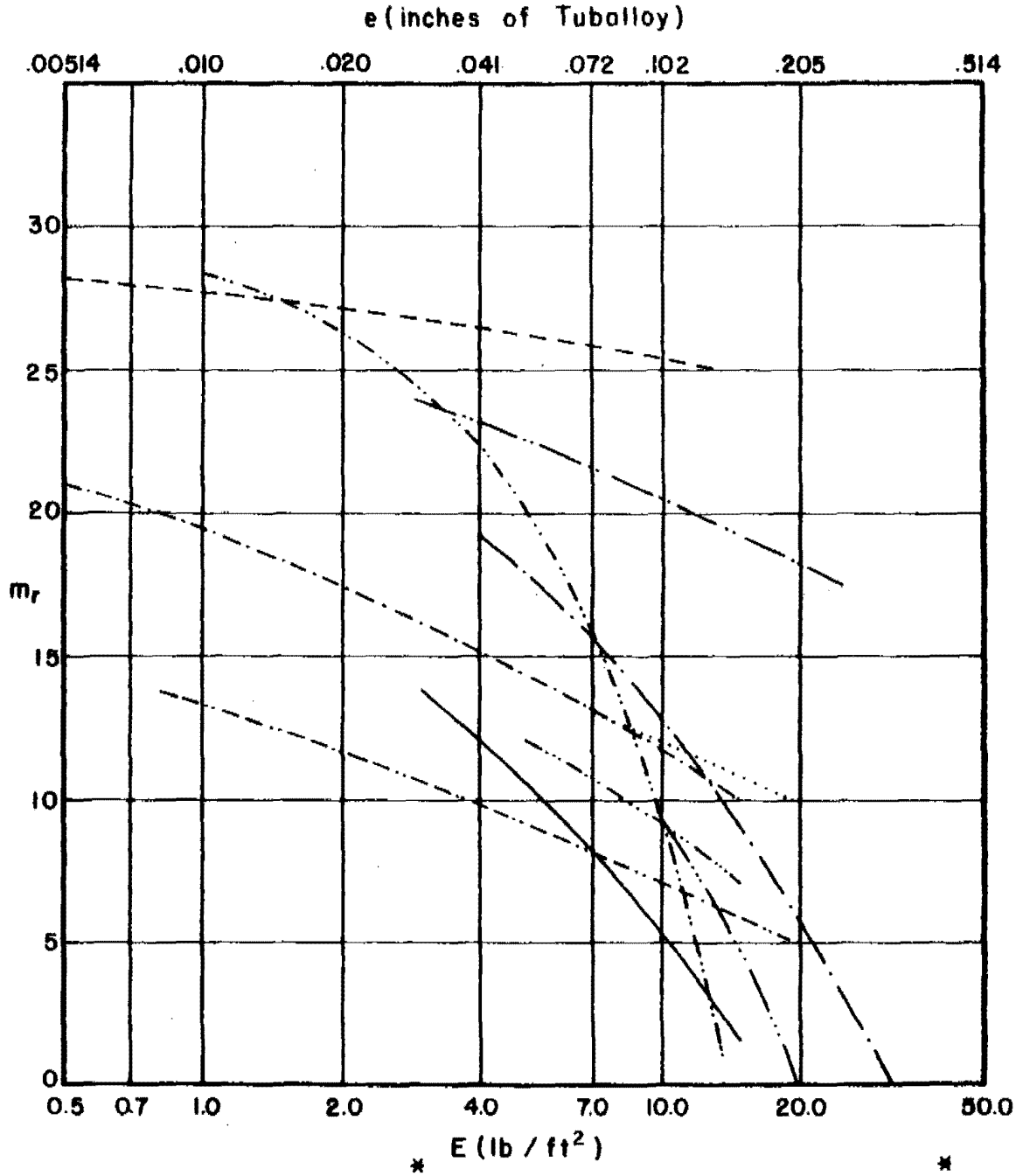

		*			*
Magnesium	— — — —	10.58	F.H. Steel	—··—··—	2.41
2024 T-3	—·—·—	6.65	Hard Steel	———	2.41
Titanium	—··—··—	4.17	Copper	—··—	2.10
Cast Iron	·····	2.59	Lead	—·—	1.70
Mild Steel	— —··— —	2.41	Tuballoy	—··—	1.00

*Ratio of Material Thickness Relative to a Unit Thickness of Tuballoy

Fig. 157

[redacted]

[redacted]

m_r vs E for Various Combinations of m_s, θ, and V_s

m_s = 100 grains θ = 0 degrees V_s = 6000 fps

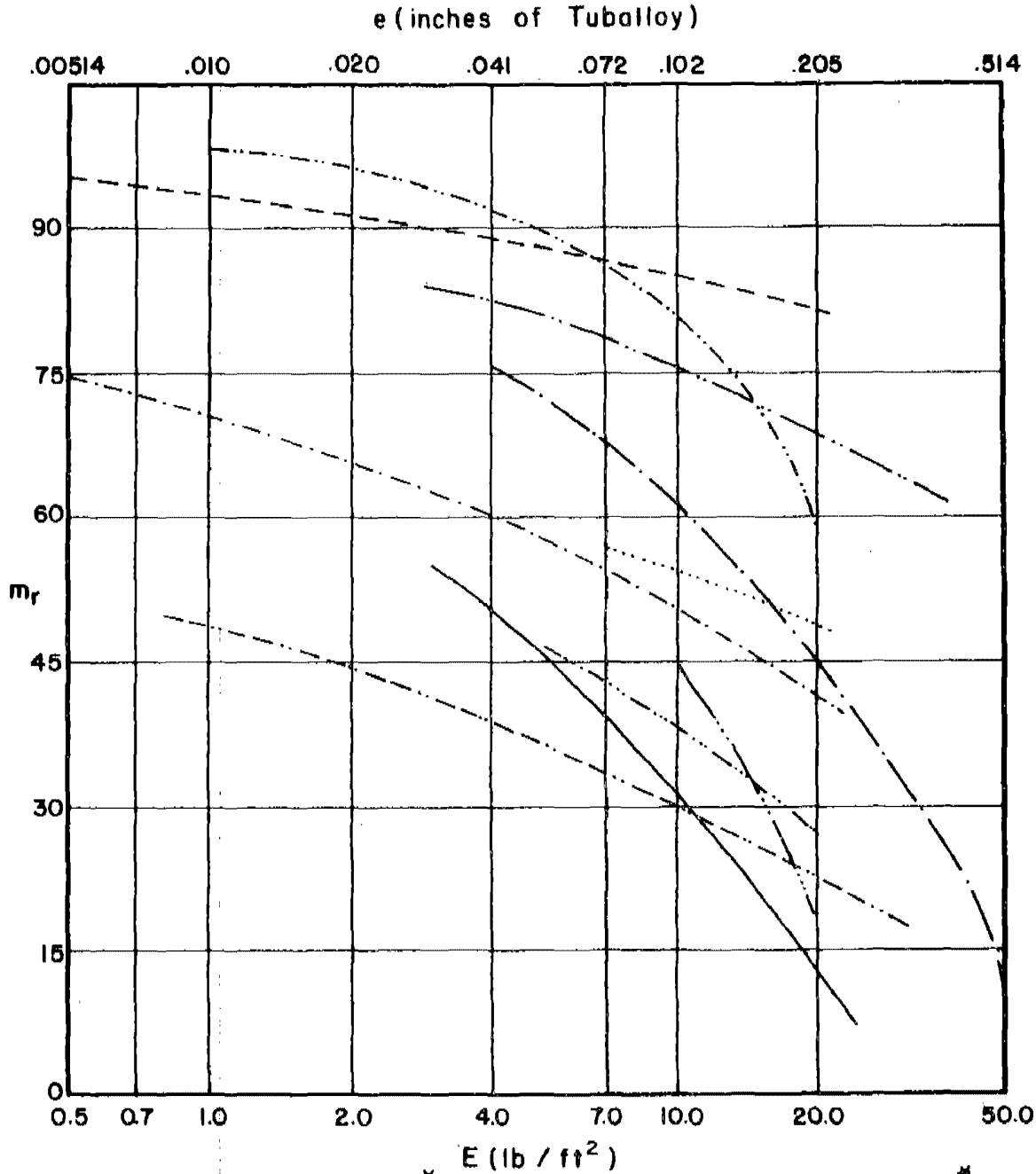

		*			*
Magnesium	— — — —	10.58	F.H. Steel	—··—··—	2.41
2024 T-3	—·—·—·—	6.65	Hard Steel	———	2.41
Titanium	—··—··—	4.17	Copper	—··—	2.10
Cast Iron	·····	2.59	Lead	—·—	1.70
Mild Steel	— —··— —	2.41	Tuballoy	—···—	1.00

*Ratio of Material Thickness Relative to a Unit Thickness of Tuballoy

Fig. 158

[redacted]

[redacted]

m_r vs E for Various Combinations of m_s, θ, and V_s

m_s = 300 grains θ = 0 degrees V_s = 6000 fps

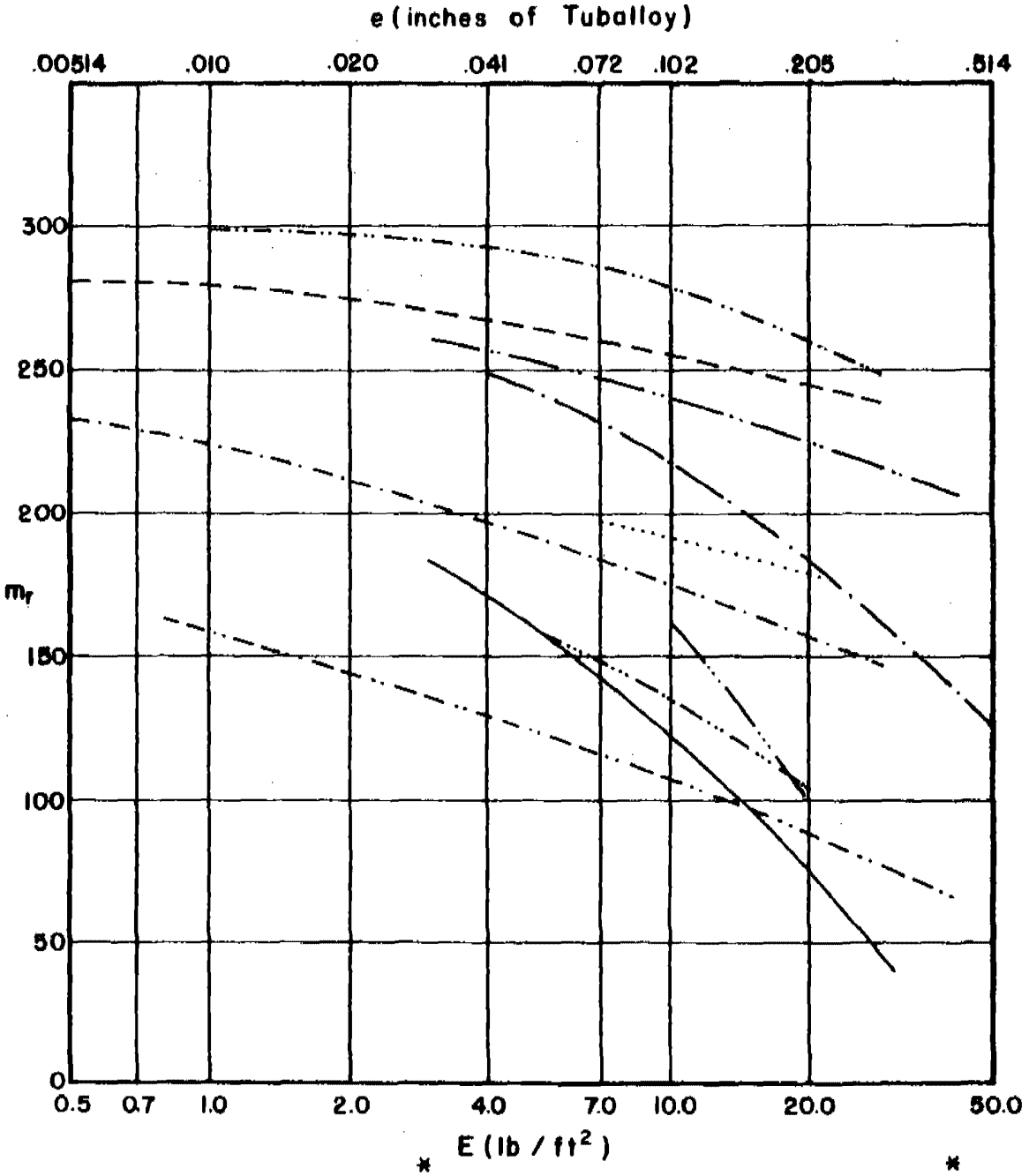

		*			*
Magnesium	— — — —	10.58	F.H. Steel	—·—·—	2.41
2024 T-3	—·—·—	6.65	Hard Steel	———	2.41
Titanium	—··—··—	4.17	Copper	—··—	2.10
Cast Iron	·····	2.59	Lead	—·—	1.70
Mild Steel	—··— —	2.41	Tuballoy	—···—	1.00

*Ratio of Material Thickness Relative to a Unit Thickness of Tuballoy

Fig. 159

[redacted]

[redacted]

m_r vs E for Various Combinations of m_s, θ, and V_s

m_s = 30 grains θ = 60 degrees V_s = 6000 fps

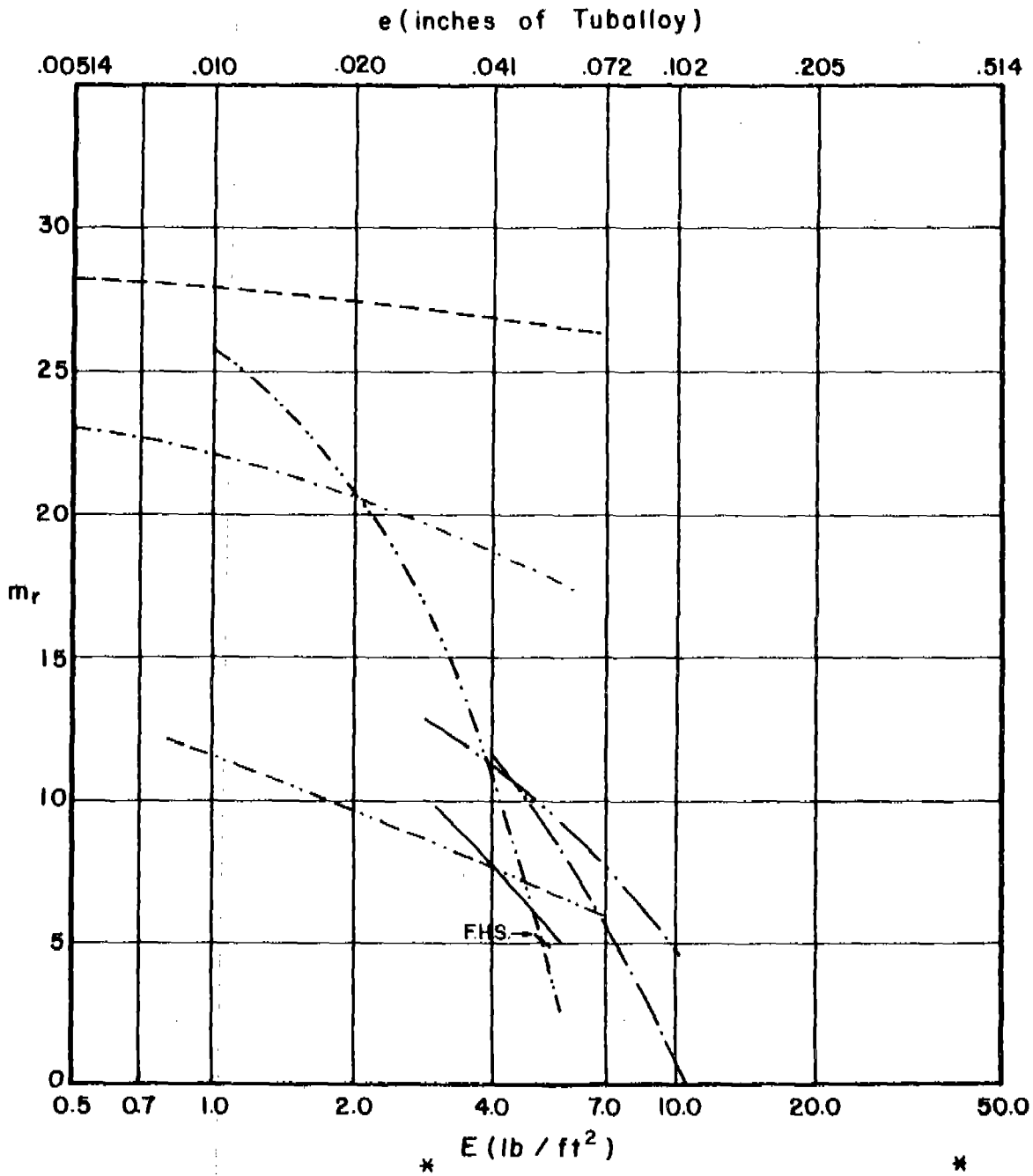

		*			*
Magnesium	— — — —	10.58	F.H. Steel	—·—·—	2.41
2024 T-3	—·—·—	6.65	Hard Steel	———	2.41
Titanium	—··—··—	4.17	Copper	—··—	2.10
Cast Iron	·····	2.59	Lead	—·—	1.70
Mild Steel	— —··— —	2.41	Tuballoy	—··—	1.00

*Ratio of Material Thickness Relative to a Unit Thickness of Tuballoy

Fig. 160

[redacted]

[redacted]

m_r vs E for Various Combinations of m_s, θ, and V_s

m_s = 100 grains θ = 60 degrees V_s = 6000 fps

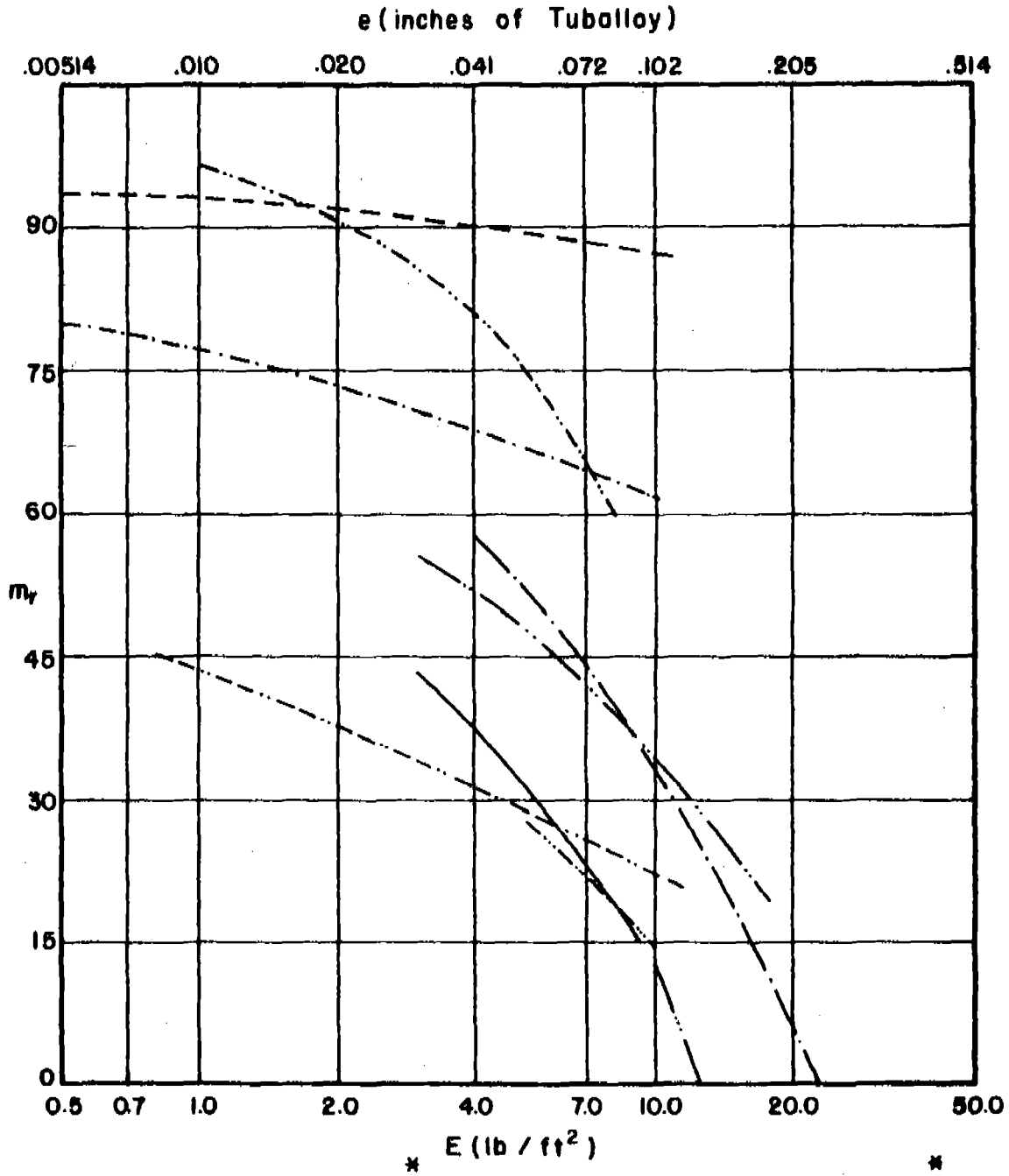

		*			*
Magnesium	———	10.58	F. H. Steel	—··—··—	2.41
2024 T-3	—·—·—	6.65	Hard Steel	———	2.41
Titanium	—··—··—	4.17	Copper	—··—	2.10
Cast Iron	·····	2.59	Lead	—·—	1.70
Mild Steel	—··—	2.41	Tuballoy	—···—	1.00

*Ratio of Material Thickness Relative to a Unit Thickness of Tuballoy

Fig. 161

[redacted]

[redacted]

m_r vs E for Various Combinations of m_s, θ, and V_s

m_s = 300 grains θ = 60 degrees V_s = 6000 fps

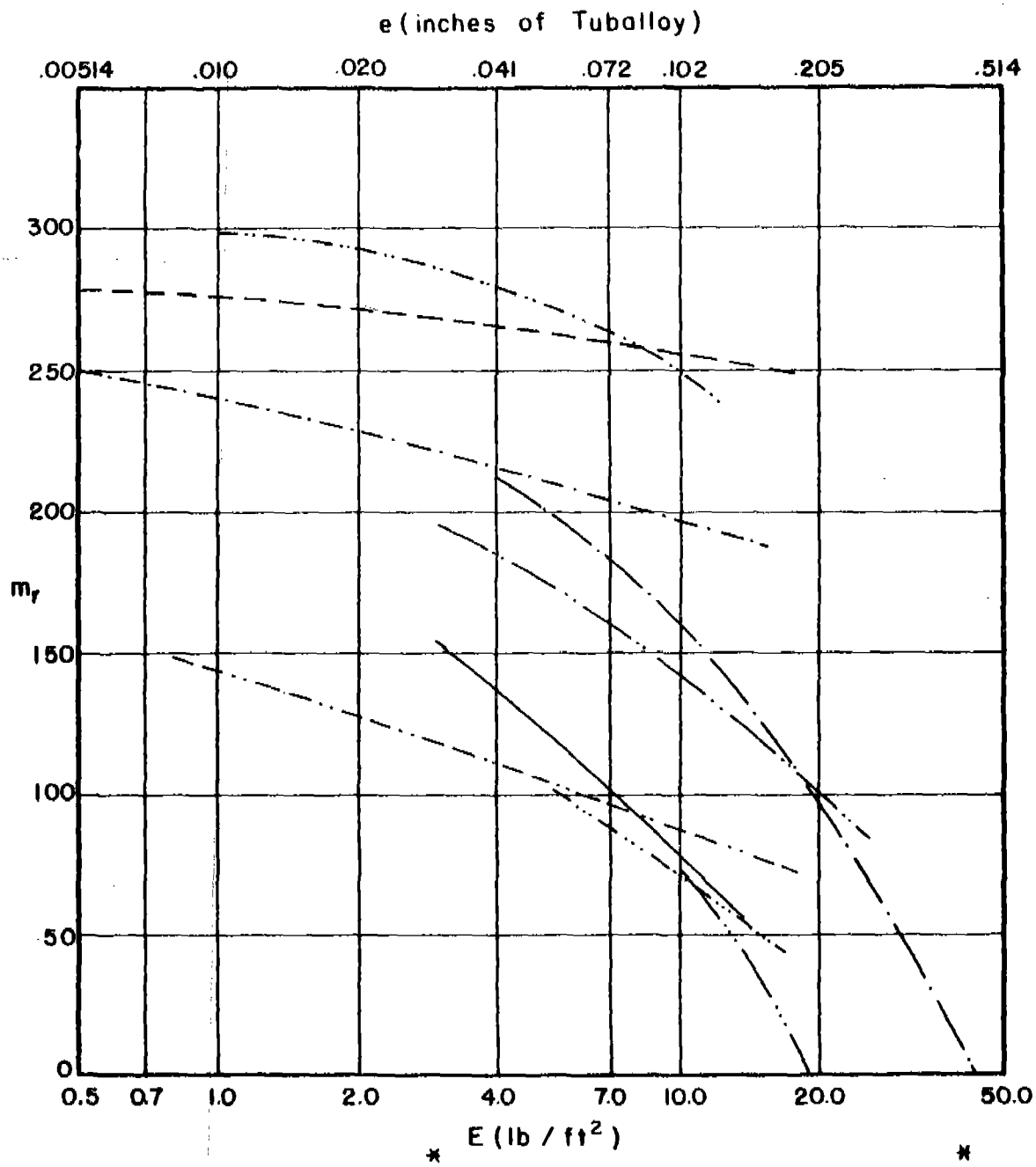

		*			*
Magnesium	— — — —	10.58	F. H. Steel	—·····—·····—	2.41
2024 T-3	—·—·—·—	6.65	Hard Steel	————	2.41
Titanium	—··—··—··—	4.17	Copper	—··—··—	2.10
Cast Iron	·····	2.59	Lead	—·—·—	1.70
Mild Steel	— —··— —	2.41	Tuballoy	—····—	1.00

*Ratio of Material Thickness Relative to a Unit Thickness of Tuballoy

Fig. 162

[redacted]

[redacted]

m_r vs E for Various Combinations of m_s, θ, and V_s

m_s = 30 grains θ = 70 degrees V_s = 6000 fps

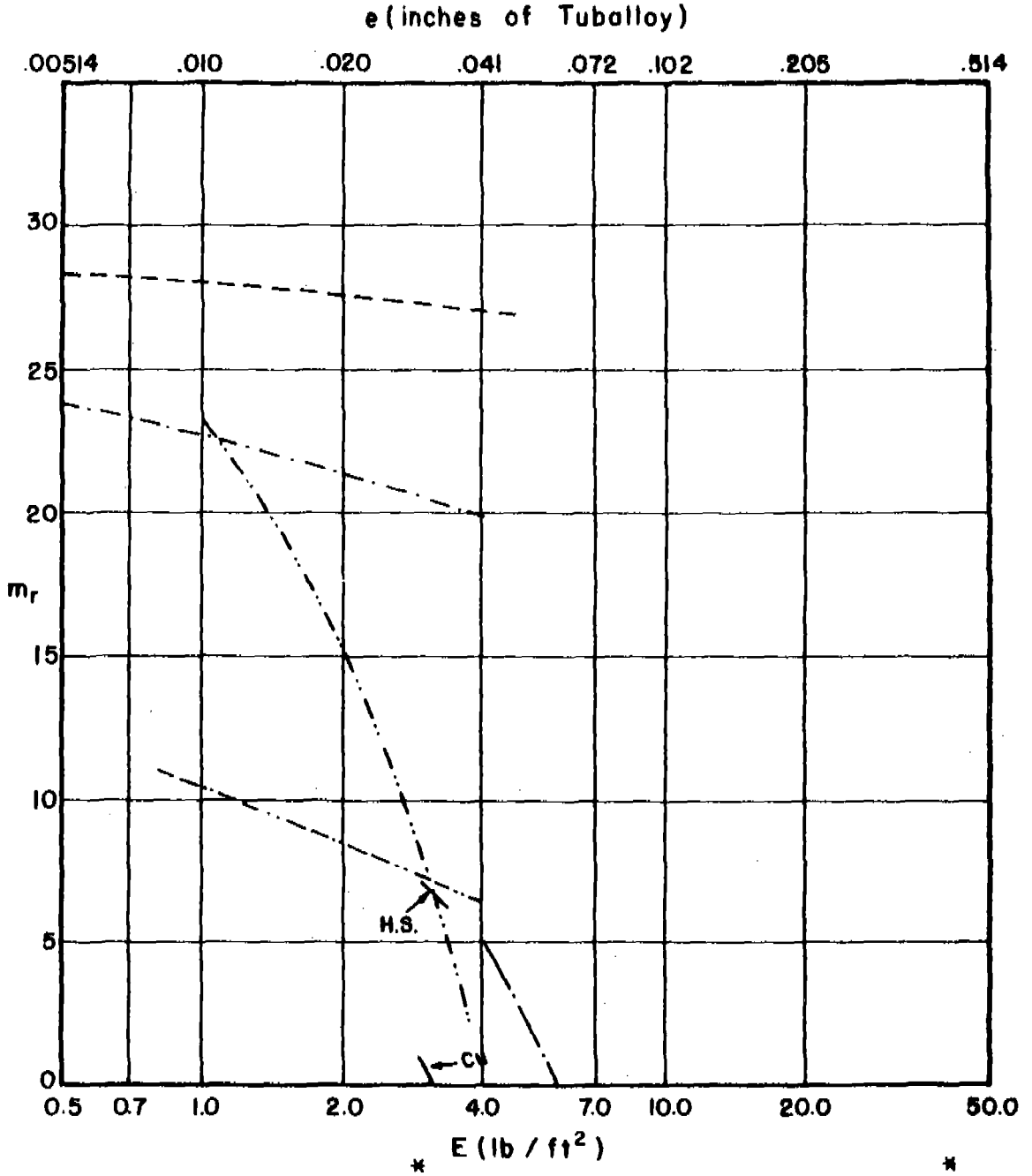

		*			*
Magnesium	- - - - -	10.58	F. H. Steel	—··—··—	2.41
2024 T-3	—·—·—	6.65	Hard Steel	———	2.41
Titanium	—··—··—	4.17	Copper	—··—	2.10
Cast Iron	·····	2.59	Lead	—·—	1.70
Mild Steel	— —··— —	2.41	Tuballoy	—···—	1.00

*Ratio of Material Thickness Relative to a Unit Thickness of Tuballoy

Fig. 163

[redacted]

[redacted]

m_r vs E for Various Combinations of m_s, θ, and V_s

m_s = 100 grains θ = 70 degrees V_s = 6000 fps

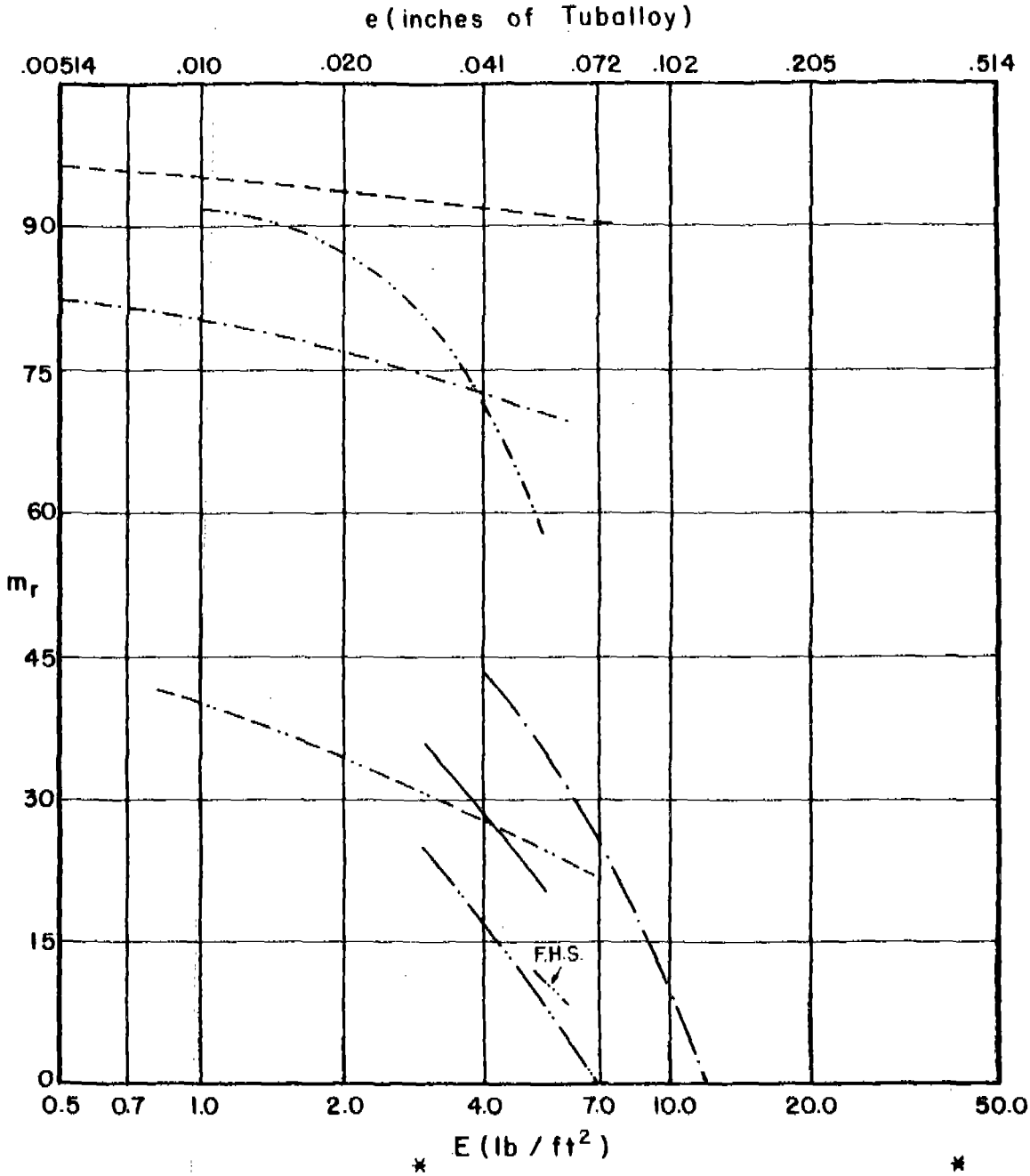

		*			*
Magnesium	— — — —	10.58	F. H. Steel	—·—·—	2.41
2024 T-3	—·—·—	6.65	Hard Steel	———	2.41
Titanium	—··—··—	4.17	Copper	—··—··—	2.10
Cast Iron	·····	2.59	Lead	—·—·—	1.70
Mild Steel	—··—··—	2.41	Tuballoy	—··—··—	1.00

*Ratio of Material Thickness Relative to a Unit Thickness of Tuballoy

Fig. 164

[redacted]

[redacted]

m_r vs E for Various Combinations of m_s, θ, and V_s

m_s = 300 grains θ = 70 degrees V_s = 6000 fps

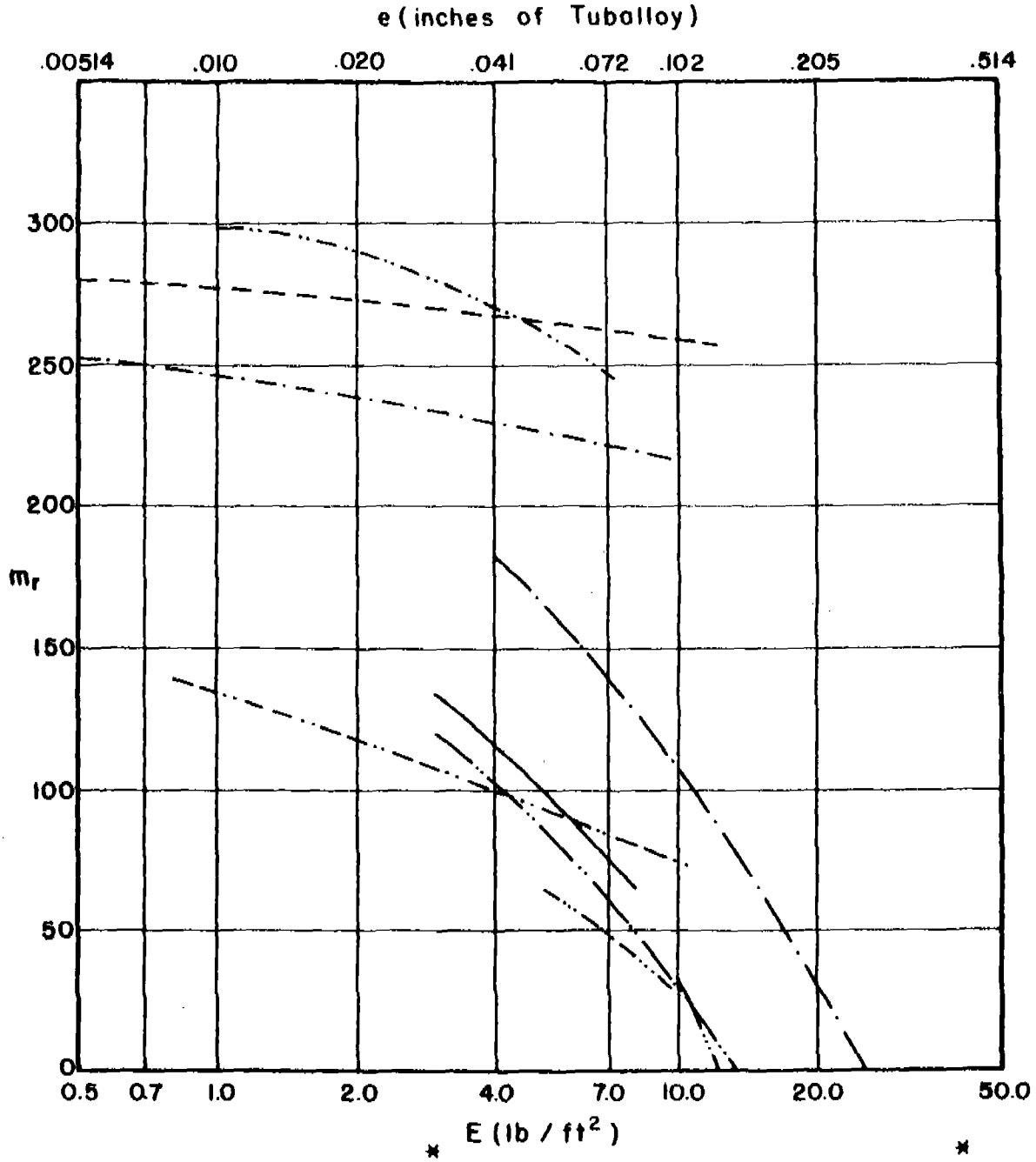

		*			*
Magnesium	— — — —	10.58	F.H. Steel	—·—·—	2.41
2024 T-3	—·—·—	6.65	Hard Steel	———	2.41
Titanium	—··—··—	4.17	Copper	—··—··—	2.10
Cast Iron	·····	2.59	Lead	—·—·—	1.70
Mild Steel	— —··— —	2.41	Tuballoy	—··—··—	1.00

*Ratio of Material Thickness Relative to a Unit Thickness of Tuballoy

Fig. 165

[redacted]

[redacted]

m_r vs E for Various Combinations of m_s, θ, and V_s

m_s = 30 grains θ = 0 degrees V_s = 9000 fps

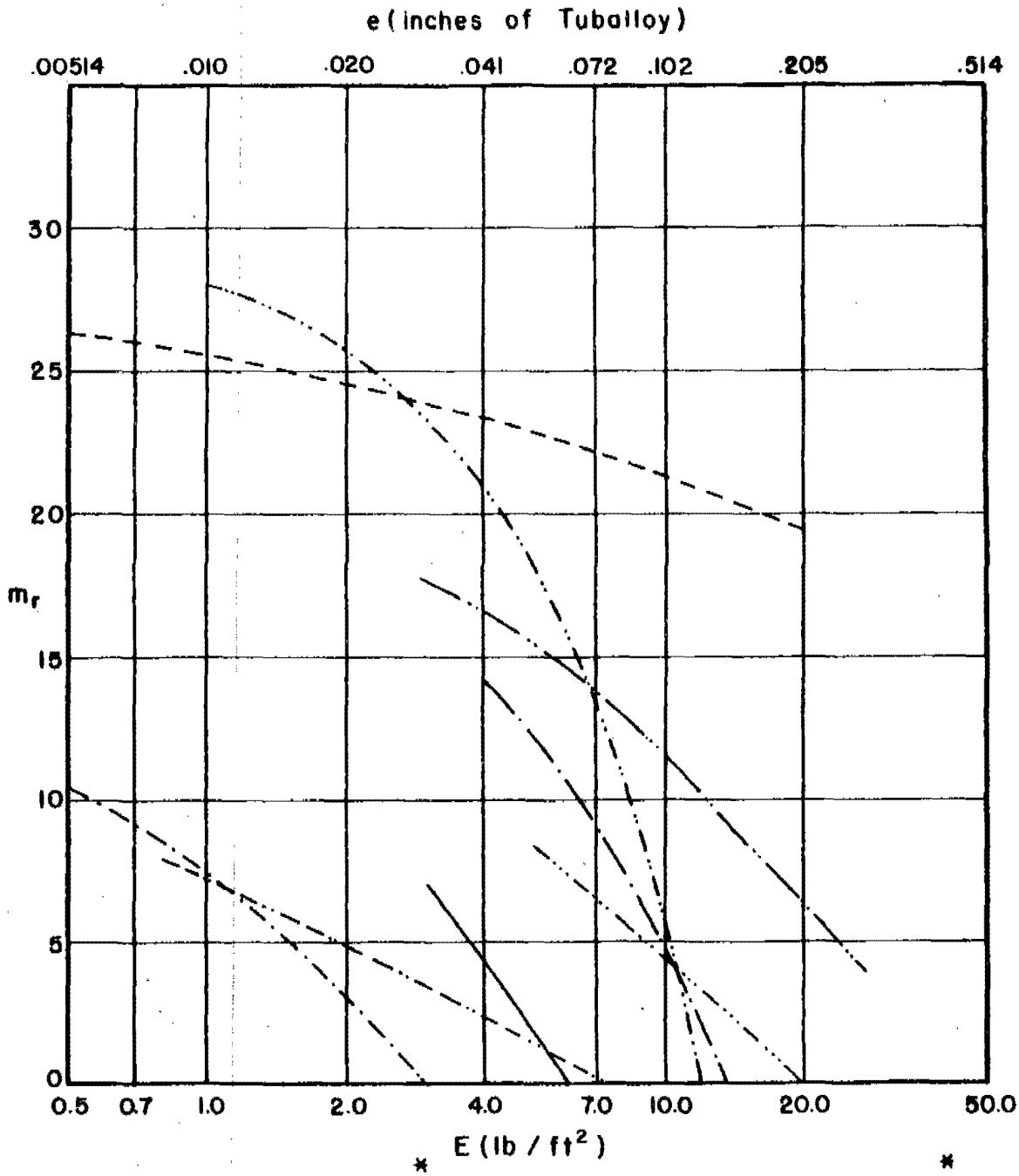

		*			*
Magnesium	— — — —	10.58	F.H. Steel	—··—··—	2.41
2024 T-3	—·—·—	6.65	Hard Steel	———	2.41
Titanium	—··—··—	4.17	Copper	—··—	2.10
Cast Iron	·····	2.59	Lead	—·—	1.70
Mild Steel	— —··— —	2.41	Tuballoy	—···—	1.00

*Ratio of Material Thickness Relative to a Unit Thickness of Tuballoy

Fig. 166

[redacted]

[redacted]

m_r vs E for Various Combinations of m_s, θ, and V_s

m_s = 100 grains θ = 0 degrees V_s = 9000 fps

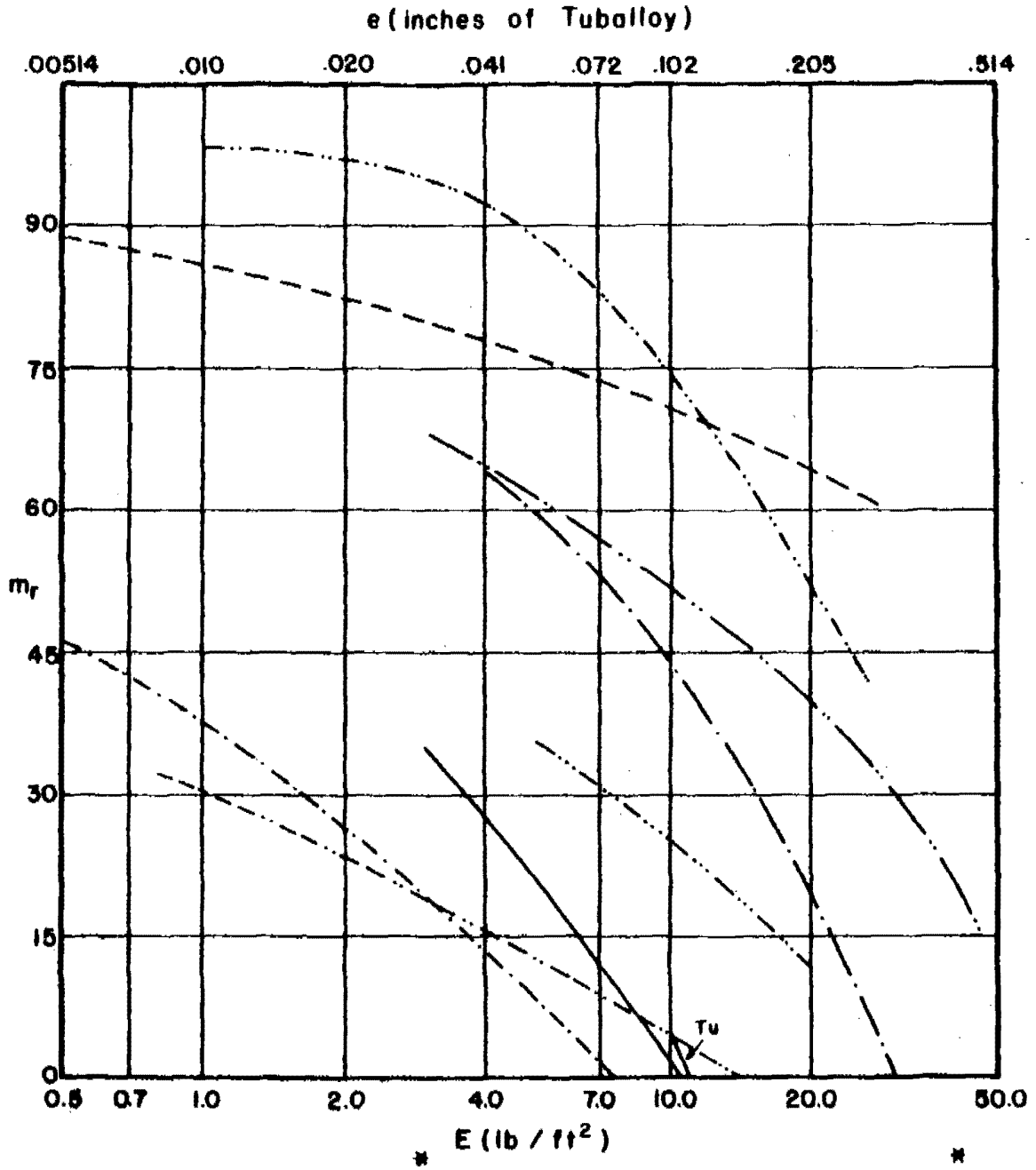

		*			*
Magnesium	— — — —	10.58	F. H. Steel	—·—·—	2.41
2024 T-3	—·—·—	6.65	Hard Steel	———	2.41
Titanium	—··—··—	4.17	Copper	—··—	2.10
Cast Iron	·····	2.59	Lead	—·—	1.70
Mild Steel	— —··— —	2.41	Tuballoy	—··—	1.00

*Ratio of Material Thickness Relative to a Unit Thickness of Tuballoy

Fig. 167

[redacted]

[redacted]

m_r vs E for Various Combinations of m_s, θ, and V_s

m_s = 300 grains θ = 0 degrees V_s = 9000 fps

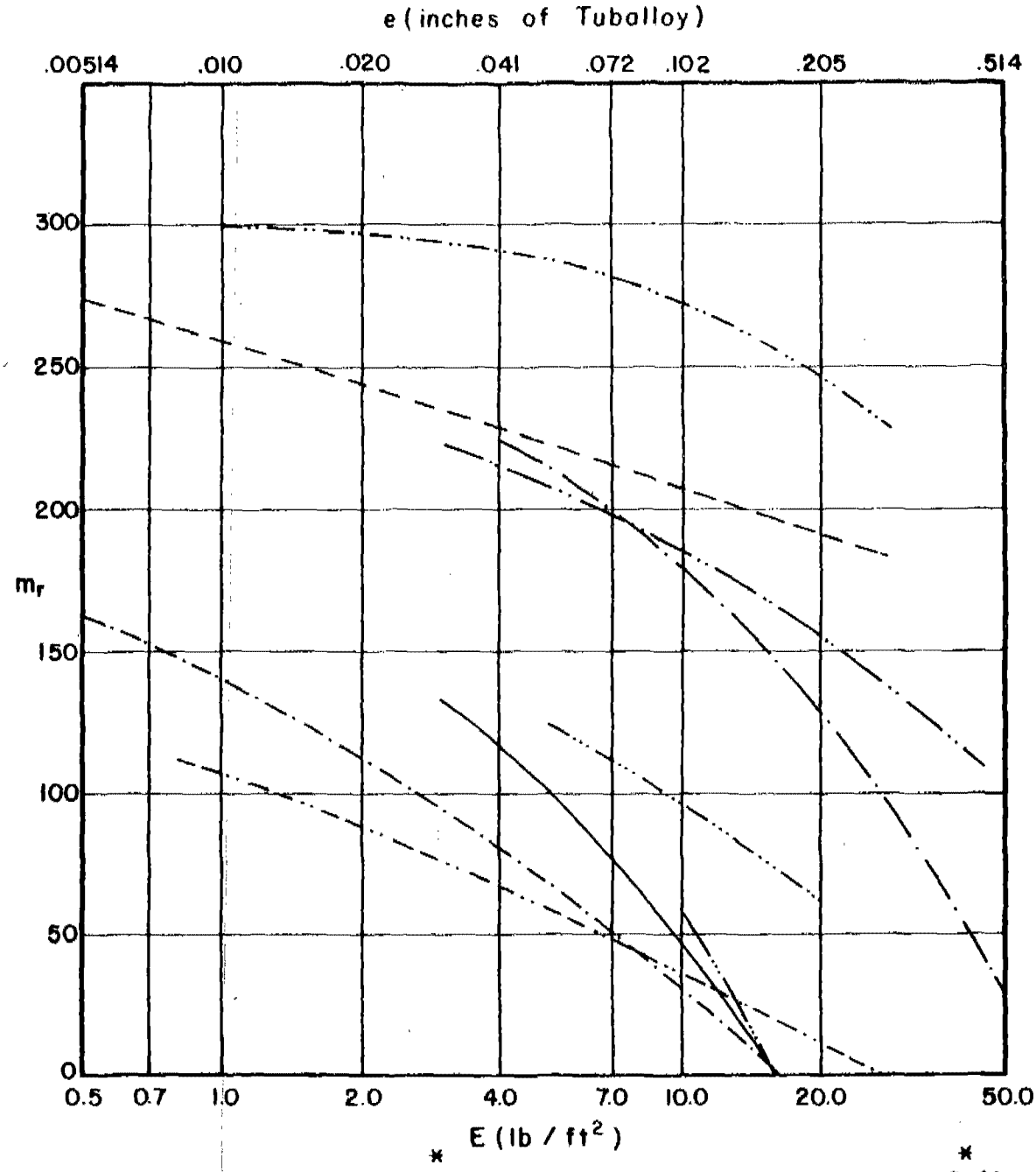

		*			*
Magnesium	— — — —	10.58	F.H. Steel	—·—·—	2.41
2024 T-3	—·—·—	6.65	Hard Steel	———	2.41
Titanium	—··—··—	4.17	Copper	—··—	2.10
Cast Iron	·····	2.59	Lead	—·—	1.70
Mild Steel	—··—··—	2.41	Tuballoy	—···—	1.00

*Ratio of Material Thickness Relative to a Unit Thickness of Tuballoy

Fig. 168

[redacted]

[redacted]

m_r vs E for Various Combinations of m_s, θ, and V_s

m_s = 30 grains θ = 60 degrees V_s = 9000 fps

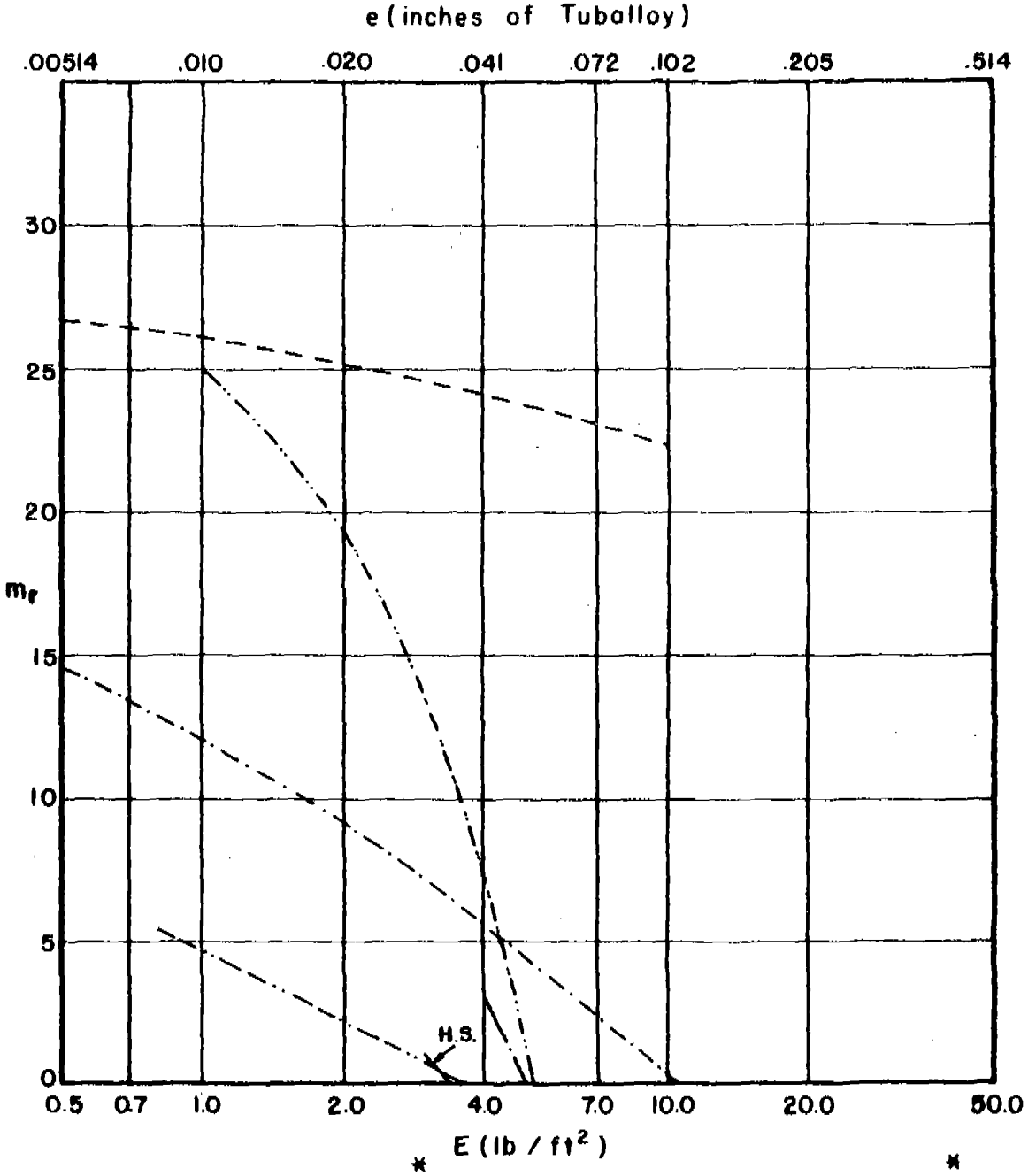

		*			*
Magnesium	— — — —	10.58	F.H. Steel	—·—·—	2.41
2024 T-3	—·—·—	6.65	Hard Steel	———	2.41
Titanium	—··—··—	4.17	Copper	—··—	2.10
Cast Iron	·····	2.59	Lead	—·—	1.70
Mild Steel	—··—··—	2.41	Tuballoy	—···—	1.00

*Ratio of Material Thickness Relative to a Unit Thickness of Tuballoy

Fig. 169

[redacted]

[redacted]

m_r vs E for Various Combinations of m_s, θ, and V_s

m_s = 100 grains θ = 60 degrees V_s = 9000 fps

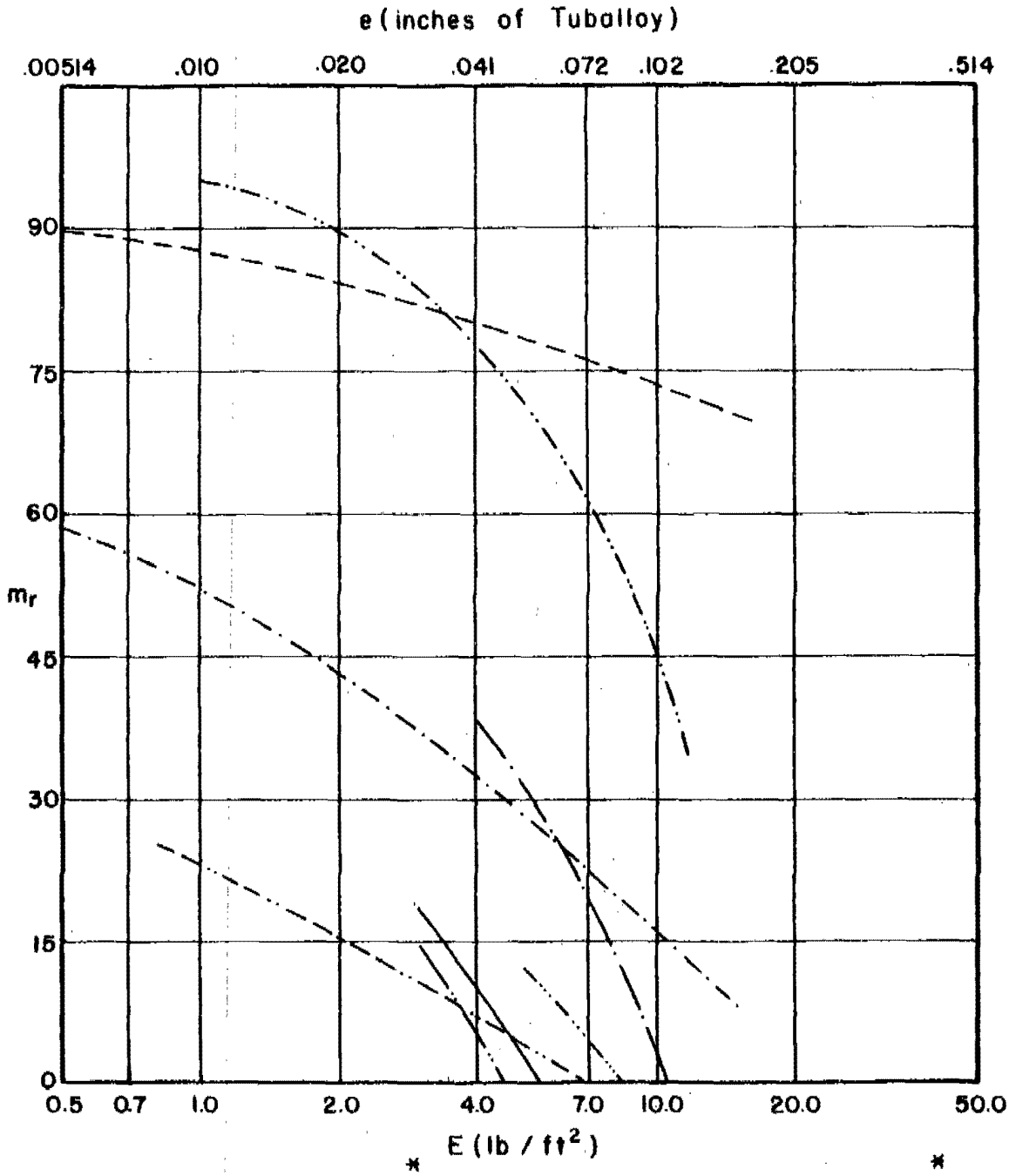

		*			*
Magnesium	— — — —	10.58	F.H. Steel	—·····—·····—	2.41
2024 T-3	—·—·—·—	6.65	Hard Steel	————	2.41
Titanium	—··—··—	4.17	Copper	—··—	2.10
Cast Iron	·····	2.59	Lead	—·—	1.70
Mild Steel	—··—·—	2.41	Tuballoy	—···—	1.00

*Ratio of Material Thickness Relative to a Unit Thickness of Tuballoy

Fig. 170

[redacted]

[redacted]

m_r vs E for Various Combinations of m_s, θ, and V_s

m_s = 300 grains θ = 60 degrees V_s = 9000 fps

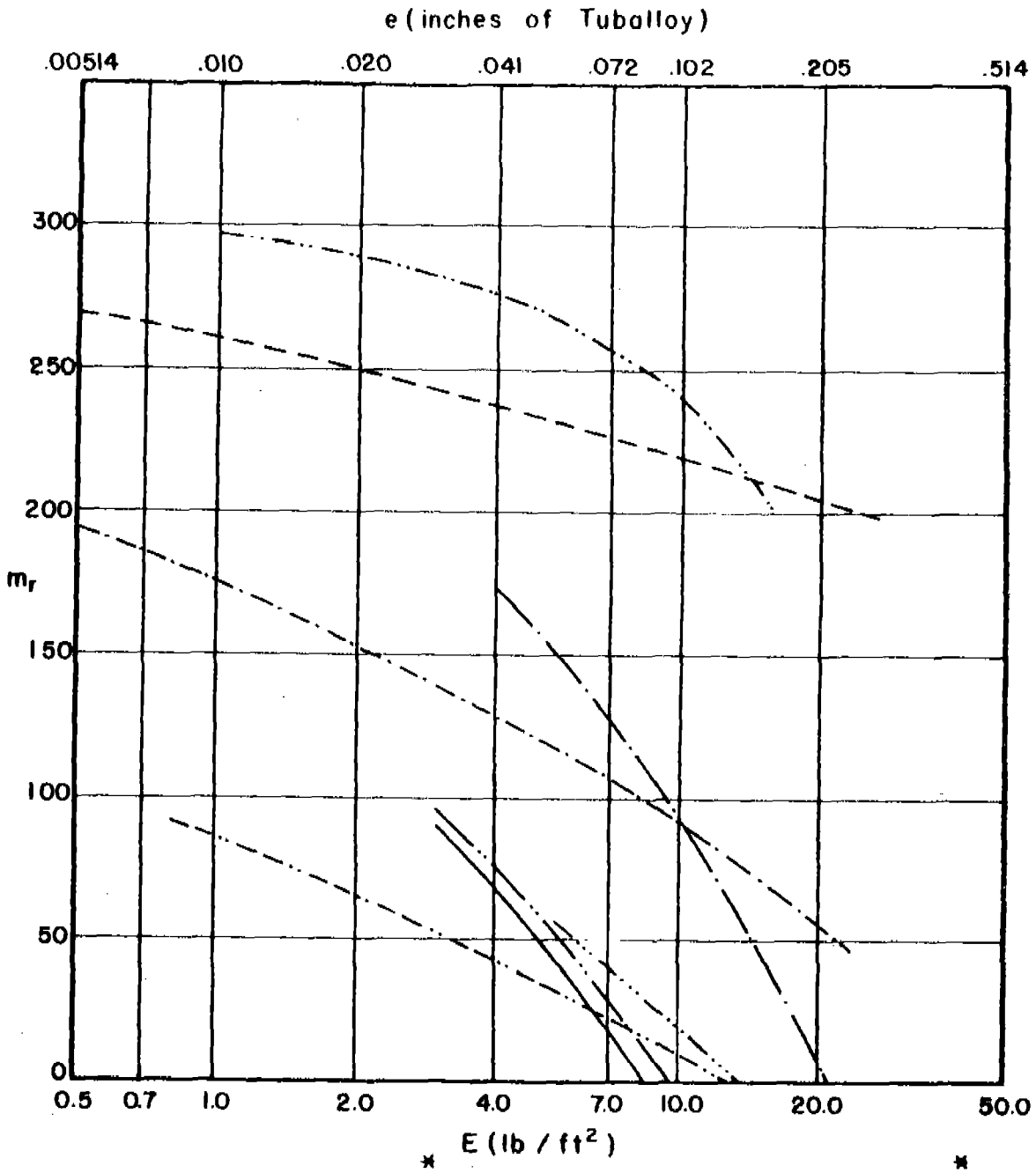

		*			*
Magnesium	— — — —	10.58	F.H. Steel	—··—··—	2.41
2024 T-3	—·—·—	6.65	Hard Steel	———	2.41
Titanium	—··—··—	4.17	Copper	—··—	2.10
Cast Iron	·····	2.59	Lead	—·—	1.70
Mild Steel	— —··— —	2.41	Tuballoy	—··—	1.00

*Ratio of Material Thickness Relative to a Unit Thickness of Tuballoy

Fig. 171

[redacted]

[redacted]

m_r vs E for Various Combinations of m_s, θ, and V_s

m_s = 30 grains θ = 70 degrees V_s = 9000 fps

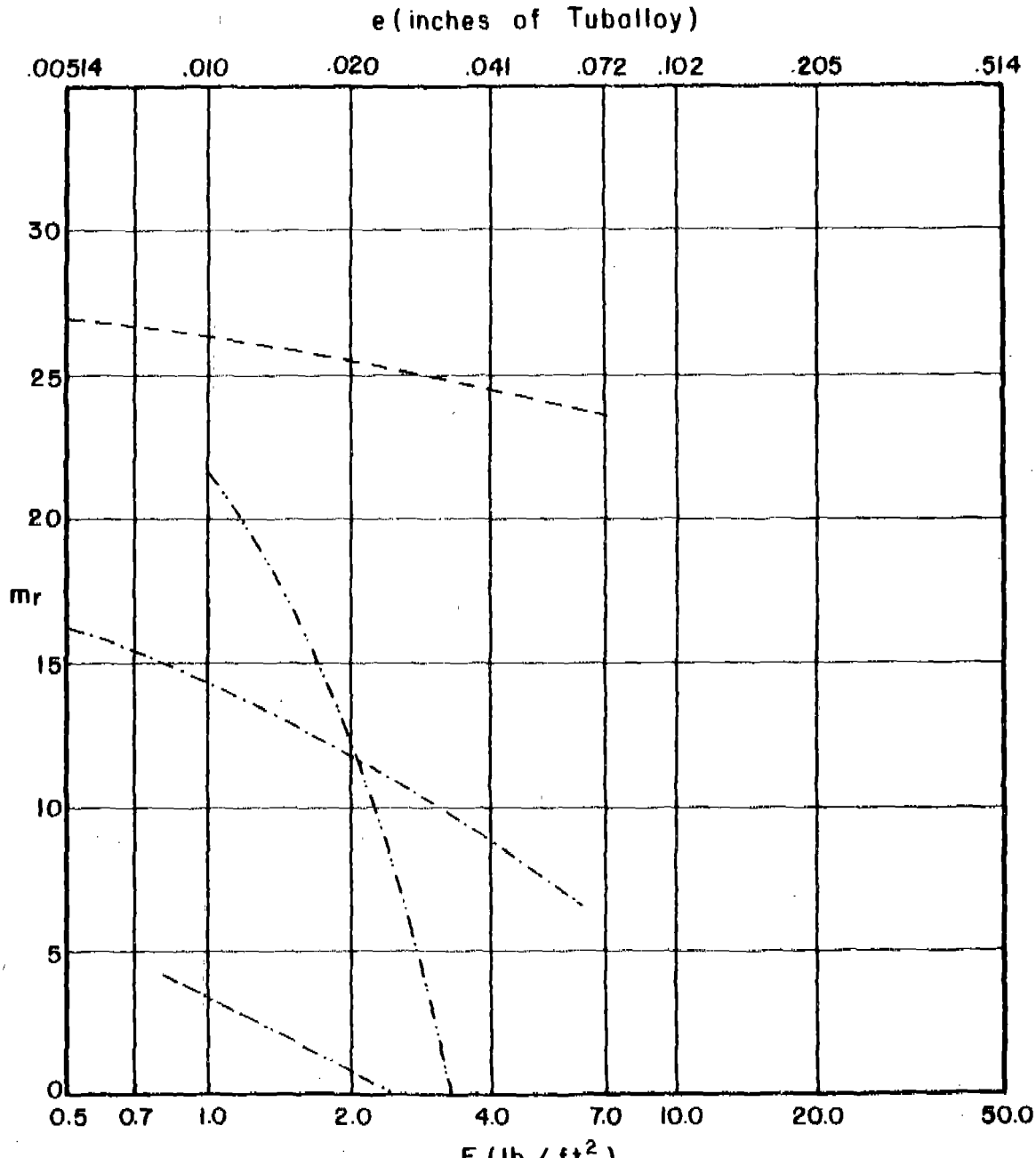

		*			*
Magnesium	— — — —	10.58	F. H. Steel	—·—·—	2.41
2024 T-3	—·—·—	6.65	Hard Steel	———	2.41
Titanium	—··—··—	4.17	Copper	—··—	2.10
Cast Iron	·····	2.59	Lead	—·—	1.70
Mild Steel	— —··— —	2.41	Tuballoy	—···—	1.00

*Ratio of Material Thickness Relative to a Unit Thickness of Tuballoy

Fig. 172

[redacted]

[redacted]

m_r vs E for Various Combinations of m_s, θ, and V_s

m_s = 100 grains θ = 70 degrees V_s = 9000 fps

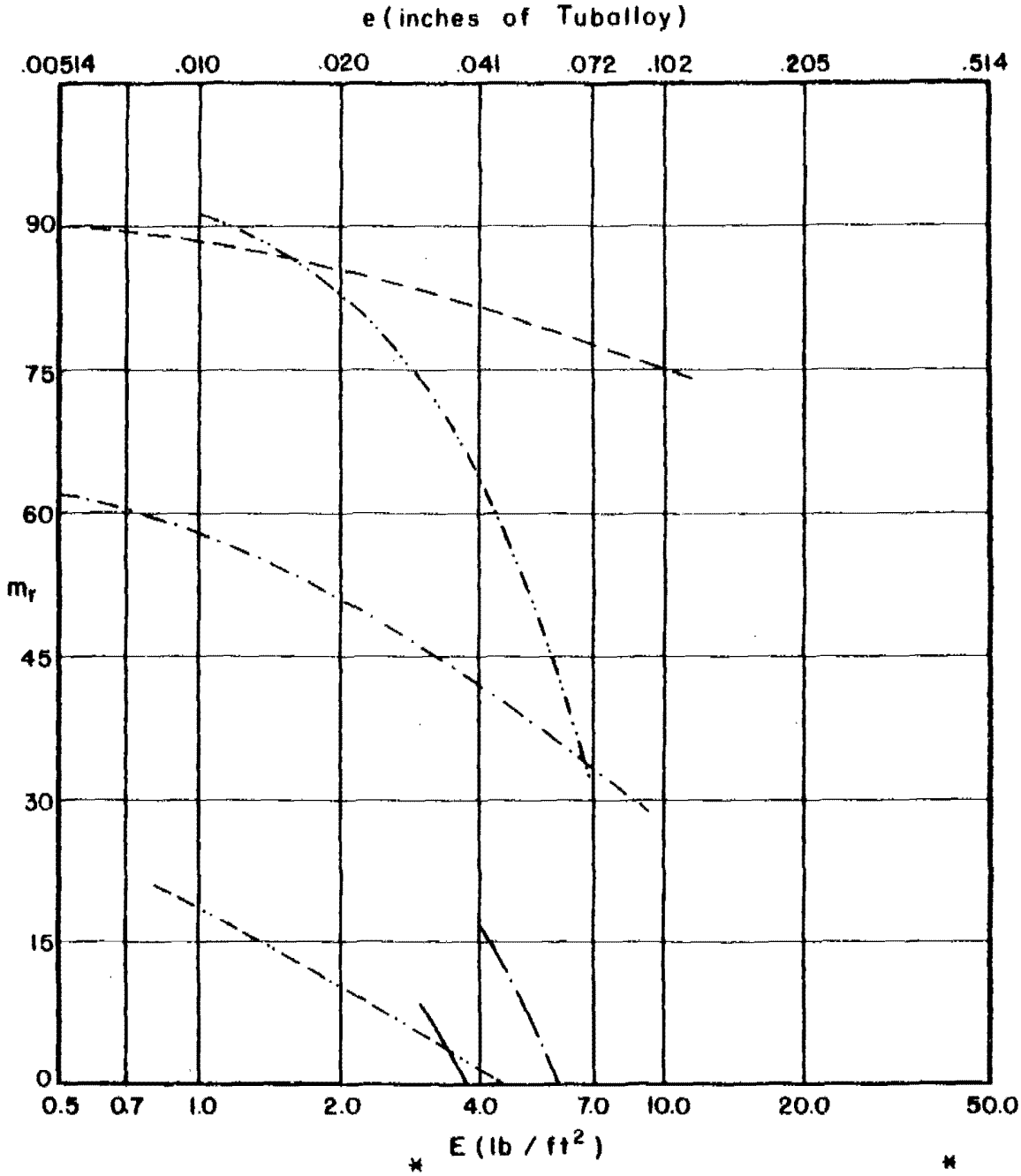

		*			*
Magnesium	———	10.58	F. H. Steel	—·—·—	2.41
2024 T-3	—·—·—	6.65	Hard Steel	———	2.41
Titanium	—··—··—	4.17	Copper	—··—	2.10
Cast Iron	·····	2.59	Lead	—·—	1.70
Mild Steel	—··—	2.41	Tuballoy	—··—	1.00

*Ratio of Material Thickness Relative to a Unit Thickness of Tuballoy

Fig. 173

[redacted]

[redacted]

m_r vs E for Various Combinations of m_s, θ, and V_s

m_s = 300 grains θ = 70 degrees V_s = 9000 fps

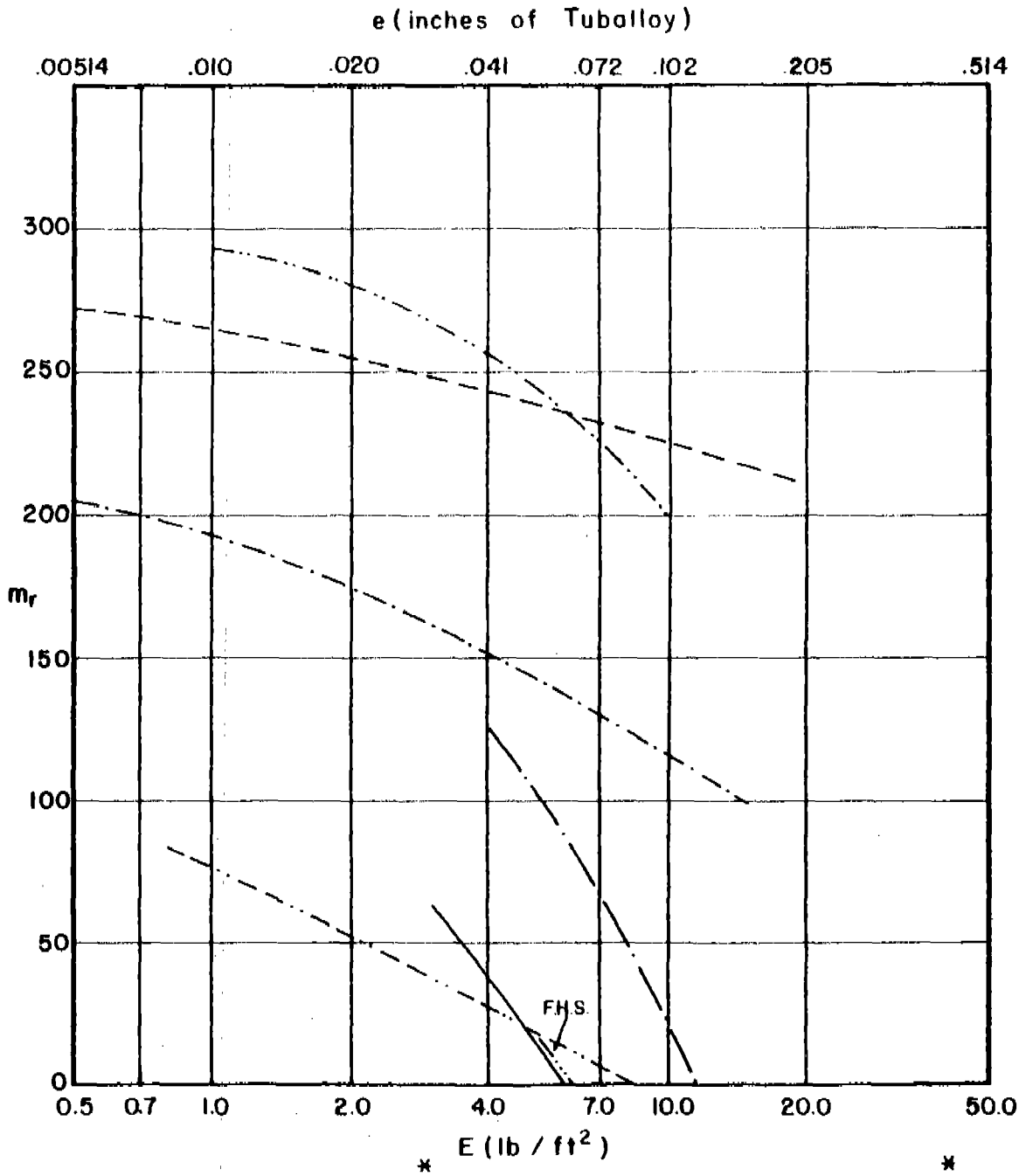

		*			*
Magnesium	— — — —	10.58	F.H. Steel	—·—·—	2.41
2024 T-3	—·—·—	6.65	Hard Steel	———	2.41
Titanium	—··—··—	4.17	Copper	—··—	2.10
Cast Iron	·····	2.59	Lead	—·—	1.70
Mild Steel	— —·— —	2.41	Tuballoy	—···—	1.00

*Ratio of Material Thickness Relative to a Unit Thickness of Tuballoy

Fig. 174

[redacted]

Appendix C

Graph Set V: $f(m_r, V_r)$ vs E for a Particular Combination of m_s, θ, V_s;

Figs. 175-178

Note: Within these sets of graphs, a contour for a particular material is shown only for those values of the abscissa for which m_r and V_r are both positive. Furthermore, the contours are not significantly extrapolated beyond the interval of thicknesses of target material employed in the basic experiments. This explains, for example, why the contours for face-hardened steel start at a value of E of 5 lb/ft^2 corresponding to a minimum experimental thickness of 0.125". No contours for cast iron appear on graphs for conditions of either 9000 fps or 70° obliquity for the reason that the experimental data did not cover these conditions. However, a contour for a given material may not appear on a graph simply because there is no permissible value of E for which both m_r and V_r are positive under the conditions for that graph.

[redacted]

$f(m_r, V_r)$ vs E for Various Combinations of m_s, θ, and V_s

m_s = 100 grains θ = 60 degrees V_s = 6000 fps

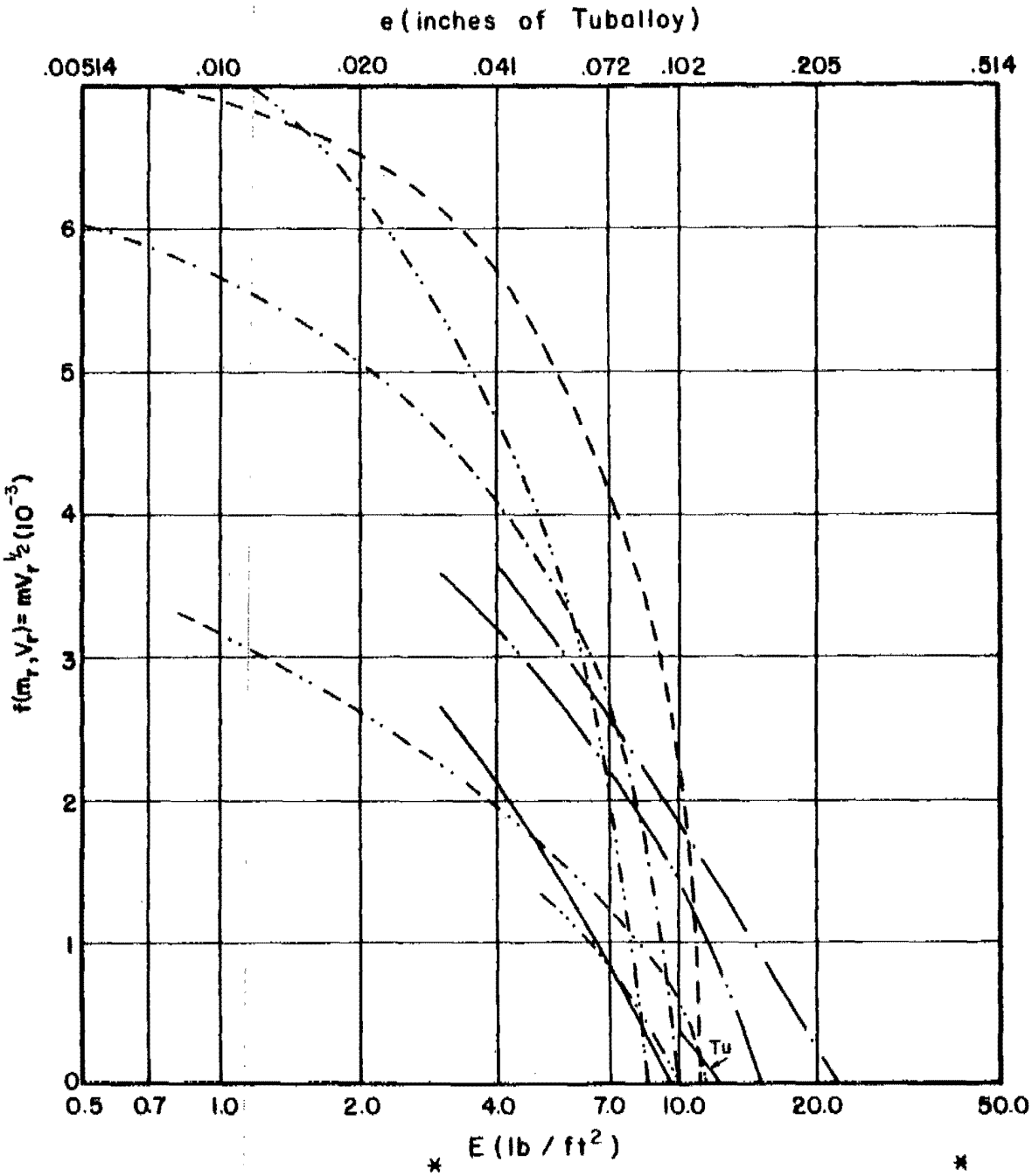

Magnesium	————	10.58*	F. H. Steel	—··—··—	2.41*
2024 T-3	—·—·—	6.65	Hard Steel	————	2.41
Titanium	—··—··—	4.17	Copper	—··—	2.10
Cast Iron	·····	2.59	Lead	—·—	1.70
Mild Steel	——··——	2.41	Tuballoy	—··—	1.00

*Ratio of Material Thickness Relative to a Unit Thickness of Tuballoy

Fig. 175

[redacted]

[redacted]

$f(m_r, V_r)$ vs E for Various Combinations of m_s, θ, and V_s

m_s = 100 grains θ = 60 degrees V_s = 6000 fps

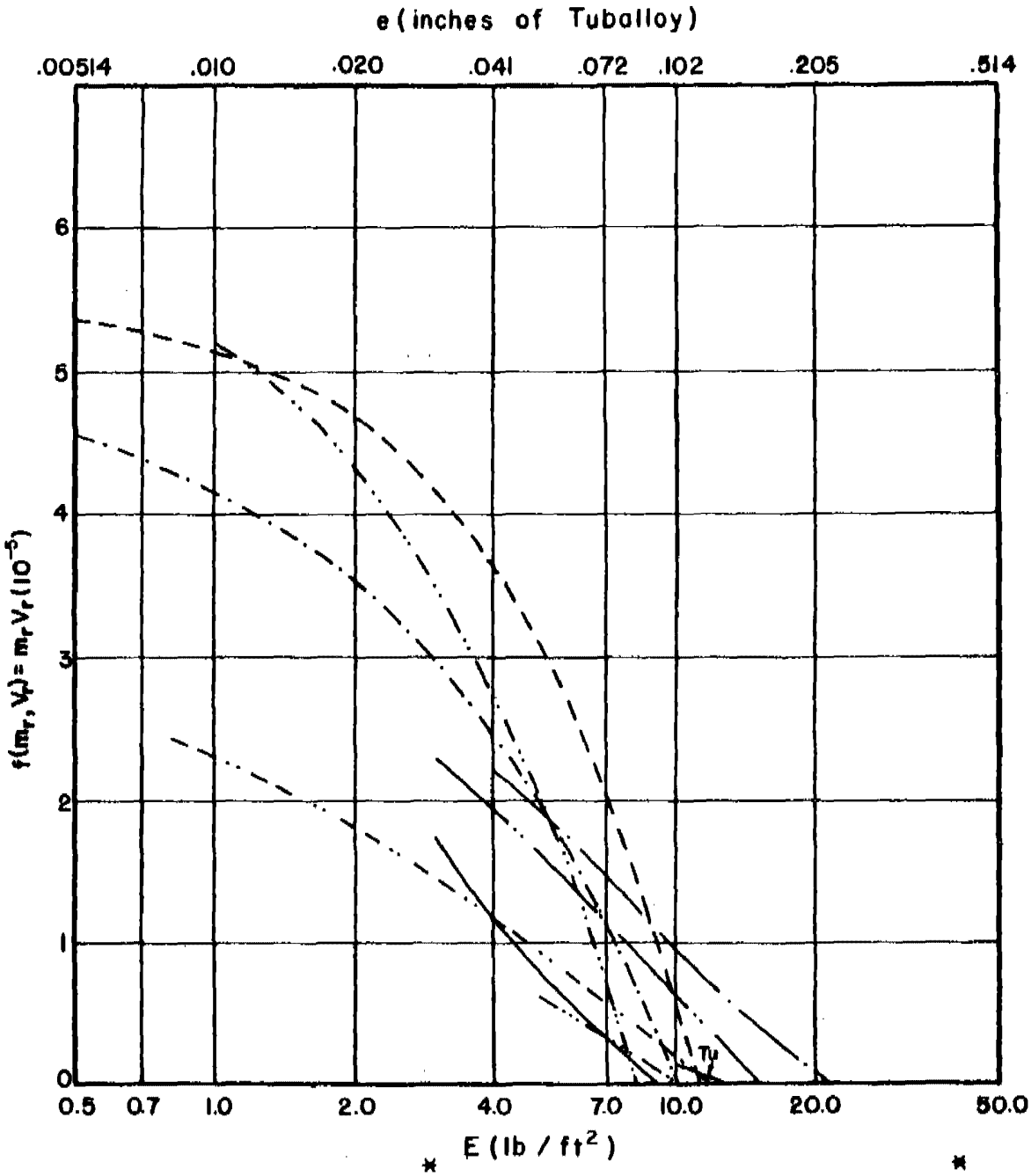

		*			*
Magnesium	— — — —	10.58	F.H. Steel	—··—··—	2.41
2024 T-3	—·—·—	6.65	Hard Steel	———	2.41
Titanium	—··—··—	4.17	Copper	—··—	2.10
Cast Iron	·····	2.59	Lead	—·—	1.70
Mild Steel	— —··— —	2.41	Tuballoy	—···—	1.00

*Ratio of Material Thickness Relative to a Unit Thickness of Tuballoy

Fig. 176

[redacted]

[redacted]

$f(m_r, V_r)$ vs E for Various Combinations of m_s, θ, and V_s

m_s = 100 grains θ = 60 degrees V_s = 6000 fps

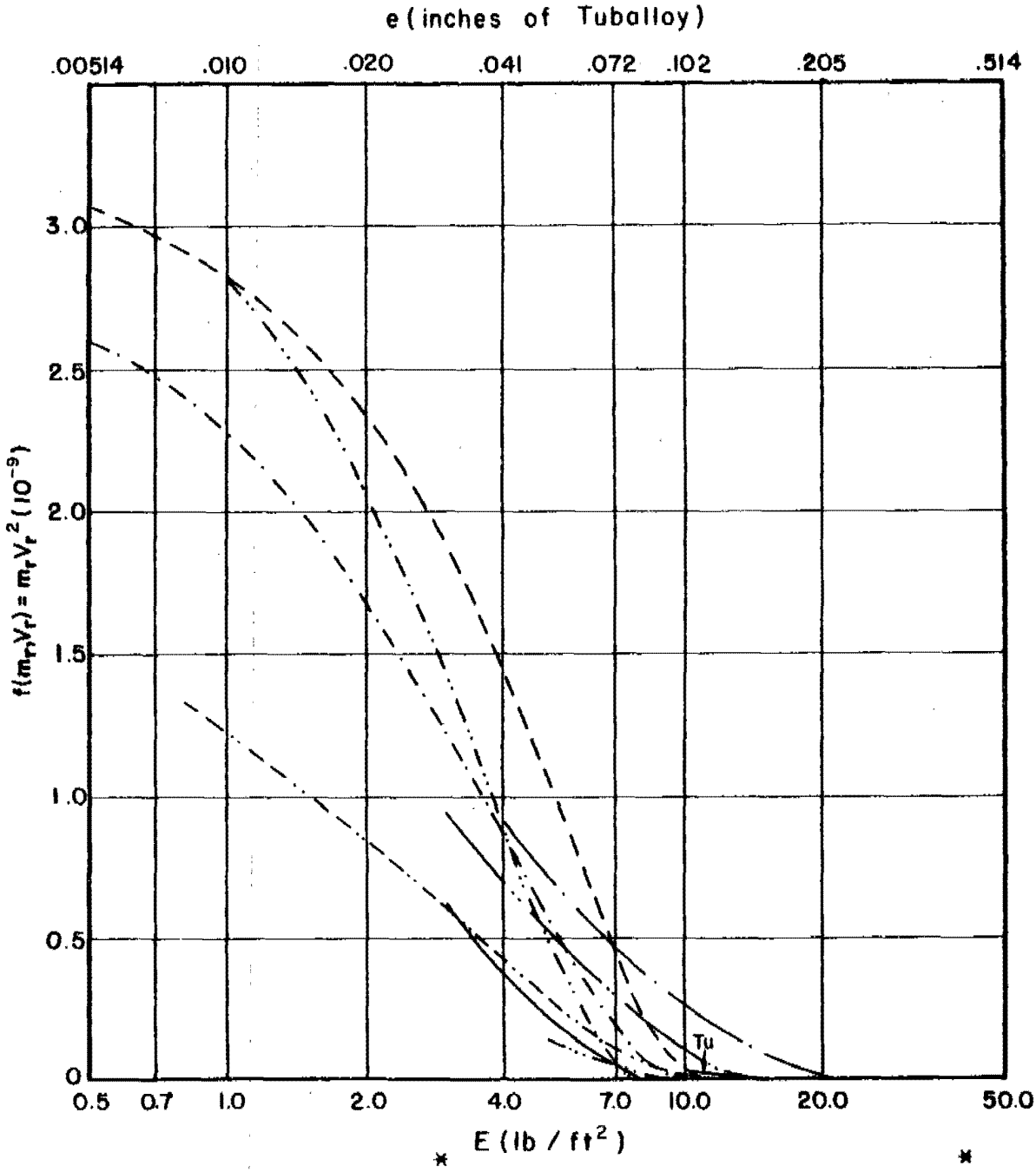

		*			*
Magnesium	— — — —	10.58	F.H. Steel	—·····—·····—	2.41
2024 T-3	—·—·—·—	6.65	Hard Steel	————	2.41
Titanium	—··—··—	4.17	Copper	—··—	2.10
Cast Iron	·····	2.59	Lead	—·—	1.70
Mild Steel	—··— —	2.41	Tuballoy	—····—	1.00

*Ratio of Material Thickness Relative to a Unit Thickness of Tuballoy

Fig. 177

[redacted]

[redacted]

$f(m_r, V_r)$ vs E for Various Combinations of m_s, θ, and V_s

m_s = 100 grains θ = 60 degrees V_s = 6000 fps

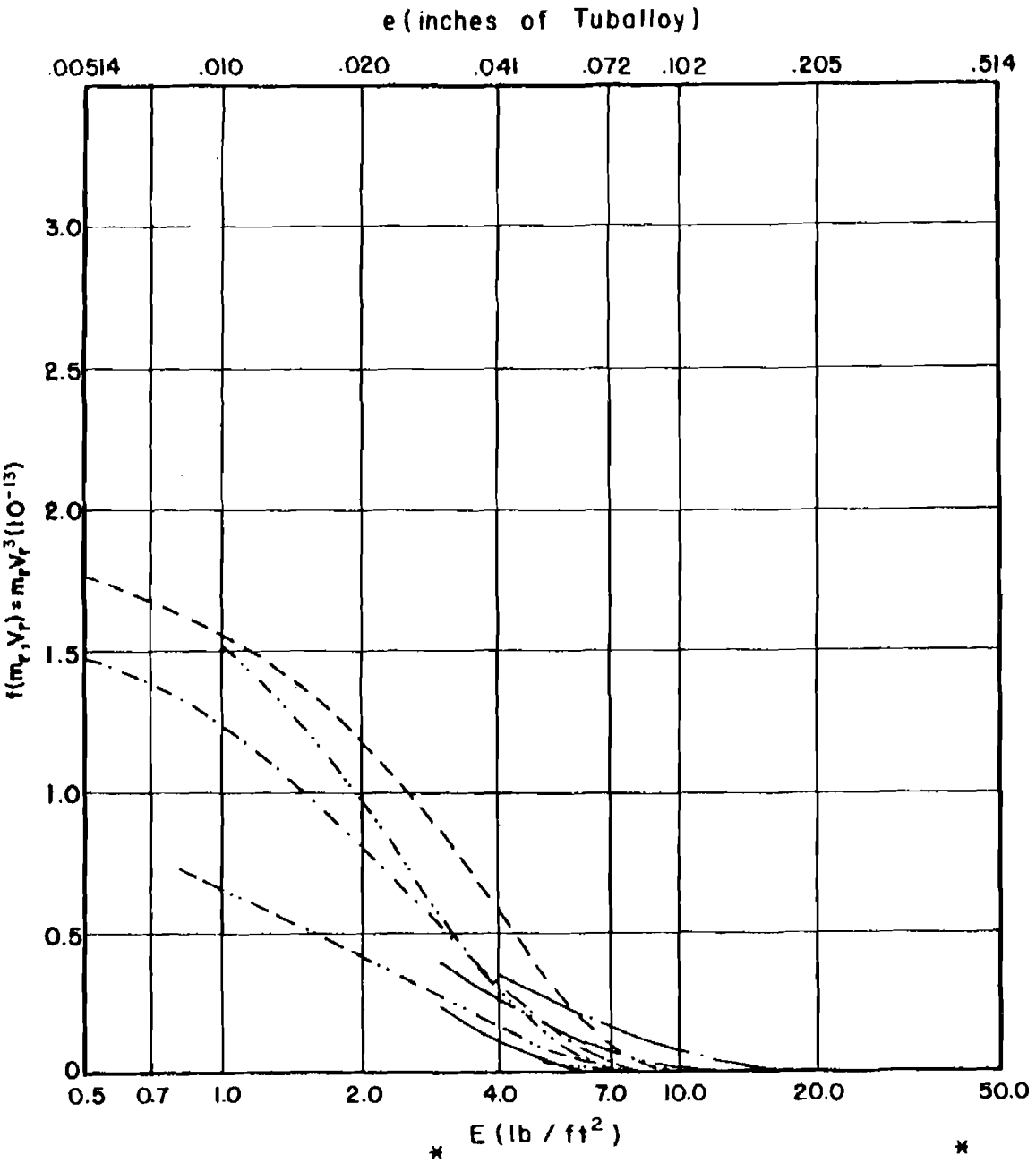

		*			*
Magnesium	— — — —	10.58	F.H. Steel	—··—··—	2.41
2024 T-3	—·—·—	6.65	Hard Steel	———	2.41
Titanium	—··—··—	4.17	Copper	—··—	2.10
Cast Iron	·····	2.59	Lead	—·—	1.70
Mild Steel	— —··— —	2.41	Tuballoy	—···—	1.00

*Ratio of Material Thickness Relative to a Unit Thickness of Tuballoy

Fig. 178

[redacted]

Following page is blank

[redacted]

Appendix D

Graph Set VI: e (inches of Celotex) vs E

for Various Combinations of m_s, θ, and V_s

Figs. 179-205

Note: The ordinate represents an estimate of the maximum thickness of calibrating material that can possibly be perforated by the largest portion of the residual fragment after the original fragment has impacted initially on one of the given metallic targets. The assumption is made that the residual fragment strikes the calibrating material at normal impact and that, furthermore, the shape of the original fragment is retained despite any loss in weight.

On each graph in this appendix there appears a value of e_o. This value is an estimate of the maximum thickness of the calibrating material that the original fragment can perforate, assuming normal impact and no intermediate barrier.

The contours are limited on these graphs to 72" of celotex and 3.0" of 2024T-3. These represent the maximum thicknesses of these materials that have been considered in BRL single-target firings. In fact, there is no instance to date of a perforation of 3.0" of 2024T-3 in BRL experimental work with pre-formed fragments.

[redacted]

[redacted]

e_{cel} vs E for Various Combinations of m_s, θ, and V_s

m_s = 30 grains θ = 0 degrees V_s = 3000 fps

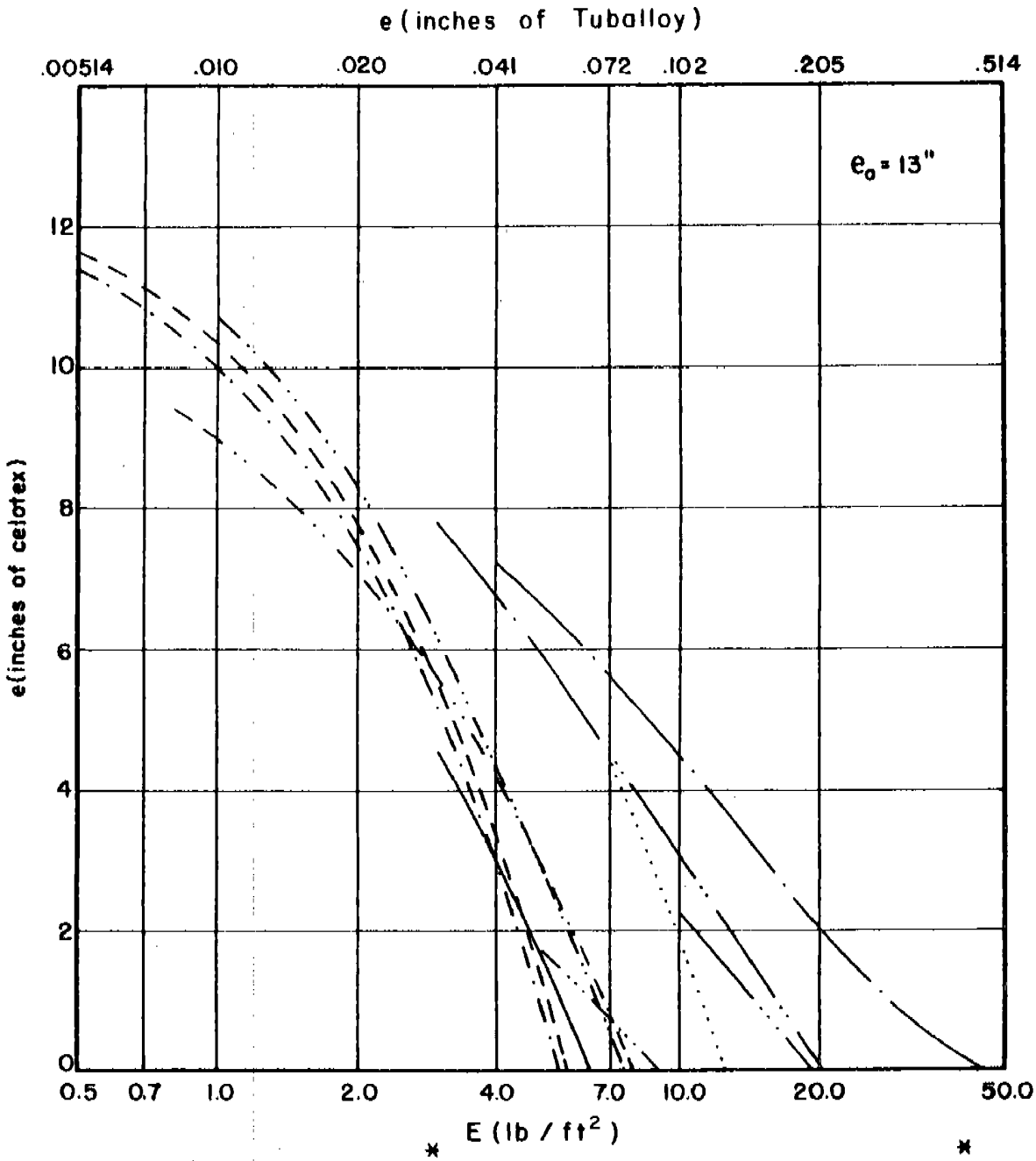

		*			*
Magnesium	— — — —	10.58	F. H. Steel	—··—··—	2.41
2024 T-3	—·—·—	6.65	Hard Steel	———	2.41
Titanium	—··—··—	4.17	Copper	—··—	2.10
Cast Iron	·····	2.59	Lead	—·—	1.70
Mild Steel	— —··— —	2.41	Tuballoy	—···—	1.00

*Ratio of Material Thickness Relative to a Unit Thickness of Tuballoy

Fig. 179

[redacted]

[redacted]

e_{cel} vs E for Various Combinations of m_s, θ, and V_s

m_s = 100 grains θ = 0 degrees V_s = 3000 fps

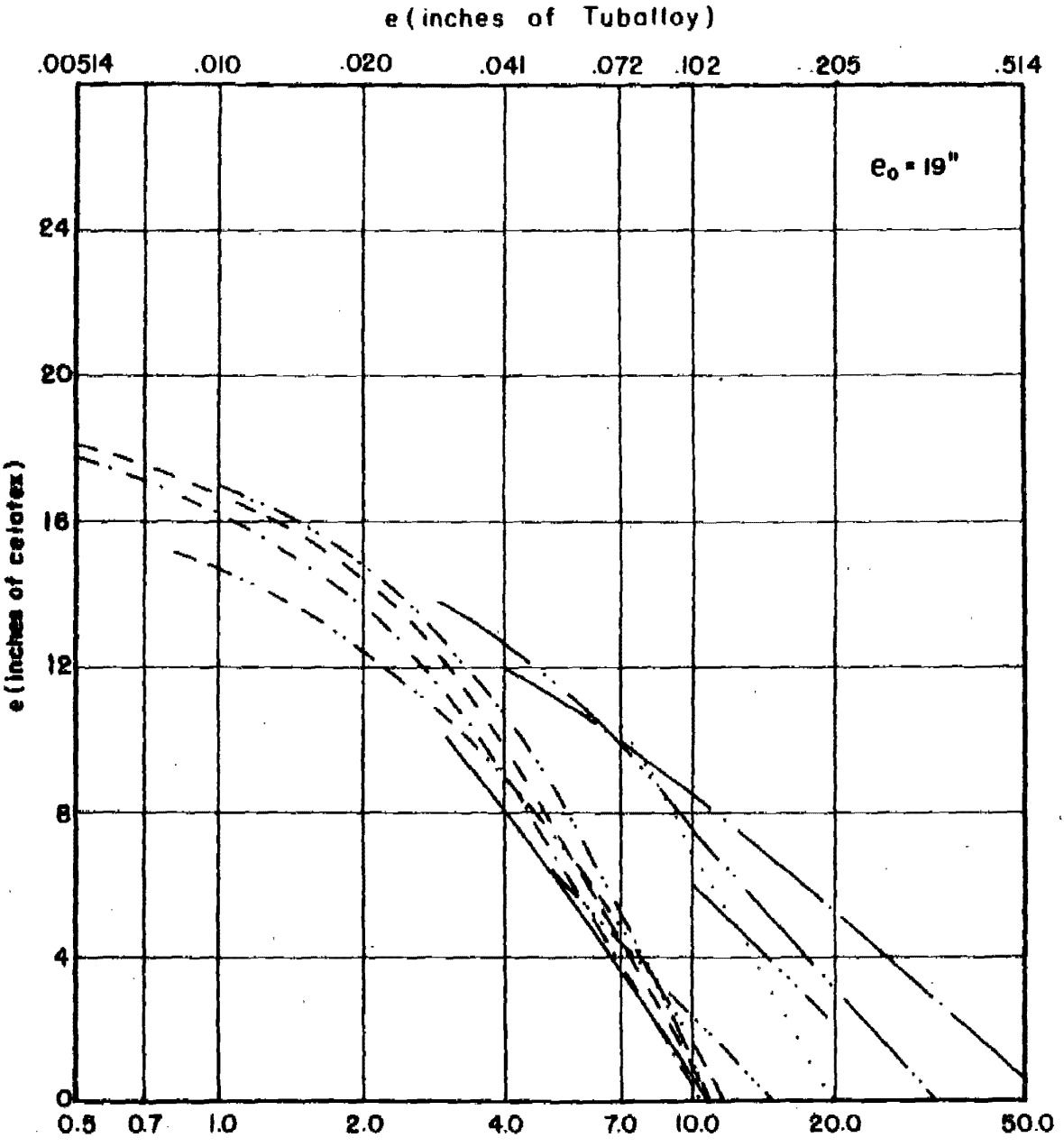

		*			*
Magnesium	— — — —	10.58	F.H. Steel	—·—·—	2.41
2024 T-3	—·—·—	6.65	Hard Steel	———	2.41
Titanium	—··—··—	4.17	Copper	—··—	2.10
Cast Iron	·····	2.59	Lead	—·—	1.70
Mild Steel	— —··— —	2.41	Tuballoy	—··—	1.00

*Ratio of Material Thickness Relative to a Unit Thickness of Tuballoy

Fig. 180

[redacted]

[redacted]

e_{cel} vs E for Various Combinations of m_s, θ, and V_s

m_s = 300 grains θ = 0 degrees V_s = 3000 fps

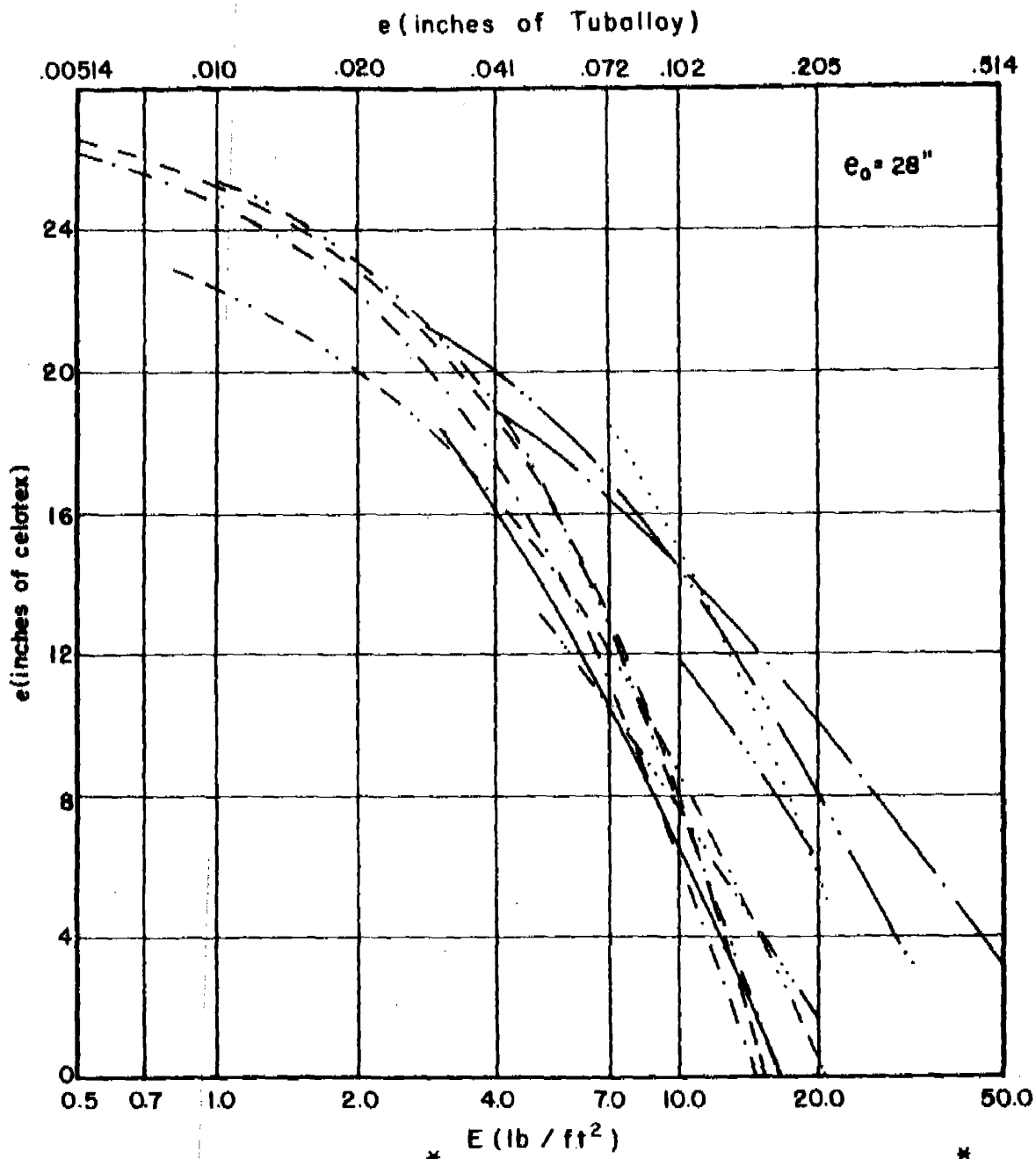

		*			*
Magnesium	— — — —	10.58	F.H. Steel	—·—·—	2.41
2024 T-3	—·—·—	6.65	Hard Steel	———	2.41
Titanium	—··—··—	4.17	Copper	—··—	2.10
Cast Iron	·····	2.59	Lead	—·—	1.70
Mild Steel	— —·— —	2.41	Tuballoy	—··—	1.00

*Ratio of Material Thickness Relative to a Unit Thickness of Tuballoy

Fig. 181

[redacted]

[redacted]

e_{cel} vs E for Various Combinations of m_s, θ, and V_s

m_s = 30 grains θ = 60 degrees V_s = 3000 fps

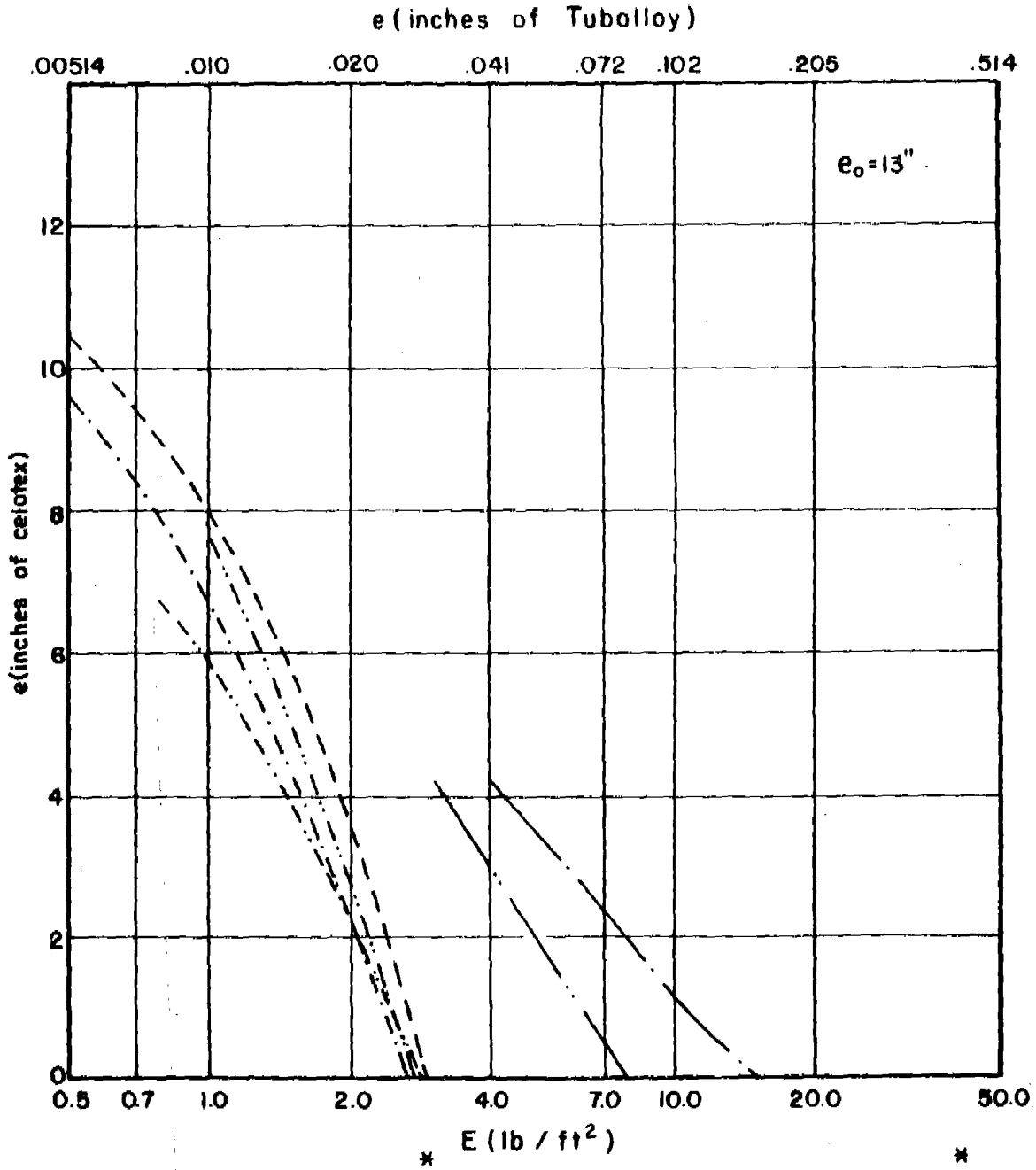

		*			*
Magnesium	— — — —	10.58	F.H. Steel	—·—·—	2.41
2024 T-3	—·—·—	6.65	Hard Steel	———	2.41
Titanium	—··—··—	4.17	Copper	—··—	2.10
Cast Iron	·····	2.59	Lead	—·—	1.70
Mild Steel	— —·· —	2.41	Tuballoy	—··—	1.00

*Ratio of Material Thickness Relative to a Unit Thickness of Tuballoy

Fig. 182

[redacted]

[redacted]

e_{cel} vs E for Various Combinations of m_s, θ, and V_s

m_s = 100 grains θ = 60 degrees V_s = 3000 fps

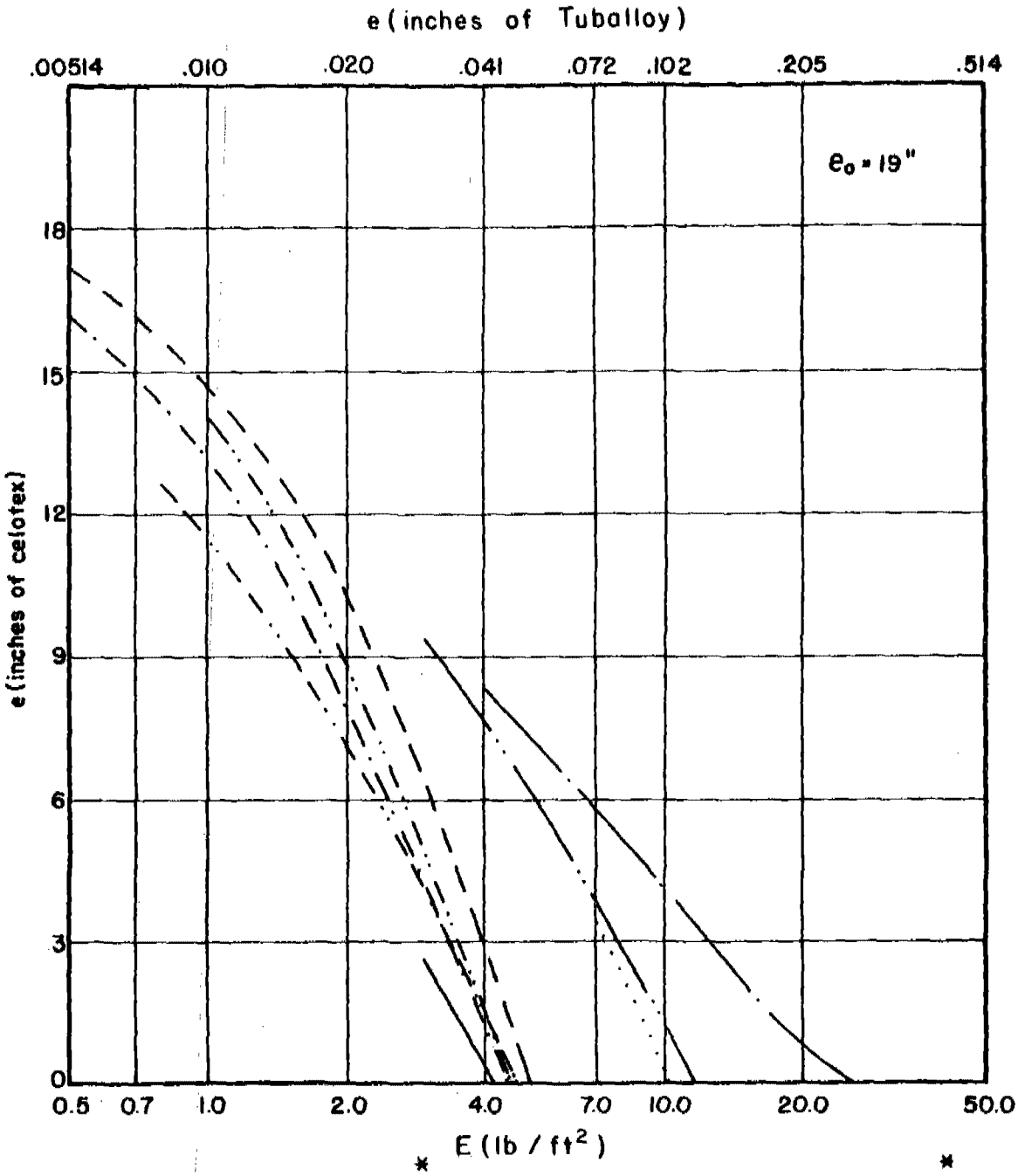

		*			*
Magnesium	------	10.58	F.H. Steel	-·-·-·-	2.41
2024 T-3	-·-·-·-	6.65	Hard Steel	———	2.41
Titanium	-··-··-	4.17	Copper	—··—	2.10
Cast Iron	·····	2.59	Lead	—·—	1.70
Mild Steel	-·-·-	2.41	Tuballoy	—··—	1.00

*Ratio of Material Thickness Relative to a Unit Thickness of Tuballoy

Fig. 183

[redacted]

[redacted]

e_{cel} vs E for Various Combinations of m_s, θ, and V_s

m_s = 300 grains θ = 60 degrees V_s = 3000 fps

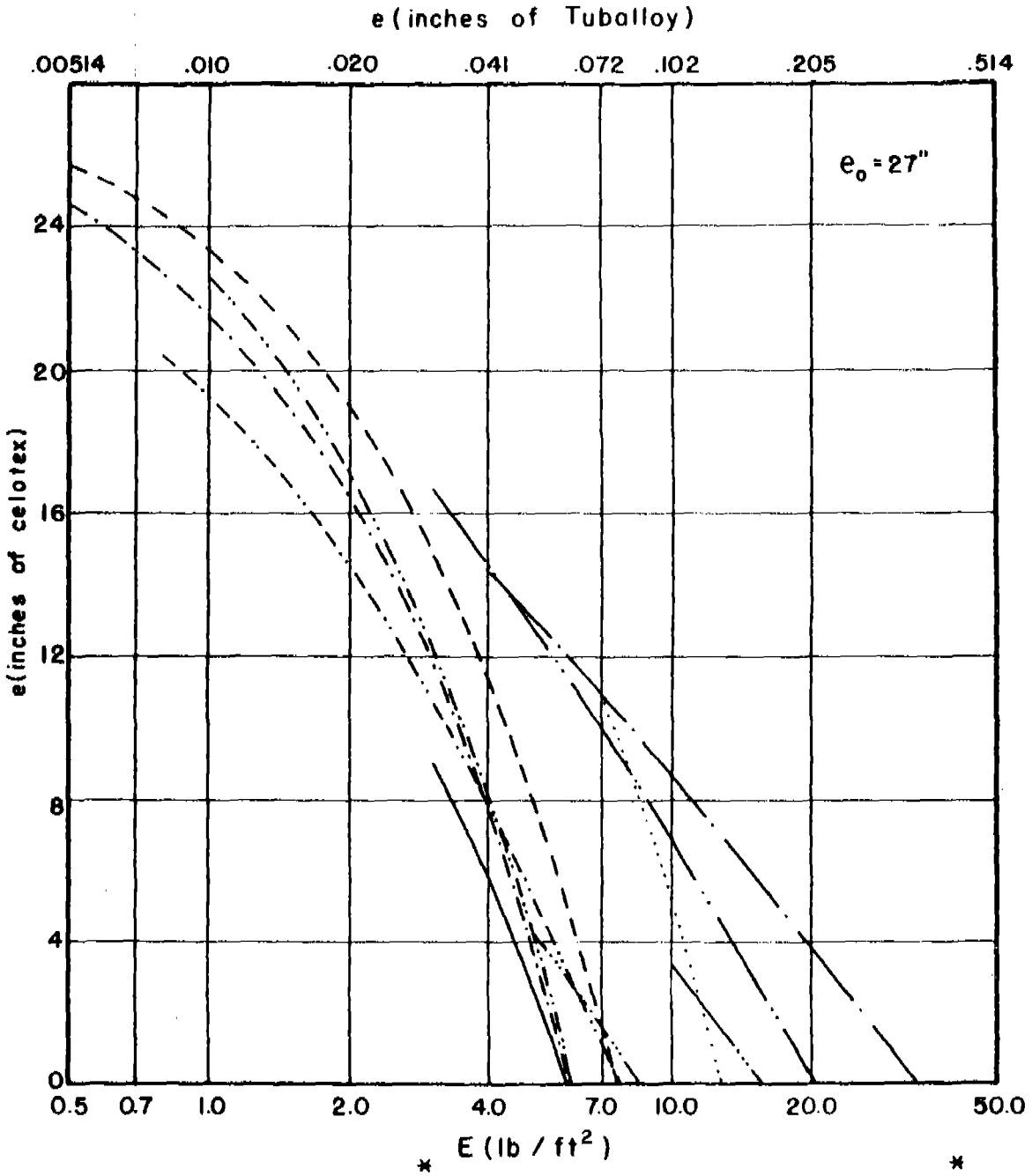

		*			*
Magnesium	— — — —	10.58	F.H. Steel	—·—·—	2.41
2024 T-3	—·—·—	6.65	Hard Steel	———	2.41
Titanium	—··—··—	4.17	Copper	—··—	2.10
Cast Iron	·····	2.59	Lead	—·—	1.70
Mild Steel	— —··— —	2.41	Tuballoy	—··—	1.00

*Ratio of Material Thickness Relative to a Unit Thickness of Tuballoy

Fig. 184

[redacted]

[redacted]

e_{cel} vs E for Various Combinations of m_s, θ, and V_s

m_s = 30 grains θ = 70 degrees V_s = 3000 fps

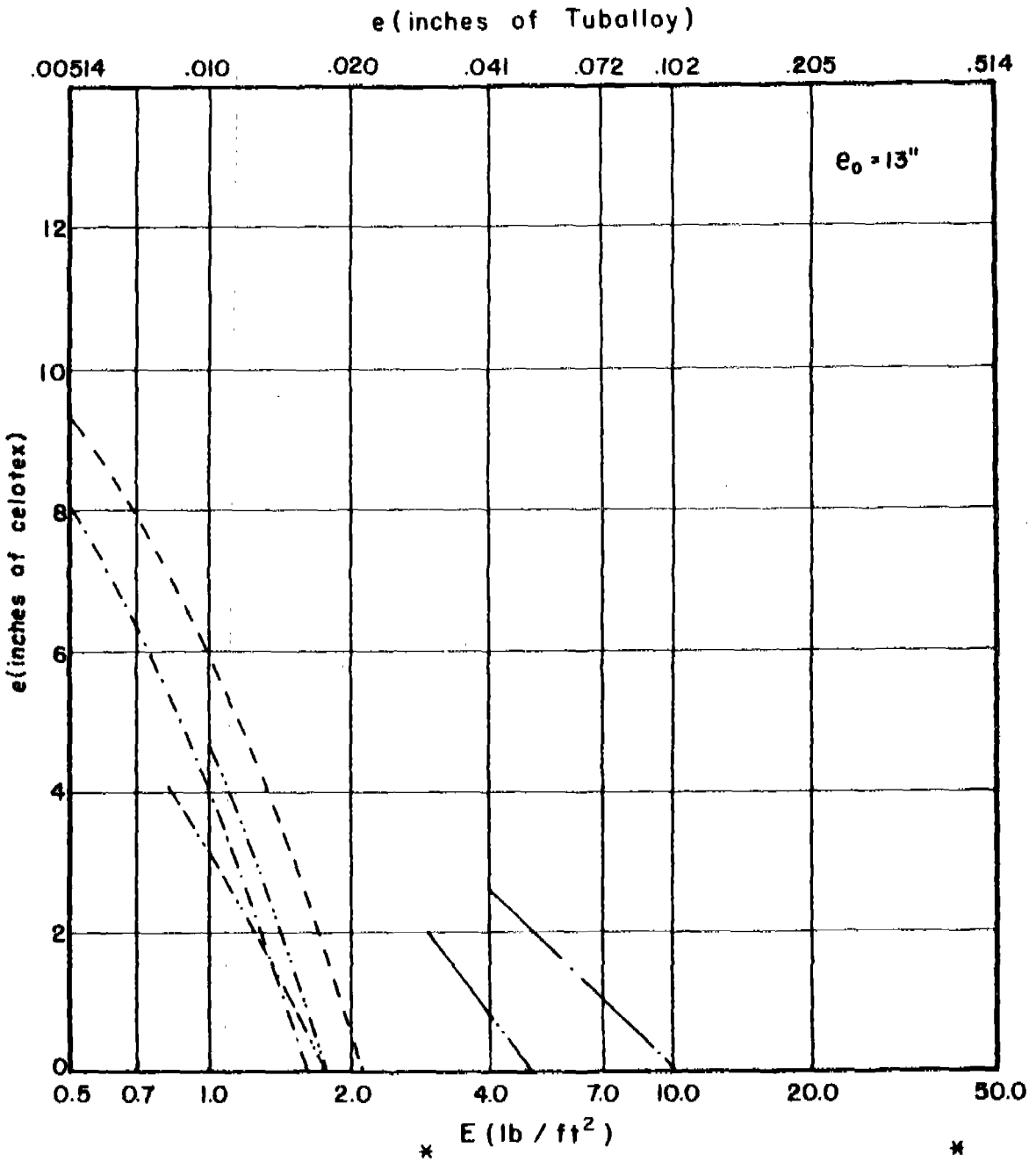

		*			*
Magnesium	— — — —	10.58	F. H. Steel	—·—·—	2.41
2024 T-3	—·—·—	6.65	Hard Steel	———	2.41
Titanium	—··—··—	4.17	Copper	—··—	2.10
Cast Iron	·····	2.59	Lead	—·—	1.70
Mild Steel	— —··— —	2.41	Tuballoy	—···—	1.00

*Ratio of Material Thickness Relative to a Unit Thickness of Tuballoy

Fig. 185

[redacted]

e_{cel} vs E for Various Combinations of m_s, θ, and V_s

m_s = 100 grains θ = 70 degrees V_s = 3000 fps

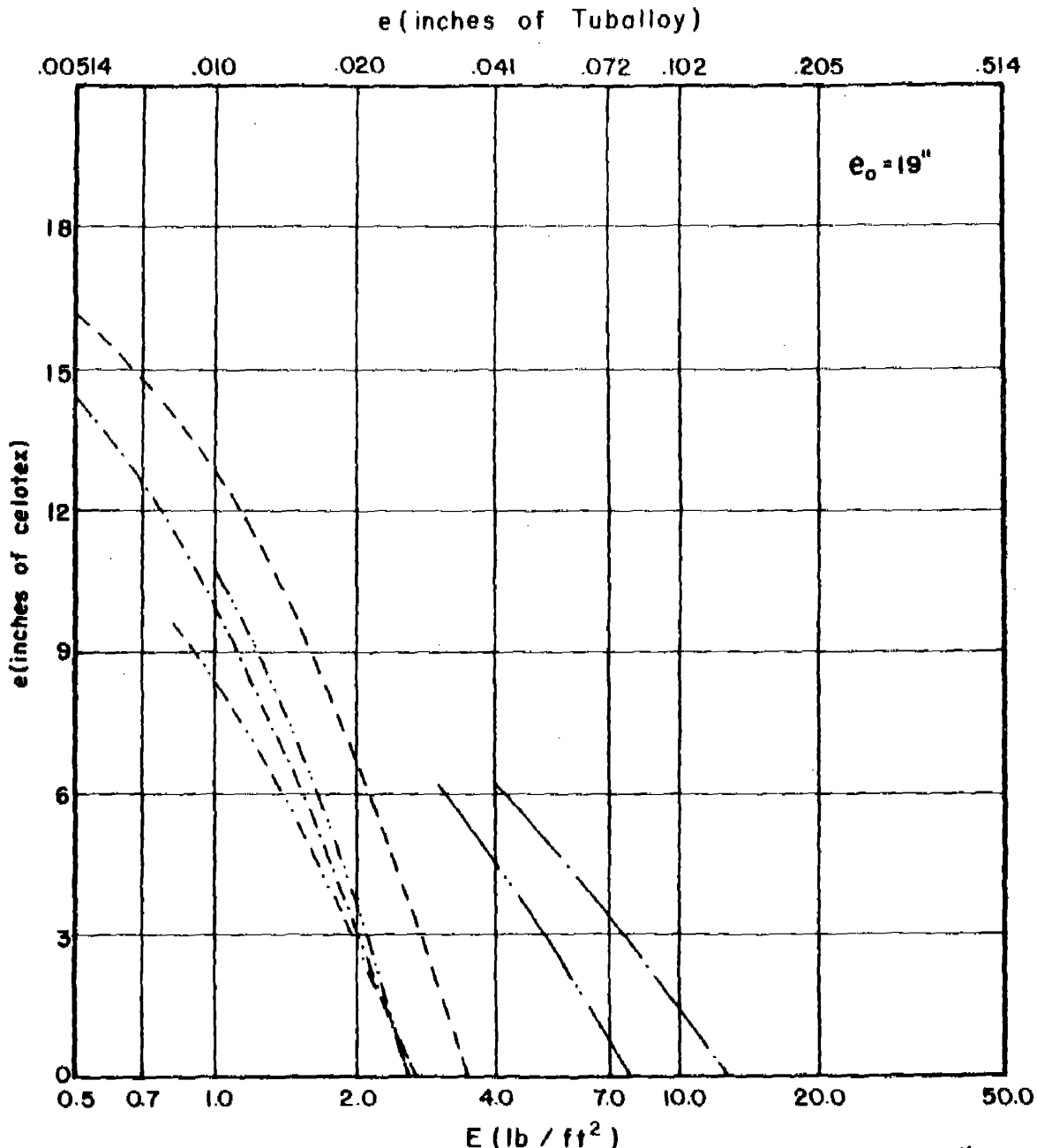

		*			*
Magnesium	———	10.58	F. H. Steel	—·—·—	2.41
2024 T-3	—·—·—	6.65	Hard Steel	———	2.41
Titanium	—··—··—	4.17	Copper	—··—	2.10
Cast Iron	·····	2.59	Lead	—·—	1.70
Mild Steel	—··—	2.41	Tuballoy	—··—	1.00

*Ratio of Material Thickness Relative to a Unit Thickness of Tuballoy

Fig. 186

[redacted]

e_{cel} vs E for Various Combinations of m_s, θ, and V_s

m_s = 300 grains θ = 70 degrees V_s = 3000 fps

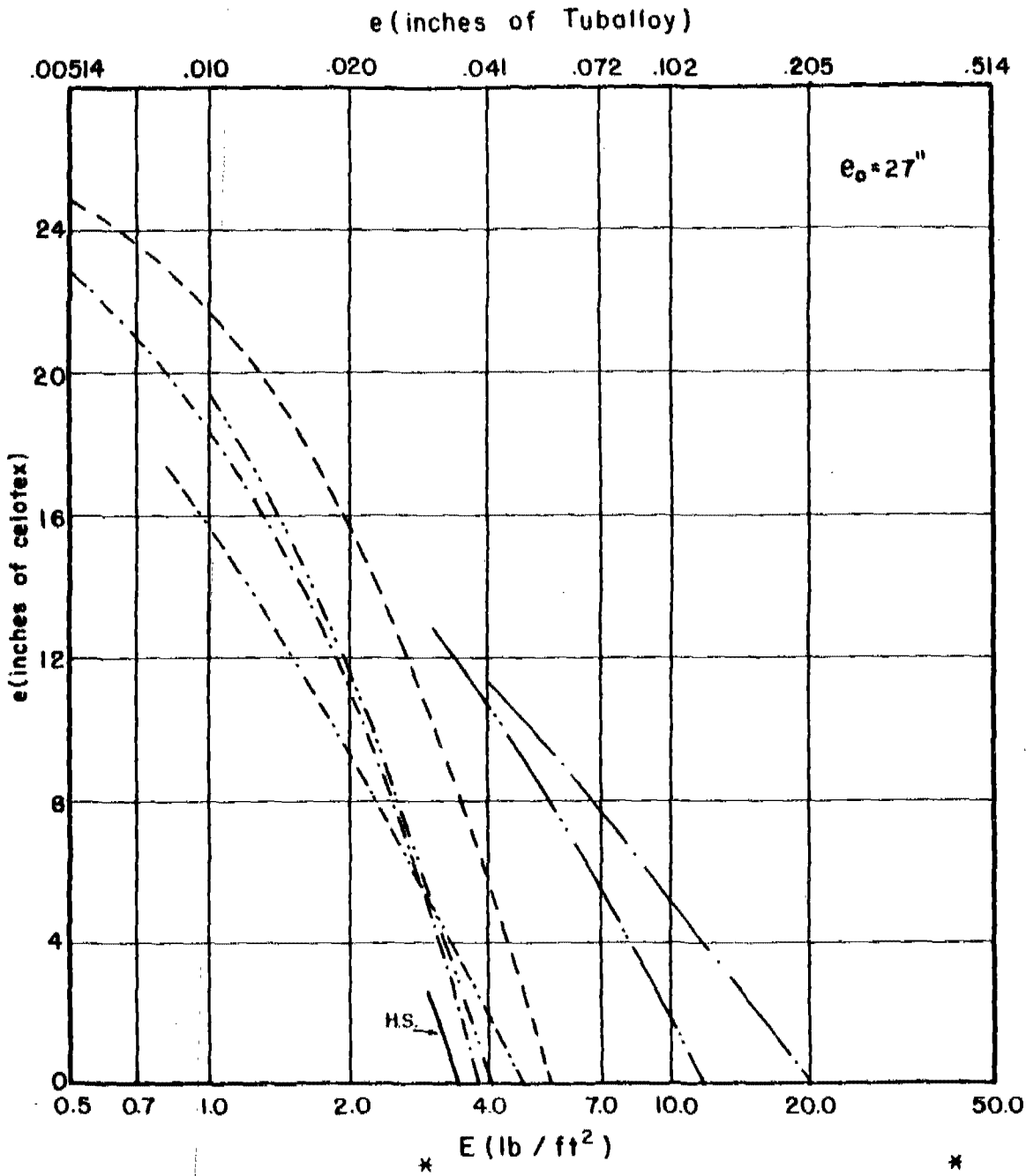

		*			*
Magnesium	— — — —	10.58	F.H. Steel	—··—··—	2.41
2024 T-3	—·—·—	6.65	Hard Steel	———	2.41
Titanium	—··—··—	4.17	Copper	—··—	2.10
Cast Iron	·····	2.59	Lead	—·—	1.70
Mild Steel	— —·— —	2.41	Tuballoy	—··—	1.00

*Ratio of Material Thickness Relative to a Unit Thickness of Tuballoy

Fig. 187

[redacted]

[redacted]

e_{cel} vs E for Various Combinations of m_s, θ, and V_s

m_s = 30 grains θ = 0 degrees V_s = 6000 fps

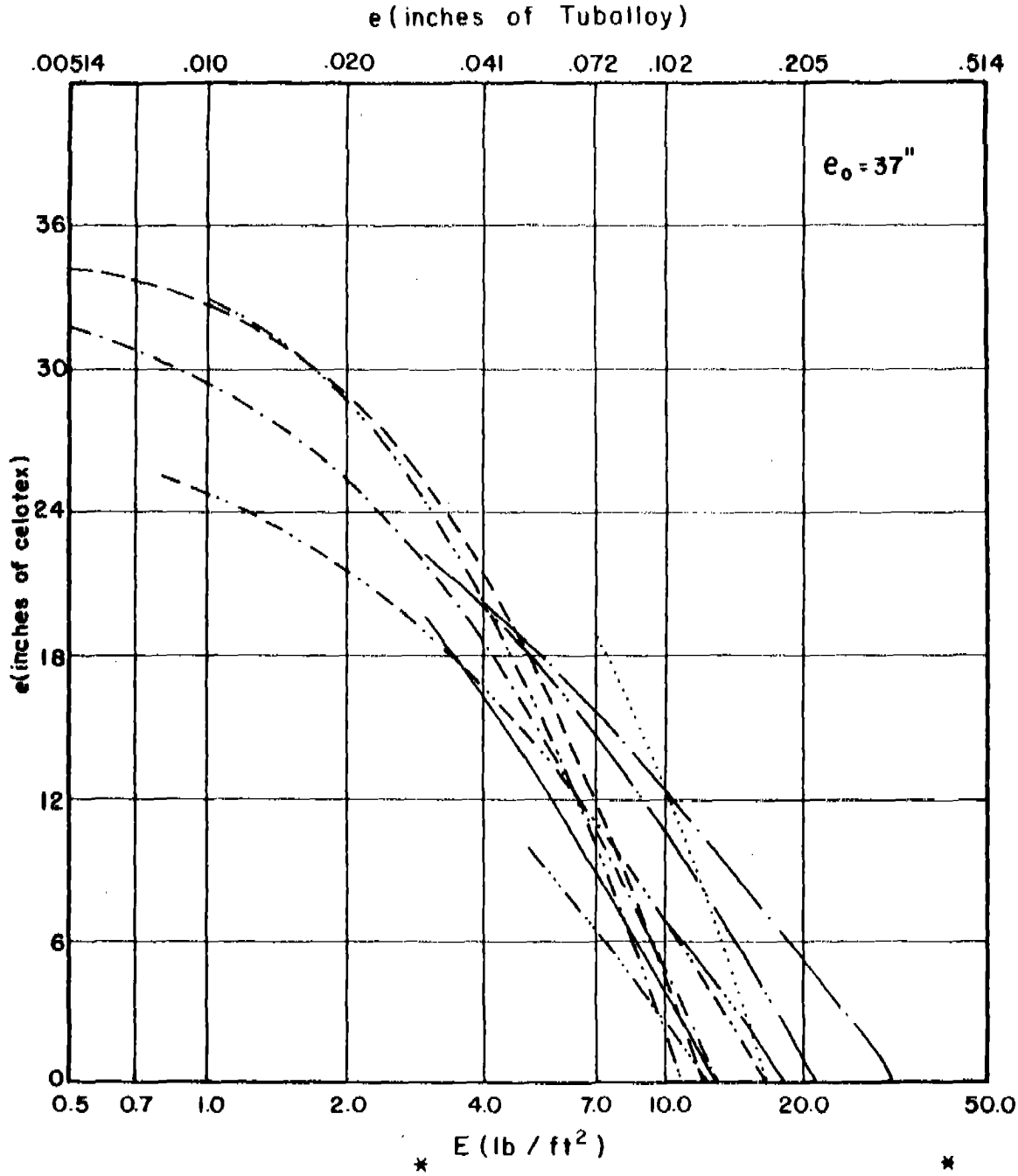

		*			*
Magnesium	— — — —	10.58	F.H. Steel	—·—·—	2.41
2024 T-3	—·—·—	6.65	Hard Steel	———	2.41
Titanium	—··—··—	4.17	Copper	—··—	2.10
Cast Iron	·····	2.59	Lead	—·—	1.70
Mild Steel	—·····—	2.41	Tuballoy	—··—	1.00

*Ratio of Material Thickness Relative to a Unit Thickness of Tuballoy

Fig. 188

[redacted]

[redacted]

e_{cel} vs E for Various Combinations of m_s, θ, and V_s

m_s = 100 grains θ = 0 degrees V_s = 6000 fps

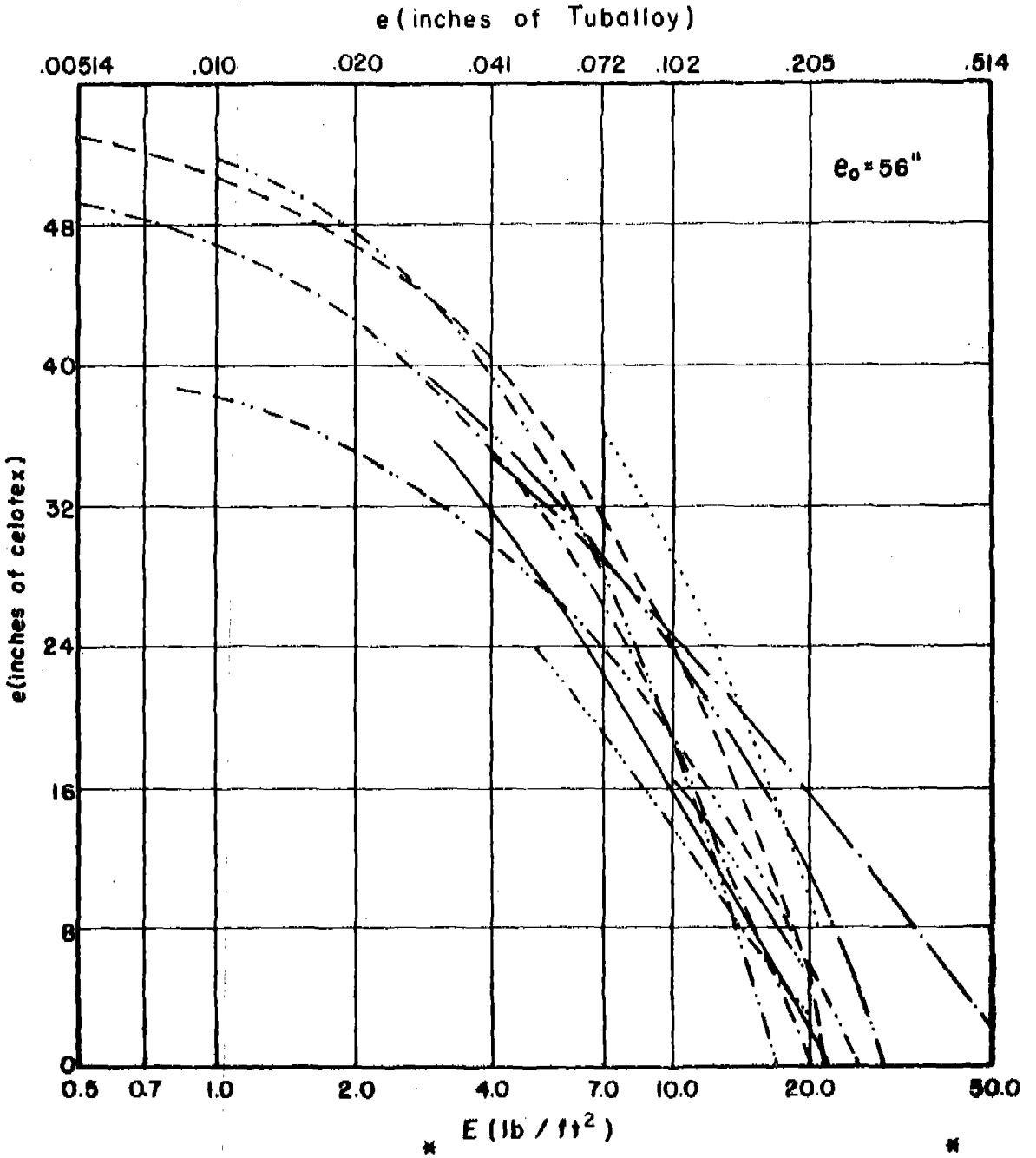

		*			*
Magnesium	———	10.58	F.H. Steel	—·—·—	2.41
2024 T-3	—·—·—	6.65	Hard Steel	———	2.41
Titanium	—··—··—	4.17	Copper	—··—	2.10
Cast Iron	·····	2.59	Lead	—·—	1.70
Mild Steel	—··—··—	2.41	Tuballoy	—··—	1.00

*Ratio of Material Thickness Relative to a Unit Thickness of Tuballoy

Fig. 189

[redacted]

e_{cel} vs E for Various Combinations of m_s, θ, and V_s

m_s = 300 grains θ = 0 degrees V_s = 6000 fps

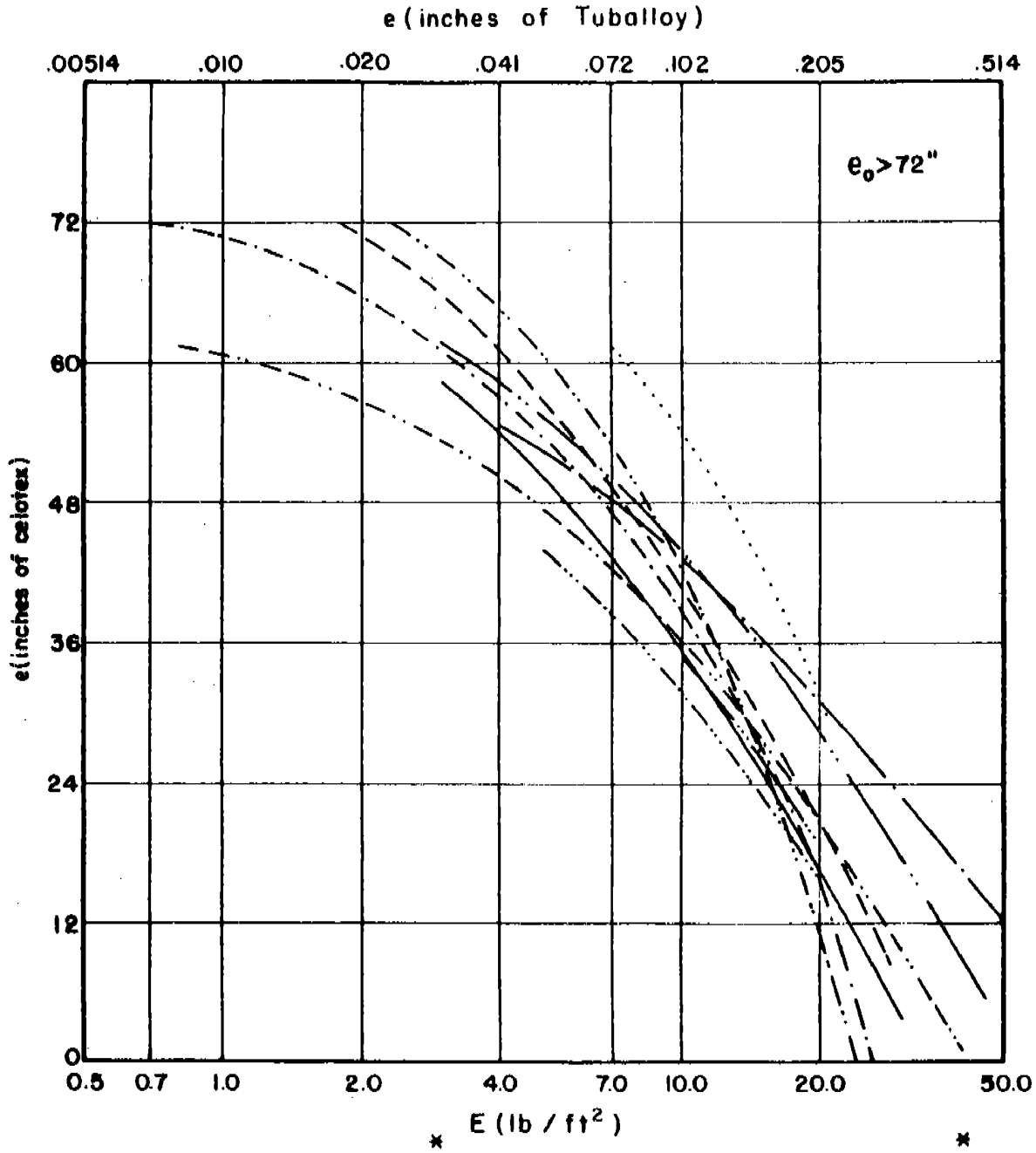

		*			*
Magnesium	— — — —	10.58	F. H. Steel	—··—··—	2.41
2024 T-3	—·—·—	6.65	Hard Steel	———	2.41
Titanium	—··—··—	4.17	Copper	—··—	2.10
Cast Iron	·····	2.59	Lead	—·—	1.70
Mild Steel	— —··— —	2.41	Tuballoy	—··—	1.00

*Ratio of Material Thickness Relative to a Unit Thickness of Tuballoy

Fig. 190

[redacted]

e_{cel} vs E for Various Combinations of m_s, θ, and V_s

$m_s = 30$ grains $\theta = 60$ degrees $V_s = 6000$ fps

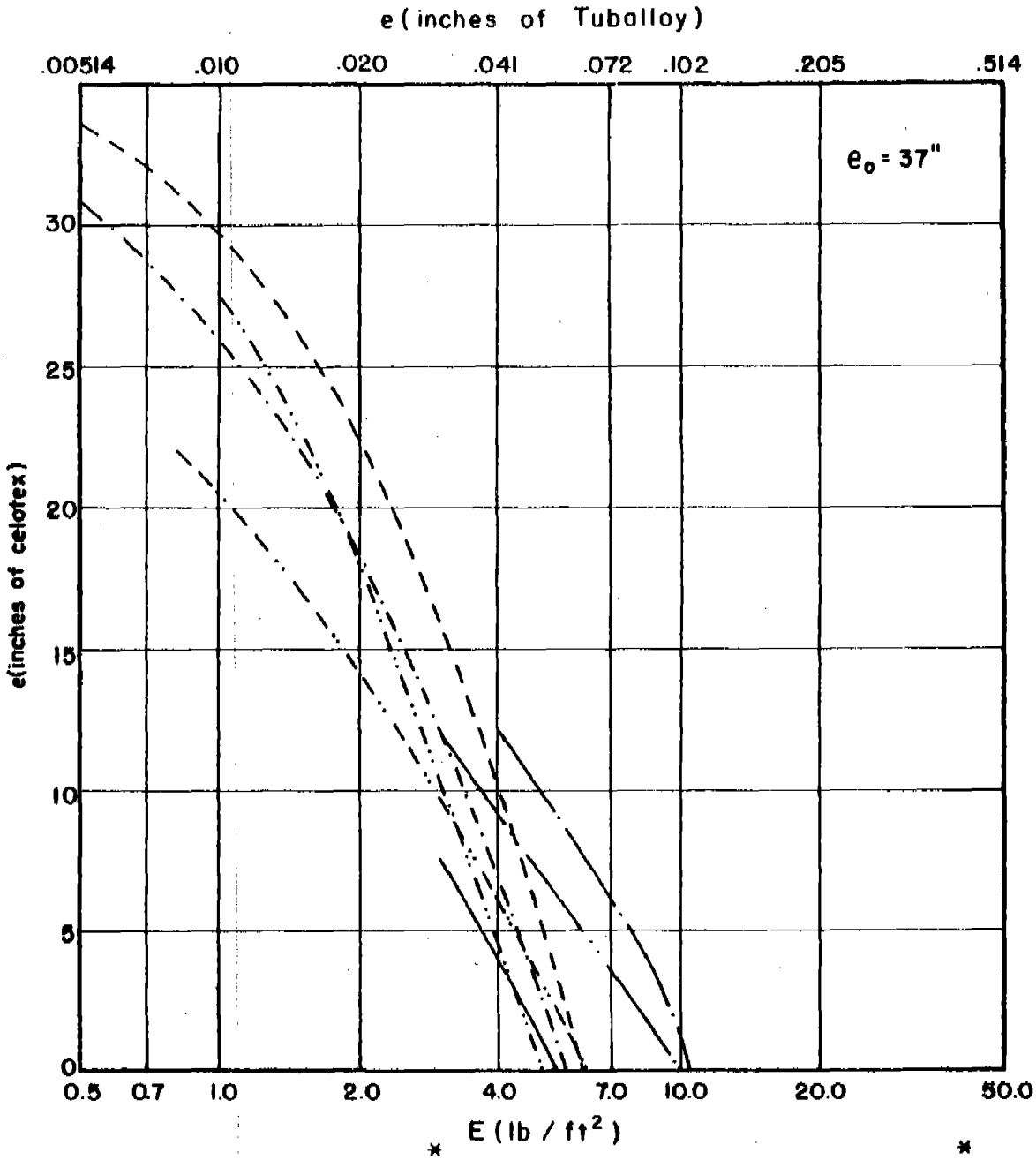

		*			*
Magnesium	— — — —	10.58	F.H. Steel	—··—··—	2.41
2024 T-3	—·—·—	6.65	Hard Steel	———	2.41
Titanium	—··—··—	4.17	Copper	—··—	2.10
Cast Iron	·····	2.59	Lead	—·—	1.70
Mild Steel	— —··— —	2.41	Tuballoy	—···—	1.00

*Ratio of Material Thickness Relative to a Unit Thickness of Tuballoy

Fig. 191

[redacted]

[redacted]

e_{cel} vs E for Various Combinations of m_s, θ, and V_s

m_s = 100 grains θ = 60 degrees V_s = 6000 fps

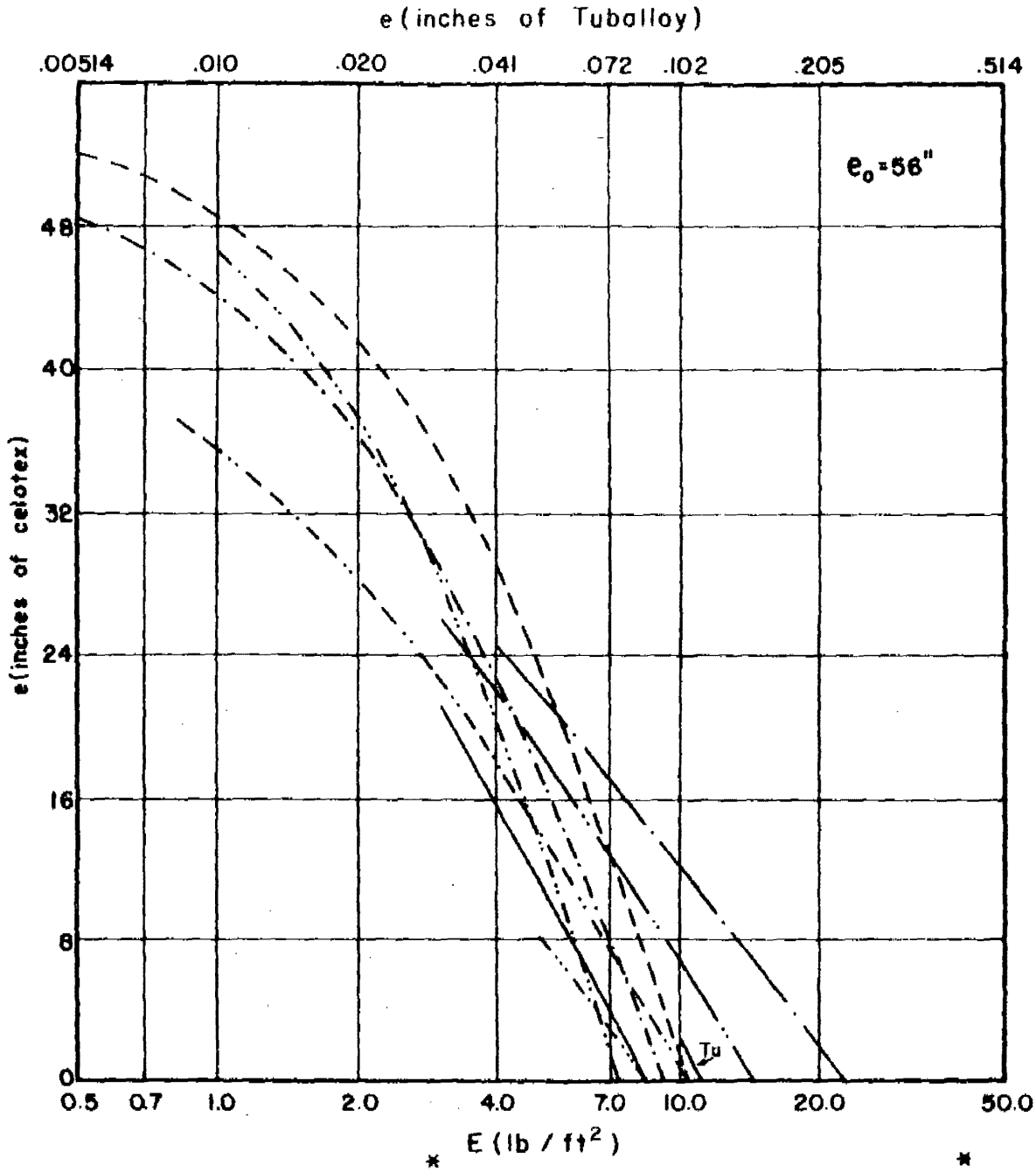

		*			*
Magnesium	———	10.58	F. H. Steel	—·—·—	2.41
2024 T-3	—·—·—	6.65	Hard Steel	———	2.41
Titanium	—··—··—	4.17	Copper	—··—	2.10
Cast Iron	·····	2.59	Lead	—·—	1.70
Mild Steel	—··—	2.41	Tuballoy	—··—	1.00

*Ratio of Material Thickness Relative to a Unit Thickness of Tuballoy

Fig. 192

[redacted]

[redacted]

e_{cel} vs E for Various Combinations of m_s, θ, and V_s

m_s = 300 grains θ = 60 degrees V_s = 6000 fps

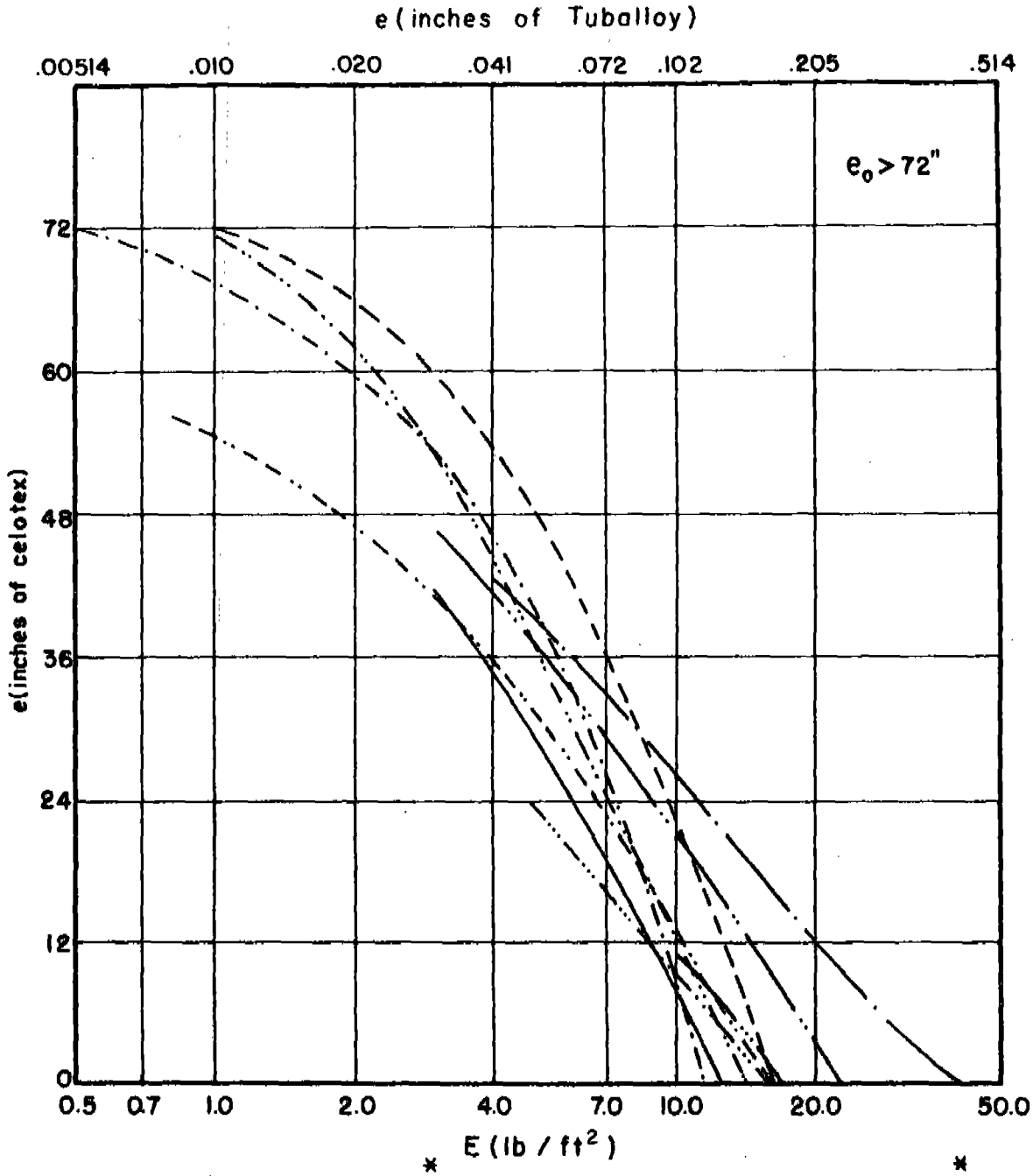

		*			*
Magnesium	— — — —	10.58	F. H. Steel	—··—··—	2.41
2024 T-3	—·—·—	6.65	Hard Steel	———	2.41
Titanium	—··—··—	4.17	Copper	—··—	2.10
Cast Iron	·····	2.59	Lead	—·—	1.70
Mild Steel	— —··— —	2.41	Tuballoy	—···—	1.00

*Ratio of Material Thickness Relative to a Unit Thickness of Tuballoy

Fig. 193

[redacted]

[redacted]

e_{cel} vs E for Various Combinations of m_s, θ, and V_s

$m_s = 30$ grains $\theta = 70$ degrees $V_s = 6000$ fps

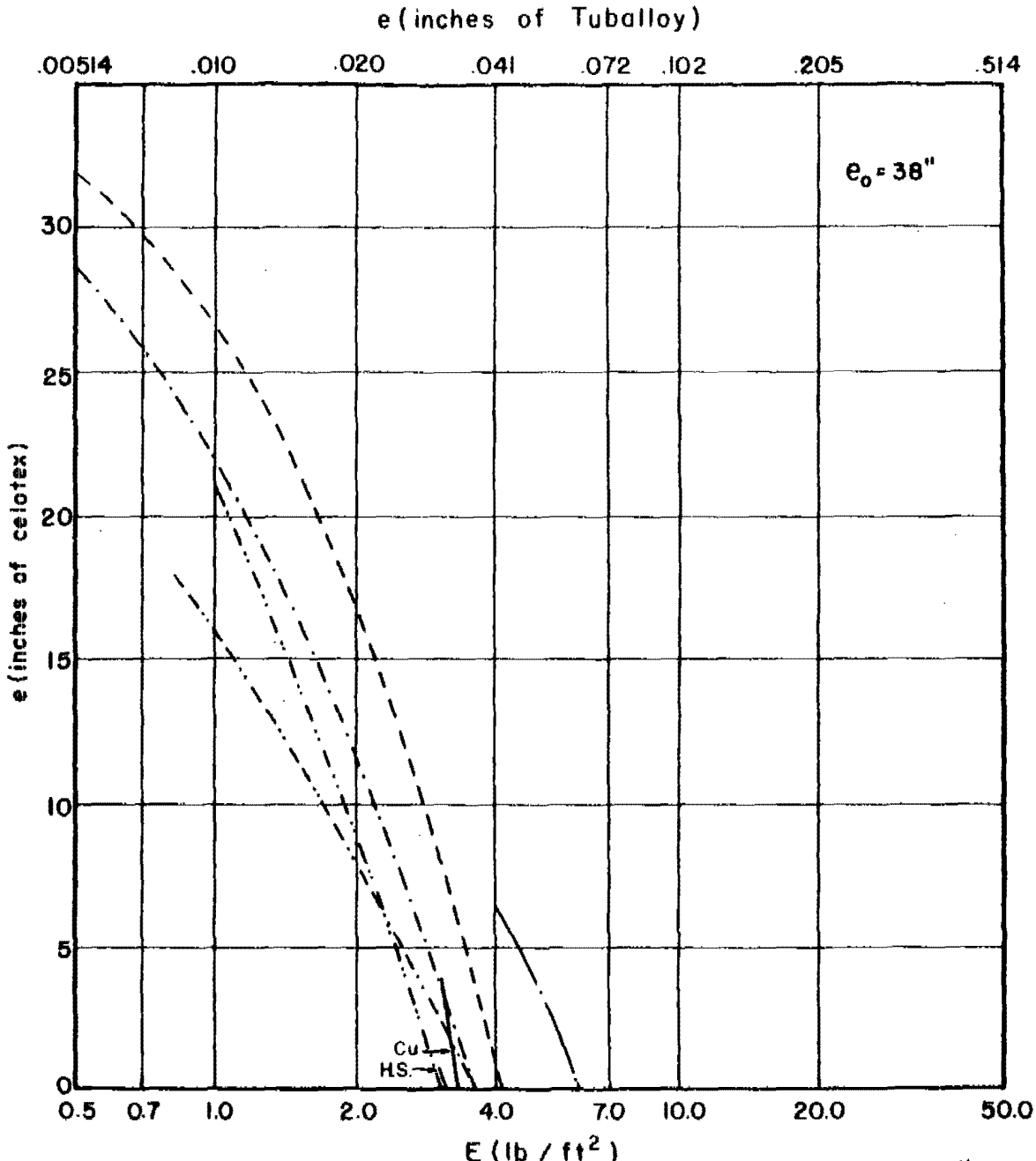

		*			*
Magnesium	— — — —	10.58	F.H. Steel	—·····—·····—	2.41
2024 T-3	—·—·—·—	6.65	Hard Steel	————	2.41
Titanium	—··—··—	4.17	Copper	—··—··—	2.10
Cast Iron	·····	2.59	Lead	—·—·—	1.70
Mild Steel	—··—··—	2.41	Tuballoy	—··—··—	1.00

*Ratio of Material Thickness Relative to a Unit Thickness of Tuballoy

Fig. 194

[redacted]

[redacted]

e_{cel} vs E for Various Combinations of m_s, θ, and V_s

m_s = 100 grains θ = 70 degrees V_s = 6000 fps

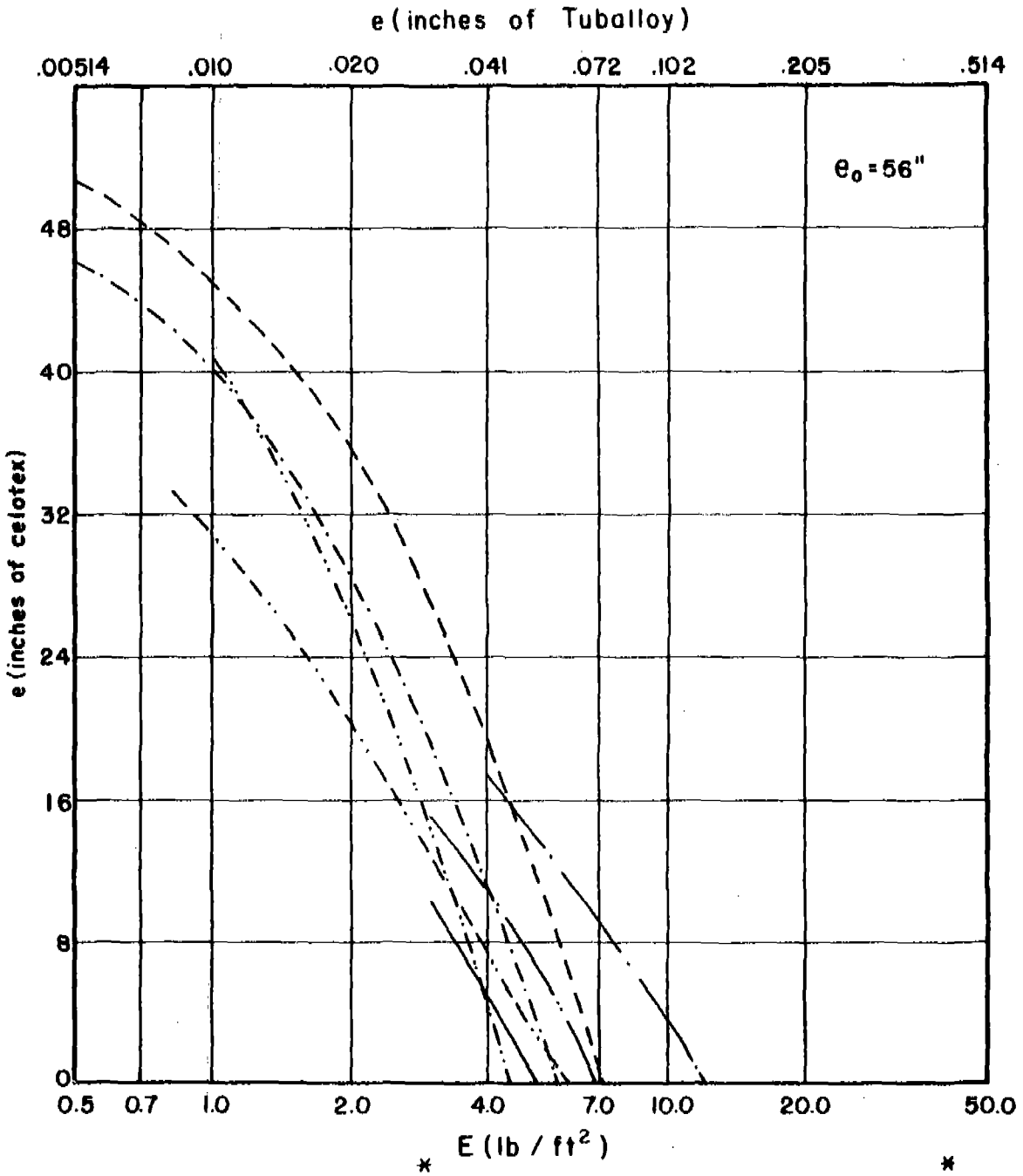

		*			*
Magnesium	— — — —	10.58	F.H. Steel	—··—··—	2.41
2024 T-3	—·—·—	6.65	Hard Steel	———	2.41
Titanium	—··—··—	4.17	Copper	—··—	2.10
Cast Iron	·····	2.59	Lead	—·—	1.70
Mild Steel	—··— —	2.41	Tuballoy	—···—	1.00

*Ratio of Material Thickness Relative to a Unit Thickness of Tuballoy

Fig. 195

[redacted]

[redacted]

e_{cel} vs E for Various Combinations of m_s, θ, and V_s

m_s = 300 grains θ = 70 degrees V_s = 6000 fps

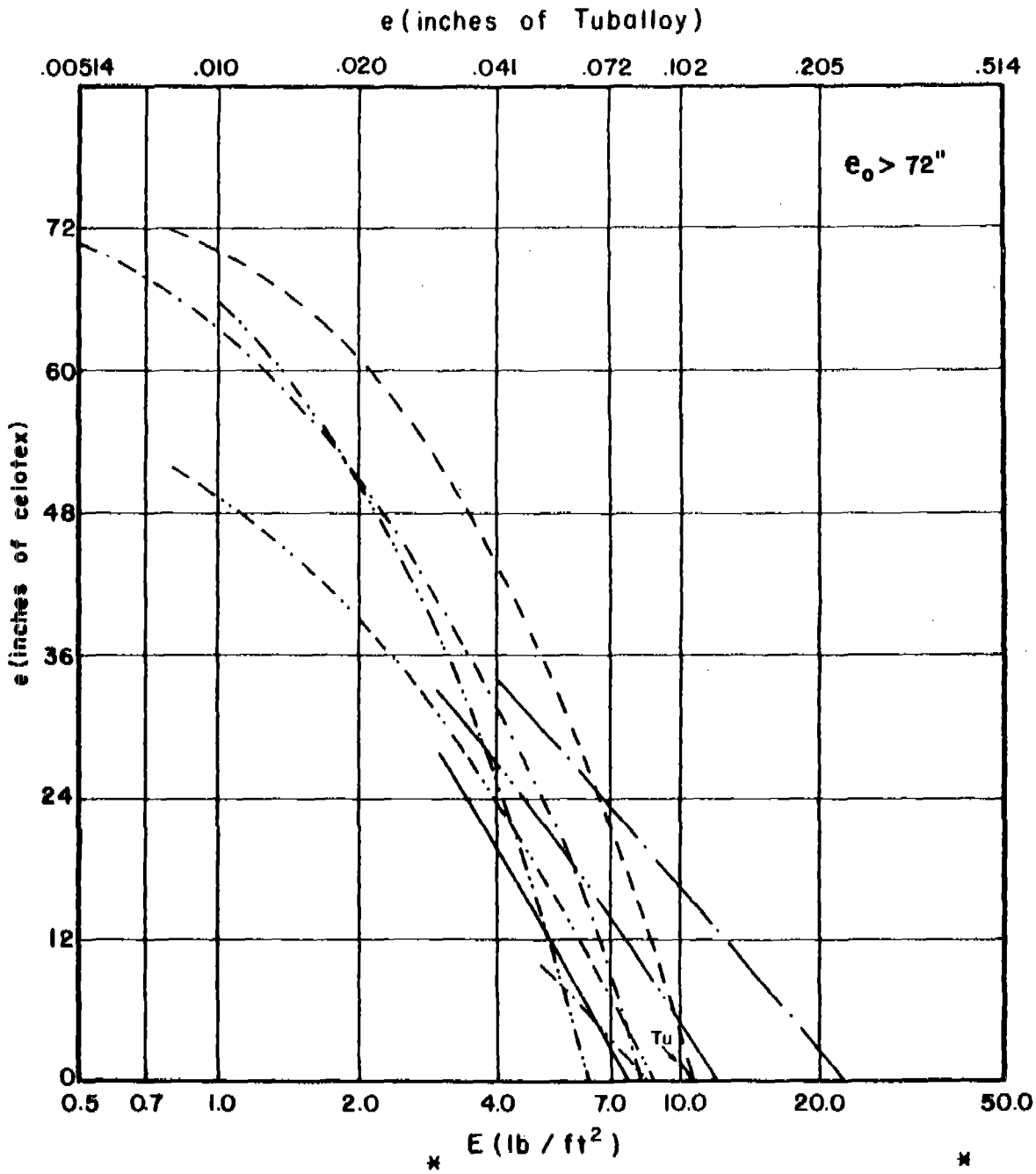

		*			*
Magnesium	— — — —	10.58	F. H. Steel	—··—··—	2.41
2024 T-3	—·—·—	6.65	Hard Steel	———	2.41
Titanium	—··—··—	4.17	Copper	—··—	2.10
Cast Iron	·····	2.59	Lead	—·—	1.70
Mild Steel	— —··— —	2.41	Tuballoy	—···—	1.00

*Ratio of Material Thickness Relative to a Unit Thickness of Tuballoy

Fig. 196

[redacted]

[redacted]

e_{cel} vs E for Various Combinations of m_s, θ, and V_s

m_s = 30 grains θ = 0 degrees V_s = 9000 fps

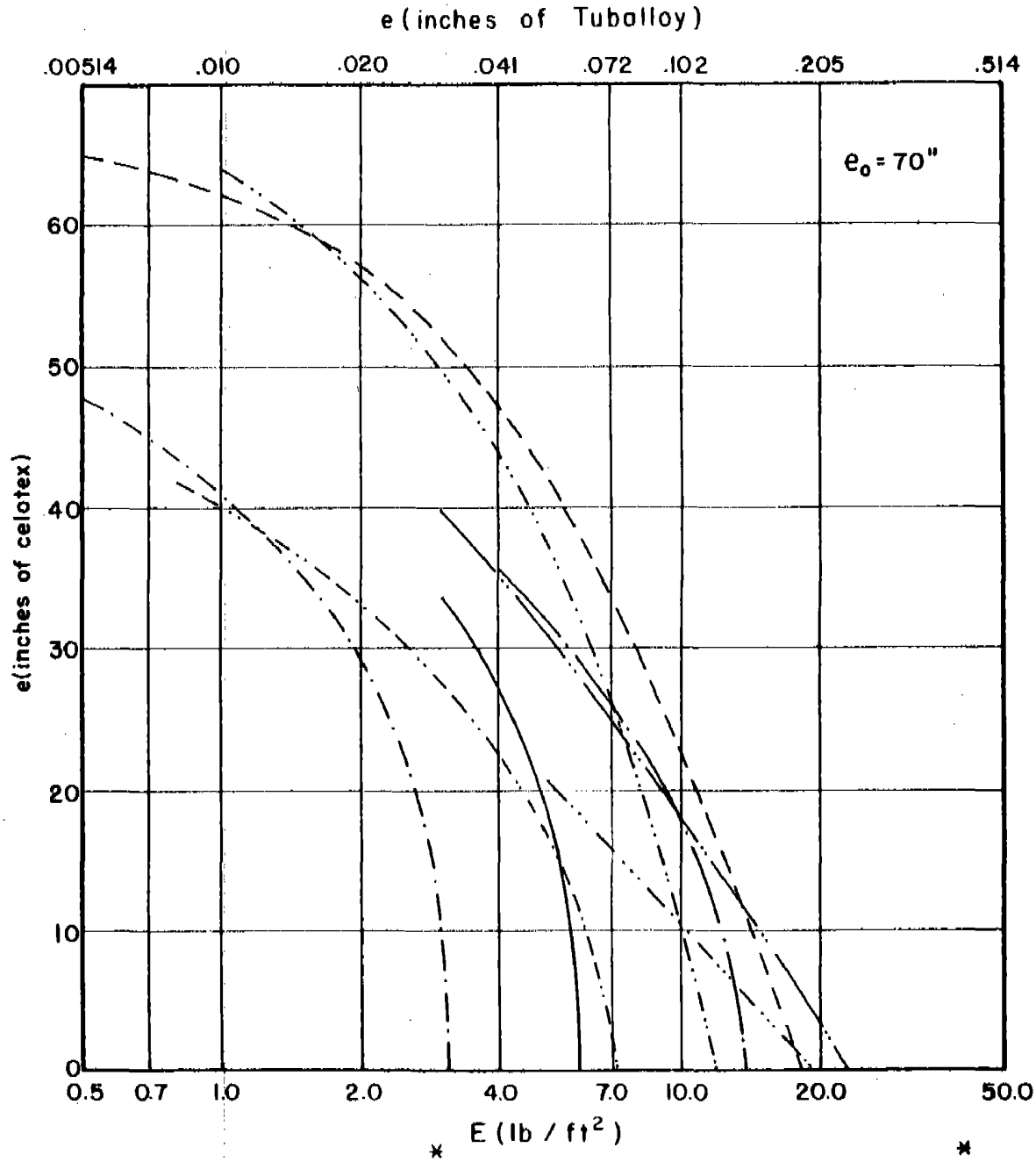

		*			*
Magnesium	— — — — —	10.58	F.H. Steel	—·—·—	2.41
2024 T-3	—·—·—	6.65	Hard Steel	———	2.41
Titanium	—··—··—	4.17	Copper	—··—	2.10
Cast Iron	·····	2.59	Lead	—·—	1.70
Mild Steel	— —··— —	2.41	Tuballoy	—··—	1.00

*Ratio of Material Thickness Relative to a Unit Thickness of Tuballoy

Fig. 197

[redacted]

[redacted]

e_{cel} vs E for Various Combinations of m_s, θ, and V_s

m_s = 100 grains θ = 0 degrees V_s = 9000 fps

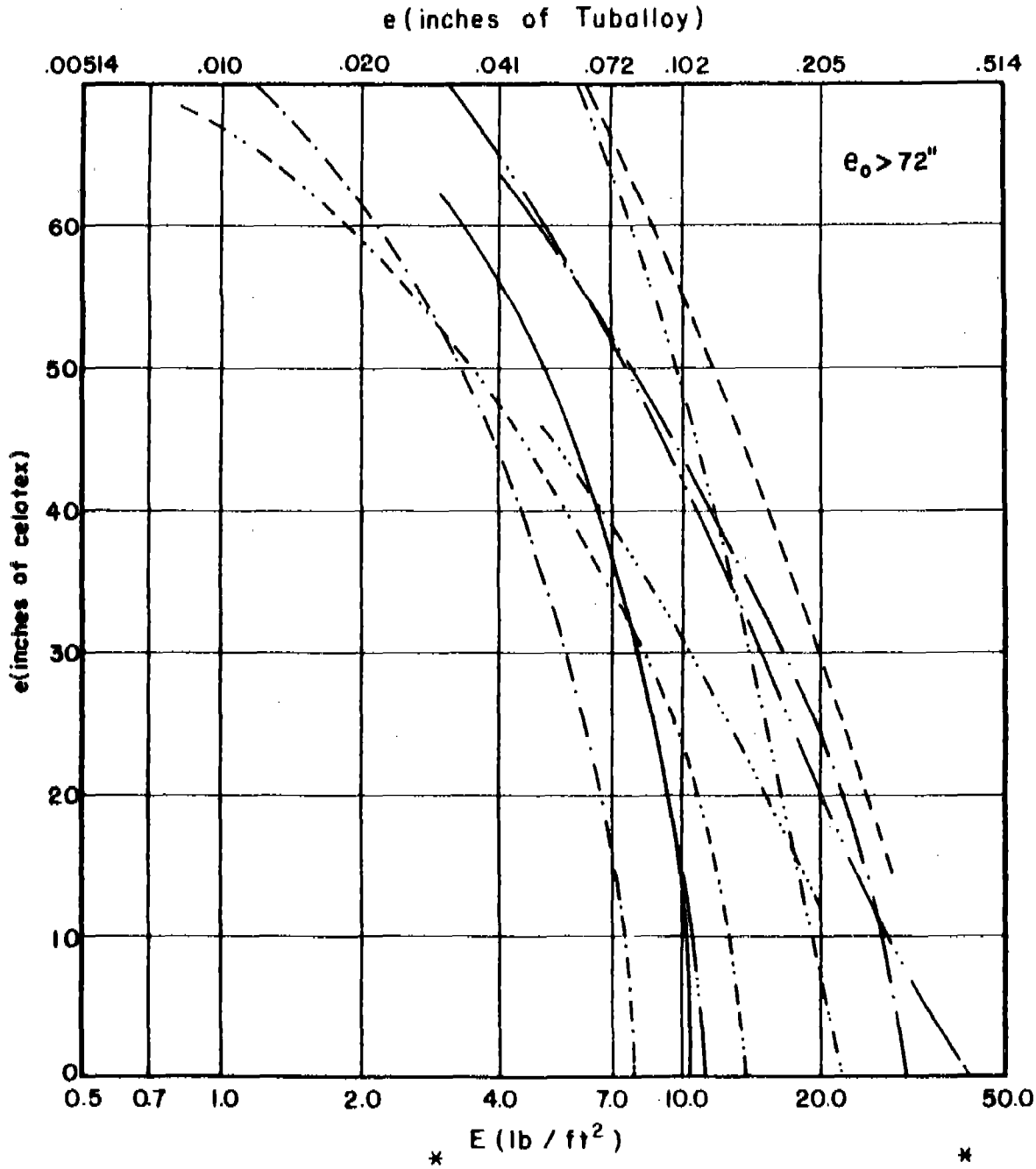

		*			*
Magnesium	— — — —	10.58	F.H. Steel	—··—··—	2.41
2024 T-3	—·—·—	6.65	Hard Steel	———	2.41
Titanium	—··—··—	4.17	Copper	—··—	2.10
Cast Iron	·····	2.59	Lead	—·—	1.70
Mild Steel	— —··— —	2.41	Tuballoy	—···—	1.00

*Ratio of Material Thickness Relative to a Unit Thickness of Tuballoy

Fig. 198

[redacted]

[redacted]

e_{cel} vs E for Various Combinations of m_s, θ, and V_s

m_s = 300 grains θ = 0 degrees V_s = 9000 fps

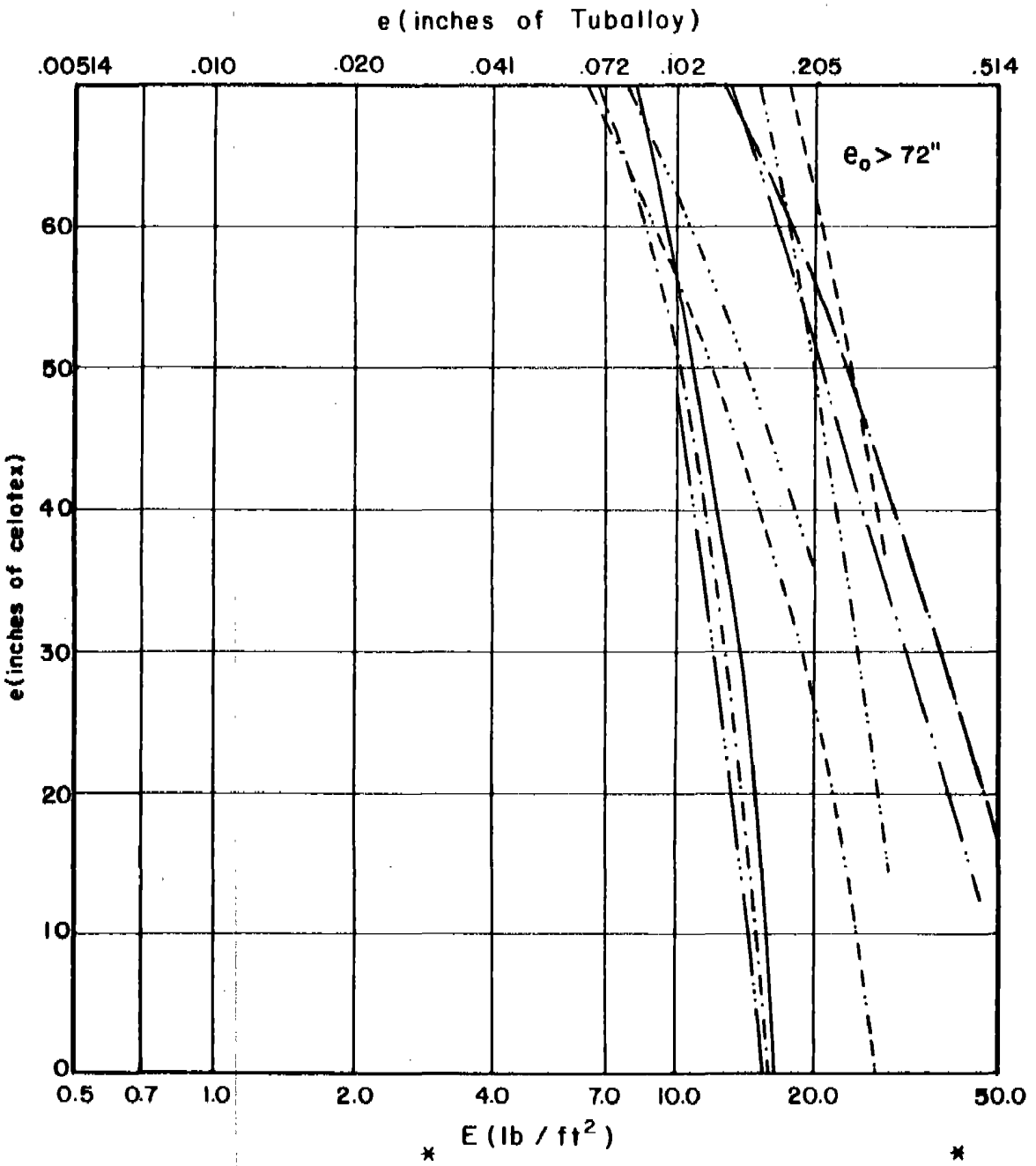

		*			*
Magnesium	— — — — —	10.58	F.H. Steel	—··—··—	2.41
2024 T-3	—·—·—·—	6.65	Hard Steel	————	2.41
Titanium	—··—··—	4.17	Copper	—··—··—	2.10
Cast Iron	·····	2.59	Lead	—·—·—	1.70
Mild Steel	— —··— —	2.41	Tuballoy	—··—··—	1.00

*Ratio of Material Thickness Relative to a Unit Thickness of Tuballoy

Fig. 199

[redacted]

[redacted]

e_{cel} vs E for Various Combinations of m_s, θ, and V_s

m_s = 30 grains θ = 60 degrees V_s = 9000 fps

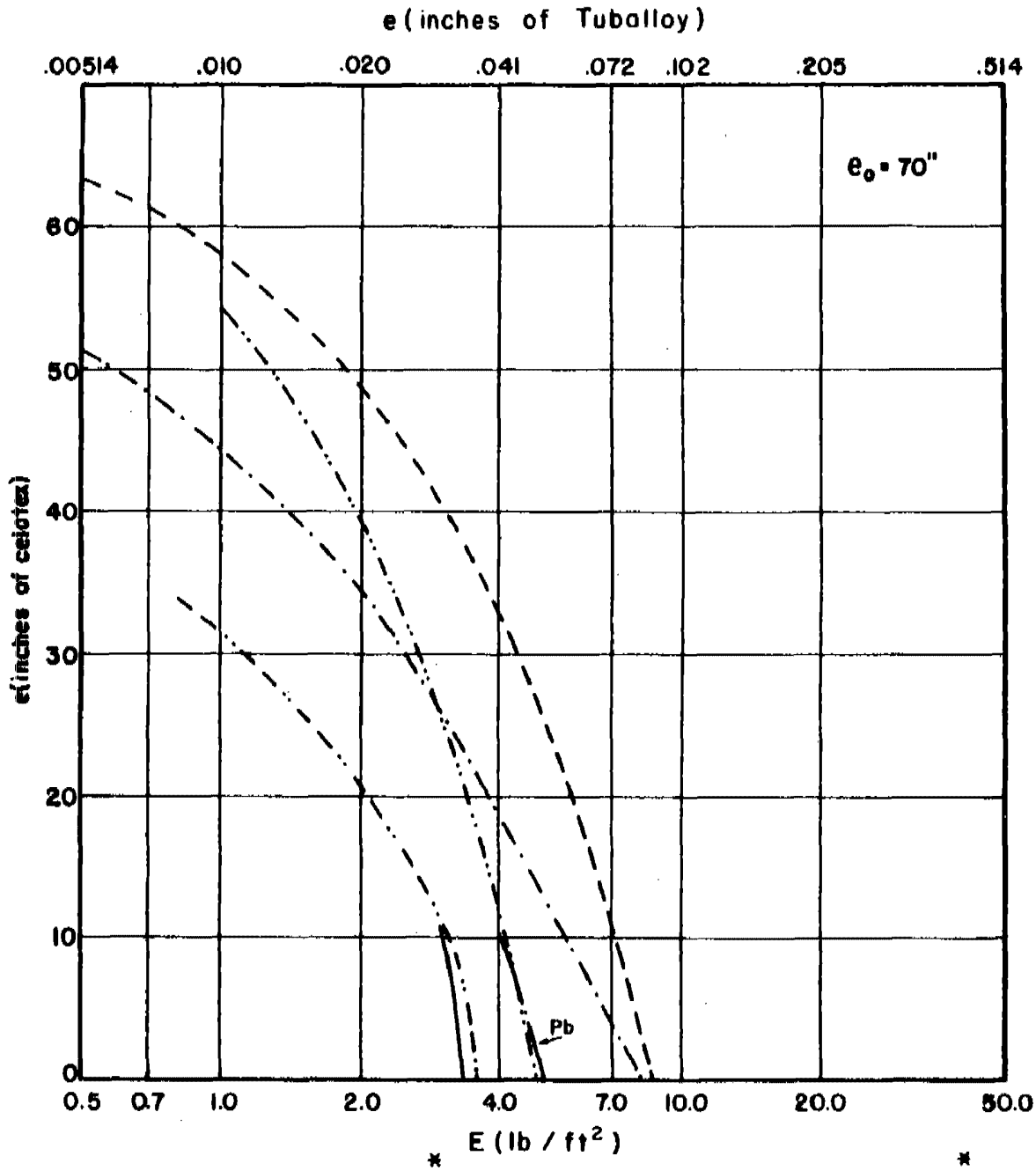

		*			*
Magnesium	— — — — —	10.58	F.H. Steel	—··—··—	2.41
2024 T-3	—·—·—·—	6.65	Hard Steel	———	2.41
Titanium	—··—··—	4.17	Copper	—··—	2.10
Cast Iron	·····	2.59	Lead	—·—	1.70
Mild Steel	— —··— —	2.41	Tuballoy	—···—	1.00

*Ratio of Material Thickness Relative to a Unit Thickness of Tuballoy

Fig. 200

[redacted]

[redacted]

e_{cel} vs E for Various Combinations of m_s, θ, and V_s

m_s = 100 grains θ = 60 degrees V_s = 9000 fps

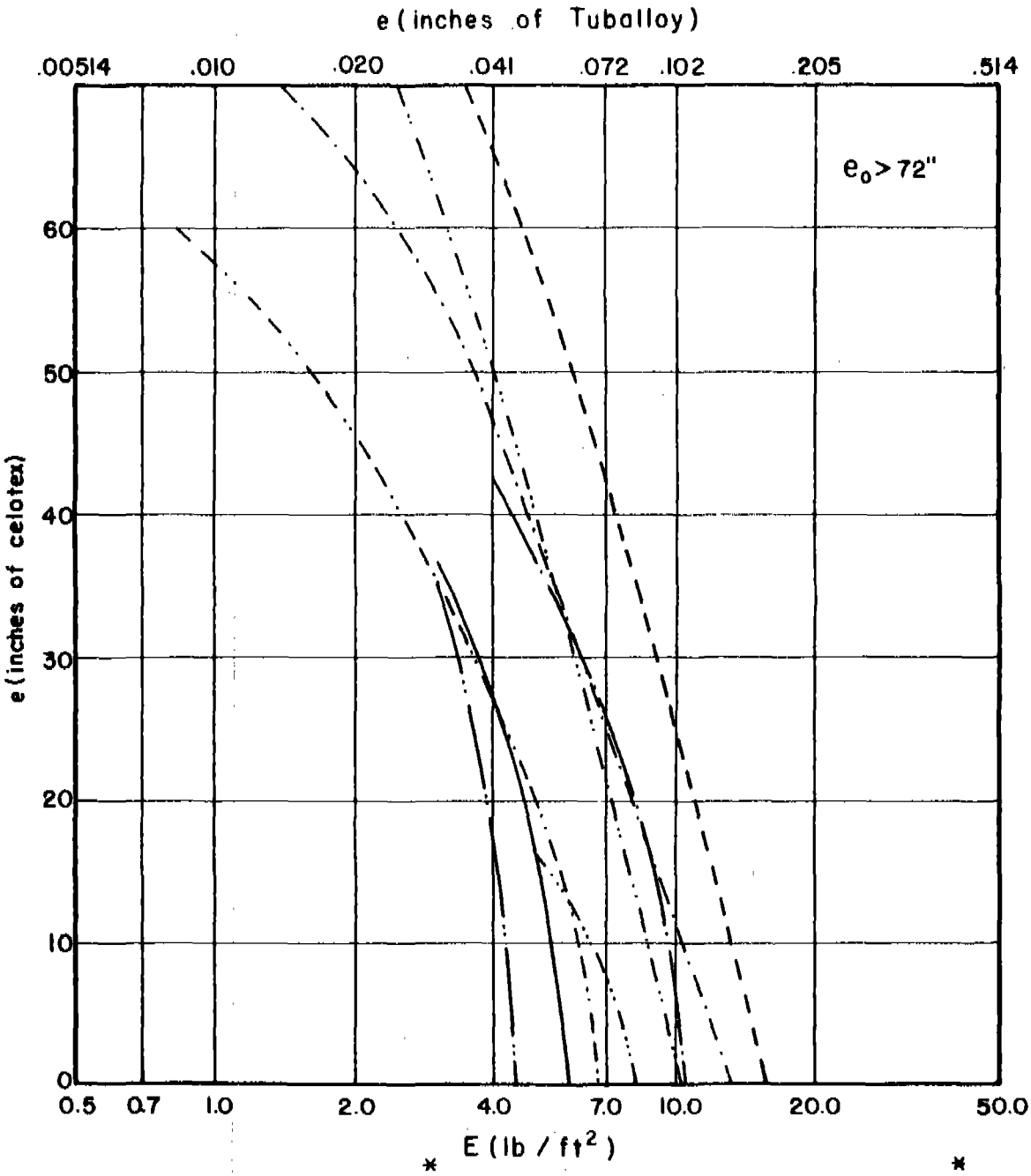

		*			*
Magnesium	— — — — —	10.58	F.H. Steel	—··—··—	2.41
2024 T-3	—·—·—·—	6.65	Hard Steel	———	2.41
Titanium	—··—··—	4.17	Copper	—··—	2.10
Cast Iron	·····	2.59	Lead	—·—	1.70
Mild Steel	— —··— —	2.41	Tuballoy	—···—	1.00

*Ratio of Material Thickness Relative to a Unit Thickness of Tuballoy

Fig. 201

[redacted]

[redacted]

e_{cel} vs E for Various Combinations of m_s, θ, and V_s

m_s = 300 grains θ = 60 degrees V_s = 9000 fps

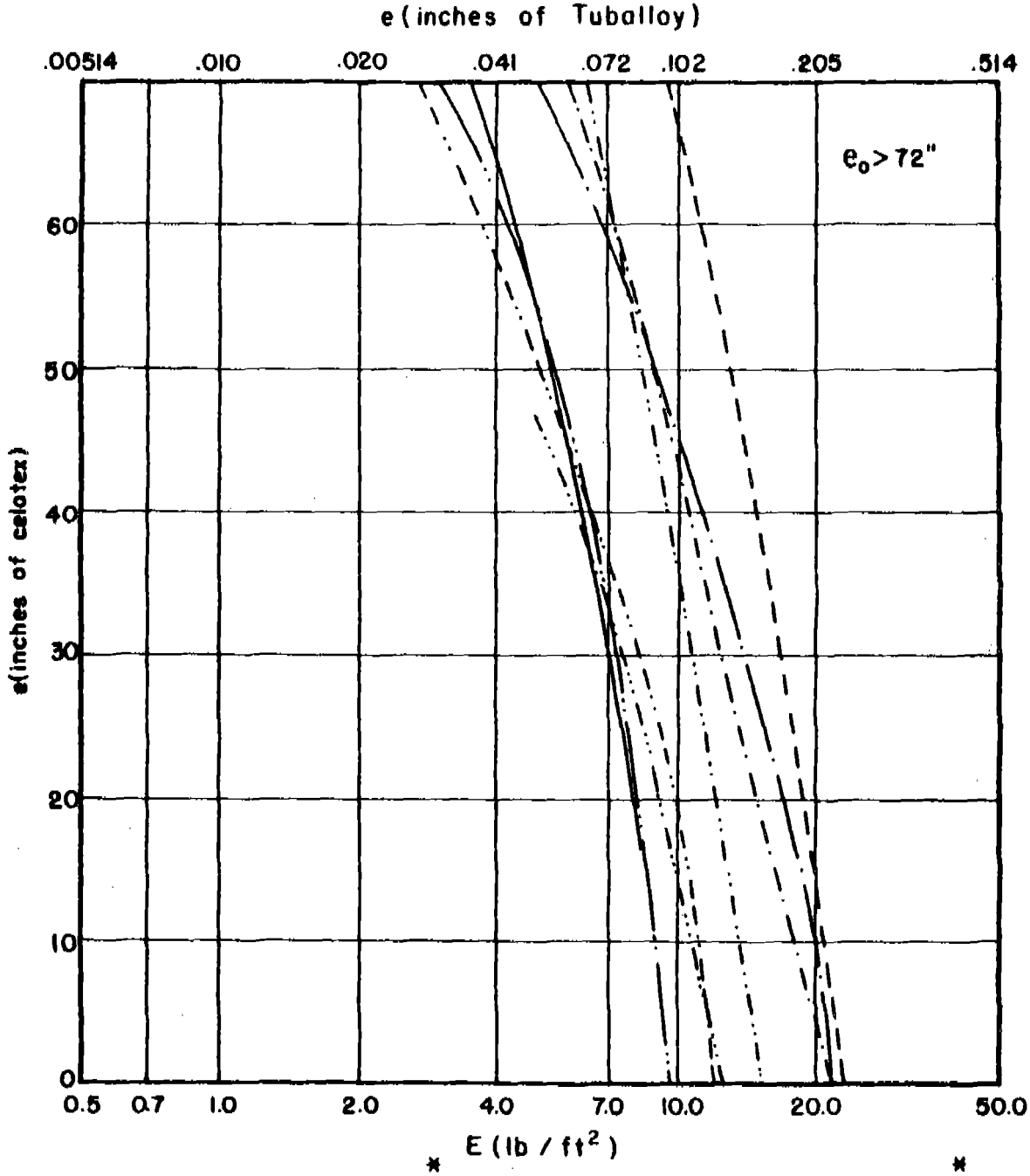

		*			*
Magnesium	— — — —	10.58	F. H. Steel	—··—··—	2.41
2024 T-3	—·—·—	6.65	Hard Steel	———	2.41
Titanium	—··—··—	4.17	Copper	—··—	2.10
Cast Iron	·····	2.59	Lead	—·—	1.70
Mild Steel	— —··— —	2.41	Tuballoy	—···—	1.00

*Ratio of Material Thickness Relative to a Unit Thickness of Tuballoy

Fig. 202

[redacted]

[redacted]

e_{cel} vs E for Various Combinations of m_s, θ, and V_s

$m_s = 30$ grains $\theta = 70$ degrees $V_s = 9000$ fps

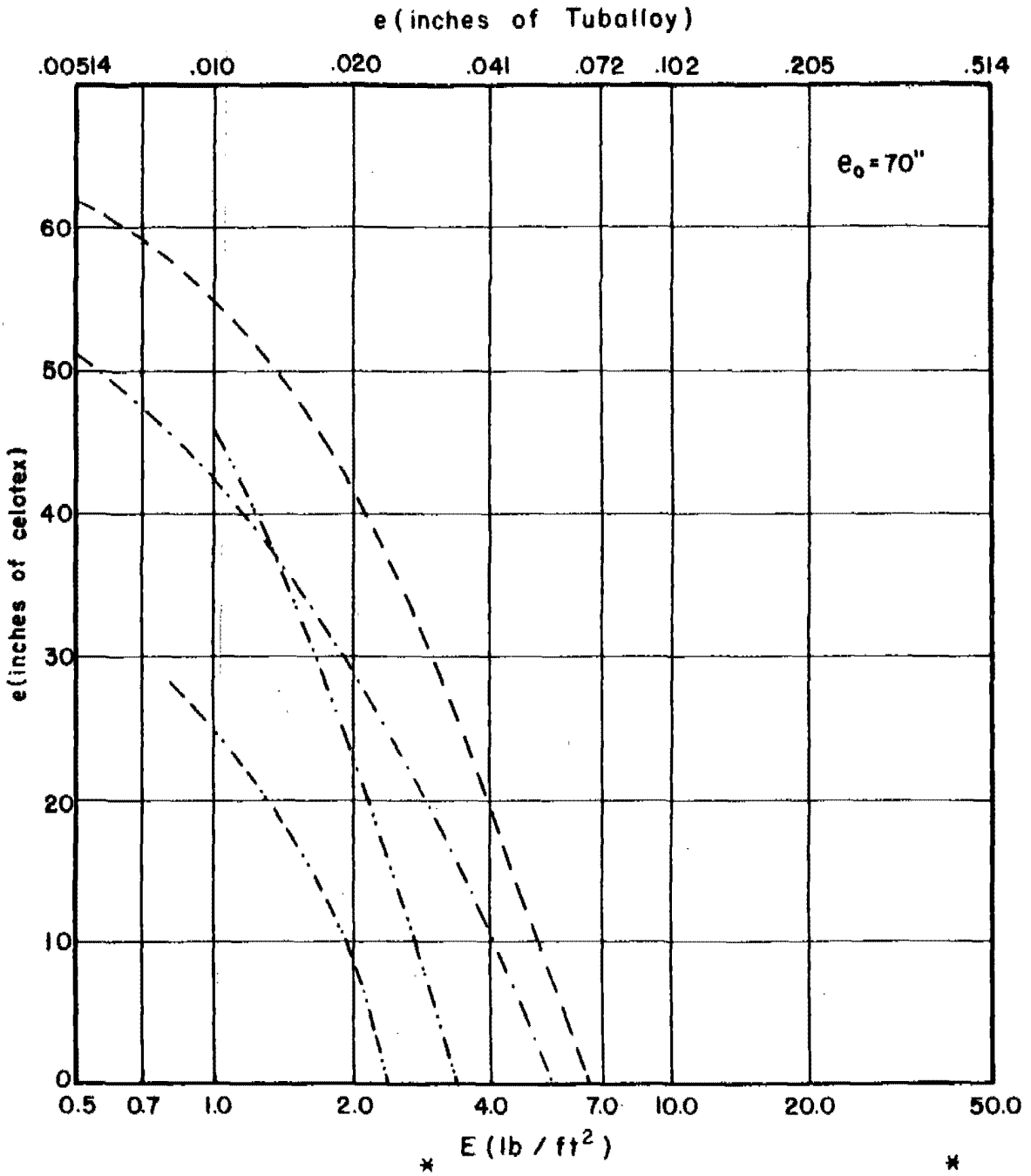

		*			*
Magnesium	— — — —	10.58	F. H. Steel	—·—·—	2.41
2024 T-3	—·—·—	6.65	Hard Steel	———	2.41
Titanium	—··—··—	4.17	Copper	—··—	2.10
Cast Iron	·····	2.59	Lead	—·—	1.70
Mild Steel	— —·— —	2.41	Tuballoy	—··—	1.00

*Ratio of Material Thickness Relative to a Unit Thickness of Tuballoy

Fig. 203

[redacted]

[redacted]

e_{cal} vs E for Various Combinations of m_s, θ, and V_s

m_s = 100 grains θ = 70 degrees V_s = 9000 fps

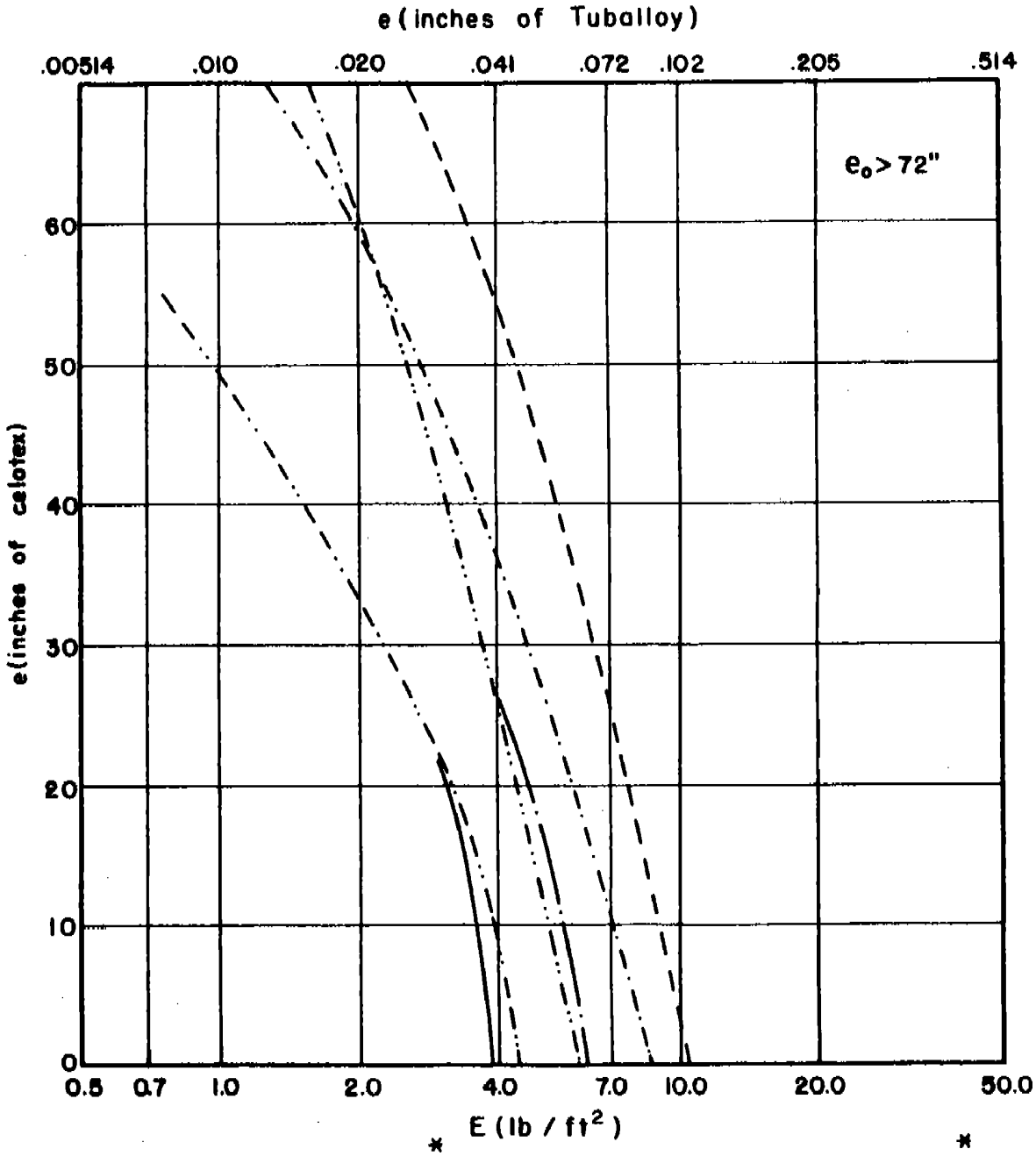

		*			*
Magnesium	------	10.58	F.H. Steel	—··—··—	2.41
2024 T-3	—·—·—	6.65	Hard Steel	———	2.41
Titanium	—··—··—	4.17	Copper	—··—	2.10
Cast Iron	·····	2.59	Lead	—·—	1.70
Mild Steel	—··—	2.41	Tuballoy	—··—	1.00

*Ratio of Material Thickness Relative to a Unit Thickness of Tuballoy

Fig. 204

[redacted]

[redacted]

e_{cel} vs E for Various Combinations of m_s, θ, and V_s

m_s = 300 grains θ = 70 degrees V_s = 9000 fps

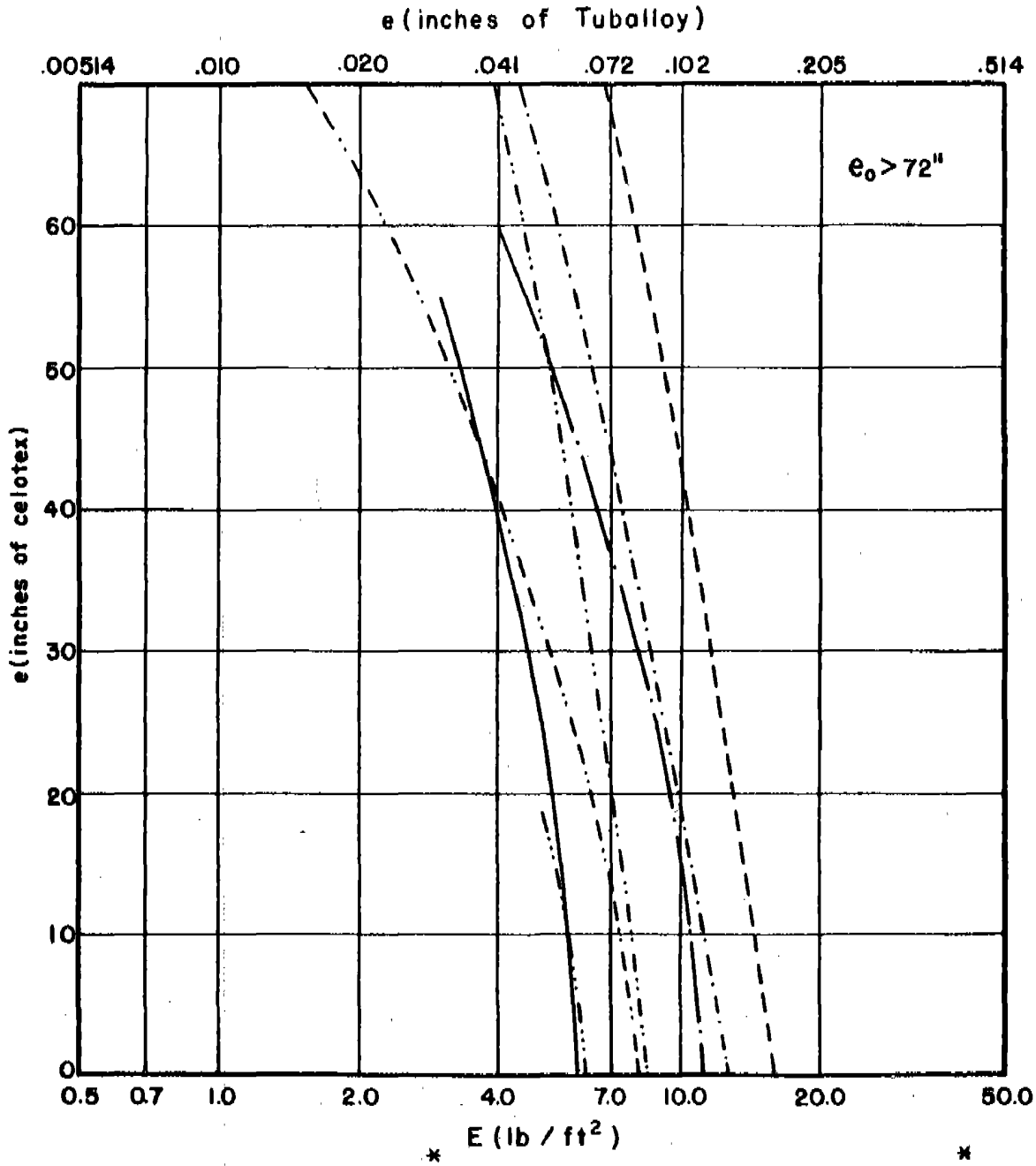

		*			*
Magnesium	— — — —	10.58	F.H. Steel	—··—··—	2.41
2024 T-3	—·—·—	6.65	Hard Steel	————	2.41
Titanium	—··—··—	4.17	Copper	—··—	2.10
Cast Iron	·····	2.59	Lead	—·—	1.70
Mild Steel	—··—	2.41	Tuballoy	—··—	1.00

*Ratio of Material Thickness Relative to a Unit Thickness of Tuballoy

Fig. 205

[redacted]

[redacted]

Appendix D

Graph Set VII: e (inches of 2024T-3) vs E

for Various Combinations of m_s, θ, and V_s

Figs. 206-232

Note: The ordinate represents an estimate of the maximum thickness of calibrating material that can possibly be perforated by the largest portion of the residual fragment after the original fragment has impacted initially on one of the given metallic targets. The assumption is made that the residual fragment strikes the calibrating material at normal impact and that, furthermore, the shape of the original fragment is retained despite any loss in weight.

On each graph in this appendix there appears a value of e_o. This value is an estimate of the maximum thickness of the calibrating material that the original fragment can perforate, assuming normal impact and no intermediate barrier.

The contours are limited on these graphs to 72" of celotex and 3.0" of 2024T-3. These represent the maximum thicknesses of these materials that have been considered in BRL single-target firings. In fact, there is no instance to date of a perforation of 3.0" of 2024T-3 in BRL experimental work with pre-formed fragments.

[redacted]

e_{2024} vs E for Various Combinations of m_s, θ, and V_s

$m_s = 30$ grains $\theta = 0$ degrees $V_s = 3000$ fps

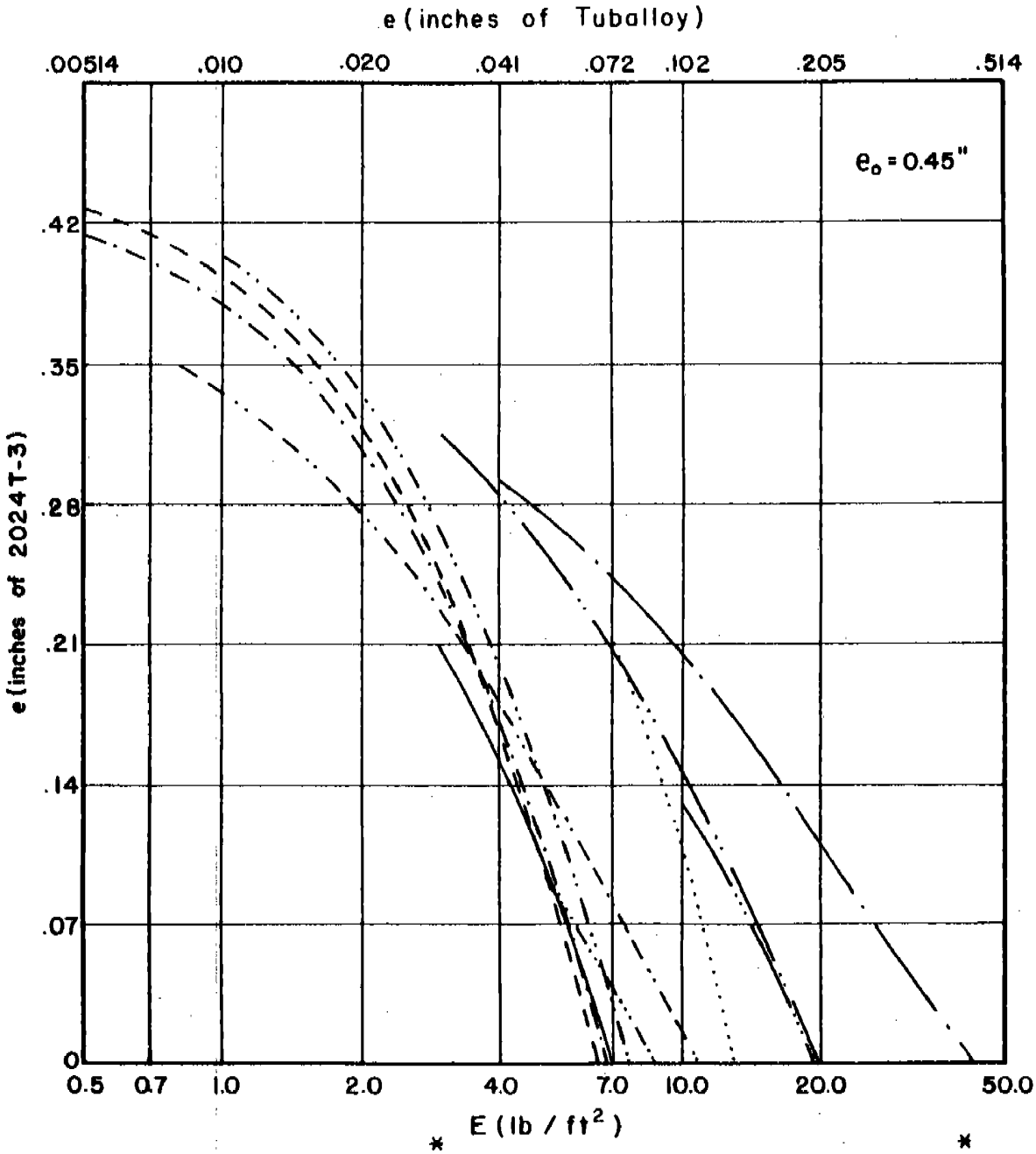

		*			*
Magnesium	———	10.58	F.H. Steel	—·—·—	2.41
2024 T-3	—·—·—	6.65	Hard Steel	———	2.41
Titanium	—··—··—	4.17	Copper	—··—	2.10
Cast Iron	·····	2.59	Lead	—·—	1.70
Mild Steel	—··—	2.41	Tuballoy	—···—	1.00

*Ratio of Material Thickness Relative to a Unit Thickness of Tuballoy

Fig. 206

[redacted]

e_{2024} vs E for Various Combinations of m_s, θ, and V_s

m_s = 100 grains θ = 0 degrees V_s = 3000 fps

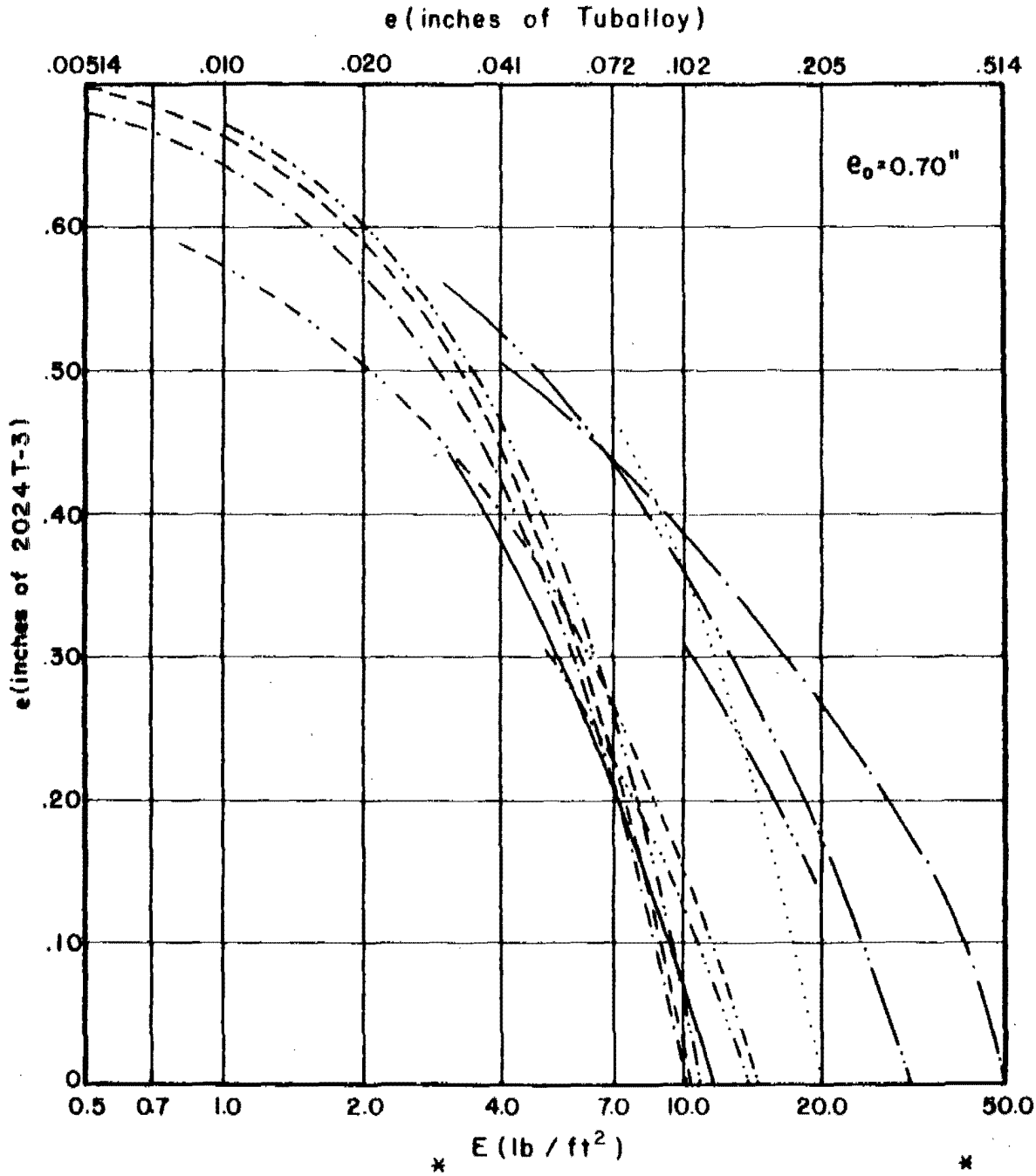

		*			*
Magnesium	— — — — —	10.58	F. H. Steel	—·—·—	2.41
2024 T-3	—·—·—	6.65	Hard Steel	———	2.41
Titanium	—··—··—	4.17	Copper	—··—	2.10
Cast Iron	·····	2.59	Lead	—·—	1.70
Mild Steel	— —·— —	2.41	Tuballoy	—··—	1.00

*Ratio of Material Thickness Relative to a Unit Thickness of Tuballoy

Fig. 207

[redacted]

[redacted]

e_{2024} vs E for Various Combinations of m_s, θ, and V_s

m_s = 300 grains θ = 0 degrees V_s = 3000 fps

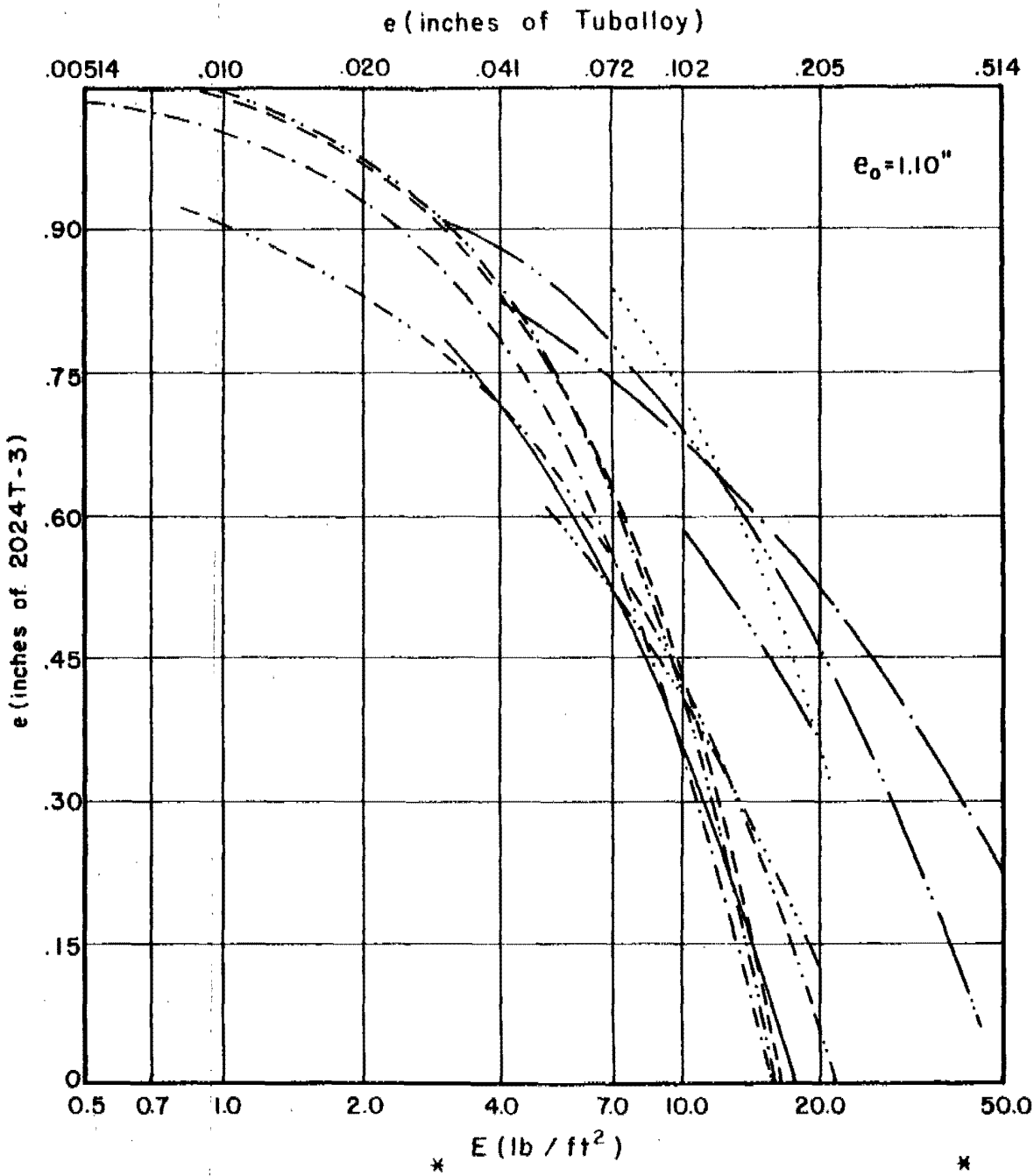

		*			*
Magnesium	— — — —	10.58	F. H. Steel	—·—·—	2.41
2024 T-3	—·—·—	6.65	Hard Steel	———	2.41
Titanium	—··—··—	4.17	Copper	—··—··—	2.10
Cast Iron	·····	2.59	Lead	—·—	1.70
Mild Steel	— —··— —	2.41	Tuballoy	—··—	1.00

*Ratio of Material Thickness Relative to a Unit Thickness of Tuballoy

Fig. 208

[redacted]

[redacted]

e_{2024} vs E for Various Combinations of m_s, θ, and V_s

m_s = 30 grains θ = 60 degrees V_s = 3000 fps

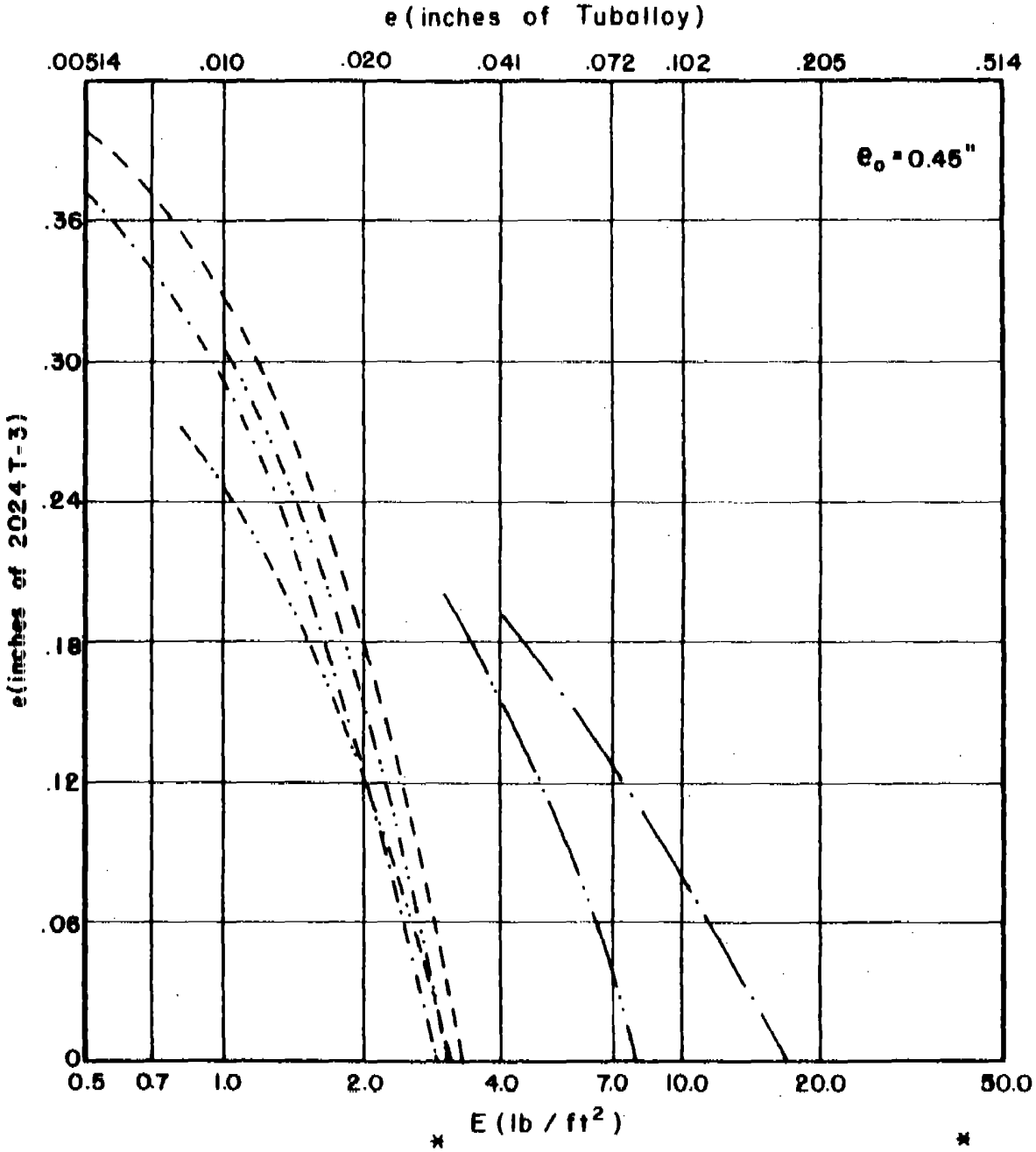

		*			*
Magnesium	— — — —	10.58	F.H. Steel	—··—··—	2.41
2024 T-3	—·—·—	6.65	Hard Steel	———	2.41
Titanium	—··—··—	4.17	Copper	—··—	2.10
Cast Iron	·····	2.59	Lead	—·—	1.70
Mild Steel	— —··— —	2.41	Tuballoy	—··—	1.00

*Ratio of Material Thickness Relative to a Unit Thickness of Tuballoy

Fig. 209

[redacted]

[redacted]

e_{2024} vs E for Various Combinations of m_s, Θ, and V_s

m_s = 100 grains Θ = 60 degrees V_s = 3000 fps

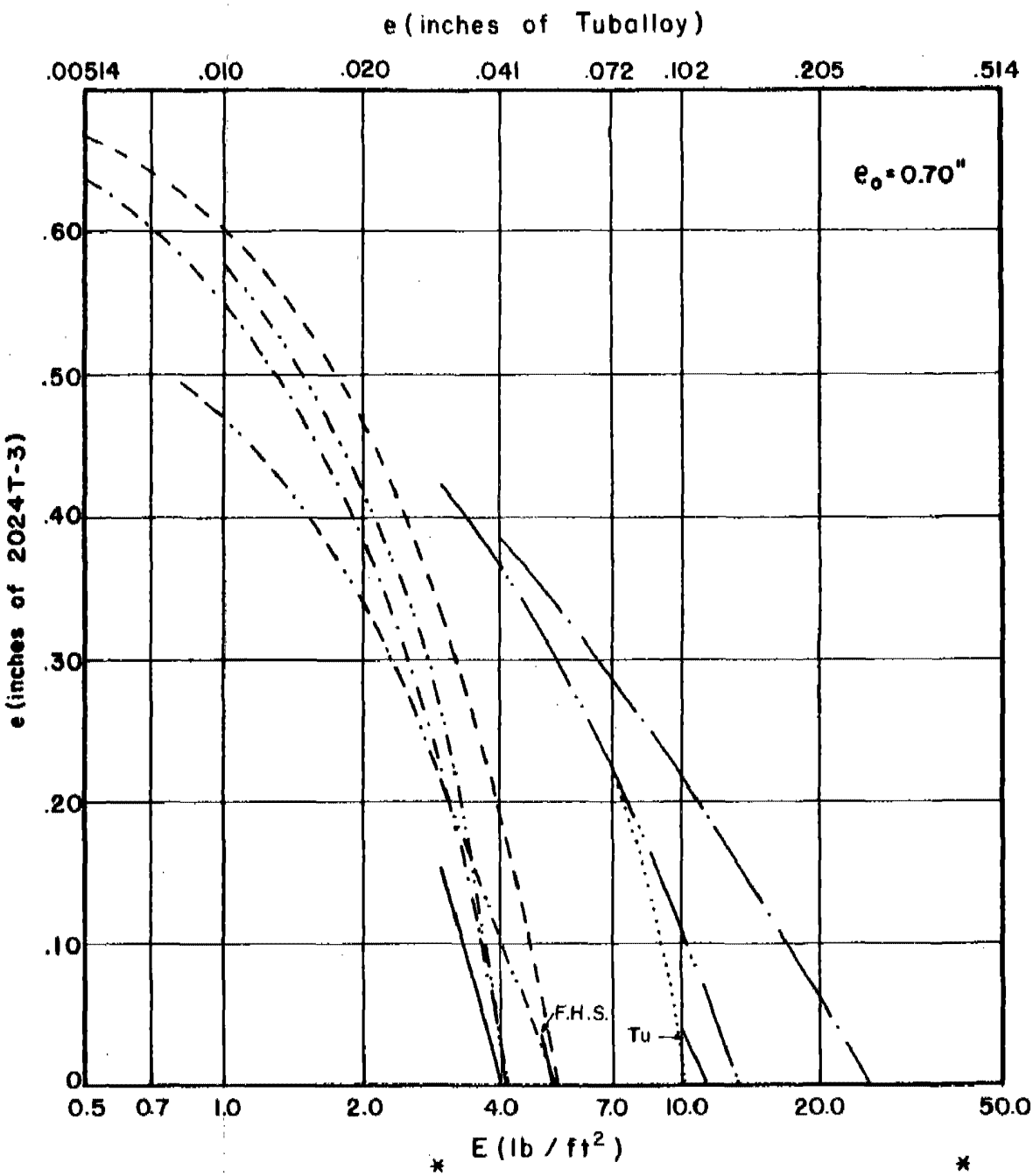

		*			*
Magnesium	— — — —	10.58	F. H. Steel	—··—··—	2.41
2024 T-3	—·—·—	6.65	Hard Steel	————	2.41
Titanium	—··—··—	4.17	Copper	—··—	2.10
Cast Iron	·····	2.59	Lead	—·—	1.70
Mild Steel	— —··— —	2.41	Tuballoy	—··—	1.00

*Ratio of Material Thickness Relative to a Unit Thickness of Tuballoy

Fig. 210

[redacted]

[redacted]

e_{2024} vs E for Various Combinations of m_s, θ, and V_s

m_s = 300 grains θ = 60 degrees V_s = 3000 fps

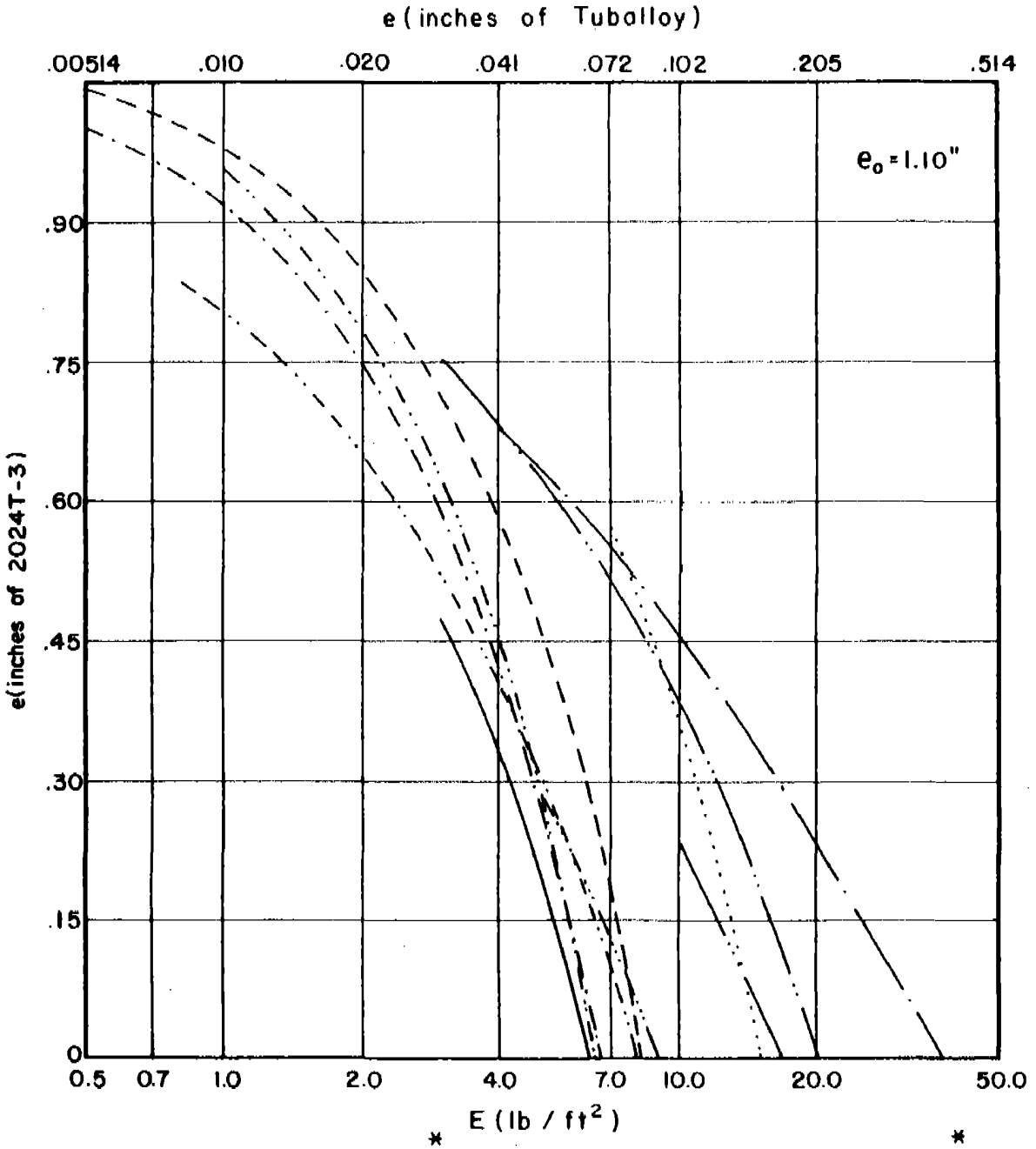

		*			*
Magnesium	— — — —	10.58	F.H. Steel	—··—··—	2.41
2024 T-3	—·—·—	6.65	Hard Steel	———	2.41
Titanium	—··—··—	4.17	Copper	—··—	2.10
Cast Iron	·····	2.59	Lead	—·—·—	1.70
Mild Steel	— —··— —	2.41	Tuballoy	—···—	1.00

*Ratio of Material Thickness Relative to a Unit Thickness of Tuballoy

Fig. 211

[redacted]

[redacted]

e_{2024} vs E for Various Combinations of m_s, θ, and V_s

$m_s = 30$ grains $\theta = 70$ degrees $V_s = 3000$ fps

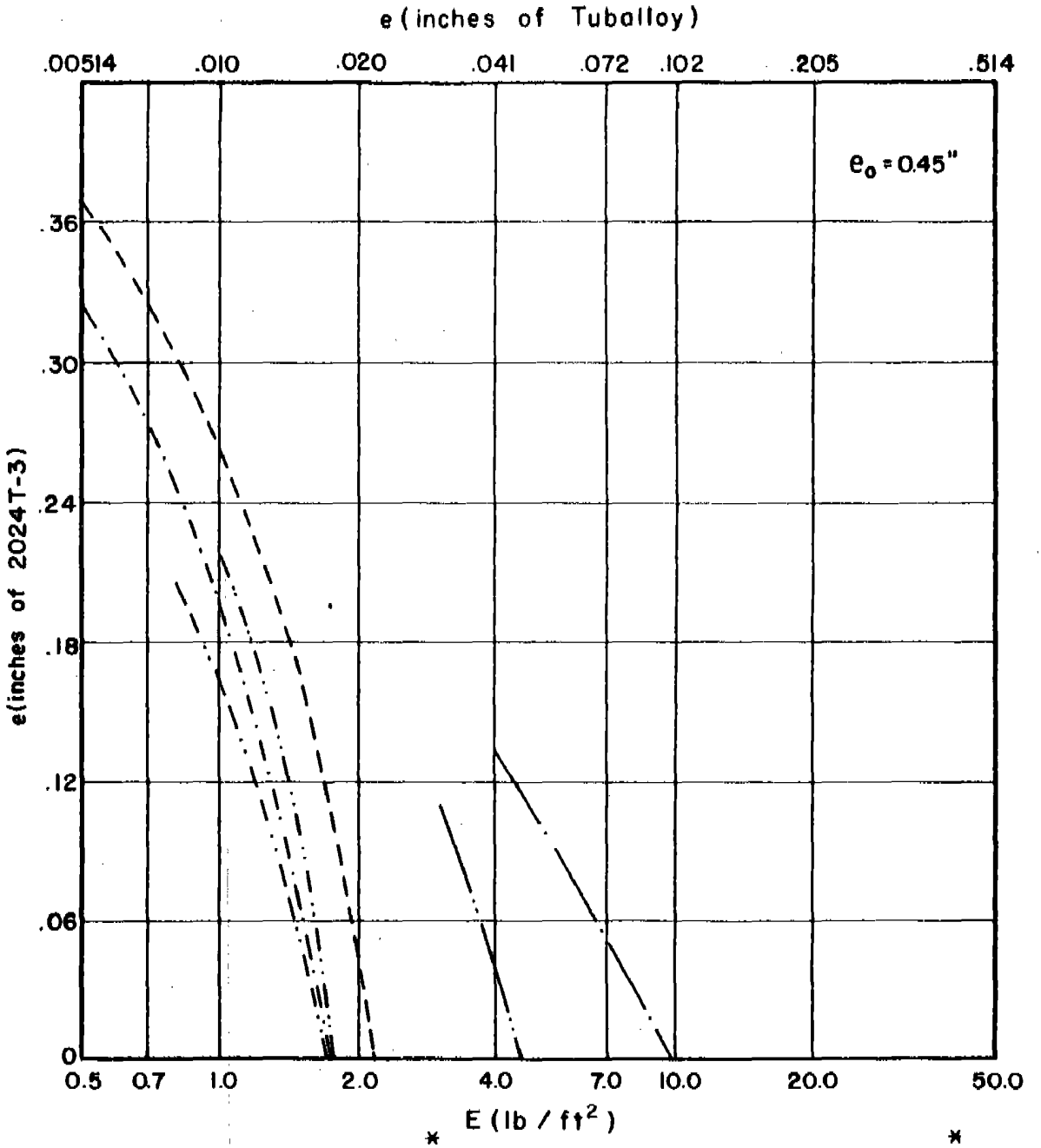

		*			*
Magnesium	— — — —	10.58	F. H. Steel	—··—··—	2.41
2024 T-3	—·—·—	6.65	Hard Steel	———	2.41
Titanium	—··—··—	4.17	Copper	—···—	2.10
Cast Iron	·····	2.59	Lead	—·—	1.70
Mild Steel	— —··— —	2.41	Tuballoy	—··—	1.00

*Ratio of Material Thickness Relative to a Unit Thickness of Tuballoy

Fig. 212

[redacted]

[redacted]

e_{2024} vs E for Various Combinations of m_s, θ, and V_s

m_s = 100 grains θ = 70 degrees V_s = 3000 fps

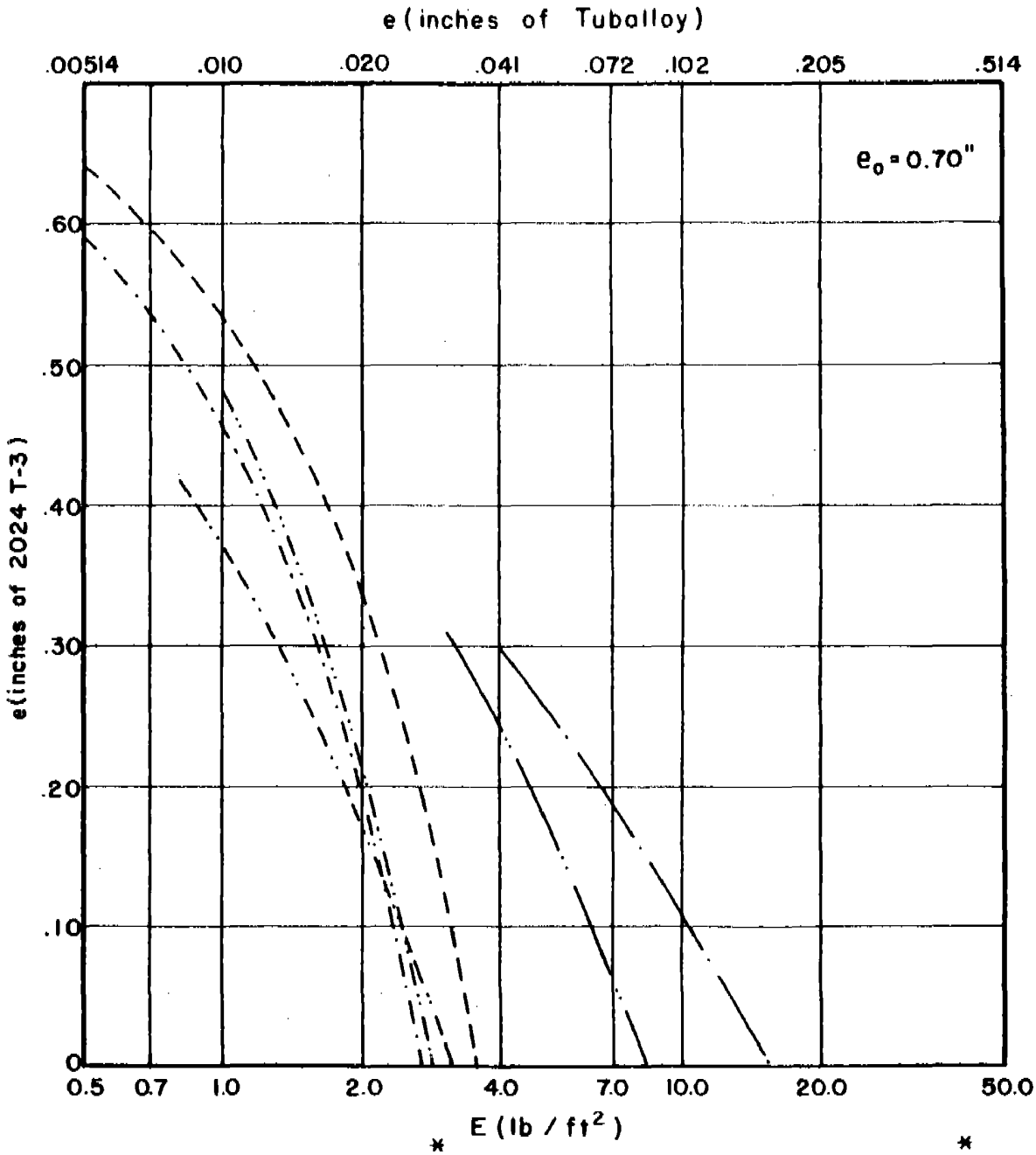

		*			*
Magnesium	— — — — —	10.58	F. H. Steel	—··—··—	2.41
2024 T-3	—·—·—·—	6.65	Hard Steel	————	2.41
Titanium	—··—··—	4.17	Copper	—— · ——	2.10
Cast Iron	·····	2.59	Lead	—— · ——	1.70
Mild Steel	— —··— —	2.41	Tuballoy	——··——	1.00

*Ratio of Material Thickness Relative to a Unit Thickness of Tuballoy

Fig. 213

[redacted]

[redacted]

e_{2024} vs E for Various Combinations of m_s, θ, and V_s

m_s = 300 grains θ = 70 degrees V_s = 3000 fps

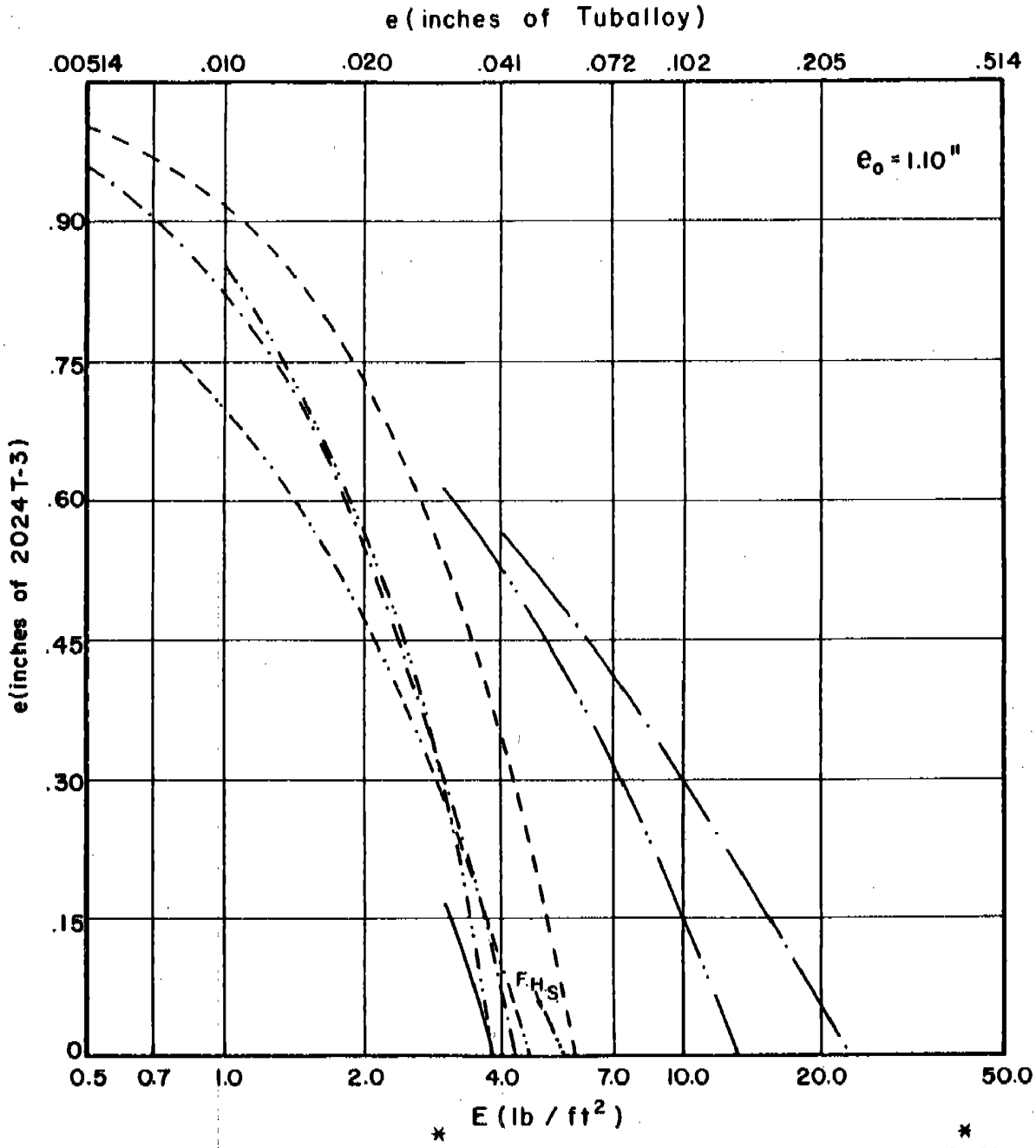

		*			*
Magnesium	— — — —	10.58	F. H. Steel	—··—··—	2.41
2024 T-3	—·—·—	6.65	Hard Steel	———	2.41
Titanium	—··—··—	4.17	Copper	—··—	2.10
Cast Iron	·····	2.59	Lead	—·—	1.70
Mild Steel	— —··— —	2.41	Tuballoy	—··—	1.00

*Ratio of Material Thickness Relative to a Unit Thickness of Tuballoy

Fig. 214

[redacted]

[redacted]

e_{2024} vs E for Various Combinations of m_s, θ, and V_s

$m_s = 30$ grains $\theta = 0$ degrees $V_s = 6000$ fps

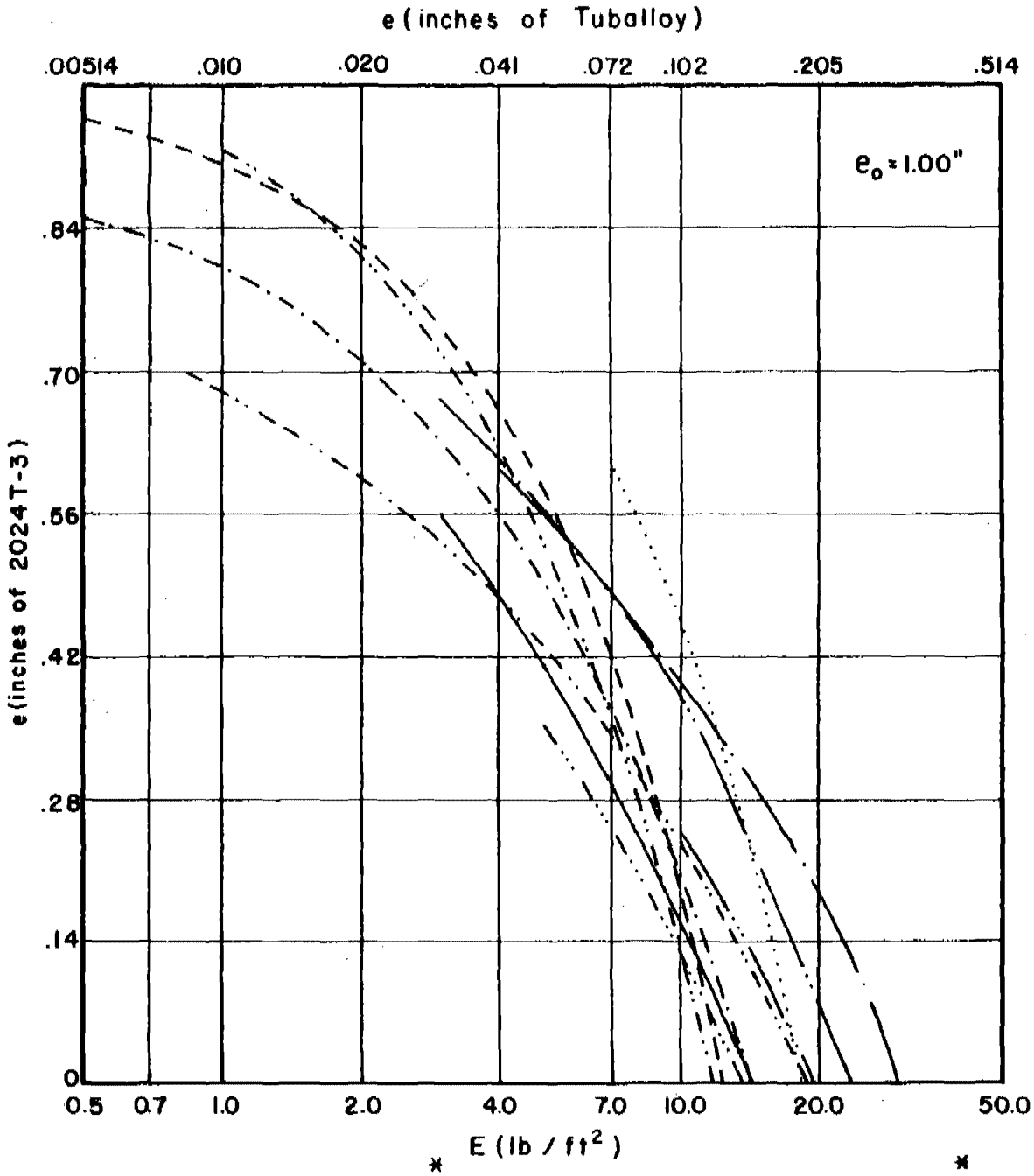

		*			*
Magnesium	------	10.58	F.H. Steel	—··—··—	2.41
2024 T-3	—·—·—	6.65	Hard Steel	———	2.41
Titanium	—··—··—	4.17	Copper	—··—	2.10
Cast Iron	·····	2.59	Lead	—·—	1.70
Mild Steel	—··—	2.41	Tuballoy	—··—	1.00

*Ratio of Material Thickness Relative to a Unit Thickness of Tuballoy

Fig. 215

[redacted]

e_{2024} vs E for Various Combinations of m_s, θ, and V_s

m_s = 100 grains θ = 0 degrees V_s = 6000 fps

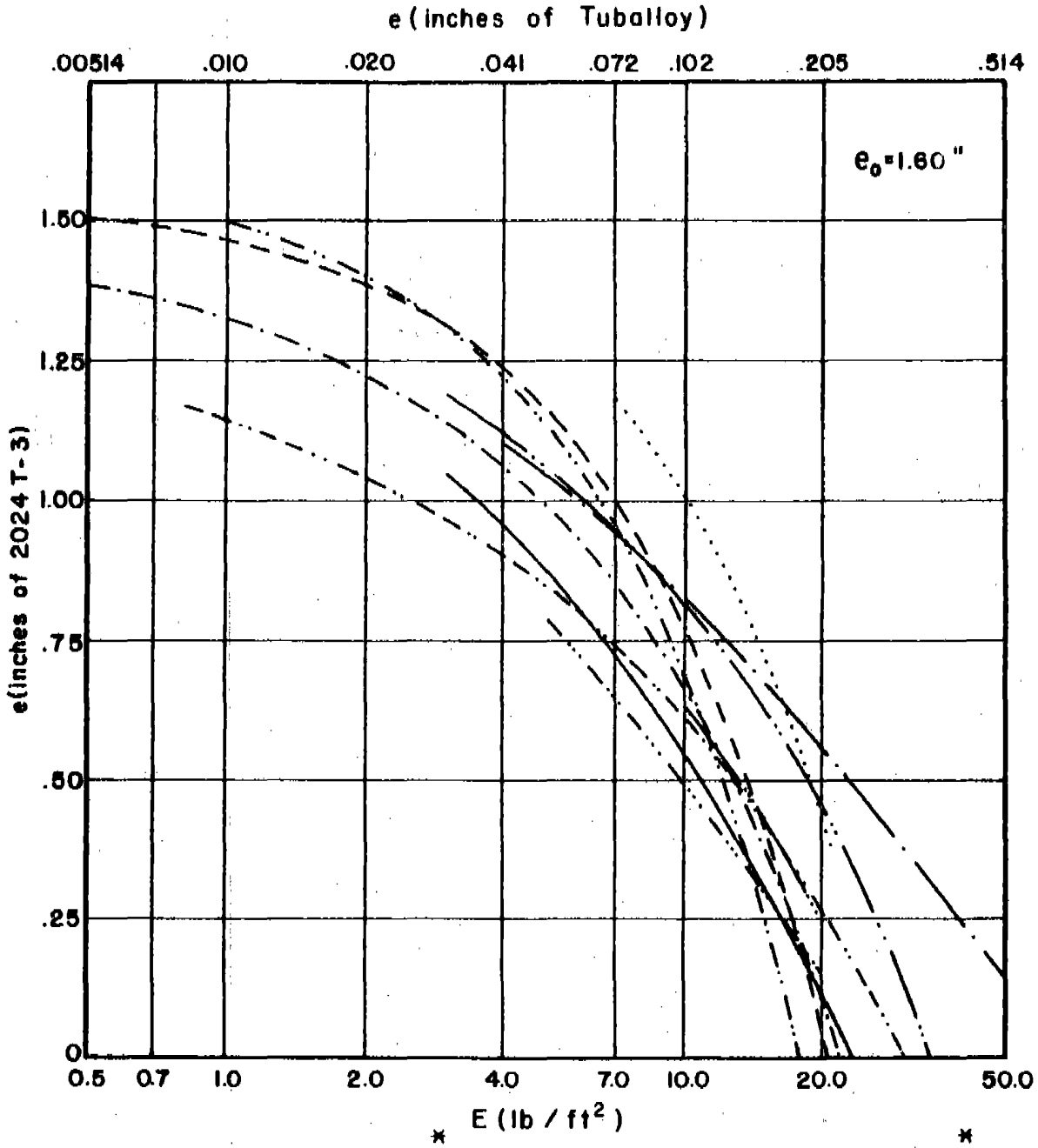

		*			*
Magnesium	— — — —	10.58	F.H. Steel	—··—··—	2.41
2024 T-3	—·—·—	6.65	Hard Steel	———	2.41
Titanium	—··—··—	4.17	Copper	—··—	2.10
Cast Iron	·····	2.59	Lead	—·—	1.70
Mild Steel	— —·· —	2.41	Tuballoy	—···—	1.00

*Ratio of Material Thickness Relative to a Unit Thickness of Tuballoy

Fig. 216

e_{2024} vs E for Various Combinations of m_s, θ, and V_s

m_s = 300 grains θ = 0 degrees V_s = 6000 fps

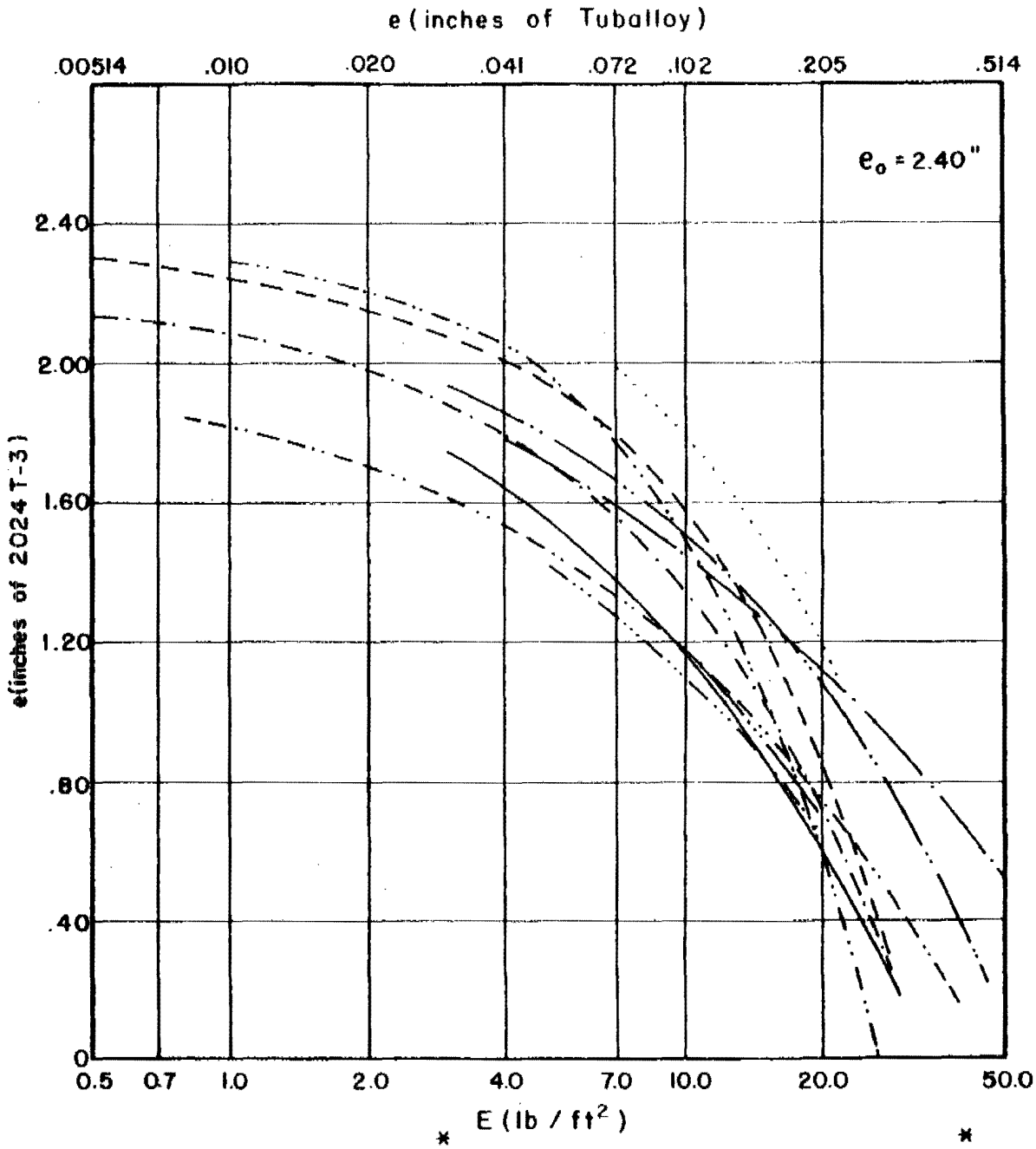

		*			*
Magnesium	— — — — —	10.58	F.H. Steel	—·—·—	2.41
2024 T-3	—·—·—·—	6.65	Hard Steel	———	2.41
Titanium	—··—··—	4.17	Copper	—··—	2.10
Cast Iron	·····	2.59	Lead	—·—	1.70
Mild Steel	—··—··—	2.41	Tuballoy	—··—	1.00

*Ratio of Material Thickness Relative to a Unit Thickness of Tuballoy

Fig. 217

e_{2024} vs E for Various Combinations of m_s, θ, and V_s

$m_s = 30$ grains $\theta = 60$ degrees $V_s = 6000$ fps

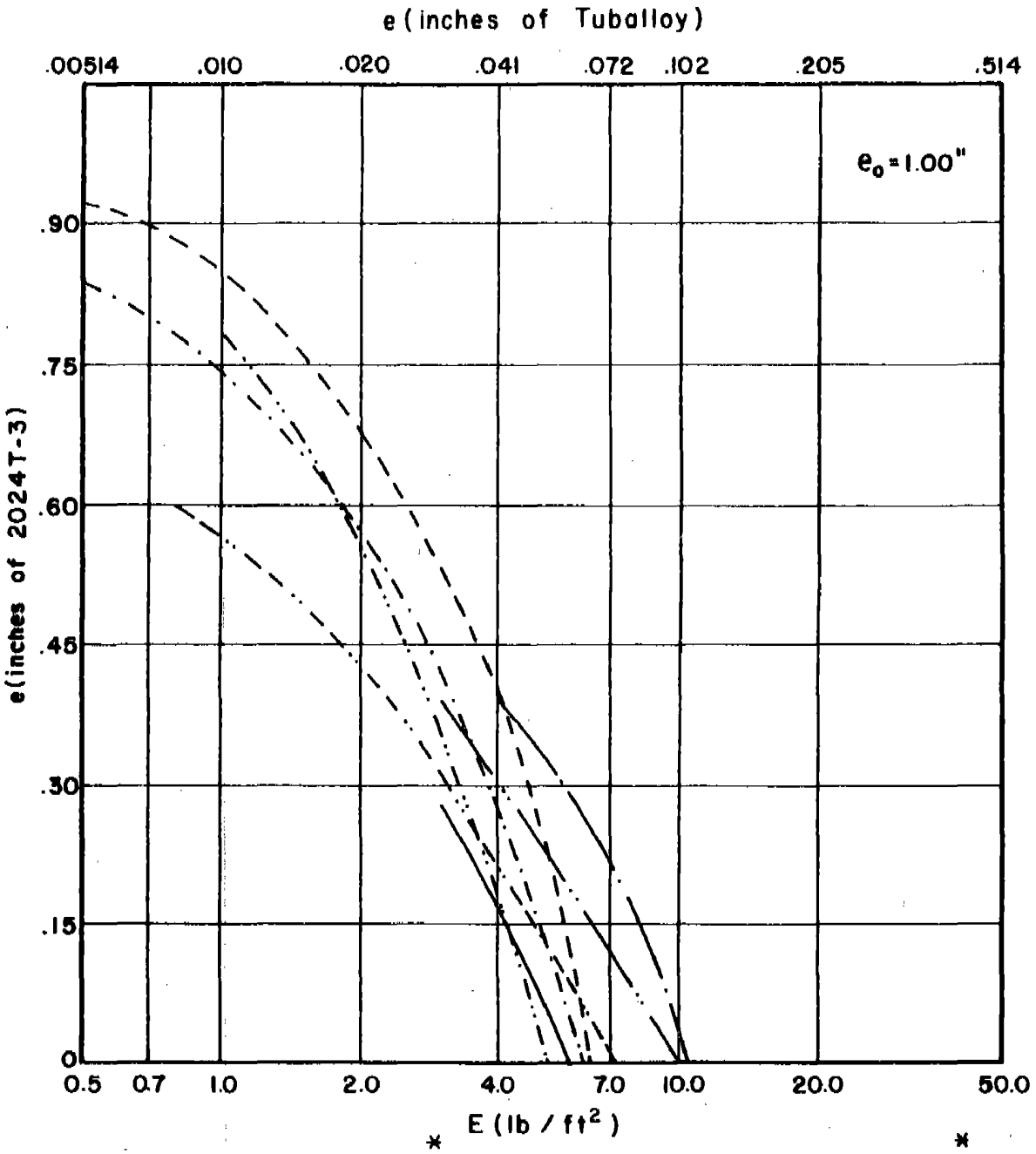

		*			*
Magnesium	— — — —	10.58	F.H. Steel	—··—··—	2.41
2024 T-3	—·—·—	6.65	Hard Steel	———	2.41
Titanium	—··—··—	4.17	Copper	—··—	2.10
Cast Iron	·····	2.59	Lead	—·—	1.70
Mild Steel	— —··— —	2.41	Tuballoy	—··—	1.00

*Ratio of Material Thickness Relative to a Unit Thickness of Tuballoy

Fig. 218

[redacted]

e_{2024} vs E for Various Combinations of m_s, θ, and V_s

m_s = 100 grains θ = 60 degrees V_s = 6000 fps

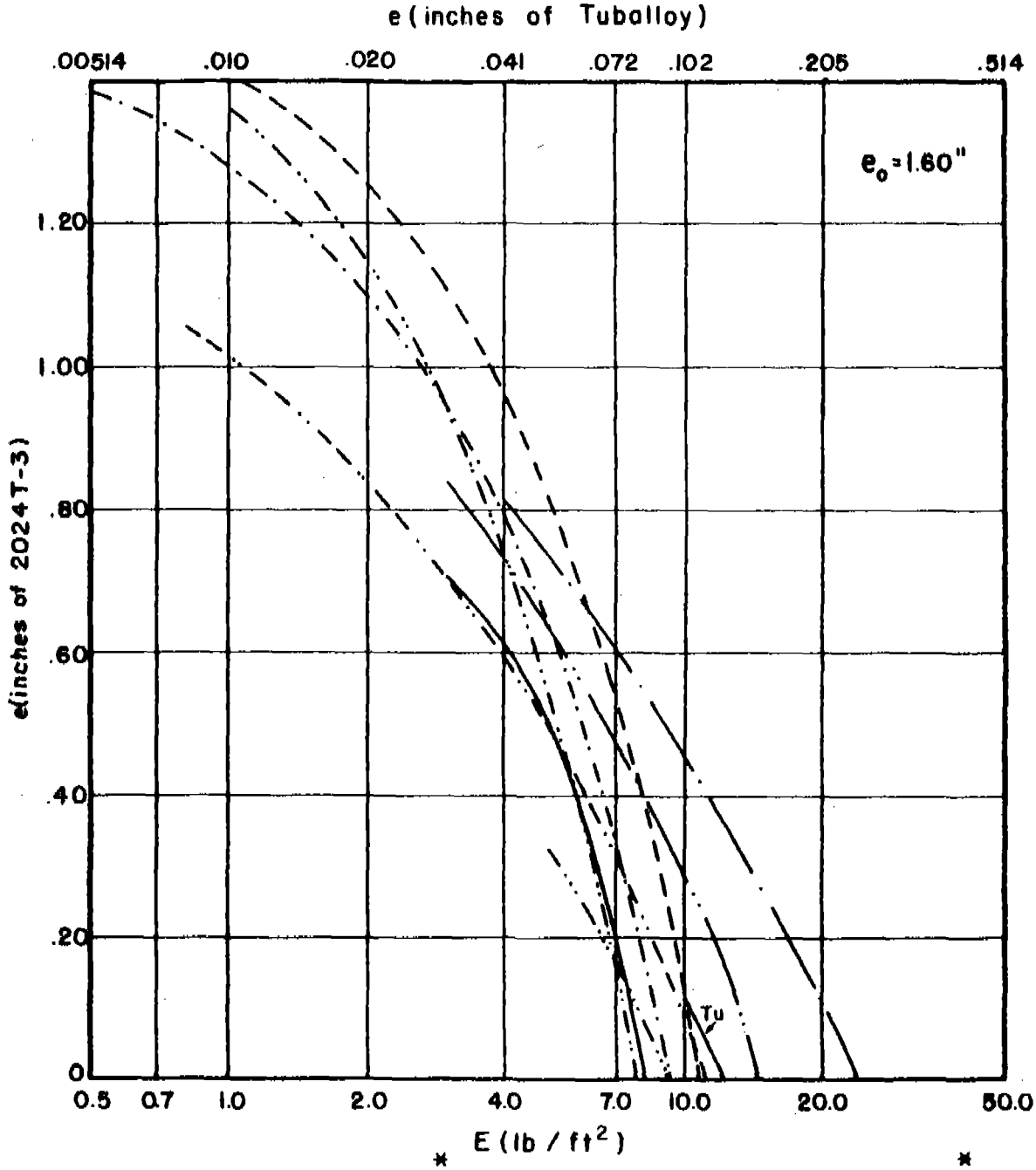

		*			*
Magnesium	— — — —	10.58	F. H. Steel	—··—··—	2.41
2024 T-3	—·—·—	6.65	Hard Steel	———	2.41
Titanium	—··—··—	4.17	Copper	—··—	2.10
Cast Iron	·····	2.59	Lead	—·—	1.70
Mild Steel	— —··— —	2.41	Tuballoy	—···—	1.00

*Ratio of Material Thickness Relative to a Unit Thickness of Tuballoy

Fig. 219

[redacted]

[redacted]

e_{2024} vs E for Various Combinations of m_s, θ, and V_s

m_s = 300 grains θ = 60 degrees V_s = 6000 fps

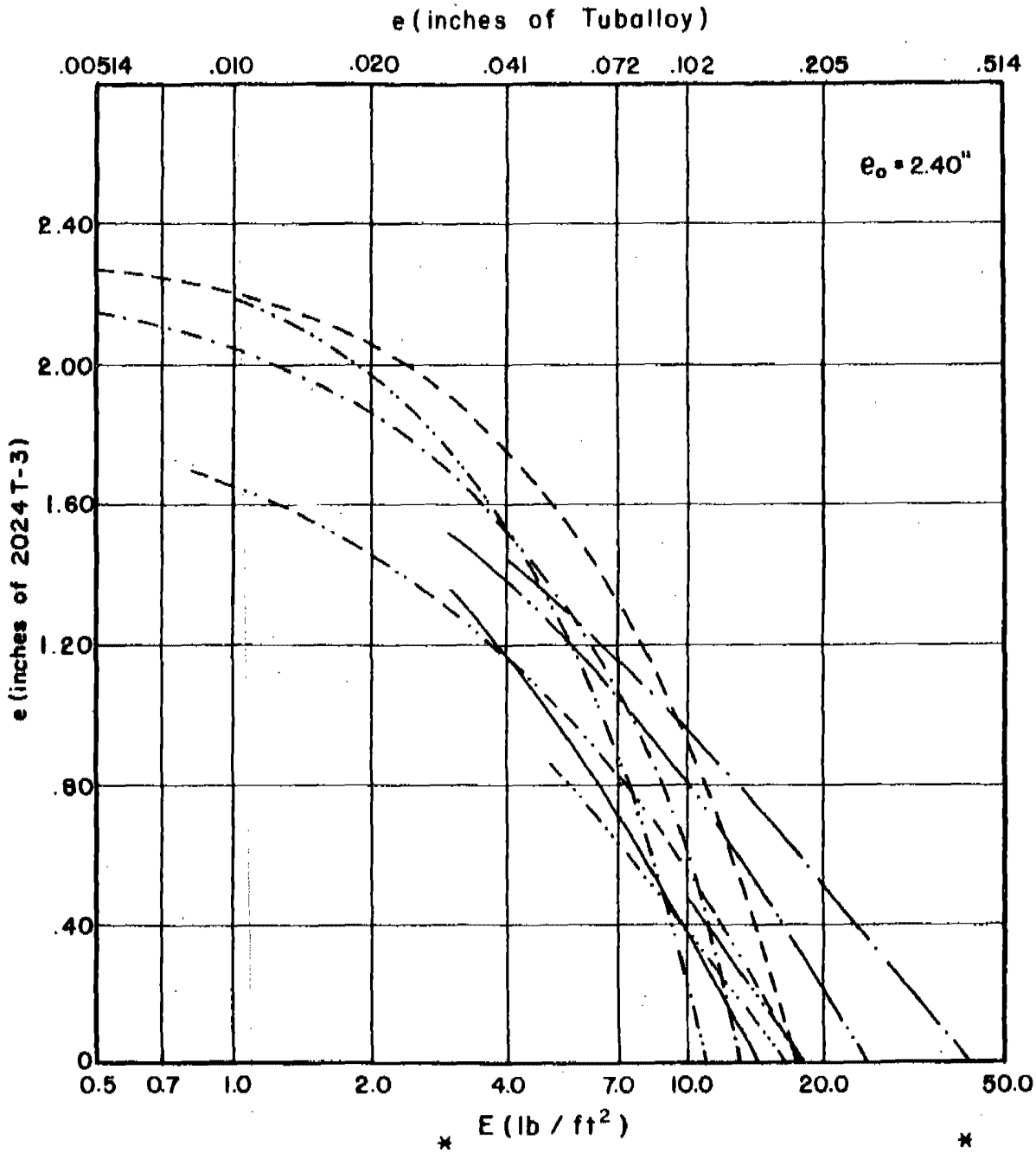

		*			*
Magnesium	———	10.58	F. H. Steel	—··—··—	2.41
2024 T-3	—·—·—	6.65	Hard Steel	———	2.41
Titanium	—··—··—	4.17	Copper	—··—	2.10
Cast Iron	·····	2.59	Lead	—·—	1.70
Mild Steel	—··—	2.41	Tuballoy	—··—	1.00

*Ratio of Material Thickness Relative to a Unit Thickness of Tuballoy

Fig. 220

[redacted]

[redacted]

e_{2024} vs E for Various Combinations of m_s, θ, and V_s

$m_s = 30$ grains $\theta = 70$ degrees $V_s = 6000$ fps

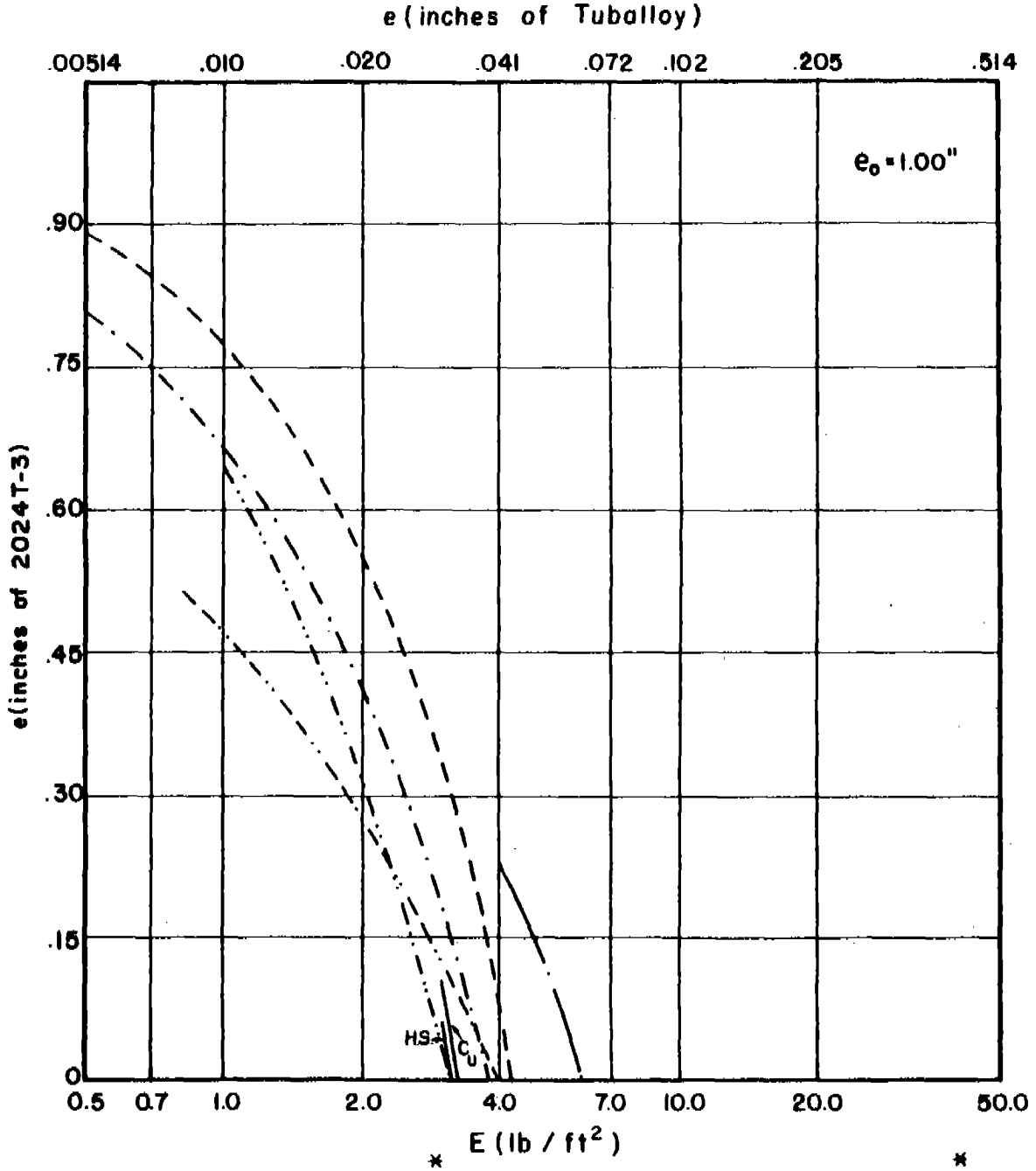

		*			*
Magnesium	— — — —	10.58	F.H. Steel	—··—··—	2.41
2024 T-3	—·—·—	6.65	Hard Steel	———	2.41
Titanium	—··—··—	4.17	Copper	—··—	2.10
Cast Iron	·····	2.59	Lead	—·—	1.70
Mild Steel	—··— —	2.41	Tuballoy	—···—	1.00

*Ratio of Material Thickness Relative to a Unit Thickness of Tuballoy

Fig. 221

[redacted]

[redacted]

e_{2024} vs E for Various Combinations of m_s, θ, and V_s

m_s = 100 grains θ = 70 degrees V_s = 6000 fps

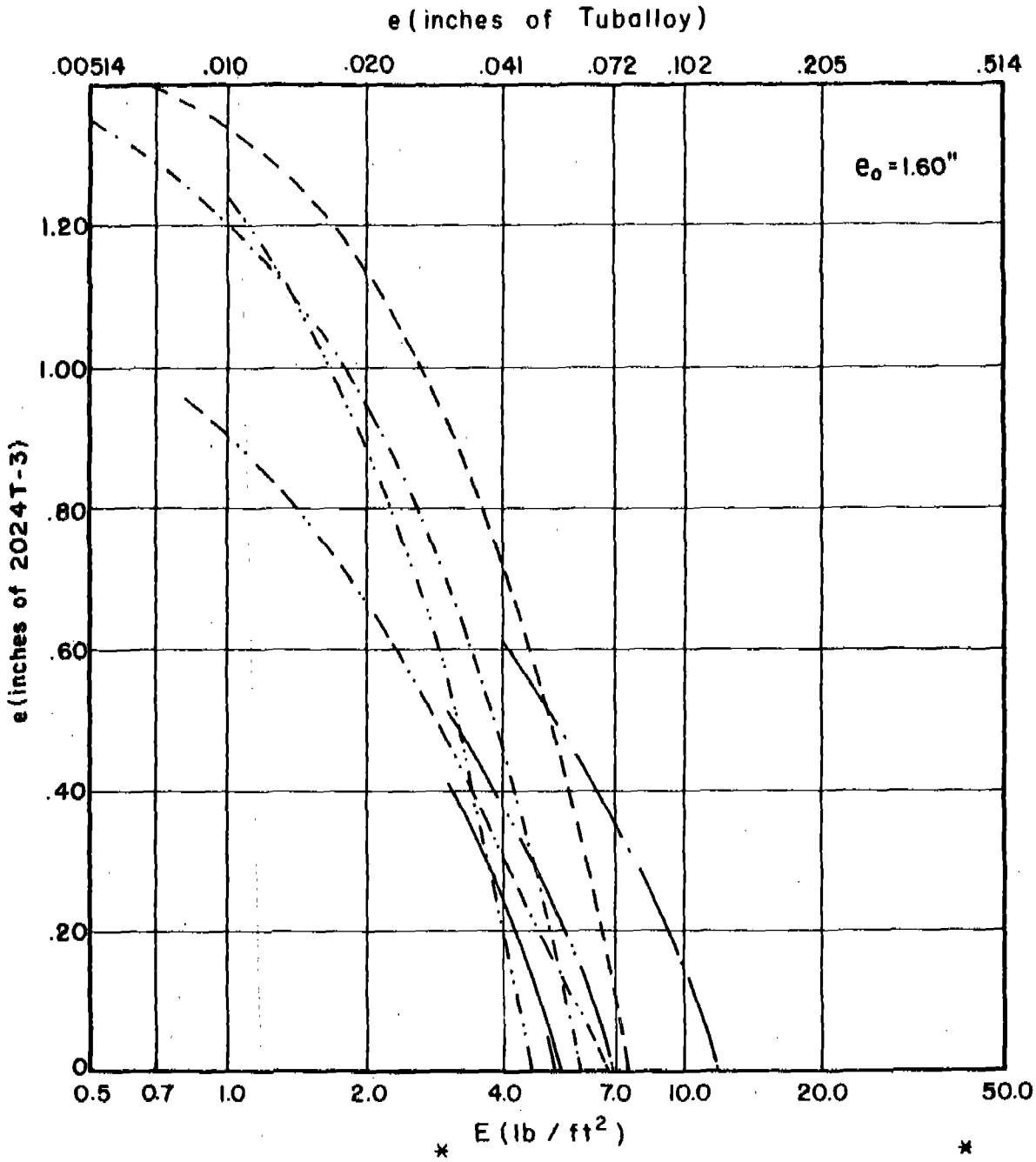

		*			*
Magnesium	— — — —	10.58	F.H. Steel	—·—·—	2.41
2024 T-3	—·—·—	6.65	Hard Steel	———	2.41
Titanium	—··—··—	4.17	Copper	—··—	2.10
Cast Iron	·····	2.59	Lead	—·—	1.70
Mild Steel	—··—	2.41	Tuballoy	—····—	1.00

*Ratio of Material Thickness Relative to a Unit Thickness of Tuballoy

Fig. 222

[redacted]

[redacted]

e_{2024} vs E for Various Combinations of m_s, θ, and V_s

m_s = 300 grains θ = 70 degrees V_s = 6000 fps

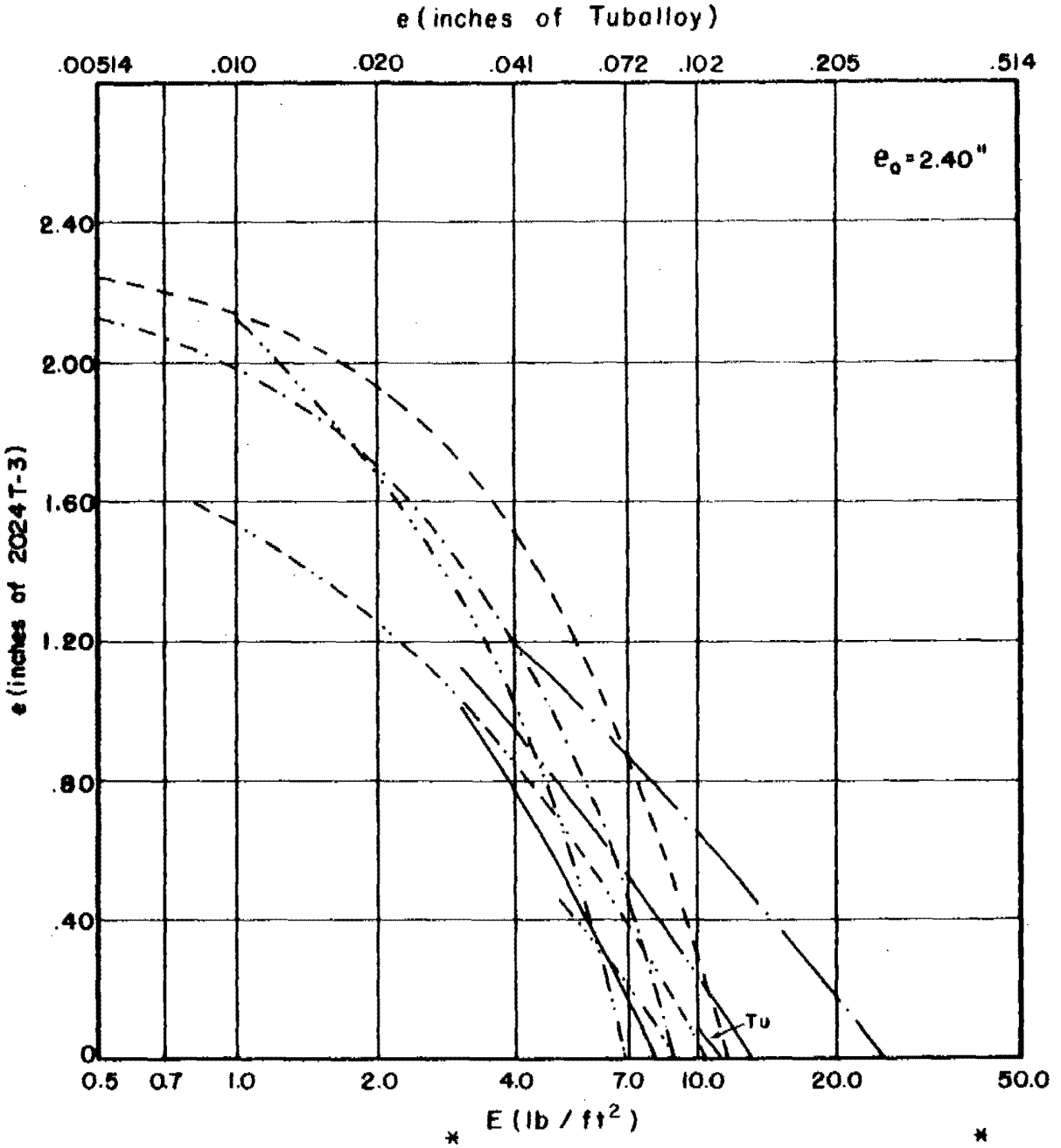

		*			*
Magnesium	— — — —	10.58	F. H. Steel	—·· —··	2.41
2024 T-3	—·—·—	6.65	Hard Steel	———	2.41
Titanium	—··—··—	4.17	Copper	—··—	2.10
Cast Iron	·····	2.59	Lead	—·—	1.70
Mild Steel	— —··— —	2.41	Tuballoy	—··—	1.00

*Ratio of Material Thickness Relative to a Unit Thickness of Tuballoy

Fig. 223

[redacted]

[redacted]

e_{2024} vs E for Various Combinations of m_s, θ, and V_s

m_s = 30 grains θ = 0 degrees V_s = 9000 fps

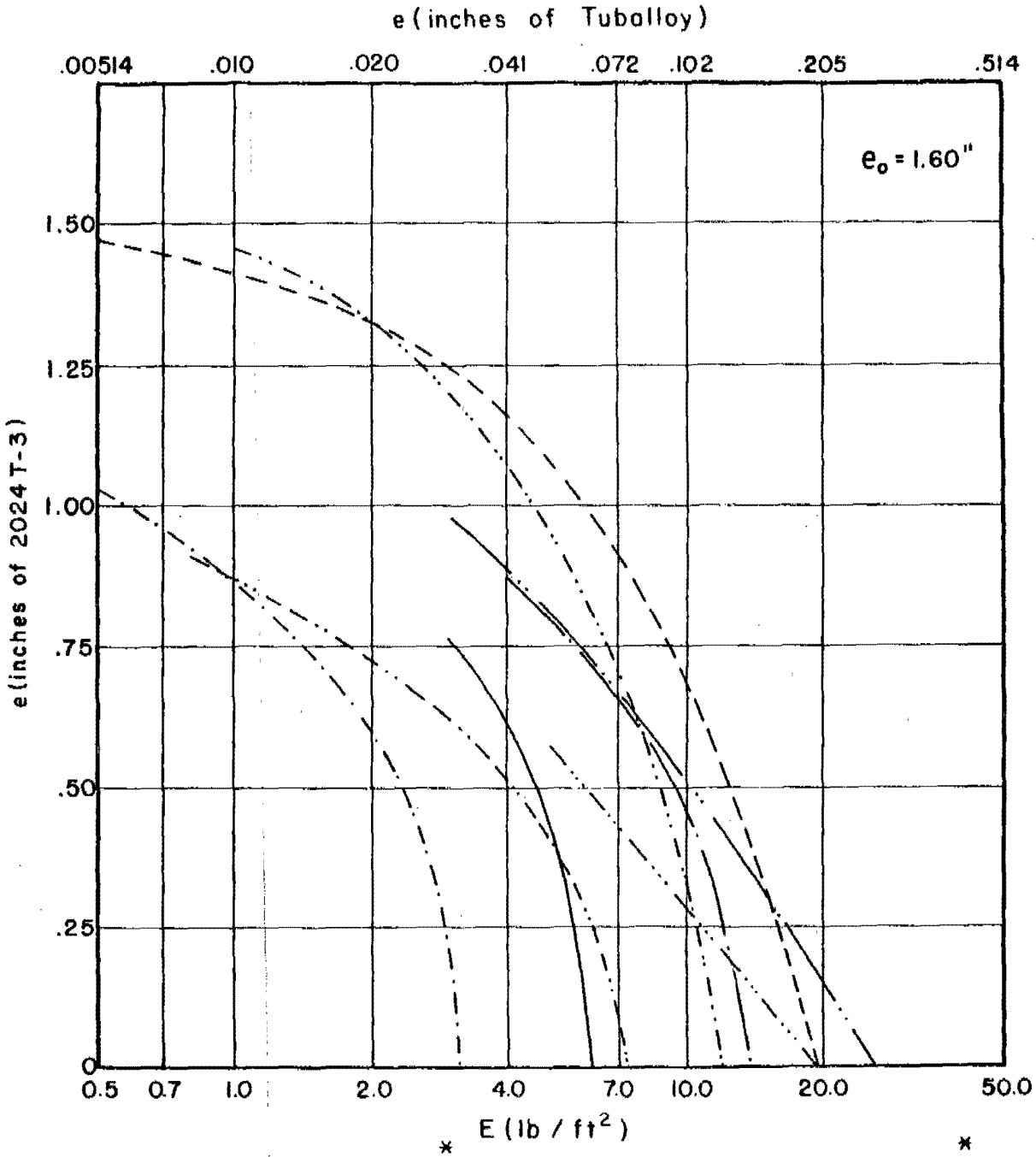

		*			*
Magnesium	— — — —	10.58	F. H. Steel	—··—··—	2.41
2024 T-3	—·—·—	6.65	Hard Steel	———	2.41
Titanium	—··—··—	4.17	Copper	—··—	2.10
Cast Iron	·····	2.59	Lead	—·—	1.70
Mild Steel	— —··— —	2.41	Tuballoy	—···—	1.00

*Ratio of Material Thickness Relative to a Unit Thickness of Tuballoy

Fig. 224

[redacted]

[redacted]

e_{2024} vs E for Various Combinations of m_s, θ, and V_s

m_s = 100 grains θ = 0 degrees V_s = 9000 fps

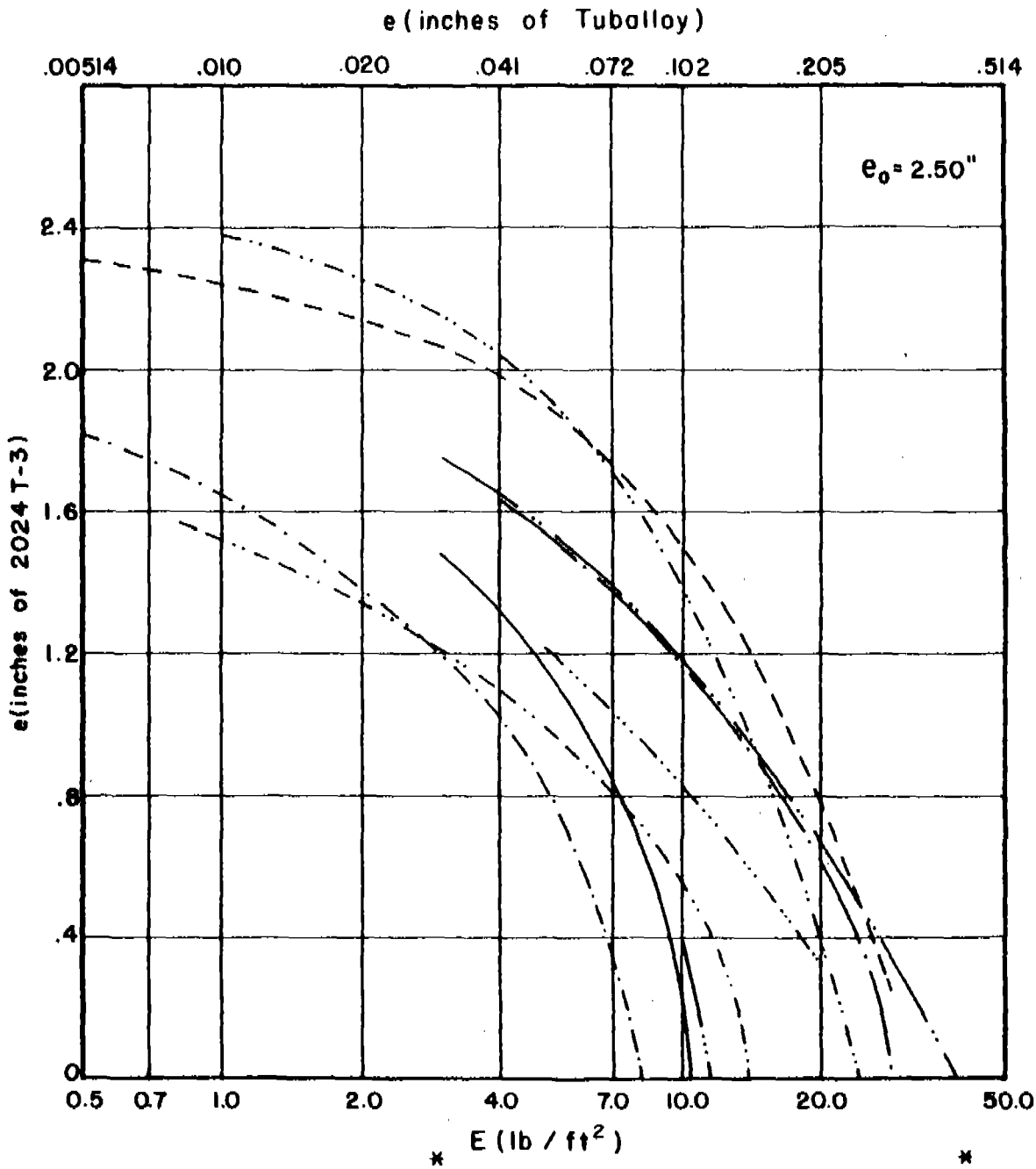

		*			*
Magnesium	— — — —	10.58	F.H. Steel	—·····—·····—	2.41
2024 T-3	—·—·—·—	6.65	Hard Steel	————	2.41
Titanium	—··—··—	4.17	Copper	—··—··—	2.10
Cast Iron	·····	2.59	Lead	—·—·—	1.70
Mild Steel	— —··— —	2.41	Tuballoy	—···—	1.00

*Ratio of Material Thickness Relative to a Unit Thickness of Tuballoy

Fig. 225

[redacted]

[redacted]

e_{2024} vs E for Various Combinations of m_s, θ, and V_s

m_s = 300 grains θ = 0 degrees V_s = 9000 fps

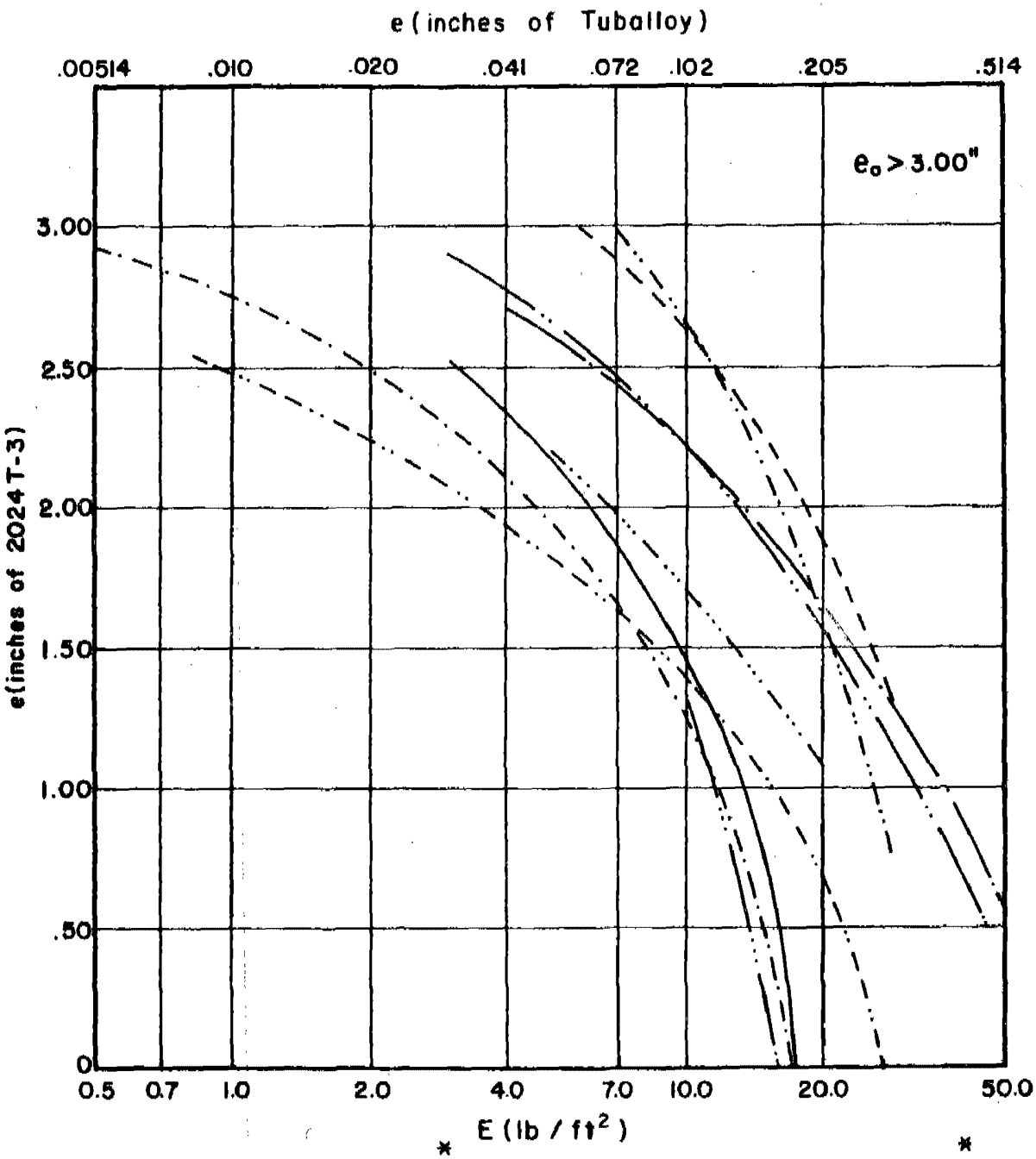

		*			*
Magnesium	— — — — —	10.58	F. H. Steel	—··—··—	2.41
2024 T-3	—·—·—·—	6.65	Hard Steel	————	2.41
Titanium	—··—··—··	4.17	Copper	—··—	2.10
Cast Iron	·····	2.59	Lead	—·—	1.70
Mild Steel	— —··— —	2.41	Tuballoy	—··—	1.00

*Ratio of Material Thickness Relative to a Unit Thickness of Tuballoy

Fig. 226

[redacted]

[redacted]

e_{2024} vs E for Various Combinations of m_s, θ, and V_s

$m_s = 30$ grains $\theta = 60$ degrees $V_s = 9000$ fps

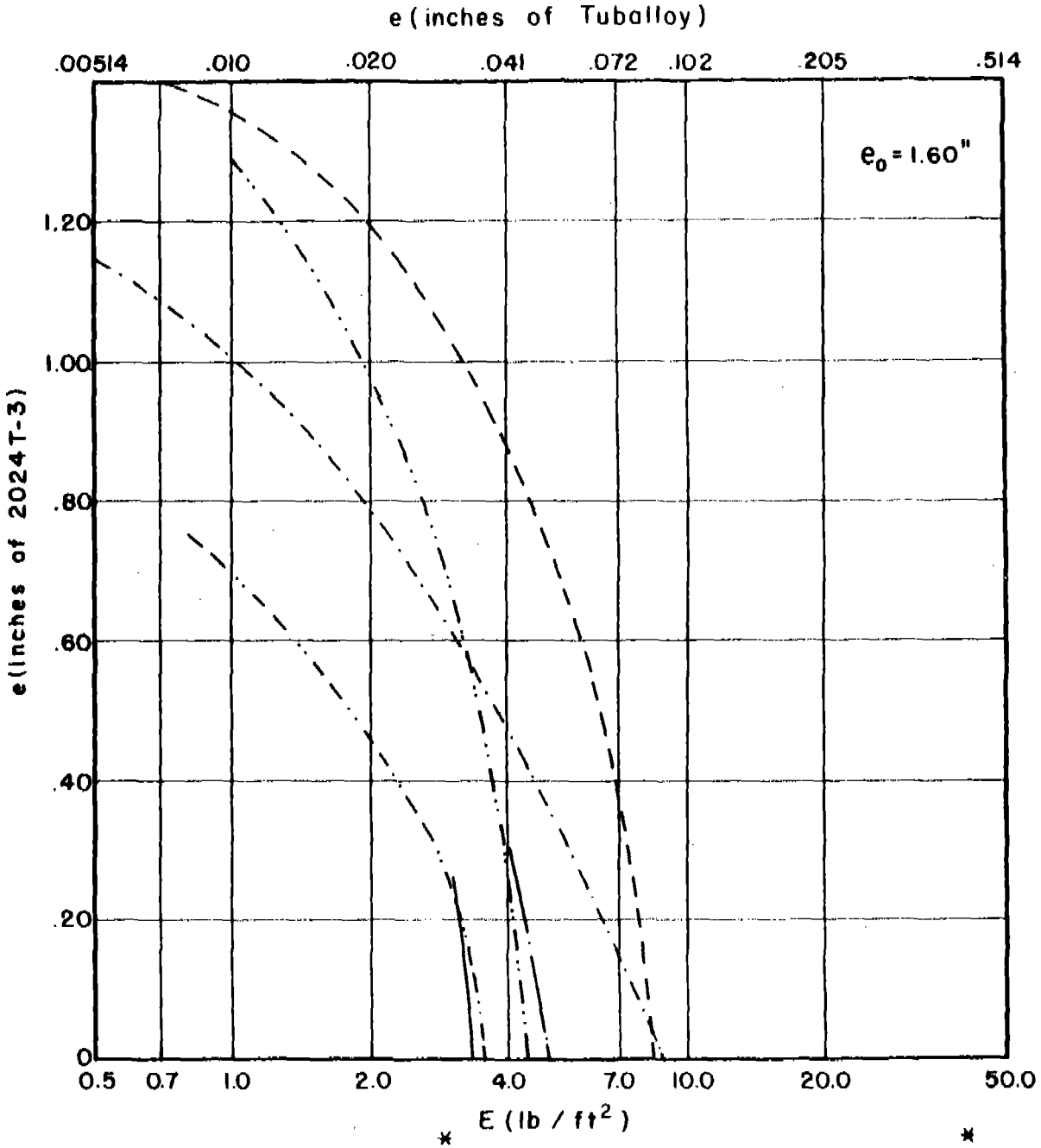

		*			*
Magnesium	------	10.58	F.H. Steel	-·-·-·-	2.41
2024 T-3	-·-·-·-	6.65	Hard Steel	———	2.41
Titanium	-··-··-	4.17	Copper	—··—	2.10
Cast Iron	·····	2.59	Lead	—·—	1.70
Mild Steel	--··--	2.41	Tuballoy	—··—	1.00

*Ratio of Material Thickness Relative to a Unit Thickness of Tuballoy

Fig. 227

[redacted]

[redacted]

e_{2024} vs E for Various Combinations of m_s, θ, and V_s

m_s = 100 grains θ = 60 degrees V_s = 9000 fps

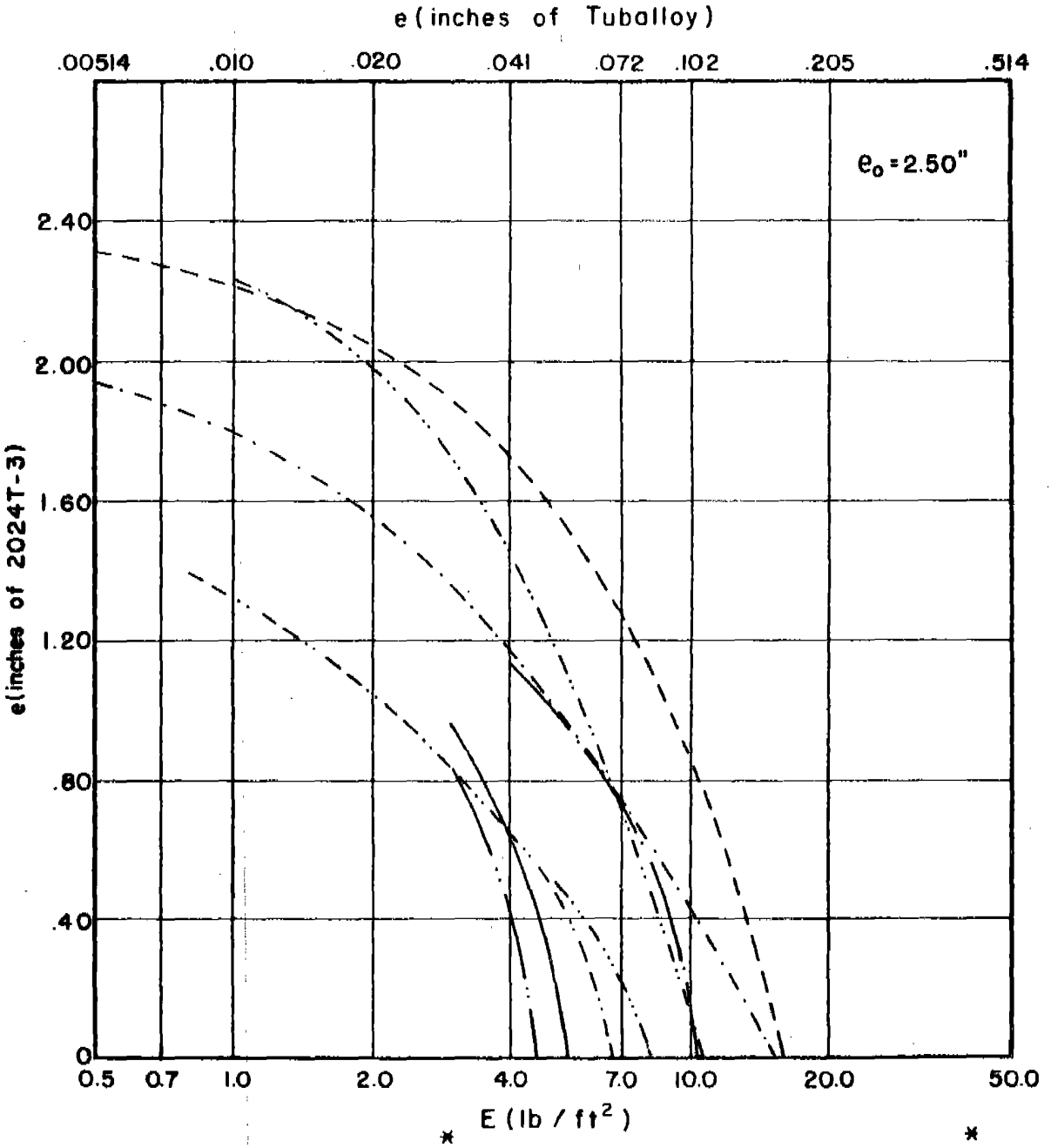

		*			*
Magnesium	— — —	10.58	F.H. Steel	—··—	2.41
2024 T-3	—·—·—	6.65	Hard Steel	———	2.41
Titanium	—··—··—	4.17	Copper	—··—	2.10
Cast Iron	·····	2.59	Lead	—·—	1.70
Mild Steel	— —··— —	2.41	Tuballoy	—··—	1.00

*Ratio of Material Thickness Relative to a Unit Thickness of Tuballoy

Fig. 228

[redacted]

[redacted]

e_{2024} vs E for Various Combinations of m_s, θ, and V_s

m_s = 300 grains θ = 60 degrees V_s = 9000 fps

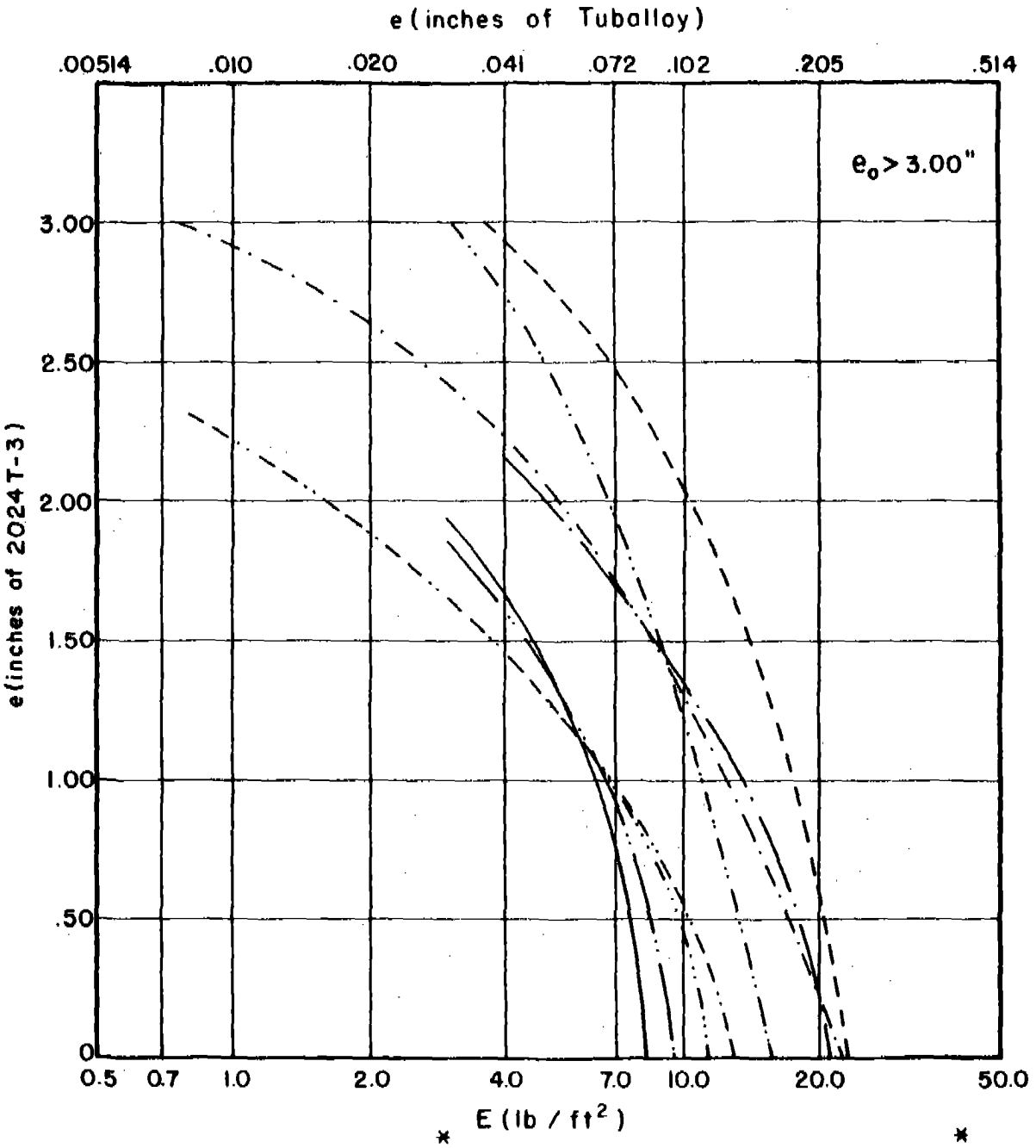

		*			*
Magnesium	— — — —	10.58	F.H. Steel	—·—·—	2.41
2024 T-3	—·—·—	6.65	Hard Steel	———	2.41
Titanium	—··—··—	4.17	Copper	—··—	2.10
Cast Iron	·····	2.59	Lead	—·—	1.70
Mild Steel	— —··— —	2.41	Tuballoy	—···—	1.00

*Ratio of Material Thickness Relative to a Unit Thickness of Tuballoy

Fig. 229

[redacted]

[redacted]

e_{2024} vs E for Various Combinations of m_s, θ, and V_s

$m_s = 30$ grains $\theta = 70$ degrees $V_s = 9000$ fps

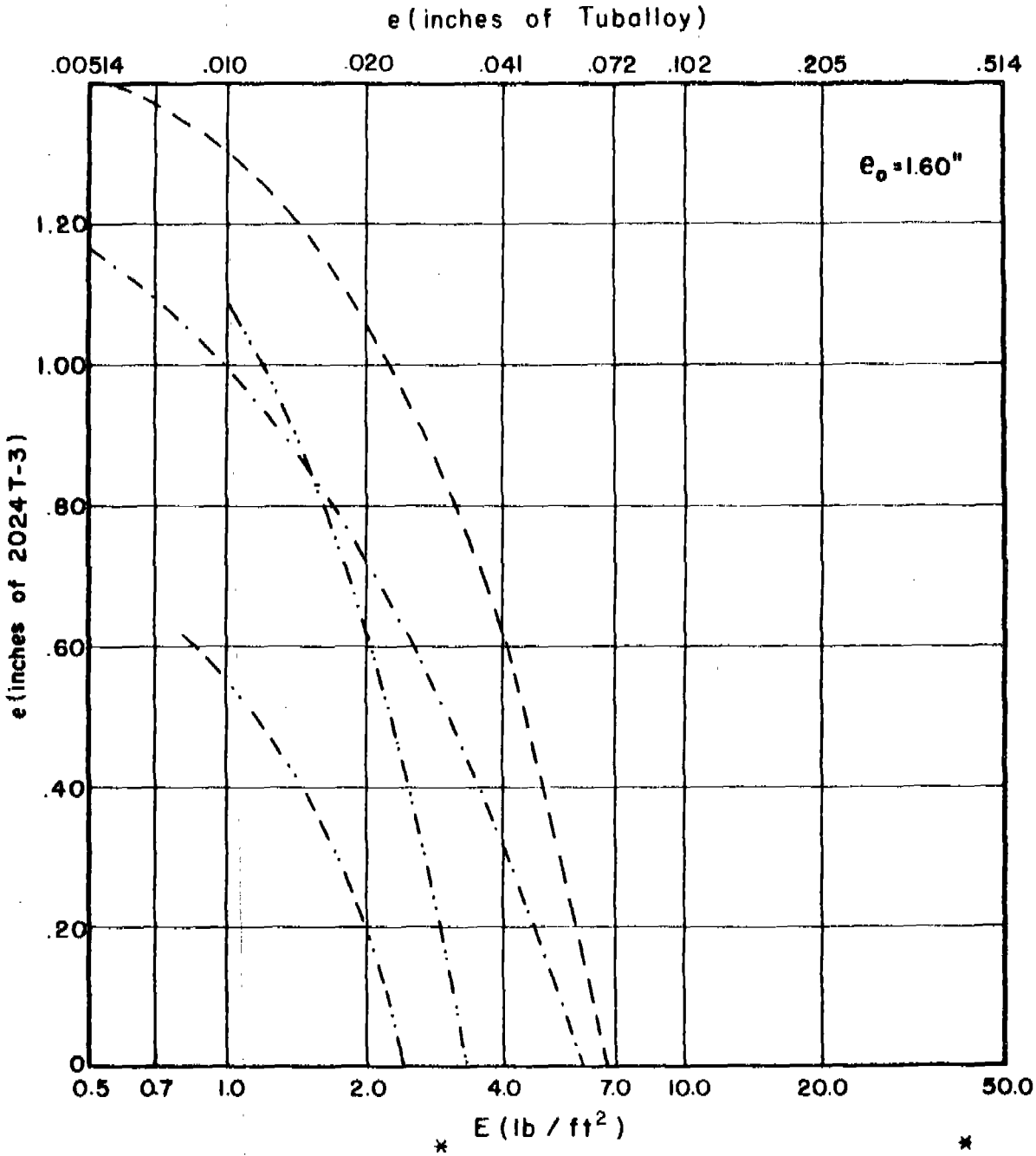

		*			*
Magnesium	— — — —	10.58	F. H. Steel	—·—·—	2.41
2024 T-3	—·—·—	6.65	Hard Steel	———	2.41
Titanium	—··—··—	4.17	Copper	—··—··—	2.10
Cast Iron	·····	2.59	Lead	—·—·—	1.70
Mild Steel	—··—··—	2.41	Tuballoy	—··—··—	1.00

*Ratio of Material Thickness Relative to a Unit Thickness of Tuballoy

Fig. 230

[redacted]

[redacted]

e_{2024} vs E for Various Combinations of m_s, θ, and V_s

m_s = 100 grains θ = 70 degrees V_s = 9000 fps

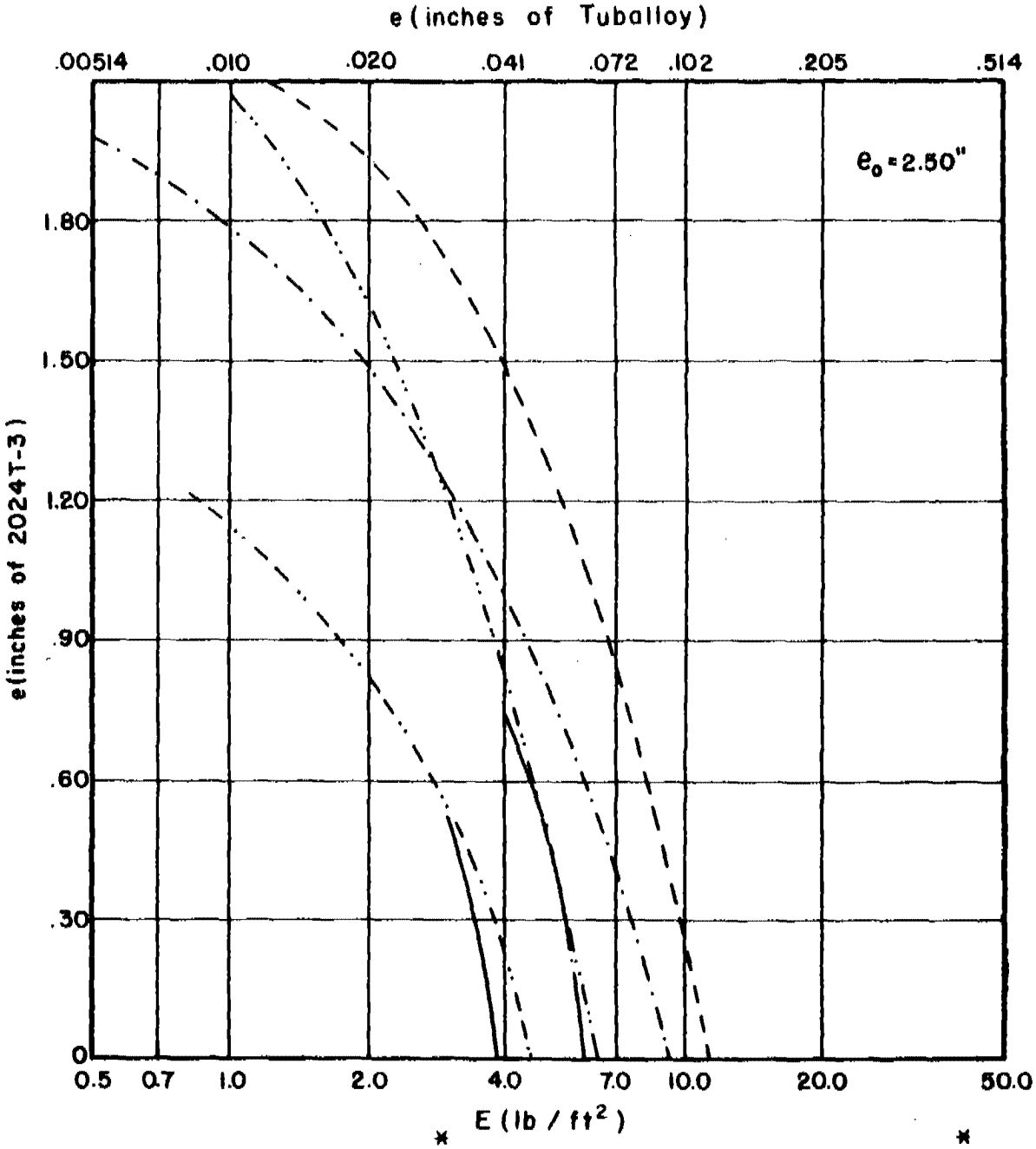

		*			*
Magnesium	— — — —	10.58	F.H. Steel	—··—··—	2.41
2024 T-3	—·—·—	6.65	Hard Steel	———	2.41
Titanium	—··—··—	4.17	Copper	—··—	2.10
Cast Iron	·····	2.59	Lead	—·—	1.70
Mild Steel	—··—	2.41	Tuballoy	—···—	1.00

*Ratio of Material Thickness Relative to a Unit Thickness of Tuballoy

Fig. 231

[redacted]

[redacted]

e_{2024} vs E for Various Combinations of m_s, θ, and V_s

m_s = 300 grains θ = 70 degrees V_s = 9000 fps

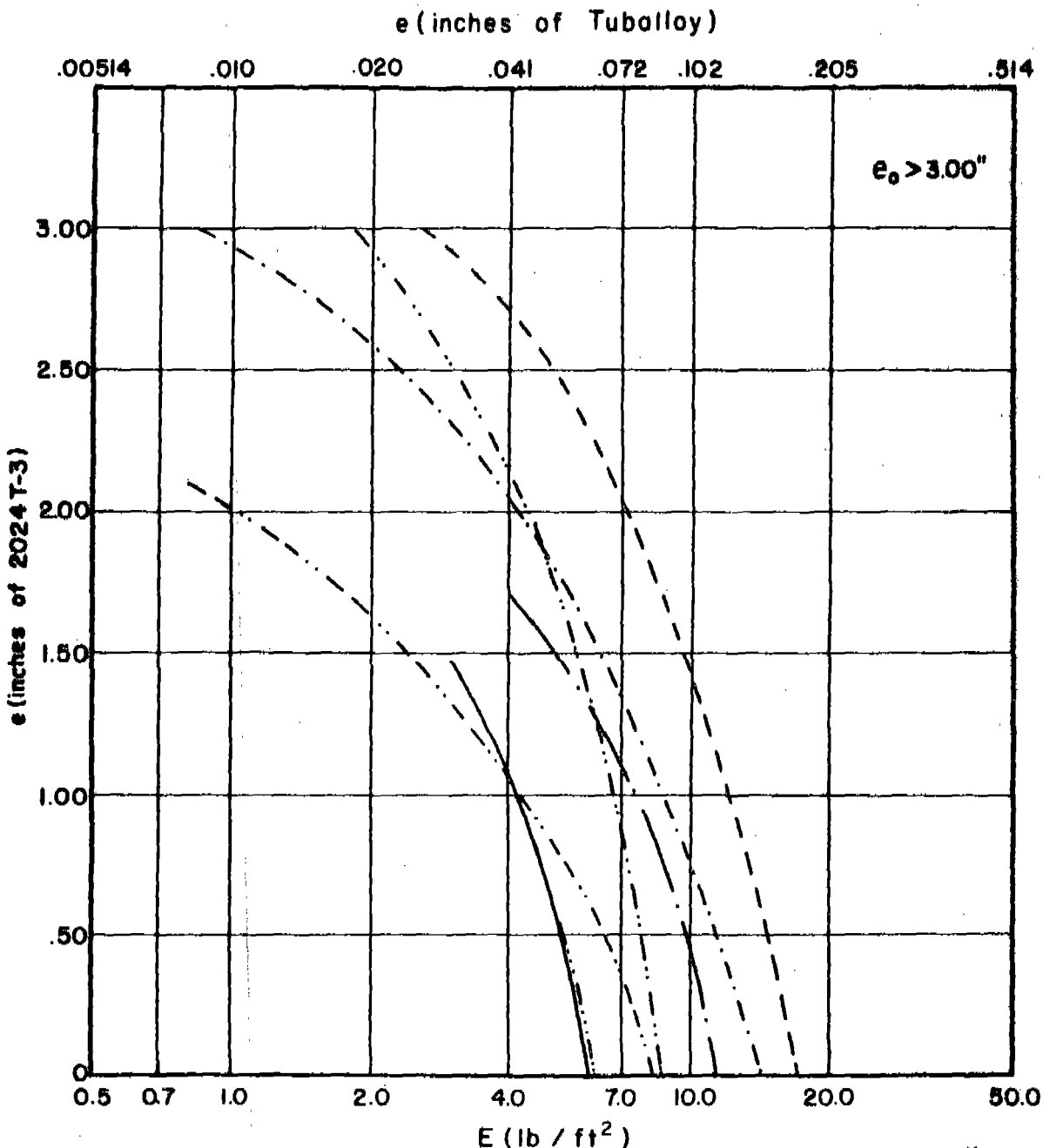

		*			*
Magnesium	— — — — —	10.58	F. H. Steel	—··—··—	2.41
2024 T-3	—·—·—·—	6.65	Hard Steel	————	2.41
Titanium	—··—··—	4.17	Copper	—·—·—	2.10
Cast Iron	·····	2.59	Lead	—·—·—	1.70
Mild Steel	— —··— —	2.41	Tuballoy	—··—··—	1.00

*Ratio of Material Thickness Relative to a Unit Thickness of Tuballoy

Fig. 232

[redacted]

[redacted]

Appendix E

Graph Set VIII: Impact Conditions for Fragment Shatter

a. Shatter Criterion: $c' = 0$

Figs. 233-241

Note: No graph for Magnesium appears within this Graph Set. The limitations of the experimental data for this material were such that extreme cases of fragment break-up are not in evidence. Still higher striker velocities would be needed to produce the break-up data necessary to warrant the predictions of impact conditions on this material for which the fragment will shatter.

[redacted]

[redacted]

Impact Conditions For Fragment Shatter

Target Material: Aluminum Alloy, 2024T-3
Shatter Criterion: $c' = m_r/m_s = 0$ ----- Extrapolated

Notes:
1) Thickness contours shown only where perforation is anticipated.
2) Blocked area shows main region of experimentation.

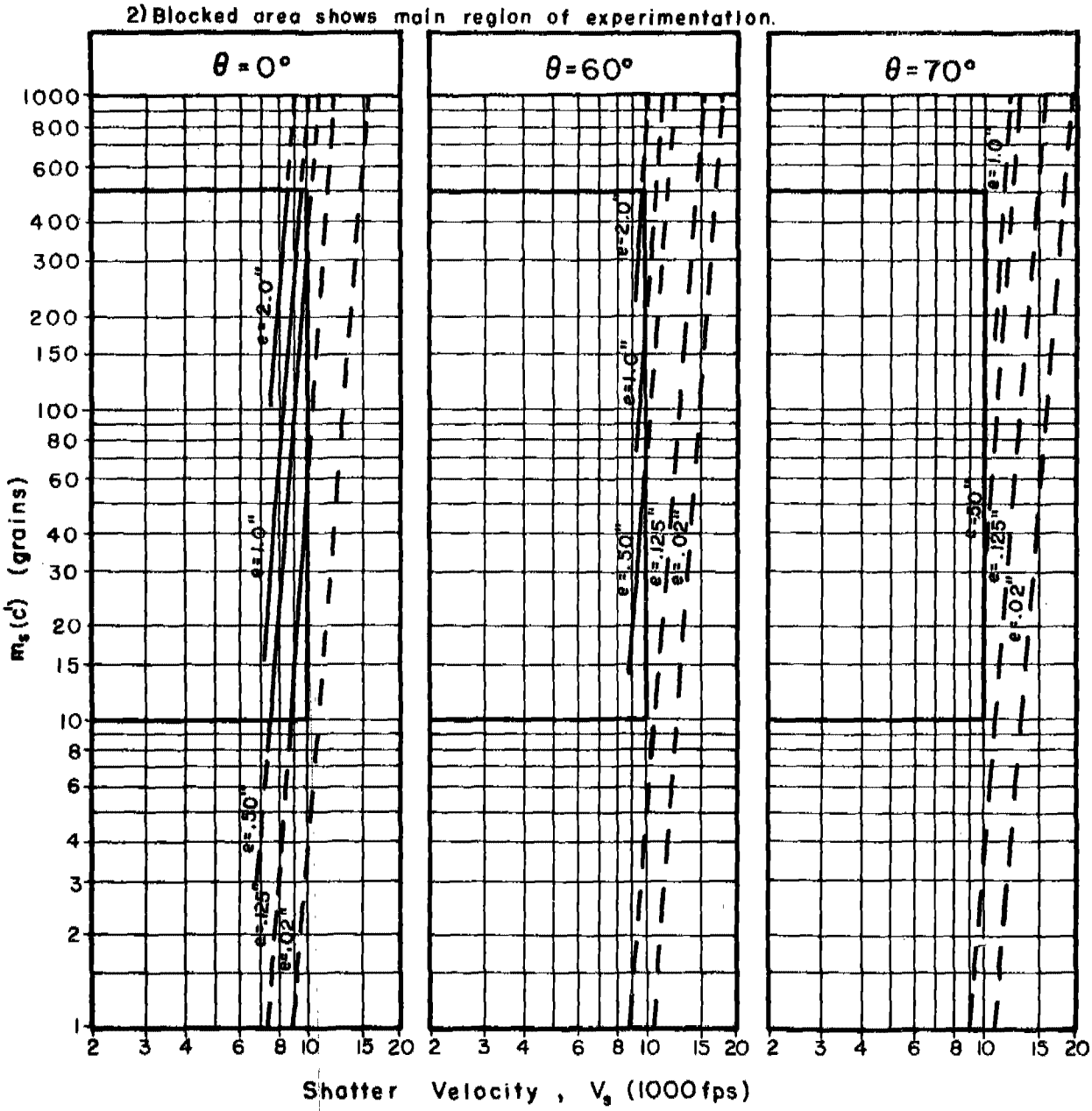

Fig. 233

[redacted]

[redacted]

Impact Conditions For Fragment Shatter

Target Material: Titanium Alloy
Shatter Criterion: $c' = m_r / m_s = 0$ ----- Extrapolated

Notes:
1) Thickness contours shown only where perforation is anticipated.
2) Blocked area shows main region of experimentation.

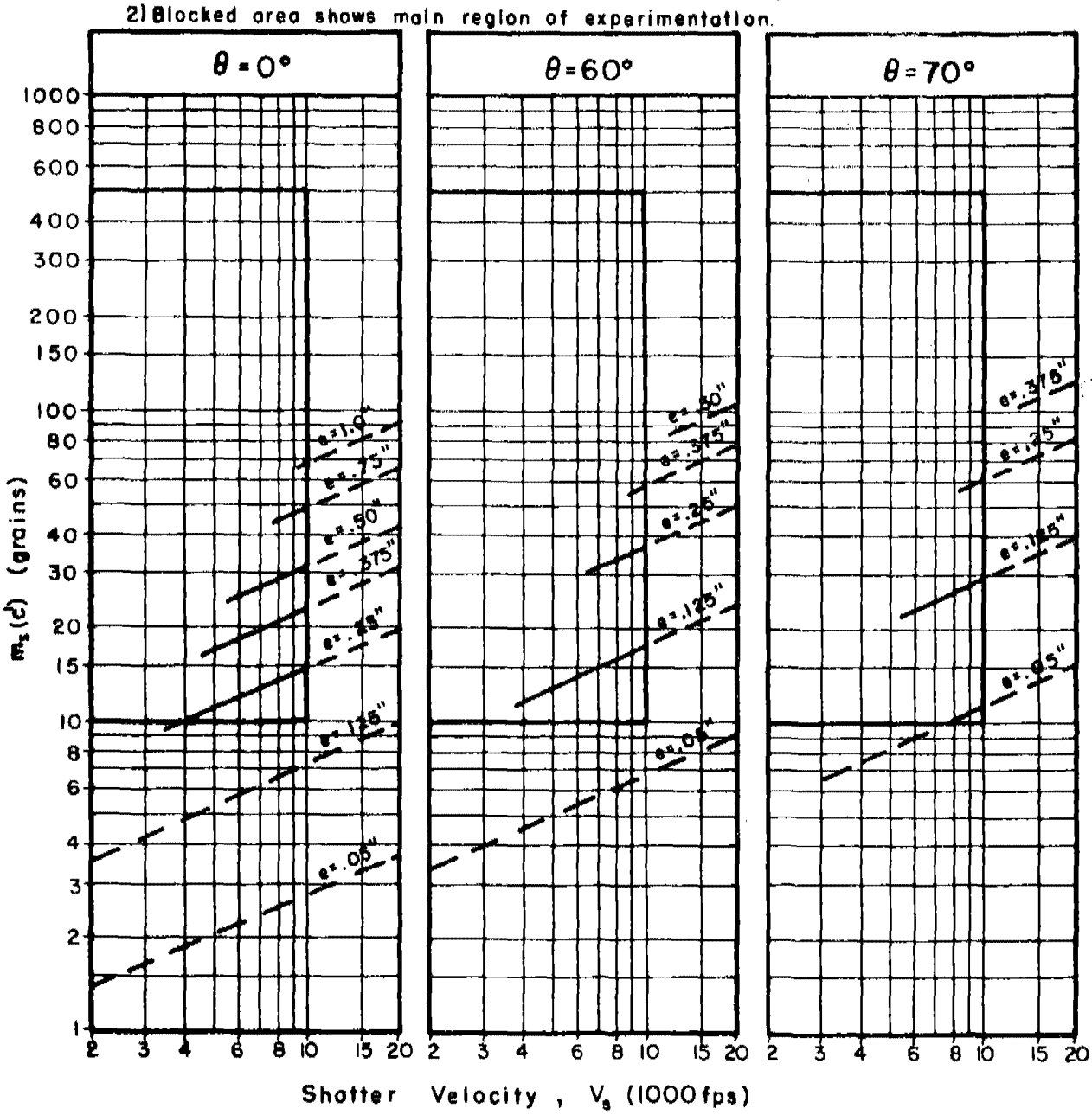

Fig. 234

[redacted]

[redacted]

Impact Conditions For Fragment Shatter

Target Material: Cast Iron
Shatter Criterion: $c' = m_r/m_s = 0$ ----- Extrapolated

Notes:
1) Thickness contours shown only where perforation is anticipated.
2) Blocked area shows main region of experimentation.

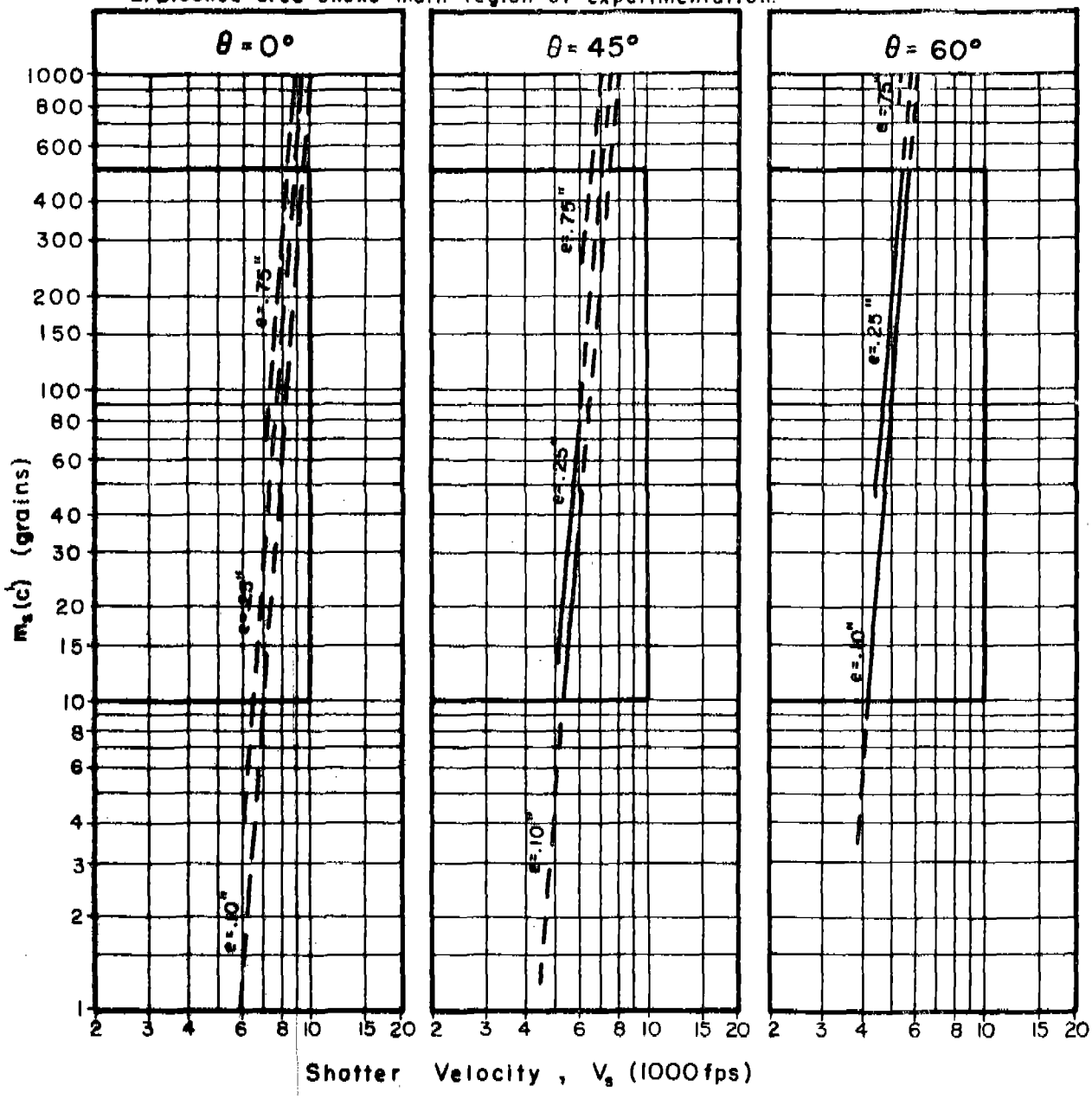

Fig. 235

[redacted]

[redacted]

Impact Conditions For Fragment Shatter

Target Material: Face-Hardened Steel
Shatter Criterion: $c' = m_r/m_s = 0$ ----- Extrapolated

Notes:
1) Thickness contours shown only where perforation is anticipated.
2) Blocked area shows main region of experimentation.

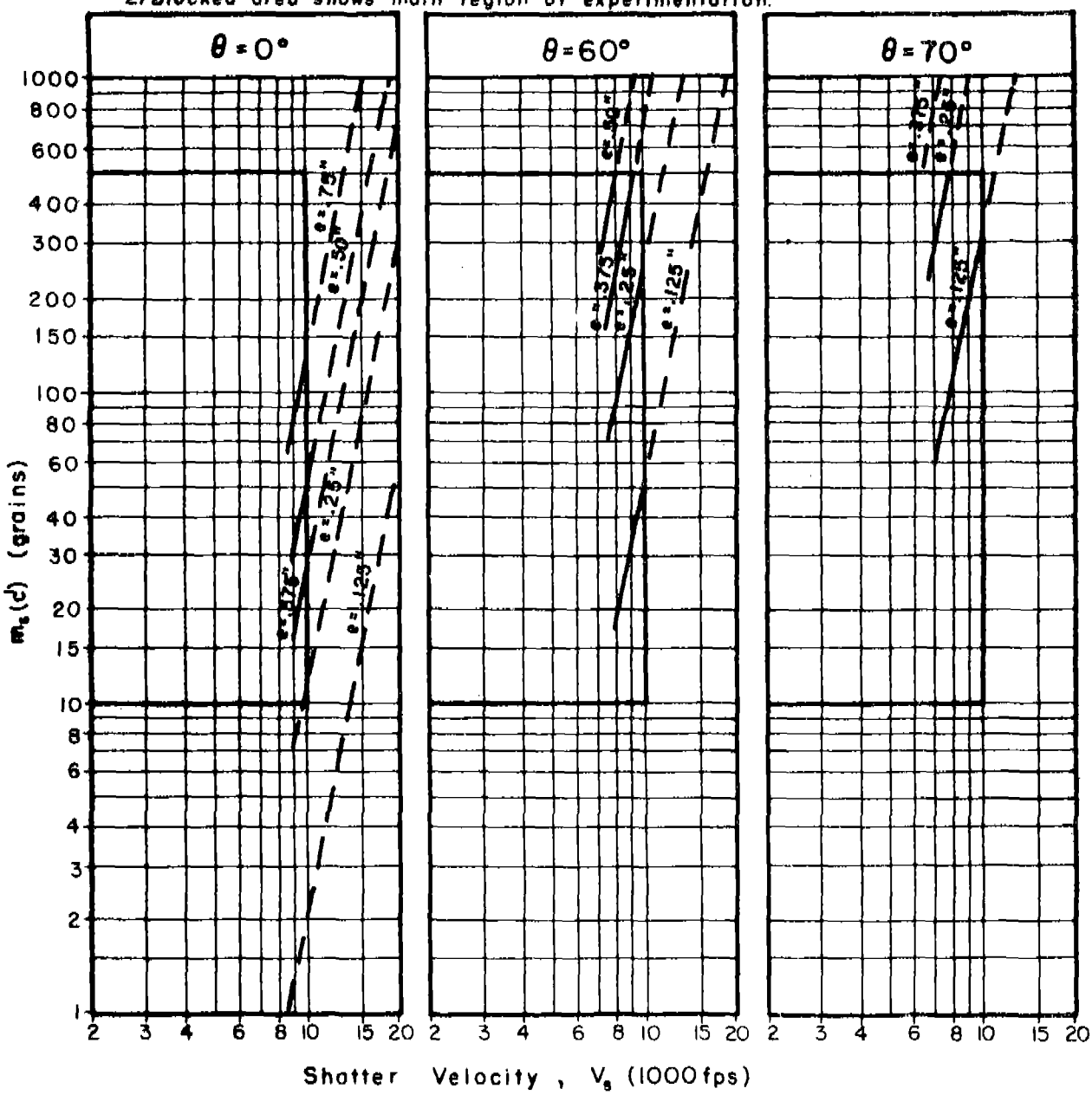

Fig. 236

[redacted]

[redacted]

Impact Conditions For Fragment Shatter

Target Material: Mild Steel
Shatter Criterion: $c' = m_r / m_s = 0$ ------ Extrapolated

Notes:
1) Thickness contours shown only where perforation is anticipated.
2) Blocked area shows main region of experimentation.

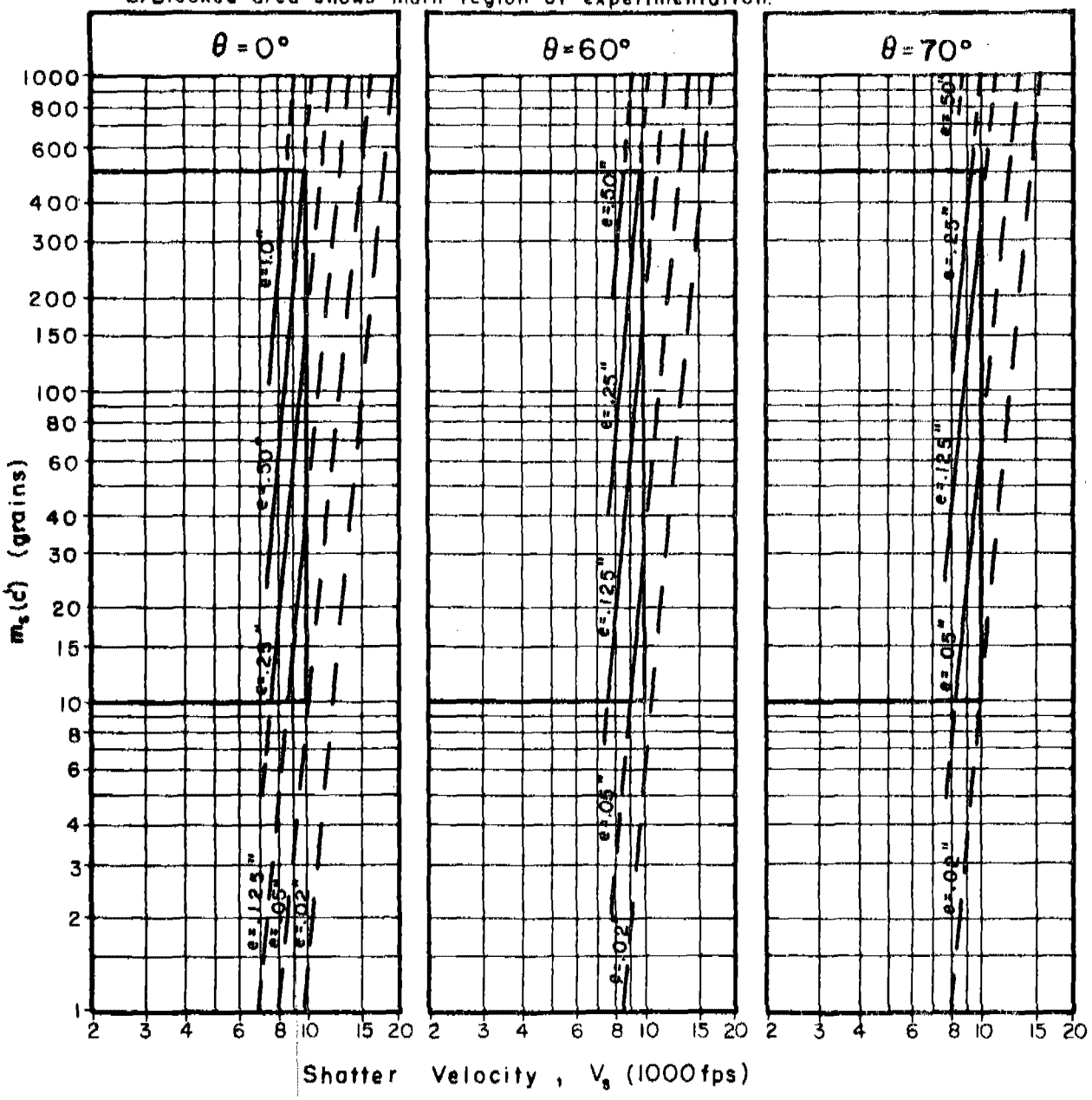

Fig. 237

[redacted]

[redacted]

Impact Conditions For Fragment Shatter

Target Material: Hard Homogeneous Steel
Shatter Criterion: $c' = m_r/m_s = 0$ ----- Extrapolated

Notes:
1) Thickness contours shown only where perforation is anticipated.
2) Blocked area shows main region of experimentation.

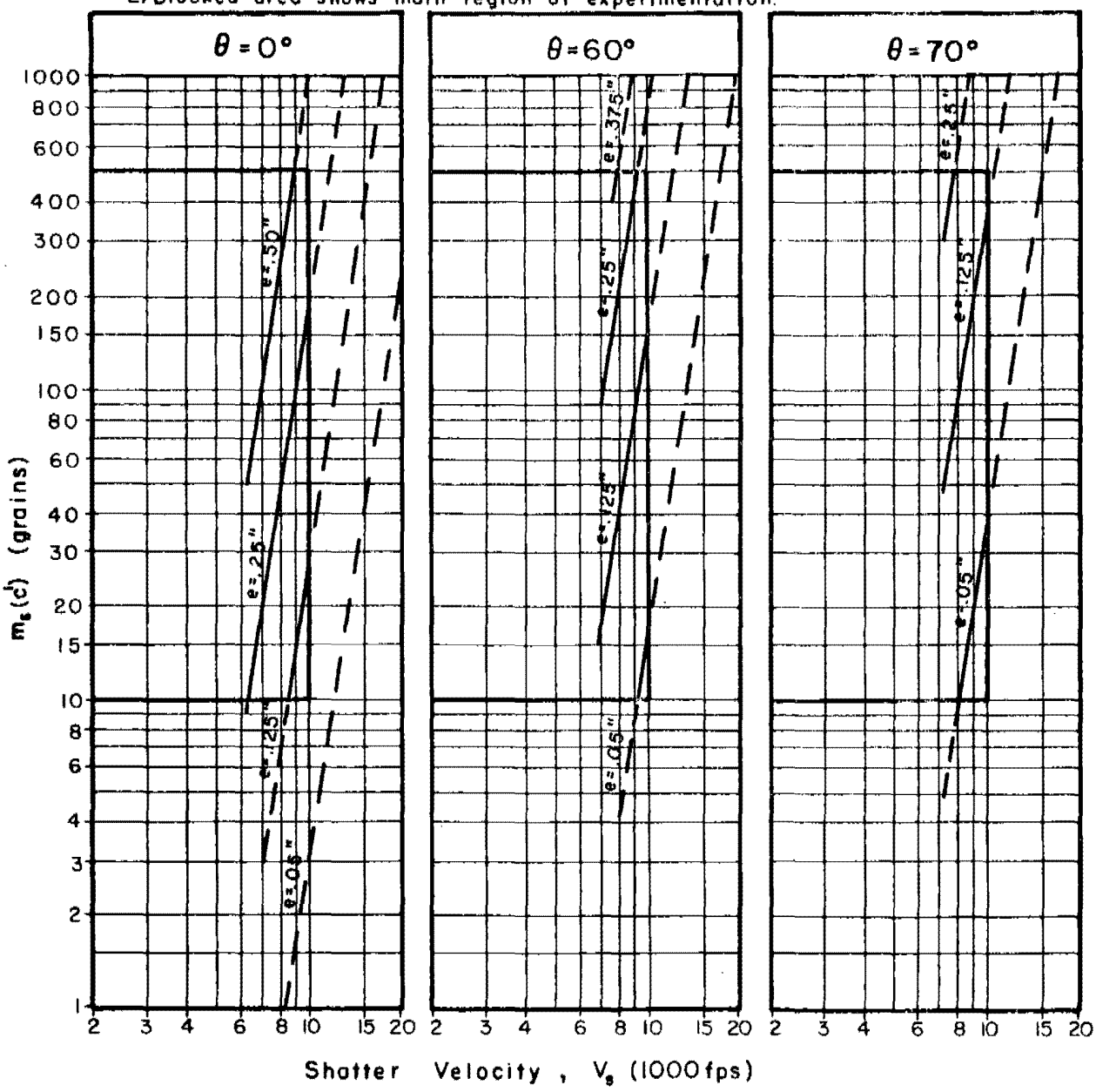

Fig. 238

[redacted]

Impact Conditions For Fragment Shatter

Target Material: Copper
Shatter Criterion: $c' = m_r/m_s = 0$ ----- Extrapolated

Notes:
1) Thickness contours shown only where perforation is anticipated.
2) Blocked area shows main region of experimentation.

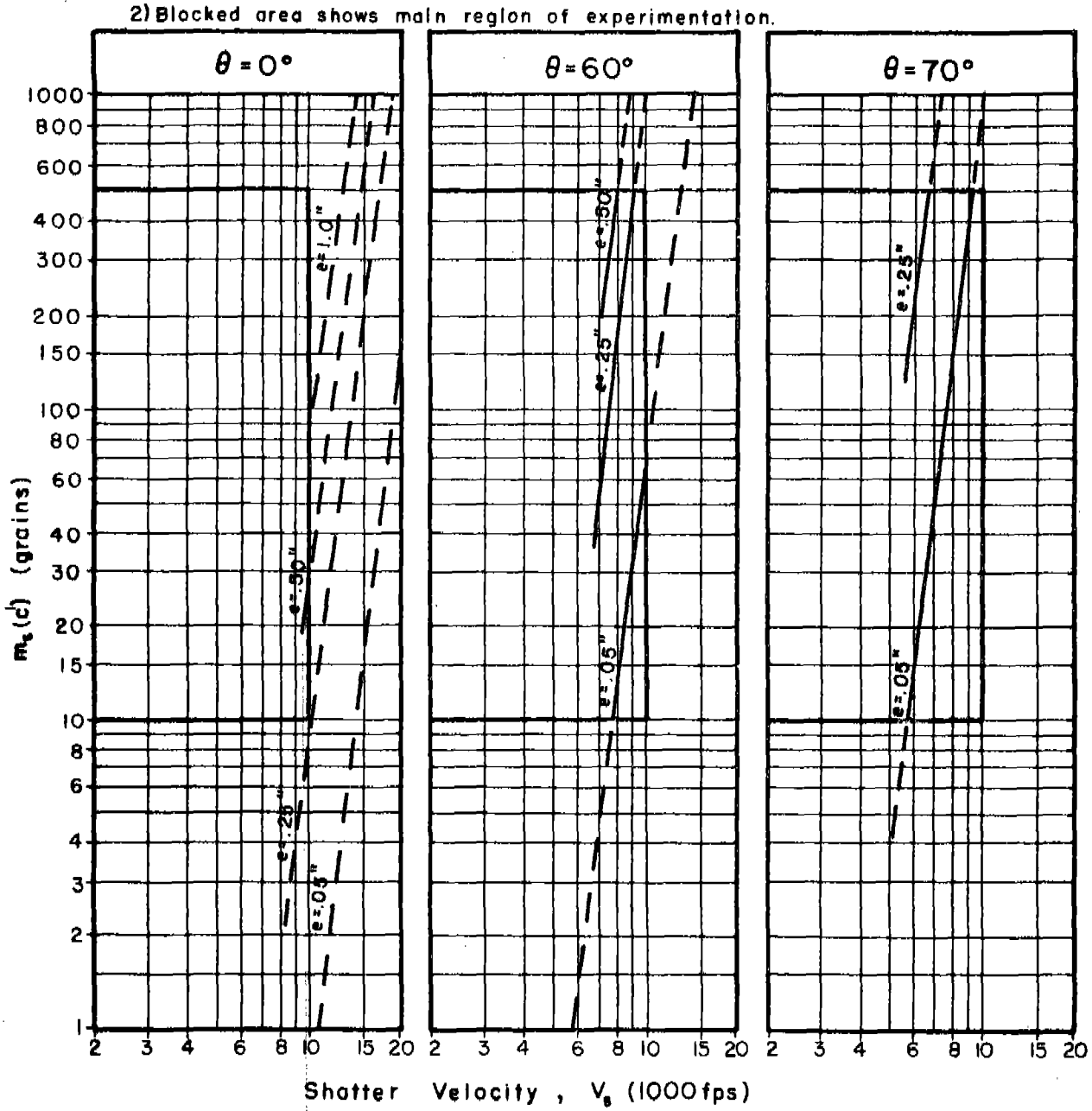

Fig. 239

[redacted]

Impact Conditions For Fragment Shatter

Target Material: Lead
Shatter Criterion: $c' = m_r/m_s = 0$ ------ Extrapolated

Notes:
1) Thickness contours shown only where perforation is anticipated.
2) Blocked area shows main region of experimentation.

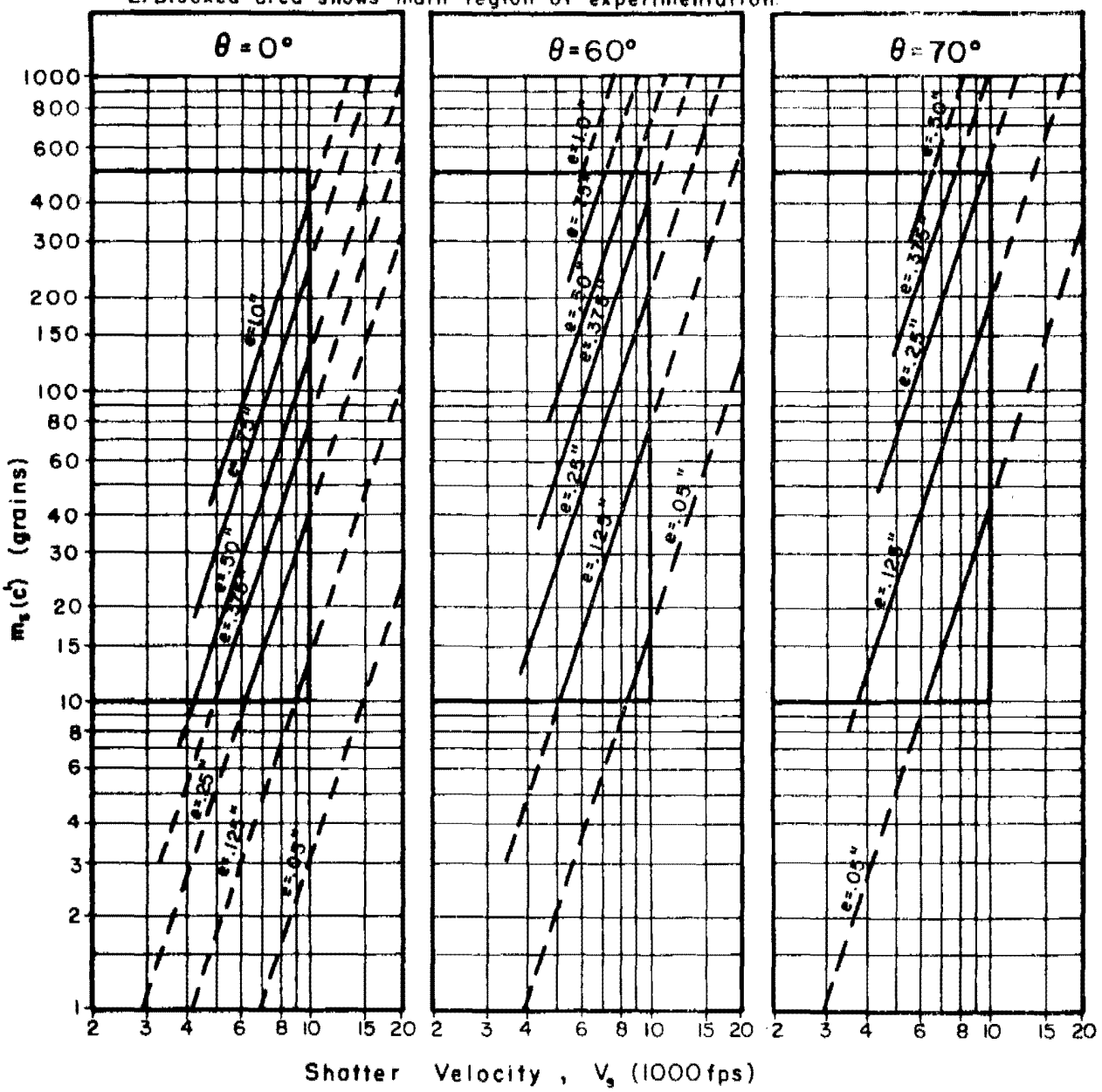

Fig. 240

[redacted]

[redacted]

Impact Conditions For Fragment Shatter

Target Material: Tuballoy
Shatter Criterion: $c' = m_r/m_s = 0$ ------ Extrapolated

Notes:
1) Thickness contours shown only where perforation is anticipated.
2) Blocked area shows main region of experimentation.

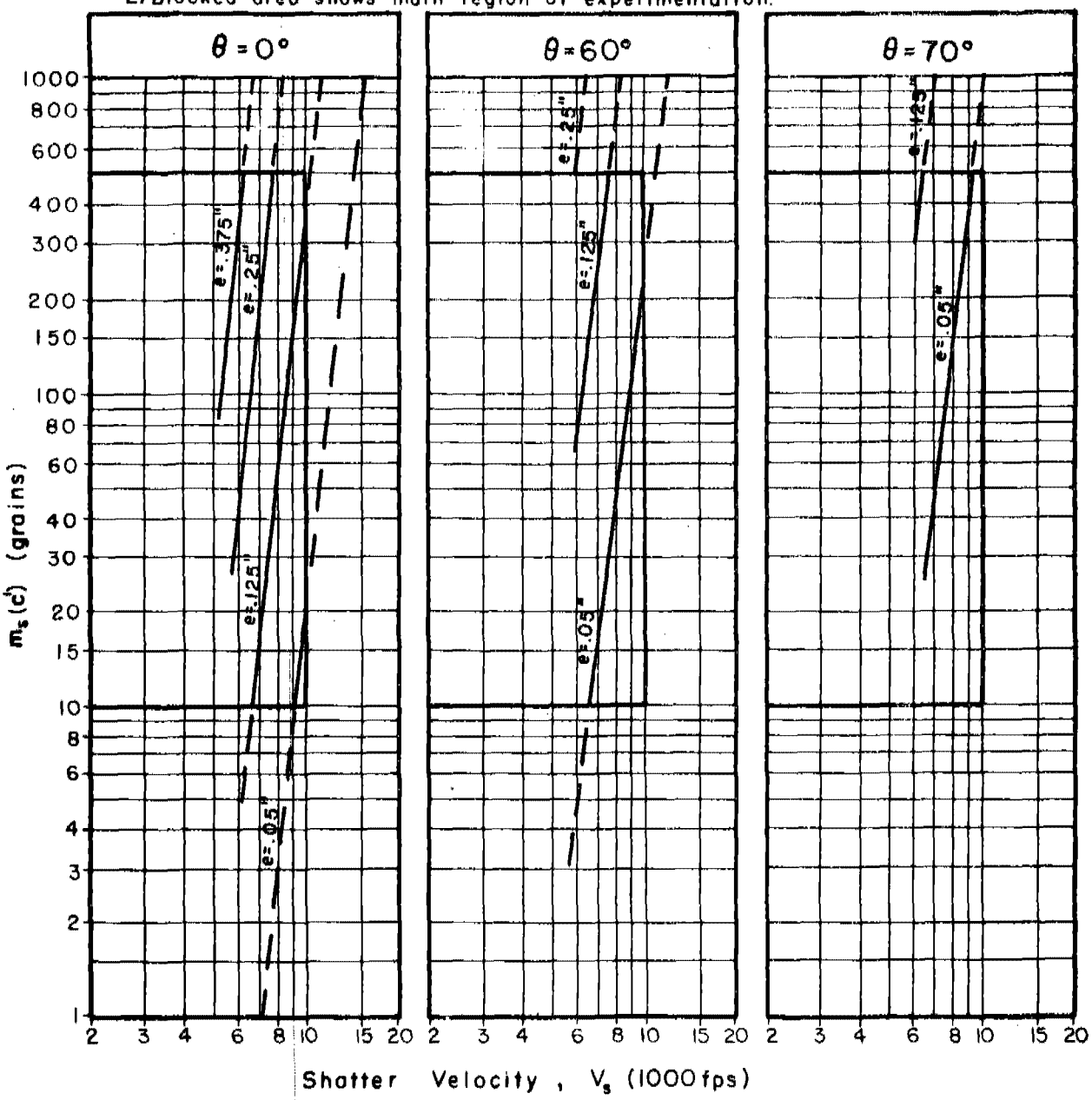

Fig. 241

[redacted]

Appendix E

Graph Set VIII: Impact Conditions for Fragment Shatter

b. Shatter Criterion: $c' = 0.25$

Figs. 242-250

Note: No graph for Magnesium appears within this Graph Set. The limitations of the experimental data for this material were such that extreme cases of fragment break-up are not in evidence. Still higher striking velocities would be needed to produce the break-up data necessary to warrant the predictions of impact conditions on this material for which the fragment will shatter.

[redacted]

Impact Conditions For Fragment Shatter

Target Material: Aluminum Alloy, 2024T-3
Shatter Criterion: $c' = m_r/m_s = 0.25$ ------ Extrapolated

Notes:
1) Thickness contours shown only where perforation is anticipated.
2) Blocked area shows main region of experimentation.

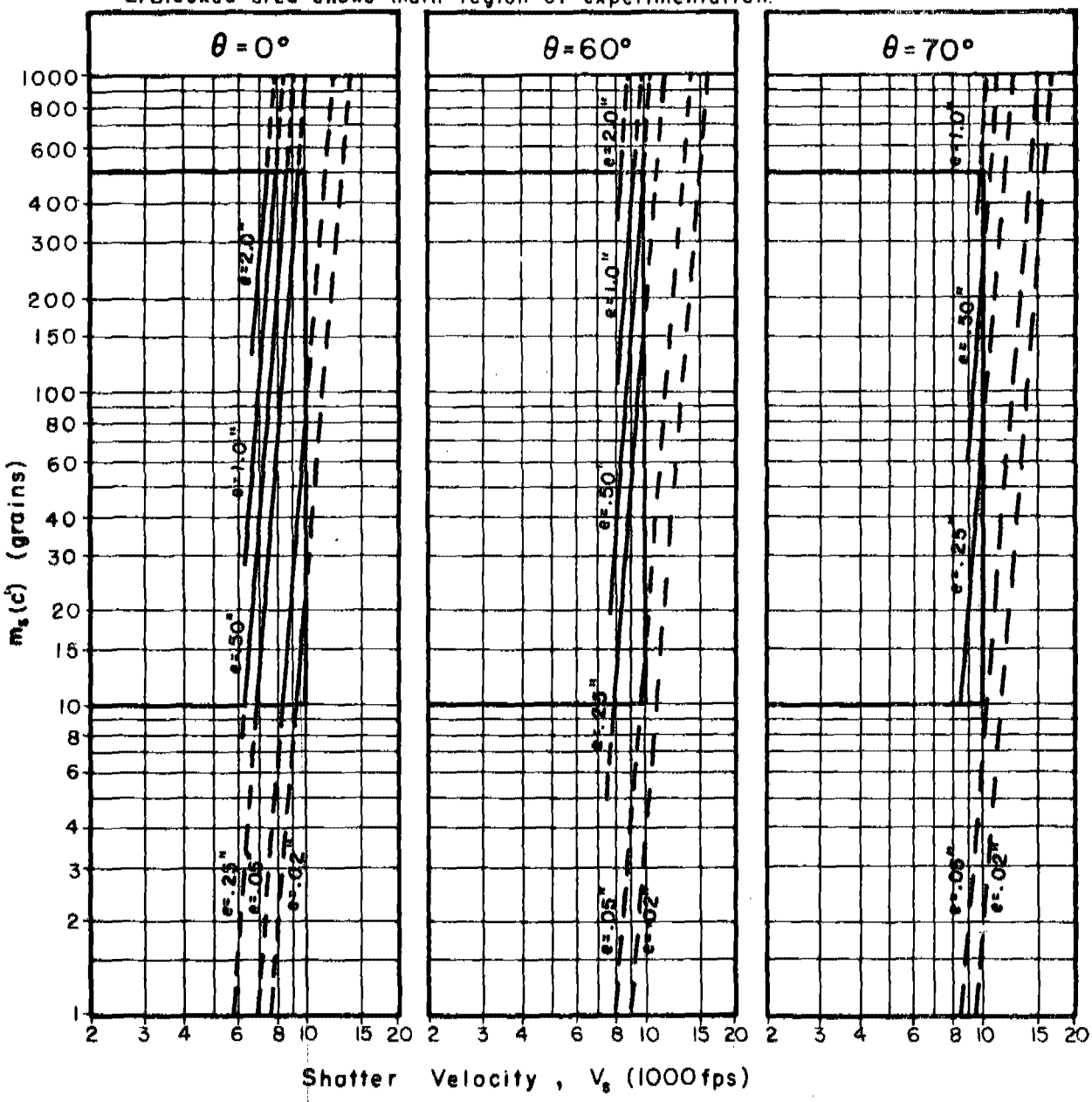

Fig. 242

[redacted]

[redacted]

Impact Conditions For Fragment Shatter

Target Material: Titanium Alloy
Shatter Criterion: $c' = m_r / m_s = 0.25$ ------ Extrapolated

Notes:
1) Thickness contours shown only where perforation is anticipated.
2) Blocked area shows main region of experimentation.

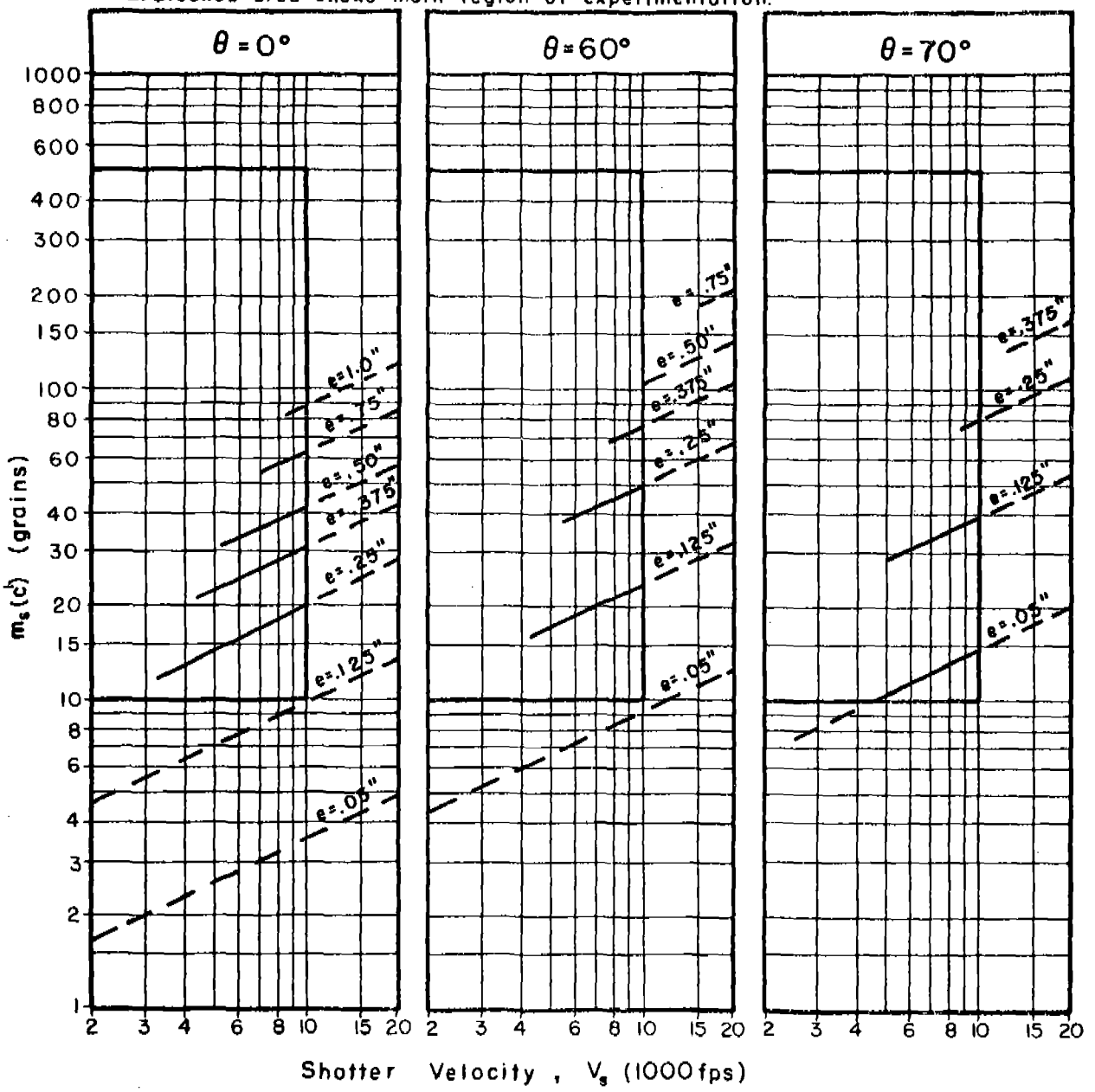

Fig. 243

[redacted]

[redacted]

Impact Conditions For Fragment Shatter

Target Material: Cast Iron
Shatter Criterion: $c' = m_r/m_s = 0.25$ ----- Extrapolated

Notes:
1) Thickness contours shown only where perforation is anticipated.
2) Blocked area shows main region of experimentation.

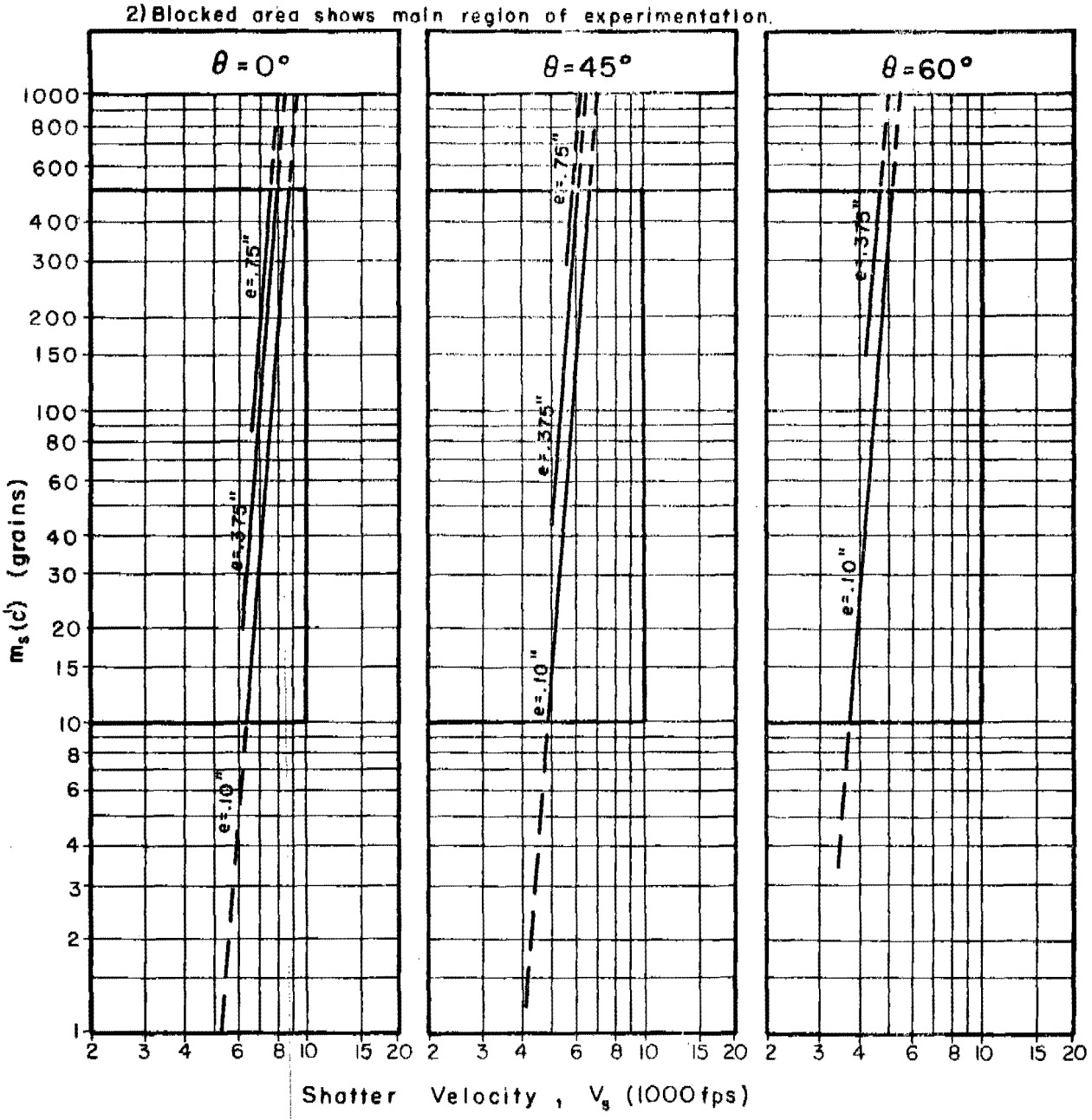

Fig. 244

[redacted]

Impact Conditions For Fragment Shatter

Target Material: Face-Hardened Steel
Shatter Criterion: $c' = m_r/m_s = 0.25$ ----- Extrapolated

Notes:
1) Thickness contours shown only where perforation is anticipated.
2) Blocked area shows main region of experimentation.

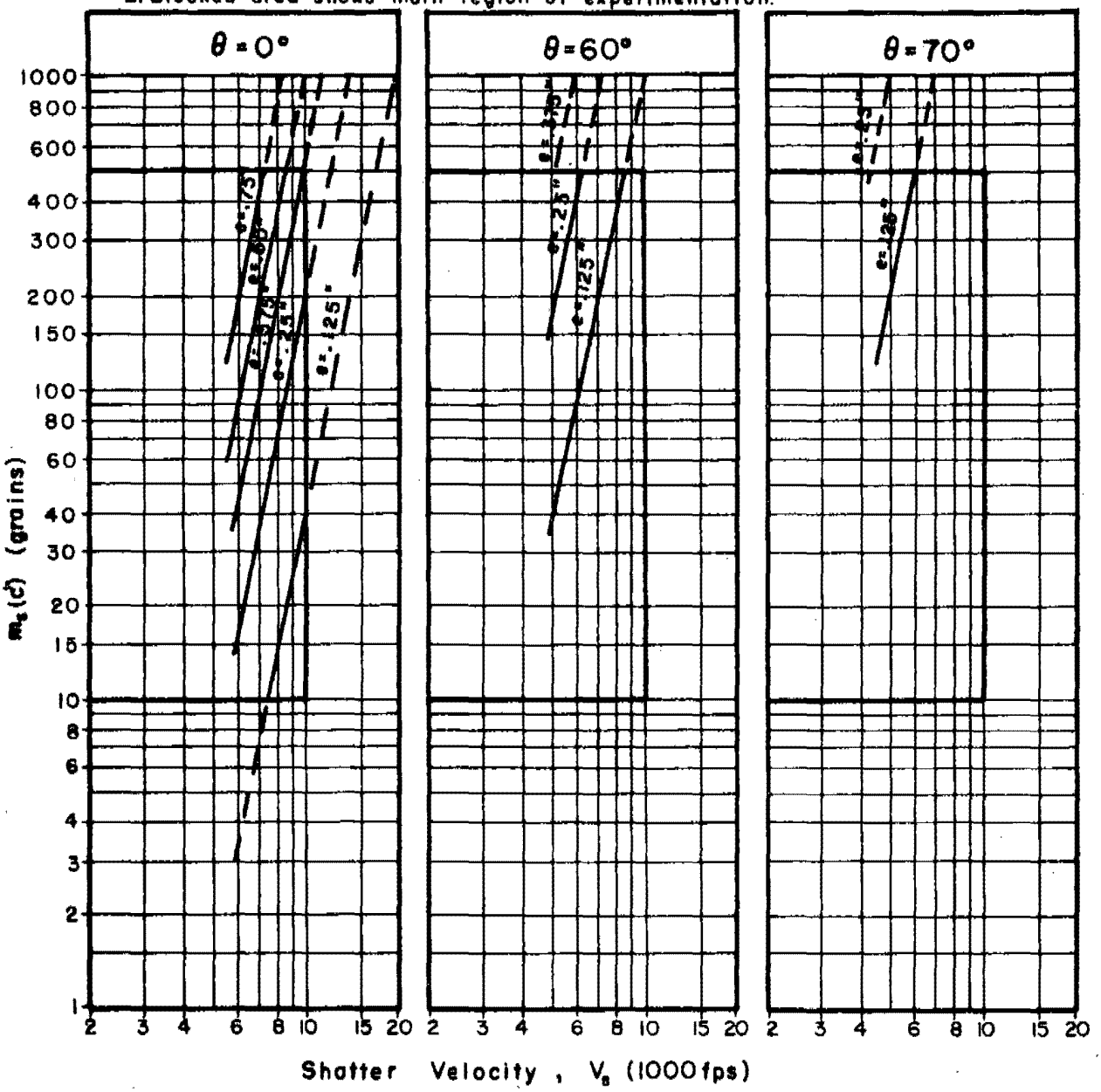

Fig. 245

[redacted]

Impact Conditions For Fragment Shatter

Target Material: Mild Steel
Shatter Criterion: $c' = m_r/m_s = 0.25$ ----- Extrapolated

Notes:
1) Thickness contours shown only where perforation is anticipated.
2) Blocked area shows main region of experimentation.

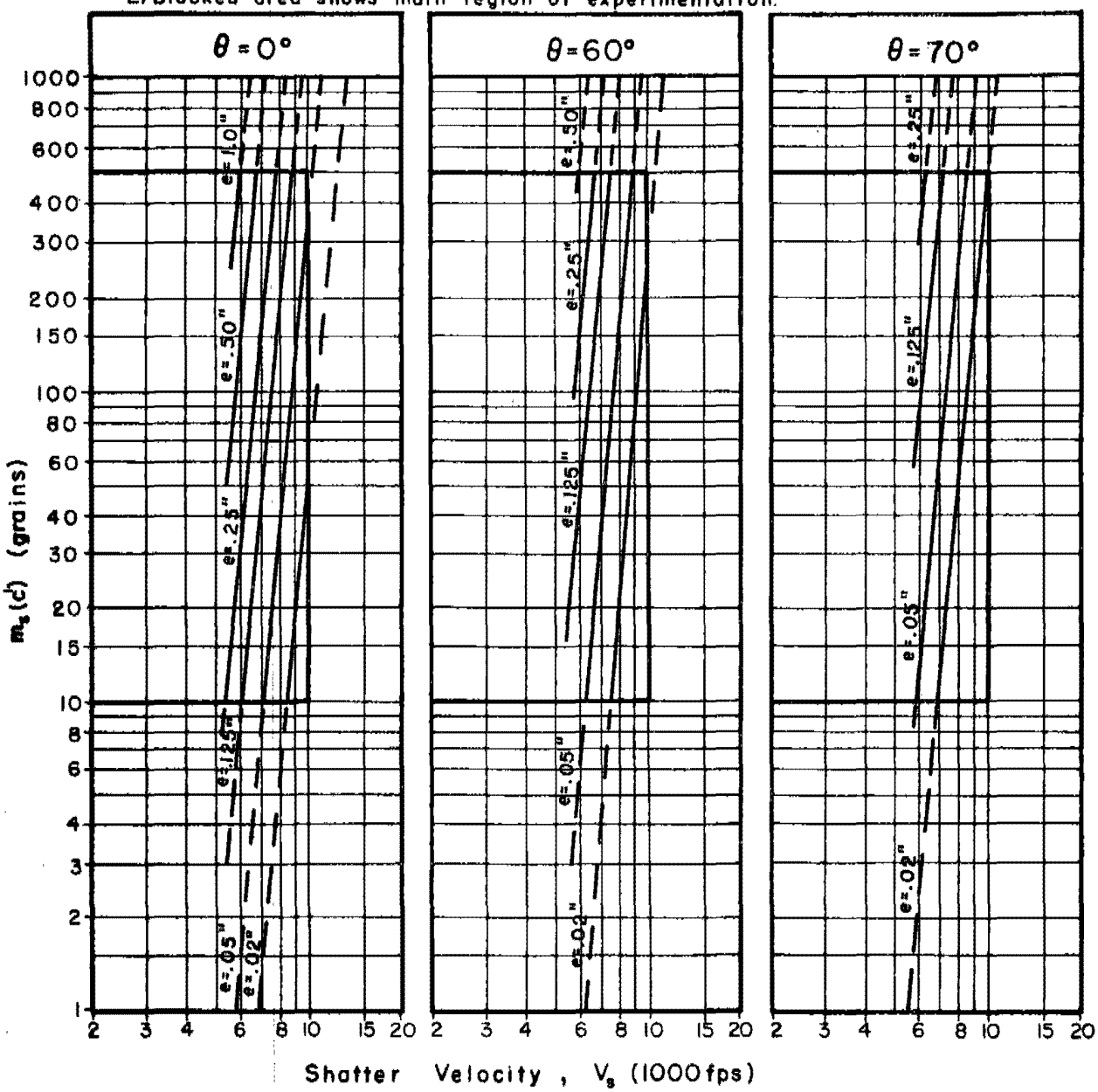

Fig. 246

[redacted]

[redacted]

Impact Conditions For Fragment Shatter

Target Material: Hard Homogeneous Steel
Shatter Criterion: $c' = m_r / m_s = 0.25$ ----- Extrapolated

Notes:
1) Thickness contours shown only where perforation is anticipated.
2) Blocked area shows main region of experimentation.

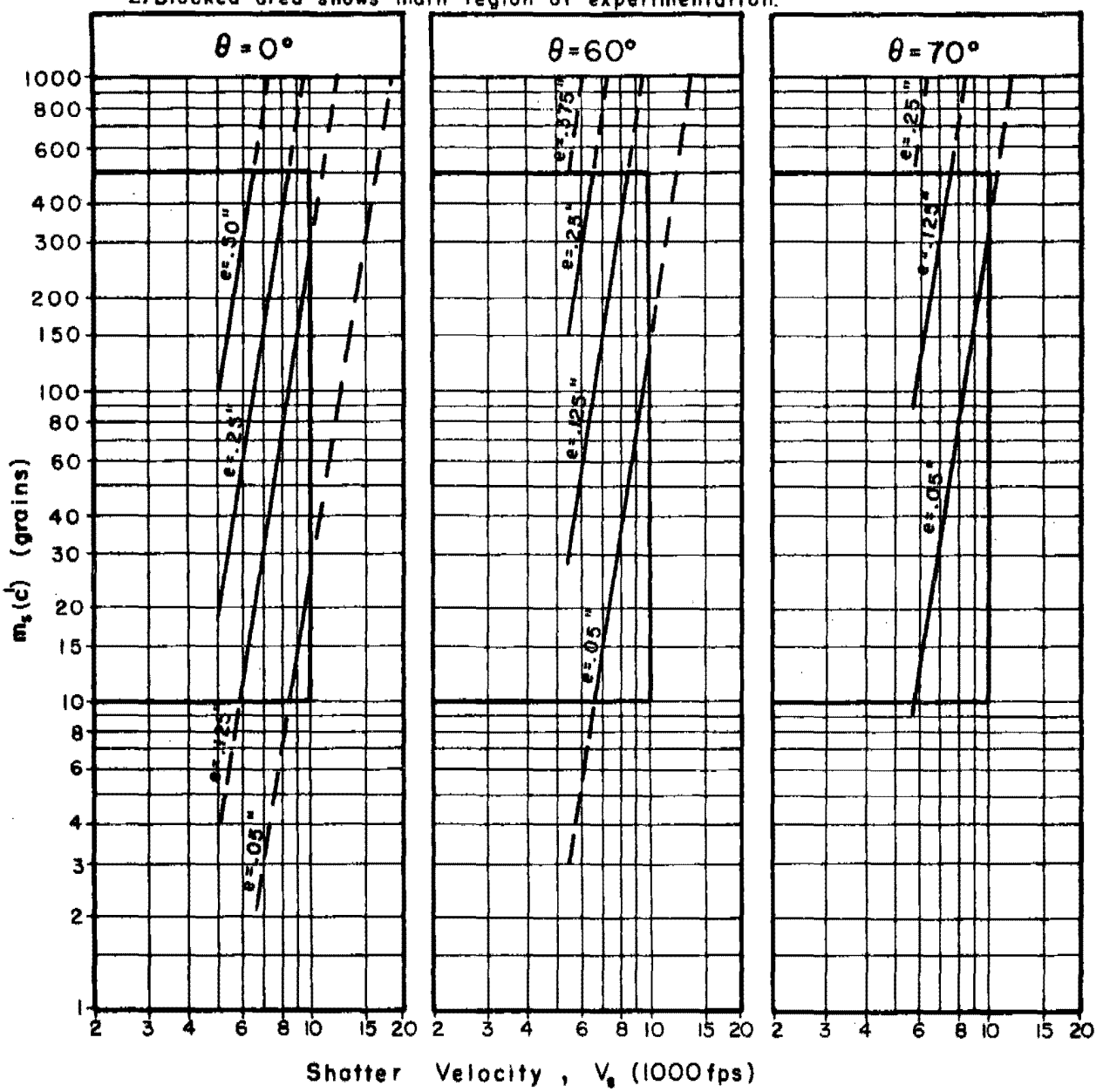

Fig. 247

[redacted]

[redacted]

Impact Conditions For Fragment Shatter

Target Material: Copper
Shatter Criterion: $c' = m_r/m_s = 0.25$ ----- Extrapolated

Notes:
1) Thickness contours shown only where perforation is anticipated.
2) Blocked area shows main region of experimentation.

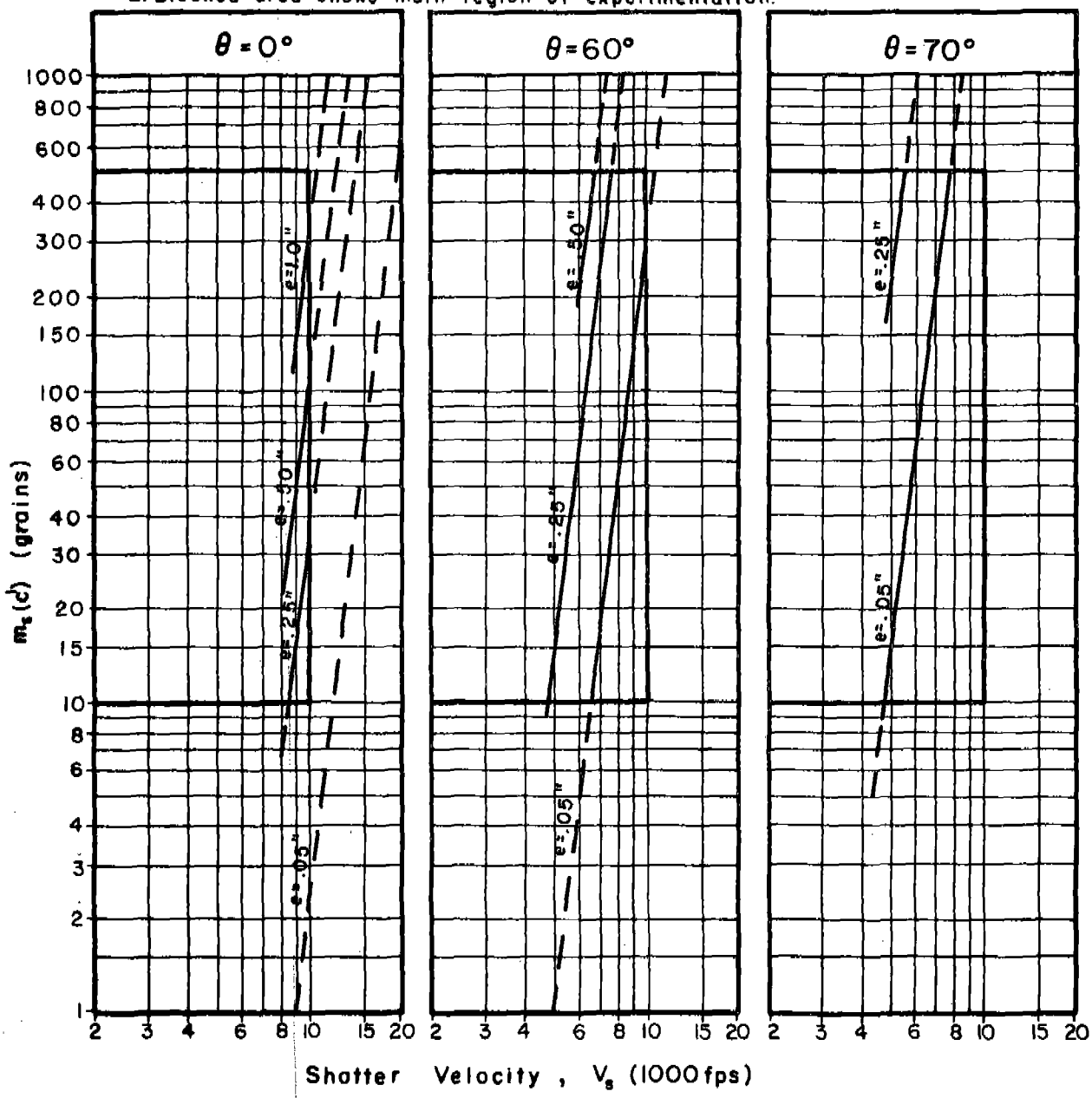

Fig. 248

[redacted]

[redacted]

Impact Conditions For Fragment Shatter

Target Material: Lead
Shatter Criterion: $c' = m_r/m_s = 0.25$ ----- Extrapolated

Notes:
1) Thickness contours shown only where perforation is anticipated.
2) Blocked area shows main region of experimentation.

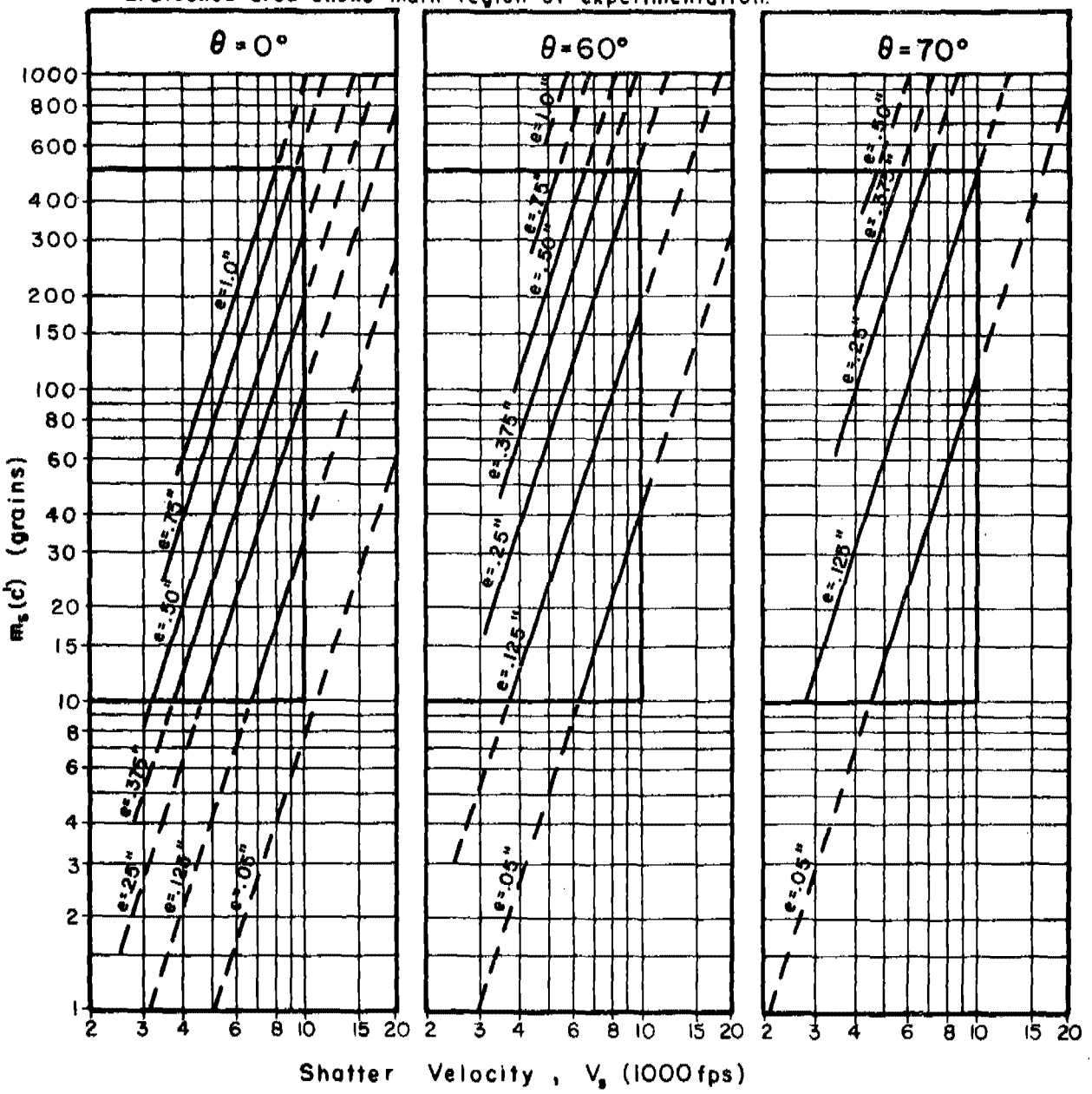

Fig. 249

[redacted]

[redacted]

Impact Conditions For Fragment Shatter

Target Material: Tuballoy
Shatter Criterion: $c' = m_r/m_s = 0.25$ ----- Extrapolated

Notes:
1) Thickness contours shown only where perforation is anticipated.
2) Blocked area shows main region of experimentation.

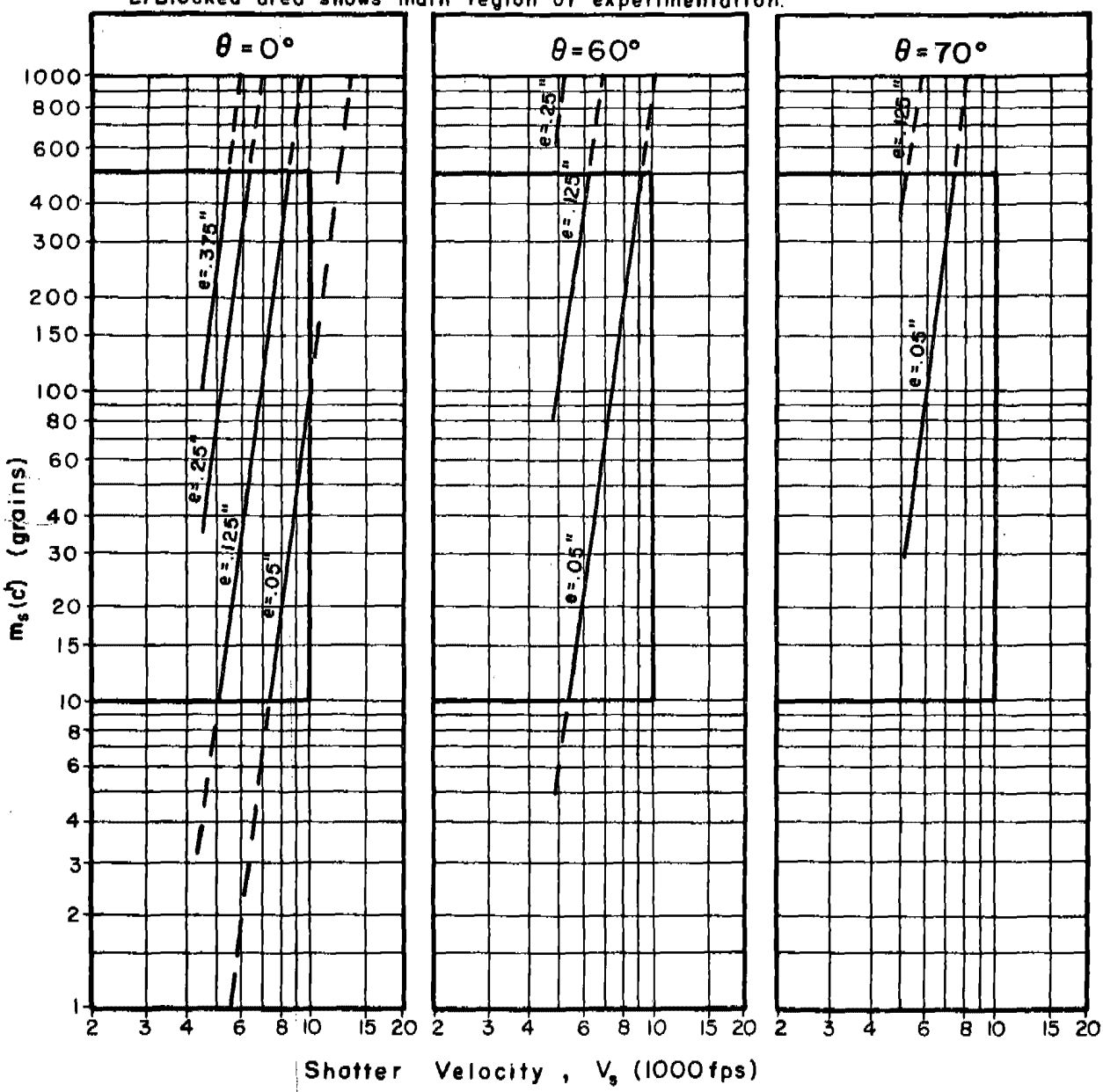

Fig. 250

[redacted]

[redacted]

Appendix F

Empirical Treatment of

Aluminum Alloys and Homogeneous Steels

[redacted]

Appendix F

Empirical Treatment of Aluminum Alloys and Homogeneous Steels

In two instances, a more complicated form of the empirical formula for estimating residual velocity was used. These instances refer to those target materials for which it was possible to vary the hardness while keeping the density essentially intact.

Impact data on three types of aluminum alloy, 2SO, 2024T-3, and 7075T-6, were supplied by BRL. The densities of these materials are 169, 173, and 175 lb/ft^3 respectively, and the corresponding Brinell Hardness values are 23, 120, and 150. The impact data on steel revealed that the Brinell Hardness values of the target samples varied from 100 to about 500.

In each case, aluminum alloys and steels, the varieties could be distinguished by many measureable characteristics, but the hardness characteristic has been selected as the one most likely to account for observed variations in target resistance to perforation. However, the effect of the change in hardness on target resistance was observed to be lacking in monotonicity. Therefore, an extension of the basic empirical form of the residual velocity estimating equation was made as follows for aluminum alloys and for steel:

$$V_r = V_s - 10^c (eA)^{\alpha} m^{\beta} (\sec \theta)^{\gamma} V_s^{\lambda} \exp (\epsilon B^2 + \omega B) \quad ,$$

where B is the Brinell Hardness Number of the material under impact, ϵ and ω are two additional constants to be determined by the least squares technique, and the other symbols are as defined previously. Actually, the constants are determined by application of the method of least squares to the linear equation relating the Briggs' logarithms:

$$\log (V_s - V_r) = c + \alpha \log (eA) + \beta \log m + \gamma \log \sec \theta + \lambda \log V_s + 0.4343 (\epsilon B^2 + \omega B).$$

The form of the hardness factor $\left[\exp (\epsilon B^2 + \omega B)\right]$ has, for $\epsilon < 0$, a maximum at $B = \frac{-\omega}{2\epsilon}$, reflecting the observation that maximum resistance occurs for an intermediate value of B. The ordinary exponential form with one unknown is a monotonic function, and hence must be adjusted to be useful here. In this manner, two master formulas, one for homogeneous steel and one for aluminum alloys, are developed.

If the residual velocity estimating equation for steel is of the form:

$$V_r = V_s - 10^c (eA)^\alpha m^\beta (\sec \theta)^\gamma V_s^\lambda \exp (\epsilon B^2 + \omega B) \quad ,$$

Using 150 BHN → MHA
350 BHN → MHA

then the resulting set of values of the constants for this material is tabulated below:

6.103

should this be -0.945?

Material	c	α	β	γ	λ	ϵ	ω
Steel	4.253	0.889	-0.352	1.262	0.019	$-8.77(10)^{-6}$	$5.41(10)^{-3}$

Note that for any particular value of Brinell Hardness, this formula reduces quickly to one of the conventional type. But is not equivalent for the above values

To accommodate the changes in density of the aluminum alloys, the form of the basic equation for these alloys was chosen to be:

$$V_r = V_s - 10^c (EA)^\alpha m^\beta (\sec \theta)^\gamma V_s^\lambda \exp (\epsilon B^2 + \omega B) \quad ,$$

where E, the areal density in lb/ft^2, is used instead of e, the target thickness in inches. The resulting set of values that corresponds to this master form is:

Material	c	α	β	γ	λ	ϵ	ω
Aluminum Alloys	5.3717	1.029	-1.0718	1.2510	-0.1394	$-1.52(10)^{-4}$	$2.75(10)^{-2}$

For any particular aluminum alloy, the values for the density and Brinell Hardness being known, it is an easy matter to transform this equation into one of the regular type, i.e., with no Brinell Hardness expression and in terms of target thickness.

Only two types of homogeneous steel were used in the attempt to relate loss of fragment weight to impact parameters. These types are distinguished by their Brinell Hardness values, 150 and 380. The estimating equations for predicting fragment residual velocities for these types were obtained by substituting these values of Brinell Hardness into the master formula.

Only one alloy of aluminum, 2024T-3, was used in the attempt to relate loss of fragment weight to impact parameters. The resistance of this alloy to perforation was determined to be greater than that of either of the two other alloys of aluminum considered, as measured by the residual velocity results.

The V_o type graphs are used to display the relative resistance of the three aluminum alloys to perforation. These composite graphs follow in Set IX.

In a similar manner, V_o type graphs are used to display the relative resistance of homogeneous steels with Brinell Hardness values of 100, 300, and 500. These composite graphs follow in Set X.

Any comparison beyond what is suggested in these graphs is hardly warranted since the corresponding information on fragment weight loss during perforation is not available to the degree necessary to fix the estimating equations.

Appendix F

Graph Set IX

V_o vs m for Selected Values of e;

Composite Graphs for 2SO, 2024T-3, and 7075T-6

Figs. 251-253

[redacted]

V_o vs Fragment Weight for Selected Target Thicknesses

Obliquity: 0°

Target Material: Aluminum Alloys

Fragment:

Type: BRL Pre-formed

Material: Steel, SAE 1020

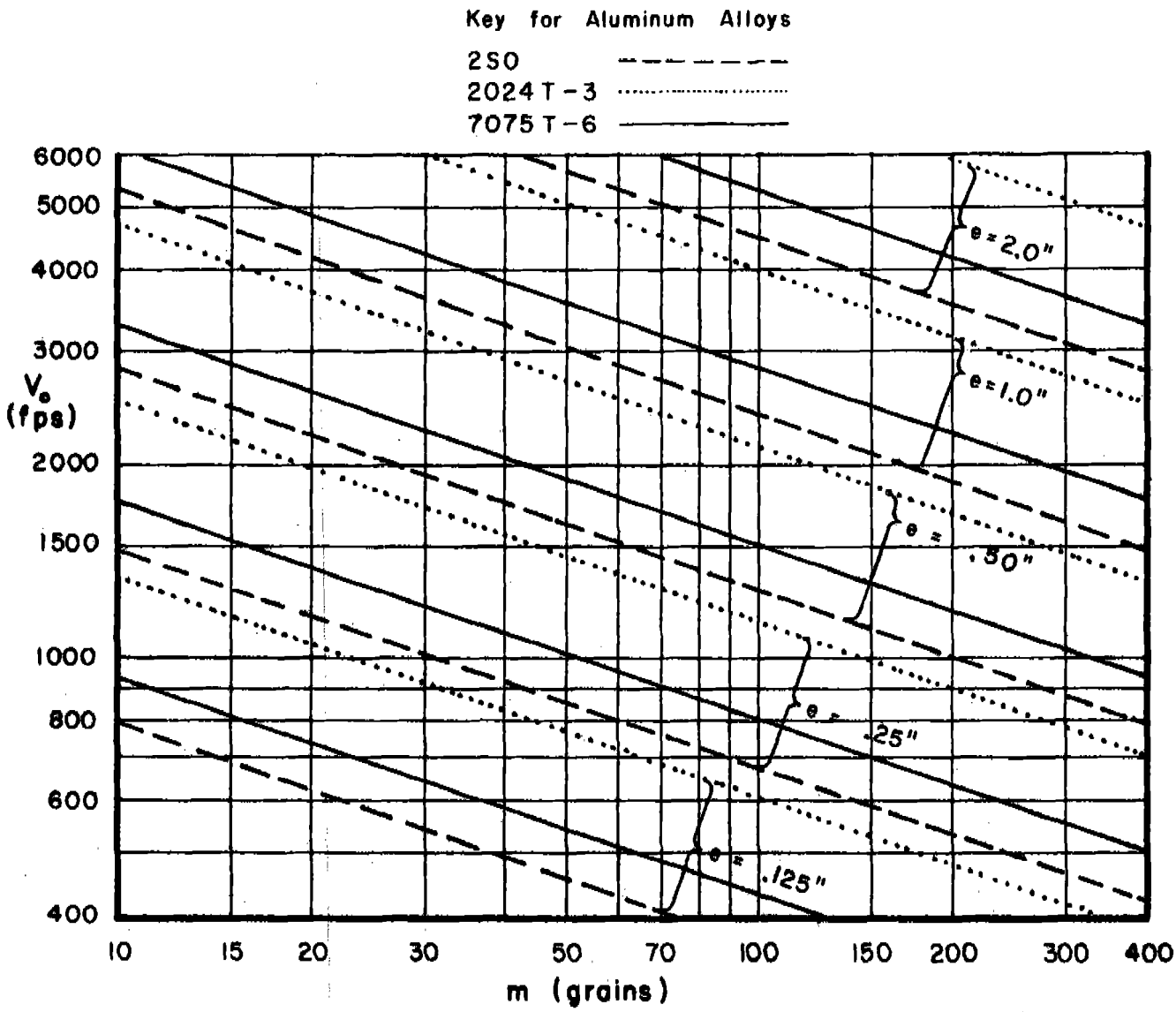

Fig. 251

[redacted]

[redacted]

V_o vs Fragment Weight for Selected Target Thicknesses

Obliquity: 60°

Target Material: Aluminum Alloys

Fragment:

Type: BRL Pre-formed

Material: Steel, SAE 1020

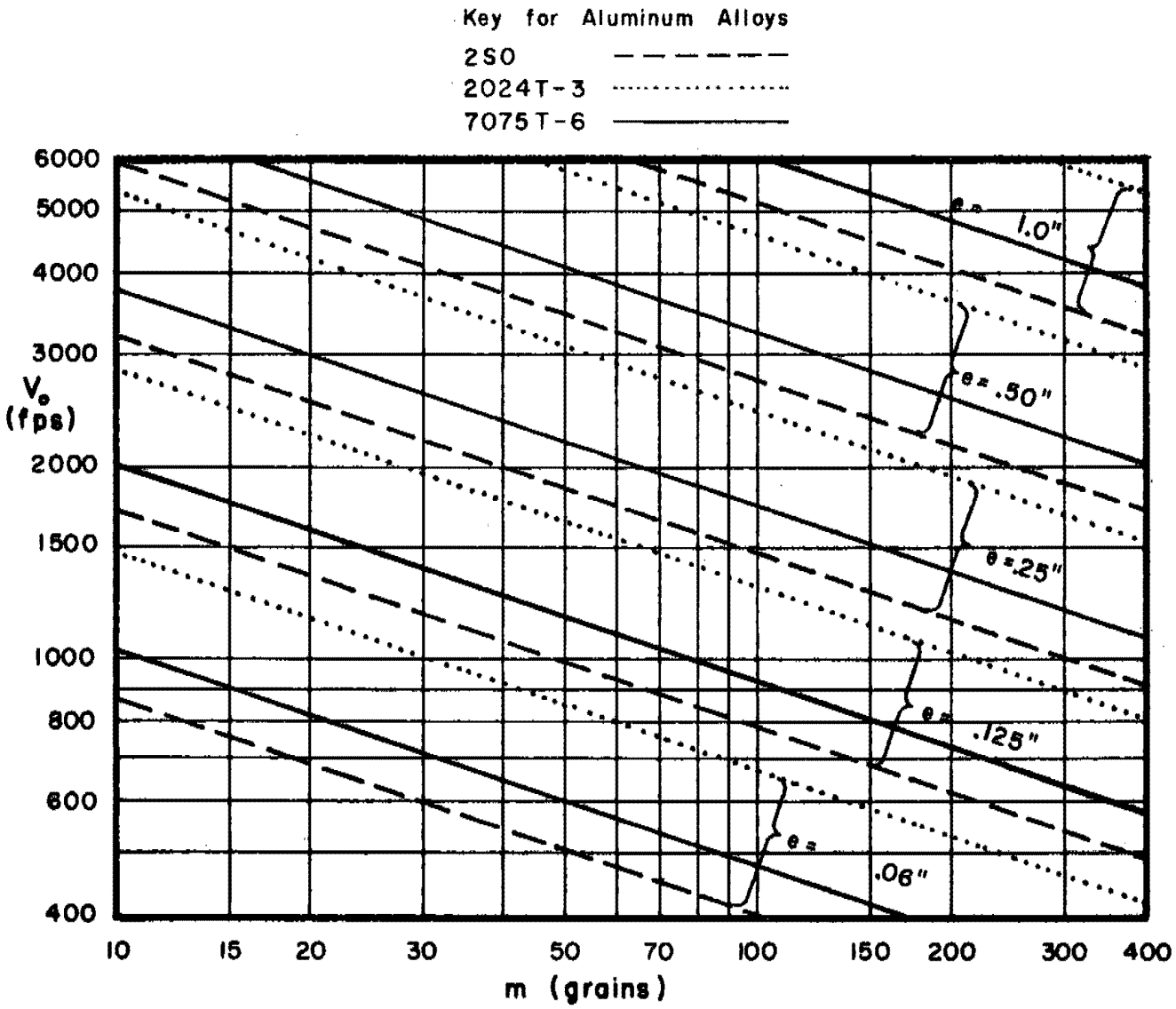

Fig. 252

[redacted]

V_o vs Fragment Weight for Selected Target Thicknesses

Obliquity: 70°

Target Material: Aluminum Alloys

Fragment:

Type: BRL Pre-formed

Material: Steel, SAE 1020

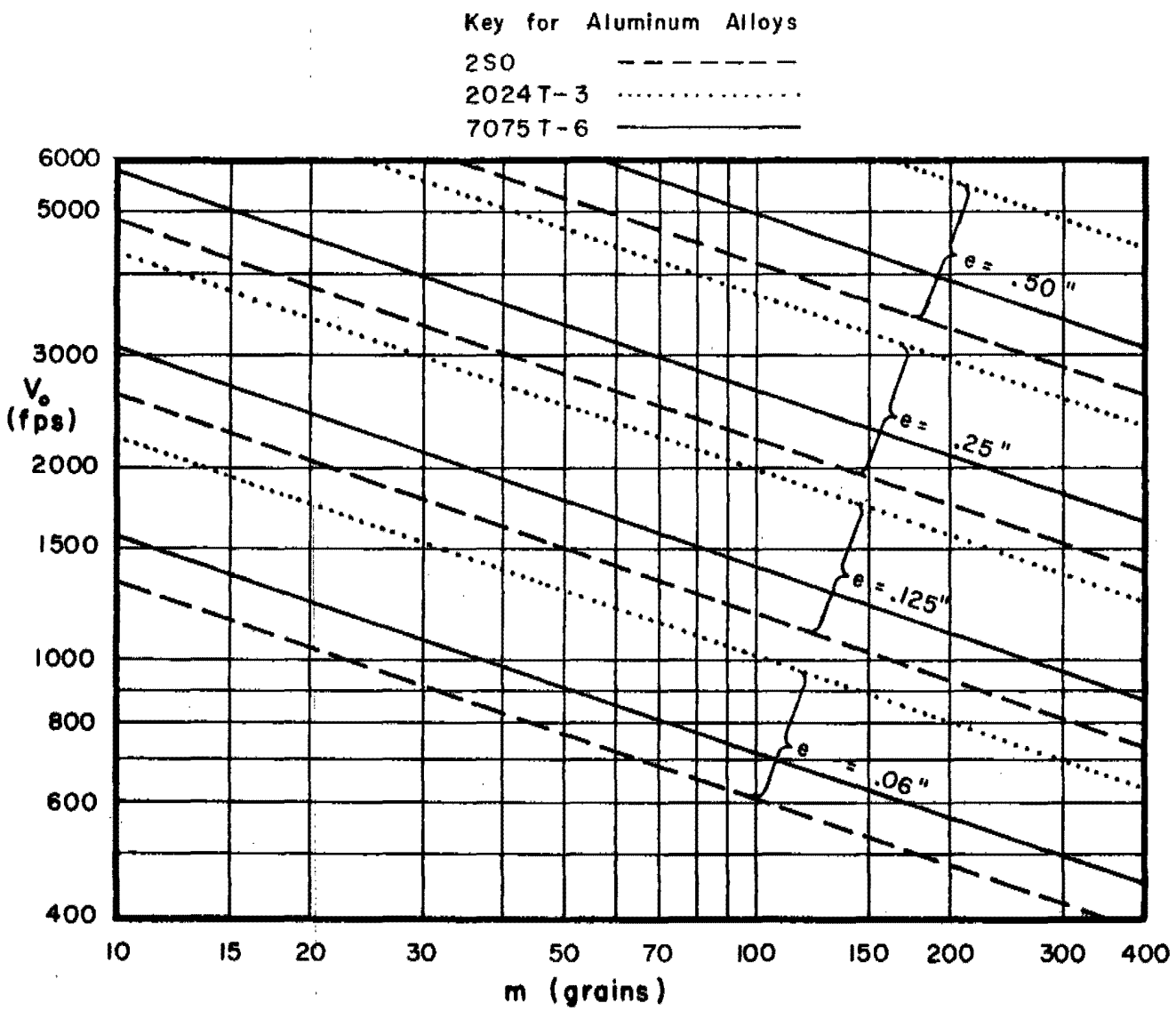

Fig. 253

[redacted]

Appendix F

Graph Set X

V_o vs m for Selected Values of e;

Composite Graphs for Homogeneous Steels

with Brinell Hardness Values of 100, 300, and 500

Figs. 254-256

[redacted]

[redacted]

V_o vs Fragment Weight for Selected Target Thicknesses

Obliquity: 0°

Target Material: Steel

Fragment:

Type: BRL Pre-formed

Material: Steel, SAE 1020

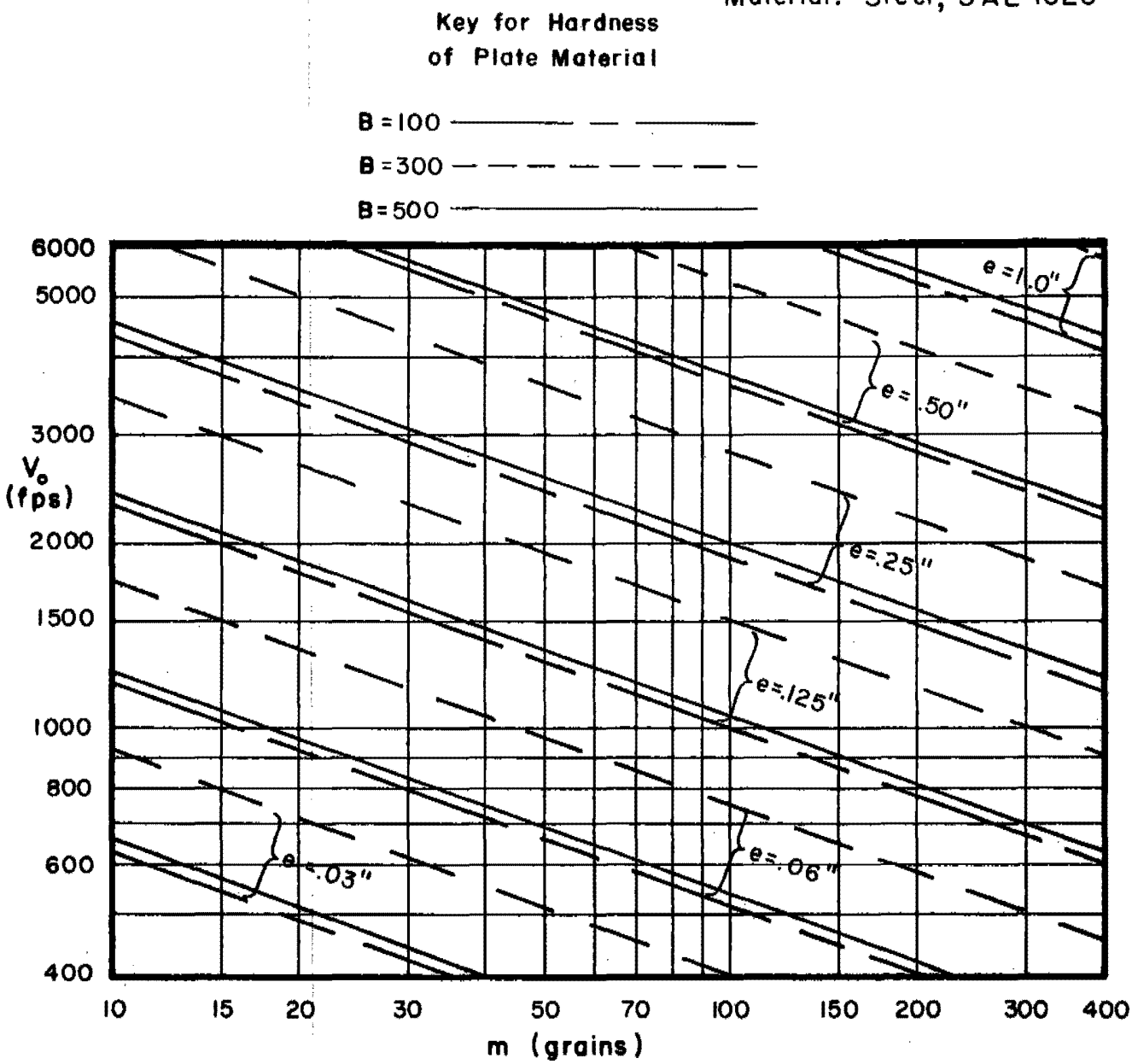

Fig. 254

[redacted]

[redacted]

V_o vs Fragment Weight for Selected Target Thicknesses

Obliquity: 60°

Target Material: Steel

Fragment:

Type: BRL Pre-formed

Material: Steel, SAE 1020

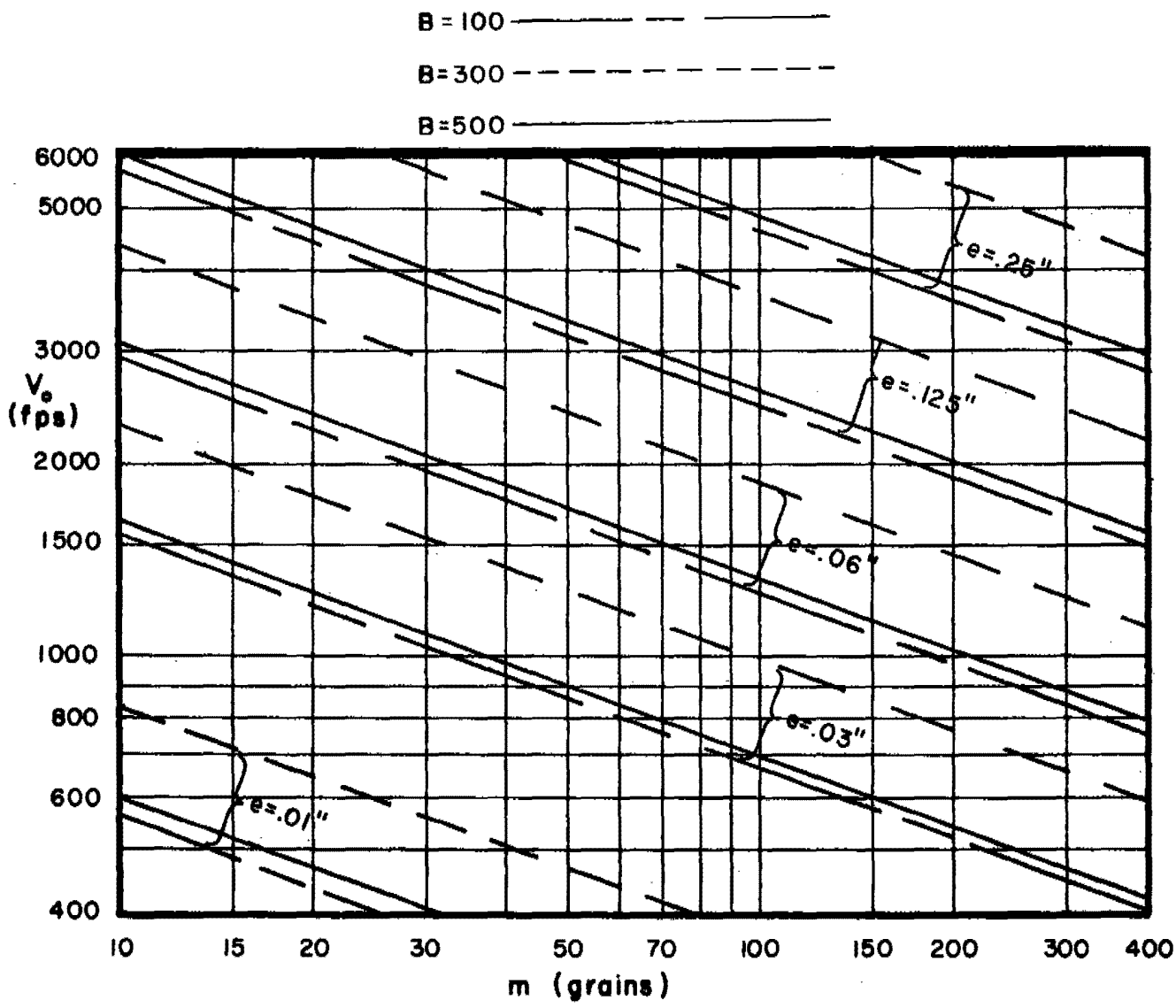

Fig. 255

[redacted]

[redacted]

V_o vs Fragment Weight for Selected Target Thicknesses

Obliquity: 70°

Target Material: Steel

Fragment:

Type: BRL Pre-formed

Material: Steel, SAE 1020

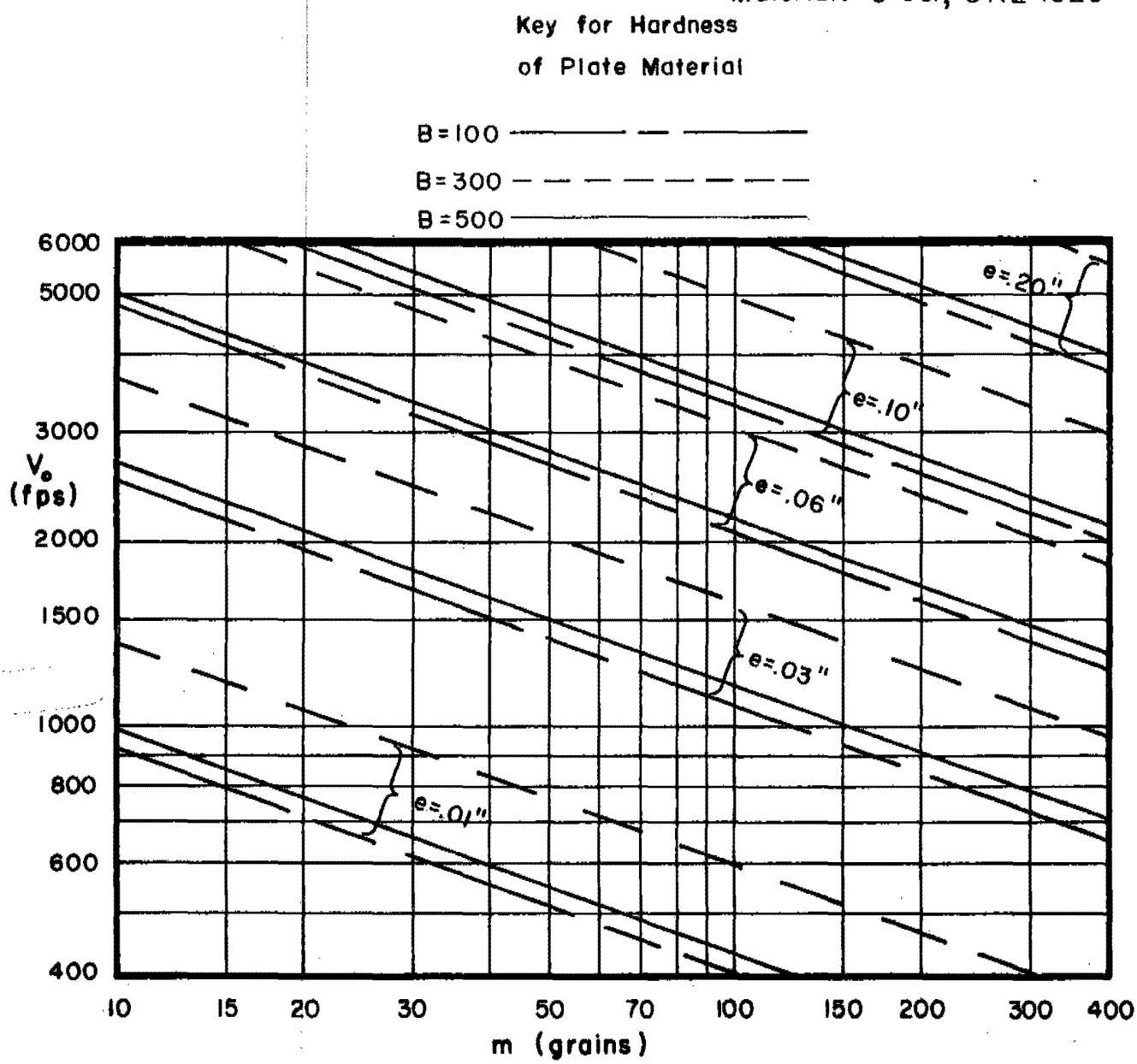

Fig. 256

[redacted]

Appendix G

Experimental Data; Steel Fragments

Impacting on Various Target Materials

Tables XIII-XXI

Experimental Data

Table XIII: Steel Fragments Impacting on Magnesium

Data No.	Material Thickness (e inches)	Fragment Weight m (grains)	Obliquity θ (degrees)	Striking Velocity V_s (fps)	Residual Velocity V_r (fps)	Residual Weight m_r (grains)	Hole Size Area ** (sq. in.)
1	.050	30	0	2000	*	29.0	
2	.050	30	45	2897	2756	29.0	
3	.050	30	45	3000	*	29.0	
4	.050	30	45	4000	*	29.0	
5	.050	30	60	2205	1916	29.0	
6	.050	30	60	5083	4743	26.2	
7	.050	30	70	2897	2461	29.0	
8	.050	60	45	2901	2767	59.0	
9	.050	60	45	3000	*	59.0	
10	.050	60	45	3000	*	59.0	
11	.050	60	45	3000	*	59.0	
12	.050	60	45	3000	*	59.0	
13	.050	60	45	3000	*	59.0	
14	.050	120	60	1000	*	119.0	
15	.050	120	60	1000	*	119.0	
16	.050	120	60	1000	*	119.0	
17	.125	30	0	2285	1598	29.0	
18	.125	30	45	3975	3456	29.0	
19	.125	60	45	3741	3310	59.0	
20	.125	60	45	4000	*	59.0	
21	.125	60	45	4000	*	59.0	
22	.125	60	45	4000	*	59.0	
23	.125	60	45	4000	*	59.0	
24	.125	60	45	4000	*	59.0	
25	.125	60	60	2972	2522	59.0	
26	.125	60	70	4868	3947	59.0	
27	.125	120	60	1500	*	119.0	
28	.125	120	60	1795	1383	119.0	

* not available

** not taken for this target material

Experimental Data

Table XIII: Steel Fragments Impacting on Magnesium (Cont)

Data No.	Material Thickness (e inches)	Fragment Weight m (grains)	Obliquity θ (degrees)	Striking Velocity V_s (fps)	Residual Velocity V_r (fps)	Residual Weight m_r (grains)	Hole Size Area ** (sq. in.)
29	.125	120	70	2844	1957	119.0	
30	.125	240	60	1000	*	239.0	
31	.125	240	60	1000	*	239.0	
32	.185	15	0	1108	0	*	
33	.185	15	45	1401	0	*	
34	.185	15	70	2528	0	*	
35	.185	60	0	701	0	*	
36	.185	60	70	1900	0	*	
37	.185	240	0	426	0	*	
38	.185	240	45	613	0	*	
39	.185	240	70	852	0	*	
40	.208	15	0	1425	0	*	
41	.261	60	0	1027	0	*	
42	.301	30	0	3016	2075	29.0	
43	.301	30	45	4961	3642	28.4	
44	.301	60	0	2821	2234	59.0	
45	.301	60	45	4841	2595	52.6	
46	.301	60	60	5100	2466	48.0	
47	.301	120	0	2878	2423	119.0	
48	.301	120	70	3957	2101	*	
49	.301	240	70	4000	*	211.7	
50	.301	240	70	4000	*	230.7	
51	.301	240	70	4000	*	233.6	
52	.301	240	70	4000	*	239.0	
53	.301	240	70	4093	2615	208.0	
54	.310	15	0	1710	0	*	
55	.310	15	70	3325	0	*	
56	.310	30	60	2090	0	*	

* not available

** not taken for this target material

Experimental Data

Table XIII: Steel Fragments Impacting on Magnesium (Cont)

Data No.	Material Thickness (e inches)	Fragment Weight m (grains)	Obliquity θ (degrees)	Striking Velocity V_s (fps)	Residual Velocity V_r (fps)	Residual Weight m_r (grains)	Hole Size Area ** (sq. in.)
57	.310	60	70	2470	0	*	
58	.310	60	80	5510	0	*	
59	.310	240	0	665	0	*	
60	.310	240	60	1235	0	*	
61	.310	240	70	1710	0	*	
62	.310	240	80	3135	0	*	
63	.492	60	70	3230	0	*	
64	.492	240	80	5890	0	*	
65	.500	15	70	5700	0	*	
66	.500	30	0	4884	2572	28.5	
67	.500	30	45	5040	1948	27.8	
68	.500	60	0	3957	2763	55.2	
69	.500	60	0	3974	2823	54.8	
70	.500	60	0	4000	*	55.1	
71	.500	60	45	10086	7037	6.9	
72	.500	120	0	3772	3112	*	
73	.500	120	60	4277	3316	105.1	
74	.500	120	60	5000	*	97.4	
75	.500	120	60	5000	*	109.9	
76	.500	120	60	5000	*	111.1	
77	.500	120	60	5000	*	111.1	
78	.500	120	60	5000	*	117.7	
79	.500	120	70	5000	*	104.9	
80	.500	120	70	5000	*	116.2	
81	.500	120	70	7174	497	*	
82	.500	240	0	4722	4065	*	
83	.500	240	60	4000	*	217.2	
84	.500	240	60	4000	*	217.4	

* not available

** not taken for this target material

Experimental Data

Table XIII: Steel Fragments Impacting on Magnesium (Cont)

Data No.	Material Thickness (e inches)	Fragment Weight m (grains)	Obliquity θ (degrees)	Striking Velocity V_s (fps)	Residual Velocity V_r (fps)	Residual Weight m_r (grains)	Hole Size Area ** (sq. in.)
85	.500	240	60	4025	2561	212.8	
86	.599	15	0	2970	0	*	
87	.599	15	70	5225	0	*	
88	.599	60	0	2031	0	*	
89	.599	240	0	950	0	*	
90	.599	240	70	2850	0	*	
91	.750	60	45	5092	2279	49.4	
92	.750	120	0	4536	3540	77.9	
93	.750	120	0	5000	*	107.6	
94	.750	120	60	5022	1978	106.8	
95	.750	120	60	1000	*	114.2	
96	.750	240	0	5021	3942	202.2	
97	.750	240	0	5400	*	195.7	
98	.750	240	0	5400	*	198.7	
99	.750	240	0	5400	*	200.8	
100	.750	240	0	5400	*	203.9	
101	.750	240	0	5400	*	212.2	
102	.750	240	0	5400	*	220.5	
103	.750	240	60	5127	2902	194.4	
104	.750	240	60	5400	*	165.4	
105	.750	240	70	5400	*	230.7	
106	.755	15	0	3420	0	*	
107	.755	30	60	5035	0	*	
108	.755	60	70	5415	0	*	
109	.755	120	70	3990	0	*	
110	.755	240	0	1425	0	*	
111	.755	240	60	2280	0	*	
112	.755	240	70	3135	0	*	

* not available

** not taken for this target material

Experimental Data

Table XIII: Steel Fragments Impacting on Magnesium (Cont)

Data No.	Material Thickness (e inches)	Fragment Weight m (grains)	Obliquity θ (degrees)	Striking Velocity V_s (fps)	Residual Velocity V_r (fps)	Residual Weight m_r (grains)	Hole Size Area ** (sq. in.)
113	.755	240	80	6840	0	*	
114	1.000	30	0	4506	1979	25.3	
115	1.000	30	0	5999	1375	23.1	
116	1.000	30	0	8194	3261	10.2	
117	1.000	30	0	9484	3822	9.1	
118	1.000	60	0	4084	1468	57.9	
119	1.000	60	0	5000	*	59.0	
120	1.000	120	0	4872	2693	104.5	
121	1.000	120	0	5000	*	98.0	
122	1.000	120	0	5000	*	104.5	
123	1.000	120	0	5000	*	119.0	
124	1.000	120	45	4847	1795	102.6	
125	1.000	120	45	5000	*	103.7	
126	1.000	120	60	5000	*	105.2	
127	1.000	120	60	5000	*	106.5	
128	1.000	120	60	7417	406	*	
129	1.000	240	0	4627	3218	220.8	
130	1.000	240	0	4649	1764	214.7	
131	1.000	240	45	4763	2731	202.2	
132	1.000	240	60	5000	*	185.0	
133	1.000	240	60	5227	2208	*	
134	1.000	240	70	9477	3640	*	
135	1.000	240	70	9498	2549	*	
136	2.000	120	0	4849	654	107.9	
137	2.000	120	0	5000	*	100.8	
138	2.000	120	0	5000	*	100.9	
139	2.000	120	0	5000	*	101.2	
140	2.000	120	0	5000	*	105.2	

* not available

** not taken for this target material

Experimental Data

Table XIII: Steel Fragments Impacting on Magnesium (Cont)

Data No.	Material Thickness (e inches)	Fragment Weight m (grains)	Obliquity θ (degrees)	Striking Velocity V_s (fps)	Residual Velocity V_r (fps)	Residual Weight m_r (grains)	Hole Size Area ** (sq. in.)
141	2.000	120	0	5000	*	106.9	
142	2.000	120	0	5000	*	112.0	
143	2.000	120	0	7280	780	*	
144	2.000	240	0	4718	1879	198.3	
145	2.000	240	0	5000	*	213.3	
146	2.000	240	0	5000	*	219.0	
147	2.000	240	45	5500	*	174.7	
148	2.000	240	45	5500	*	190.1	
149	2.000	240	45	9639	5846	*	
150	3.000	240	0	10403	4186	*	

* not available

** not taken for this target material

Experimental Data

Table XIV: Steel Fragments Impacting on Aluminum Alloys

Data No.	Alloy	Material Thickness e (inches)	Fragment Weight m (grains)	Obliquity θ (degrees)	Striking Velocity V_s (fps)	Residual Velocity V_r (fps)	Residual Weight m_r (grains)	Hole Size Area (sq. in.)
1	2SO	.125	30	0	1897	1648	**	**
2	2SO	.125	30	0	1913	1674	**	**
3	2SO	.125	30	0	4665	4337	**	**
4	2SO	.125	30	0	4668	4386	**	**
5	2SO	.125	30	60	4906	3749	**	**
6	2SO	.125	30	60	4908	3621	**	**
7	2SO	.125	30	70	4967	3360	**	**
8	2SO	.125	30	70	4981	3324	**	**
9	2SO	.125	60	0	5037	4620	**	**
10	2SO	.125	60	0	5082	4731	**	**
11	2SO	.125	240	0	4051	3919	**	**
12	2SO	.125	240	0	4129	4024	**	**
13	2SO	1.000	240	0	5038	3278	**	**
14	2SO	1.000	240	0	5042	3348	**	**
15	2SO	2.000	240	0	6032	1590	**	**
16	2SO	2.000	240	0	6056	116	**	**
17	2SO	2.000	240	0	6065	119	**	**
18	2SO	2.000	240	0	6086	1771	**	**
19	2024T-3	.020	5	60	2108	**	4.0	.018
20	2024T-3	.020	5	70	2740	**	4.0	.031
21	2024T-3	.020	5	70	3080	**	4.0	.037
22	2024T-3	.020	5	70	3333	**	4.0	.037
23	2024T-3	.020	30	0	8160	**	13.2	.077
24	2024T-3	.020	30	60	7656	**	26.1	.221
25	2024T-3	.020	30	70	9185	**	17.8	.387
26	2024T-3	.020	30	80	600	0	**	**
27	2024T-3	.020	60	0	8280	**	54.7	.129
28	2024T-3	.020	120	0	9457	**	36.7	.221
29	2024T-3	.020	240	80	280	0	**	**
30	2024T-3	.072	15	70	5722	**	5.3	.230

** not taken

Experimental Data

Table XIV: Steel Fragments Impacting on Aluminum Alloys (Cont)

Data No.	Alloy	Material Thickness e (inches)	Fragment Weight m (grains)	Obliquity θ (degrees)	Striking Velocity V_s (fps)	Residual Velocity V_r (fps)	Residual Weight m_r (grains)	Hole Size Area (sq. in.)
31	2024T-3	.072	30	0	8202	**	2.0	.150
32	2024T-3	.072	30	0	8240	**	26.7	.107
33	2024T-3	.072	30	60	9240	**	7.5	.500
34	2024T-3	.072	30	70	3702	**	29.0	.370
35	2024T-3	.072	30	70	5468	4278	**	**
36	2024T-3	.072	30	70	5543	3742	**	**
37	2024T-3	.072	30	70	9662	**	4.6	.408
38	2024T-3	.072	30	80	2986	**	29.0	**
39	2024T-3	.072	30	80	3200	0	**	**
40	2024T-3	.072	30	80	3202	**	29.0	**
41	2024T-3	.072	30	80	3280	**	29.0	**
42	2024T-3	.072	30	80	3409	**	29.0	**
43	2024T-3	.072	30	80	3486	**	29.0	**
44	2024T-3	.072	60	0	10049	**	9.9	.190
45	2024T-3	.072	60	60	8178	**	17.1	.497
46	2024T-3	.072	60	70	2949	**	55.6	.690
47	2024T-3	.072	60	70	5125	3688	**	**
48	2024T-3	.072	60	70	5191	3590	**	**
49	2024T-3	.072	60	70	8496	**	9.5	.828
50	2024T-3	.072	120	70	5918	4505	**	**
51	2024T-3	.072	120	70	6020	4510	**	**
52	2024T-3	.072	240	0	9847	**	14.3	.442
53	2024T-3	.072	240	70	5942	5066	**	**
54	2024T-3	.072	240	70	5953	5135	**	**
55	2024T-3	.072	240	80	850	0	**	**
56	2024T-3	.091	30	70	2500	0	**	**
57	2024T-3	.091	30	70	2508	**	28.8	**
58	2024T-3	.091	30	70	2510	**	28.8	**
59	2024T-3	.091	30	70	2627	**	28.6	**
60	2024T-3	.091	30	70	2714	**	28.5	**

** not taken

Experimental Data

Table XIV: Steel Fragments Impacting on Aluminum Alloys (Cont)

Data No.	Alloy	Material Thickness e (inches)	Fragment Weight m (grains)	Obliquity θ (degrees)	Striking Velocity V_s (fps)	Residual Velocity V_r (fps)	Residual Weight m_r (grains)	Hole Size Area (sq. in.)
61	2024T-3	.091	30	70	2915	**	29.0	**
62	2024T-3	.091	30	70	3013	**	28.9	**
63	2024T-3	.091	60	0	736	**	59.0	**
64	2024T-3	.091	60	0	835	**	59.0	**
65	2024T-3	.091	60	0	843	**	59.0	**
66	2024T-3	.091	60	0	983	**	59.0	**
67	2024T-3	.091	60	0	1064	**	59.0	**
68	2024T-3	.091	60	45	797	**	59.0	**
69	2024T-3	.091	60	45	799	**	59.0	**
70	2024T-3	.091	60	45	859	**	59.0	**
71	2024T-3	.091	60	45	1039	**	59.0	**
72	2024T-3	.091	60	45	1081	**	59.0	**
73	2024T-3	.091	60	45	1223	**	59.0	**
74	2024T-3	.091	60	60	1176	**	59.0	**
75	2024T-3	.091	60	60	1244	**	59.0	**
76	2024T-3	.091	60	60	1250	0	**	**
77	2024T-3	.091	60	60	1268	**	59.0	**
78	2024T-3	.091	60	60	1273	**	59.0	**
79	2024T-3	.091	60	60	1315	**	59.0	**
80	2024T-3	.091	60	60	1319	**	59.0	**
81	2024T-3	.091	60	70	1409	**	59.0	**
82	2024T-3	.091	60	70	1609	**	59.0	**
83	2024T-3	.091	60	70	1718	**	59.0	**
84	2024T-3	.091	60	70	1790	**	59.0	**
85	2024T-3	.091	60	70	1797	**	58.8	**
86	2024T-3	.091	60	70	1800	0	**	**
87	2024T-3	.091	60	70	1801	**	58.7	**
88	2024T-3	.091	60	70	1819	**	58.9	**
89	2024T-3	.091	60	70	1821	**	59.0	**
90	2024T-3	.091	60	70	1825	**	59.0	**

** not taken

Experimental Data

Table XIV: Steel Fragments Impacting on Aluminum Alloys (Cont)

Data No.	Alloy	Material Thickness e (inches)	Fragment Weight m (grains)	Obliquity θ (degrees)	Striking Velocity V_s (fps)	Residual Velocity V_r (fps)	Residual Weight m_r (grains)	Hole Size Area (sq. in.)
91	2024T-3	.091	60	70	1830	**	58.8	**
92	2024T-3	.091	60	70	1841	**	59.0	**
93	2024T-3	.091	60	70	1850	0	**	**
94	2024T-3	.091	60	70	1850	0	**	**
95	2024T-3	.091	60	70	1852	**	59.0	**
96	2024T-3	.091	60	70	1897	**	59.0	**
97	2024T-3	.091	60	70	1916	**	59.0	**
98	2024T-3	.091	60	70	1923	**	59.0	**
99	2024T-3	.091	60	70	1995	**	58.8	**
100	2024T-3	.091	60	70	1999	**	59.0	**
101	2024T-3	.091	60	70	2001	**	59.0	**
102	2024T-3	.091	60	70	2030	**	59.0	**
103	2024T-3	.091	60	70	2040	**	59.0	**
104	2024T-3	.091	60	70	2083	**	59.0	**
105	2024T-3	.091	60	70	2177	**	59.0	**
106	2024T-3	.091	60	70	2241	**	59.0	**
107	2024T-3	.091	60	70	2938	**	59.0	**
108	2024T-3	.091	120	0	553	**	119.0	**
109	2024T-3	.091	120	0	636	**	119.0	**
110	2024T-3	.091	120	0	762	**	119.0	**
111	2024T-3	.091	120	0	851	**	119.0	**
112	2024T-3	.091	120	0	907	**	119.0	**
113	2024T-3	.091	120	70	1208	**	119.0	**
114	2024T-3	.091	120	70	1242	**	119.0	**
115	2024T-3	.091	120	70	1262	**	119.0	**
116	2024T-3	.091	120	70	1300	0	**	**
117	2024T-3	.091	120	70	1358	**	119.0	**
118	2024T-3	.091	120	70	1380	**	119.0	**
119	2024T-3	.091	120	70	1481	**	119.0	**
120	2024T-3	.091	240	70	965	0	**	**

** not taken

Experimental Data

Table XIV: Steel Fragments Impacting on Aluminum Alloys (Cont)

Data No.	Alloy	Material Thickness e (inches)	Fragment Weight m (grains)	Obliquity θ (degrees)	Striking Velocity V_s (fps)	Residual Velocity V_r (fps)	Residual Weight m_r (grains)	Hole Size Area (sq. in.)
121	2024T-3	.091	240	80	1150	0	**	**
122	2024T-3	.091	240	80	4262	**	238.3	**
123	2024T-3	.091	240	80	5767	**	217.1	**
124	2024T-3	.125	5	0	4737	**	4.0	.028
125	2024T-3	.125	15	60	5784	**	7.5	.240
126	2024T-3	.125	15	70	6041	**	1.4	.221
127	2024T-3	.125	30	0	1109	854	**	**
128	2024T-3	.125	30	0	1791	1302	**	**
129	2024T-3	.125	30	0	2992	2372	**	**
130	2024T-3	.125	30	0	3661	3124	**	**
131	2024T-3	.125	30	0	8464	**	19.3	.172
132	2024T-3	.125	30	0	8793	**	1.4	.260
133	2024T-3	.125	30	0	9389	**	2.6	.371
134	2024T-3	.125	60	60	9505	**	4.4	.877
135	2024T-3	.125	60	70	8377	**	13.7	.828
136	2024T-3	.125	60	70	8602	**	5.6	.730
137	2024T-3	.125	60	70	8891	**	1.2	.920
138	2024T-3	.125	60	70	9683	**	0.0	.466
139	2024T-3	.125	120	0	1828	1471	**	**
140	2024T-3	.125	120	0	3011	2694	**	**
141	2024T-3	.125	120	0	3939	3461	**	**
142	2024T-3	.125	120	70	3794	2524	**	**
143	2024T-3	.125	120	70	4972	2847	**	**
144	2024T-3	.125	120	70	5654	3330	**	**
145	2024T-3	.125	120	70	5923	3563	**	**
146	2024T-3	.125	240	70	5955	4208	**	**
147	2024T-3	.125	240	70	5965	4089	**	**
148	2024T-3	.125	240	70	6064	4527	**	**
149	2024T-3	.188	30	0	1791	1024	**	**
150	2024T-3	.188	30	0	2862	1890	**	**

** not taken

Experimental Data

Table XIV: Steel Fragments Impacting on Aluminum Alloys (Cont)

Data No.	Alloy	Material Thickness e (inches)	Fragment Weight m (grains)	Obliquity θ (degrees)	Striking Velocity V_s (fps)	Residual Velocity V_r (fps)	Residual Weight m_r (grains)	Hole Size Area (sq. in.)
151	2024T-3	.188	30	0	2889	2064	**	**
152	2024T-3	.188	30	0	2893	2035	**	**
153	2024T-3	.188	30	0	3880	3021	**	**
154	2024T-3	.188	30	0	5302	4455	**	**
155	2024T-3	.188	30	0	5388	4547	**	**
156	2024T-3	.188	30	45	5369	4001	**	**
157	2024T-3	.188	30	45	5488	4029	**	**
158	2024T-3	.188	30	70	3000	0	**	**
159	2024T-3	.188	120	0	1904	1460	**	**
160	2024T-3	.188	120	0	3034	2531	**	**
161	2024T-3	.188	120	0	3930	3390	**	**
162	2024T-3	.188	120	70	6022	2983	**	**
163	2024T-3	.188	120	70	6044	2945	**	**
164	2024T-3	.188	240	0	5707	5199	**	**
165	2024T-3	.188	240	0	5828	5167	**	**
166	2024T-3	.188	240	0	5877	5283	**	**
167	2024T-3	.188	240	70	5965	4436	**	**
168	2024T-3	.188	240	70	5983	3883	**	**
169	2024T-3	.188	240	70	6055	3421	**	**
170	2024T-3	.188	240	75	2900	0	**	**
171	2024T-3	.250	5	0	5338	**	4.0	**
172	2024T-3	.250	15	60	6525	**	0.9	.190
173	2024T-3	.250	30	0	1961	949	**	**
174	2024T-3	.250	30	0	1994	972	**	**
175	2024T-3	.250	30	0	2014	951	**	**
176	2024T-3	.250	30	0	3334	2110	**	**
177	2024T-3	.250	30	0	3356	2100	**	**
178	2024T-3	.250	30	0	3502	2145	**	**
179	2024T-3	.250	30	0	4677	3326	**	**
180	2024T-3	.250	30	0	4701	3376	**	**

** not taken

Experimental Data

Table XIV: Steel Fragments Impacting on Aluminum Alloys (Cont)

Data No.	Alloy	Material Thickness e (inches)	Fragment Weight m (grains)	Obliquity θ (degrees)	Striking Velocity V_s (fps)	Residual Velocity V_r (fps)	Residual Weight m_r (grains)	Hole Size Area (sq. in.)
181	2024T-3	.250	30	0	4747	3453	**	**
182	2024T-3	.250	30	0	5416	2709	**	**
183	2024T-3	.250	30	0	5478	2501	**	**
184	2024T-3	.250	30	70	4000	0	**	**
185	2024T-3	.250	30	70	5296	**	7.4	**
186	2024T-3	.250	30	70	6535	**	1.1	**
187	2024T-3	.250	60	0	2078	1240	**	**
188	2024T-3	.250	60	0	2388	1503	**	**
189	2024T-3	.250	60	0	2891	1854	**	**
190	2024T-3	.250	60	0	3829	2891	**	**
191	2024T-3	.250	60	0	4033	2991	**	**
192	2024T-3	.250	60	0	4860	3925	**	**
193	2024T-3	.250	60	60	3187	**	59.0	**
194	2024T-3	.250	60	60	3482	**	59.0	**
195	2024T-3	.250	60	60	3483	**	47.6	**
196	2024T-3	.250	60	60	3500	0	**	**
197	2024T-3	.250	60	60	3552	**	50.5	**
198	2024T-3	.250	60	60	3552	**	59.0	**
199	2024T-3	.250	60	60	3580	**	47.1	**
200	2024T-3	.250	60	60	3608	**	58.3	**
201	2024T-3	.250	60	60	3700	**	47.8	**
202	2024T-3	.250	60	60	3717	**	46.9	**
203	2024T-3	.250	60	60	6012	**	5.9	.552
204	2024T-3	.250	60	70	5296	**	7.4	**
205	2024T-3	.250	120	0	1779	1245	**	**
206	2024T-3	.250	120	0	1813	1331	**	**
207	2024T-3	.250	120	0	3092	2339	**	**
208	2024T-3	.250	120	0	3403	2541	**	**
209	2024T-3	.250	120	0	4993	4207	**	**
210	2024T-3	.250	120	0	5148	4374	**	**

** not taken

Experimental Data

Table XIV: Steel Fragments Impacting on Aluminum Alloys (Cont)

Data No.	Alloy	Material Thickness e (inches)	Fragment Weight m (grains)	Obliquity θ (degrees)	Striking Velocity V_s (fps)	Residual Velocity V_r (fps)	Residual Weight m_r (grains)	Hole Size Area (sq. in.)
211	2024T-3	.250	120	0	5196	4196	**	**
212	2024T-3	.250	120	70	6013	**	2.5	.700
213	2024T-3	.250	240	0	1978	1685	**	**
214	2024T-3	.250	240	0	2083	1739	**	**
215	2024T-3	.250	240	0	3594	3017	**	**
216	2024T-3	.250	240	0	3672	3105	**	**
217	2024T-3	.250	240	0	4884	4251	**	**
218	2024T-3	.250	240	0	4908	4330	**	**
219	2024T-3	.250	240	70	2526	**	238.8	**
220	2024T-3	.250	240	70	2845	**	223.4	**
221	2024T-3	.250	240	70	3030	**	239.0	**
222	2024T-3	.250	240	70	3058	**	222.5	**
223	2024T-3	.250	240	70	3200	0	**	**
224	2024T-3	.250	240	70	3227	**	180.4	**
225	2024T-3	.250	240	70	3261	**	168.9	**
226	2024T-3	.250	240	70	3623	**	163.4	**
227	2024T-3	.250	240	70	6128	3053	**	**
228	2024T-3	.250	240	70	6182	3257	**	**
229	2024T-3	.375	30	60	4300	0	**	**
230	2024T-3	.375	30	60	4500	0	**	**
231	2024T-3	.375	30	70	5600	0	**	**
232	2024T-3	.375	60	70	7890	**	11.6	**
233	2024T-3	.375	240	70	3292	**	165.2	**
234	2024T-3	.500	30	0	3786	1083	**	**
235	2024T-3	.500	30	0	3808	1135	**	**
236	2024T-3	.500	30	0	4732	2267	**	**
237	2024T-3	.500	30	0	4576	2057	**	**
238	2024T-3	.500	30	60	8685	**	0.8	**
239	2024T-3	.500	60	0	3064	928	**	**
240	2024T-3	.500	60	0	3568	1328	**	**

** not taken

Experimental Data

Table XIV: Steel Fragments Impacting on Aluminum Alloys (Cont)

Data No.	Alloy	Material Thickness e (inches)	Fragment Weight m (grains)	Obliquity θ (degrees)	Striking Velocity V_s (fps)	Residual Velocity V_r (fps)	Residual Weight m_r (grains)	Hole Size Area (sq. in.)
241	2024T-3	.500	60	0	4853	2730	**	**
242	2024T-3	.500	60	0	4890	2851	**	**
243	2024T-3	.500	60	0	5977	**	28.2	.371
244	2024T-3	.500	60	45	1951	**	58.9	**
245	2024T-3	.500	60	45	3344	**	54.0	**
246	2024T-3	.500	60	45	3483	**	49.2	**
247	2024T-3	.500	60	45	3584	**	44.2	**
248	2024T-3	.500	60	45	3670	**	45.3	**
249	2024T-3	.500	60	45	3719	**	57.0	**
250	2024T-3	.500	60	45	3726	**	46.6	**
251	2024T-3	.500	60	45	3837	**	50.3	**
252	2024T-3	.500	60	45	4015	**	53.3	**
253	2024T-3	.500	60	45	4217	**	48.2	**
254	2024T-3	.500	60	45	4295	**	47.2	**
255	2024T-3	.500	60	45	4420	**	56.0	**
256	2024T-3	.500	60	60	4533	**	222.1	**
257	2024T-3	.500	60	60	4908	**	175.6	**
258	2024T-3	.500	60	60	5300	0	**	**
259	2024T-3	.500	60	60	5369	**	37.9	**
260	2024T-3	.500	120	0	3446	1764	**	**
261	2024T-3	.500	120	0	3509	1785	**	**
262	2024T-3	.500	120	0	4932	3226	**	**
263	2024T-3	.500	120	0	5001	3258	**	**
264	2024T-3	.500	120	60	5926	**	20.4	.230
265	2024T-3	.500	240	0	2070	1151	**	**
266	2024T-3	.500	240	0	2079	1183	**	**
267	2024T-3	.500	240	0	3479	2378	**	**
268	2024T-3	.500	240	0	3503	2344	**	**
269	2024T-3	.500	240	0	4905	3857	**	**
270	2024T-3	.500	240	0	4908	3736	**	**

** not taken

Experimental Data

Table XIV: Steel Fragments Impacting on Aluminum Alloys (Cont)

Data No.	Alloy	Material Thickness e (inches)	Fragment Weight m (grains)	Obliquity θ (degrees)	Striking Velocity V_s (fps)	Residual Velocity V_r (fps)	Residual Weight m_r (grains)	Hole Size Area (sq. in.)
271	2024T-3	.500	240	45	2662	**	229.8	**
272	2024T-3	.500	240	45	2756	**	216.1	**
273	2024T-3	.500	240	45	2766	**	219.5	**
274	2024T-3	.500	240	45	2775	**	238.6	**
275	2024T-3	.500	240	45	2812	**	226.9	**
276	2024T-3	.500	240	45	2842	**	237.2	**
277	2024T-3	.500	240	60	2557	**	175.6	**
278	2024T-3	.500	240	60	2638	**	222.1	**
279	2024T-3	.500	240	60	3083	**	174.9	**
280	2024T-3	.500	240	60	3280	**	179.0	**
281	2024T-3	.500	240	60	3300	0	**	**
282	2024T-3	.500	240	60	3310	**	184.1	**
283	2024T-3	.500	240	60	3361	**	179.9	**
284	2024T-3	.500	240	60	3421	**	182.1	**
285	2024T-3	.500	240	60	4837	**	94.7	**
286	2024T-3	.500	240	60	4869	**	73.2	**
287	2024T-3	.500	240	60	4935	**	94.0	**
288	2024T-3	.500	240	70	4700	0	**	**
289	2024T-3	.750	60	0	4845	1183	**	**
290	2024T-3	.750	60	0	4866	1421	**	**
291	2024T-3	.750	120	0	3302	661	**	**
292	2024T-3	.750	120	0	3482	521	**	**
293	2024T-3	.750	120	0	4942	2159	**	**
294	2024T-3	.750	120	0	4990	2187	**	**
295	2024T-3	.750	240	0	3422	1747	**	**
296	2024T-3	.750	240	0	3500	1618	**	**
297	2024T-3	.750	240	0	3547	1750	**	**
298	2024T-3	.750	240	0	4911	3119	**	**
299	2024T-3	.750	240	0	4940	3086	**	**
300	2024T-3	.750	240	60	4537	**	159.5	**

** not taken

Experimental Data

Table XIV: Steel Fragments Impacting on Aluminum Alloys (Cont)

Data No.	Alloy	Material Thickness e (inches)	Fragment Weight m (grains)	Obliquity θ (degrees)	Striking Velocity V_s (fps)	Residual Velocity V_r (fps)	Residual Weight m_r (grains)	Hole Size Area (sq. in.)
301	2024T-3	.750	240	60	4850	0	**	**
302	2024T-3	.750	240	60	4866	**	143.6	**
303	2024T-3	.750	240	60	4893	**	156.3	**
304	2024T-3	.750	240	60	4920	**	159.3	**
305	2024T-3	.750	240	60	5083	**	151.9	**
306	2024T-3	1.000	30	0	6840	0	**	**
307	2024T-3	1.000	30	0	8748	**	9.0	.129
308	2024T-3	1.000	30	45	12000	0	**	**
309	2024T-3	1.000	60	0	7511	**	1.9	.249
310	2024T-3	1.000	120	0	3850	0	**	**
311	2024T-3	1.000	120	0	4857	**	116.1	**
312	2024T-3	1.000	120	0	4878	**	59.3	**
313	2024T-3	1.000	120	0	4894	**	66.8	**
314	2024T-3	1.000	120	0	4931	**	105.1	**
315	2024T-3	1.000	120	0	4968	1380	**	**
316	2024T-3	1.000	120	0	5024	**	57.1	**
317	2024T-3	1.000	120	0	5085	**	63.5	**
318	2024T-3	1.000	120	0	5575	**	28.7	.519
319	2024T-3	1.000	120	0	9990	1058	**	**
320	2024T-3	1.000	120	45	6500	0	**	**
321	2024T-3	1.000	120	60	8800	0	**	**
322	2024T-3	1.000	240	0	3200	0	**	**
323	2024T-3	1.000	240	0	3483	754	**	**
324	2024T-3	1.000	240	0	3502	806	**	**
325	2024T-3	1.000	240	0	3508	493	**	**
326	2024T-3	1.000	240	0	3586	706	**	**
327	2024T-3	1.000	240	0	4949	2187	**	**
328	2024T-3	1.000	240	0	4980	2209	**	**
329	2024T-3	1.000	240	45	4300	0	**	**
330	2024T-3	1.000	240	45	4500	0	**	**

** not taken

Experimental Data

Table XIV: Steel Fragments Impacting on Aluminum Alloys (Cont)

Data No.	Alloy	Material Thickness e (inches)	Fragment Weight m (grains)	Obliquity θ (degrees)	Striking Velocity V_s (fps)	Residual Velocity V_r (fps)	Residual Weight m_r (grains)	Hole Size Area (sq. in.)
331	2024T-3	1.000	240	60	5600	0	**	**
332	2024T-3	1.000	240	70	8000	0	**	**
333	2024T-3	1.250	60	60	3562	**	54.9	.344
334	2024T-3	1.250	60	70	4042	**	18.9	**
335	2024T-3	1.250	30	0	12000	0	**	**
336	2024T-3	1.500	120	0	7800	0	**	**
337	2024T-3	2.000	120	0	12000	0	**	**
338	2024T-3	2.000	240	0	7000	0	**	**
339	2024T-3	2.000	240	45	10000	0	**	**
340	2024T-3	3.000	240	0	12500***	0	**	**
341	7075T-6	.125	30	0	1859	1593	**	**
342	7075T-6	.125	30	0	1886	1589	**	**
343	7075T-6	.125	30	0	4596	4170	**	**
344	7075T-6	.125	30	0	4787	4347	**	**
345	7075T-6	.125	30	60	4773	3326	**	**
346	7075T-6	.125	30	60	4796	3392	**	**
347	7075T-6	.125	30	70	4795	2243	**	**
348	7075T-6	.125	30	70	4897	2054	**	**
349	7075T-6	.125	60	0	4887	4504	**	**
350	7075T-6	.125	60	0	4914	4516	**	**
351	7075T-6	.125	240	0	4070	3895	**	**
352	7075T-6	.125	240	0	4113	3955	**	**
353	7075T-6	.125	240	0	5046	4829	**	**
354	7075T-6	.125	240	0	5070	4917	**	**
355	7075T-6	.250	30	0	4797	3772	**	**
356	7075T-6	.250	30	0	4923	3840	**	**
357	7075T-6	.500	30	0	4921	2226	**	**
358	7075T-6	.500	30	0	4994	2260	**	**

** not taken

*** extrapolated

Experimental Data

Table XV: Steel Fragments Impacting on Titanium Alloy

Data No.	Material Thickness e (inches)	Fragment Weight m (grains)	Obliquity θ (degrees)	Striking Velocity V_s (fps)	Residual Velocity V_r (fps)	Residual Weight m_r (grains)	Hole Size Area ** (sq. in.)
1	.038	30	70	1350	0	*	
2	.050	30	0	1863	1710	29.0	
3	.050	30	0	2000	*	28.7	
4	.050	30	0	2000	*	29.0	
5	.050	30	0	2000	*	29.0	
6	.050	30	0	2000	*	29.0	
7	.050	30	0	2000	*	29.0	
8	.050	30	0	2000	*	29.0	
9	.050	30	0	4796	4246	14.0	
10	.050	30	0	5000	*	20.8	
11	.050	30	45	4511	3900	27.9	
12	.050	30	60	2950	1945	24.7	
13	.050	30	60	2989	2073	25.9	
14	.050	30	70	2970	1461	21.3	
15	.050	30	70	3000	*	24.5	
16	.050	30	70	3000	*	25.5	
17	.050	60	0	2621	2207	59.0	
18	.050	60	0	3000	*	59.0	
19	.050	60	0	3000	*	59.0	
20	.050	60	0	3000	*	59.0	
21	.050	60	0	3388	3142	26.5	
22	.050	60	0	5500	*	44.4	
23	.050	60	0	5500	*	49.1	
24	.050	60	0	5500	*	51.9	
25	.050	60	0	5500	*	55.6	
26	.050	60	60	2500	1803	58.3	
27	.050	60	60	3000	*	58.3	
28	.050	60	70	2398	1467	59.0	

* not available

** not taken for this target material

Table XV: Steel Fragments Impacting on Titanium Alloy (Cont)

Data No.	Material Thickness e (inches)	Fragment Weight m (grains)	Obliquity θ (degrees)	Striking Velocity V_s (fps)	Residual Velocity V_r (fps)	Residual Weight m_r (grains)	Hole Size Area ** (sq. in.)
29	.050	120	0	2000	*	119.0	
30	.050	120	0	2000	*	119.0	
31	.050	120	0	2000	*	119.0	
32	.050	120	0	2000	*	119.0	
33	.050	120	0	2000	*	119.0	
34	.050	120	0	2000	*	119.0	
35	.050	120	0	2000	*	119.0	
36	.050	120	0	2000	*	119.0	
37	.050	120	0	2103	1842	119.0	
38	.050	120	0	3147	2870	119.0	
39	.050	120	0	5000	*	32.3	
40	.050	120	45	2755	2349	118.7	
41	.050	120	45	3000	*	119.0	
42	.050	120	60	2240	1686	119.0	
43	.050	120	70	2179	1303	*	
44	.050	240	0	3500	*	230.6	
45	.050	240	0	3500	*	239.0	
46	.059	30	60	1500	0	*	
47	.059	30	70	2000	0	*	
48	.059	30	80	4800	0	*	
49	.059	240	60	700	0	*	
50	.059	240	70	925	0	*	
51	.059	240	80	1800	0	*	
52	.082	240	70	1150	0	*	
53	.100	30	0	3000	*	29.0	
54	.100	30	0	3000	*	29.0	
55	.100	30	0	3000	*	29.0	
56	.100	30	0	5000	*	26.4	

* not available

** not taken for this target material

[redacted]

[redacted]

Experimental Data

Table XV: Steel Fragments Impacting on Titanium Alloy (Cont)

Data No.	Material Thickness e (inches)	Fragment Weight m (grains)	Obliquity θ (degrees)	Striking Velocity V_s (fps)	Residual Velocity V_r (fps)	Residual Weight m_r (grains)	Hole Size Area ** (sq. in.)
57	.100	30	60	5000	*	14.5	
58	.100	30	60	5000	*	16.7	
59	.100	60	60	4000	*	54.2	
60	.100	120	0	2500	*	119.0	
61	.100	120	0	2500	*	119.0	
62	.100	120	0	5000	*	60.3	
63	.100	120	60	3000	*	50.5	
64	.125	30	0	2888	1937	*	
65	.125	30	0	3000	*	25.3	
66	.125	30	0	3000	*	29.0	
67	.125	30	0	4447	3555	25.1	
68	.125	30	45	4491	3156	25.8	
69	.125	30	70	10223	*	0.4	
70	.125	60	0	2035	1643	59.0	
71	.125	60	0	2537	1912	58.8	
72	.125	60	0	3000	*	56.9	
73	.125	60	0	3000	*	59.0	
74	.125	60	0	3000	*	59.0	
75	.125	60	0	3000	*	59.0	
76	.125	60	0	4918	4107	37.5	
77	.125	60	60	3474	1746	46.5	
78	.125	60	60	5000	*	43.2	
79	.125	120	0	2000	*	119.0	
80	.125	120	0	2000	*	119.0	
81	.125	120	0	2000	*	119.0	
82	.125	120	0	3202	2577	119.0	
83	.125	120	0	3500	*	118.2	
84	.125	120	0	3500	*	118.4	
85	.125	120	0	3500	*	119.0	

* not available

** not taken for this target material

Table XV: Steel Fragments Impacting on Titanium Alloy (Cont)

Data No.	Material Thickness e (inches)	Fragment Weight m (grains)	Obliquity θ (degrees)	Striking Velocity V_s (fps)	Residual Velocity V_r (fps)	Residual Weight m_r (grains)	Hole Size Area ** (sq. in.)
86	.125	120	0	4000	*	115.1	
87	.125	120	0	4000	*	117.3	
88	.125	120	0	4000	*	117.4	
89	.125	120	0	5000	*	33.4	
90	.125	120	45	3896	2910	108.5	
91	.125	120	60	3000	*	30.6	
92	.125	120	60	3000	*	96.1	
93	.125	120	70	2500	*	118.8	
94	.125	120	70	3500	*	87.7	
95	.125	240	0	2000	*	239.0	
96	.125	240	0	2000	*	239.0	
97	.125	240	0	3500	*	237.0	
98	.125	240	0	3500	*	238.3	
99	.125	240	0	3500	*	238.4	
100	.125	240	0	3500	*	239.0	
101	.125	240	45	4000	*	224.6	
102	.125	240	45	4337	3388	218.5	
103	.125	240	60	3103	1549	42.7	
104	.125	240	60	3157	2498	189.5	
105	.250	30	0	4892	2242	26.7	
106	.250	30	0	6517	3698	8.6	
107	.250	30	60	10447	2636	4.3	
108	.250	60	0	4940	2541	50.0	
109	.250	60	0	5007	3213	*	
110	.250	60	0	5500	*	45.4	
111	.250	60	0	8055	4486	1.9	
112	.250	60	60	9963	3112	*	
113	.250	120	0	4870	3264	*	

* not available

** not taken for this target material

[redacted]

[redacted]

Experimental Data

Table XV: Steel Fragments Impacting on Titanium Alloy (Cont)

Data No.	Material Thickness e (inches)	Fragment Weight m (grains)	Obliquity θ (degrees)	Striking Velocity V_s (fps)	Residual Velocity V_r (fps)	Residual Weight m_r (grains)	Hole Size Area ** (sq. in.)
114	.250	120	0	5000	*	69.9	
115	.250	120	0	5000	*	91.7	
116	.250	120	0	5000	*	102.9	
117	.250	120	0	5000	*	105.8	
118	.250	120	0	5000	*	106.0	
119	.250	120	0	5000	*	107.6	
120	.250	120	0	5000	*	108.0	
121	.250	120	45	4999	1136	74.5	
122	.250	240	45	5000	*	187.3	
123	.250	240	60	5056	2644	69.9	
124	.500	30	0	7781	1252	*	
125	.500	30	0	11142	*	1.2	
126	.500	60	0	8372	3825	8.8	
127	.500	60	60	9832	0	*	
128	.500	120	0	5000	*	83.0	
129	.500	240	45	4928	631	*	
130	.500	240	45	5000	*	117.6	
131	.985	240	0	5800	0	*	
132	1.202	240	45	8194	124	*	

* not available

** not taken for this target material

Experimental Data

Table XVI: Steel Fragments Impacting on Cast Iron

Data No.	Material Thickness e (inches)	Fragment Weight m (grains)	Obliquity θ (degrees)	Striking Velocity V_s (fps)	Residual Velocity V_r (fps)	Residual Weight m_r (grains)	Hole Size Area* (sq. in.)
1	.188	15	0	4316	1872	10.8	
2	.188	30	0	1880	634	29.5	
3	.188	30	0	3882	2191	23.3	
4	.188	30	0	5693	3770	13.7	
5	.188	30	45	3894	1275	19.3	
6	.188	60	0	2050	1243	59.1	
7	.188	60	0	4250	2934	50.1	
8	.188	60	0	5912	4281	36.6	
9	.188	60	45	4072	2309	14.1	
10	.188	60	45	5876	3375	31.0	
11	.188	240	0	1994	1392	235.8	
12	.188	240	0	3488	2795	214.9	
13	.188	240	0	5224	4291	183.1	
14	.188	240	45	4238	3301	181.8	
15	.188	240	45	6045	4635	160.8	
16	.375	30	0	3920	486	24.4	
17	.375	30	0	5778	1811	3.4	
18	.375	60	0	4099	1172	41.9	
19	.375	60	0	5826	2477	32.2	
20	.375	240	0	3890	2304	194.3	
21	.375	240	0	5912	3542	170.8	
22	.375	240	45	3547	1119	162.4	
23	.375	240	45	4091	1740	lost	
24	.375	240	45	6093	2915	lost	
25	.562	60	0	5822	1314	24.2	
26	.562	240	0	4057	1595	182.8	
27	.562	240	0	5957	2657	120.9	
28	.562	240	45	6103	1611	41.1	

* not taken for this target material.

Experimental Data

Table XVII: Steel Fragments Impacting on Face-Hardened Steel

Data No.	Material Thickness e (inches)	Fragment Weight m (grains)	Obliquity θ (degrees)	Striking Velocity V_s (fps)	Residual Velocity V_r (fps)	Residual Weight m_r (grains)	Hole Size Area (sq. in.)
1	.136	15	70	8789	*	0.0	.074
2	.136	30	0	2455	0	*	**
3	.136	30	0	3338	1221	25.4	.092
4	.136	30	0	3549	0	24.2	.110
5	.136	30	0	11067	*	1.7	.196
6	.136	30	45	5038	810	0.0	.147
7	.136	30	60	5673	0	*	.074
8	.136	30	70	8357	*	0.0	.092
9	.136	60	60	5173	0	*	.202
10	.136	60	70	6027	0	*	.049
11	.136	120	60	3272	0	*	.245
12	.136	120	60	3418	0	*	.515
13	.136	120	70	5350	0	*	.172
14	.136	120	70	5481	0	*	.730
15	.136	240	70	2367	0	*	.123
16	.136	240	70	3568	0	*	1.964
17	.136	240	70	5896	1617	0.0	1.117
18	.140	30	30	5213	1750	15.3	.147
19	.140	30	45	4889	1100	10.6	.171
20	.140	240	45	3903	2180	46.2	.430
21	.140	240	45	4004	2535	170.2	.589
22	.250	5	0	9500	0	*	.028
23	.250	15	0	7243	1859	2.0	.077
24	.250	15	0	10289	*	0.0	.150
25	.250	30	0	3521	*	7.3	**
26	.250	30	0	4209	*	7.3	**
27	.250	30	0	4284	*	16.0	**
28	.250	30	0	4500	*	9.8	**
29	.250	30	0	5791	1808	13.0	**
30	.250	30	0	5970	2351	6.6	**

* not available

** not taken

Experimental Data

Table XVII: Steel Fragments Impacting on Face-Hardened Steel (Cont)

Data No.	Material Thickness e (inches)	Fragment Weight m (grains)	Obliquity θ (degrees)	Striking Velocity V_s (fps)	Residual Velocity V_r (fps)	Residual Weight m_r (grains)	Hole Size Area (sq. in.)
31	.250	30	0	9454	3661	1.0	.249
32	.250	30	0	9633	4145	3.4	.249
33	.250	30	30	5196	1268	*	.150
34	.250	60	0	3053	*	10.0	**
35	.250	60	0	3173	*	11.2	**
36	.250	60	0	3279	*	10.8	**
37	.250	60	0	3500	0	*	*
38	.250	60	0	3818	1086	30.7	**
39	.250	60	0	5858	2517	5.3	**
40	.250	60	0	7058	2957	10.6	.307
41	.250	60	0	9184	4969	4.8	.307
42	.250	60	60	8359	*	0.0	**
43	.250	120	0	2508	*	16.0	**
44	.250	120	0	2857	*	22.5	**
45	.250	120	0	3776	1587	99.4	**
46	.250	120	0	5794	2856	21.5	**
47	.250	120	0	6225	3150	9.3	1.239
48	.250	120	0	9794	6704	3.4	.785
49	.250	120	45	4018	828	*	.368
50	.250	120	60	6926	0	*	**
51	.250	120	60	10069	1719	0.0	**
52	.250	240	0	3906	2294	146.0	**
53	.250	240	0	5369	3410	23.6	**
54	.250	240	45	5098	2000	103.8	.766
55	.250	240	45	5112	2137	104.5	.766
56	.250	240	60	5930	*	0.0	**
57	.250	240	70	9046	2875	1.4	.663
58	.250	240	70	9297	6059	*	**
59	.500	30	0	10665	*	1.8	.442
60	.500	60	0	5876	0	*	**

* not available

** not taken

Experimental Data

Table XVII: Steel Fragments Impacting on Face-Hardened Steel (Cont)

Data No.	Material Thickness e (inches)	Fragment Weight m (grains)	Obliquity θ (degrees)	Striking Velocity V_s (fps)	Residual Velocity V_r (fps)	Residual Weight m_r (grains)	Hole Size Area (sq. in.)
61	.500	60	0	7466	1000	17.7	.371
62	.500	60	0	8838	2276	2.0	.307
63	.500	120	0	5912	1211	101.1	**
64	.500	120	0	6845	1724	11.3	.479
65	.500	120	0	7300	2512	15.4	.515
66	.500	120	0	9453	3210	6.2	.601
67	.500	120	30	6034	672	12.1	.601
68	.500	240	0	3938	950	189.8	**
69	.500	240	0	6036	2330	115.3	**
70	.500	240	0	9032	4434	7.6	**
71	.500	240	30	5703	700	69.2	.785
72	.500	240	45	8051	*	0.0	.785
73	.500	240	60	8468	1827	1.5	.540

* not available

** not taken

Experimental Data

Table XVIII: Steel Fragments Impacting on Homogeneous Steel of Various Hardnesses

Data No.	Brinell Hardness Number	Material Thickness (e inches)	Fragment Weight m (grains)	Obliquity θ (degrees)	Striking Velocity V_s (fps)	Residual Velocity V_r (fps)	Residual Weight m_r (grains)	Hole Size Area (sq. in.)
1	90	.029	30	0	600	0	*	**
2	90	.061	30	0	900	0	*	**
3	92	.250	30	0	3200	0	*	**
4	100	.029	30	60	5325	4339	*	**
5	100	.029	30	60	5410	4674	*	**
6	100	.029	30	70	5340	3478	*	**
7	100	.029	30	70	5448	2576	*	**
8	100	.029	30	70	5570	3838	*	**
9	100	.060	60	60	5094	3280	*	**
10	100	.060	60	60	5135	3281	*	**
11	100	.060	120	60	5760	3782	*	**
12	100	.060	120	60	6007	3976	*	**
13	100	.060	120	70	5893	3384	*	**
14	100	.060	120	70	5979	2395	*	**
15	100	.060	120	70	6007	2981	*	**
16	100	.060	240	60	6050	4863	*	**
17	100	.060	240	60	6067	4866	*	**
18	100	.060	240	70	6016	4443	*	**
19	100	.060	240	70	6079	4158	*	**
20	100	.132	120	60	5944	2549	*	**
21	100	.132	120	60	5953	2600	*	**
22	100	.132	240	60	6064	3958	*	**
23	100	.132	240	60	6108	4075	*	**
24	100	.132	240	70	5902	3166	*	**
25	100	.132	240	70	6045	3291	*	**
26	105	.132	30	0	1650	0	*	**
27	105	.750	60	0	10,006	*	3.5	.601
28	107	.247	30	0	3250	0	*	**

* not available

** not taken

Experimental Data

Table XVIII: Steel Fragments Impacting on Homogeneous Steel of Various Hardnesses (Cont)

Data No.	Brinell Hardness Number	Material Thickness (e inches)	Fragment Weight m (grains)	Obliquity θ (degrees)	Striking Velocity V_s (fps)	Residual Velocity V_r (fps)	Residual Weight m_r (grains)	Hole Size Area (sq. in.)
29	110	.032	5	0	3562	*	4.0	.028
30	110	.032	15	0	4182	*	4.9	.150
31	110	.032	15	60	4272	*	9.9	.169
32	110	.032	15	70	5553	*	1.8	.387
33	110	.032	30	70	4823	*	12.0	.344
34	110	.032	60	70	4900	*	20.9	.736
35	110	.032	120	70	3718	*	93.9	1.930
36	110	.032	240	70	4216	*	186.6	1.632
37	110	.065	240	70	1100	0	*	**
38	110	1.000	120	0	9282	*	0.0	.442
39	110	1.000	240	0	9189	*	25.2	.982
40	115	.100	15	0	5573	*	0.4	.767
41	115	.100	15	0	8408	*	0.0	.150
42	115	.100	30	0	5330	*	1.0	.196
43	115	.100	30	60	5401	*	1.9	.258
44	115	.100	30	70	8791	*	0.0	.301
45	115	.100	60	60	5183	*	9.8	.442
46	115	.100	60	70	6803	*	0.0	.442
47	115	.100	120	70	6052	*	0.0	.957
48	115	.100	240	70	4947	*	26.4	1.571
49	120	.250	30	0	5085	*	6.8	.196
50	120	.250	30	60	9969	*	0.0	.202
51	120	.250	60	0	5200	*	2.6	.371
52	120	.250	60	60	9286	*	0.0	.442
53	120	.250	120	45	5987	*	19.0	.626
54	120	.250	240	70	8751	*	0.0	1.178
55	120	.500	60	0	8534	*	11.1	.601
56	120	.500	120	0	5986	*	8.2	.601

* not available

** not taken

Experimental Data

Table XVIII: Steel Fragments Impacting on Homogeneous Steel of Various Hardnesses (Cont)

Data No.	Brinell Hardness Number	Material Thickness (e inches)	Fragment Weight m (grains)	Obliquity θ (degrees)	Striking Velocity V_s (fps)	Residual Velocity V_r (fps)	Residual Weight m_r (grains)	Hole Size Area (sq. in.)
57	120	.500	240	0	5760	*	57.4	.887
58	125	.375	30	0	6351	*	14.1	.196
59	125	.375	30	0	7880	*	2.0	.249
60	128	1.000	30	0	12000	0	*	**
61	128	1.000	60	0	10500	0	*	**
62	128	1.000	120	0	9000	0	*	**
63	128	1.000	240	0	6400	0	*	**
64	128	1.000	240	45	9000	0	*	**
65	135	.018	30	0	2915	2785	*	**
66	135	.018	30	70	2933	2400	*	**
67	135	.018	60	0	991	910	*	**
68	135	.018	60	70	2088	1425	*	**
69	135	.060	30	0	3975	3330	*	**
70	135	.060	30	60	3572	1615	*	**
71	135	.060	60	0	1291	840	*	**
72	135	.060	60	60	3935	2680	*	**
73	135	.060	120	60	2642	1830	*	**
74	135	.060	120	70	3919	2450	*	**
75	135	.125	60	0	2899	1780	*	**
76	135	.125	120	60	4894	2815	*	**
77	141	1.500	240	0	9500	0	*	**
78	150	.055	30	60	10553	*	4.6	.368
79	150	.055	30	70	9766	*	1.7	.258
80	150	.100	30	0	10603	*	0.8	.307
81	150	.250	60	0	8676	*	3.0	.442
82	150	.250	60	0	9734	*	3.0	.601
83	200	.500	30	0	9000	0	*	**
84	200	.500	120	70	9400	0	*	**
85	200	.500	240	60	7071	0	*	**
86	300	.125	30	0	4991	3925	*	**

* not available

** not taken

Experimental Data

Table XVIII: Steel Fragments Impacting on Homogeneous Steel of Various Hardnesses (Cont)

Data No.	Brinell Hardness Number	Material Thickness (e inches)	Fragment Weight m (grains)	Obliquity θ (degrees)	Striking Velocity V_s (fps)	Residual Velocity V_r (fps)	Residual Weight m_r (grains)	Hole Size Area (sq. in.)
87	300	.125	60	0	2886	1915	*	**
88	300	.125	60	0	4810	3820	*	**
89	300	.125	120	0	2984	2265	*	**
90	300	.125	240	0	3007	2475	*	**
91	300	.125	240	0	4677	3870	*	**
92	300	.125	240	60	4945	3440	*	**
93	300	.250	60	0	4810	2255	*	**
94	300	.250	240	0	4700	3405	*	**
95	300	.250	240	60	4695	1475	*	**
96	300	.260	17	0	4895	0	*	**
97	300	.260	17	30	5900	0	*	**
98	300	.270	44	0	3600	0	*	**
99	300	.270	44	30	4259	0	*	**
100	300	.270	44	45	4954	0	*	**
101	300	.270	207	0	2254	0	*	**
102	300	.270	207	0	2276	0	*	**
103	300	.270	207	30	2550	0	*	**
104	300	.270	207	30	2619	0	*	**
105	300	.270	207	45	3014	0	*	**
106	300	.270	207	45	3016	0	*	**
107	300	.270	207	60	3726	0	*	**
108	300	.270	207	60	4041	0	*	**
109	300	.270	825	0	1544	0	*	**
110	300	.270	825	30	1695	0	*	**
111	300	.270	825	45	2099	0	*	**
112	300	.270	825	60	2507	0	*	**
113	300	.280	17	0	5101	0	*	**
114	300	.280	17	30	5946	0	*	**
115	300	.520	207	0	3766	0	*	**
116	300	.520	207	30	4722	0	*	**

* not available

** not taken

Experimental Data

Table XVIII: Steel Fragments Impacting on Homogeneous Steel of Various Hardnesses (Cont)

Data No.	Brinell Hardness Number	Material Thickness (e inches)	Fragment Weight m (grains)	Obliquity θ (degrees)	Striking Velocity V_s (fps)	Residual Velocity V_r (fps)	Residual Weight* m_r (grains)	Hole Size Area (sq. in.)
117	300	.520	207	45	5925	0	*	**
118	300	.520	825	0	2584	0	*	**
119	300	.520	825	30	2973	0	*	**
120	300	.520	825	45	3437	0	*	**
121	305	.250	30	0	4575	1510	*	**
122	305	.250	240	0	5105	3640	*	**
123	332	.500	240	0	5448	2492	*	**
124	350	.078	30	60	3300	0	*	**
125	350	.078	120	60	1900	0	*	**
126	350	.078	240	70	1750	0	*	**
127	350	.125	30	60	4800	0	*	**
128	350	.125	120	60	3600	0	*	**
129	350	.125	120	70	7000	0	*	**
130	350	.125	240	70	3000	0	*	**
131	350	.250	120	60	6500	0	*	**
132	350	.250	240	70	5000	0	*	**
133	370	.080	30	0	3268	*	27.0	.110
134	370	.080	30	0	11341	*	0.4	.196
135	370	.080	30	60	5092	*	1.4	.221
136	370	.080	30	70	8111	*	2.2	.215
137	370	.080	60	60	5088	*	7.7	.365
138	370	.080	60	70	6813	*	4.7	.552
139	370	.080	120	70	5955	*	33.8	.945
140	370	.080	120	70	6089	*	10.3	.859
141	370	.125	240	60	4254	2843	*	**
142	371	.125	30	0	5285	*	1.1	.150
143	371	.125	30	60	7874	*	0.0	.258
144	371	.125	60	45	5138	*	32.4	.442
145	371	.125	60	70	7971	*	1.8	.258
146	371	.125	120	45	6121	*	61.9	.589

* not available

** not taken

Experimental Data

Table XVIII: Steel Fragments Impacting on Homogeneous Steel of Various Hardnesses (Cont)

Data No.	Brinell Hardness Number	Material Thickness (e inches)	Fragment Weight m (grains)	Obliquity θ (degrees)	Striking Velocity V_s (fps)	Residual Velocity V_r (fps)	Residual Weight m_r (grains)	Hole Size Area (sq. in.)
147	371	.125	120	60	5918	*	21.5	.522
148	371	.125	240	45	4853	*	173.1	.663
149	371	.125	240	60	4820	*	67.0	.844
150	371	.125	240	70	5098	*	156.6	.614
151	380	.080	30	70	10534	*	1.1	.279
152	380	.125	60	60	9575	*	6.0	.430
153	380	.127	60	60	9877	*	2.5	.574
154	380	.250	30	0	10269	*	2.5	.391
155	390	.250	30	0	6038	*	6.3	.196
156	390	.250	60	0	4957	*	8.8	.307
157	390	.250	120	0	5161	*	22.1	.442
158	390	.250	120	70	8975	*	1.0	.086
159	390	.250	240	0	4519	*	35.7	.644
160	390	.250	240	60	5115	*	0.0	.709
161	390	.250	240	70	8402	*	1.0	.810
162	390	.500	60	0	8436	*	1.7	.442
163	390	.500	120	0	6038	*	18.5	.442
164	390	.500	240	0	8764	*	1.0	1.227
165	390	.500	240	45	8101	*	1.0	.834
166	393	.060	30	0	2001	1207	*	**
167	393	.060	120	70	4174	2517	*	**
168	393	.060	240	70	5078	3751	*	**
169	400	.270	17	0	4806	0	*	**
170	400	.270	17	30	5317	0	*	**
171	400	.270	44	0	3300	0	*	**
172	400	.270	44	30	3876	0	*	**
173	400	.270	44	45	4574	0	*	**
174	400	.270	207	0	2087	0	*	**
175	400	.270	207	30	2515	0	*	**
176	400	.270	207	45	2885	0	*	**

* not available

** not taken

Experimental Data

Table XVIII: Steel Fragments Impacting on Homogeneous Steel of Various Hardnesses (Cont)

Data No.	Brinell Hardness Number	Material Thickness (e inches)	Fragment Weight m (grains)	Obliquity θ (degrees)	Striking Velocity V_s (fps)	Residual Velocity V_r (fps)	Residual Weight m_r (grains)	Hole Size Area (sq. in.)
177	400	.270	207	60	4014	0	*	**
178	400	.270	825	0	1394	0	*	**
179	400	.270	825	30	1660	0	*	**
180	400	.270	825	45	1591	0	*	**
181	400	.502	207	0	3461	0	*	**
182	400	.502	207	30	4008	0	*	**
183	400	.510	825	0	2346	0	*	**
184	400	.510	825	30	2399	0	*	**
185	410	.625	30	0	11500	0	*	**

* not available

** not taken

Experimental Data

Table XIX: Steel Fragments Impacting on Copper

Data No.	Material Thickness e (inches)	Fragment Weight m (grains)	Obliquity θ (degrees)	Striking Velocity V_s (fps)	Residual Velocity V_r (fps)	Residual Weight m_r (grains)	Hole Size Area (sq. in.)
1	.055	30	60	7569	**	9.5	.387
2	.055	30	60	8266	**	3.7	.368
3	.060	15	0	1350	*	14.0	**
4	.060	15	0	1350	*	14.0	**
5	.060	15	0	1357	786	*	**
6	.060	15	0	1500	*	14.0	**
7	.060	15	0	1500	*	14.0	**
8	.060	15	0	2828	2005	14.0	**
9	.060	15	0	3000	*	14.0	**
10	.060	15	0	3600	*	14.0	**
11	.060	15	0	4700	*	8.5	**
12	.060	15	0	4744	3632	*	**
13	.060	15	60	3427	1597	*	**
14	.060	15	60	4792	1899	4.9	**
15	.060	30	0	1000	*	29.0	**
16	.060	30	60	2798	1689	29.0	**
17	.060	30	60	3000	*	26.7	**
18	.060	30	60	7081	**	8.3	.295
19	.060	30	70	5960	**	5.0	.387
20	.060	30	70	8648	**	1.4	.491
21	.060	60	0	1210	870	59.0	**
22	.060	60	0	2593	2043	54.3	**
23	.060	60	60	2600	1722	*	**
24	.060	60	70	4223	*	14.5	**
25	.060	60	70	4223	2920	21.0	**
26	.060	60	70	8198	**	0	.798
27	.060	60	70	9672	**	1.0	.675
28	.060	120	0	1000	*	119.0	**
29	.060	120	0	1146	857	119.0	**
30	.060	240	0	1000	*	239.0	**

* not available

** not taken

Experimental Data

Table XIX: Steel Fragments Impacting on Copper (Cont)

Data No.	Material Thickness e (inches)	Fragment Weight m (grains)	Obliquity θ (degrees)	Striking Velocity V_s (fps)	Residual Velocity V_r (fps)	Residual Weight m_r (grains)	Hole Size Area (sq. in.)
31	.060	240	0	1000	*	239.0	**
32	.060	240	0	1000	*	239.0	**
33	.060	240	0	1000	*	239.0	**
34	.060	240	0	1300	*	239.0	**
35	.060	240	0	1318	1087	239.0	**
36	.060	240	0	1318	1087	239.0	**
37	.125	15	0	2786	1347	14.0	**
38	.125	15	0	2800	*	13.1	**
39	.125	15	0	3000	*	14.1	**
40	.125	15	0	4720	2974	10.0	**
41	.125	15	0	4750	*	7.7	**
42	.125	15	0	5000	*	2.3	**
43	.125	15	0	5000	*	14.0	**
44	.125	30	0	2500	*	26.7	**
45	.125	30	0	2543	1444	27.5	**
46	.125	30	60	4887	2050	8.0	**
47	.125	30	60	8986	**	1.5	.460
48	.125	30	70	11366	**	0	.414
49	.125	60	0	3713	2640	54.3	**
50	.125	60	60	4168	1313	32.6	**
51	.125	60	70	8118	**	0	1.516
52	.125	60	70	9879	**	0	.742
53	.125	120	0	2000	*	117.6	**
54	.125	120	0	2446	1646	115.0	**
55	.125	120	60	2984	1101	90.7	**
56	.125	120	60	2984	*	92.0	**
57	.125	240	0	1522	1068	*	**
58	.125	240	0	2000	*	239.0	**
59	.125	240	0	2000	*	239.0	**
60	.125	240	70	4254	1614	82.6	**

* not available

** not taken

Experimental Data

Table XIX: Steel Fragments Impacting on Copper (Cont)

Data No.	Material Thickness e (inches)	Fragment Weight m (grains)	Obliquity θ (degrees)	Striking Velocity V_s (fps)	Residual Velocity V_r (fps)	Residual Weight m_r (grains)	Hole Size Area (sq. in.)
61	.125	240	70	9936	**	0.9	2.099
62	.250	15	0	10589	3159	*	**
63	.250	30	0	3840	2185	29.0	**
64	.250	30	0	11418	4348	*	**
65	.250	60	45	8185	1814	6.8	**
66	.250	60	45	9753	2760	*	**
67	.250	60	45	10092	4282	*	**
68	.250	60	60	10502	2330	*	**
69	.250	120	0	2993	*	95.7	**
70	.250	120	0	2993	1288	119.0	**
71	.250	120	0	3000	*	110.7	**
72	.250	120	60	8665	1035	*	**
73	.250	240	0	3000	*	179.2	**
74	.250	240	0	3000	*	198.6	**
75	.250	240	0	3000	*	239.0	**
76	.250	240	0	3347	2315	196.6	**
77	.250	240	60	4254	1716	71.4	**
78	.250	240	60	4700	*	140.6	**
79	.250	240	60	4800	*	141.4	**
80	.250	240	60	4830	*	71.4	**
81	.250	240	60	4830	1564	142.3	**
82	.250	240	60	5000	*	123.8	**
83	.250	240	70	7825	500	*	**
84	.500	30	0	8776	1266	3.2	**
85	.500	30	0	10529	1534	1.0	**
86	.500	60	0	4800	*	59.0	**
87	.500	60	0	4950	915	59.0	**
88	.500	60	0	10866	2624	2.8	**
89	.500	120	0	5000	*	111.3	**
90	.500	120	0	5001	1237	5.4	**

* not available

** not taken

Experimental Data

Table XIX: Steel Fragments Impacting on Copper (Cont)

Data No.	Material Thickness e (inches)	Fragment Weight m (grains)	Obliquity θ (degrees)	Striking Velocity V_s (fps)	Residual Velocity V_r (fps)	Residual Weight m_r (grains)	Hole Size Area (sq. in.)
91	.500	120	0	8645	2825	*	**
92	.500	120	45	10346	900	*	**
93	.500	240	0	4604	1994	239.0	**
94	.500	240	0	4718	1834	*	**
95	.500	240	45	4604	1177	155.2	**
96	.500	240	70	8943	5926	6.5	**
97	1.000	240	0	5135	735	*	**
98	1.000	240	0	5169	743	*	**

* not available

** not taken

Experimental Data

Table XX: Steel Fragments Impacting on Lead

Data No.	Material Thickness e (inches)	Fragment Weight m (grains)	Obliquity θ (degrees)	Striking Velocity V_s (fps)	Residual Velocity V_r (fps)	Residual Weight m_r (grains)	Hole Size Area (sq. in.)
1	.065	15	60	2928	800	6.9	.393
2	.065	15	60	2930	1200	14.0	.344
3	.065	15	60	3037	800	4.0	.319
4	.125	30	0	7878	3500	1.5	.887
5	.125	30	0	8005	3000	1.2	.884
6	.125	30	60	8200	*	0.3	.773
7	.125	30	60	8926	*	0	.859
8	.125	30	60	10303	3394	0.9	.874
9	.125	60	0	7617	*	4.7	.994
10	.125	60	60	9551	*	3.0	1.534
11	.125	120	0	5940	3615	12.9	2.405
12	.130	15	0	2856	1554	**	**
13	.130	15	0	3287	1692	**	**
14	.130	30	0	4000	**	21.6	**
15	.130	30	0	4000	**	22.5	**
16	.130	30	0	4053	2850	21.6	**
17	.130	30	60	1316	75	**	**
18	.130	30	60	2783	762	**	**
19	.130	30	60	2784	697	**	**
20	.130	30	60	2970	594	**	**
21	.130	30	60	3777	*	0	**
22	.130	120	60	1190	580	**	**
23	.130	240	0	3934	3300	204.5	**
24	.130	240	0	4000	**	204.3	**
25	.130	240	0	4000	**	207.2	**
26	.130	240	60	1070	880	**	**
27	.130	240	70	4000	**	48.4	**
28	.130	240	70	4000	**	55.4	**

* not available

** not taken

Experimental Data

Table XX: Steel Fragments Impacting on Lead (Cont)

Data No.	Material Thickness e (inches)	Fragment Weight m (grains)	Obliquity θ (degrees)	Striking Velocity V_s (fps)	Residual Velocity V_r (fps)	Residual Weight m_r (grains)	Hole Size Area (sq. in.)
29	.137	15	0	2375	1700	14.0	.249
30	.137	15	0	4774	2500	2.0	.442
31	.137	15	0	4811	2000	0.5	.442
32	.137	30	0	3142	1500	27.5	.338
33	.137	30	0	3431	2000	10.6	.405
34	.137	30	0	5648	2500	3.2	.601
35	.235	60	0	4819	2500	7.3	1.353
36	.250	30	0	9150	*	0.6	1.623
37	.250	30	60	9905	*	0	1.289
38	.250	60	0	2623	1200	19.8	1.617
39	.250	60	60	8706	*	0	1.675
40	.250	240	0	8559	3300	5.3	4.080
41	.250	240	60	8545	1700	1.0	3.497
42	.260	15	0	1266	0	**	**
43	.260	15	60	4992	**	2.0	**
44	.260	30	0	3900	**	12.0	**
45	.260	30	0	3900	**	22.0	**
46	.260	30	0	5751	*	0	**
47	.260	30	60	3158	**	2.0	**
48	.260	30	70	7294	303	**	**
49	.260	60	60	2047	0	**	**
50	.260	60	60	8924	3922	**	**
51	.260	60	60	9110	2749	**	**
52	.260	60	70	9011	690	**	**
53	.260	120	0	2362	1204	**	**
54	.260	120	0	2404	1224	**	**
55	.260	120	0	3995	2100	98.0	**
56	.260	120	0	4056	2300	**	**

* not available

** not taken

Experimental Data

Table XX: Steel Fragments Impacting on Lead (Cont)

Data No.	Material Thickness e (inches)	Fragment Weight m (grains)	Obliquity θ (degrees)	Striking Velocity V_s (fps)	Residual Velocity V_r (fps)	Residual Weight m_r (grains)	Hole Size Area (sq. in.)
57	.260	120	70	6512	2318	**	**
58	.260	240	0	550	0	**	**
59	.260	240	0	6206	*	54.0	**
60	.260	240	60	1980	142	**	**
61	.260	240	70	4000	**	76.5	**
62	.275	60	0	2486	1750	27.5	.601
63	.304	60	60	3920	1678	23.3	.945
64	.309	60	60	3676	2438	17.7	.699
65	.375	30	45	7481	3058	**	**
66	.500	30	0	6436	854	**	**
67	.500	30	45	10393	1197	**	**
68	.500	60	0	2868	694	**	**
69	.500	60	0	2901	573	**	**
70	.500	60	45	9357	1427	**	**
71	.500	120	0	3075	976	20.0	**
72	.500	120	0	3973	1207	**	**
73	.500	120	0	4008	1103	**	**
74	.500	120	0	4156	1887	45.0	2.074
75	.500	120	45	5054	*	40.0	**
76	.500	120	60	6814	0	**	**
77	.500	120	60	7602	0	**	**
78	.500	240	0	2929	1216	112.0	**
79	.500	240	0	2944	1238	110.0	**
80	.500	240	0	3092	1266	237.0	1.917
81	.500	240	0	5676	2000	22.0	3.976
82	.500	240	60	3990	0	**	**
83	.500	240	60	5914	1300	10.0	2.921
84	.500	240	60	6220	*	2.0	**

* not available

** not taken

Experimental Data

Table XX : Steel Fragments Impacting on Lead (Cont)

Data No.	Material Thickness e (inches)	Fragment Weight m (grains)	Obliquity θ (degrees)	Striking Velocity V_s (fps)	Residual Velocity V_r (fps)	Residual Weight m_r (grains)	Hole Size Area (sq. in.)
85	.500	240	70	8784	1774	**	**
86	1.000	30	0	8323	1815	**	**
87	1.000	60	0	4956	0	**	**
88	1.000	120	0	3890	400	**	**
89	1.000	240	0	3076	645	173.0	**
90	1.000	240	0	3192	555	128.0	1.767
91	1.000	240	0	4146	2500	171.0	**
92	1.000	240	0	4800	**	98.8	**
93	1.000	240	0	4858	925	99.0	**
94	1.000	240	0	5896	1105	47.8	4.909
95	1.000	240	45	8541	3546	**	**

* not available

** not taken

Experimental Data

Table XXI: Steel Fragments Impacting on Tuballoy

Data No.	Material Thickness e (inches)	Fragment Weight m (grains)	Obliquity θ (degrees)	Striking Velocity V_s (fps)	Residual Velocity V_r (fps)	Residual Weight m_r (grains)	Hole Size Area (sq. in.)
1	.100	30	0	3578	1427	23.0	.150
2	.100	30	0	4746	1800	16.0	**
3	.100	30	0	9408	4500	1.0	**
4	.100	30	30	4460	1359	12.3	.129
5	.100	30	45	5452	*	0	**
6	.100	60	0	3037	1053	14.0	.249
7	.100	60	0	4828	2700	5.0	**
8	.100	60	30	3737	1338	43.0	.221
9	.100	60	30	4450	1873	35.0	.276
10	.100	60	60	5588	*	0	**
11	.100	120	0	1625	572	117.0	.472
12	.100	120	0	2250	1269	85.0	.129
13	.100	120	30	3960	2187	87.0	.439
14	.100	120	60	5670	*	0	**
15	.100	120	60	5900	2281	*	**
16	.100	120	60	9352	3000	1.0	.626
17	.100	240	0	2400	1452	220.0	.371
18	.100	240	30	3150	1809	200.0	.515
19	.100	240	45	9642	3400	24.5	.920
20	.100	240	60	5962	1800	1.0	**
21	.100	461	45	5310	2500	214.0	1.252
22	.100	465	0	3200	2300	165.0	.690
23	.100	465	60	7345	2900	21.0	1.460
24	.125	30	0	5692	1600	3.5	**
25	.125	30	45	5484	*	0	**
26	.125	30	45	5948	3000	1.0	**
27	.125	60	45	5625	800	1.0	**
28	.125	240	0	4653	2500	225.0	**
29	.125	240	45	4844	1300	88.0	**
30	.125	240	45	4962	2000	1.0	**

* not available

** not taken

Table XXI: Steel Fragments Impacting on Tuballoy (Cont)

Data No.	Material Thickness e (inches)	Fragment Weight m (grains)	Obliquity θ (degrees)	Striking Velocity V_s (fps)	Residual Velocity V_r (fps)	Residual Weight m_r (grains)	Hole Size Area (sq. in.)
31	.125	240	45	5566	2000	1.0	**
32	.125	240	60	5779	1800	1.0	**
33	.150	30	0	5311	1500	5.0	**
34	.150	60	0	4871	1360	8.0	**
35	.150	120	0	4575	3000	3.0	**
36	.150	120	45	5073	900	2.0	**
37	.150	240	0	5866	2600	4.0	**
38	.150	240	45	5090	2500	90.0	**
39	.150	465	30	4300	1700	110.0	.884
40	.150	467	45	5078	2300	120.5	1.200
41	.150	468	30	5374	2300	155.0	1.043
42	.150	471	30	3400	2300	355.0	.828
43	.200	30	0	9319	2500	1.0	**
44	.200	30	45	10091	*	0	**
45	.200	30	60	9138	*	0	**
46	.200	60	0	5638	2000	2.0	**
47	.200	60	0	8318	2600	3.0	**
48	.200	60	45	5839	*	0	**
49	.200	120	0	5577	4000	1.0	**
50	.200	120	0	6048	3157	1.0	**
51	.200	120	45	6121	900	2.0	**
52	.200	240	0	5837	2400	12.0	**
53	.200	240	0	6100	4000	1.0	**
54	.200	240	45	4962	2000	1.0	**
55	.200	465	45	7664	3100	5.0	1.105
56	.200	465	0	7124	2100	21.0	1.325
57	.200	466	45	5024	1500	58.0	1.688
58	.200	467	45	5161	2200	80.0	1.304
59	.200	468	0	5120	2650	83.5	1.105

* not available

** not taken

Following page is blank

[redacted]

Appendix H

Other Ballistic Analysis Laboratory Reports

on Studies of the Perforation

of Target Materials by Fragments and Projectiles

[redacted]

Other Ballistic Analysis Laboratory Reports on Studies of the Perforation of Target Materials by Fragments and Projectiles

Report No.	Date	Title	Classification
14	Sept. 1954	A Suggested Technique for Predicting the Performance of Armor-Piercing Projectiles Acting on Rolled Homogeneous Armor (U)	C
25	July 1956	A Comparison of Various Materials in Their Resistance to Perforation by Steel Fragments; Empirical Relationships (U)	C
36	April 1958	A Study of Residual Velocity Data for Steel Fragments Impacting on Four Materials; Empirical Relationships (U)	C
41	May 1959	A Comparison of the Performance of Fragments of Four Materials Impacting on Various Plates (U)	C
44	Jan. 1960	The Resistance of Two Nose-Cone Materials to Perforation by Steel Fragments; Empirical Relationships for Fragment Residual Velocity and Residual Weight (U)	S

[redacted]

DISTRIBUTION LIST

No. of Copies	Organization
6	Chief of Ordnance Department of the Army Washington 25, D.C. Attn: ORDTB-Ball Sec
10	Chief of Ordnance Washington 25, D.C. Attn: ORDTB (6 for United Kingdom) (4 for Canada)
1	Chief of Ordnance Washington 25, D.C. Attn: ORDTP-Maj. D.R. Balfour Canadian Liaison Office
1	Army Ord Representative U.S. Nav Ord Test Sta Annex 3202 E. Foothill Blvd. Pasadena 8, California Attn: Mr. Z.A. Typaldos
1	Commanding Officer Diamond Ordnance Fuze Labs. Washington 25, D.C. Attn: Tech Ref Section ORDTL 06.33
1	Commanding General U.S. Army Ord Missile Command Redstone Arsenal, Alabama Attn: Library Section
1	Commanding Officer Ord Material Res Office Watertown Arsenal Watertown 72, Mass. Attn: Mr. B. Goldberg
2	Commanding Officer U.S. Army Ord District 128 North Broad Street Philadelphia, Pennsylvania Attn: OD, R&D Branch
2	Commanding General Ord Tank-Automotive Command 1501 Beard Street Detroit 9, Michigan Attn: Mr. H. Spiro Mr. Charles Saulter
1	Canad. Arm Res & Dev Est. Box 1247 Quebec, Canada VIA: Major J.J. Vallaster ARGMA, Project Office
1	ABMA Field Office U.S.Army Ord Missile Command Lockheed Missile & Space Div P.O. Box 504, Sunnyvale, Cal Attn: Mr. A.E. Papazoni VIA: Bu Weap Rep
3	Commander Army Rocket & G. Missile Agcy Redstone Arsenal, Alabama Attn: Mr. P. Mullowney (1) Mr. C. Cockrell (1) Library Section (1)
3	Com, Army Ball Miss Agcy Redstone Arsenal, Alabama Attn: ORDAB-DV, Mr.H.L. Martin Mr.J.P. Heaman, Aerob Lab ORDAB-RRT, Mr.G.R.Emanuel
1	Director Marshall Space Flight Center Nat'l Aeron & Space Admin Redstone Arsenal, Alabama Attn: Library Section
4	Commanding Officer Picatinny Arsenal Dover, New Jersey Attn: Messrs. F. Saxe J. Killen, W.J. Kuhn Dr. N. Clarke
1	Commanding Officer Frankford Arsenal Philadelphia 37, Pennsylvania Attn: Mr. H. Markus
1	Commanding Officer Watertown Arsenal Watertown 72, Massachusetts Attn: Watertown Arsenal Lab Armor Section

[redacted]

[redacted]

DISTRIBUTION LIST (Cont)

No. of Copies	Organization
1	Office of the Chief Q.M. Gen Washington 25, D.C. Attn: OMGRE-O Mr. Herbert Maisel
2	Commanding General Q.M. Res & Eng Command Natick, Massachusetts Attn: Capt. Josef Senna Mr. A. Alessi
1	Commanding Officer U.S. Army Art & Missile Sch Fort Sill, Oklahoma Attn: Librarian O. Willard Hollaway
10	Armed Services Tech Info Agcy Documents Service Center Arlington Hall Station Arlington 12, Virginia
1	Commander Field Command Defense Atomic Support Agency P.O. Box 5100 Sandia Base Albuquerque, New Mexico Attn: FCDR/4
2	U.S. Atomic Energy Commission Sandia Corporation Sandia Base Albuquerque, New Mexico Attn: W.F. Hartman, Div 126 F.J. Weibell, Div 1285
1	Commanding General U.S.Army Transp Materiel Comm 12th & Spruce Streets St. Louis, Missouri Attn: TC MAC-EPP
1	Commanding Officer U.S. Army Chemical Center, Md. Attn: Mr. George Stewart
1	Commanding Officer U.S.Army Transp Res Command Fort Eustis, Virginia Attn: E.V. Merritt
16	Director Ballistic Research Labs Aberdeen Proving Ground, Md. Attn: Mr. R.G. Bernier, WSL Mr. J.J. Dailey, WSL Mr. J.W. Gehring, TBL Mr. D. Dunn, TBL Mr. R. O'Brien, WSL Mr. H. Peaker, WSL Reports Dist Sect (10)
1	Director Development & Proof Services Aberdeen Proving Ground, Md. Attn: Mr. W.C. Pless
2	Commanding General Aberdeen Proving Ground, Md. Attn: Tech Info Branch
3	Chief Bureau of Nav Weapons Department of the Navy Washington 25, D.C. Code: A, RMMO-5
1	Commander Naval Air Development Center Johnsville, Pennsylvania Attn: WR-4
1	Commander Naval Ord Laboratory Corona, California Attn: Fuze Department
1	Commander Naval Ord Laboratory White Oak Silver Spring, Maryland
2	Commanding Officer U.S. Nav Ord Test Station China Lake, California Attn: Code 12, Mr. Naufeld Code 4057, Mr. Zeitlin
1	Office of Naval Research Navy Department Washington 25, D.C. Attn: M483 (Sc. Let. Br)

[redacted]

[redacted]

DISTRIBUTION LIST (Cont)

No. of Copies	Organization
2	Commander Naval Research Laboratory Anacostia, Maryland Attn: Dr. S. Thompson, Code 6235 Mr. W.W. Atkins
3	Commanding Officer Naval Proving Ground Dahlgren, Virginia Attn: Dr. A.V. Hershey KBT-3S Code W4-1; Missile Safety Staff
1	Marine Corps Liaison Officer Office Chief of Ordnance Washington 25, D.C. Attn: Major Paul Sanders
2	Commander Air Proving Ground Center Eglin Air Force Base, Florida Attn: PGRE PGTZM
1	Commander Aerospace Tech Intell Center Wright-Patterson AFB, Ohio
1	Commander Kirtland Air Force Base Albuquerque, New Mexico Attn: AF Space Weapons Center
1	Commander U.S.Navy Nuclear Ord Eval Unit Kirtland Air Force Base Albuquerque, New Mexico Attn: Code 40
1	Commander H.Q. Ogden Air Materiel Area Hill Air Force Base, Utah Attn: OOGSS
1	Applied Physics Laboratory The Johns Hopkins University 8621 Georgia Avenue Silver Spring, Maryland Attn: Mr. G.L. Seielstad for H.R. Holt VIA: Bur of Nav Weap Rep
1	Institute for Coop Research The Johns Hopkins University 34th & Charles Streets Baltimore 18, Maryland Attn: H.R. Warfield, Dir
1	Armour Research Foundation 33rd & Dearborn Streets Chicago, Illinois Attn: Librarian of Documents VIA: Commanding Officer Chicago Air Proc Dist 165 N. Canal Street Chicago 6, Illinois
1	University of Denver Industrial Research Institute Denver 10, Colorado Attn: Mr. L.E. Smith VIA: Commanding Officer St. Louis Ord Dist 4300 Goodfellow Blvd. St. Louis 20, Missouri
1	Stanford Research Institute Menlo Park, California Attn: T.C. Poulter VIA: Commanding Officer San Francisco Ord Dist 1615 Clay Street P.O. Box 1829 Oakland 12, California
1	Colorado School of Mines Golden, Colorado Attn: John S. Rinehart VIA: Commanding Officer St. Louis Ord Dist 4300 Goodfellow Blvd. St. Louis 20, Miss.

[redacted]

[redacted]

DISTRIBUTION LIST (Cont)

UNCLASSIFIED

No. of Copies	Organization
1	University of Utah Salt Lake City, Utah Attn: Explosives Res Group VIA: Commanding Officer Los Angeles Ord Dist 55 S. Grand Avenue Pasadena 2, California
1	Cornell Aeronautical Lab Buffalo, New York VIA: Commanding Officer New York Ordnance Dist 770 Broadway New York 3, New York
1	Director Operations Research Office 6935 Arlington Road Bethesda, Maryland Washington 14, D.C.
1	Lincoln Laboratory Mass. Inst of Tech Cambridge, Massachusetts Attn: Mr. W. Herrmann Room 41-219 VIA: Boston Ordnance Dist Boston Army Base Boston 10, Mass.
1	Carnegie Institute of Tech Schenley Park Pittsburgh 13, Pennsylvania VIA: Commanding Officer Philadelphia Ord Dist 128 N. Broad Street Philadelphia 2, Pa.
2	Space Technology Lab. Inc. Box 95001, Los Angeles 45, Cal Attn: Dr. Morris Rosen (1) VIA: AF Ball Missile Div AF Unit Post Office Los Angeles 45, Cal Attn: Lt Eibling (WDTVV-3-1) (1)
1	McDonnell Aircraft Company Box 516, St. Louis 66, Miss. VIA: U.S. AF Plant Rep

No. of Copies	Organization
2	Aerojet General Corporation Azusa, California Attn: K.N. Krezenhagen Ann R. Chase, Libr at Downey, Calif. VIA: Bureau of Nav Weap Rep
1	Aircraft Armaments Inc. Cockeysville, Maryland VIA: Philadelphia Ord Dist 128 North Broad Street Philadelphia 2, Pa.
1	AVCO Manufacturing Corp Res & Advanced Development Wilmington, Massachusetts Attn: Mrs. H.M. Page VIA: Commanding Officer Boston Ord District Boston Army Base Boston 10, Mass.
1	Bell Helicopter Corporation P.O. Box 482 Fort Worth 1, Texas Attn: Mr. M. Kawa VIA: Bureau of Nav Weap Rep
1	Boeing Airplane Company P.O. Box 3707 Seattle 24, Washington Attn: Mr. Val Deriugin, Mail Stop 14-60 VIA: AF Plant Rep
1	Chrysler Corporation Missile Division Attn: Mr. Hertler (Aerophysics) VIA: Detroit Ord Dist 574 E. Woodbridge Detroit 31, Michigan
2	Convair Div of Gen Dyn Corp P.O. Box 1950 Pomona, California Attn: J. Benish G.D. Goldshine VIA: Resident ARGMA Rep

UNCLASSIFIED

[redacted]

No. of Copies	Organization
1	Raytheon Manufacturing Co. Missile System Division Bedford, Massachusetts Attn: Mr. Bud Hurd VIA: Boston Ordnance Dist Boston Army Base Boston 10, Mass.
1	Republic Aviation Corporation Scientific Research Staff Farmingdale, New York VIA: U.S. AF Plant Rep
1	Sylvania Electrical System Waltham 54, Massachusetts VIA: Boston Ordnance Dist Boston Army Base Boston 10, Mass.
1	Vertol Air Corporation Morton, Pennsylvania Attn: Mrs. L.M. Rankin VIA: Bureau of Nav Weap Rep
1	Grumman Aircraft Eng Corp Bethpage, Long Island, N.Y. Attn: E.J. Bonan VIA: Bur of Nav Weap Rep
1	The RAND Corporation 1700 Main Street Santa Monica, California Attn: Dr. R.L. Bjork VIA: U.S. AF Plant Rep
1	Convair, Div of Gen Dyn Corp San Diego Division Mail Zone 6-157 San Diego 12, California Attn: Chief Librarian VIA: Bur of Nav Weap Rep
1	General Electric Company Burlington, Vermont VIA: Boston Ordnance Dist Boston Army Base Boston 10, Mass.
1	North American Aviation Corp Los Angeles 45, California VIA: Bur of Nav Weap Rep

No. of Copies	Organization
1	General Electric Company Radnor, Pennsylvania VIA: Philadelphia Ord Dist 128 North Broad Street Philadelphia 2, Pa.
1	Goodyear Aircraft Corporation 1210 Massillon Road Akron 15, Ohio Attn: Robert Shumaker VIA: Bur of Nav Weap Rep
1	Hughes Aircraft Company Fullerton, California Attn: D.A. Secrist Ground Systems Group Mail Station 600/F-231 VIA: Los Angeles Ord Dist 55 S. Grand Avenue Pasadena 2, California
1	Arthur D. Little, Inc. 35 Acorn Park Cambridge, Massachusetts Attn: Mr. D.B. Lull VIA: Boston Ordnance Dist Boston Army Base Boston 10, Mass.
1	The Martin Company Orlando, Florida Attn: Mr. M. Meyerson VIA: Birmingham Ord Dist 2120 N. Seventh Ave. Birmingham, Alabama
1	Nortronics 500 East Orangethorpe Avenue Anaheim, California VIA: Los Angeles Ord Dist 55 S. Grand Avenue Pasadena 2, California
1	General Electric Company Missile & Space Vehicle Div Philadelphia 4, Pennsylvania Attn: A.M. Smith VIA: Philadelphia Ord Dist 128 North Broad Street Philadelphia 2, Pa.